Characterization of *Vibrio cholerae* regulatory protein CytR in chitin utilization and pathogenesis

Thesis submitted for the degree of
Doctor of Philosophy (Science)
in
Life Science & Bio-technology

by

SUMAN DAS, M.Sc.

(JU Index No.: 49/18/Life. Sc./25)

Department of Life Science and Bio-technology
Jadavpur University
Kolkata, India

2022

CERTIFICATE FROM THE SUPERVISOR

This is to certify that the thesis entitled **"Characterization of *Vibrio cholerae* regulatory protein CytR in chitin utilization and pathogenesis"** Submitted by Sri / ~~Smt.~~ **SUMAN DAS** who got his / ~~her~~ name registered on 13.02.2018 For the award of Ph. D. (Science) degree of Jadavpur University, is absolutely based upon his own work under the supervision of **Dr. NABENDU SEKHAR CHATTERJEE** and that neither this thesis nor any part of it has been submitted for either any degree / diploma or any other academic award anywhere before.

NSChattyu 22-02-2022

(Signature of the Supervisor date with official seal)

नबेन्दु शेखर चटर्जी / Nabendu Sekhar Chatterjee
(वैज्ञानिक - एफ / Scientist F)
आई.सी.एम.आर राष्ट्रीय कॉलरा और आंत्र रोग संस्थान
ICMR National Institute of Cholera & Enteric Diseases
पी-३३, सी.आई.टी. रोड, स्कीम-१०एम, बेलियाघाटा
P-33, CIT Road, Scheme-XM, Beliaghata
कोलकाता-७०००१० / Kolkata-700010

DECLARATION

I do, hereby, declare that the work embodied in this thesis entitled **"Characterization of *Vibrio cholerae* regulatory protein CytR in chitin utilization and pathogenesis"** submitted for the award of Doctorate of Philosophy (Science) in Life Science and Bio-technology, is the completion of work carried out under the supervision of Dr. Nabendu Sekhar Chatterjee, Scientist – F, at the Division of Biochemistry, ICMR-National Institute of Cholera and Enteric Diseases, Kolkata. Neither this thesis nor any part of it has been submitted for either any equivalent degree/diploma or any other academic award elsewhere.

Date: 22-02-2022

Place: Kolkata

....
Signature of the candidate

Suman Das

to…

Baba & Maa

Contents

Acknowledgement

Acknowledgement

Standing at the verge of completion of my Doctoral research, perhaps no words are sufficient to express my gratitude, sincere appreciation and praise for all those who have contributed both professionally and emotionally in this journey and helped this dissertation take its present shape. I would like to express the deepest appreciation to my esteemed guide Dr. Nabendu Sekhar Chatterjee, Biochemistry Division, Indian Council of Medical Research – National Institute of Cholera and Enteric Diseases (ICMR-NICED), Kolkata, who has given me the opportunity to pursue my PhD career and giving me the freedom to think and implement my ideas. He has taught me the intricacies of research with great patience while critically analyzing the results which eventually guided me to enter a fruitful and exciting field of research. He has always encouraged me to be involved with various scientific activities out of the sphere of my research which helped me to great extent to be matured as a student of science. His guidance has ultimately helped me to formulate my dissertation to its present status.

I am thankful to Dr. Shanta Dutta, present director of ICMR-NICED, for granting me the privilege to continue my work in this esteemed institute. I would also express my sincere gratitude to Dr. Asish Kumar Mukhopadhyay, Dr. Sushmita Bhattacharya, Dr. Hemanta Koley, Dr. Sandipan Ganguly, Dr. Provash Chandra Sadhukhan, Dr. Amit Pal, Dr. Santasabuj Das, Dr. Moumita Dutta, Dr. Sulagna Basu for their help and allowing me to use their laboratory facilities.

Apart from the faculty, I wish to convey my gratitude to my seniors, friends and colleagues for their continuous help and co-operation that created a perfect laboratory environment. Amongst all, first and foremost I express my heartfelt thanks to my lab seniors Dr. Rhishita Chourashi, Dr. Sudipto Mandal, Dr. Amarshi Mukherjee, Dr. Anusuya Debnath, Dr. Moumita Mondal, and my all-time lab partner-cum-colleague Mr. Debjyoti Bhakat, all of whom taught me the basic and finer arts of microbiology, molecular biology and provided continuous advice, assistance and encouragement to complete my work, even at the darkest hours of scientific failures. A special thanks to Dr. Priyadarshini Mukherjee for her help in animal experiments. I would also like to thank my lab friend Mr. Indranil Mondal and lab juniors Mrs. Priyanka Basak, Ms. Uzma Khan, Ms. Priyanka Maitra, Ms. Sushmita Kundu, for their unquestioned support and assistance throughout the course of this study. I desire to extend my appreciation to the lab interns Swastik, Saurav, Rounack, Pritha, Priyanka, Symphony, Ditam who have been exceptionally helpful throughout and I sincerely appreciate their friendship and assistance.

I shall treasure the camaraderie that has developed amongst us. I would also like to thank my other seniors Sagar da, Abhishek da, Amlan da, Asim da, Abhijeet da, Arindam da, Piyali di, Prosenjit da, Bipul da, Tanmoy da, Gautam da, Subhankar da, Subhoshree di, Tanushree di, Sraborni di, Nilakshi di, Tania di, Sayan Da, Nirmalya da, Shreya di, Rituparna di, and Punam di and my collegues Rudra Narayan, Sangita, Debjani, Sreeja, Puja, Sanjeeb da, Tapas, Maruf, Ajanta, Amrita, Priyanka, Krishnendu da, Suparna, Mainak, Sohini, Bani, Payel, Pralay, Suhrid, Vivek, Suprodip, Sagnik, Urbi and Subhrotoa for their selfless encouragement and support which helped to overcome the tough times during my work.

I shall remain grateful to Animesh, Arpita di and Bibhas da for their technical assistance mainly through their contributions with confocal microscopy, electron microscopic sample preparations and microtomy of histological slide preparations. The staff members of this institute Ananda da, Alam da, Chinmoy da, Malay da, Manas da, Dipak da, Subho da, Prosenjit da and Gouri di have always come forward with helping hands, for which I sincerely thank them all. I am grateful to all the members and the staff of the Institute for their friendly behaviour, cooperation, good wishes throughout the course of my study.

My heartfelt gratitude goes to Dr. Keinosuke Okamoto and Mrs. Miki Hidaka of Okayama University, Japan, for extending their hands of assistance and providing partial financial support to our lab.

I owe my deepest gratitude to all the authors of literatures reviewed, as their work provided me information and knowledge to carry out my thesis work. I earnestly appeal them to please excuse me for using some of their illustrations with proper citation and acknowledgement in my writing for academic purpose only.

I would like to thank all my teachers in school, college and university who have allowed me to grow and learn with them.

This dissertation would not have been possible without the generous support, encouragement and patience of my family members during the course of this journey. I pay my sincere respect to my Baba, Mr. Biswanath Das and Maa, Mrs. Ila Das who had to sacrifice a routine life in order to accommodate my long hour at the laboratory and who have been the unequivocal pillars of strength throughout my life. Words cannot express my heartiest gratitude for my wife Dipanwita for her unquestioned and sustained support throughout this endeavour. I thank the almighty and the departed souls of my grandparents, Dadu, Dida, Late Mrs. Jyotsna Das, for their eternal love and blessings which helped me sail through the tumultuous journey.

Finally, thank you everybody (including all the people I have mentioned above and if I have forgotten anyone else to talk about) for your help and cooperation, what made me reach this height in my career.

Dated: **Suman Das**

Place: Kolkata

Abbreviations

Abbreviations

°C	Degree Celsius
β-ME	β-mercaptoethanol
µg	Microgram
µl	Microlitre
µM	Micromolar
µm	Micrometre

A

aa	Amino acid
A_{260}	Absorbance at 260 nm
A_{280}	Absorbance at 280 nm
AC	Adenylate cyclase
Ace	Accessory cholera enterotoxin
ADP	Adenosine diphosphate
AHL	Acyl homoserine lactone
AI	Autoinducer
AI-1	Autoinducer-1
AI-2	Autoinducer-2
AMP	Adenosine monophosphate
Amp^R	Ampicillin resistant
Amp^S	Ampicillin sensitive
APS	Ammonium Persulphate
ATP	Adenosine triphosphate

B

bp	Base pairs
BSA	Bovine serum albumin
BLASTN	Basic local alignment search tool, nucleotides
BLASTP	Basic local alignment search tool, proteins

C

CFU	Colony forming unit
cm	Centimetre
CRP	cAMP receptor protein
CT	Cholera toxin
CTAB	Cetyl trimethyl ammonium bromide
CTXΦ	Cholera toxin phage
cAMP	Cyclic AMP

CAI-1	Cholera autoinducer-1
c-di-GMP	Cyclic di-GMP
cDNA	Complementary DNA
CFTR	Cystic fibrosis transmembrane conductance regulator
CV	Column Volume

D

Da	Dalton
DMF	Dimethyl formamide
DNA	Deoxyribonucleic acid
dNTP	Deoxyribonucleotide
DMSO	Dimethyl sulphoxide
DMEM	Dulbecco's modified eagle's medium
DNS	Dinitrosalicylic acid
DTT	Dithiothreitol

E

EDTA	Ethylenediaminetetraacetic acid
EF	Elongation factor
ELISA	Enzyme-linked immunosorbent assay

F

FA	Fluid Accumulation
FBS	Fetal Bovine Serum
Fig	Figure(s)

G

g	Gram
GlcNAc	N-acetylglucosamine
GM1	Monosialoganglioside
GDP	Guanosine diphosphate
GTP	Guanosine triphosphate
GFP	Green Fluorescent Protein

H

h	Hour
H₃PO₄	Phosphoric acid
HA	Haemagglutinin
HK	Histidine kinase
HAP	Haemagglutinin protease A
HCD	High cell density
HRP	Horseradish peroxidase
HTH	Helix-turn-helix
HEPES	4-(2-hydroxyethyl)-1piperazineethanesulphonic acid
HT-29	Human colorectal adenocarcinoma cell line

I

IPTG	Isopropyl-β-Dthiogalactopyranoside
IMAC	Immobilised metal ion affinity chromatography
IL	Interleukin

K

kb	Kilobase pairs
kDa	KiloDalton
kV	Kilovolt
Kan^R	Kanamycin resistant
KEGG	Kyoto encyclopedia of genes and genomes

L

LA	Luria agar
LB	Luria-Bertani Broth
LCD	Low cell density
LPS	Lipopolysaccharides
LDH	Lactate dehydrogenase

M

M	Molar
MeOH	Methanol
M9M	M9 minimal medium
MCS	Multiple cloning sites
mg	Milligram
min	Minutes
ml	Millilitre
mm	Millimeter
mM	Millimolar
mmol	Millimole

mRNA	Messenger RNA
MIC	Minimum Inhibitory Concentration
MBC	Minimum Bactericidal Concentration

N

N	Normal
ng	Nanogram
nm	Nanometer
NBT	Nitro Blue Tetrazolium
NEB	New England Biolabs
NCBI	National Centre for Biotechnology Information
NCCS	National Centre for Cell Sciences

O

OD	Optical density
OMP	Outer membrane protein
ORF	Open reading frame
ori	Origin of replication
ORS	Oral rehydration solution

P

PAGE	Polyacrylamide gel electrophoresis
PBP	Periplasmic binding protein
PBS	Phosphate buffer saline
PBS-T	Phosphate buffer saline-Tween 20
PCR	Polymerase chain reaction
PVDF	Polyvinylidene fluoride
PMSF	Phenylmethane sulphonylfluoride

Q

qRT-PCR	Quantitative RT-PCR
QS	Quorum sensing

R

RNA	Ribonucleic acid
rpm	Revolution(s) per minute
RT	Reverse transcriptase

RTX   Repeats in toxin

S

sec   Second(s)
SD   Standard deviation
SEM   Standard Error of Mean
SDS   Sodium dodecyl sulfate
Str^R   Streptomycin resistant

T

TAE   Tris-HCl-acetate-EDTA
TBS   Tris Buffer Saline
TCA   Trichloroacetic acid
TE   Tris-HCl-EDTA
TCBS   Thiosulphate-Citrate-Bile salt-Sucrose
TCP   Toxin-coregulated pilus
TCEP   Tris (2-carboxyethyl) phosphine
TEMED   N,N,N',N'-tetramethyl ethylene diamine
TMB   3,3',5,5'-tetramethylbenzidine
tRNA   Transfer RNA
TEV protease Tobacco Etch Virus protease
TNF   Tumor necrosis factor

U

U   Unit
UV   Ultraviolet

V

V   Volt
v/v   Volume by volume
VBNC   Viable but non-culturable
VPI   *Vibrio* pathogenicity island
VPS   Vibrio polysccharide

W

w/v   Weight by volume
WHO   World Health Organization
WT   Wild-type

X

X-gal   5-Bromo-4-chloro-3-D-galactoside

Z

Zot   Zonula occludens toxin

Chapter 1

Review of Literature

Review of Literature

1.1. Vibrio cholerae

Vibrios are Gram-negative, facultative anaerobes, single or united in spirals, non-spore-forming curved rods, about 1.04 – 2.06 µm long and they are motile by means of a single polar flagellum (Thompson et al., 2005) *(Fig.1.1).* The name 'vibrio' is derived from the characteristic vibratory motility (from *vibrare* meaning *to vibrate*). They are heterotrophic, varying greatly in nutritious requirement; non-capsulated and are widely distributed as saprophytic forms in saltwater, freshwater, and soil, they also occur as parasites and pathogens. *Vibrio cholerae* was first isolated as the cause of cholera by Italian anatomist Filippo Pacini
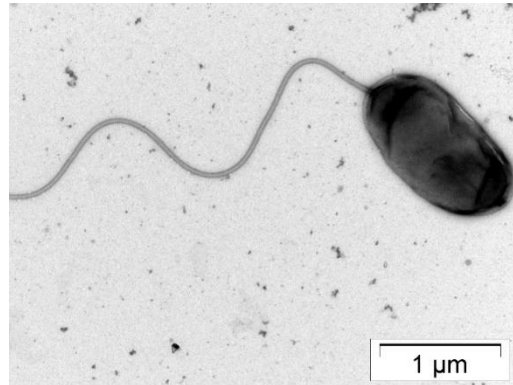
Fig.1.1. *Vibrio cholerae* **with its single polar flagellum.** Electron micrograph of *V. cholerae* by Moumita Dutta, Division of Electron microscope, ICMR-NICED, Kolkata.
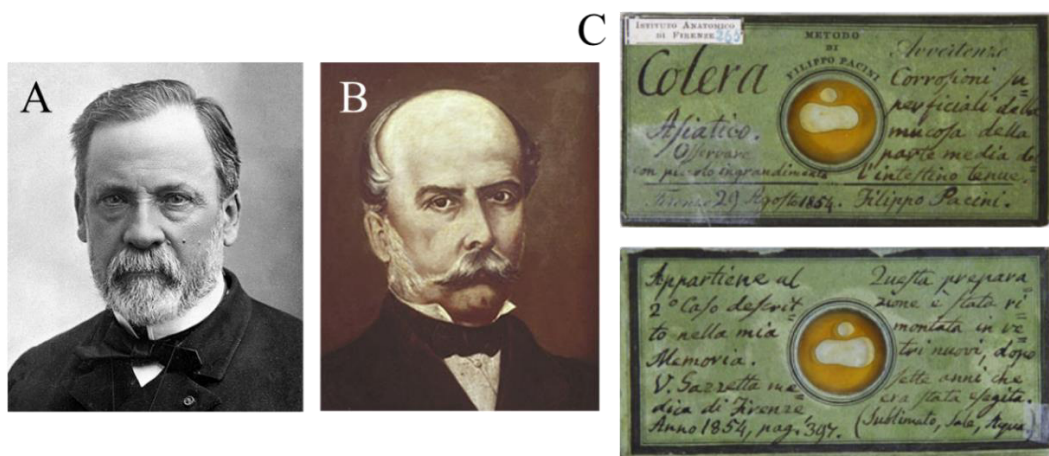
Fig.1.2. Early scholars whose contribution played a pivotal role in the discovery of the etiological agent of cholera. (A) Robert Koch **(B)** Filippo Pacini **(C)** Unpublished memoirs of Pacini's observation where the discovery of Vibrions was described step by step (University of Florence, Museum of natural History, Biomedical section).

in 1854 (Lippi & Gotuzzo, 2014) and later in 1983, it was established as the causative

agent of cholera by Robert Koch *(Fig.1.2)*. Koch isolated the bacteria in pure culture from the rice-water stools of cholera patients and named them "comma bacilli", because of the shape of the bacteria. The subsequent name *Vibrio comma* was used for several decades before being changed to *Vibrio cholerae* (Lippi & Gotuzzo, 2014).

1.2. Microbiology

Vibrio cholerae (Type Strain: ATCC 14035) is a member of the Vibrionaceae family along with Aeromonas, Photobacterium, and Plesiomonas Spp (Farmer, 2006; P I Watnick et al., 1999). It is capable of respiratory and fermentative metabolism. The bacterium is oxidase-positive, reduces nitrate, and is motile by a single, sheathed, polar flagellum. The *Vibrio* stains readily with aniline dyes and are Gram-negative, non-acid-fast. *Vibrio cholerae* is strongly aerobic and it grows within a temperature range of 16^0C to 40^0C. Organism tolerates high alkalinity with optimum pH of 7.6 to 8.2 which is useful for selective culturing of *V. cholerae* in alkaline peptone water. It grows well in general laboratory medium. On nutrient agar, after overnight growth colonies are moist, translucent, round discs and 1-2mm in diameter. The colonies and liquid culture of *Vibrio cholerae* had a distinctive odour. The growth of *V. cholerae* is stimulated by the addition of 1% sodium chloride (NaCl). However, an important distinction from other *Vibrio* spp. is the ability of *V. cholerae* to grow in nutrient broth without added NaCl, and growth is inhibited by 7% NaCl.

1.3. V. cholerae genome

The complete genomic sequence of the Gram-negative, γ-Proteobacterium *Vibrio cholerae* El-Tor N16961 to be 4,033,460 base pairs (bp). *V. cholerae* possesses two circular chromosomes; chromosome I is 2.96×10^6 bp and chromosome II is having 1.07×10^6 bp *(Fig.1.3)*. The genome of *V. cholerae* comprised a total of 3885 predicted open reading frames distributed in its two chromosomes. Most of the genes required for growth and viability are present on chromosome I, although some genes that are found only on chromosome II are also thought to be essential for normal cell function. This genomic sequence analysis of *V. cholerae* established the presence of a large integron island (a gene capture system) located on chromosome II (Baker-Austin et al., 2018; Hall et al., 1991) DNA replication, repair, transcription, translation, cell-wall biosynthesis, and various central catabolic and biosynthetic pathways are encoded by chromosome 1. Again, most genes that are known to be required for bacterial

pathogenicity (those encoding the toxin co-regulated pilus, cholera toxin, lipopolysaccharide, and the extracellular protein secretion machinery) are also located on chromosome I.
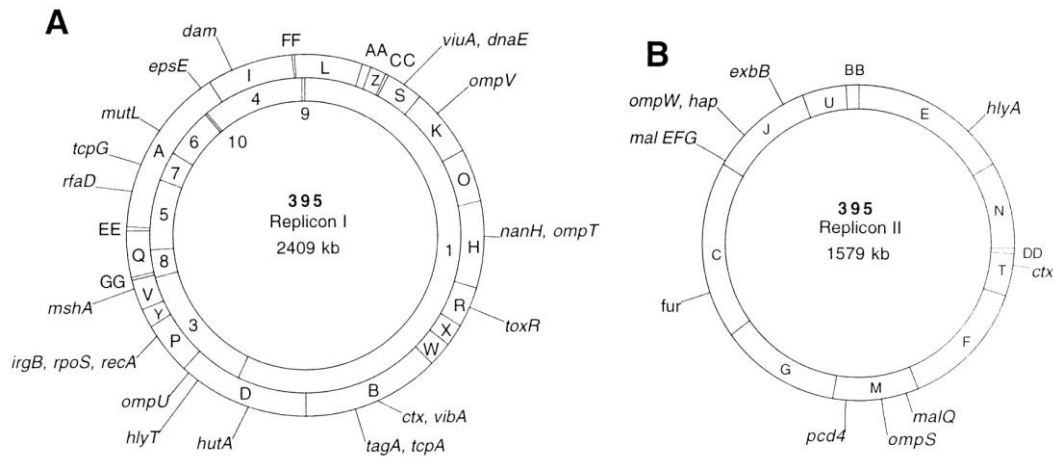
Fig.1.3. *V. cholerae* **genome showing two (large and small) chromosomes.** [Source: Trucksis et al., 1998]

1.4. Comparative Genomics

The majority of the *V. cholerae* genes are very close to *E. coli* genes (1,454 ORFs). 499 of the *V. cholerae* ORFs exhibit the highest similarity to other *V. cholerae* genes, suggesting duplications. Most of the duplicated ORFs encode products engaged in regulatory functions, chemotaxis, transport, adherence, transposition, pathogenicity, or unknown functions encoded by conserved hypothetical proteins. There are a significant number of duplications with at least one of each ORF on each chromosome suggesting there has been a crossover between chromosomes. The extensive duplication of genes involved in scavenging property (chemotaxis and solute transport) indicates the importance of these gene products in *V. cholerae* biology, especially its ability to inhabit diverse environments. Additionally, El Tor strain N16961 carries a single copy of the cholera toxin prophage, other *V. cholerae* strains carry multiple copies of this element (Davis et al., 1999; Mekalanos et al., 1983). Strains of the classical biotype have a second copy of the prophage that is localized on chromosome II (Trucksis et al., 1998). Thus, virulence genes are presumed to be under selective pressure, affecting copy number and chromosomal location.

1.5. Genome evolution of choleragenic V. cholerae

The origin and evolution of many bacterial diseases are directly related to genome fluidity. Horizontally acquired genetic elements containing fitness traits are a major source of bacterial evolution. The genome of *Vibrio cholerae* contains several mobile genetic elements (MGEs), which are critical for disease progression and survival (Pant et al., 2020). Only O1 and O139 isolates of *V. cholerae* have been reported to be choleragenic out of 206 distinct serovers. Surprisingly, their two key virulence determinants are encoded within mobile genetic components acquired by horizontal gene transfer. CT is encoded within the filamentous phage CTXϕ.
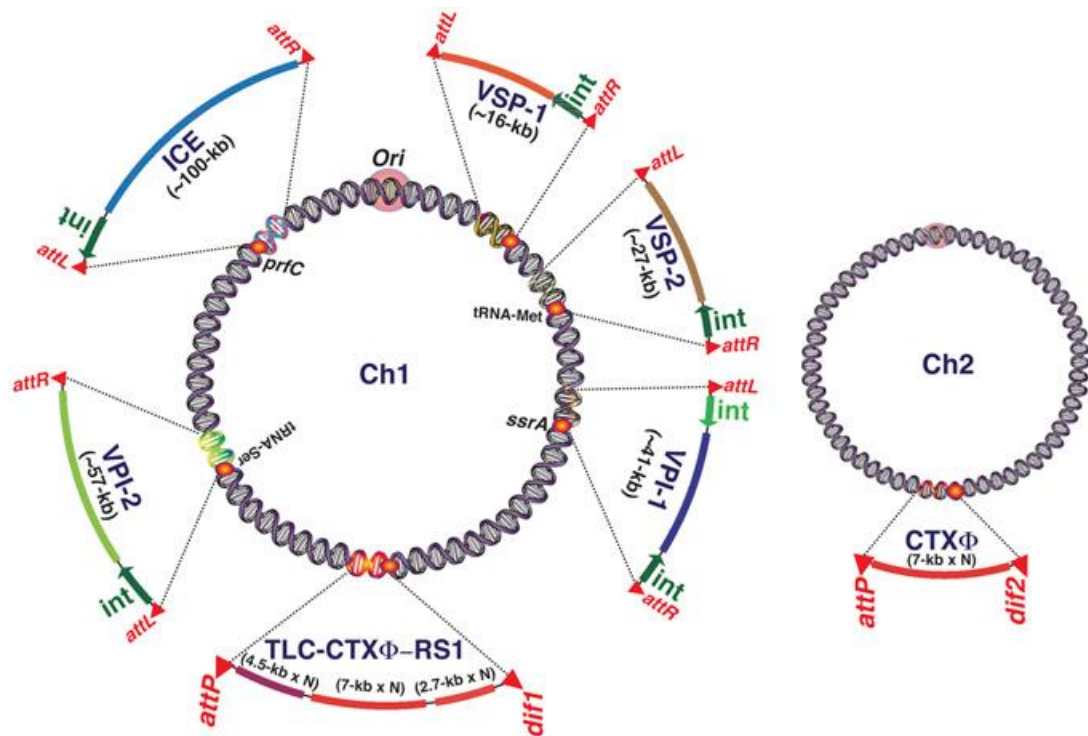
Fig.1.4. Distribution of genomic islands (GIs), prophages, and integrative conjugative element (ICE) in the genome of *V. cholerae* clinical isolates. Each of the genetic elements except prophages is linked with different mobility functions like integrase and repeat sequences. VPI-1, *Vibrio* pathogenicity island-1; VPI-2, *Vibrio* pathogenicity island-2; VSP-1, *Vibrio* seventh pandemic island-1; VSP-2, *Vibrio* seventh pandemic island-2; int, integrase [Source: Pant et al., 2020].

The CTXϕ phage has been demonstrated to be transferable between *V. cholerae* strains, with TCP acting as the phage receptor. TCP is encoded within the *Vibrio* pathogenicity island-1 (VPI-1). Other mobile genetic elements have been associated

with virulence in choleragenic isolates of *V. cholerae*: the SXT integrative conjugative element, VPI-2, and *Vibrio* seventh pandemic island-1 (VSP-1) and -2 (VSP-2). The SXT element is self-transmissible and confers to *V. cholerae* isolates resistance to streptomycin, sulfamethoxazole, and trimethoprim *(Fig.1.4)*.

VPI-2 is found only in pathogenic *V. cholerae* isolates and encodes a group of genes involved in sialic acid transport and catabolism. The capacity to utilize sialic acid as a carbon source gives choleragenic vibrios a competitive advantage in the mouse intestine. VSP-1 encodes the transcription factor VspR, which is controlled by a ToxT-regulated small RNA. VspR regulates the expression of several VSP-1-encoded genes, one of which, DncV, encodes a new class of dinucleotide cyclase. DncV produces a hybrid cyclic AMP-GMP molecule that is essential for successful intestinal colonization and downregulates *V. cholerae* chemotaxis, a trait linked with hyperinfectivity. VSP-2 has yet to be connected with a potential function. VPI-1, VPI-2, VSP-1, and VSP-2, the four pathogenicity islands encoded by choleragenic *V. cholerae*, can excise from their host's genome and form circular intermediates, which could possibly allow the transfer of virulence genes to other non-pathogenic *V. cholerae* strains (Banerjee et al., 2014).

Interestingly, it has been repeatedly found that some non-O1, non- O139 environmental strains carry virulence genes. These strains have the potential of acting as reservoirs of virulence genes for non-choleragenic strains of *V. cholerae*. It was recently found that the major component of the shell of crustaceans, chitin, induces the natural competence of *V. cholerae*. *V. cholerae* has been found associated with copepods in its natural environment, where it forms biofilms while attached to their chitinous surface.

The remarkable discovery that *V. cholerae* becomes naturally competent when thriving on chitin, combined with the existence of numerous hybrid strains of *V. cholerae* that encode some of the mobile genetic elements associated with virulence, strongly suggests that the shell of copepods is a critical location where genetic material exchange occurs among *V. cholerae* strains and novel pathogenic isolates may emerge.

1.6. Taxonomy

The genus Vibrio includes many different species of which few are pathogenic. The classic example of a pathogenic species of this genus is *V. cholerae*, others being

V. parahaemolyticus, *V. alginolyticus*, *V. mimicus*, *V. vulnificus* and certain non-agglutinable vibrios (Sakazaki , Gomez, 1967) (previously termed as NAG vibrios). The present systematic position of *V. cholerae* is as follows,

Systematic position of *Vibrio cholerae*

Domain	Bacteria
Phylum	Proteobacteria
Class	Gamma proteobacteria
Order	Vibrionales
Family	Vibrionaceae
Genus	*Vibrio*
Species	*V. cholerae*

1.7. Phenotypic fingerprinting and classification of V. cholerae

The phenotypic fingerprinting and classification scheme of *V. cholerae* can be divided into five major types, which include biochemical tests, serological classification, biotyping, phage typing, and anti-microbial susceptibility testing *(Fig.1.5)*.
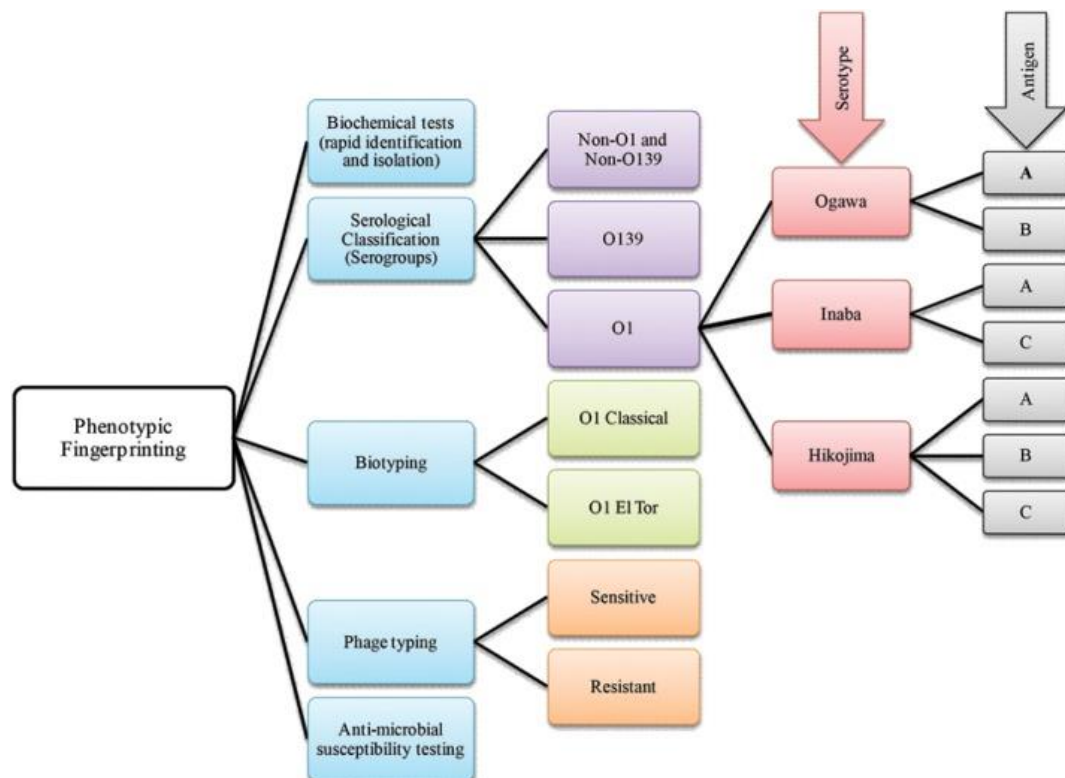
Fig.1.5. Scheme of classification of *V. cholerae*

1.7.1. Biochemical tests

V. cholerae and the other species belonging to the Vibrio and related genera can be differentiated for all practical purposes by a variety of simple tests as shown in *Table 1.1* (below) (S. N. Chatterjee & Chaudhuri, 2003; Kaper et al., 1995).

Table 1.1. Differentiation of *V. cholerae* from related species.

Tests	*V. cholerae*	Other Vibrio species	Enterobacteriaceae
Oxidase[1]	+	+ a	−
String test[2]	+	+/−	−
Acid from mannitol[3]	+	+/−	+/−
Acid from sucrose[3]	+	+/−	+/−
Lysine decarboxylase[4]	+	+/−	+/−
Ornithine decarboxylase[4]	+	+/−	+/−
Growth in 0% NaCl[5]	+	− b	−
Mol % G+C[6]	47-49	38-51	38-60

a, except for *V. metchnikovii*; **b**, except for *V. mimicus*; positive response means: **1**, test for the presence in bacteria of certain oxidase that will catalyze the transport of electrons between donors in bacteria and a redox dye which is reduced to a deep purple colour; **2**, a mucoid string is formed when an inoculating loop is drawn slowly away from a drop of 0.5% aqueous solution of sodium deoxycholate in which a 24-h growth of the organism is suspended. The string is formed because the organisms are lysed, DNA released and the mixture made viscous; **3**, the ability of the organism to ferment the particular sugar added to the growth medium and produce acid which changes colour of an indicator (phenol red, bromothymol blue, etc.); **4**, the ability of the organism to decarboxylate a particular amino acid added to the growth medium with the liberation of carbon dioxide and change of colour of the medium to violet; **5**, the ability of the organism to grow in the absence of NaCl in the medium; **6**, DNA base composition given in terms of mol% G+ C. [Source: Chatterjee & Chaudhuri, 2003]

1.7.2. Serological classification (Serotyping)

The classification system of *V. cholerae* depends on the type of O-antigen present. O-antigen is a homopolymer made of amino acid sugar D-perosamine (4-amino-4, 6-dideoxy-D-mannose), in which the amino groups are acetylated by 3-deoxy-

L- glycero-tetronic acid (Redmond, 1979; Kenne et al, 1982; Manning et al, 1994). The most widely used classification system for the O-antigen of *V. cholerae* is developed by Sakazaki and Shimada (Sakazaki & Shimada, 1977). This method of typing is made up of 138 different O-groups to which the newly discovered O139 group was added recently (Shimada et al., 1994). The different O groups are referred to as serogroups or serovars *(Fig.1.6)*.

The O1 serogroup is classified into three antigenic forms called Inaba, Ogawa, and Hikojima. These antigenic types are known as serotypes or subtypes. The O antigen of *V. cholerae* O1 consists of three factors designated A, B, C. The A factor probably is the D-perosamine homopolymer but the nature of B and C factor is not known (Martinez et al., 2001). The differences among the subtypes are mainly quantitative; Ogawa strains can generate the A and B and a small amount of C antigen, while Inaba strains produce only the A and C antigens (Shimada et al., 1994). The Hikojima subtype has all three factors. The O139 strain is a hybrid of O1 and non-O1 strains. It does not produce the O1 LPS and are lacking some of the genes essential for O1 antigen, but is similar to O1 El Tor strains in relation to cholera enterotoxin and toxin co-regulated pilus (TCP).
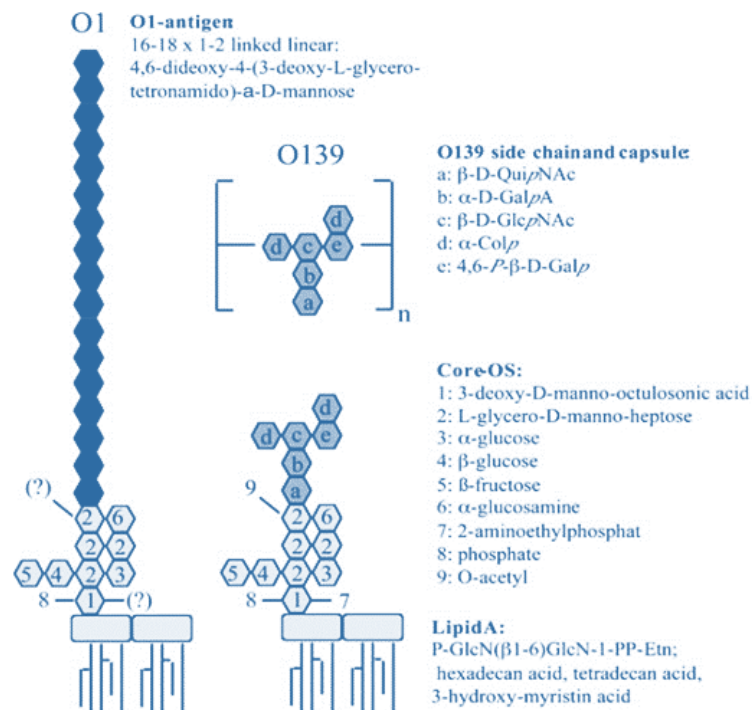
Fig.1.6. LPS structure of *V. cholerae* serogroup O1 and O139. The deduced structure of *V. cholerae* serogroupO1 (left) and O139 (right); shown are the different O antigen and capsule structures, and the similar core-OS and lipid A structures.

1.7.3. Biotyping

There are two biotypes of *V. cholerae* O1 strains namely Classical and El Tor. These two biotypes are classified on the basis of hemolysis, hemagglutination, phage, and polymixin B sensitivity and the Voges-Proskauer reaction, as well as with genetic methods such as multiplex PCR and restriction fragment length polymorphism (RFLP) (Alm & Manning, 1990). Isolates from the sixth pandemic were found of classical biotype. However, the majority of isolates of the seventh pandemic have been of the El Tor biotype (S. N. Chatterjee & Chaudhuri, 2003).

Tests used	Responses of the Two biotypes	
	Classical	El Tor
Hemolysis of sheep erythrocytes	−	+/ −
Agglutination of chicken erythrocytes	−	+
Voges-Proskauer reaction	−	+
Inhibition of Polymixin B (50-µg disk)	+	−
Lysis by Gr IV cholera phage	+	−
Lysis by FK cholera phage	+	−

1.8. Isolation and identification of V. cholerae

The transport medium used for *V. cholerae* in a stool sample is the Cary-Blair medium. Alkaline peptone water (APW) is generally used as enrichment broth (Pal et al, 1992) and thiosulfate-citrate-bile salt-sucrose (TCBS) agar is the most commonly used plating medium for *V. cholerae* (Kaper et al., 1995) *(Fig.1.7)*. TCBS agar is green when prepared. Overnight growth (18 to 24 hours) of *V. cholerae* produces large (2 to 4 mm in diameter), slightly
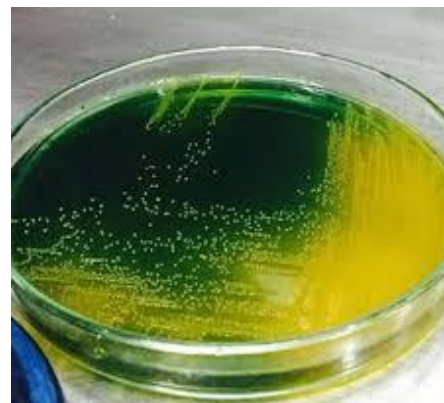
Fig.1.7. *V. cholerae* **grown on TCBS agar, selective media for** *V. cholerae***.** Overnight colonies of *V. cholerae* on TCBS agar are large (2-4 mm) and yellow because of the fermentation of sucrose. They are characteristically round, smooth, glistening, and slightly flattened

flattened, yellow colonies with opaque centers and translucent peripheries. The yellow color is caused by the fermentation of sucrose in the medium. Sucrose nonfermenting

organisms, such as *V. parahaemolyticus*, produce green to blue-green colonies. Another media for isolation of *V. cholerae* is Taurocholate Tellurite Gelatin Agar (TTGA or Monsur's agar). Overnight growth of *V. cholerae* on TTGA agar appears as small opaque colonies with slightly dark centers. After 24 hours, the centers of the colonies become darker, and eventually, the entire colony becomes "gunmetal" grey in color. In addition to the dark coloration, which is due to the reduction of tellurite, there is also an opaque zone around colonies that resembles a halo. The halo effect, which is due to the production of the enzyme gelatinase, can be intensified by brief (15- to 30-minute) refrigeration of the plate. On MacConkey's agar, the Vibrio colonies are colorless at first but become reddish on prolonged incubation due to the late fermentation of lactose. On blood agar colonies are initially surrounded by a zone of greening and which later become clear due to hemolysis. *V. cholerae* is routinely identified by biochemical tests, direct specimen examination, agglutination in antisera against O1 antigen, and by using DNA probes and PCR.

1.9. Ecology and environmental reservoirs of V. cholerae

V. cholerae ecology is extremely important in the emergence of more toxigenic and virulent *V. cholerae* strains. The requirement of salt for *V. cholerae* to develop shows that it originated at sea. The striking resemblance of *Vibrio* spp. isolated from deep-sea hydrothermal vents in the East Pacific region shows that this species is indigenous to the deep sea (Colwell, 2004). Later *V. cholerae* genome sequencing investigations proved that *V. cholerae* is a versatile bacterium capable of living in a variety of habitats and infecting the human gastro-intestinal tract (Luigi Vezzulli et al., 2010).

In an aquatic habitat, lateral transfer of genetic material results in the dispersion of virulence genes in environmental strains of *V. cholerae* from multiple serogroups, providing an environmental reservoir for such genes (K. De et al., 2004). The novel toxigenic variations of *V. cholerae* result from phage infection, which allows *V. cholerae* to gain antibiotic resistance genes, giving rise to multi-drug resistance *V. cholerae* (Colwell, 2002; Lipp et al., 2002).

V. cholerae is an aquatic autochthonous pathogen that can be found in brackish water, marine water, and fresh water. It can survive for months to years in some aquatic habitats by interacting with zooplankton and other aquatic species (A. Huq et al., 1983)

(Fig.1.8). Colwell and colleagues were the first to report *V. cholerae*'s commensal or symbiotic connection with aquatic planktons (A. Huq et al., 1983; Luigi Vezzulli et al., 2010). *V. cholerae* O1 and non-O1 serogroups were identified adhered to the surface of live copepods, with the mouth region and egg sac being the most intensively colonized. Low temperature and nutrient conditions can induce the Viable But Non-Culturable (VBNC) state, from which it can be resuscitated under more favourable conditions. *V. cholerae* can also adhere to autotrophic organisms such as phytoplankton or macroalgae, which can serve as a carbon source. Attachment to chitinous zooplankton and gelatinous egg masses (e.g., chironomids) supplies nutrition while also facilitating HGT. Fish and birds consume plankton or mussels that may host *V. cholerae* and can potentially spread the bacterium over great distances.
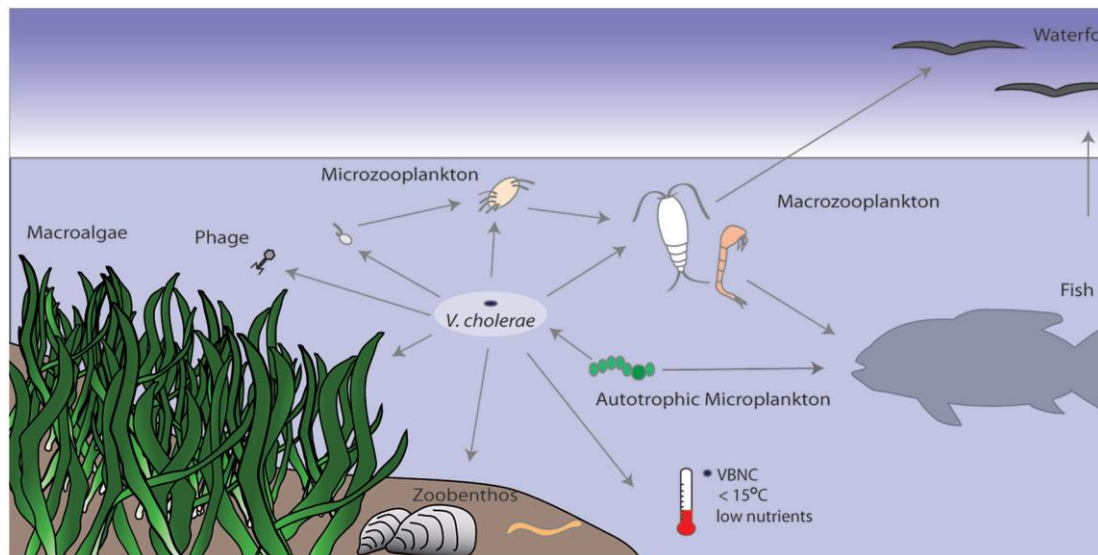
Fig.1.8. *Vibrio cholerae* **interactions with other organisms and the environment** [Source: Lutz et al., 2013].

V. cholerae outcompetes other bacterial taxa associated with zooplankton, such as γ-proteobacteria and *Vibrio photobacterium*, in aquatic environments and is commensal with copepods (Luigi Vezzulli et al., 2010). *V. cholerae* linked with zooplankton survives longer in sea water than free-living cells (Alam et al., 2017). The association of *V. cholerae* with copepods offers the bacterium a number of benefits, including food availability, adaption to environmental nutrient gradients, stress tolerance, and predator protection. Cladocerans, *Monia spp.*, and *Diphanosoma spp.*, as well as the rotifer *Brachionus angularies*, are significantly correlated with the prevalence of *V. cholerae* and cholera outbreaks. Furthermore, *V. cholerae* has been found to be connected with the copepod *Acatina tonsa*, which appears to contain a

greater amount of *V. cholerae* than other co-occurring copepods (Binsztein et al., 2004; A. Huq et al., 1983; Pruzzo et al., 2008; Rawlings et al., 2007).

1.10. Environmental factors that influence V. cholerae growth

The occurrence of *V. cholerae* in the environment is dependent on a number of environmental factors such as temperature, pH, salinity, and phyto- as well as zooplankton (Lutz et al., 2013; Turner et al., 2014).

1.10.1. Temperature

V. cholerae is most commonly found in warmer water (over 15 °C) (C. N. Johnson et al., 2012; Sullivan & Neigel, 2018). Many investigations have shown that the abundance of *V. cholerae* follows a seasonal pattern that is mostly determined by temperature. Increased temperature influences *V. cholerae* attachment to chitinous zooplankton via increased expression of colonization factors such as MSHA, pillus, and GbpA (Castro-Rosas & Escartín, 2000; Turner et al., 2009).

1.10.2. pH

pH is a key parameter for the isolation of *V. cholerae* from environmental materials (using alkaline peptone water of pH 8- 8.6). *V. cholerae* thrives in high pH environments in aquatic environments. Elevated pH can affect the attachment of *V. cholerae* to the chitinous surface of copepods (Lipp et al., 2002).

1.10.3. Salinity

Seasonal changes in temperature (El-Niño effect) as well as fresh water intake, can have a significant impact on the salinity of marine water bodies. The average salinity of open ocean water is 35 ppm. However, salinity can diminish near coastal and estuarine areas due to fresh water influx from rivers or precipitation. *V. cholerae* grows best at salinities around 25 ppt (Baker-Austin et al., 2010; Thomas et al., 2006). *V. cholerae* enhances the formation of the protective pigment melanin in high saline settings (Coyne & Al-Harthi, 1992), which gives UV tolerance (Valeru et al., 2012).

1.10.4. Biotic factors

Higher phytoplankton and zooplankton abundance in spring and autumn provide chitinous surfaces that harbour bacteria such as *V. cholerae* (Anwar Huq et al., 2005; Lobitz et al., 2000). This may allow the organism's overall population to increase in the environment despite the presence of more bacterivorous predators.

1.10.5. Conductivity

Water conductivity has been reported as a critical element influencing *V. cholerae* persistence in aquatic environments. An increase in a lake or estuarine water conductivity leads to an increase in cholera cases (Anwar Huq et al., 2005).

1.10.6. Rainfall

Rainfall has been linked to epidemics of waterborne diseases (Curriero et al., 2001). Rainfall events were found to be the cause of 51 percent of water-borne disease outbreaks. Heavy rains can also cause a decrease in salinity, an increase in sea level, and changes in ocean circulation, all of which can affect *V. cholerae* proliferation in aquatic environments. Some sources also suggest a decrease in the number of cholera cases as a result of increasing rainfall (Louis et al., 2003).

1.10.7. Sunlight

The seasonal and inter-annual variability of sunlight affects the persistence and spread of *V. cholerae* as it is associated with phytoplankton. Excessive evaporation due to sunlight can cause an increase in water salinity affecting *V. cholerae* growth in the marine environment. UV ray that comes with sunlight may cause damage to the nucleic acid (Sedas, 2007).

1.10.8. Fe^{3+} ion

V. cholerae exhibits adaptive features that allow it to persist in the environment for extended periods of time when soluble iron is scarce. *V. cholerae* has the ability to create iron-chelating siderophores in order to absorb insoluble iron from the environment. When insoluble iron (Fe_2O_3) is accessible, the survival of *V. cholerae* improves much more. The Fe3+ ion also promotes *V. cholerae* proliferation and influences CT expression (Lipp et al., 2002).

1.10.9. Water depth

Huq *et al,* in the year 2005 mentioned increased cases of cholera with a decrease in pond or estuarine water depth.

1.10.10. El Niño

El Niño Southern Oscillation (ENSO) has a positive effect on cholera and the occurrence of *V. cholerae* (Pascual et al., 2000). The inter-annual climate variability due to EL Niño is an important cause of cholera incidence.

1.11. The role played by V. cholerae in the environment

In order to survive and adapt to the environment, *V. cholerae* has multiple functional roles to play. Most of these features are initialized or activated in the presence of chitin present in the exoskeleton of zooplanktons in the aquatic reservoirs. As already mentioned, *V. cholerae* uses them as an adhesion matrix, the other functions are interconnected to each other.

1.11.1. Chemotaxis

Chemotaxis of *V. cholerae* toward chitin oligosaccharides has been reported by Li and Roseman (Li & Roseman, 2004). the secreted chitinase of starving cells comes into contact with chitin in the microenvironment and generates a disaccharide and/or a $(GlcNAc)_n$ gradient, causing the cells to swim up the gradient to the cuticle or chitin. Once attached *V. cholerae* cells are able to utilize chitin as a source of carbon and nitrogen (Cottingham et al., 2003).

1.11.2. Surface colonization

V. cholerae strains possess multiple strategies for surface attachment to persist in the nutrient-limited aquatic environment and to get nutrients from the biotic surfaces attached with it. *V. cholerae* in the aquatic environment has been detected as attached to many abiotic and biotic surfaces including ship hulls (Shikuma & Hadfield, 2010), zooplankton (Anwar Huq et al., 2005; Tamplin et al., 1990), macroalgae (Hood & Winter, 2006) and as floating aggregates (Alam et al., 2006). On coming in close proximity to chitin it binds to chitin oligomers. Binding to chitin is a complex process involving hydrophobic and ionic bonds (L. Vezzulli et al., 2007). There are few surface proteins of *V. cholerae* that are known to bind the Chitinous exoskeleton of zooplanktons. These are as follows:-

Mannose-sensitive haemagglutinin (MSHA)- is a type 4 pilus produced by *V. cholerae* O1 El Tor and O139 has been reported to be involved in colonization and subsequent biofilm formation on nutritive (cellulose) and non-nutritive (borosilicate glass) surfaces (Paula I. Watnick & Kolter, 1999). It is a thin flexible pilus composed of subunits with a molecular mass of 17 kDa. MSHA is a type IV pilus encoded by a gene named *mshA*. MSHA also helps *V. cholerae* to adhere to the intestinal lumen in animal models (Osek et al., 1992).

N-acetylglucosamine binding protein A (GbpA)- is a 53 kDa secreted protein that mediated adherence of *V. cholerae* to chitin surfaces and *Daphnia magna*, has been described by Kirn and co-workers (2005), who has termed this protein as GlcNAc-binding protein A (GbpA). GbpA was first discovered as a colonization factor to promote bacterial attachment to natural substrates, chitin as well as host intestinal epithelium (R. Bhowmick et al., 2007; Kirn et al., 2005). Thus, this novel colonization factor of *V. cholerae* can be used by the bacteria for adherence to both types of surfaces, chitin and intestinal surface (Tarsi & Pruzzo, 1999).

ChiRP- The chitin-regulated pilus contributes to colonization of chitin in *V. cholerae* O1 El Tor (Meibom et al., 2004). ChiRP plays a vital role in adhesion on previously colonized chitin surfaces. In these cases, the established gradients of GlcNAc and (GlcNAc)2 direct bacteria to the chitin surface and induce synthesis of ChiRP, promoting further colonization (Meibom et al., 2004).

1.12. Motility

Swimming motility of *Vibrio* spp. is achieved through the rotation of "whip" - like appendages flagella. Flagellar-mediated motility is closely related to processes such as chemotaxis, colonization, biofilm formation, and virulence of *Vibrio* spp. (Butler & Camilli, 2005; McCarter, 2004; Yildiz & Visick, 2009). Thus, motility plays a significant role in the lifestyle of Vibrios, both in the aquatic environment as well as during host colonization. Many *Vibrio* spp. are monotrichous with a single, sheathed polar flagellum (e.g., *V. cholerae* and *V. alginolyticus*); however, some Vibrios can also be peritrichous or lophotrichous.

There are three major structural components of a flagellum: the basal body, the hook, and the filament. Each component is assembled in a hierarchical manner starting at the inner cytoplasmic membrane, proceeding to the outer membrane, and ultimately outside the cell *(Fig.1.9)*.
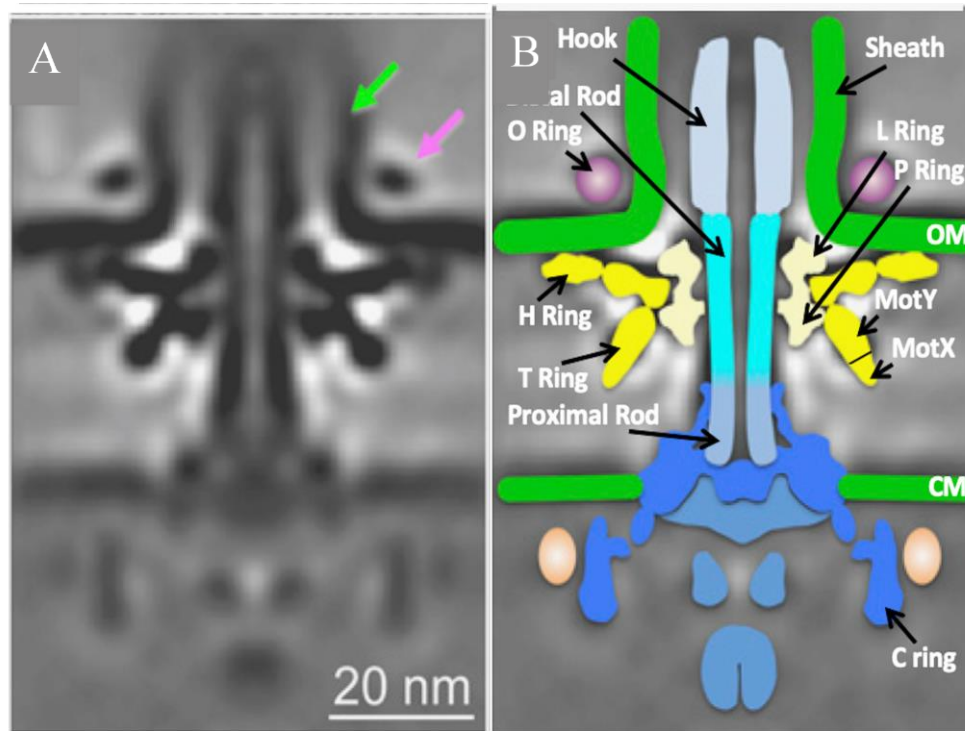
Fig.1.9. Structure of *V. cholerae* flagellar complex. (A) Electron microscopy rendering of the sheathed Vibrio flagellar complex. Vibrio specific attributes are depicted by arrows: the sheath (green arrow) and the O ring (purple arrow). **(B)** Schematic of the sheathed Vibrio flagellar complex. [Source: Echazarreta & Klose, 2019]

More than 50 genes are involved in the synthesis and regulation of flagella in *V. cholerae.* The expression of flagella-synthesis genes in *V. cholerae* is categorized into a four-tier transcriptional hierarchy (Echazarreta & Klose, 2019) *(Fig.1.10)*. The σ54-dependent transcriptional activator FlrA is the only class I gene in this hierarchy. FlrA is the master regulator of the *V. cholerae* flagellar transcription hierarchy because it is important for the expression of the rest of the flagellar genes. FlrA, along with the RpoN (sigma factor σ54), activates class II flagellar genes. Class II flagellar protein histidine kinase FlrB and its response regulator FlrC regulates the synthesis of class III flagellar genes, which encodes the different structural components of flagella including the major flagellin subunit (FlaA), proximal and distal transmembrane helical rod (FlgB/G), H-ring protein (FlgT), H-ring-associated protein (FlgP), flagellar-hook-associated protein (FlgK) and T-ring motor protein (MotY) (Klose & Mekalanos, 1998; Syed et al., 2009).

Fig.1.10. A schematic of the flagellar transcription hierarchy of *Vibrio cholerae*. The sole Class I gene of the Vibrio hierarchy is the σ54-dependent transcriptional activator, flrA, which is the master regulator of the flagellar hierarchy. The FlrA- and σ54-dependent Class II genes encode components of the MS ring, C ring, ATPase, and export apparatus. The FlrC- and σ54-dependent Class III genes encode additional components of the C- ring, inner membrane export apparatus, the rod, rod cap, PLH and T rings, torque generator, hook components, filament cap, the FlaA flagellin, the flagellin chaperone, a chemotaxis protein, and proteins of unknown function. The σ28-dependent Class IV genes encode additional flagellins, motor components, chemotaxis proteins, and methyl-accepting chemoreceptors (MCPs).

1.13. Quorum sensing

Quorum sensing, or the control of gene expression in response to cell density, involves the production and detection of extracellular signalling molecules known as autoinducers (AI). Quorum sensing controls processes that include virulence, biofilm formation, and natural competence in *V. cholerae* (Liu et al., 2007). *V. cholerae* produces and responds to two AIs using two parallel QS circuits. One AI is (S)-3-hyroxytridecan-4-one (CAI-1). The second AI, AI-2, is synthesized by LuxS (Higgins et al., 2007; Ng et al., 2011; Wei et al., 2012). *V. cholerae* detects CAI-1 and AI-2 using two parallel membrane-bound two-component receptors as shown in *(Fig.1.11)*. At high cell density (HCD), AIs results in increased hapR expression, which is a quorum-

sensing response regulator that positively regulates the transcription of *hapA* (J. Zhu et al., 2002), *cytR*, a repressor of biofilm development, flagellum biosynthesis genes (Yildiz et al., 2004)and represses VPS production and the virulence regulator ToxR production (J. Zhu et al., 2002; Jun Zhu & Mekalanos, 2003). At low cell density (LCD) just the opposite regulation takes place due to repression of hapR.

At HCD, QS inhibition of biofilms and virulence factor production facilitates *V. cholerae* dispersal back into the environment, in contrast to LCD, where activation of the biofilm lifestyle permits *V. cholerae* to remain attached to host tissue when virulence factors are expressed. This strategy allows *V. cholerae* to compete for nutrients in the host at LCD while also maximizing its potential to escape and propagate to new hosts once it reaches HCD. Furthermore, when free-swimming *V. cholerae* cells converted to an attached lifestyle (Fong et al., 2010; Yildiz & Visick, 2009), natural competence and horizontal gene transfer (HGT) (Lo Scrudato & Blokesch, 2012) were allowed, as well as enhanced predation resistance.
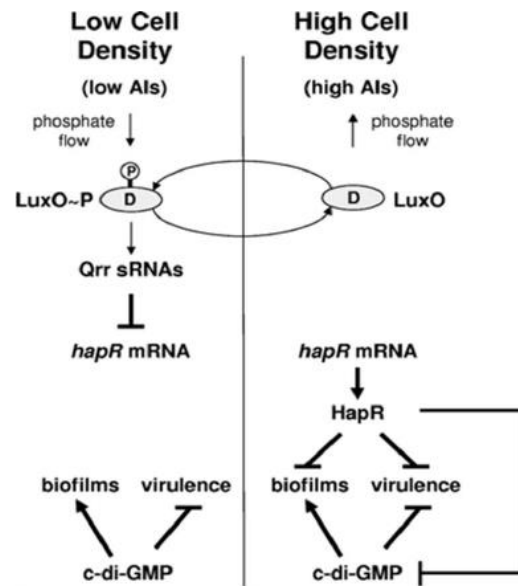
Fig.1.11. Simplified model of the interaction between Quorum sensing and c-di-GMP in the regulation of gene expression in *V. cholerae*. When concentrations of AIs are low (left side), the response regulator LuxO is phosphorylated, resulting in expression of multiple genes encoding the Qrr sRNAs that repress translation of the master transcriptional regulator, HapR. When concentrations of AIs are high (right side), LuxO is dephosphorylated which leads to termination of qrr expression. In the absence of the Qrr sRNAs, HapR is produced. HapR represses both biofilm formation and virulence factor expression. Like HapR, c-di-GMP also represses virulence factor expression, but unlike HapR, c-di-GMP activates biofilm formation. Here, HapR is shown to repress biofilm formation both directly (via controlling vpsT) and indirectly by reducing the levels of c-di-GMP [Source: Waters et al., 2008]

1.14. Biofilm formation

Biofilm formation is crucial for *Vibrio cholerae* environmental survival as well as host colonization. The production of biofilm allows *V. cholerae* to survive and stay in aquatic conditions, as well as to get through the gastric acid barrier and gain access to the small intestine. In aquatic environments, biofilms are formed on the chitinous surface to promote nutrient acquisition, as shown in *(Fig.1.12)*. The transcriptional activators vpsR and vpsT, which are transcriptionally regulated by a variety of environmental cues, regulate the genes involved in biofilm formation. Furthermore, VPS helps in cell immobilization, microcolony formation, and biofilm maturation (P I Watnick et al., 1999; Paula I. Watnick & Kolter, 1999). High and low VPS producing *V. cholerae* colony types are known as "rugose" and "smooth," respectively, with the rugose having a highly protective effect against a variety of stresses, including chlorine (Morris et al., 1996), low pH (Jun Zhu & Mekalanos, 2003), osmotic and oxidative stress (Wai, 1999), anti-bacterial serum (Morris et al., 1996), phage (Nesper et al., 2001) and heterotrophic protists (Sun et al., 2013).
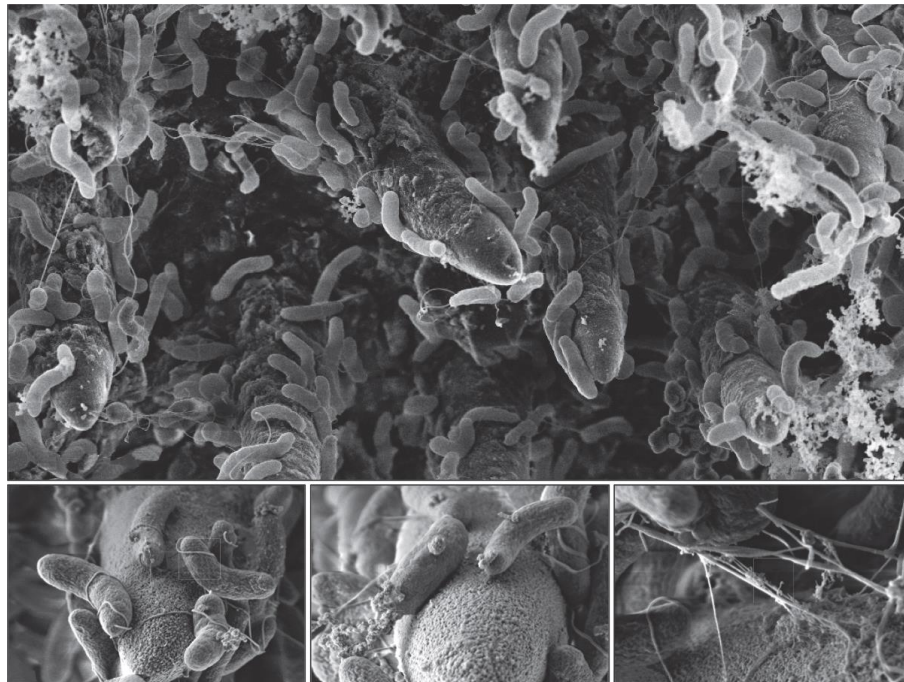
Fig.1.12. *V. cholerae* forms biofilms on chitinous surfaces. Biofilm-forming *V. cholerae* cells bound to chitinous surfaces are illustrated in these scanning electron micrographs. In the lower row bacteria that are attached to chitinous spikes (porous-looking surface) are shown at higher magnification, which allows the visualization of detailed structures such as the polar flagellum, unidentified pili/fibers, and biofilm matrix components.

1.15. Natural competence

"Why" bacteria, such as *V. cholerae*, become naturally competent to take up extracellular DNA is a question that has remained unanswered since the pioneering studies of the "transforming principle" by Griffith and later Avery, McLeod, and McCarthy, who established *S. pneumoniae* as a model organism for studying natural competence for DNA uptake.
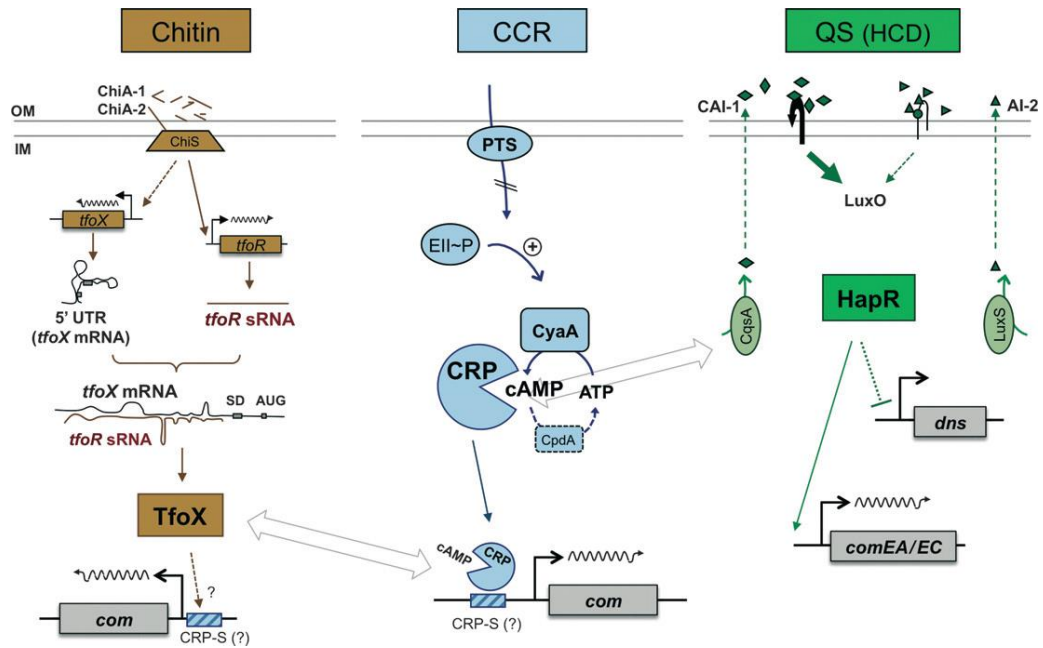
Fig.1.13. A complex, threefold regulatory network is involved in the natural transformation of *V. cholerae*. The induction of natural competence and transformation in *V. cholerae* is linked with three of the common environmental cues: (1) the chitinous surface as the sole carbon source for this bacterium and other *Vibrio* spp. (brown pathway); (2) Carbon Catabolite Repression (CCR) and the induction of competence after starvation for preferred PTS(Phosphotransferase System)-transported sugars (blue pathways); and (3) cell-to-cell communication, such as that exerted by the quorum-sensing systems (green pathway). **Left** – Extracellular chitinase (e.g. ChiA-1 and ChiA-2 directly secreted by *V. cholerae* degrades the insoluble (GlcNAc) polymer chitin and releases diacetylchitobiose units as the major product (together with some triacetylchitotriose). These chitin oligomers are recognized by a sensory histidine kinase, ChiS, and a signal transduction pathway subsequently leads to the induction of tfoX and tfoR expression. tfoR encodes for a small regulatory RNA, which enhances the translation of the tfoX mRNA. TfoX, as the major regulator of transformation, is involved in the induction of competence genes. **Middle** – In the absence of preferred PTS-transported sugars (such as glucose or the chitin monomer GlcNAc), the PTS systems are not saturated, and the phosphoryl group is kept by enzyme II (EII). EII–P is a direct activator of the cAMP-producing enzyme CyaA. Accumulating cAMP, together with its binding protein (CRP), leads to the induction of the competence genes. This complex might interact with TfoX to allow for the binding of cAMP-CRP to competence-specific CRP-S sites. **Right** – high cell density, as measured by

QS, is required for competence induction and transformation. At high cell density (HCD), the binding of the autoinducer to the respective receptors initiates a signalling cascade (simplified), which conclusively results in the production of the major regulator of QS, HapR. HapR acts as repressor of the extracellular nuclease gene dns and as a positive regulator of the competence genes comEA and comEC. The encoded proteins of all three genes are expected to be in direct contact with transforming DNA; these proteins either induce the degradation of external DNA at low cell density (Dns) or are part of the DNA-uptake machinery (ComEA and ComEC).

As DNA uptake was later uncovered in diverse bacterial species, hypotheses developed that natural competence evolved to aid in three major processes: HGT, nutrition, and DNA repair. It is recognized that DNA taken up by bacteria may not be used solely for one function or another, as extracellular DNA scavenged as food may also be available for chromosome recombination and DNA repair *(Fig.1.13)*. Current natural competence research indicates that DNA taken up by the competence apparatus may perform several functions in the marine pathogen *V. cholerae*.

Upon growth on chitinous surfaces, *V. cholerae* initiates a developmental program termed "natural competence for genetic transformation". Natural competence is a mode of horizontal gene transfer in bacteria and contributes to the maintenance and evolution of bacterial genomes. The genes required for natural competence are reported to get activated by chitin (Meibom et al., 2004). The authors of an earlier study proposed a model that involved at least three inter-connected regulatory pathways: 1) induction by chitin, 2) catabolite repression, and 3) quorum sensing (qs) based on bacterial metabolism and group behavior. Recently, it has been reported that in *V. cholerae*, TfoX is dependent on cAMP-CRP (Antonova et al., 2012; Blokesch, 2012) and it positively regulates competence genes upon exposure to chitin as already mentioned earlier (Shouji Yamamoto et al., 2010, 2011)

1.16. Chitin

Chitin is a linear stable polymer of β-1,4-N-acetylglucosamine (GlcNAc), which is 2-acetamido-2-deoxy-D-glucose, and is the second-highest occurring biopolymer on the planet after cellulose. It is present in the exoskeleton of an insect, crabs, shrimp, lobsters, fungi, yeast, diatoms, nematodes, crustaceans, and other invertebrates *(Fig.1.14)*.
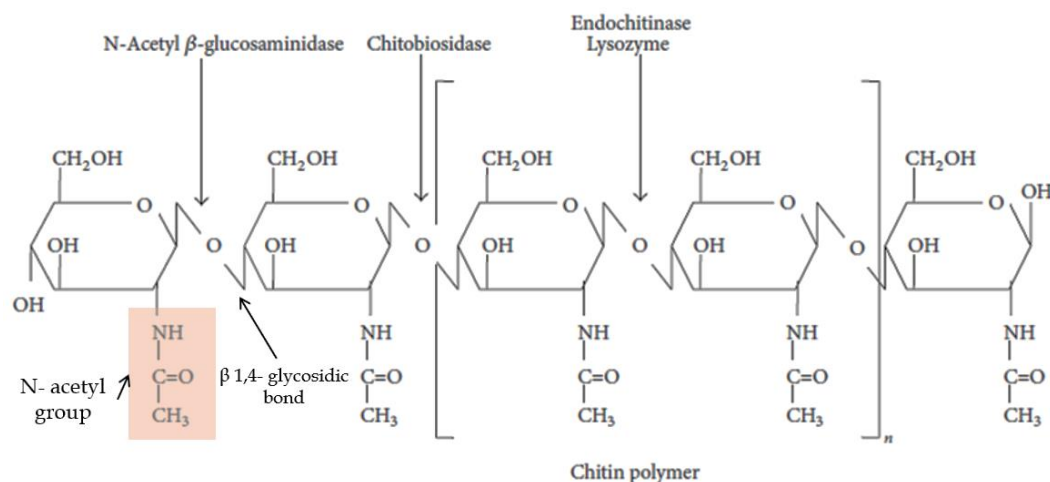
Fig.1.14. The biochemical structure of chitin and specificity of different chitinases towards chitin polymer.

The percentage of chitin present varies depending on the organism. Crabs and shrimps contain the highest percentage of chitin, accounting for 90 percent of chitinous waste. It is a crystalline polysaccharide found in nature in three forms: α-chitin, β-chitin, and γ-chitin. α-Chitin, produced by the crustaceans, is the most common, isomorphic, and compact form because of the antiparallel orientation of chitin chains, which encourages strong hydrogen bonding. β-Chitin, produced by diatoms, is loosely packed and chains are organized in parallel with weaker intermolecular interactions, resulting in a less stable form. The third polymorphic form is γ-chitin, which is a combination of α- and β-chitins. Chitinases catalyze the hydrolysis of chitin's glycosidic linkages, which degrades chitin into disaccharides and longer oligosaccharides. When compared to α-chitin, β-chitin is more easily hydrolyzed and soluble. It may be dissolved in formic acid. Chitinolytic bacteria, particularly members of the Vibrionaceae family, recycle the vast majority of chitin in the aquatic biosphere (Hunt et al., 2008a; Keyhani & Roseman, 1999; Meibom et al., 2004). Chitinolytic bacteria use chitin as a source of both carbon and nitrogen through a complex process that includes detection of chitin, attachment to a chitinaceous surface, and degradation of chitin.

1.17. Chitinases

Chitinase genes are found in a wide range of bacteria, fungi, plants, and also in some viruses, and also in humans. These enzymes have different functions depending on the organism of origin. The chitinolytic enzymes are glycosyl hydrolases and are generally divided into two main categories; Endochitinases (EC 3.2.1.14) and Exochitinases. Endochitinases cleave chitin randomly at internal sites, generating

soluble low molecular weight oligomers of GlcNAc (Sahai & Manocha, 1993). Exochitinases are subdivided into two categories: chitobiosidases (EC 3.2.1.29) that catalyze the release of di acetyl chitobiose and 1,4- β N acetyl glucosaminidases (EC 3.2.1.30) which cleave oligomeric products of GlcNAc (Sahai & Manocha, 1993). The types of chitinases most extensively studied in plants are endochitinases (Roberts & Selitrennikoff, 1988) of which many show some degree of lysozyme (EC 3.2.1.17) activity, i.e. they can hydrolyze β-1,4 linkages between N-acetyl-muramic acid and GlcNAc residues in peptidoglycan (Schultz et al., 1998). Bacteria produce a different kind of chitinase mainly to meet their nutritional requirement, probably to hydrolyze the diverse type of chitin found in nature. Fungal chitinases like bacterial chitinases also play an important role in nutrition but are also active in the fungal developmental process and morphogenesis (Gooday, 1994). In higher animals and plants, chitinases mainly play a role in defence against pathogen attacks (Patil et al., 2000).

1.18. Utilization of Chitin by V. cholerae

Annual chitin production in aquatic biospheres is estimated to be more than 10^{11} tonnes, primarily from copepods and other organisms, resulting in a constant "marine snow" of organic matter down through the water column. Chitinolytic bacteria, which include members of the Vibrionaceae family, rapidly recycle chitin by breaking it down into its soluble constituents GlcNAc and chitobiose $(GlcNAc)_2$. This chitin utilization process enables chitinolytic bacteria to maintain the nitrogen and carbon biogeochemical cycles in marine environments.

The *V. cholerae* chitin degradation genes appear to be universally conserved (Hunt et al., 2008b). After attaching to chitin, the organism degrades it to oligosaccharides that can reach the periplasmic space, and then further degrades the oligosaccharides to GlcNAc. The combined action of chitinase (EC 3.2.1.14) and -N-acetylglucosaminidase (EC 3.2.1.30) is thought to be required for full hydrolysis of chitin to GlcNAc (Beier & Bertilsson, 2013; Gooday, 1994).
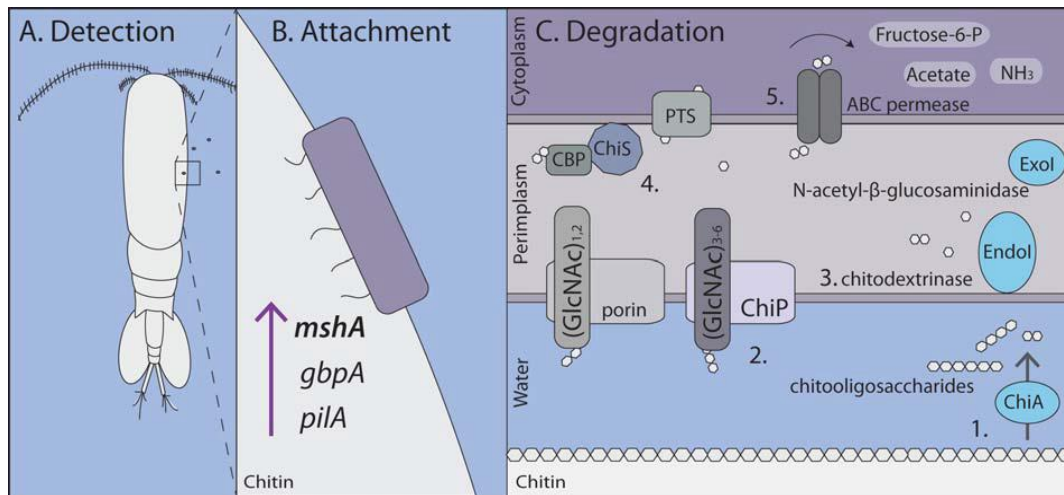
Fig.1.15. Utilization of chitin by *Vibrio* spp. (A) Chemotaxis towards chitin occurs when chitin oligosaccharides are detected by two independent receptors. **(B)** Attachment to chitin occurs via GbpA, MshA pilus, or chitin-regulated pilus encoded by pilA. (C1) Attachment to chitin leads to the extracellular secretion of chitinases such as ChiA, which degrade chitin polymer to chito oligosaccharides. (C2) These enter the periplasm through specific porins such as ChiP and nonspecific porins. The chitooligosaccharides are hydrolyzed by various enzymes into GlcNAc and (GlcNAc)2 (C3) and are transported into the cytoplasm (C4 and C5). The oligosaccharides are further phosphorylated into the final products acetate, NH3, and fructose-6-P (C5) [Source: Erken et al., 2015].

Chitinases are enzymes that cleave GlcNAc glycosidic linkages at random to create soluble oligosaccharides, primarily chitobiose, which is then hydrolyzed to GlcNAc by -N-acetyl glucosaminidases *(Fig.1.15)*. Among these enzymes, chitinases play a critical role in the bacterial breakdown (Keyhani & Roseman, 1999). GlcNAc is then taken up via the phospho-enol pyruvate: GlcNAc phosphotransferase system (PTS). A second, independent system known as ABC-type transporter is used for the uptake and catabolism of (GlcNAc)2. The GlcNAc-6-P generated in the cytoplasm by either the PTS or the N, N -deacetylchitobiose phosphorylase route for (GlcNAc)2 is transformed in two steps to fructose-6-P and ammonia, which enters the Pentose Phosphate Pathway. Suzuki et al. described the hydrolyzing activities of chitinases like ChiA, ChiB, and ChiC1 against diverse chitinous substrates in the case of other marine bacteria like Serratia marcescens (Suzuki et al., 2002). In another marine bacterium, *Alteromonas sp*. strain O-7, numerous chitinases (ChiA, ChiB, ChiC, and ChiD) are produced for efficient chitin breakdown in the natural environment (Orikoshi et al., 2005). Therefore, in the aquatic environment, marine bacteria have evolved efficient chitin utilization strategies to survive under nutrient-poor conditions.

1.19. Vibrio cholerae chitinases

Marine bacteria including the members of the family vibrionaceae, are excellent sources of chitinase (Meibom et al., 2004). Many Vibrio species including pathogenic *V. cholerae* have chitinase activity (R. Bhowmick et al., 2007). They are common inhabitants of marine and estuarine waters and live in association with a chitinous exoskeleton of copepods utilizing chitin as the sole carbon and nitrogen source in the environment (Meibom et al., 2005). *V. cholerae* possess five chitinase genes with locus names VC 0769, VC 1073, VC 1952, VCA 0027, and VCA 0811 (Rudra Bhowmick et al., 2008; Heidelberg et al., 2000) which hydrolyses chitin (Jorgensen & Pfallerc, 2015).

1.20. Role of chitin-binding protein and sensor histidine kinase ChiS in chitin utilization

The *V. cholerae* interaction with chitin has a profound influence on the life cycle of this bacterium, inside and outside its human host, as well as its ecological function in the natural environment (Colwell, 2002). Association of chitin with *V. cholerae* has provided the microorganism with multiple properties at different levels in the environment that include cell metabolic and physiological responses e.g- chemotaxis, cell multiplication, induction of competence, quorum sensing, biofilm formation, commensal and symbiotic relationship with higher organisms, cycling of nutrients and pathogenicity for humans and aquatic animals thus making it advantage, in case of food availability, adaptation to environmental nutrient gradients, tolerance to stress and protection from predators. Chitin utilization by *V. cholerae* is a complex process including steps such as chitin sensing, attachment, and degradation. The two extracellular chitinases, ChiA1 (VC1952) and ChiA2(VCA0027) play an important role in the initialization of *V. cholerae* chitin catabolic cascade (Hunt et al., 2008a) as shown in *(Fig.1.16)*. When *V. cholerae* comes in contact with chitin, these enzymes play a collective but differential activity to degrade chitin into $(GlcNAc)_{n>2}$ oligosaccharides that are transported into periplasmic space via chitoporin (Svitil et al., 1997).
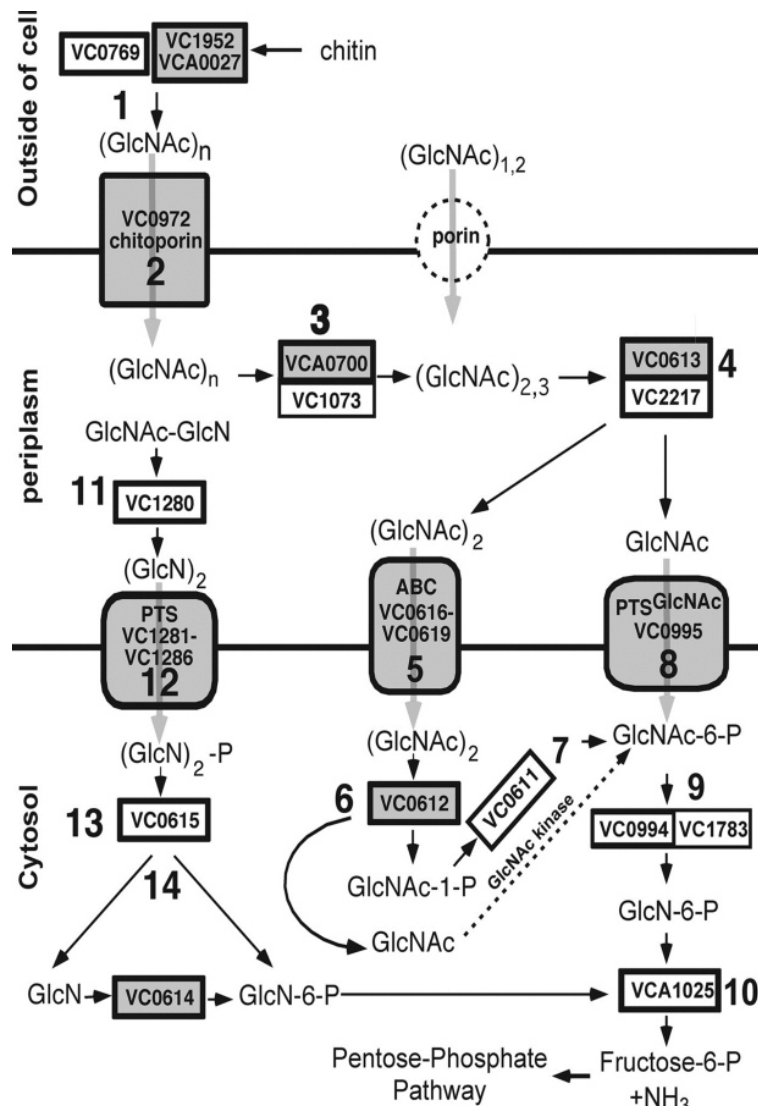
Fig. 1.16. Schematic diagram of the chitin catabolic cascade in *V. cholerae*. The GlcNAc residues are transported and utilized by transporters and enzymes and finally get metabolized to Fructose-6-P which enters into the Pentose phosphate pathway to be utilized as a carbon source. [Source: Hunt et al., 2008a]

1.21. The role played by *V. cholerae* CytR in chitin utilization

CytR, **Cyt**idine **R**egulator, is a transcription factor required for the transport and utilization of ribonucleosides and deoxyribonucleosides. CytR was first mentioned in 1975 (Hammer-Jespersen & Munch-Petersen, 1975) and identified in 1985 (Singer et al., 1985). The repressor CytR and the activator CRP, two dimeric proteins, interact to form a complex repressor nucleoprotein in the intergenic region. When only CRP is bound to this promoter, it functions as an activator, and then, when CytR binds to DNA and CRP, the activation is repressed because CytR masks an activating region of CRP

that otherwise would contact the RNA polymerase to activate transcription (Meibom et al., 2000; Valentin-Hansen et al., 1996). The CytR protein cannot act alone; the synergistic DNA binding is increased by direct interaction with CRP (Sogaard-Andersen et al., 1990). Footprinting analyses showed that the dimers of CytR are flanked or sandwiched by two dimers of CRP. Perini and co-workers showed that CytR binds in tandem in the regulated intergenic region (Perini et al., 1996). On the other hand, in 1997, Pedersen and Valentin-Hanses showed that CytR binds to octamer repeats, GTTGCATT in either the direct or inverted orientation and preferably separated by 2 or 3 bp (Kallipolitis & Valentin-Hansen, 2004). Nine *Escherichia coli* genes were experimentally shown to be regulated by CytR and form the CytR regulon: deoC, cytR itself, tsx, cdd, ppiA, nupC, nupG, udp, rpoH. Since among the gamma-proteobacteria CytR is present only in *E. coli* and its close relatives (up to Vibrionales), it has been suggested that CytR appeared in the Enterobacteriales due to horizontal transfer from the delta Proteobacteria (*Geobacillus* sp. or *Caulobacter sp*.) (Price et al., 2007).

1.22. Structure of CytR

CytR is a 335 amino acid long, 37 kDa protein located in the cytoplasm of *V. cholerae* and is produced from the locus VC_2677 of Chromosome I. CytR is an atypical representative of the LacI-family (Weickert & Adhya, 1992). Like the other members of LacI family, CytR has an N-terminal domain that contains a helix-turn-helix (HTH) motif for DNA binding and a C-terminal domain for dimerization, inducer binding, and protein interaction with CRP (cAMP receptor protein) *(Fig.1.17)*. Its affinity to its operators is rather weak and because of that, in contrast to most prokaryotic repressors, CytR alone is not capable to repress transcription. CytR functions in a complex with a multifunctional transcription factor (TF), CRP. The mechanism of the CytR action is anti-activation rather than direct repression (Sernova & Gelfand, 2012).

1.22. Functions of CytR in nutrient uptake and extracellular nucleoside acquisition in V. cholerae

The complex response to nutrient starvation controlled by (cAMP receptor protein) CRP incorporates other regulatory proteins that allow bacteria to use not only different sugars but also nucleic acids. Many genes in *E. coli* that scavenge and

metabolize extracellular pyrimidine nucleosides are negatively controlled by the cytidine repressor CytR (Valentin-Hansen et al., 1996). CytR binds to CRP and functions as an 'anti-activator' of the promoters of specific CRP-activated genes involved in nucleoside transport and degradation when free nucleosides are scarce.
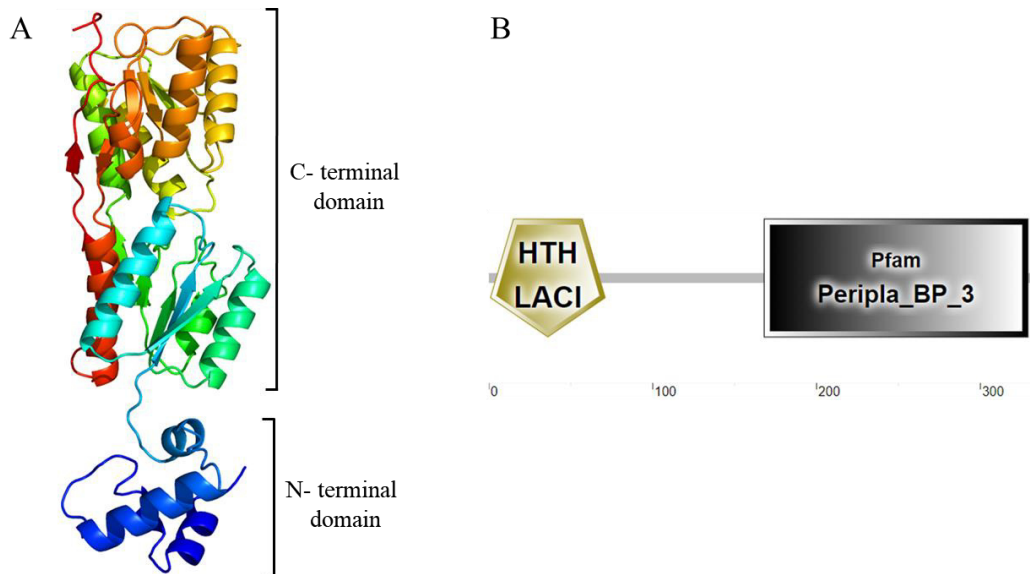
Fig.1.17. Structure prediction of *V. cholerae* **CytR by homology modelling (A)** CytR has an N-terminal domain that contains a helix-turn-helix (HTH) motif for DNA binding and a C-terminal domain for dimerization, inducer binding, and protein interaction **(B)** HTH-LacI domain – 1-71 amino acid; Periplasmic binding protein superfamily domain- 168-329 amino acid.

Cytidine, on the other hand, enters the cell and binds allosterically to CytR. When CytR is complexed with cytidine, conformational alterations in CytR impede interaction with CRP and, as a result, CytR-dependent anti-activation of CRP-regulated genes is eliminated. CRP can then trigger promoter expression by engaging RNA polymerase (Barbier et al., 1997). As a result, genes essential for nucleoside uptake and metabolism are only expressed in the presence of nucleosides.

The availability of nucleotides such as purine has also been found to have a role in controlling natural competence in *H. influenzae* (Macfadyen et al., 2001; Sinha et al., 2013). However, the *H. influenzae* genome lacks a CytR homologue, and a functionally comparable protein, PurR, was found to be independent to purine-mediated competence repression (Sinha et al., 2013). Interestingly, cytR was originally identified as a TfoX-regulated *V. cholerae* gene (Meibom et al., 2005).

However, its specific role in natural competence was just recently discovered, when a cytR mutant was demonstrated to be non-transformable and displayed reduced expression of *comEA*, *chiA-1*, and *pilA*. (Antonova et al., 2012). The presence of nucleosides, specifically cytidine, directly suppressed both transformation and comEA expression, implying a regulatory mechanism similar to that proposed for *H. influenzae* (Antonova & Hammer, 2011) *(Fig.1.18)*.

Mutants having CytR variants that were unable to bind to CRP were impaired for transformation, implying that the CytR–CRP protein-protein interactions required for nucleoside scavenging in *E. coli* are likewise required for activating natural competence genes in *V. cholerae* (Antonova et al., 2012). Although the precise role of nucleotide scavenging in natural competence has yet to be identified, these findings
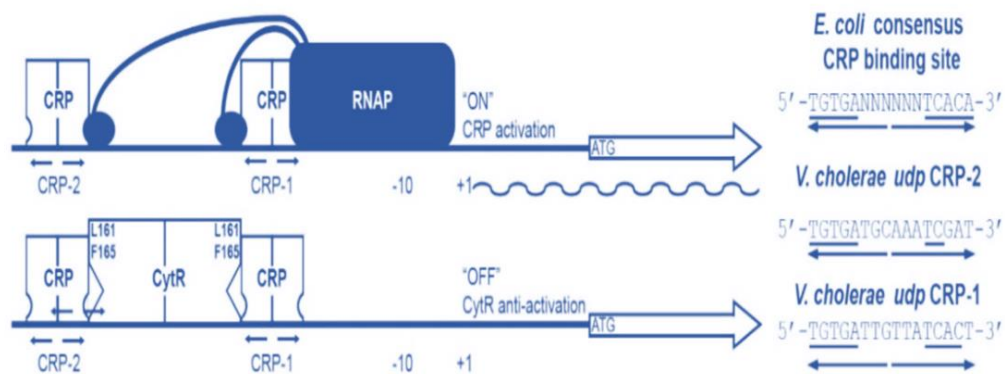
Fig.1.18. *V. cholerae* CytR is a CRP-dependent anti-activator. (A) Top: Model of promoter region of *V. cholerae* genes transcriptionally activated when a CRP dimer binds to both a proximal (CRP-1) and distal (CRP-2) binding site, and recruits RNA polymerase by association with each αCTD of RNAP (black ovals). Bottom: CytR makes protein-protein interactions via L161 and F165 with each CRP dimer blocking CRP-dependent activation of transcription at the promoter via an "anti-activation" mechanism. Arrows at each CRP binding site highlight that the sequence is an inverted repeat. **(B)** The *E. coli* consensus binding site for one CRP dimer, and the predicted distal (CRP-2) and proximal (CRP-1) binding sites in the *udp* promoter region of *V. cholerae*. Arrows highlight the inverted repeat sequence, and underlined nucleotides indicate the critical nucleotides of the 5'-TGTGA(N6)TCACA-3' consensus.

suggest that natural competence in the Vibrionaceae may be deployed not only for HGT but also for nutrient acquisition.

TfoX has recently been found to positively influence the expression of two transcription factors, CytR and QstR. (Lo Scrudato & Blokesch, 2013; Meibom et al.,

2005). CytR, as previously characterized, is a nucleoside scavenging cytidine repressor that inhibits the expression of *comEA*, *pilA*, and *chiA-1* in *V. cholerae* (Antonova et al., 2012). TfoX also promotes the transcription of qstR, which encodes a transcription factor required for the production of *comEA* and *comEC* (Lo Scrudato & Blokesch, 2013). The key quorum-sensing regulator, HapR, is also required for QstR activation (Lo Scrudato & Blokesch, 2013), which accounts for the subset of TfoX-regulated genes that are also controlled by quorum sensing (Lo Scrudato & Blokesch, 2012). These findings highlight the intricate roles of TfoX in coordinating the expression of the genes essential for *V. cholerae* competence.

1.24. The function of CytR in other aspects

CytR negatively regulates a small group of nucleoside scavenging and metabolism genes in *E. coli*, including *udp*, *cdd*, *ompK*, and *cytR* itself, through a cAMP receptor protein (CRP)-dependent anti-activation mechanism (Valentin-Hansen et al., 1996). *V. cholerae* CytR is a functionally diverse protein and a global regulator. It represses several nucleoside catabolism and scavenging genes, positively regulate competence and the majority of natural transformation genes, induces bacterial killing by activating T6SS gene clusters, and co-regulates chitinase genes alongside TfoX. Recently it has been discovered that among many other roles CytR is involved in the regulation of *V. cholerae* extracellular chitinase *chiA1* (Antonova et al., 2012) and *chiA2* (Watve et al., 2015).

In the intestine, *V. cholerae* secretes chitinases in order to degrade mucin to gain access to the epithelial cells as well as to get nutrients. There are reports that indicate the involvement of bacterial chitinases in virulence (Frederiksen et al., 2013; Mondal et al., 2014; Tran et al., 2011). The pathogenesis of *V. cholerae* within the human host is controlled by a complex signalling cascade of virulence genes and regulatory factors that has been studied for several decades. Although the role of *V. cholerae* CytR in chitin metabolism and degradation has been studied well its role in pathogenesis is still lacking.

1.25. Transmission of V. cholerae from the environment to the host

Toxigenic strains of *V. cholerae* persist in aquatic environments alongside non-toxigenic strains, aided by biofilm formation on biological surfaces and the use of chitin as a carbon and nitrogen source *(Fig.1.19)*. On ingestion of these aquatic-environment-

adapted bacteria in contaminated food or water, toxigenic strains colonize the small intestine, multiply, secrete cholera toxin, and are shed back into the environment by the host in secretory diarrhoea. The stool-shed pathogens are in a transient hyper infectious state that serves to amplify the outbreak through the transmission to subsequent hosts. (Antonova et al., 2012; Lo Scrudato & Blokesch, 2012, 2013; Meibom et al., 2004, 2005).
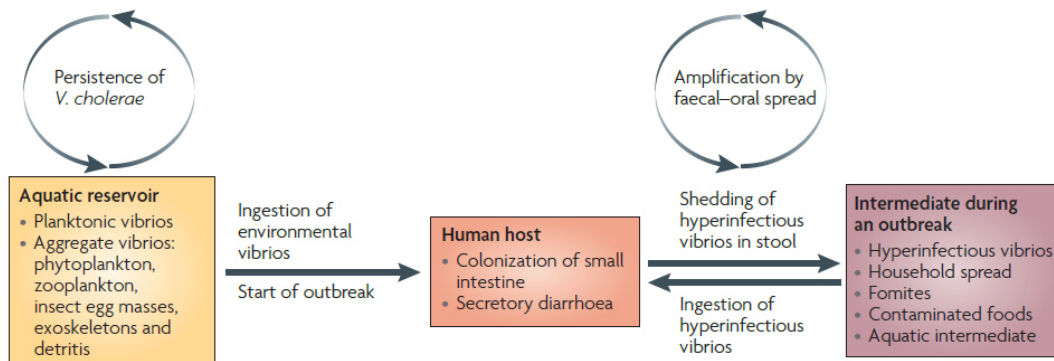
Fig.1.19. The life cycle of pathogenic *Vibrio cholerae*. Toxigenic strains of *Vibrio cholerae* persist in aquatic environments alongside non-toxigenic strains, aided by biofilm formation on biological surfaces and the use of chitin as a carbon and nitrogen source. On ingestion of these aquatic-environment-adapted bacteria in contaminated food or water, toxigenic strains colonize the small intestine, multiply, secrete cholera toxin, and are shed back into the environment by the host in secretory diarrhoea. The stool-shed pathogens are in a transient hyper-infectious state that serves to amplify the outbreak through the transmission to subsequent hosts.

1.26. V. cholerae pathogenesis

Cholera is characterized by severe, watery diarrhea, which can rapidly lead to dehydration and death in untreated patients. *V. cholerae* of the O1 and O139 serotypes are responsible for epidemic cholera in humans. All other serotypes are grouped as "non-O1" strains; they are associated with sporadic cases of gastroenteritis *(Fig.1.20)*.

Infection due to *V. cholerae* begins with the ingestion of contaminated water or food. After passage through the acid barrier of the stomach, the organism colonizes the epithelium of the small intestine by means of the toxin-coregulated pili (Taylor et al., 1987) and possibly other colonization factors such as the different haemagglutinins, accessory colonization factor, and core-encoded pilus, all of which are thought to play a role in pathogenesis *(Fig.1.21)*.
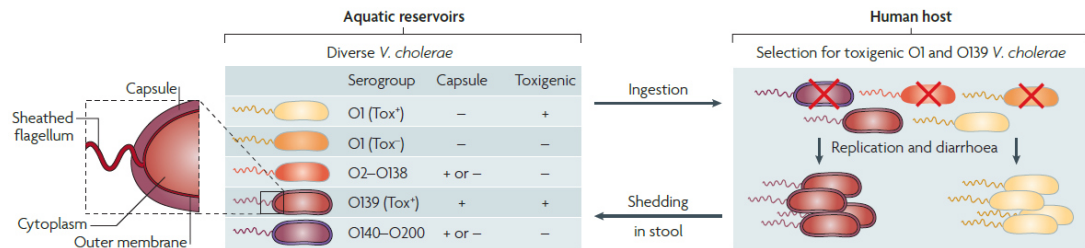
Fig.1.20. **Phylogenetic relationship of *Vibrio cholerae* strains.** On the basis of the antigenicity of the O antigen component of the outer membrane lipopolysaccharide, more than 200 serogroups (O1–O200) of *Vibrio cholerae* exist in aquatic environments. Only a subset of O1 and O139 serogroup strains are toxigenic (Tox$^+$) and therefore capable of causing cholera when ingested; such strains are selected for in the host. Other strains are non-toxigenic (Tox$^-$) and are selected against. Different O antigen types are indicated by the colour of the outer membrane and sheathed flagellum. Capsules are present in a subset of strains.
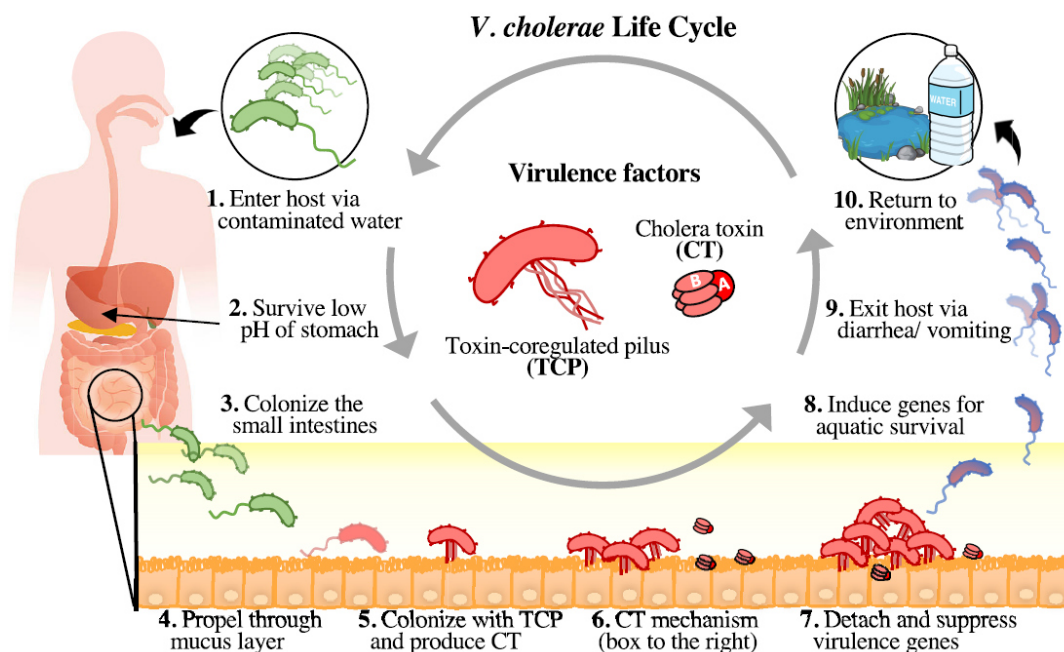
Fig.1.21. *V. cholerae* life cycle and pathogenesis. *V. cholerae* is a waterborne disease that causes cholera and is a human-restricted pathogen. (1) *V. cholerae* is introduced to the human host through contaminated water. (2) In the stomach, *V. cholerae* encounters a low pH environment. (3) To induce disease, *V. cholerae* colonizes the small intestine. (4) *V. cholerae* uses a single flagellum to propel through the mucus and reaches the epithelial surface. *V. cholerae* responds to host signals including bile, mucins, pH, and oxygen availability to induce virulence factors such as toxin coregulated pilus (TCP) and cholera toxin (CT). (5) TCP facilitates the colonization of the epithelial surface, and CT is produced, binding GM1 on the host cells. (6) CT is then endocytosed and induces cyclic AMP (cAMP). High cAMP levels cause the efflux of electrolytes and water, resulting in the characteristic watery diarrhea

of cholera. (7) Microcolonies form and *V. cholerae* produces extracellular matrix components including Vibrio polysaccharides, biofilm proteins, and extracellular DNA. At high cell density, *V. cholerae* represses virulence genes through quorum sensing. (8) At this high density, *V. cholerae* detaches from the epithelial surface and migrates to the lumen. Genes required for transitioning into the aquatic environment are upregulated. (9) *V. cholerae* is excreted from the host in diarrheal stool and vomitus. (10) *V. cholerae* returns to the environment, where contamination of drinking water may infect another host. [Source: Chac et al., 2021]

1.27. Cholera: The most fearsome waterborne infection

Cholera is an acute enteric infection caused by the ingestion of the bacterium *Vibrio cholerae* present in fecally contaminated water or food, primarily linked to insufficient access to safe water and proper sanitation. Every year 3-5 million people around the world are infected with cholera and 100,000- 120,000 people die from the infectious disease, according to estimates by the World Health Organization (WHO '2015).

Fig.1.22. A child, lying on a cholera cot, is showing typical signs of severe dehydration from cholera. The patient has sunken eyes, a lethargic appearance, and poor skin turgor; however, these symptoms could be reversed to near normal within 2 h if adequately rehydrated [Source: Sack et al., 2004].

Cholera is characterized in its most severe form by a sudden onset of acute watery diarrhoea that can cause a massive loss of bodily fluids leading to sunken eyes, blue-grey skin, and eventually death *(Fig.1.22)*. The extremely short incubation period - two hours to five days - enhances the potentially explosive pattern of outbreaks, as the number of cases can rise very quickly. About 75% of people infected with cholera do not develop any symptoms. However, the pathogens stay in their faeces for 7 to 14 days and are shed back into the environment, possibly infecting other individuals.

1.28. Epidemiology of V. cholerae

Cholera first emerged from the Ganges Delta of the Indian subcontinent as early as the nineteenth century. Over the centuries, seven well-defined pandemics have been reported, with an eighth pandemic suspected to have occurred since 1992 *(Table 1.2)*. El Tor biotype of *V. cholerae* serogroup O1 triggered the seventh pandemic, which began in Indonesia in 1961 and spread to Africa and the Americas in 1970 and 1991, respectively. In 1992, a new serotype, O139, developed in India and quickly spread to Bangladesh and surrounding Asian countries. In recent years, massive and prolonged outbreaks have occurred in countries that have been free of cholera for decades.
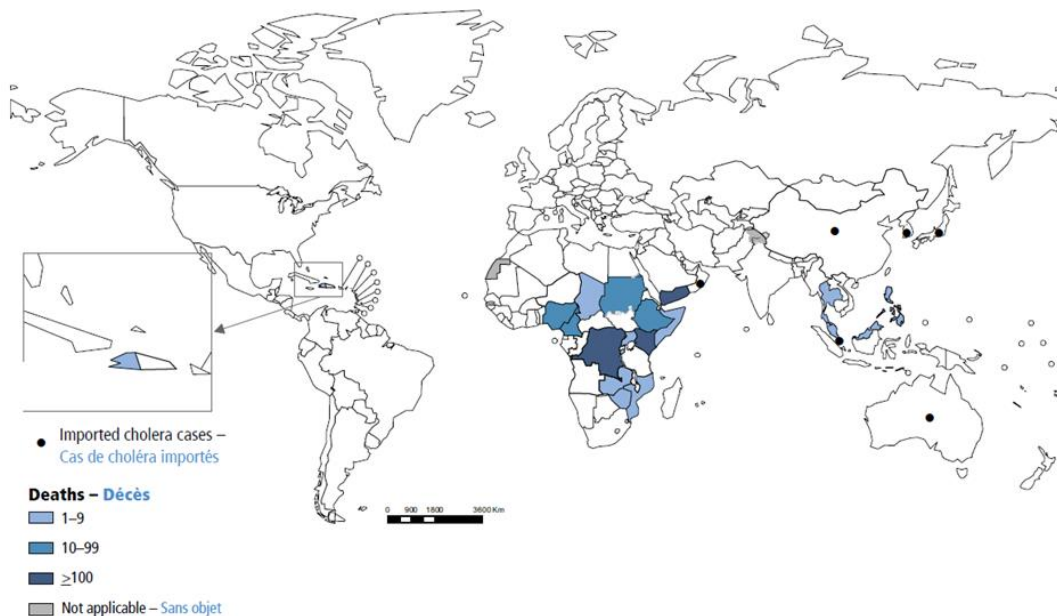
Fig.1.23. Countries reporting cholera cases and deaths in 2019
[Source: Weekly Epidemiological Record, WHO cholera report 2019]

A near-doubling in the global number of cholera cases reported to WHO during 2019 (923 037) over that in 2018 (499 447) might appear to be a step backward in cholera control; however, there is highly positive news, in that the total number of reported deaths from cholera decreased by 36%, from 2990 in 2018 to 1911 in 2019; Africa reported the fewest annual numbers of cases and deaths in the 21st century, and the Americas reported the fewest cases and deaths since the disease was introduced into Haiti in 2010. In 2019, a sharp increase in reported cholera cases is due to the increase in the number of cases in Yemen (8,61,096) *(Fig.1.24)*, the Democratic Republic of the

Congo (30,304), and Mozambique (7,010) which accounted for 97% of the cases reported globally in 2019 (WHO, 2019). The recent global distribution of cholera is depicted in *Fig.1.23*.

"Yemen has been devastated by a brutal war which started in early 2015. Twenty one million people (75% of the total population) require humanitarian assistance, 7.3 million are severely food insecure, and 3.3 million are internally displaced. Moreover, the health-care system is on the brink of collapse as more than 55% of health facilities are partially functioning or destroyed. This situation, which is already a complex web of challenges, is exacerbated by the airport closures, severe shortages of fuel, food, drinking water and medication, and non-payment of public employees for 15 months since September 2016. In addition, sewage and drainage systems are clogged and rubbish is piled high in the streets. The underground water in all Yemeni cities is contaminated with sewage and treatment plants are not functioning because of lack of fuel and maintenance."

-excerpt from *Al-Mekhlafi Hesham*, 2018 on Recent cholera outbreak in Yemen.

Fig.1.24. (A) People gather to collect drinking water from a charity tanker truck in the midst of the cholera epidemic in Taiz governorate, **(B)** rubbish piles up on the main street in Sana'a city, and **(C)** cholera-infected patients lie on the ground while receiving treatment at a temporary health station in Hajjah governorate, Yemen. [Source: Al-Mekhlafi, 2018]

Table 1.2. History of cholera pandemics

Cholera Pandemics	Years	Countries
First	1817-1823	The first pandemic originated in the Ganges River delta in India. the disease spread to Southeast Asia, central Asia, Middle East, eastern Africa, and the Mediterranean coast.
Second	1829-1849	It started also in India and reached Russia by 1830 and spread in countries Finland, Poland, Europe, North America.
Third	1852-1859	Originated once again in India. It devastated large swaths of Asia, Europe, North America and Africa. In 1854, the worst year, 23,000 died in Britain alone.
Fourth	1863-1879	The fourth pandemic began in the Bengal region from which Indian Muslim pilgrims visiting Mecca spread the disease to the Middle East. From there it migrated to Europe, Africa and North America. Cholera claimed 90,000 lives in Russia in 1866.
Fifth	1881-1896	Again, originated in the Bengal region of India and swept through Asia, Africa, South America and parts of France and Germany.
Sixth	1899-1923	The sixth pandemic killed more than 8,00,000 people in India before moving into the Middle East, northern Africa, Russia and parts of Europe.
Seventh	1961 to present	Unlike other pandemics the seventh pandemic originated in Indonesia then spread to Italy, Africa and ravaged populations across Asia and the Middle East. Later an outbreak among Rwandan refugee in 1994, Zimbawe in 2008, Haiti in 2010 took many lives.

1.29. *V. cholerae and human intestine*

Intake of contaminated water or food with *V. cholerae* is the major route of *V. cholerae* ingestion by a human. After ingestion, in order to cause infection *V. cholerae* must thrive in the hostile acidic environment of the host stomach, and then penetrate the mucus lining that coats intestinal epithelia. Due to the acid intolerance of *V. cholerae* cells, a relatively high infectious dose (10^6 to 10^{11} CFU/ml) is required to cause infection in humans (Cash et al., 1974). In the human intestine, *V. cholerae* adhere and colonize on the intestinal epithelial cells, eventually producing CT and the resulting manifestation of cholera symptoms. During the habitat switching from aquatic environment to human intestine *V. cholerae* cells come into contact with low pH environment present in the gastric juice (Cash et al., 1974). The cells, that overcome

such gastric barrier further colonize the intestinal epithelial cells, eventually producing CT and causing cholera.

1.30. Mechanisms of intestinal colonization

Vibrio cholerae pathogenesis is multifactorial and relies on both host and bacterial counterparts. *V. cholerae* after being introduced into the intestinal lumen requires attachment to intestinal linings. This initial attachment is the key step in the pathogenesis of *V. cholerae*. A number of colonization factors have been documented which serve as important adhesion molecules in interaction with the host cell surface. Colonization of the small intestinal epithelium is necessary for *V. cholerae* to cause disease. Factors that may contribute to this process include bacterial pili, hemagglutinins, an accessory colonizing factor, porin-like proteins, *rfb*-encoded enzymes, and a chitin-binding protein.

1.31. Impact of host factors

After ingestion in order to survive and cause infection *V. cholerae* must pass through certain barriers. In addition, there are some factors that help the bacterium to colonize and cause cholera.

1.31.1. pH

V. cholerae must pass through and survive the gastric acid barrier of the stomach, then penetrate the mucus lining that coats intestinal epithelia. Due to the acid sensitivity of *V. cholerae,* the infectious dose needs to be relatively high (10^6 to 10^{11} CFU/ml) to cause cholera infection in humans (Kaper et al., 1995). The pH here is as low as 2, rapidly changed from highly acid in the stomach to about pH 6 in the duodenum. The pH gradually increases in the small intestine from pH 6 to about pH 7.4 in the terminal ileum. There as soon as the bacterium reaches the small intestine, it gets its required pH that helps in successful infection as the optimal pH is about 7.6.

1.31.2. Mucin

It is a glycoprotein that is present extracellular to and coating the intestinal epithelia which prevent most microorganisms from reaching and persisting on the intestinal surface. It is highly glycosylated consisting of ~80% carbohydrates primarily N-acetylgalactosamine, N-acetylglucosamine, fucose, galactose, and sialic acid, and

traces of mannose and sulfate. The oligosaccharide chains of mucin exhibit moderate branching and are attached to the protein core by O-oligosaccharide bonds to the hydroxyl side chains of serine and threonines and arranged in a bottle brush configuration about the protein core (Bansil & Turner, 2006; Dekker et al., 2002). The remaining 20% consists of the protein core with a molecular mass of ~200 to 500 kDa. The abundance of intestinal mucin appears to be an important factor explaining at least some of the regiospecific aspects of *V. cholerae* intestinal colonization. As already mentioned the chitin-binding protein GbpA of *Vibrio cholerae* has been previously described as a common adherence factor for chitin and intestinal surface (Kirn et al., 2005). In addition, it has been also reported that there is a coordinated interaction between GbpA and mucin to upregulate each other in a cooperative manner, leading to increased levels of expression of both of these interactive factors and ultimately allowing successful intestinal colonization and pathogenesis by *V. cholerae*. This was a novel colonization factor applicable to both the surfaces due to the fact that both chitin and mucin possess a common adhesion factor recognized by GbpA i.e, N-Acetyl glucosamine. Counter to the above report recently, it has been demonstrated that host mucins are a key factor limiting *V. cholerae* intestinal colonization, particularly in the proximal part of the small intestine where there appears to be a more abundant mucus layer.

1.31.3. Bicarbonate

A previous study says that bicarbonate stimulates virulence gene expression by enhancing ToxT activity. ToxT is a regulatory protein that directly activates transcription of the genes encoding cholera toxin (CT), toxin-coregulated pilus (TCP), and other virulence genes that shall be discussed later. Both the classical and El Tor biotypes produce inactive ToxT protein when they are cultured statically in the absence of bicarbonate. The addition of bicarbonate to the culture medium does not affect ToxT production but causes a significant increase in CT and TCP expression in both biotypes. Thus, bicarbonate is the first positive effector for ToxT activity to be identified (Abuaita & Withey, 2009). Given that bicarbonate is present at high concentration in the upper small intestine where *V. cholerae* colonizes, bicarbonate is likely an important chemical stimulus that *V. cholerae* senses and that induces virulence during the natural course of infection.

1.31.4. Bile salts

Bile is a complex mixture of organic and inorganic molecules in the form of sodium taurocholate, glycocholate, etc that is stored in the gallbladder and released into the proximal small intestine to promote lipid absorption after a fatty meal. The sole function of conjugated bile acids in the small intestine is to solubilize polar lipids during digestion. The second function of bile acids in the intestine is to inhibit the growth of bacteria in the small intestine (Inagaki et al., 2006). Previous studies have shown that bile and its unsaturated fatty acid components released in the small intestine, reduce virulence gene expression and therefore are likely important signals upon entering the host. Further studies on the effects of bile on *V. cholerae* virulence factor transcription revealed that unsaturated fatty acids (arachidonic, linoleic, and oleic acids) within bile repressed *ctxAB* and *tcpA* expression, suggesting that these components may be directly interacting with ToxT to repress its activity. The presence of high levels of bile within the intestinal lumen may prevent premature ToxT activity prior to the organisms' arrival within intestinal crypts (A. Chatterjee et al., 2007; Gupta & Chowdhury, 1997). Recently, the mechanism for bile-mediated reduction of virulence gene expression has also been clearly defined (Withey et al., 2015).

1.32. Virulence factors of V. cholerae

In *V. cholerae*, the two main virulence factors responsible for cholera disease are cholera toxin (CT) and toxin co-regulated pilus (TCP). A filamentous bacteriophage (designated CTXΦ) contains genes encoding cholera toxin, and a 41-kb pathogenicity island on the chromosome encodes the toxin co-regulated pilus (TCP). Cholera toxin, encoded by the *ctx*AB genes of lysogenic CTXΦ is a potent enterotoxin of the A-B toxin type. It consists of one enzymatic A subunit and five receptor binding B-subunits and is secreted by a bacterial type II secretion system. After secretion, the CT-B subunit binds to ganglioside GM1 receptors in lipid rafts on the plasma membrane of the target cells. The entire toxin complex is endocytosed by the cell and moved through the Golgi apparatus to the endoplasmic reticulum, where the A subunit dissociates from the toxin complex. CT-A is transported to the cytoplasm of the target cell where it ADP-ribosylates a GTP-binding protein that activates adenyl cyclase. This event leads to an increase in the intracellular cAMP level, resulting in an imbalance in electrolyte movement in the epithelial cell. This in turn leads to increased secretion of NaCl, which

further enhances the osmotic movement of water into the intestinal lumen, resulting in the watery diarrheal disease cholera which is a hallmark of cholera.

1.33. Regulation of Virulence factors

Many *V. cholerae* virulence genes are coordinately regulated in response to environmental signals. Although the conditions that affect toxin production in the human intestine are not known, in vitro factors increasing toxin production are low temperature (25º to 30ºC), osmolarity (NaCl concentration of 50 to 60 mmol), high aeration, acidic pH (6.5), and the presence of certain amino acids (asparagine, serine, glutamate, and arginine), phosphate, and trace elements *(Fig.1.25)*.

1.33.1. ToxR regulon

ToxR, a 32-kDa transmembrane protein is the master key for the control of virulence factors for *V. cholerae* O1 (Miller et al, 1987). It regulates by binding to the upstream of the *ctx*AB genes and upregulates their transcription. ToxS enhances the activity of ToxR by stabilizing the ToxR dimeric form (Victor J. DiRita, 1992). ToxR in association with CT (Taylor et al., 1987) also controls the expression of TCP, accessory colonization factor, and the outer membrane proteins OmpT and OmpU. At least 17 genes are found under the regulation of ToxR, which construct the "ToxR regulon". There is another regulatory protein ToxT which also regulates certain genes of this regulon (V. J. DiRita et al., 2006). ToxR regulates transcription of *tox*T gene, which leads to activation of other genes in the ToxR regulon. Thus, there is a regulatory cascade mechanism that controls the expression of crucial virulence factors in *V. cholerae*. A heat shock protein of *V. cholerae*, *htp*G also plays important role in the control of the ToxR regulon. ToxT is a 32-kDa protein, which is a member of the AraC family of transcriptional activators. ToxT activates transcription of ctxAB, as well as the tcp genes, the acf genes, and the aldA gene. There are both ToxT-dependent and ToxT-independent branches of the ToxR regulon; transcription of the genes encoding two major outer membrane proteins, OmpT and OmpU, is regulated directly by ToxR, as are genes involved in motility and chemotaxis.
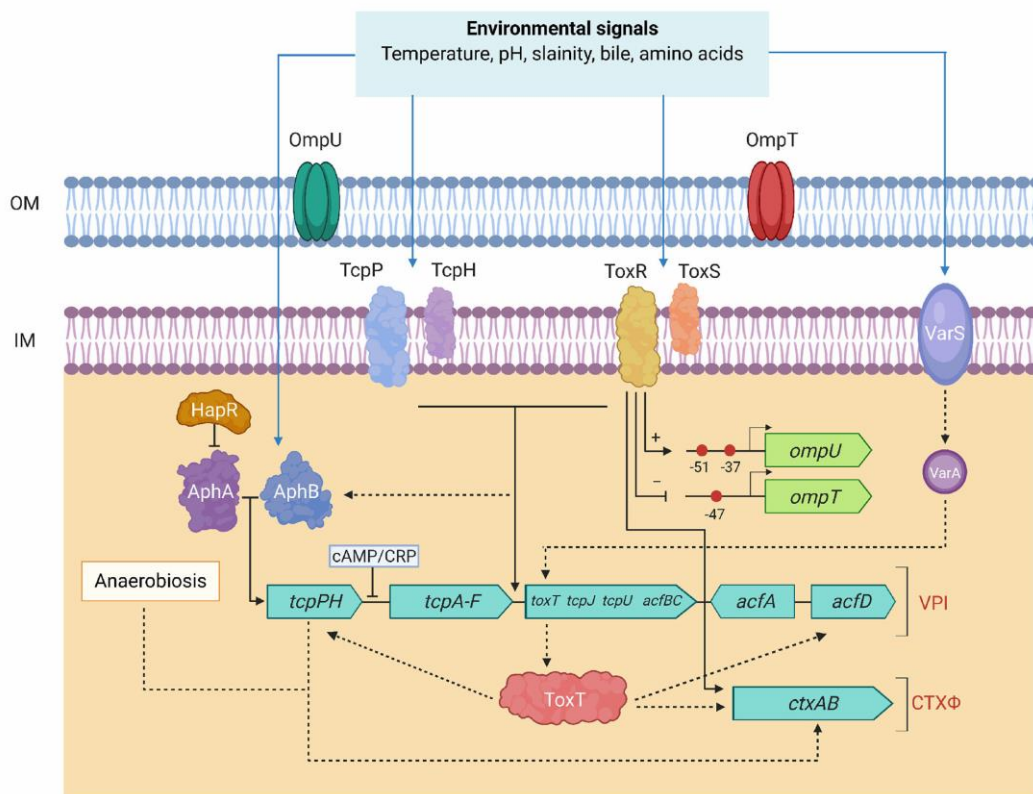
Fig.1.25. Regulation model of Tox-mediated virulence genes in *V. cholerae*.
TcpP/TcpH and ToxR/ToxS function together in activating transcription of *toxT*.
ToxR and TcpP need accessory proteins (ToxS and TcpH, respectively) for
maximal activity. ToxT initiates transcription of the full *tcp* operon, *ctxAB*, and
acf. AphA and AphB activate transcription of the *tcpPH* operon in response to
environmental conditions. *tcpPH* promoter is negatively influenced by the global
regulator, CRP. ToxR/ToxS, and AphA/AphB also regulate genes other than *ctx*
and *acf*. ToxRS, AphAB, TcpPH, and ToxT coordinately regulate the transcription
of *ctx* and *tcp*. AphA and AphB activates the expression of the *tcpPH*. TcpPH and
ToxRS regulate *ctx* and *tcp* genes through ToxT. AphB has been linked to the
expression of *tcpPH* for anaerobiosis that enhances the production of CT. The
direct activator and the second activator are differentiated by black solid and dotted
arrows, respectively. Blue arrows indicate different environmental conditions
sensed by the ToxRS and TcpPH, AphAB, and VarS regulatory systems. The two-
component VarS-VarA system responds to environmental factors and signals *toxT*.
ToxR, independently activates and represses transcription of *ompU* and *ompT*.
ToxR modulation was shown by an arrow (*ompU*) and line with base (*ompT*)
through + for the transcription of *ompU* and—for repressing the transcription of
ompT. Red circles in *ompU* and *ompT* indicate the ToxR binding sites and the
transcriptional start sites are marked with arrows for each promoter.

ToxR has different activities if it is expressed in *Escherichia coli* or in its native
host, *V. cholerae (Fig.1.26)*. In experimental systems in *E. coli*, ToxR acts as a
transcriptional activator of ctxAB by binding to a 7-bp repetitive region in the ctxAB
promoter; the more tandem repeats that are present, the more toxin is produced. In *V.*

cholerae, however, ToxR does not directly activate the ctxAB promoter but acts to control toxin expression through activation of toxT (Matson et al., 2007). The difference in the ability of ToxR to activate ctxAB in *E. coli* and *V. cholerae* is not yet understood.
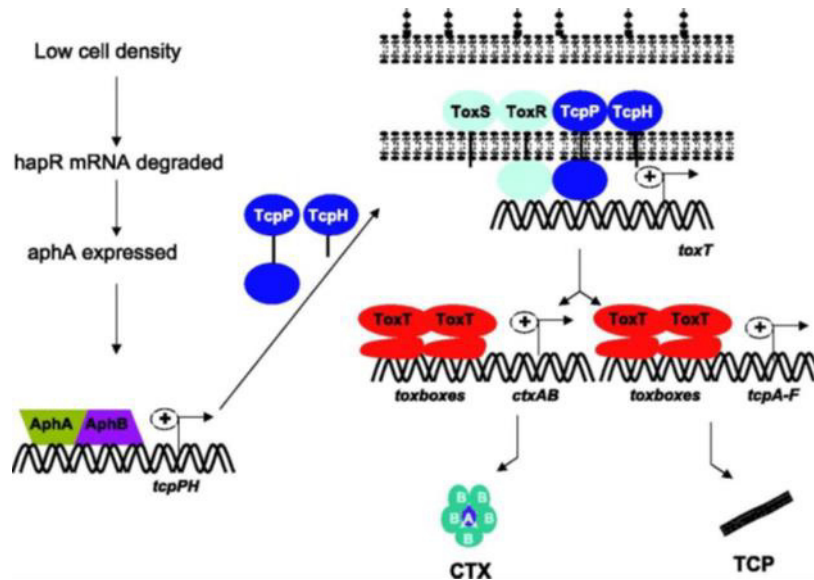
Fig.1.26. Schematic representation of ToxR regulon showing the different components regulating the production of two major virulence determinants CT and TCP. [Source: Matson et al., 2007**]**

The proteins involved in directly sensing the environmental changes that regulate gene expression are not known. Production of TcpP and TcpH is controlled by environmental changes; transcription of the tcpPH genes is regulated by temperature and pH in a ToxR-independent manner. The ability of TcpP/H to activate ToxT is significantly reduced when the growth medium contains a high NaCl concentration; both exogenous and endogenous sodium appear to affect virulence factors in *V. cholerae* in a complex fashion.

The regulatory protein AphA is required for activation of the tcpPH promoter, and may act to regulate the expression of tcpPH in response to environmental changes. It may be that other yet undefined regulatory proteins affect TcpPH and/or ToxR expression, or that TcpPH and/or ToxR directly sense external signals. However, ToxR expression itself is not influenced by most environmental changes. One exception is the reduced expression of ToxR at high temperatures (37ºC), which may relate to control at the promoter level by the divergently transcribed heat shock gene, *htpG*.

The response of *V. cholerae* strains to environmental conditions varies by biotype. Variations in control over the expression of ToxT appear to be important in

these biotype differences. Other genes may also be important in the regulation of virulence genes. The cAMP-CRP system, a global regulator in many bacteria that responds to carbon sources through cAMP expression, also influences the expression of ToxR-regulated virulence genes. *V. cholerae* has a virulence locus, *varA*, which is a homologue of the conserved global regulatory gene *gacA*. GacA belongs to the family of two-component signal-transducing molecules. Transcription of the *varA* gene is independent of ToxR; *varA* mutants produce less TCP and CT, and are attenuated in colonization. Finally, phage induction and replication may be an additional mechanism for the regulation of CT production *in vivo*. Expression of CT from the replicative form of CTXΦ is largely independent of ToxR and ToxT.

1.33.2. TfoX: an integral regulator

The *tfoX* gene was originally identified among other *V. cholerae* genes that display elevated expression levels in response to chitin. When constitutively expressed, TfoX can induce genetic competence in the absence of chitin. Chitin, in the form of either crab shells or oligosaccharides, enhances the production of TfoX, at both transcriptional and post-transcriptional levels. Genetic studies in *V. cholerae* have shown that chitin sensed by the hybrid sensor kinase ChiS, promotes the production of a small regulatory RNA named TfoR *(Fig.1.27)*. The signaling pathway initiated by ChiS that leads to *tfoR* expression remains unclear. TfoR is predicted to base-pair with the 5′-untranslated region (5′-UTR) of the *tfoX* transcript, thus preventing the formation of an inhibitory secondary structure that sequesters the predicted Shine–Dalgarno sequence for *tfoX*. Translational activation of *tfoX* by TfoR also requires the RNA chaperone Hfq, which is often a crucial player in trans-encoded small RNA-mediated regulation. A transcriptional repressor element was also identified within the *tfoX* promoter in *V. cholerae*. However, in contrast to the strong translational regulation described above, the transcriptional derepression of *tfoX* by chitin and (GlcNAc)n is moderate, and the transcription factor involved in this process remains unknown. CRP–cAMP was recently shown to also directly induce *tfoX* transcription in *V. cholerae*, suggesting conserved regulation among these Gram-negative bacteria. Future studies of *tfoX* regulation will greatly help our understanding of how the *Vibrionaceae* process the external chitin signal to turn on complex phenotypes like competence and T6S.
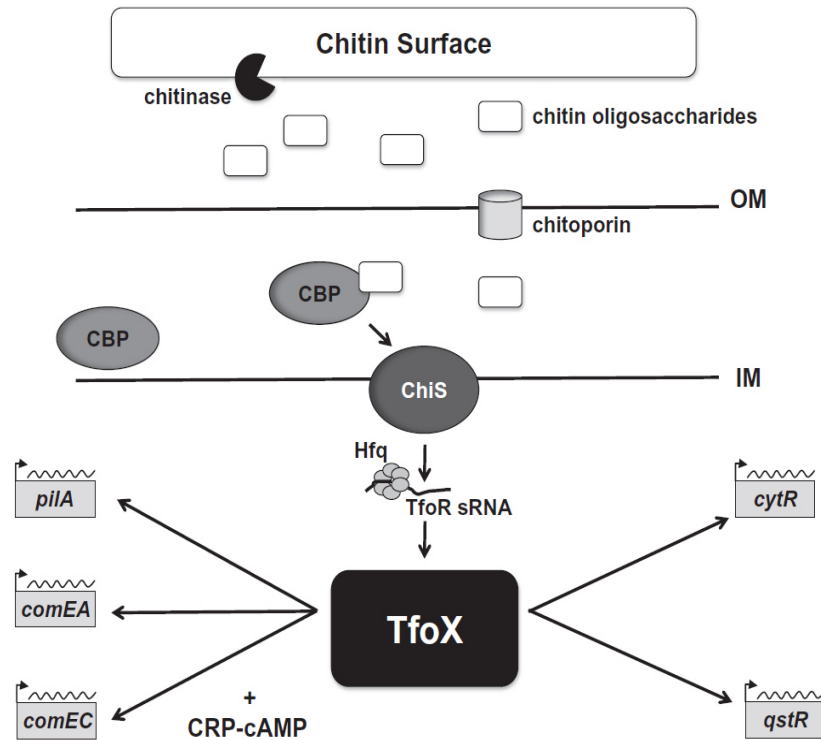
Fig.1.27. Chitin-dependent signaling pathways for natural transformation and Type 6 Secretion in *V. cholerae*. Chitin is degraded by extracellular chitinases into oligosaccharide fragments, which enter the periplasm through a chitoporin. With the help of CBP, ChiS senses the presence of chitin oligosaccharides and activates the TfoR sRNA via the RNA chaperone Hfq. TfoR then initiates translation of TfoX. It upregulates the expression of other competence genes (e.g. *pilA*, *comEA* and *comEC*) and two genes encoding transcription factors (*cytR* and *qstR*). Regulation of the competence genes by TfoX also requires the cAMP–CRP complex. IM, inner membrane; OM, outer membrane.

Members of the chitin-dependent TfoX regulon include the *pilQ*, *pilA*, *comEA*, and *comEC* genes *(Fig.1.27)*, whose gene products play essential roles in the uptake and transport of exogenous DNA. In addition, the expression of a gene encoding a homolog of DprA, which plays a crucial role in the integration of exogenous DNA, was reported to be elevated in response to induction of *tfoX* expression. cAMP, presumably in complex formation with CRP, is required for chitin-dependent induction of *comEA* and *pilA* in *V. cholerae* highlights that TfoX may also serve as an accessory factor. A common motif ACTCG(A/C)AA was identified in most of the 19 TfoX-induced promoter regions by means of a phylogenetic footprint analysis. At this time, whether TfoX binds DNA in complex with CRP has not yet been determined by experimental approaches.

1.34. Various toxins of V. cholerae

1.34.1. Cholera enterotoxin (CT)

Cholera toxin (choleragen) (PDB ID. 1XTC) is the sole cause of the clinical disease *(Fig.1.28)*. This substance induces the enterocytes to increase secretion of electrolytes, above all Cl^- ions, whereby passive water loss also occurs. Cholera enterotoxin produced by the adherent vibrios is secreted across the bacterial outer membrane into the extracellular environment and disrupts ion transport by intestinal epithelial cells. The subsequent loss of water and electrolytes leads to the severe diarrhea characteristic of cholera. The existence of cholera enterotoxin (CT) was first suggested by Robert Koch in 1884 and demonstrated 75 years later (S. N. De & Chatterje, 1953; Dutta et al., 1959). CT is encoded by the gene ctxAB. Many

Fig.1.28. Crystallographic structure of Cholera enterotoxin.

strains of *V. cholerae* O1 contain multiple copies of the ctx operon. The toxin belongs to the group of AB toxins. Analysis of purified toxin shows that it is consist of an A subunit and 5 smaller identical B subunits (Finkelstein & LoSpalluto, 1969). The B subunit serves to bind the toxin to the eukaryotic cell receptor, ganglioside GM1.

The A subunit possesses a specific enzymatic function and acts intracellularly, raising the cellular level of cAMP and thereby changing the net absorptive tendency of the small intestine to one of net secretion. As a result, cholera toxin stimulates hypersecretion of water and chloride ions while inhibiting the absorption of sodium ions. The patient loses massive fluid and electrolytes. The binding of CT to epithelial cells is enhanced by neuraminidase. An alternative mechanism of cholera toxin also exists which says that prostaglandin and the enteric nervous system (ENS) are involved in the response to CT. CT is a potent oral antigen by itself and with another unrelated antigen (Holmgren et al., 1993). The B subunit of CT has an adjuvant-like effect probably due to the binding of this subunit with G_{MI} ganglioside (Czerkinsky et al., 1989) *(Fig.1.29)*.
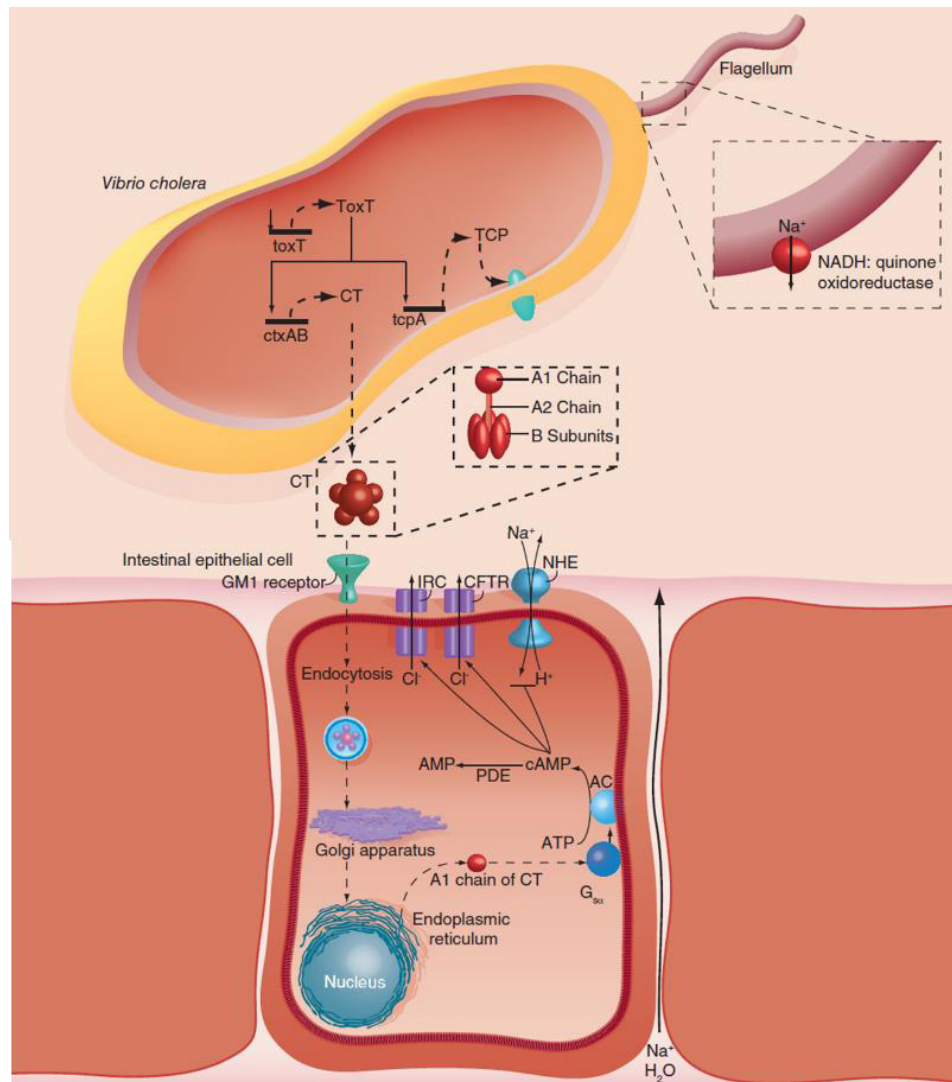
Fig.1.29. Schematic overview of mode of action of cholera enterotoxin (CT). Cholera toxin approaches target cell surface. B subunits bind to oligosaccharide of G_{M1} ganglioside (the first-ever structurally defined mammalian cell receptors). Conformational alteration of holotoxin occurs, allowing the presentation of the A subunit to cell surface. The A subunit enters the cell. The disulfide bond of the A subunit is reduced by intracellular glutathione, freeing A_1 and A_2. NAD is hydrolyzed by A_1, yielding ADP-ribose and nicotinamide. One of the G_s proteins of adenylate cyclase is ADP-ribosylated, inhibiting the action of GTPase and locking adenylate cyclase (AC) in the "on" mode (Fishman,1980) and elevation of intracellular cAMP occurs. Increased intracellular cAMP then causes stimulation of cystic fibrosis transmembrane conductance regulator and/or inwardly rectifying Cl-channel-dependent Cl- secretion and inhibition of Na+ absorption through NHE, resulting in effluxes of Na+ and water and, hence, secretory diarrhea. CFTR: Cystic fibrosis transmembrane conductance regulator; CT: Cholera toxin; IRC: Inwardly rectifying Cl- channel; NHE: Na+–H+ exchanger; TCP: Toxin-coregulated pilus.

1.34.2. Zonula occludens toxin (Zot)

Another toxin of *V. cholerae* is Zot, which was first described by Fasano et al in 1991 (Fasano et al., 1991). This toxin acts by increasing the permeability of small

intestinal mucosa by affecting the structure of the intracellular tight junction, or zonula occludens resulting in loosening of the junction (Baudry et al., 1991)**.** Zot causes diarrhea by leakage of water and electrolytes into the lumen under the force of hydrostatic pressure. The *zot* gene was found to be located immediately of the *ctx* locus (Baudry et al., 1991)**.** The zot genes are present in both *V. cholerae* O1 and non-O1 strains (Faruque et al., 1994)**.** The zot gene is comprised of a 1.3 kb open reading frame that encodes a protein product of 44.8 kDa molecular weight. The amino acid sequence of Zot protein does not show homology to any other bacterial toxin.

1.34.3. Accessory cholera toxin (Ace)

Ace protein of *V. cholerae* was first reported by Trucksis et al, 1993. The open reading frame of Ace is positioned exactly upstream of the Zot. Like CT and in contrast to Zot this new toxin increases potential difference rather than tissue conductivity. The ace gene encodes a 96-residue peptide with a predicted molecular weight of 11.3kDa (Trucksis et al., 1998). The amino acid sequence of Ace shares sequence similarity with a family of eukaryotic ion transporting ATPases such as human plasma membrane calcium pump, calcium transporting ATPase from rat brain, and the Cystic Fibrosis Transmembrane Regulator (CFTR) (Bear et al., 1992).

1.34.4. Hemolysin/ *Vibrio cholerae* cytolysin (VCC)

The hemolytic activity of strains of the El Tor biotype of *V. cholerae* toward sheep erythrocytes was known in the early 1960s and was used as a phenotypic marker to distinguish them from strains of the classical biotype (Kaper et al., 1995). The toxin is absent in classical strains of *V. cholerae* due to an 11bp deletion in the structural gene for the toxin. The toxin was purified from the culture of *V. cholerae* grown in brain heart infusion broth (BHI) and partially characterized (Honda & Finkelstein, 1979). The structural gene consists of a 2,223 nucleotide long open reading frame which codes for a 741 amino acid long protein, pre-prohemolysin, of molecular weight 81,961 (K. Yamamoto et al., 1990). The pore-forming toxin hemolysin was first purified by Honda and Finkelstein. It has a cytolytic activity for a variety of erythrocytes and mammalian cells in culture and is quite lethal for mice. The pre-mature protein is an 82kDa protein and it is processed in two steps to a mature 65 kDa active cytolysin (Shigeo Yamamoto et al., 1993). The gene *hlyA* codes for the hemolysin is present in classical, El Tor, and non-O1 strains of *V. cholerae*. VCC is capable of causing fluid accumulation in ligated

rabbit ileal loops (Ichinose et al., 1987). Unlike the watery fluid produced in response to CT, the accumulated fluid produced in response to hemolysin was found bloody with mucous (Ichinose et al., 1987).

1.34.5. Miscellaneous toxins

In addition to CT, Zot, Ace, and hemolysin which are widely distributed in *V. cholerae*, several other toxins have been reported for this pathogen such as Shiga-like toxin (ST), Cholix toxin, new cholera toxin sodium channel inhibitor, and thermo-stable direct hemolysin.

1.35. Prevention and control of V. cholerae

A multifaceted approach is a key to preventing and controlling cholera and reducing deaths. A combination of surveillance, water, sanitation and hygiene, social mobilization, treatment, and oral cholera vaccines are used.

1.35.1. Surveillance

Cholera cases are identified clinically in patients who present with severe acute watery diarrhoea. *V. cholerae* is then identified in stool samples from infected patients, confirming the suspicion. Local capacity to detect (diagnose) and monitor cholera occurrence (collect, assemble, and analyze data) is critical for an effective surveillance system and the planning of control actions.

1.35.2. Water and Sanitation interventions

Economic development and universal access to safe drinking water and proper sanitation are the long-term solutions for cholera control (which benefits all diseases spread by the fecal-oral pathway). The following precautions are taken to prevent both epidemic and endemic cholera. Development of piped water systems with water treatment facilities (chlorination), interventions at the household level (water filtration, chemical or solar water disinfection, safe water storage), and installation of safe sewage disposal systems, including latrines.

1.35.3. Treatment

Cholera is an easily treatable disease. The majority of patients can be successfully treated if oral rehydration solution is administered promptly (ORS). In

1 litre (L) of clean water, WHO/UNICEF ORS standard sachet is dissolved and adult patients with mild dehydration may require up to 6 L of ORS *(Table 1.3)*.

Table 1.3. Composition of the new ORS formulation

New ORS	Grams/litre	%	New ORS	Mmol/litre
Sodium chloride	2.6	12.683	Sodium	75
Glucose, anhydrous	13.5	65.854	Chloride	65
Potassium chloride	1.5	7.317	Glucose, anhydrous	75
Trisodium citrate, dihydrate	2.9	14.146	Potassium	20
			Citrate	10
Total	20.5	100.00	Total Osmolarity	245

1.36. Vaccines – present and future

Oral Cholera Vaccines (OCVs) are now a cornerstone of the action plan "Ending Cholera: A Global Roadmap to 2030," launched in 2017 by WHO's Global Task Force on Cholera Control (GTFCC) and 50 other organizations. By 2030, the goal is to reduce cholera deaths by at least 90% and abolish cholera transmission in the majority of currently affected nations. There are currently three WHO-approved oral cholera vaccines: Dukoral®, Shanchol™, and Euvichol® (Holmgren J., 2021).

Dukoral™ (Valneva, Sweden): The first effective OCV that was developed was the inactivated whole-cell/ cholera toxin B subunit vaccine Dukoral™. It contains a mixture of formalin- and heat-killed *V. cholerae* O1 bacteria, representing both the Ogawa and Inaba serotypes and the classical and El Tor biotypes, and a recombinantly produced cholera toxin B subunit. Dukoral is widely used as a travelers' vaccine for both cholera and ETEC diarrhea. Dukoral® provides approximately 65% protection against cholera for 2 years.

Shanchol™ (Sanofi-Shantha Biotechnics, India): In the late 1980s, Sweden supplied OCV manufacturing technology to Vietnam for the local production of an orally killed whole-cell OCV. This vaccine comprised the same *V. cholerae* O1 components as Dukoral but excluded the cholera toxin B subunit to

reduce production costs and complexity. A two-dose immunization against cholera was found to provide 66 percent protection in adults and children as young as one year old. Following the development of O139 in India and Bangladesh in 1992, the vaccine was modified to include killed *V. cholerae* O139 cells and was approved nationally, first as OrcVax™ and later as mOrcvax™. In endemic locations, individuals vaccinated with Shanchol™ or Euvichol® have around 65 percent protection against cholera for up to 5 years after immunization.

Euvichol™/Euvichol-Plus™ (Eubiologics, S. Korea): To address the increasing demand for OCVs, IVI also transferred the reformulated OCV technology to Eubiologics, Seoul, Republic of Korea. This has led to the successful production of Euvichol™ OCVs, which has an identical composition as Shanchol™

Other nationally licensed OCVs

The Vietnamese mOraVax™; Bangladeshi Cholvax™ (produced by Incepta); Chinese OraVacs™ (produced by Shanghai United cell Biotechnology) and United Sates' Vaxchora™ (produced by PaxVax), consists of lyophilized *V. cholerae* "CVD 103-HgR" O1 bacteria that are derived from a classical Inaba strain (569B).

1.37. The emergence of drug resistance in V. cholerae

In the last few decades, *V. cholerae* that causes acute watery diarrhoeal disease cholera has emerged as a notorious multidrug-resistant (MDR) enteric pathogen (Kitaoka et al., 2011). Although chromosomal mutations can play a role in antimicrobial resistance (AMR), the frequent acquisition of extrachromosomal mobile genetic elements (MGEs) from closely/distantly related bacterial species is a significant aspect in *V. cholerae* drug resistance. Antimicrobial resistance genes found in *V. cholerae* can contribute to antibiotic resistance through one of three mechanisms: (i) reduced permeability or active efflux of the antibiotics, (ii) alteration of the antibiotic targets by introducing post-transcriptional/translational modifications, and (iii) hydrolysis or chemical modification of antibiotics.

Antibiotic treatment is suggested in cholera patients after the restoration of the initial fluid loss and prevention of vomiting. The emergence of MDR (Multi-drug resistance) and XDR (Extremely-drug resistance) *V. cholerae* is excellent evidence of recent bacterial evolution. Recent research indicates that horizontal gene transfer (HGT) via self-transmissible, autonomously replicating plasmids or integrative IMGEs such as Integrating Conjugative Elements (ICEs), Insertion Sequences (IS), and transposable genetic elements are primarily responsible for the emergence of MDR and XDR *V. cholerae* (Verma et al., 2019).

During the 1960s, resistance to one or a few antibiotics was largely attributable to the acquisition of spontaneous mutations in the drug's target, such as DNA gyrase, topoisomerase, b-subunit of RNA polymerase (RpoB), and small subunit ribosomal protein12. MDR *V. cholerae* isolates from serogroup O1 showing resistance to tetracycline, streptomycin, and chloramphenicol were first reported in 1970. Resistance to ampicillin, nalidixic acid, chloramphenicol, and tetracycline began to rise rapidly since the early 1990s. Most clinical isolates of *V. cholerae* are now resistant to practically all commonly used antibiotics, according to a recent trend.

The emergence of MDR *V. cholerae* serogroup O139 was first reported in 1996. Resistance was found to be caused by the **SXT** element, a 100-Kb ICE (Integrating conjugative element) that carries numerous resistance genes against **S**ulfametho**x**azole, **T**rimethoprim, and Streptomycin (Das et al., 2020).

1.38. Anti-bacterial vs Anti-virulence approach

The ongoing rise of antibiotic-resistant bacterial infections has prompted the development of novel approaches to disease diagnosis and treatment. Instead of directly targeting viability or growth, anti-virulence therapies work by inhibiting in vivo essential virulence components in order to disarm the pathogen. This strategy to treating bacteria-mediated disorders may be superior to standard antibiotics since it targets pathogenesis-specific factors, potentially reducing selection for resistance and limiting collateral damage to the resident microbiota. With more annual fatalities from antibiotic-resistant diseases anticipated by 2050 than cancer, we urgently need effective solutions to address this catastrophe.

1.39. Phytochemicals, Small molecules, and other types of inhibitors

The world is currently facing an antibiotic-resistance crisis, and the discovery of alternative medicines is a critical strategy for treating drug-resistant bacteria (S. B. Johnson et al., 2018; Langeveld et al., 2014; Rasko & Sperandio, 2010). Anti-virulence methods offer new and novel approaches to combat infectious diseases by expanding the study of antimicrobial targets beyond those required for growth. There is growing interest in the antimicrobial capabilities of phytochemicals and Essential Oils in particular, which has encouraged us to investigate the function of phytochemicals in bacterial pathogenicity. The potential for use of small molecules, monosaccharides, and chitinase inhibitors were also studied here (Aminov, 2010; Aminzare et al., 2018; Burt, 2004).

Chapter 2

Objectives

Objectives

$\mathcal{T}$he overall goal of this thesis work is to understand the role of *V. cholerae* regulatory protein CytR in the natural environment and in the host intestine. The specific objectives are-

1. *To study the role of CytR in chitin utilization pathway in Vibrio cholerae.*

The effect of different environmental factors on CytR is unknown. Environmental factors such as temperature, pH, salinity, and different nutrient medium on the expression of CytR will be studied. How these environmental factors affect different chitin utilization pathway genes at the transcription level will be an important aspect of the study.

2. *To understand the role of CytR in pathogenesis.*

The significance of *Vibrio cholerae* in the environment and chitin utilization is well documented. Chitinases are an integral part of chitin utilization and it has been already known that chitinases are important for the survival of *V. cholerae* in the intestine. Therefore, it is important to explore whether CytR has any role inside the intestine and in pathogenesis. In addition, we investigated the role of several bioactive compounds that may be capable of inhibiting disease pathogenesis.

3. *To study the effect of host intestine on CytR during pathogenesis.*

Apart from the natural environment, CytR might also be affected by host factors like mucin, crude bile, and bile salts. This study will help us to understand its relation with host factors and characterize CytR further.

Chapter 3

Material & Methods

Materials and Methods

3.1. Bacterial strains, their maintenance and culture conditions

The streptomycin-resistant *V. Cholerae* O1 El Tor Inaba strain N16961 was used in this study (Heidelberg et al., 2000). The suicide vector pCVD442 (please see appendix) was maintained in *E. coli* strain DH5αλpir (Philippe et al., 2004). For TA cloning, we have used pGEMT-Easy vector (please see appendix) (Promega, Madison, WI, USA) and maintained it in *E. coli* JM109 (Promega, Madison, WI, USA). Different *Escherichia coli* strains such as Sm10λpir, MG1655, Top10, BL21-DE3 (Clontech, CA, USA) were used in cloning, expression, and mutation studies. All strains were maintained at -80°C in Luria broth (LB) (please see appendix) containing 15% glycerol in a total volume of 2 ml. The *V. cholerae* strains were streaked from the -80°C stock and incubated overnight at 37ºC on TCBS agar plates. The characteristic large, yellow, single colonies were taken for further work. Strains were grown in LB medium (BD, Difco, Franklin Lake, NJ) at 37°C with appropriate antibiotics [streptomycin (100 μg/ml) or ampicillin (100 μg/ml) whenever necessary] under constant shaking at 180 rpm, or in M9 minimal–lactate media (please see appendix) with or without mucin (Sigma, St. Louis, MO, USA) as a sole source of carbon. To study the expression of virulence genes, bacteria were also cultured in AKI media (please see appendix) at 37°C under static conditions. For studies related to different environmental factors, *V. cholerae* strains were also grown in DASW-defined artificial sea-water media (please see appendix) supplemented with chitin. Sodium lactate was added to support equal growth of wild-type and mutant strains.

3.2. Primer design for PCR

All the primers used in this study were designed based on the sequences of *V. cholerae* El Tor strain N16961 (NCBI Reference sequence: NC_002505.1 for Chromosome 1 and NC_002506.1 for Chromosome 2) available in the GenBank *(https://www.ncbi.nlm.nih.gov/)*. The primers and the sequences were tested for primer dimer formation, degeneracy, and cross-reactivity with any other genes present in *V. cholerae* using the BLAST programme *(https://blast.ncbi.nlm.nih.gov/Blast.cgi)*. For Real-Time PCR the primers were designed using IDT software

(PrimerQuest™ Tool). All the primers used in this study are listed in the appendix section.

3.3. Growth conditions used for expression studies of cytR, chitinases, and chiS

To study the impact of the environment on CytR, chitinases (ChiA1, ChiA2, VC_1073, VC_0769) and ChiS, *V. cholerae* was grown overnight in defined artificial seawater media known as DASW (please see appendix) and any one of the 4 environmental parameters such as temperature, pH, salinity and the amount of chitin was varied while keeping the others fixed. The temperature was varied at a range of 16ºC to 42ºC and pH was varied at a range of 6.5 to 9.0. In the case of salinity varying concentrations of NaCl were used at a range of 100 mM to 600 mM. The amount of chitin was varied from 0.2% to 2.5%. For studying the effect of host factors, *V. cholerae* was also grown in minimal media supplemented with varying concentrations of mucin (0.2% to 2.5%) and different bile components like Cholate, Deoxycholate, Chenodeoxycholate, Taurocholate hydrate, Glycocholic acid hydrate (at 0.5mM and 5mM concentration) and crude bile.

3.4. Total RNA isolation for expressional studies

Bacteria were harvested from log-phase cultures and centrifuged at $8000 \times g$ at 4 ºC for 10 min. Bacterial pellets were washed thrice in PBS and then used for RNA isolation. Total RNA was isolated using TRIzol (Invitrogen, Carlsbad, CA) following the manufacturer's protocol. Briefly, TRIzol (Invitrogen, Carlsbad, CA) (monophasic solution of phenol and guanidine isothiocyanate) was added to the cell pellet (at the rate of 0.5 ml/ 5 ml culture of OD 1 at 600 nm) and cells were resuspended by slow pipetting. Samples were incubated for 20 min at room temperature to allow for complete dissociation of nucleoprotein complexes. Chloroform (0.2 ml/ ml of TRIzol) was added to the mixture, shaken vigorously for 15 s, and was incubated for 2-3 min at room temperature. The mixture was then centrifuged at $12,000 \times g$ for 20 min at 4ºC and the aqueous phase was transferred to a DNase, RNase-free microcentrifuge tube (Axygen, Union City, CA). Isopropanol was added (at the rate of 0.5 ml/ ml of TRIzol) and the mixture was incubated at room temperature for 10 min. RNA was precipitated by centrifugation at $12,000 \times g$ for 10 min at 4 ºC. The pellet was washed with 0.5 ml (1 ml/ ml of TRIzol) of 75% (v/v) ethanol, air-dried, and dissolved in

nuclease-free water. RNA thus isolated was treated with DNase of Ambion® DNA-*free*™ kit (Ambion, Texas, USA) for the elimination of contaminating genomic DNA following the supplier's protocol. Isolated total RNA was stored at -80ºC till use. The purity of RNA was checked by spectrophotometrically at 260 nm.

3.5. Measurement of the RNA concentration and purity

The concentration of RNA was quantified by measuring the absorbance at 260 nm and using the following formula: $(A_{260} \times DF \times 40)/ 1000$ µg/µl, where A_{260} is the absorbance of the diluted RNA at 260 nm and DF is the dilution factor of RNA in nuclease-free water. For RNA, A_{260} of 1.0 corresponds to 40 µg/ml concentration. The purity of RNA was determined from the ratio of absorbance at both 260 and 280 nm. Ideally, the purest form of RNA has an A_{260}/A_{280} ratio of 2.

3.6. Reverse transcription reaction

First-strand cDNA, reverse transcription (RT) was prepared by using a Verso cDNA synthesis (Thermo) kit. Briefly, 1µg of total RNA was heated at 70ºC for 10 min to denature the secondary structures and chilled immediately at the ice. 1µg RNA was mixed with the reaction components in a 0.2 ml PCR tube as described in *Table 3.1.* The components were assembled gently and spun briefly. The mixture was incubated at first at room temperature for 10 minutes then at 42ºC for 15 min. Enzymes were heat-inactivated by incubating at 95ºC for 5 min and kept at 4ºC for at least 5 min. the RT products were stored at -20ºC till further use.

Table 3.1. Composition of the reaction mixture for reverse transcriptase PCR

Components	Volume added
5X cDNA synthesis buffer*	4 µl
dNTP Mix	1 µl
RNA primer (Random Hexamer)	1 µl
RT Enhancer	1 µl
Verso Enzyme Mix	1 µl
Template (RNA)	1-5 µl
Nuclease Free Water	To make up the volume of 20 µl
Final volume	20 µl

*The reverse transcriptase buffer contains 100 mM tris-HCL (pH 9.0 at 25ºC), 500 mM KCL and 1% Triton X-100.

3.7. Quantitative Real-Time PCR

V. cholerae was grown up to log phase with varying environmental conditions. The total RNA isolated from *V. cholerae* was converted to cDNA using Reverse Transcription System (Promega, Madison, WI, USA) and was used as a template. The mRNA transcript levels were quantified by quantitative PCR (qPCR) using $2\times$SYBR green PCR master mix (Applied Biosystems, Foster City, California) and 0.2 µM of specific forward and reverse primers designed using PrimerQuest from Integrated DNA Technologies (IDT) for each transcript (Please see Appendix). The composition of the real-time PCR reaction mixture is depicted in *Table 3.2* and Real-time PCR cycling conditions in *Fig.3.1.* Data analysis was done using a 7500 Real-Time PCR detection system (Applied Biosystems, Foster City, California) with 40 cycles of a two-step cycle followed by a melting curve. The relative expression of the target transcripts was calculated according to Livak's $2^{-\Delta\Delta C_T}$ method (Livak & Schmittgen, 2001) using *recA* (VC_0543) as an internal control.

Table 3.2. Composition of the Real-Time PCR reaction mixture

Components	Volume added
SYBR® Green Master Mix	10 µl
Real-Time Forward Primer, 10µM	1 µl
Real-Time Reverse Primer, 10µM	1 µl
Template (cDNA)	1-5 µl
Nuclease Free Water	To make up the volume of 20 µl
Final volume	**20 µl**
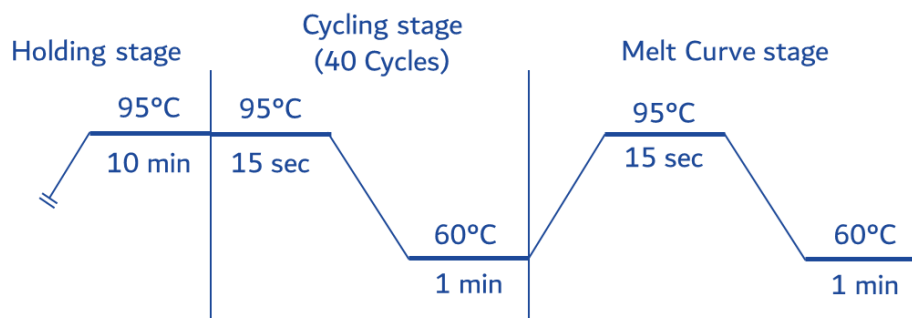
Fig.3.1. Schematic diagram of real-time PCR conditions for all transcripts.

3.8. Polymerase Chain Reaction (PCR)

Polymerase chain reaction throughout the study wherever required was done in 0.2 ml PCR tubes with the following reaction mixture as described below *(Table 3.3).*

Table 3.3. Composition of the Real-Time PCR reaction mixture (For each reaction)

Components	Volume added
MgCl$_2$, 25 mM	2 µl
5X Reaction buffer	4 µl
Forward primer, 10µM	0.4 µl
Reverse primer, 10µM	0.4 µl
dNTP mix, 10mM	0.8 µl
Taq DNA polymerase, 5U/µl	0.2 µl
Template (DNA)	2 µl
Nuclease Free Water	To make up the volume up to 20 µl
Final Volume	**20µl**

The components were mixed gently and spun briefly and PCR was done by using a thermal cycler (Bio-Rad). The annealing temperature for each set of forward and reverse primers were set 2ºC below the T$_m$ (melting temperature) of each primer and the period of extension for the Taq DNA polymerase was calculated according to 1000bp per minute synthesis rate. PCR conditions for *CytR* demonstrated schematically in *Fig.3.2.*

Amplification of CytR with Internal Primers

Cycle 1		Cycle 2 (x 30)			Cycle 3
95 ℃	95 ℃		72 ℃	72 ℃	
5 mins	1 mins	54 ℃	40 sec	4 mins	
		30 sec			4 ℃
					Hold
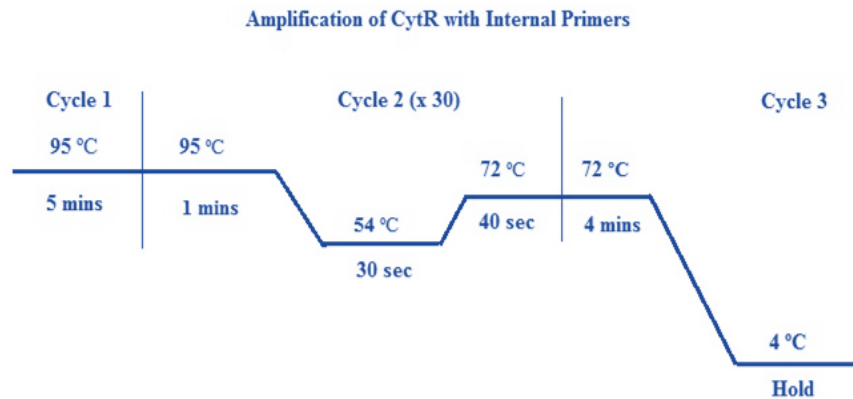
Fig.3.2. Schematic diagram of PCR conditions used to amplify CytR.

3.9. Agarose gel electrophoresis

The amplified DNA fragments were resolved in 1.2% agarose gel electrophoresis. Briefly, agarose was mixed with 1X TAE buffer (Please see Appendix) and heated to dissolve the agarose. The dissolved agarose was poured into the gel caster. Run was performed and the PCR products are stained either using Ethidium Bromide (EtBr) or SYBR Safe DNA gel stain (Invitrogen) and finally visualized under UV transilluminator. The images were captured using a gel documentation system (Bio-Rad). Densitometric analysis from agarose gel was done from the band intensities of amplified test samples using Bio-Rad QUANTITY 1 software.

3.10. Generation of the isogenic ΔCytR mutant strain and its complement

3.10.1. Sequence of CytR gene

The CytR gene (VC 2677) was searched out from the NCBI GenBank genome sequence of *Vibrio cholerae* O1 Biovar El Tor strain N16961 of chromosome 1 (NCBI Reference Sequence: NC_002505.1)

3.10.2. Primer design

The isogenic *ΔCytR* mutant was constructed as previously described method (Philippe et al., 2004). In brief, 500-bp fragment upstream and downstream of *CytR* was PCR-amplified using the primer pairs CytR FP *XbaI* (A) and CytR RP Fusion (B); CytR FP Fusion (C), and CytR RP *SacI* (D) (Please see Appendix). The primers were designed to delete the 876 bp region from the middle of the CytR gene sequence. A fusion tag "CCCATCCACTATAAACTAACA" was added to the 5' ends of the fusion primers (primer B & C).

3.10.3. Construction of the deleted gene (CytR) construct: by Fusion PCR

Amplified fragment AB (PCR amplified with primer A and B) contains a 3' Fusion tag overhang and fragment CD (PCR amplified with primer C and D) contains a 5' Fusion tag overhang, the sequence of which is complementary to each other. Both the PCR amplified PCR fragment AB and CD were mixed in a 1:1 molar ratio and used for making fusion construct *(Fig.3.3)*. The fusion construct is 954 bps long *(Fig.3.4. A)*.

The fused gene was then amplified by PCR again and the amplified product was ligated to a pGEMT-Easy cloning vector. The ligated construct was transformed into *E. coli* JM109, competent host cells. The positively cloned cells were selected by using ampicillin as a selective marker. The selected cells were confirmed further by colony PCR by using the external forward (A) and reverse primers (B).
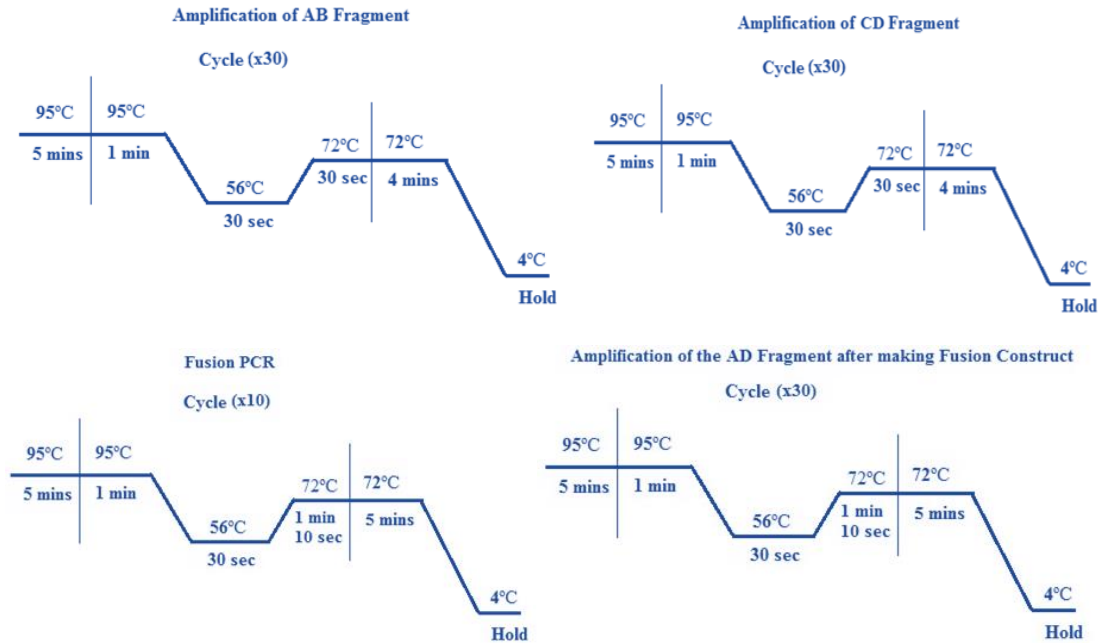
Fig.3.3. Schematic diagram of the PCR conditions used to construct the deleted CytR region.

A   B
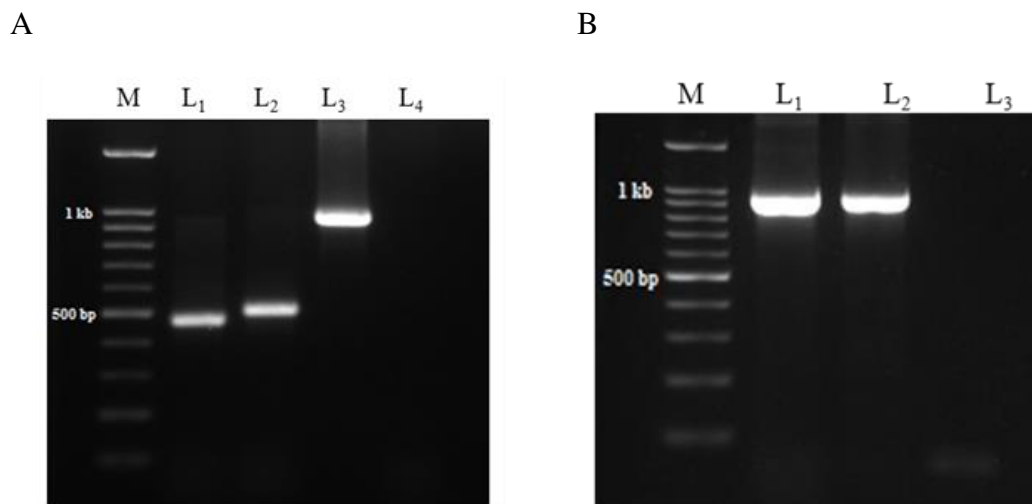
Fig.3.4. (A) 1.2% Agarose gel of the amplified gene product (M, 100bp molecular marker; L_1, fragment AB, 450 bp; L_2, fragment CD, 483 bp; L_3, fusion PCR construct AD, 954 bp; L_4, negative control), **(B) 1.2% Agarose gel of the transformed *E. coli* JM109 colony with CytR deleted construct in pGEMT-Easy vector** (M, 100bp molecular marker; L_1, CytR deleted construct in pGEMT-Easy in *E. coli* JM109, 954 bp; L_2, fusion PCR construct AD, 954 bp; L_3, negative control)

3.10.4. Cloning of the fusion construction in the Suicidal vector pCVD442

On confirmation of the presence of the fusion construct in the ligated pGEMT-Easy vector that was cloned into *E. coli* JM109, plasmid isolation was done by the Vacuum manifold method (Promega, Madison, Wisconsin, US). The fusion construct (amplicon) and the pCVD442 suicide vector were digested with *Sac1* and *Xba1* (New England Biolabs, Massachusetts, US), to produce complementary staggered ends in the amplicon and the vector. For the restriction digestion, 10 µg of the sample (both the pCVD442 and CytR deleted construct in pGEMT-Easy vector, in separate reaction setup) was incubated with 1U enzyme at 37ºC for 3 hr. After digestion, the products were run in 1% agarose gel, desired cut bands were gel purified by the Promega SV gel clean-up system. Vector plasmid pCVD442 and pGEMT containing the CytR deleted construct (insert) were then ligated overnight. The ligated vector was then transformed into *E. coli* DH5αλpir competent host cell. The positively cloned cells were selected by using ampicillin as a selective marker. The selected cells were confirmed further by colony PCR using the external primers A and D *(Fig.3.4. B)*.

3.10.5. Preparation of competent *E. coli* SM10λpir

10 ml of fresh LB was inoculated with 100µl of the overnight culture of SM10λpir and grown-up to OD_{600} = 0.5 at 37ºC with shaking. The cells were then harvested by centrifugation at 4000 rpm for 15 min at 4ºC. The harvested cells were thoroughly suspended in equal volume (initial culture) of ice-cold 100mM Calcium Chloride. The cell suspension was kept on ice for 45 mins and then centrifuged at 4000 rpm for 15 min at 4ºC. Then the pellet was suspended in 1ml ice cold Calcium Chloride – Glycerol (85% 100mM $CaCl_2$ +15% glycerol) with cold micro tips and aliquot with 50 µl each in a microcentrifuge tube and stored till use at -80ºC.

3.10.6. Transformation of the deleted CytR construct into SM10λpir by electroporation

The cloned plasmid was isolated from the same transformed *E. coli* DH5αλpir cells and the resultant chimeric plasmid was transformed and maintained in *E. coli* SM10λ*pir* (Skorupski & Taylor, 1996) *(Fig.3.5)*. The competent SM10λpir was used for transformation. ~1µg of the purified deleted construct was mixed with the competent SM10λpir while keeping in ice and kept for 30 min without any

disturbance. After that, the cell and plasmid mixture was transferred in a 2 mm gap electroporation cuvette (BTX electroporation cuvettes plus; part no. 45-0125; model no. 620) and the deletion construct was transformed by electroporation. The electroporation conditions used here were; Voltage: 1.8 kV, resistance: 200-ohm, pulse: 3, capacitance: 25 μF with a time constant of 3-3.5ms. Following electroporation, the cells were immediately placed on ice for 1-2 min and 500 μl of SOC medium (Invitrogen, Carlsbad, CA) was added to the electroporated mixture. Next, the cells were incubated at 37 ℃ for 1 h with shaking at 200 rpm, and the cells were plated on LB plates. The positively cloned cells were selected by using ampicillin as a selective marker and further confirmed by colony PCR *(Fig.3.6)*.
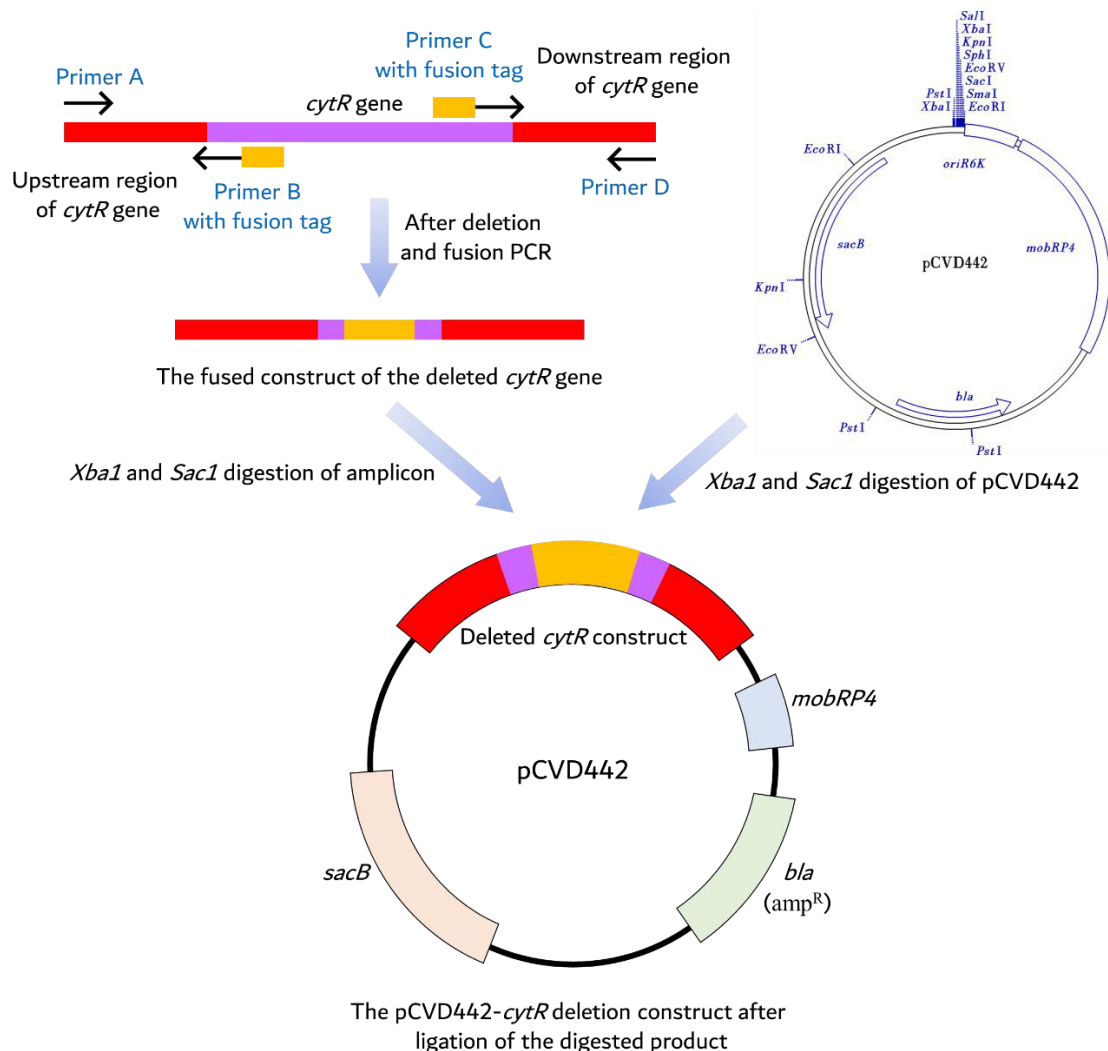
Fig.3.5. Schematic diagram of generation of the cytR-pCVD442 construct

3.10.7. Conjugation of transformed SM10λpir cells with *V. cholerae* (first recombination)

Finally, the deletion construct in pCVD442 was mobilized conjugally from *E. coli* SM10λ*pir* to *V. cholerae* N16961. The conjugation was done in LA plates by streaking the donor (SM10λpir) and the recipient (*V. cholerae* N16961) strains with an angle of 90º to each other. After 6 hr incubation the transconjugants were selected in ampicillin (100μg/ml) and Streptomycin (100μg/ml) double antibiotic Luria Bertani (LB) agar plates. Here, Streptomycin is used to eliminate the donor strain SM10λpir. After overnight incubation at 37°C, one colony was picked and streaked onto double antibiotic (streptomycin and ampicillin) LB agar plates the positive clones were confirmed further by colony PCR.
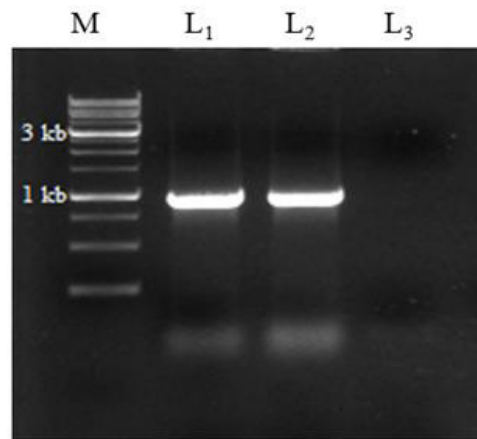
Fig.3.6. 1.2% Agarose gel of colony PCR product to confirm insertion of pCVD442 containing CytR deleted construct in *E. coli* SM10λpir (M, 1Kb molecular marker; L_1, transformed SM10λpir colony with construct size 954 bp; L_2, Positive colony of pCVD442 CytR deleted construct inserted DH5αλpir colony with construct size 954 bp; L_3, negative control.

3.10.8. Second recombination of the transconjugants in sucrose media and confirmation of the deletion mutant

Finally, the transconjugants from the ampicillin and streptomycin double antibiotic plates were grown in sucrose selection media (1% tryptone, 0.5% yeast extract, 10% sucrose, and 1.5% agar) (Philippe et al., 2004) to identify the clones where pCVD442 plasmid loss has occurred *(Fig.3.7)*. This step allowed the selection of plasmid excision from the chromosome by a second crossover (Reyrat et al., 1998). After overnight incubation at 30°C, colonies were picked from the Sucrose plates and

streaked on both ampicillin-containing LA plates and Streptomycin-containing LA plates.
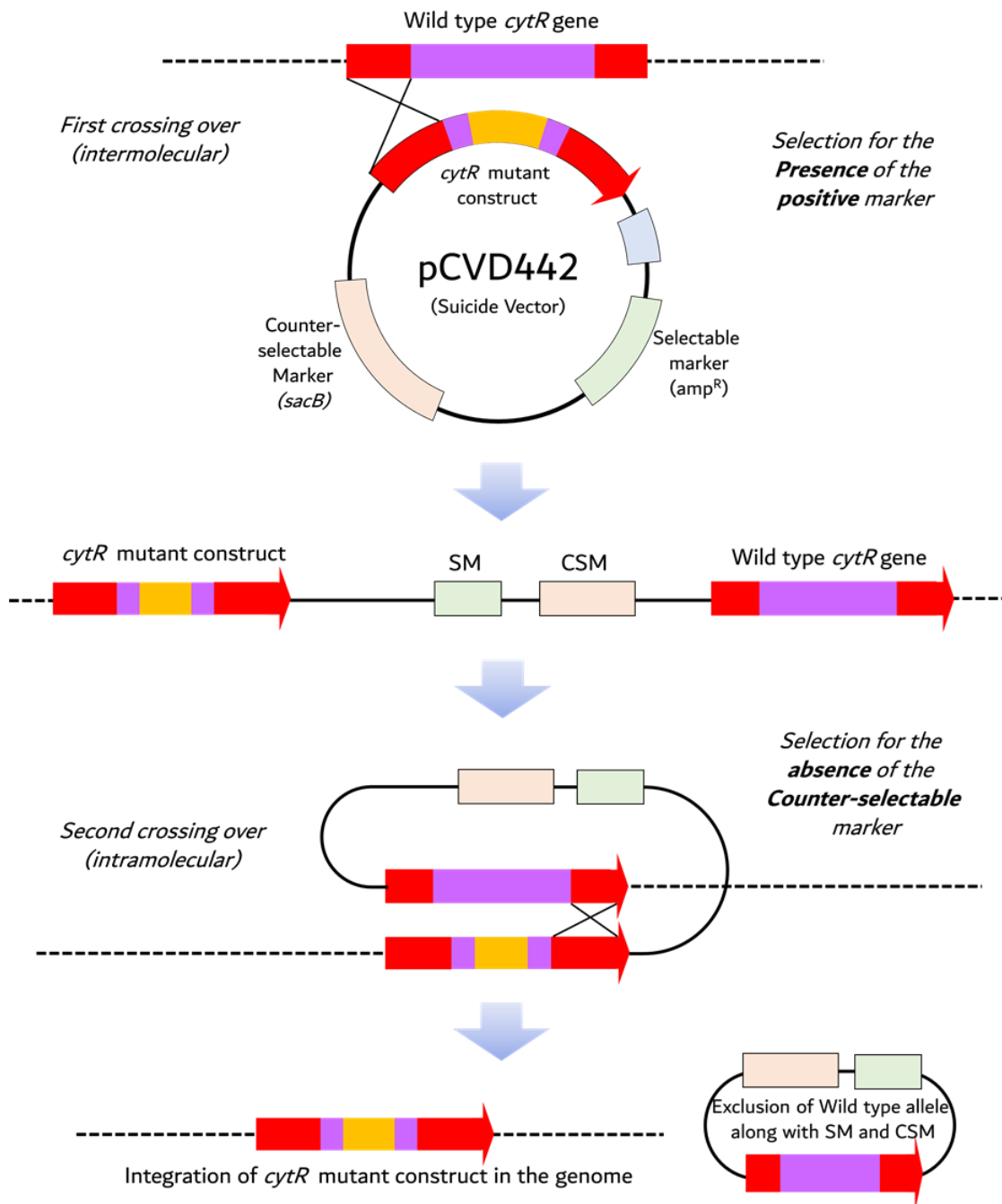
Fig.3.7. Double-selection strategy. Positive selection of allelic exchange mutants in a two-step selection strategy, using a counter-selectable marker. First, the entire plasmid is integrated into the chromosome by a single crossover between the homologous genes, producing a chromosomal duplication. Second, the chromosomal duplication is segregated by homologous recombination between the flanking direct repeats, ultimately leaving one copy of the gene on the chromosome - either the wild-type copy or the mutant copy. Expression of the *sacB* gene is toxic for gram-negative bacteria when grown in the presence of 5% sucrose, providing a direct selection for loss of the

plasmid. If one of the two copies of the duplicated region has a mutation, a certain percentage of segregants will have lost the wild-type sequence and left the mutation in the chromosome (modified from Reyrat et al. 1998). CSM, Counter Selectable-Marker; SM, Selectable Marker.

The $Str^{S}Amp^{R}$ colonies were then selected and in-frame deletion of *CytR* was confirmed by PCR using *CytR* external primers (Primers A &D) and Internal primers. PCR confirmation using external primers showed only 954 bps amplicon for *CytR* isogenic mutant instead of 1809 bp amplicon (wild type N16961). Since allelic exchange depends on the second crossover event, many clones were screened by colony PCR with external and internal primers. Clones that gave positive results *(Fig.3.8)* with external primers and negative results with internal primers were finally selected to be ΔCytR mutants of N16961 strain and stored in glycerol suspension in -80°C.
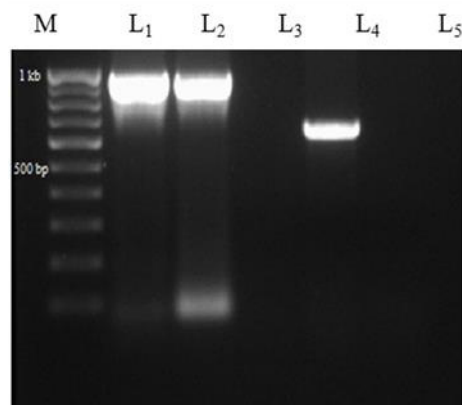
Fig.3.8. 1.2% Agarose gel of colony PCR product to confirm in-frame deletion of CytR gene in *V. cholerae* El Tor strain N16961. (M, 100 bp molecular marker; L_1, colony PCR product of CytR deleted construct in SM10λpir, 954 bp; L_2, colony PCR product of ΔCytR N16961 colony with primer pair A and D, 954 bp; L_3, ΔCytR colony PCR with CytR internal primer pair; L_4, WT N16961 colony PCR with CytR internal primer pair as a positive control, 653bp; L_5, negative control.

3.10.9. Complementation of *cytR* mutant

For complementation of *cytR* mutant, the open reading frame of *cytR* was PCR amplified by using Taq polymerase and Pfu polymerase (Promega, Madison, WI, USA) at a ratio of 2:1 and primers mentioned in (Please see appendix) and cloned into pBAD-TOPO TA (For map see appendix) (Invitrogen, Carlsbad, CA) expression vector along with its signal sequence using the primers mentioned in Table (Please

see appendix). The cloned vector was transformed into *cytR* mutant strain (CytR⁻) of N16961 and the complemented strain was denoted as CytRᶜ.

3.11. Expression and purification of Recombinant protein rCytR

For making recombinant Protein of CytR, pET151 expression vector (Invitrogen, Carlsbad, CA) was used. In brief, the procedure is as follows.

3.11.1. Designing PCR primers for cloning.

The sequence of *Vibrio cholerae* O1 biovar El Tor Strain N16961 CytR gene was obtained from NCBI Database (Reference No. NC_002505.1, gene locus VC2677). To enable directional cloning 'CACC' is added to the 5' end of the Forward Primer. And to include the 6xHistidine tag at the N-terminal region of the cloning vector Reverse primer is designed excluding the gene termination codon (in this case 'TAA'). The sequence of the primers is included in the Appendix.

3.11.2. Production of Blunt end PCR products

Using the following primers, a Polymerase Chain Reaction was set up using thermostable proofreading DNA polymerase (*Pfu* DNA polymerase) and *Vibrio cholerae* Wild type N16961 DNA as a PCR template. The quality and quantity of the amplified Blunt end PCR product were checked using agarose gel electrophoresis.

3.11.3. Performing TOPO cloning reaction

The desired PCR product is now ready to be cloned directly into the pET151 TOPO vector. For optimal result 2:1 molar ratio of CytR PCR product: pET151 vector is used. For transformation of the ligated vector, a chemically competent *E. coli* Top10 cell is used. TOPO cloning reaction and the procedure are as follows *(Table.3.4)*.

Table 3.4. Composition of the Real-Time PCR reaction mixture

Reagents	For Chemically competent *E. coli*
Fresh PCR Product	0.5 – 4μl
Salt Solution	1 μl
Sterile Water	Add to a final volume of 5 μl
pET151 TOPO® Vector	1 μl
Total volume	**6 μl**

All the reagents of the reaction were mixed gently in a 0.2 ml microcentrifuge tube and incubated at room temperature (22ºC - 24ºC) for 5 minutes. After that, the reaction mixture was kept on ice.

3.11.4. Transformation of the cloned product in Chemically competent *E. coli* Top10 cell

3μl of the pET151 TOPO cloning reaction was added to 50μl chemically competent *E. coli* TOP10 and mixed gently by hand tapping. The reaction tube was incubated in ice for 20mins. And heat shock at 42ºC was given for 30 sec was given. The tubes were transferred to ice immediately and then 250μl S.O.C. medium was added. The tubes were kept at 37ºC horizontal shaker incubator for 1 hr. After the incubation, 100μl of the transformation reaction was spread on Luria-Bertani agar plate supplemented with 100μg/ml Ampicillin. Plates were kept at 37ºC incubator overnight.

3.11.5. Analyzing transformants by PCR

10 colonies were picked from the overnight grown plates. The positive clone was selected by doing colony PCR with high fidelity polymerase using the primers listed in the Appendix (pET151 d-TOPO Forward Primer and pET151 d-TOPO Reverse Primer). The positive colony was freshly streaked on a LA plate with 100μg/ml Ampicillin. A 15% glycerol stock of CytR-pET151-TOP10 cell was prepared for storing the strain at -80˚C for future use.

3.11.6. Expressing rCytR-pET151 clone

Firstly rCytR-pET151 plasmid was isolated from *E. coli* TOP10 cell by standard plasmid isolation procedure. Isolated plasmids were checked for a single band at 1008 bp region on 1.2% agarose gel. Then the quantitation was also done by spectrophotometric analysis. Then the transformation of rCytR-pET151 construct was done in *E. coli* BL21 (DE3) chemically competent cells using standard procedure. The entire transformation reaction was added to 10 ml of LB (broth) with 100μg/ml Ampicillin and grown overnight at 37ºC with shaking. Pilot expression: 500μl of the overnight culture was inoculated in 10 ml LB broth containing 100μg/ml Ampicillin. And grown for 2 hours at 37ºC with shaking until OD_{600} reaches the mid-log phase. Then the culture was split into two 20ml LB broth containing 100μg/ml Ampicillin. One flask is induced with 0.4mM or 0.8mM IPTG (Isopropyl β-D-1-

thiogalactopyranoside) and kept at 37ºC with shaking for 6 hours. And another flask is left untreated which is also grown for the same time.

3.11.7. Analyzing the induced expressed sample

500µl of the induced and uninduced culture samples were taken. samples were centrifuged and pellet dissolved in 20mM Tris-HCl (pH 7.5) buffer and boiled in a water bath for 10 min with SDS-PAGE loading dye. Then the proteins samples were separated and analyzed by 12.5% SDS Poly Acrylamide Gel Electrophoresis *(Fig.3.9. A)*. Further presence of 6xHistidine Tag was analyzed by Western Blot using Alkaline phosphatase tagged Poly-His Tag Monoclonal Primary antibody *(Fig. 3.9.B).*

A   B
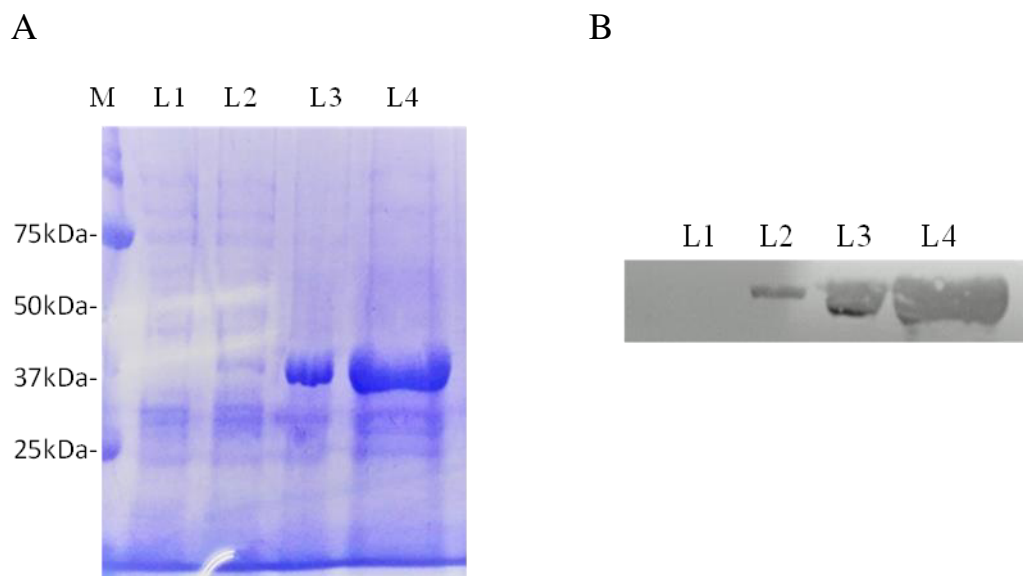
Fig.3.9. (A) 12.5% SDS-PAGE of the protein samples. (B) Western Blot of proteins on nitrocellulose membrane. (M, Protein marker; L₁, *E. coli* BL21(DE3) without transformation of cloned vector; L₂, uninduced *E. coli* BL21(DE3) with rCytR-pET151 cloned construct; L₃, 0.4mM IPTG induced *E. coli* BL21(DE3) with rCytR-pET151 cloned construct; L₄, 0.8mM IPTG induced *E. coli* BL21(DE3) with rCytR-pET151 cloned construct.

3.11.8. Expression of rCytR

This cloned recombinant CytR plasmid will be used for induced expression of the Protein on large scale. rCytR-BL21 strain having the plasmid of r*CytR*-pET151 was cultured overnight in LB. From overnight culture, the strain was again sub-cultured at a dilution of 1: 100 in LB containing ampicillin (100µg/ ml) and grown to OD 0.5 at 600 nm. At this stage, 0.4 mM IPTG was added (Calbiochem, San Diego, CA) to induce the expression of the recombinant protein. After 24 h induction at 37

ºC, cells were harvested and lysed by sonication in Tris buffer pH-8 (please see appendix). The lysed cells were centrifuged at 16000 ×g for 10 min to separate the lysate and the lysed cell pellet. The lysate and the lysed cell pellet were analyzed in SDS-PAGE to detect the presence of rCytR.

3.11.9. Preparation of inclusion bodies (IB)

For the preparation of the inclusion bodies (IB) the rCytR-BL21 cells were resuspended in resuspension buffer (please see appendix) at the rate of 10 ml/g of cell pellet. Cells were lysed by sonication. After lysis NDSB-201 was added to the lysed cells at a final concentration of 0.125 M and rotationally stirred slowly for 15 min at room temperature. Then the suspension was centrifuged at 8000 ×g for 15 min at 10 ºC. The supernatant was discarded. The IB pellet was washed in wash buffer (please see appendix) (10 ml/ g of cell pellet) and again centrifuged at 8000 ×g for 15 min. To remove the residual NDSB-201 from the IB pellet, the pellet was resuspended and washed twice in cell resuspension buffer at the rate of 10 ml/ g of pellet and centrifuged again at 8000 ×g for 15 min at 10 °C.

3.11.10. Denaturation of the inclusion bodies

The IB denaturation buffer (see appendix) was added to the IB pellet (5 ml/ 0.5 g). 50 μl of 1M TCEP / 0.5 g IB pellet was then added to the solution. The IB pellet was disrupted by brief sonication in a case where the pellet did not dissolve properly. The IB pellet was then stirred for 1h at room temperature until the solution was clear. This denatured IB pellet was next used for purification.

3.11.11. Purification of the denatured rCytR by IMAC sepharose

The high-performance Ni^{2+} charged sepharose column (GE Healthcare) was used for purification of the denatured rCytR using the principle of affinity chromatography. First, the column was equilibrated with 2-5 column volume (CV) of binding buffer (see appendix for composition) at a linear flow rate of 150 cm/ h. After that, the currently prepared denatured IB sample was passed through the equilibrated column. The column was washed with at least 15 CV of the binding buffer until the absorbance becomes a near baseline. The washing was done to remove the unbound material. After washing, the bound rCytR was eluted by using 5 CV of elution buffer (Please see appendix).

3.11.12. Re-folding of the purified denatured rCytR

The re-folding of the purified denatured rCytR was done by repeated slow dialysis of the denatured protein in refolding buffer (please see appendix) at 4°C with a gradual decrease of the guanidine hydrochloride concentration.

3.11.13. Antibody generation

To raise an antibody against the rCytR the purified individual protein bands were sliced from the 10% SDS-PAGE, crushed in phosphate buffer saline (pH 7.4) and approximately 5µg of protein was injected into the peritoneal cavity of each 6-week-old female BALB/C mice. After four subsequent booster doses, the blood was collected and the serum was prepared.

3.12. ELISA

The CytR protein levels were measured quantitatively by indirect ELISA. 96-well flat-bottom ELISA plates (Maxisorp® Nunc, Roskilde, Denmark) were coated overnight with 100µl of the total bacterial lysates. The next day, the wells were washed with 4X PBS-T (0.1% Tween-20 in PBS) and blocked using 5% non-fat dry milk was added at a dilution of 1:500 and incubated for 2 h. The plates were washed with 4X PBS-T. HRP conjugated anti-mouse secondary antibody (Sigma, St. Louis, MO, USA) was added at a dilution of 1: 2000 and incubated for 30 min. The plates were further washed with 4X PBS-T. 3, 3′, 5, 5′ - Tetramethyl benzidine (TMB) (BD, Difco, Franklin Lake, NJ) was added, and after the reaction mixture turned blue, the reaction was stopped by adding 1 M H_2SO_4. Absorbance at 450 nm was recorded by an ELISA reader (Biorad, USA).

Estimation of the human interleukin-8 (IL-8) and TNF (Tumor Necrosis Factor) secreted from the Caco2 cell line after treatment with wild type *V. cholerae, ΔcytR* mutant was also done by ELISA. The ELISA was carried out using a Human IL-8 and TNF ELISA Kit II (BD, OptEIA, BD, Biosciences, San Jose, CA) following the manufacturer's protocol. Briefly, 50 µl of ELISA diluent (12 ml of buffered protein base with 0.09% sodium-azide as preservative) was added to each well. After that, 100 µl of the sample was added to the wells. The mixture was incubated for 2 h at room temperature and after incubation washed 5 times. After the wash, 100 µl of the working detector (enzyme concentrate + detection antibody) was added to each well and incubated for 1 h at room temperature. After incubation, the wells were

washed 5 times. 100 µl of TMB was added to each well and again incubated up to 30 min at room temperature. After incubation 50 µl of the stop solution was added to each well and the OD was measured at 450 nm using a microplate reader, 550 (BioRad, Hercules, CA). A standard curve was generated using 2 fold serial dilution of purified IL-8 and TNF and this curve was used to get unknown IL-8 and TNF concentrations.

GM1 ganglioside – Cholera toxin (CT) ELISA: The ability to secrete cholera toxin (CT) by *V. cholerae* strains was assayed by GM1 enzyme-linked immunosorbent assay (ELISA) following the previously described method (Holmgren, 1973) with minor modifications (Patra et al., 2012). CT expression was measured by cell-free culture supernatants from AKI-grown *V. cholerae* cultures harvested after 18 h of static incubation at 37°C as well as from *in vivo* rabbit ileal loop culture. Culture supernatants were added to the wells of MaxiSorp ELISA plates (Nunc) that were coated with 1.5µg/ml GM1 ganglioside in 60mM Na_2CO_3 (Sigma). After incubation of 2 h at room temperature, wells were washed five times with PBS followed by the addition of 100µl of polyclonal α-CT antibody (Sigma) diluted in Solution 1 [1X PBS, 2% BSA, 0.05% TWEEN-20] in a 1:1000 ratio. Again after 1 h incubation at room temperature, each well is washed with PBS five times. Next, 100µl of HRP-conjugated anti-rabbit secondary antibody was added to each well making a dilution of the secondary antibody in PBS in a 1:2000 ratio. After 1 h of incubation at room temperature, the plate was washed with PBST (PBS + 0.05% TWEEN 20) five times. Later 100 µl of TMB substrate (BD Biosciences) was added to each well (Kit solution 1 and 2 in 1:1 ratio) and incubation for a few minutes was done to develop the color. Finally, 100 µl of 6N H_2SO_4 was added to each well to stop the reaction. In each set of assays, known amounts of purified CT were used in different concentrations to generate a standard curve. The amount of CT secreted by *V. cholerae* strains was done by extrapolating the optical density value of the samples at 450nm in the standard curve. The OD_{450} average obtained from triplicate wells of each experimental set was considered to estimate the amount of CT present and expressed as ng of CT/ml.

3.13. Genomic DNA isolation

3.13.1. Boil lysis method

Total genomic DNA was isolated by the boiled template method (Ghosal et al., 2007). In brief, overnight grown *V. cholerae* samples were pelleted down by centrifugation for 5 min at 6000 rpm, resuspended in TE buffer, boiled for 10 mins, and followed by centrifugation for 5 min at 6000 rpm. The supernatant served as a template for PCR experiments.

3.13.2. CTAB method

The CTAB (Cetyl-Trimethyl Ammonium Bromide) approach (William et al., 2004) was used to isolate genomic DNA of *V. cholerae*, which later serves as template DNA for different cloning experiments. Briefly, the late log phase or early stationary cells were pellet down at 10,000 rpm for 5 min and the supernatant was discarded. The pellet was resuspended in TE buffer. 10% SDS and Proteinase-K (10mg/ml) was added and incubated for 1-3 hours at 60°C. After the cells were lysed (as seen by cleared solution with increased viscosity) 5 M NaCl was added. CTAB (heated to 65°C) was added at 100µl /1 ml culture and incubated at 65°C for 1 hour with occasional shaking (see below for the preparation of CTAB). Chloroform: Isoamyl alcohol (24:1) at 500 µl/1 ml was added and mixed for 20 minutes on ice. Centrifuged at 16,000 ×*g* for 10 minutes at room temperature and the aqueous phase was transferred to a clean microcentrifuge tube to which phenol: chloroform: isoamyl alcohol was added at the ratio of 25: 24: 1 at 500 µl/ 1 ml and mixed well. Centrifuged at 16,000 ×*g* for 10 min at room temperature. To the aqueous phase 0.6 volume isopropanol (-20°C) was added and incubated at -20°C for 2 hours. Next, Centrifugation was done at 10000 ×*g* for 15 minutes at 4°C. The pellet was washed with cold 70% ethanol and again centrifuged at 10000 ×*g* for 5 minutes at 4°C. The supernatant was discarded and the pellet was air-dried at room temperature. Then the pellet was resuspended in DNase-free water. Then RNase I at 10U/µl was added and incubated at 37°C for 1 hour. The enzyme was heat inactivate at 70°C for 15 minutes followed by placing the tube in ice. The DNA was ethanol precipitated and finally, the DNA was eluted in TE buffer and stored at –20˚C.

CTAB/NaCl (hexade- ceyltrimethyl ammonium bromide)

4.1 g of NaCl was dissolved in 80 ml of water and slowly 10 g CTAB (Sigma) was added while heating ($\approx$65°C) and stirring. This takes more than 3 hrs to dissolve CTAB. Adjust final volume to 100 ml and sterilize by filter or autoclave.

Ethanol precipitation:

DNA and PCR products were ethanol precipitated. Briefly, the salt concentration of the DNA sample was adjusted by adding 1/10th volume of 3.2 M sodium acetate, pH 5.2, or an equal volume of 5 M ammonium acetate. Then, 2-2.5 volume 100% ice-cold ethanol was added and mixed well. The mixture was kept at -20°C for 30 min and spun down at 16,000 $\times g$ for 15 minutes at 4°C. The supernatant was carefully separated and 70% ice-cold ethanol was added and mixed by vortexing. It was again centrifuged for 10 min at 16,000 $\times g$ at 4°C. The supernatant was discarded and the precipitated DNA was air-dried. Finally, the DNA was eluted in TE buffer.

3.14. Plasmid DNA isolation

Plasmids were isolated using Wizard® plus Minipreps DNA purification system (Promega, USA). Briefly, 1-10 ml of overnight grown bacterial culture was pelleted by centrifugation at 1,400 $\times g$ for 10 min. The bacterial pellet was dissolved in 400 µl of cell resuspension solution (50 mM Tris-HCl, pH 7.5; 10 mM EDTA; 100 µg/ml RNase A). Next, 400 µl of cell lysis solution (0.2 M NaOH; 1% SDS) was added and the cell suspension became clear. After the addition of 400 µl of neutralization solution (1.32 M potassium acetate, pH 4.8) the lysate was centrifuged at 10,000 $\times g$ for 15 min. The supernatant was mixed with 1 ml of resin and a vacuum of 15 inches of Hg was applied to pull the resin/lysate completely through the Minicolumn. The resin was then thoroughly washed with wash buffer (80 mM potassium acetate; 8.3 mM Tris- HCl, pH 7.5; 40 µM EDTA; 55% ethanol). Plasmid bound to the membrane was recovered with nuclease-free water.

3.15. Purification of PCR products

The PCR or gel-cut products were purified using Wizard SV Gel and PCR clean-up system (Promega, USA). Briefly, an equal volume of membrane binding solution (4.5 M guanidine isothiocyanate; 0.5 M potassium acetate, pH 5.0) was

mixed with the PCR product. For gel-cut products, a membrane-binding solution was added at 1 µl/mg and heated at 65°C to dissolve the agarose gel. The mixture was poured into SV Minicolumn and incubated for 1 min at room temperature. The vacuum was applied (at least 15 inches of Hg) to pull the solution completely and the membrane was washed by adding 700 µl followed by 500 µl membrane wash solution (10 mM potassium acetate, pH 5.0; 80% ethanol; 16.7 µM EDTA, pH 8.0). To remove the residual amount of ethanol the Minicolumns were spun down at 16,000 $\times g$ for 5 min. The membrane was incubated at room temperature with 30 µl nuclease-free water for 1 min. The DNA was eluted by centrifugation at 16,000 $\times g$ for 1 min in a fresh tube. The absorbance was measured at 260 nm to determine the concentration of the eluted product.

3.16. Measurement of DNA concentration and purity

The concentration of RNA was quantified by measuring the absorbance at 260 nm and using the following formula: $(A_{260} \times DF \times 50)/ 1000$ µg/µl, where A_{260} is the absorbance of the diluted DNA at 260 nm and DF is the dilution factor of DNA in nuclease-free water. For dsDNA, A_{260} of 1.0 corresponds to 50µg/ml concentration. The purity of DNA was determined from the ratio of absorbance at both 260 and 280 nm. Ideally, the purest form of DNA has an A_{260}/A_{280} ratio of 1.8.

3.17. Polyacrylamide gel electrophoresis (PAGE)

The purity of the protein samples was determined by SDS-PAGE (Raymond *et al.,* 1959). The sample was heated with loading dye (please see appendix) at 100 °C for 5 min before loading and the run was performed at 80-120 V at room temperature in an Atto gel running system. For the composition of the running buffer please see the appendix. For the composition of the SDS-PAGE gel please see *Table 3.5*.

3.18. Coomassie staining

Following the SDS-PAGE, the gel was first fixed in 50% methanol (MeOH) and 5% glacial acetic acid (AcOH) for 30 min, and the gel was then incubated with staining solution (50% MeOH, 50% AcOH, and 0.1% Coomassie brilliant blue R250) at room temperature for 30 min. To visualize the protein bands, the gel was destained with 5% MeOH and 7.5% AcOH (Meyer *et al.*, 1965).

Table 3.5. Composition of the SDS-PAGE gel

	Separating gel (pH 8.8)						Stacking gel (pH 6.8)
	5%	**7.5%**	**10%**	**12.5%**	**15%**	**20%**	
A (ml)*	1.7	2.5	3.33	4.2	5	6.7	1.5
B (ml)*	2.5	2.5	2.5	2.5	2.5	2.5	-
C (ml)*	-	-	-	-	-	-	1.8
H$_2$O (ml)	5.8	5	4.2	3.33	2.5	0.8	
10% APS (µl)	23	23	23	23	23	23	10
TEMED (µl)	5.5	5.5	5.5	5.5	5.5	5.5	7.0

*A, B, C denotes the composition of different solutions. Please see the appendix.

3.19. Silver staining

The gel was first incubated in 50% MeOH overnight (at least 1 h) and then with a fixing solution (40% MeOH and 13.5% HCHO) for 10 min. The gel was then washed twice with Milli-Q water for 20 sec and soaked for 1 min in 0.2% $Na_2S_2O_3$. The gel was then washed twice with Milli-Q water for 20 sec and soaked with 0.1% silver nitrate in dark for 10 min. Using the developing solution (3% Na_2CO_3, 0.05% HCHO, and 0.000016% $Na_2S_2O_3$) until the band was developed and 2.3 M citric acid was used to stop the reaction (Switzer et al., 1979).

3.20. Protein estimation by modified Lowry method

The concentration of the protein sample was measured by the modified Lowry method (Lowry *et al*., 1951). The following three types of reagents were used for the estimation method:

Reagent A: 2% Na_2CO_3 in 0.1 M NaOH containing 0.16% Na-K tartrate + 0.1% SDS

Reagent B: 4% $CuSO_4$. $5H_2O$

Reagent C: 100 : 1= A : B (10 ml + 100 µl)

200 µl of the protein sample was incubated with 600 µl of reagent C at room temperature for 15 min. Then 1 N Folin Ciocalteu's reagent was added to the mixture and re-incubated at 37 ºC for 30 min. the OD was measured at 660 nm. The

concentration of the protein was estimated from the equation; concentration = OD_{660}/ 0.0026, which was obtained from a standard curve of BSA.

3.21. Western immunoblotting

For western blotting, the electrophoretic transfer of proteins from SDS-PAGE to nitrocellulose or polyvinylidene fluoride (PVDF) membrane was done. To transfer the proteins from polyacrylamide gel to nitrocellulose membrane (Towbin et al., 1979), the membrane, gel, and the filter pads were incubated in transfer buffer (48 mM Tris; 39 mM Glycine; 0.05% SDS; 20% MeOH) for 30 min at RT. The assembly for semi-dry transfer was shown in *Fig.3.10.A* and the run was performed at 200 mA for 1 h. The transfer cassette was assembled for wet transfer as shown in *Fig.3.10.B* and the run was performed at 100 V for 1 h under cold conditions.

A
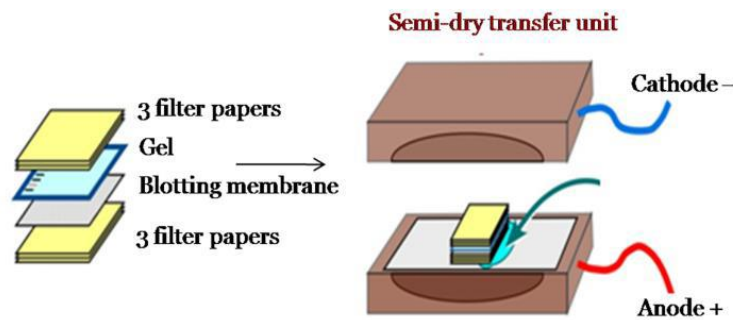
B

Fig.3.10. Arrangement of filter paper, gel, and membrane for western blot. (A) Semi-dry transfer **(B)** Wet transfer

After the transfer, the membrane was incubated in blocking buffer [5% skimmed milk in TBST (19.8 mM Tris, pH 7.5; 50 mM NaCl and 0.1% Tween 20)] overnight at 4°C to block non-specific sites. The next day the membrane was washed with TBS-T thrice. A primary antibody with suitable dilution was incubated for 2 h at RT in blocking buffer. After washing the secondary antibody was added in TBS-T either

tagged with alkaline phosphatase or (AP) horseradish peroxidase (HRP) was incubated. For AP-conjugated antibody, NBT (nitro blue tetrazolium) /BCIP (5-Bromo-4-chloro-3-indolyl phosphate) and for HRP conjugated antibody, luminal and peroxide were used as substrates. Briefly, for alkaline phosphate NBT solution (7.5 mg NBT dissolved in 175 μl DMF, dimethylformamide and 75 μl water) and BCIP (3.75 mg BCIP dissolved in 250 μl DMF) were mixed with 24.5 ml of bicarbonate buffer (210 mg Na_2CO_3 and 5.07 mg $MgCl_2$, pH 9.8 in 25 ml water) freshly and the mixture was incubated with the membrane in the dark until the desired bands appear.

3.22. Generation of V. cholerae growth curve

Cultures of wild type *V. cholerae* CytR$^+$, CytR$^-$ mutant, and its complement CytR^C were taken from the log phase and centrifuged, washed in PBS, and O.D was adjusted to 1×10^9 cells/ml. An inoculum of 1×10^5 cells/ml was given in fresh DASW media supplemented either with 0.5% sodium lactate or with 0.8% chitin (Sigma, St. Louis, MO, USA). The cultures were maintained at 30°C under constant shaking at 150 rpm for 48 h (Mondal et al., 2014). We also used log-phase cultures of wild type. *V. cholerae* CytR$^+$, CytR$^-$ mutant, and its complement CytR^C and mixed at the same dilution mentioned before in the mucin supplemented (1%) M9 minimal medium. The cultures were grown at 37°C under constant shaking at 180 rpm for 60 h. The viable cell counts were enumerated by dilution plating of the cultures at different time points (between 0 to 60 h) onto LB agar plates supplemented with streptomycin followed by colony count (Vercruysse M. *et al*., 2014). For inhibitor study, different concentrations of phytochemicals at the MIC level or below the MIC level were added to the growth media alongside the inoculation with *V. cholerae*.

3.23. β-Hexosaminidase assay

The activity of the β-Hexosaminidase enzyme was estimated by a previously described procedure (Li & Roseman, 2004) with *p*-nitrophenyl-β, D-*N*-acetylglucosaminide (PNP-GlcNAc) (Sigma). In brief, *V. cholerae* cells wild-type CytR$^+$, mutant CytR$^-$, and its complement CytR^C were grown in either DASW media with or without 0.8% chitin media or in minimal-lactate media with or without 1% porcine mucin up to the log phase. The bacterial cell density was adjusted to 5×10^8 cells/ml, they were washed and treated with toluene at a ratio of 10μl/ml of culture. After vigorous shaking for 10 sec, the mixture was kept at room temperature for 20

mins. 0.1 ml of these treated cultures were mixed 0.1 ml of 1mM PNP-GlcNAc in 20 mM Tris-HCl (pH 7.5) and incubated at 37°C for 60 mins. The reaction was stopped with 0.8 ml of 1M Tris base (pH 11). Cell debris was removed by centrifugation and the optical density of the supernatant was analyzed at 400nm. Total hexosaminidase activity was analyzed after measuring total protein by the Lowry method and then expressed as *p*-nitrophenol produced per minute per mg of protein. For determining *in vivo* hexosaminidase activity, rabbit ileal loop intestinal fluid was collected after incubation. The samples were then washed and centrifuged to collect the bacterial cells and total hexosaminidase activity was measured as described above (Chourashi et al., 2016).

3.24. Chitinase activity assay

The N-acetylglucosamine concentration in the reaction mixture and the chitinase activity were determined by the previously followed di-nitrosalicylic acid (DNS) method (Mondal et al., 2014). This method tests the free carbonyl groups in the reducing sugars. Chitinase activity was assayed here by estimating reducing sugars. Equal no bacteria were inoculated in minimal medium supplemented with mucin (pH-7.5). 0.5% sodium lactate (Sigma, St. Louis, MO, USA) was also added to support equal growth of all the strains. Log phase cultures were taken, bacteria were pelleted by centrifugation and the crude supernatant from each of the bacterial culture were used as samples for the enzymatic assay. The samples were used to incubate with 0.5 mg/ml porcine mucin (Sigma, St. Louis, MO, USA) or colloidal assay grade chitin (Sigma, St. Louis, MO, USA) for 1 h at 37°C. In each case, the control was done by using heat-inactivated samples. The reaction was stopped by adding a DNS solution. The mixture was boiled at 100°C for 10 min and cooled by keeping it on ice immediately after boiling. The amount of reducing sugar was estimated by measuring the OD at 540 nm. The amount of reducing sugar was calculated from a known standard curve. Total enzymatic activity was analyzed after measuring total protein by the lowry method and then calculated by measuring the amount of GlcNAc produced in nmoles /mg of protein/ min.

3.25. Mucin penetration assay

The assay was performed according to a previously published method (Liu et al., 2008). In brief, mucin columns were prepared in 1ml syringes by adding different

concentrations of porcine mucin (1%, 1.5%, and 2%) (Sigma). Bacteria were grown up to the mid-log phase and their concentration was adjusted to 5×10^8 cells/ml using PBS. 0.1 ml of the culture was loaded on the top of the mucin columns. Columns were then allowed to settle for 1 h at 37°C under static conditions. 100 μl fractions were collected from the bottom of the columns. Bacterial numbers were measured by serially diluting the samples and plating them onto LB agar and counting the Colony-forming Units (CFU). While performing the inhibitor study, different concentrations of the phytochemicals were added to each of the mucin columns. The untreated mucin column was used as a control.

3.26. Motility assay

The surface motility of all *V. cholerae* strains used in this study was done by a previously described procedure (Yeung et al., 2012). Bacterial strains were grown up to the mid-log phase in LB broth. The culture was resuspended in PBS and O.D. adjusted to 5×10^8 cells/ml. 1μl of this culture was spotted on soft agar plates containing 0.4% porcine mucin (Sigma) in minimal M9 media (BD Difco) and 0.3% bacto agar (BD Difco). And the plates were incubated for 18h at 37°C. Bacterial motility was analyzed by measuring the diameter of the motility zone on the plate surface. While studying the effect of inhibitors, specific inhibitors were added to the soft agar plate media just before preparing the plate.

3.27. Determination of Minimum Inhibitory Concentration (MIC) and Minimum Bactericidal Concentration (MBC) of inhibitors

The Minimum Inhibitory Concentration (MIC) of carvacrol was determined by the broth microdilution method according to CLSI guidelines (Clinical Laboratory Standards Institute, 2000) in 96-well flat-bottomed polystyrene microtitre plates (Costar Corning). Bacterial strain suspension was adjusted to Optical density values 0.08-0.12 at 600 nm (equivalent to 0.5 McFarland standard turbidity) with a spectrophotometer. 200 μl cell suspensions were inoculated into the wells of 96-well microplates and carvacrol was dissolved in DMSO and then in Muller Hinton Broth (MHB) as required and transferred to the microplate well to obtain a 2-fold serial dilution ranging from 1200μg/ml to 1μg/ml. MHB only and MHB with bacteria containing wells were used as negative and positive controls, respectively. Plates were incubated for 24 h at 37°C and bacterial growth was evaluated by the presence of

turbidity and a pellet on the bottom. The MIC value was recorded as the lowest concentration of the tested compound that had no macroscopically visible growth of bacteria (Burt, 2004). To determine the minimum bactericidal concentration (MBC) values, 100μl of each well medium with no visible growth was inoculated in Muller Hinton Agar (MHA) plates. After 24 h of incubation at 37°C, the number of surviving organisms was determined. MBC was defined as the lowest concentration of compounds at which 99 % of the bacteria were killed. Each experiment was repeated twice separately (Magina et al., 2009). To verify that the anti-microbial effect was from the carvacrol and not from DMSO (that was used as the solvent for carvacrol), we used DMSO as negative control and it did not inhibit bacterial growth.

3.28. Medium additives for inhibitor study

For the inhibitor study, the following phytochemicals were used, Curcumin (CC), Carvacrol (CV) (Sigma-Aldrich) and Trans-cinnamaldehyde (TC) (Sigma-Aldrich); N-acetyl D-glucosamine (GlcNAc) (Sigma-Aldrich), Xylose (Sigma-Aldrich), Xylitol (Sigma-Aldrich), Allose (Sigma-Aldrich) and Mannitol (Sigma-Aldrich) as monosaccharide; Na-3-hydroxy Butyrate (3HB) (Sigma-Aldrich) and NH125 (Calbiochem) as a small molecule. Pentoxifylline (PEN) (Cayman chemicals), Caffeine (CF) (Cayman chemicals), Dequalinium chloride (DQ) (Cayman chemicals), and Theophylline (TH) (Cayman chemicals) as Family-18 chitinase inhibitors. Appropriate dilutions were made during stock preparations and during experiments by dissolving the compounds in DNA/RNA-free water or in polar solvent DMSO (Dimethyl Sulfoxide) and filter sterilizing it (0.2μm). Additives were supplemented in LB or minimal M9 media in different concentrations. Media with no additive added was used as control.

3.29. Cell culture

Human intestinal cell line HT-29 (ATCC HTB-38) and CaCo2 (ATCC HTB-37) were used in the experiments in this study. HT-29 cell line was maintained as per American Type Culture Collection (ATCC) cell culture guidelines. The HT-29 cell line was cultured in Corning T-25 flasks using Dulbecco's Modified Eagle's medium (DMEM) (Sigma-Aldrich) containing 4.5 g/ L glucose and 110 mg/ L sodium pyruvate and 10% heat-inactivated fetal bovine serum (FBS) (South American origin, PAN Biotech, Germany) at 37°C with 5% CO_2 using a HERAcell® 150 humidified

incubator (Thermo Scientific, USA) to form a monolayer. Complete DMEM media supplemented with 3.7 g/ L sodium bicarbonate, 50 U/ ml penicillin, and 50 mg/ ml streptomycin (Sigma, St. Louis, CA) was used for maintaining the cell line and for infection studies, incomplete media lacking penicillin-streptomycin and 0.5% FBS was used. The spent culture media was replaced with a fresh one on alternate days and the monolayer was used after achieving ~90% confluency. The stock of the cultured epithelial cell was prepared by using 95% complete growth media and 5% DMSO (Sigma-Aldrich, USA) and kept in liquid nitrogen. To keep anchorage-dependent cell lines growing in monolayers in exponential development, they are sub-cultured at regular intervals. The cells are ready to be sub-cultured when they are nearing the end of exponential development (approximately 70% to 90% confluent). The used media was discarded and washed with PBS (37°C) without calcium or magnesium. Then 2 mL to 3 mL of the 0.25% trypsin-EDTA solution (37°C) was added and kept at 37°C for cells to be detached. Then complete growth medium was added to inactivate the trypsin. After centrifugation, the cells are suspended in complete media and dispensed in a routine split ratio.

3.30. *In vitro growth assay in HT-29 cell line*

Mucin secreting human intestinal cell line HT-29 and CaCo2 cell lines were maintained in Dulbecco's Modified Eagle's Medium (DMEM, Sigma, St. Louis, MO, USA), supplemented with 10% fetal bovine serum (FBS) (HiMedia, Mumbai, India), 1% (vol/vol) non-essential amino acid (DMEM, Sigma, St. Louis, MO, USA) and 1% (vol/vol) penicillin/streptomycin (Sigma, St. Louis, MO, USA) mixture at 37°C under 5% CO_2. The survival of *V. cholerae* in the presence of mucin secreting HT-29 cells was analyzed by using the previously described protocol (Mondal et al., 2014). The 80% confluent, serum-starved HT-29 cells in 12-well plates were infected with log-phase cultures of all *V. cholerae* N16961 strains (wild type CytR[+], mutant CytR[−], and its complement CytR[C]) at an infectious dose of 10^7 c.f.u/ml. After a varying period of incubation, unbound cells were collected from the supernatant, and cells were then treated with 0.1 % Triton X-100 for 2–3 min to detach the bound bacteria. Both the unbound and the bound bacteria were collected, washed in PBS, serially diluted, and plated onto LB agar to get a viable bacterial count.

3.31. HT-29 and Caco2 cell adhesion assay

Adhesion of *V. cholerae* (WT CytR$^+$, mutant CytR$^-$, and its complement CytR^c) to the human colon adenocarcinoma cell line HT-29 and Caco2 was done according to the previously described method (Chourashi et al., 2016). As mentioned earlier HT-29 cells were split into 12 well cell culture plates and maintained in DMEM with 10% FBS. Upon reaching 80% confluency, 1.2×10^8 freshly grown mid-log phase bacterial inoculum (washed in PBS, numerated by CFU counting, ratio, 100 bacteria:1 HT-29 cells, MOI 100) was given to 1.2×10^6 cells in DMEM culture medium with 0.5% FBS and without antibiotics. Adhesion assay was conducted by incubating the bacteria/cell at 37°C for 1 h under conditions of 5% CO_2 and 90% relative humidity. Cells were washed thrice with prewarmed PBS pH 7.4 and were detached using 0.1% Triton X-100. Adherent bacteria were counted after serial dilution by plating on LB agar plates supplemented with 100 µg/ml streptomycin.

3.32. In vivo intestinal epithelium adhesion assay

In vivo adhesion of bacterial strains with the rabbit intestinal lumen was also evaluated. Intestinal loop sections recovered 18 h after the rabbit ileal loop experiment was washed in PBS three times and then homogenized and serially diluted in PBS. The adherent bacterial count was determined by plating and counting these bacterial cultures on LB agar supplemented with 100 µg/ml streptomycin.

3.33. Suckling mice colonization competition assay

The *in vivo* infant mouse colonization assay was performed as described previously (Zheng et al., 2010). Log phase culture of *V. cholerae* mutant strain (LacZ$^-$) was mixed with each of the wild-type strains (LacZ$^+$) i.e., CytR$^+$, CytR$^-$, and CytR^c at a ratio of 1:1. 2 h prior to giving inoculum 4 to 5 days old suckling Swiss albino mice *(Fig.3.11)* were separated from their mothers. Each mouse was then orally gavaged with 50µl of 5×10^8 CFU/ml of the mixed bacterial culture. Negative control mice were fed with 50µl PBS. Mice were kept at 26°C in isolation. 18 h after infection they were sacrificed and the intestine was harvested, washed in PBS, mechanically homogenized, and diluted serially to plate on LB agar supplemented with 100µg/ml streptomycin. Competitive Index (CI) was calculated by the following equation: - ratio out $_{(mutant/wild-type)}$ / ratio in $_{(mutant/wild-type)}$. The CI value of < 1 indicates

a fitness defect and that of > 1 indicates an increased fitness. Seven mice per group were used in this study.

Fig.3.11. 4 to 5 days old infant mice

3.34. Rabbit ileal loop assay for fluid accumulation and bacterial recovery

This assay was performed in New Zealand White Rabbits weighing approx. 2.5 kg by a detailed method described previously (Koley et al., 1999). In brief, a bacterial inoculum of all three strains was adjusted to 1×10^9 CFU/ml and 1ml of these cultures were introduced into the ligated loops of the ileum. The negative control loop was inoculated with PBS. The animal was sacrificed after about 18 h and loops were taken out. The volume of the accumulated fluid and the length of the loops were measured. The extent of the fluid accumulation (FA) was expressed as loop fluid volume (ml)/length (cm) ratio. PBS was used as a negative control. Bacteria were counted by homogenizing the intestinal sections in 1 ml PBS. To determine the actual bacterial c.f.u at the time of intestinal harvest, bacteria were collected from the intestine, washed, serially diluted, and plated on LB agar supplemented with streptomycin (100 µg/ml). In the inhibitor study, 1 ml of 1×10^9 CFU/ml *V. cholerae* culture with or without carvacrol (at 150µg/ml, 75µg/ml, 37.5µg/ml) were introduced into each ileal loop. Bacterial recovery and other measurements were done as stated earlier.

3.35. Histological studies

Histological analysis was done by collecting tissue samples (1 cm in length) from rabbit ileal loop assays. They were fixed in 10% neutral buffered formalin. Further, the samples were embedded in paraffin. 3-4 µm thin sections were cut in a microtomy rotor (Leica, Germany) and were stained with hematoxylin and eosin and examined under a compound light microscope. Photographs were taken under different magnifications with a Carl Zeiss PrimoStar microscope (Oberkochen, Germany), equipped with a digital imaging system.

3.36. Cell staining and fluorescence microscopy

For fluorescence microscopy, all *V. cholerae* strains (WT CytR$^+$, mutant CytR$^-$, and its complement CytR^c) were transformed with Ampicillin resistant GFP expressing plasmid, pGFPuv (Clontech, TaKaRa bioscience) by electroporation. Adhesion assay with this GFP expressing *V. cholerae* strain was done on a grease-free, sterile coverslip, washed in PBS, and mounted with VECTASHIELD antifade mounting medium (Vector laboratories) to view under a fluorescence microscope (Olympus AX-70) to show the GFP labeled bacteria bound to HT-29 cells.

The effect of carvacrol on human adenocarcinoma cell line HT-29 was visualized by fluorescence microscopy. HT-29 cells were seeded on sterile borosilicate cover glass (Blue star) in 6-well cell culture plates. Upon reaching 80% confluency, HT-29 cells were incubated in serum-free DMEM and carvacrol treatment at different concentrations (0µg/ml to 250µg/ml) was done for 4 h. After removing the media HT-29 cells were washed in PBS and stained with Hoechst 33342 (5µg/ml) (Sigma-Aldrich) for 10 mins. Cells were then washed in PBS twice and subsequently counterstained and mounted with PI containing mounting medium (VectaShield, Vector laboratories). Each carvacrol treated and the untreated cell was visualized under a confocal laser scanning microscope. Propidium Iodide (PI) is a membrane impermeant dye while Hoechst H33342 is a membrane-permeable stain, therefore HT-29 cells exhibiting membrane permeability upon carvacrol treatment displays red (PI) intensity.

3.37. LDH cytotoxicity assay

The effect of different inhibitors on the cytotoxicity of the HT-29 cell line was estimated by lactate dehydrogenase (LDH) release assay following the manufacturer's protocol (LDH cytotoxicity detection kit, TaKaRa Biosciences). In brief, HT-29 cells were grown in 6-well cell culture plates up to 80% confluency and then co-incubation with carvacrol at different concentrations was done for 12 h at 37°C humid cell culture incubator. Cell culture supernatants were analyzed for the release of lactate dehydrogenase (LDH). The percent cytotoxicity value was calculated using the following formula, $\text{Cytotoxicity (\%)} = \left(\frac{EX-LC}{HC-LC} - BC\right) \times 100$; where EX = Experimental value, LC = Low control or spontaneous LDH release from the untreated normal HT-29 cells, HC = High control or maximum releasable LDH in the HT-29 cells by the addition of 1% Triton X-100, BC = Background control or LDH activity in the assay medium. Treatment with 1% (v/v) Triton X-100 represented maximum LDH release hence representing 100% cytotoxicity.

3.38. Biofilm assay

Assays to quantify biofilms were performed as previously described method (Zhu & Mekalanos, 2003). In brief, a 1:100 dilution of the overnight grown culture of *V. cholerae* was inoculated in LB broth into 10- by 75-mm borosilicate glass tubes and incubated for 30 hrs at 37°C. Subsequently, the tubes were rinsed three times with phosphate-buffered saline (PBS) and then filled with 1% crystal violet stain. After 5 min, the excess stain was rinsed off with deionized water. The biofilm-associated crystal violet was solubilized in dimethyl sulfoxide (DMSO), and the optical density at 570 nm (OD_{570}) of the resulting suspension was measured.

3.39. Transmission Electron Microscopy (TEM)

Negatively stained whole-cell mounts were prepared to visualize bacterial morphology. In brief CytR⁺, CytR⁻ strains of *V. cholerae* were grown in LB broth, and in the case of inhibitors, *V. cholerae* was grown with or without different concentrations (150µg/ml, 75µg/ml, 37.5µg/ml) of carvacrol. From the culture, 5µl of bacterial suspension was gently placed on glow-discharged carbon-coated 300 mesh copper grids. After about 1 min, the remaining solution on the grids was wicked away with the help of a filter paper followed by washing with two drops of distilled water.

The grid was then stained with 2% (w/v) uranyl acetate and air-dried. The negatively stained cells were visualized with an FEI Tecnai 12 BioTWIN Transmission electron microscope (FEI, Hillsboro, OR, USA) at an operating voltage of 100 kV.

3.40. Whole-genome transcriptome analysis

Different *V. cholerae* strains CytR$^+$, CytR$^-$ were grown in the presence or absence of 1% mucin in minimal media up to the mid-log phase, and then bacterial samples were harvested. Samples were dissolved in RNAsol and processed for quality check. The RNA samples were quality checked using Nanodrop and quantitated using Qubit dsDNA BR assay (Thermo Scientific, USA). The quality was checked using a 1% Agarose TAE gel. The samples were also checked for degradation using Agilent Bioanalyzer RNA 6000 nano kit. The samples that had passed QC were taken further for analysis.

Library QC: 1) Illumina library: To achieve the highest quality of data on Illumina sequencing platforms, optimum cluster densities across every lane of every flow cell were created which required accurate quantitation of library templates. So, we quantified prepared libraries using qPCR according to the Illumina qPCR Quantification Protocol Guide. 2) GS FLX library: To generate a standard curve of fluorescence readings and calculate the library sample concentration, we use Roche's Rapid library standard Quantification solution and calculator. The samples which had passed library QC were taken further for sequencing.

Basic statistics of raw sequences were done to get the information of the total number of raw reads, read length, and percentage of GC content. Differential Gene Expression (DGE) was calculated by edgeR using the TPM value. We calculated Log2 fold change, two-tailed P-value, and false discovery rate (FDR). A volcano plot was done to compare the data sets. Heat Map of the top and bottom 10 genes of each sample were generated.

3.41. Statistical analysis

All the experiments were analyzed by Student's t-test. Each of the experiments was repeated at least three times. Data were represented as mean ± standard error of the mean (SEM). Statistical analysis and data plotting for suckling mice colonization

competition assay were done by two-way ANOVA using GraphPad Prism software (Version 5). A 'P-value of <0.05 was considered as statistically significant.

3.42. Ethics statement

Animal experiments were conducted following the standard operating procedure framed by the Committee for the Purpose of Control and Supervision of Experiments on Animal (CPCSEA), Government of India. All the animal experiments performed here were approved by the Institutional Animal Ethics Committee of National Institute of Cholera and Enteric Diseases (Registration no: PRO/120/April 2016 - March 2019). Intestinal colonization competitive index assay was performed using four to five days old infant Swiss mice. For fluid accumulation and other *in vivo* studies, New Zealand white rabbits weighing about 2.5 kg were used. Animals were euthanized in the CO_2 chamber assuring minimum pain to the animals during the intestinal harvest.

3.43. Safety statement

All experiments with bacteria, cell culture and with animal models were conducted following the standard operating procedure of a Bio-Safety level 2 (BSL2) laboratory and with proper disposal of biohazard waste as outlined by Department of Biotechnology, Government of India Handbook and was approved by the Institutional Bio Safety Committee (IBSC), Indian Council of Medical Research- National Institute of Cholera and Enteric Diseases, Kolkata, India. (Approval No. NICED/BS/NSC- 004/2016 dated 27/04/2016).

Chapter 4

Results

To study the role of CytR in chitin utilization pathway in Vibrio cholerae

Results

The effect of abiotic environmental factors like temperature, pH, NaCl concentration (salinity), and different concentrations of crab shell chitin was used to study the gene expression of *cytR* at the RNA level by qPCR. CytR Protein levels were also studied by ELISA. Next, we have done a comparative study on time-dependent growth of wild type *V. cholerae* (CytR$^+$), CytR mutated *V. cholerae* (CytR$^-$), and with complemented strain (CytR^c) in presence of insoluble chitin or other carbon sources. The role of CytR in chitin utilization has also been elucidated by studying the expressional analysis of *V. cholerae* chitinase genes. Further, we have studied other upstream chitin degradation pathway genes like sensor histidine kinase ChiS and a master regulator TfoX. Additionally, we have also measured the chitinase activity and activity of ChiS by β-hexosaminidase activity and *p*-nitrophenyl-β, D-*N*-acetylglucosaminidine (PNP-GlcNAc) following the previously described procedure (Li & Roseman, 2004; Mondal et al., 2014).

4.1. Effect of temperature on CytR expression
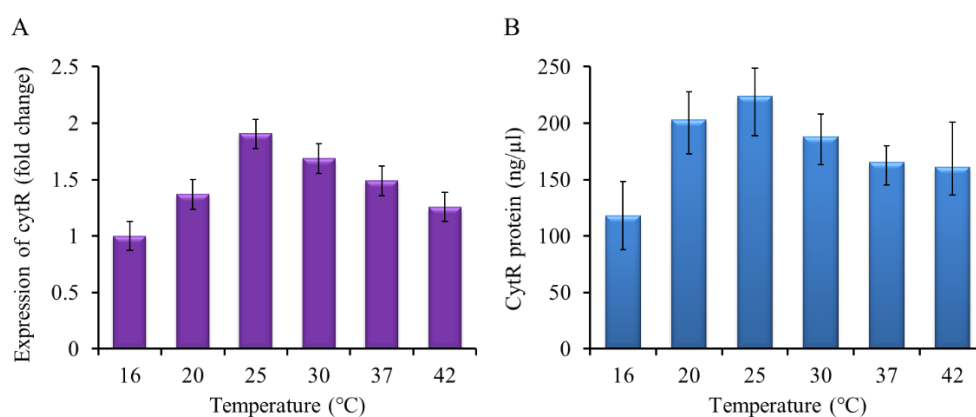

Fig.4.1. Effect of temperature on CytR expression. *V. cholerae* N16961 was grown to log phase under varying temperature. mRNA expression was analysed by qPCR and protein levels by ELISA. **(A)** Relative mRNA expression of cytR, **(B)** Relative protein level expression of cytR. Each of the experiment was repeated three times (n=3) and the data were expressed as Mean ± SEM.

V. cholerae was grown in different temperatures between 16°C to 42°C keeping a fixed pH 8.0 and 300mM salinity in a medium of seawater (Please see Appendix) supplemented with 1% chitin. First, the cytR RNA expression was studied by qRT-PCR *(Fig.4.1A)*. The cytR RNA expression was lowest at 16°C, hence, considering it as the basal level of expression. RNA expression gradually increased with the temperature shift. It was the highest at 25°C, showing a maximum of 1.9-fold increase in the cytR expression *(Fig. 4.1A)* compared to the basal level of expression. Decreased RNA expression was observed with further temperature shifts.

Next, the CytR protein levels were analyzed *(Fig.4.1B)*. CytR protein expression pattern in the same temperature range corroborated with the RNA expression. The highest level was observed at 25°C with 224ng/µl of protein. At 16°C and 42°C, the protein expression was 118ng/µl and 161ng/µl respectively.

4.2. Effect of pH on CytR expression
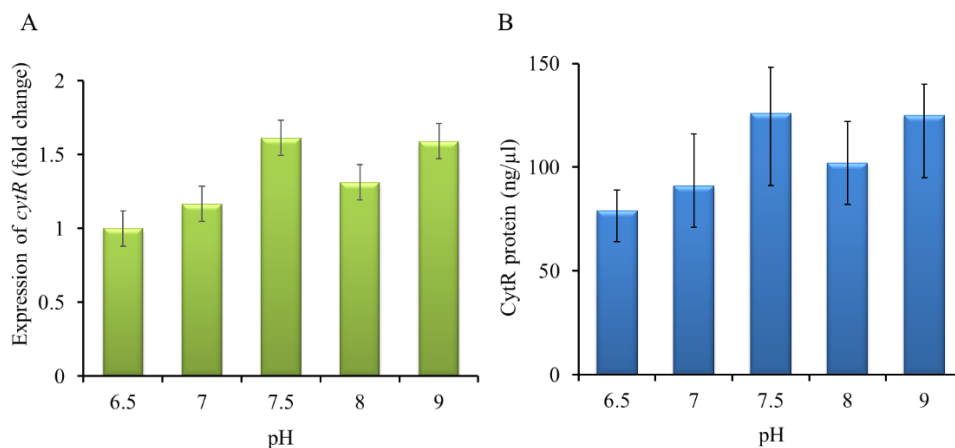
Fig.4.2. Effect of pH on CytR expression. *V. cholerae* N16961 was grown to log phase under varying pH. mRNA expression was analyzed by qPCR and protein levels by ELISA. **(A)** Relative mRNA expression of cytR, **(B)** Relative protein level expression of cytR. Each of the experiments was repeated three times (n=3) and the data were expressed as Mean ± SEM.

The effect of pH was studied under varying pH of 6.5 to 9 with fixed temperature (30°C) and salinity (300mM) in sea-water media supplemented with 1% chitin. The study of cytR RNA expression by qRT-PCR showed that at pH 6.5, the expression was lowest *(Fig.4.2A)*. Maximum expression of cytR was observed at pH 7.5 with an increase of 1.61-fold than the expression observed at pH 6.5. Interestingly,

at pH 9 the cytR expression showed a 1.59-fold increase which was almost comparable to the expression levels at pH 7.5.

The protein expression pattern also showed similarity with the RNA expression *(Fig.4.2B)*. The protein expression was lowest at pH 6.5 showing 79 ng/µl expression. At pH 7.5 and pH 9.0, the amount of protein produced was 126 ng/µl and 125 ng/µl respectively.

4.3. Effect of salinity on CytR expression

Fig.4.3. Effect of salinity on CytR expression. *V. cholerae* N16961 was grown to log phase under the varying concentration of sodium chloride. mRNA expression was analyzed by qPCR and protein levels by ELISA. **(A)** Relative mRNA expression of cytR, **(B)** Relative protein level expression of cytR. Each of the experiments was repeated three times (n=3) and the data were expressed as Mean ± SEM.

The effect of salinity on the expression of cytR was studied under the varying concentration of salt (NaCl) starting from 0 mM to 600 mM in an artificial seawater medium supplemented with 0.8% chitin. *V. cholerae* was grown under varying salt supplemented with chitin keeping the temperature and pH fixed at 30°C and pH 8 respectively. The optimum salt concentration for maximum expression of cytR was observed to be at 300mM NaCl, which is 1.37-fold more than the condition where no salt is present *(Fig.4.3A)*.

The CytR protein expression pattern as an effect of salt concentration was also similar to RNA expression *(Fig.4.3B)*. The maximum CytR expression was at 300 mM concentration measuring 145 ng/µl. At 100 mM salt concentration, the CytR expression was only 95 ng/µl and observed as lowest. The protein expression increased with increasing salinity up to 300mM salt concentration. After 300 mM salt

concentration the CytR expression decreased gradually with increasing salinity. At 600 mM salt concentration, the protein expression level was 120 ng/µl.

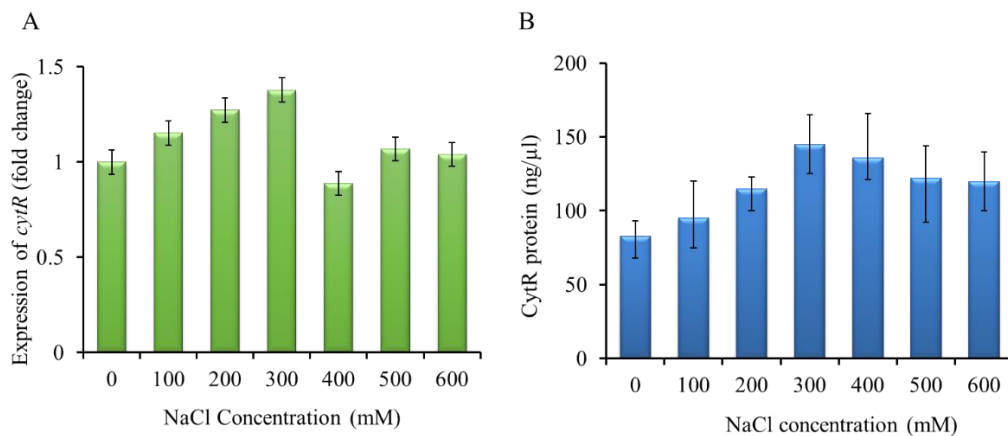## 4.4. Effect of chitin on CytR expression
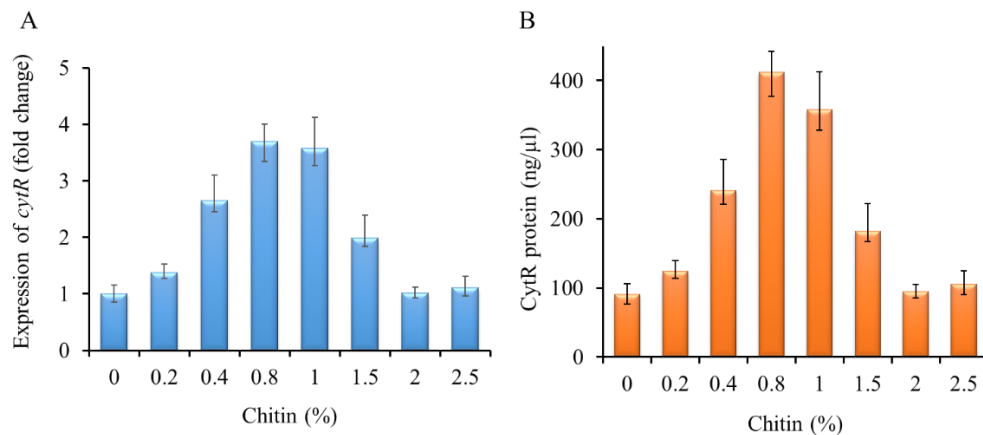
Fig.4.4. Effect of chitin on CytR expression. *V. cholerae* N16961 was grown to log phase under the varying concentration of crab shell chitin. mRNA expression was analyzed by qPCR and protein levels by ELISA. **(A)** Relative mRNA expression of cytR, **(B)** Relative protein level expression of cytR. Each of the experiments was repeated three times (n=3) and the data were expressed as Mean ± SEM.

V. cholerae was grown in different concentrations of chitin between 0 to 2.5% keeping a fixed pH 8.0 and 300mM salinity and 30°C temperature in a medium of seawater. First, the cytR RNA expression was studied by qRT-PCR *(Fig.4.4A)*. Analysis of cytR expression under different amounts of chitin showed 0.8% chitin was optimum for cytR expression. Significant expression was also observed at a chitin concentration of 1%. *V. cholerae* produces 3.7-fold more cytR mRNA in presence of 0.8% chitin. Very low (0.2%) or high (>1.5%) chitin decreased the expression of cytR.

The CytR protein expression pattern under the varying amount of chitin was also similar to RNA expression *(Fig.4.4B)*. The expression increased with the increasing amount of chitin. At 0.8% chitin, the CytR protein expression was maximum measuring 412 ng/µl compared to the expression of 91 ng/µl in absence of chitin. Beyond 1.5% chitin, the CytR expression decreased gradually with the increasing amount of chitin.

4.5. V. cholerae upregulates all four chitinase genes in presence of chitin

Next, we have studied the role of *V. cholerae* chitinases in chitin degradation. *V. cholerae* was grown to mid-log phase in defined artificial water media with optimum salinity (i.e., 300mM), optimum temperature (i.e., 25°C), optimum pH (i.e., pH 7.5), and in presence or absence of chitin (0.8%). RNA expression was studied by qRT-PCR. Four *V. cholerae* chitinases namely, ChiA1, ChiA2, VC_1073 (ChiC), and VC_0769 were studied here. The result showed that in presence of chitin, *V. cholerae* expresses 5.5-fold, 6.5-fold, 3.4-fold, and, 4.6-fold increased levels of *chiA1*, *chiA2*, *vc_1073* (*chiC*), and *vc_0769* respectively *(Fig.4.5A)*.
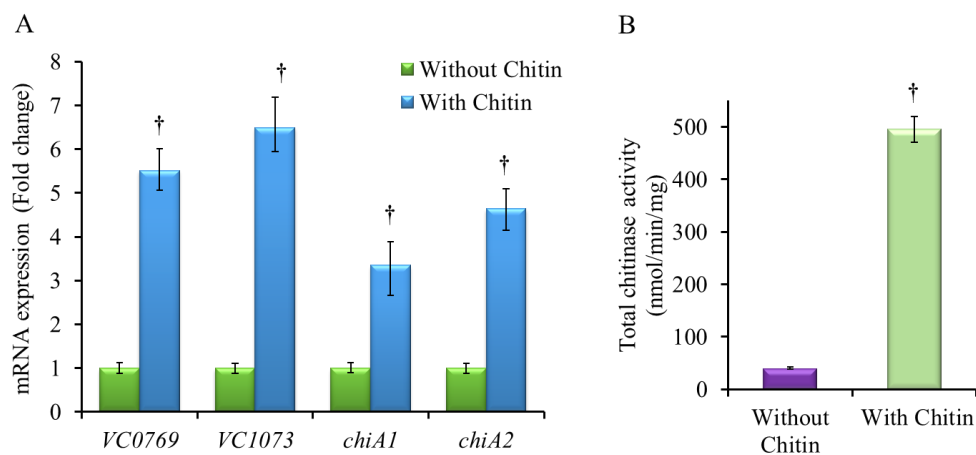
Fig.4.5. Relative expression of chitinase genes and chitinase activity. *V. cholerae* N16961 was grown to log phase in the artificial seawater media in the presence or absence of 0.8% chitin. **(A)** Relative mRNA expression of different chitinase genes was analyzed by qRT-PCR **(B)** Total chitinase activity was measured by the DNS method (Mondal *et al.*, 2014) from the culture supernatant of *V. cholerae* grown in the presence or absence of chitin. Each of the experiments was repeated three times (n=3) and the data were expressed as Mean ± SEM; †, P-value <0.05

We have also checked the total chitinase activity from the culture supernatant by the previously described DNS method (Mondal et al., 2014). The result showed that the total chitinase activity of the *V. cholerae* increased by 12-fold in presence of chitin in the culture media *(Fig.4.5B)*.

4.6. *V. cholerae CytR plays an important role in chitin utilization*

A

B
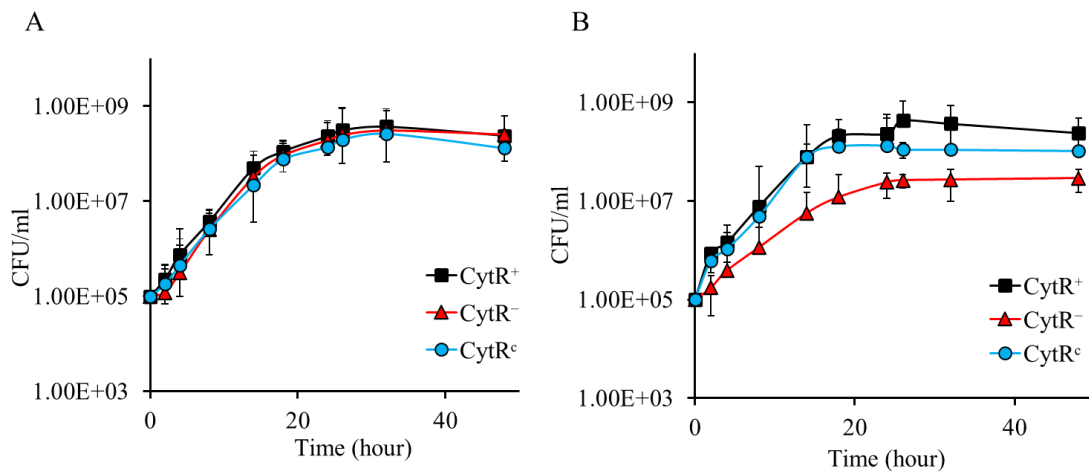
Fig.4.6. CytR helps *V. cholerae* to utilize chitin as a sole nutrient source. All *V. cholerae* N16961 strains, CytR$^+$ (wild type) (■), CytR$^-$ (isogenic CytR mutant) (▲) and CytR^c (CytR$^-$ strain complemented with CytR clone) (●) strains were inoculated separately in **(A)** Defined artificial seawater media with 0.5% sodium lactate as sole carbon source and **(B)** Defined artificial seawater media supplemented with 0.8% chitin only. The viable bacterial counts in colony-forming units (c.f.u.)/ml were detected by plate count method, taking culture samples from different time points and represented graphically. Each of the experiments was repeated three times (n=3) and the data were expressed as Mean ± SEM.

In order to understand the role of CytR in chitin utilization we have measured the growth rate of all the *V. cholerae* strains *i.e.*, CytR$^+$ (wild type), CytR$^-$ (isogenic CytR mutant), and CytR^c (CytR$^-$ strain complemented with CytR clone) in defined artificial seawater (DASW) media in the absence *(Fig.4.6A)* or presence of 0.8% chitin *(Fig. 4.6B)*. The CytR$^-$ mutant strain grew poorly in chitin-supplemented DASW media compared to the wild-type CytR$^+$ strain. At 48 h, the total viable count of wild type *V. cholerae* CytR$^+$ strain in chitin supplemented media was 2.4 ×10^8 CFU/ml, whereas it was 2.9×10^7 CFU/ml in the CytR$^-$ mutant strain, showing an 8.2-fold difference in growth *(Fig. 4.6B)*. The complemented CytR^c strain showed similar growth as of the wild-type CytR$^+$ strain in chitin supplemented media. In contrast, all the strains showed an almost similar growth pattern in presence of sodium lactate supplemented DASW media in absence of chitin *(Fig. 4.6A)* which indicates equal fitness of all the strains. This result indicates *V. cholerae* could utilize chitin as the sole nutrient source and CytR contributes to utilizing it.

4.7. *V. cholerae CytR controls the expression of chitinase genes and other chitin utilization pathway regulators*
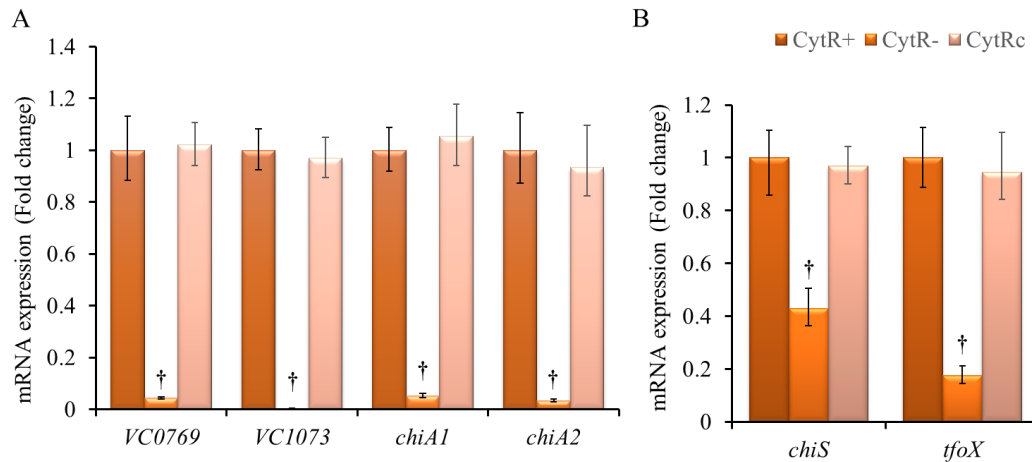
Fig. 4.7. CytR is important for *V. cholerae* to express chitinase genes and other upstream regulators. All *V. cholerae* N16961 strains, CytR⁺ (wild type) (■), CytR⁻ (isogenic CytR mutant) (■) and CytRᶜ (CytR⁻ strain complemented with CytR clone) (■) strains were inoculated separately in Defined artificial seawater media supplemented with 0.8% chitin. RNA was isolated from the mid-log phase culture and subsequently, cDNA was prepared. Expressional analysis was done by qRT-PCR. **(A)** Relative expression of chitinase genes in all three *V. cholerae* strains was shown graphically. **(B)** Relative expressional analysis of *chiS* and *tfoX* was also done. Each of the experiments was repeated three times (n=3) and the data were expressed as Mean ± SEM; †, P-value <0.05

We have seen previously that chitinases are an essential part to degrade chitin in the marine environment and *V. cholerae* upregulates the expression of extracellular chitinases *(Section 4.5)* that in turn degrades chitin and *V. cholerae* uses that as a carbon source. Here, we aim to study the role of cytR in chitin utilization. For that, we have taken the isogenic deletion mutant of CytR (CytR⁻) along with the wild type (CytR⁺) and complemented strain (CytRᶜ). All strains were grown separately in DASW media supplemented with 0.8% chitin. qRT-PCR analysis was performed with the RNA isolated from the mid-log phase culture. The result showed that the CytR⁻ mutant strain is 23.8-fold, 52-fold, 19.6-fold, 29.4-fold less efficient to express chitinase genes *vc_0769, vc_1073, chiA1, chiA2* respectively than the wild type bacteria *(Fig.4.7A)*. We have also studied the expression of sensor histidine kinase, *chiS*, and a regulator of *V. cholerae* chitin utilization pathway, *tfoX*. Both of these genes were downregulated by 2.3-fold and 5.7-fold respectively in CytR mutant strain *(Fig.4.7B)*. In both, the cases complemented CytR strain (CytRᶜ) showed comparable gene expression as the wild type *V. cholerae*.

4.8. Sensor histidine kinase ChiS is positively controlled by CytR
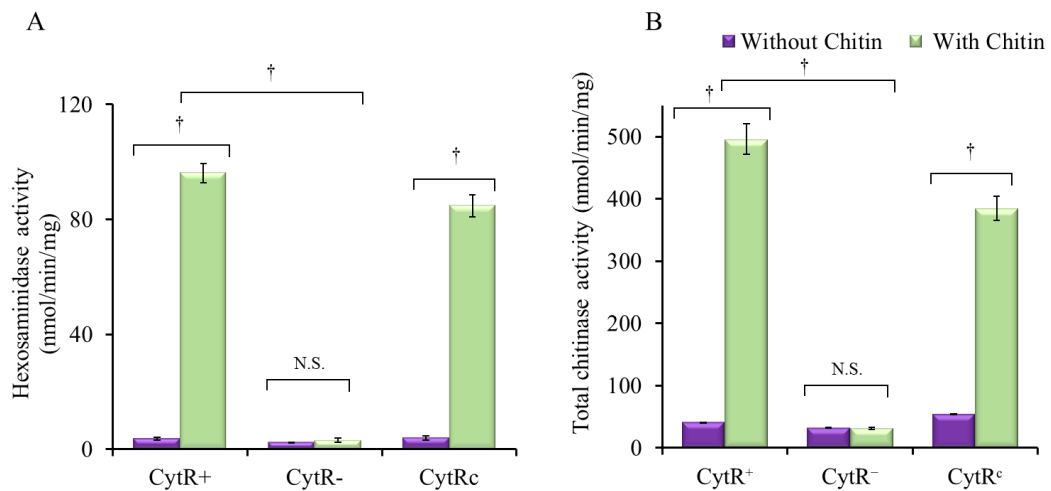
Fig.4.8. Role of CytR in hexosaminidase and total chitinase enzyme activity in *V. cholerae*. All bacterial strains of *V. cholerae*, CytR⁺ (wild type), CytR⁻ (isogenic CytR mutant), and CytRᶜ (CytR⁻ strain complemented with CytR clone) were grown in DASW media in the presence (■) or absence (■) of 0.8% chitin. **(A)** Hexosaminidase enzyme activity was measured by taking log-phase cultures and **(B)** Total chitinase activity was measured from the bacterial culture supernatant. Each of the experiments was repeated three times (n=3) and the data were expressed as Mean ± SEM; †, P-value <0.05

The activity of periplasmic two-component chitin sensing histidine kinase, ChiS is measured by the amount of production of β-hexosaminidase enzyme per unit time per mg of protein, located downstream of ChiS (Li & Roseman, 2004). Total β-hexosaminidase enzyme activity in all the *V. cholerae* strains in the presence or absence of 0.8% chitin as a sole nutrient source was measured here. The activity of hexosaminidase enzyme in wild-type CytR⁺ strain in presence of chitin was 96 nmol/min/mg, whereas in CytR⁻ mutant strain it was 3 nmol/min/mg. So, the CytR⁻ mutant strain showed 26-fold less hexosaminidase activity than the wild-type CytR⁺ strain *(Fig.4.8A)*. However, the enzyme activity was negligibly small in absence of chitin in all the strains, suggesting that it is triggered in presence of chitin. On the other hand, complemented CytRᶜ strain also showed comparable hexosaminidase enzyme activity with respect to the CytR⁺ strain in presence of chitin. CytR regulates the activity of the hexosaminidase enzyme by means of activating the ChiS in presence of chitin.

V. cholerae CytR is also important for chitinase activity. Total chitinase activity was measured from the culture supernatant. The activity of chitinases in wild-

type CytR$^+$ strain in presence of chitin was 495 nmol/min/mg, whereas in CytR$^-$ mutant strain it was 31 nmol/min/mg. So, the CytR$^-$ mutant strain showed 16-fold less activity than the wild-type CytR$^+$ strain *(Fig.4.8B)*. The chitinase activity was negligibly small in absence of chitin in all the strains.

Chapter 5

Results

To understand the role of CytR in pathogenesis.

Results

To understand the role of CytR in pathogenesis, the following experiments were done using the following *V. cholerae* strains [wild type *V. cholerae* (CytR+), CytR mutated *V. cholerae* (CytR-) and complemented strain (CytRᶜ)].

5.1. CytR helps V. cholerae to utilize mucin
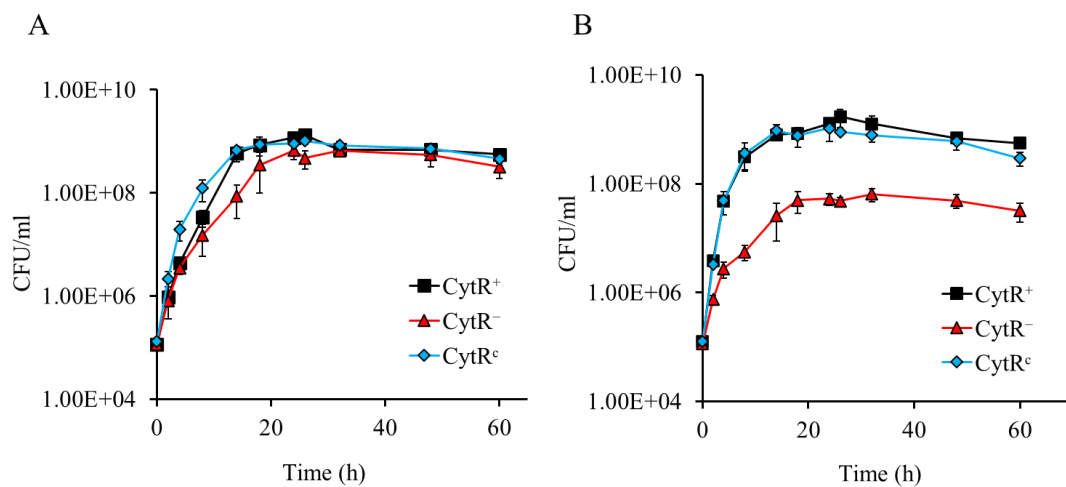
Fig.5.1. CytR contributes in the utilization of mucin as a sole nutrient source in *V. cholerae*. All *V. cholerae* N16961 strains, CytR+ (wild type) (■), CytR- (isogenic CytR mutant) (▲) and CytRᶜ (CytR- strain complemented with CytR clone) (♦) strains were inoculated separately in **(A)** M9 minimal media with 0.5% sodium lactate as sole carbon source and **(B)** M9 minimal media supplemented with 1% (w/v) porcine mucin only. The viable bacterial counts in CFU/ml were detected by plate count method taking culture samples from different time points and represented graphically. Each of the experiments was repeated three times (n=3) and the data were expressed as Mean ± SEM.

We first measured the growth rate of all the *V. cholerae* in M9 minimal media in the absence *(Fig.5.1A)* or presence of mucin *(Fig.5.1B)*. The CytR- mutant strain grew poorly in mucin supplemented M9 minimal media compared to the wild-type CytR+ strain. At 60 h, the total viable count of wild type *V. cholerae* CytR+ strain in mucin supplemented media was 5.57×10^8 CFU/ml, whereas it was 3.18×10^7 CFU/ml in the CytR- mutant strain, showing a 17.5-fold difference in growth. The complemented CytRᶜ strain showed similar growth as of the wild-type CytR+ strain in mucin supplemented media. In contrast, all the strains showed an almost similar growth

pattern in presence of sodium lactate supplemented M9 minimal media in absence of mucin *(Fig. 5.1A)* which indicates equal fitness of all the strains. This result indicates *V. cholerae* could utilize mucin as the sole nutrient source and CytR contributes in utilizing it.

5.2. CytR plays an important role in motility and mucin penetration in V. cholerae
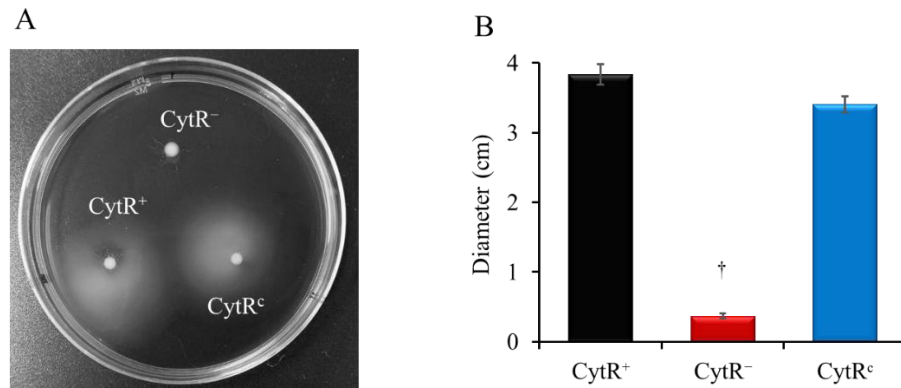
Fig. 5.2. Surface motility in *V. cholerae* is affected by CytR. CytR⁺ (wild type), CytR⁻ (isogenic CytR mutant), and CytRᶜ (CytR⁻ strain complemented with CytR clone) were grown separately in LB broth till mid-log phase. 1 µl of 5×10^8 CFU/ml different bacterial samples were spotted on 0.3% agar plates containing 0.4% mucin. Plates were incubated at 37°C for 18 h. **(A)** Plate showing motility zone of different bacteria. **(B)** The diameter of bacterial surface motility zones is graphically represented as mean ± SEM by measuring the zone of three independent biological replicates. Each of the experiments was repeated three times (n=3); †, P-value <0.05

We investigated the surface motility of different *V. cholerae* strains on soft agar mucin plates. We found that CytR⁻ strain showed reduced motility with a zone of 0.36 ± 0.03 cm, whereas CytR⁺ strain showed a motility zone of 3.8 ± 0.14 cm *(Fig.5.2A, 5.2B)*. Therefore, the motility of CytR⁻ strain was reduced to 10.5-fold compared to the CytR⁺ strain. The complemented CytRᶜ strain showed a similar motility zone of 3.4 ± 0.11 cm when compared to the wild-type strain.

Further, *in vitro* mucin layer penetration experiment supports the above observation. Here we have studied the time-dependent mucin penetrating ability of *V. cholerae* in different concentrations of mucin in a mucin column. Our observation showed that motility of CytR⁻ *V. cholerae* strain decreased severely in all the conditions.
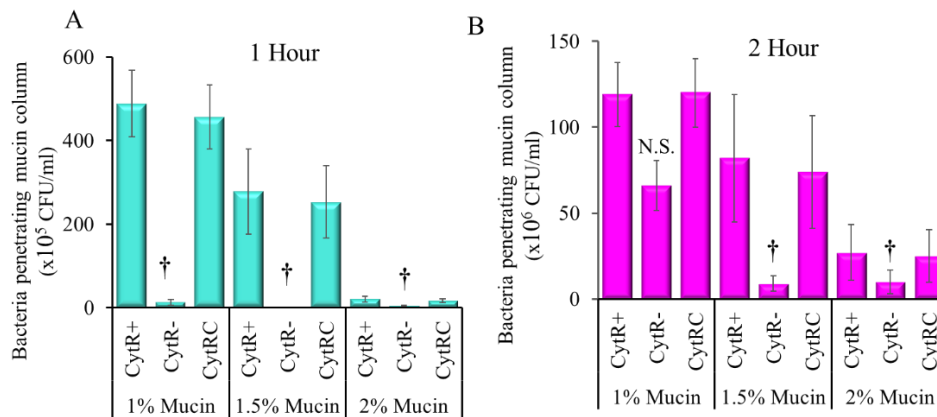
Fig. 5.3. Mucin penetration is promoted by CytR in *V. cholerae*. CytR$^+$ (wild type), CytR$^-$ (isogenic CytR mutant), and CytR^c (CytR$^-$ strain complemented with CytR clone) were grown separately in LB broth till mid-log phase. 100µl of 5×10^8 CFU/ml bacterial culture CytR$^+$ (wild type), CytR$^-$ (isogenic CytR mutant), and CytR^c (CytR$^-$ strain complemented with CytR clone) were loaded on top of the 1ml mucin column of containing 1%, 1.5% and 2% porcine mucin. Bacterial samples of 100µl were collected from the bottom of the column after 1 h (■) **(A)** or 2 h (■) **(B)** incubation at 37°C. The samples were serially diluted and plated on LB agar supplemented with proper antibiotics and the bacterial numbers were counted and graphically represented. Each of the experiments was repeated three times (n=3) and the data were expressed as Mean ± SEM; †, P-value <0.05

Out of total 5×10^8 CFU/ml bacteria loaded on top of the mucin column, 4.89×10^7 CFU/ml, 2.72×10^7 CFU/ml, and 2.1×10^6 CFU/ml wild type CytR$^+$ bacteria were able to penetrate through the 1%, 1.5 %, and 2% mucin column respectively after 1 h incubation *(Fig.5.3A)*. However, only 1.3×10^6 CFU/ml, 2×10^5 CFU/ml, and 2×10^5 CFU/ml mutant CytR$^-$ bacteria were able to penetrate the 1%, 1.5%, and 2% mucin column respectively. This clearly showed that CytR$^-$ strain was 37.6-fold, 136-fold, and 10.5-fold less competent in motility than the wild-type bacteria respectively in 1%, 1.5%, and 2% mucin columns. CytR^c strain showed almost similar mucin penetrating ability compared to the CytR$^+$ strain.

Again, out of total 5×10^8 CFU/ml bacteria loaded on top of the mucin column, 11.9×10^7 CFU/ml, 8.2×10^7 CFU/ml, and 2.7×10^7 CFU/ml wild type CytR$^+$ bacteria were able to penetrate through the 1%, 1.5 %, and 2% mucin column respectively after 2 h incubation *(Fig.5.3B)*. However, only 6.6×10^7 CFU/ml, 9×10^6 CFU/ml, and 10×10^6 CFU/ml mutant CytR$^-$ bacteria were able to penetrate the 1%, 1.5%, and 2% mucin column respectively. This clearly showed that CytR$^-$ strain was 1.8-fold, 9.1-fold, and

2.7-fold less competent in motility than the wild-type bacteria respectively in 1%, 1.5%, and 2% mucin column. Here also CytR^c strain showed almost similar mucin penetrating ability compared to the CytR$^+$ strain.

5.3. CytR in V. cholerae plays an important role in adhesion to epithelial cells
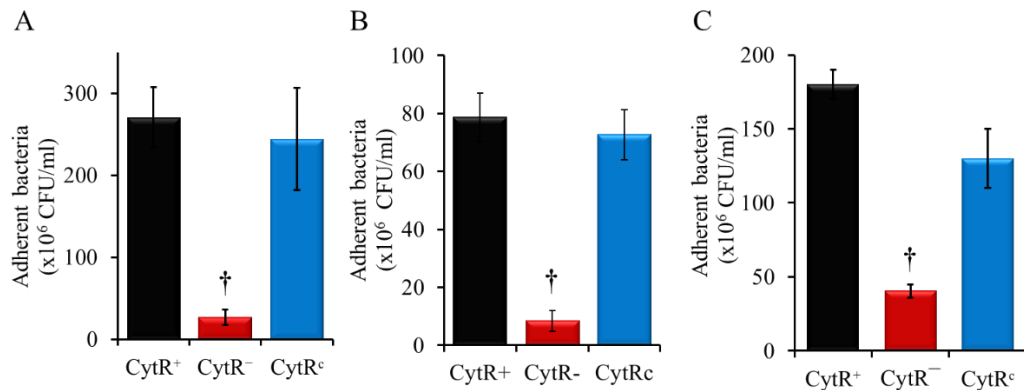
Fig.5.4. CytR plays an important role in the adhesion of *V. cholerae* with the epithelial cells. All three experimental strains were grown to mid-log phase and optical density was adjusted to 1. Tissue culture cell line was grown in 12-well cell culture plate to 80% confluency. The cell line was then infected at 100 MOI. After incubation at humidified 37°C incubator for 1 h, cell culture plate was washed with PBS to remove unbound bacteria and bound bacteria were collected and enumerated by plating on streptomycin supplemented LB agar. **(A)** Graphical representation of different strains of *V. cholerae* bound to the colon carcinoma cell line HT-29 under cell culture conditions, **(B)** Graphical representation of different strains of *V. cholerae* bound to intestinal Caco2 cell line under cell culture conditions, **(C)** Bacterial adhesion was assayed from the samples recovered from *in-vivo* rabbit ileal loop tissue samples, where the bound bacterial count was determined after washing and homogenizing the tissue samples. Bound bacteria were collected, plated, and the number of bacteria was enumerated by the plate count method. Each of the experiments was repeated three times (n=3) and the data were expressed as Mean ± SEM; †, P-value <0.05

Further, we have studied the effect of CytR in adherence capability of *V. cholerae* to the mucin secreting intestinal epithelial cell line, HT-29, and Caco2 in tissue culture conditions. Adherent wild-type CytR$^+$ *V. cholerae* strain count after one-hour incubation with HT-29 cell was 2.7×10^8 CFU/ml, whereas CytR$^-$ strain was 2.6×10^7 CFU/ml *(Fig.5.4A)*. Therefore, CytR$^-$ *V. cholerae* strain was 10.5-fold less adherent with HT-29 cells than the wild type. CytR^c complemented strain showed similar adhering ability when compared to the wild-type CytR$^+$. GFP- labeled CytR$^-$ mutant bacteria were less visible in adhered form when compared to the wild-type CytR$^+$ strain under fluorescence microscopy *(Fig.5.5)*, whereas complemented CytR^c strain adhered

similarly like the wild type *V. cholerae*. This adherence study was also done in intestinal cell line Caco2. Similar results were also observed here. After one hour of incubation with Caco2, the adhered wild-type CytR$^+$ *V. cholerae* count was 7.8×10^7 CFU/ml, whereas CytR$^-$ strain was 8×10^6 CFU/ml *(Fig.5.4B)*. Therefore, CytR$^-$ *V. cholerae* strain was 9.7-fold less adherent with Caco2 cells than the wild type. CytR^c complemented strain showed similar adhering ability when compared to the wild-type CytR$^+$.

We further tested the adherence in rabbit ileal loop conditions. Our result suggested that 1.8×10^8 CFU/ml wild-type CytR$^+$ *V. cholerae* adhered to the intestinal lumen *(Fig.5.4C)*. In contrast, only 4.0×10^7 CFU/ml CytR$^-$ bacteria were adherent, showing ~ 4.5-fold decrease in adherence efficiency of the CytR$^-$ mutant compared to the wild-type bacteria. CytR^c complemented strain adhered similarly to the wild-type CytR$^+$.
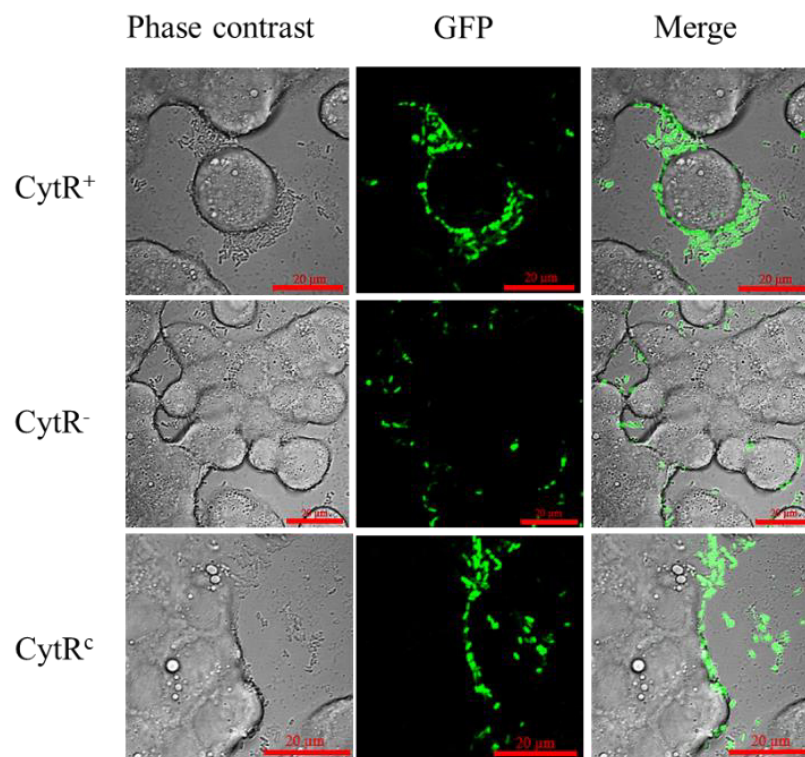
Fig.5.5. Representative photograph of fluorescence microscopy of *V. cholerae*'s adhesion to the HT-29 cell line. All three experimental strains were transformed with ampicillin-resistant GFP expressing plasmid pGFPuv and were grown to mid-log phase and optical density was adjusted to 1. HT-39 cell line was grown on a cover-slip in 35mm cell culture dishes to 80% confluency. The cell line was then infected with at 100 MOI. After incubation at 5% humidified 37°C CO$_2$ incubator for 1 h, the cell culture coverslip was washed with PBS to remove unbound bacteria and the bound bacteria were mounted to a glass slide to view under the fluorescence microscope. Scale: Red bar equals 20 µm.

5.4. CytR plays a role in V. cholerae ex vivo survival

Growth phenotype study of *V. cholerae* in mucin supplemented minimal media suggested that *V. cholerae* utilized mucin as a nutrient source. When *V. cholerae* was incubated for 16 h with HT-29 and Caco2 cell line which is human intestinal cell line specializing in synthesis and secretion of mucin, the multiplication of the wild type CytR+ cells were 3-fold more than that of the CytR− mutant bacteria when incubated with 5×10^5 bacteria *(Fig. 5.6)*. The complemented strain grew normally indicating a reversal of the phenotype. However, in the Caco2 cell line, the growth difference between the wild type and mutant bacteria did not reduce significantly.
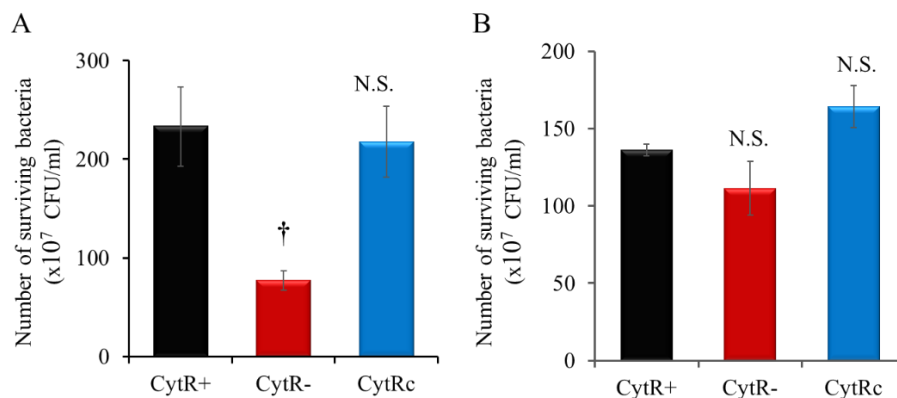
Fig.5.6. Role of CytR in *V. cholerae ex-vivo* proliferation. Comparative study of the survival of the wild type and isogenic ΔCytR mutant in human intestinal **(A)** HT-29 and **(B)** Caco2 cell line in cell culture conditions. The incubation was done at humidified 37°C incubator for 16 h. Then, both the bound and unbound bacteria were removed and enumerated by plating on streptomycin supplemented LB agar. Each of the experiments was repeated three times (n=3) and the data were expressed as Mean ± SEM; †, P-value <0.05; N.S. Not Significant.

5.5. CytR mutant shows colonization defect in suckling mice

Bacterial binding to intestinal epithelial cells facilitates bacterial colonization in the intestine. We have already shown that the CytR− strain is defective in adhesion to the *ex vivo* epithelial cells in cell culture conditions. To further examine the role of CytR in colonization, we used the 5-6 days old suckling mice for the intestinal colonization ability of the mutant CytR− strain along with complemented CytR^c and the wild type *V. cholerae* N16961 (CytR+LacZ−). During bacterial infection, the input ratio of mutant (CytR−) to wild type N16961 (CytR+LacZ−) was 1:1. CytR− strain showed an output

ratio (Competitive Index, CI) (CytR⁻ LacZ⁺/ CytR⁺ LacZ⁻) of 0.034 ± 0.01 at 18 h post-infection *(Fig. 5.7)*. Whereas, CI between CytR⁺ LacZ⁻/ CytR⁺ LacZ⁺ was 0.84 ± 0.06, indicating no or negligibly low fitness defect of the LacZ⁻ mutant strain over wild type LacZ⁺ *V. cholerae*. This clearly indicates that deletion in CytR in *V. cholerae* significantly decreased its colonization fitness to 24.5-fold. In contrast, complemented CytRᶜ strain showed CI, CytRᶜ LacZ⁺/ CytR⁺ LacZ⁻ value of 0.71 ± 0.07 with almost no competitive disadvantage. Taken together, this indicated that the CytR⁺ strain outcompeted CytR⁻ strain in the infant mice colonization. Therefore, we concluded that *V. cholerae* CytR contributes to intestinal colonization.
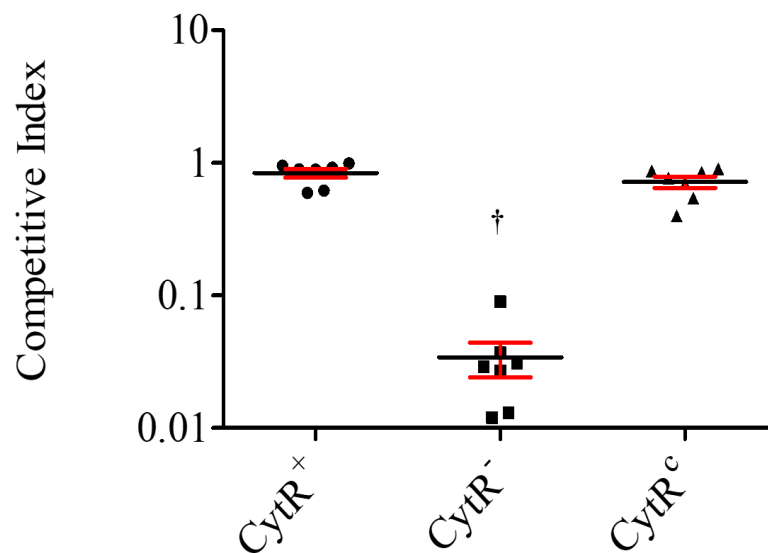
Fig.5.7. Colonization of *V. cholerae* in the infant mice intestine is affected by CytR. Competitive indices of CytR deletion mutant shows less colonization fitness compared to wild type *V. cholerae*. Comparative colonization studies of three experimental strains were done in 5-6 days old suckling mice. 50µl of 5× 10^8 CFU/ml bacteria of *V. cholerae* (LacZ⁻) strain were mixed at a ratio of 1:1 with each of the strains i.e., CytR⁺ (LacZ⁺), CytR⁻ (LacZ⁺) and CytRᶜ (LacZ⁺) and orally gavaged to each mouse. After 18 h incubation, mouse intestine was harvested, washed, homogenized, serially diluted, and plated on LB agar. The competitive index (CI) was calculated and plotted to represent in the graph. CI = ratio out(mutant/wild-type)/ratio in(mutant/wild-type). Each data point represents an individual animal infected with *V. cholerae*. Seven animals were sacrificed in each set. Horizontal bars indicate the mean ± SEM. CI<1 indicates fitness defect; CI>1 indicates increased fitness, whereas CI≈1 indicates no fitness defect. Experiments were done in seven biological replicates (n=7) and the data were expressed as Mean ± SEM; †, P-value <0.05

5.6. CytR depletion in V. cholerae results in reduced fluid accumulation in rabbit intestine

Till now, we have shown that CytR affects *V. cholerae* colonization efficiency. In this experiment, we have quantitatively shown and measured the intestinal fluid accumulation in ligated rabbit ileal loop model by evaluating the FA ratio *(Fig.5.8)*.

In this experiment, we have measured the amount of fluid secreted per unit area (FA ratio) in each loop 18 h post-infection. Loop Infected with CytR⁻ strain showed 3-fold less fluid accumulation compared to the wild-type CytR⁺ strain *(Fig.5.8)*. Infection with CytRᶜ complemented strain showed fluid accumulation similar to CytR⁺. This indicated that CytR is involved in fluid accumulation in the host intestine, which is one of the critical aspects of *V. cholerae* pathogenesis.
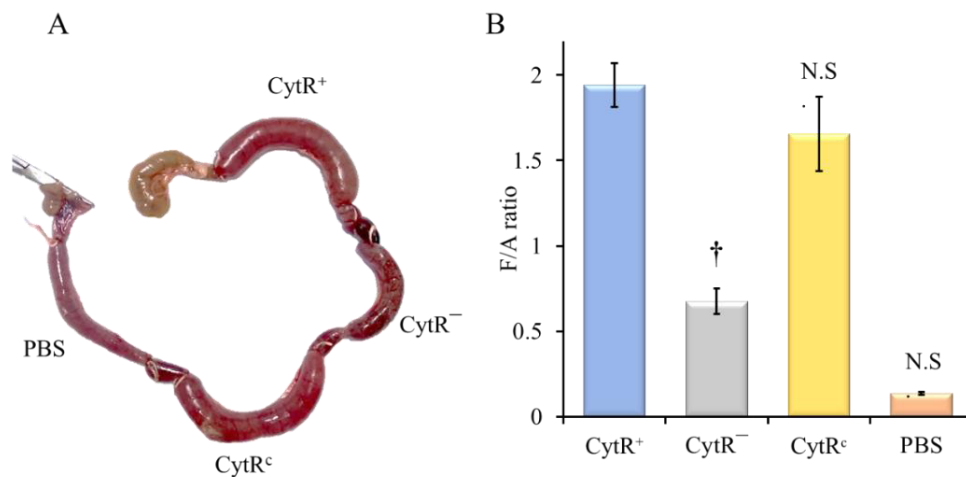
Fig.5.8. Fluid accumulation studies of the rabbit intestine. All *V. cholerae* experimental strains i.e., CytR⁺ (wild type), CytR⁻ (isogenic CytR mutant), and CytRᶜ (CytR⁻ strain complemented with CytR clone) were grown separately in LB broth till mid-log phase, and O.D. was adjusted to 1.0 and 1 ml of 10^9 CFU/ml were inoculated in each of the ligated loops of rabbit intestine. **(A)** Retrieved rabbit intestinal portion showing infected loop 18 h post-infection. Each loop was separated by an uninfected interloop region. A negative control loop was inoculated with PBS. **(B)** The fluid accumulation ratio in the rabbit intestine of three different experiments was measured and represented graphically as mean ± SEM.†, P-value <0.05; N.S. Not Significant.

5.7. CytR plays a role in Cholera Toxin (CT) production in V. cholerae

Next, we analyzed Cholera Toxin (CT) production, which is primarily responsible for fluid accumulation in the rabbit intestine. We found that the rabbit ileal loop samples infected with CytR⁻ mutant contained 3-fold less CT (215 ng/ml) than the fluid from wild-type CytR⁺ infected loop (665 ng/ml) *(Fig.5.9B)*. Fluid from CytRᶜ

infected loop showed similar CT (574 ng/ml) production compared to the wild type. *In-vitro,* AKI-bicarbonate grown *V. cholerae* culture also showed similar results where the mutant CytR⁻ culture produced 3.8-fold less CT compared to wild type culture *(Fig. 5.9A).* Complemented CytRᶜ strain in this case also did not show much difference in CT production compared to wild type *V. cholerae.*
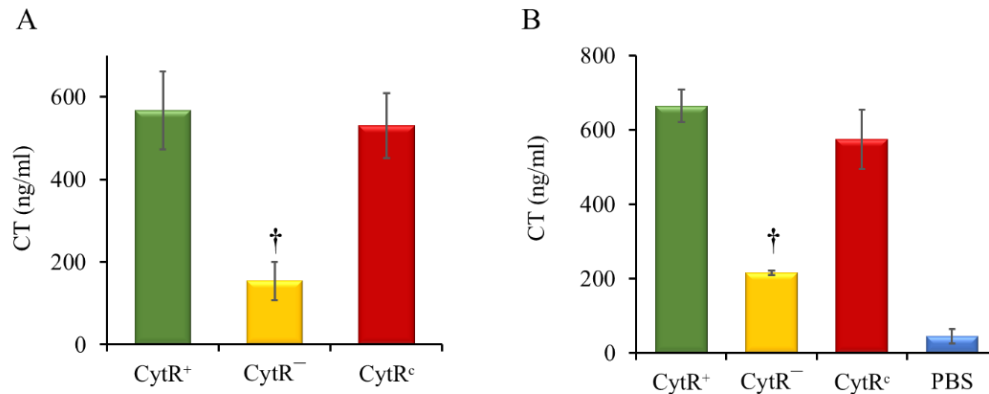
Fig.5.9. Cholera toxin production is affected by CytR mutation. (A) Log phase cultures of *V. cholerae* experimental strains were inoculated (1:100) in AKI media and grown statically at 37°C for 18 h. Culture supernatant was collected, Cholera Toxin (CT) was measured by ELISA and represented graphically. **(B)** *In-vivo* CT production was also measured by ELISA from the accumulated fluid samples of ligated rabbit ileal loops. Each of the experiments was repeated three times (n=3) and the data were expressed as Mean ± SEM; †, P-value <0.05

5.8. CytR regulates other virulence-associated genes
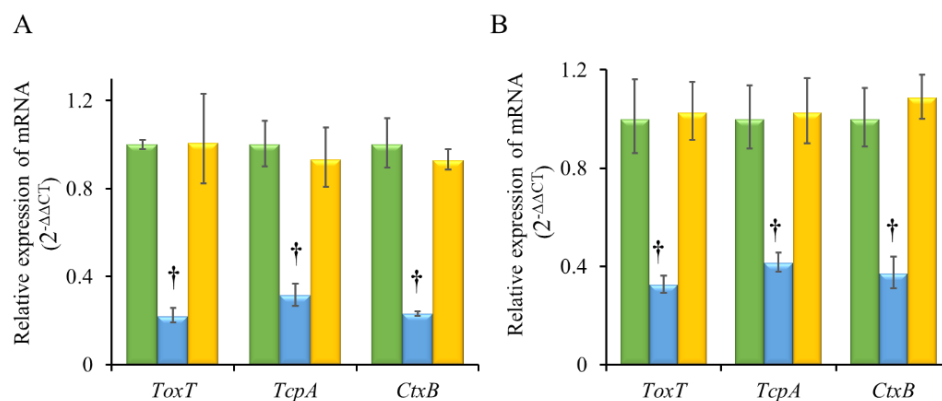
Fig.5.10. Virulence gene expression is affected by isogenic deletion mutation of CytR. (A) Relative expression of virulence genes from rabbit ileal loop samples CytR⁺ (wild type) (🟩), CytR⁻ (isogenic CytR mutant) (🟦) and CytRᶜ (CytR⁻ strain complemented with CytR clone) (🟨) was measured by qRT-PCR. **(B)** Bacterial RNA from AKI-grown culture was also harvested and processed. Data were represented by the comparative $\Delta\Delta C_T$ method, using *recA* as an internal control. Each of the experiments was repeated three times (n=3) and the data were expressed as Mean ± SEM; †, P-value <0.05

Since we found differential colonization, less fluid accumulation, and less toxin production in the rabbit intestine, we then measured and analyzed the expression level of different virulence genes (*toxT*, *tcpA,* and *ctxB*) by qPCR. We found expression of these genes was significantly reduced by 5-fold, 3.5-fold, and 4.5-fold respectively in CytR⁻ mutant infected ileal loop samples relating to the infection with wild-type *V. cholerae (Fig.5.10A)*. Similarly, in AKI media, CytR⁻ strain showed a significant decrease in RNA levels of these virulence genes by 3-fold, 2.5-fold, and 2.5-fold respectively for *toxT*, *tcpA* and *ctxB* genes *(Fig.5.10B)*. CytR^c strain showed *toxT*, *tcpA,* and *ctxB* RNA levels like the CytR⁺ strain.

5.9. CytR mutant causes less damage to the rabbit intestine compared to the infection with wild type V. cholerae
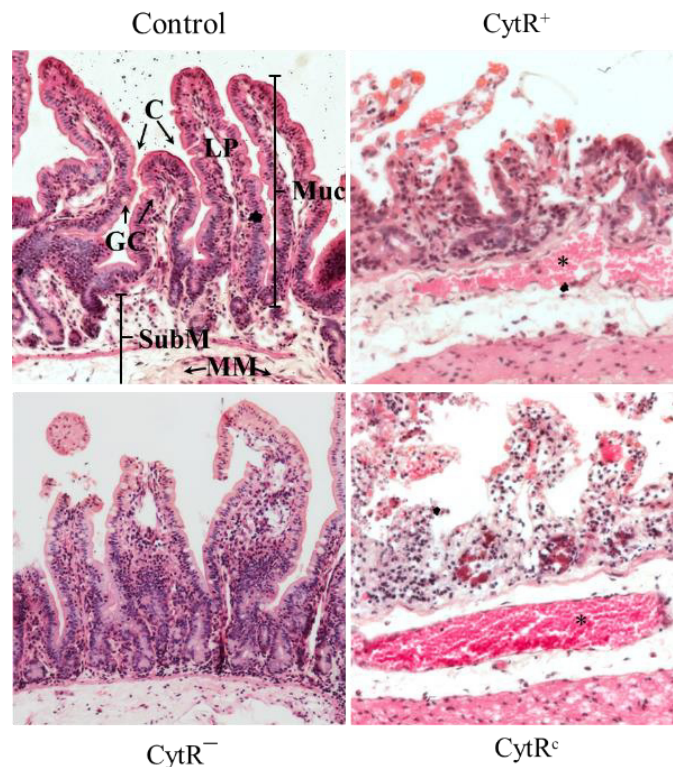
Fig.5.11. Histological examination of rabbit intestine showed CytR mutant infected loop causes less damage to the intestinal lining. All *V. cholerae* strains CytR⁺ (wild type), CytR⁻ (isogenic CytR mutant), and CytR^c (CytR⁻ strain complemented with CytR clone) were grown separately in LB broth till mid-log phase and O.D. was adjusted to 1.0 and 1 ml of 10⁹ CFU/ml were inoculated in each of the ligated loops of rabbit intestine. 18 h post-infection tissue sections from each loop were collected, processed, and stained with Haematoxylin and Eosin. Representative images were taken under a 20X objective lens. PBS treated ileal loop was considered as control. C, Crypts; GC, Goblet Cells; LP, Lamina Propria; Muc, Mucosa; MM, Muscularis Mucosae; SubM, Submucosa, *, indicating the site of haemorrhage.

The intestinal fluid accumulation assay result encouraged us to investigate the microscopic changes of the rabbit intestinal tissues. Histological staining of rabbit ileum showed that the wild-type CytR$^+$ strain of *V. cholerae* caused gross structural alteration with distorted villus epithelium, extensive damage to mucosa, sub-mucosa, and lamina propria were seen *(Fig.5.11)*. Haemorrhage in muscularis mucosa was also seen. CytR$^-$ strain treated loop section showed almost normal villi structure. Although dilated and extended lamina propria with scattered haemorrhagic changes were observed. Mucosa and sub-mucosal layers also did not show much noticeable change. Complemented CytR^c strain treatment showed a similar effect on villi and mucosal structure alike wild type *V. cholerae* treatment. PBS treated ileal loop tissue showed normal crypts and villi structure and did not show any alteration to the gut mucosae.

5.10. Sensor histidine kinase ChiS and chitinases are positively controlled by CytR both in vitro and in vivo conditions
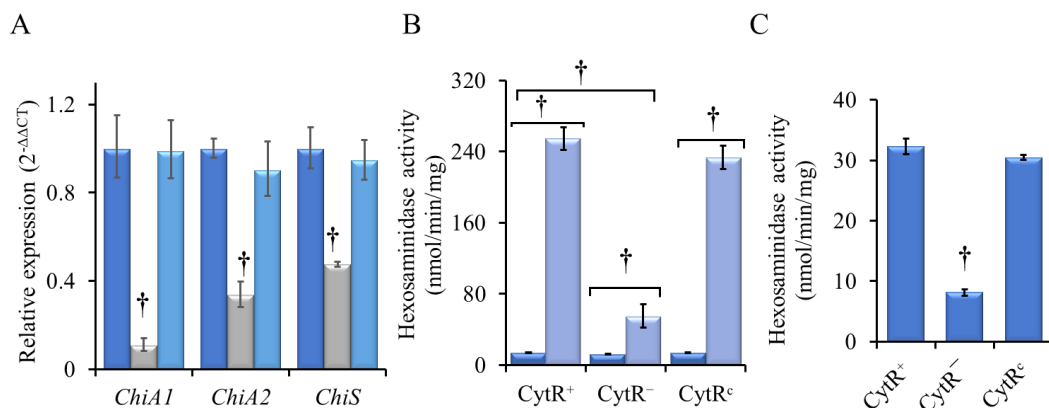
Fig.5.12. *V. cholerae* CytR regulates the expression and activity of chitinases and sensor histidine kinase. (A) CytR affects the expression of *V. cholerae* chitinase *chiA1*, *chiA2,* and sensor histidine kinase *chiS* gene. *V. cholerae* strains, CytR$^+$ (wild type) (■), CytR$^-$ (isogenic CytR mutant) (■) and CytR^c (CytR$^-$ strain complemented with CytR clone) (■) were grown in 1% porcine mucin supplemented M9 minimal media. Bacterial samples were collected from the mid-log phase and RNA was isolated using the TriZol method. mRNA transcript levels were analyzed by qRT-PCR and graphically represented, using *recA* as an internal control gene. **(B)** CytR regulates the activity of the hexosaminidase enzyme by means of activating ChiS in presence of mucin. All bacterial strains of *V. cholerae* were grown in M9 minimal media with 0.5% sodium lactate in the presence (■) or absence (■) of 1% porcine mucin. Total hexosaminidase enzyme activity was measured by taking log-phase cultures. **(C)** *V. cholerae* CytR affects β–hexosaminidase activity *in-vivo.* β–hexosaminidase enzyme activity was performed from the accumulated fluid samples collected after 18 h of infection. Each of the experiments was repeated three times (n=3) and the data were expressed as Mean ± SEM; †, P-value <0.05

The activity of periplasmic two-component chitin sensing histidine kinase, ChiS is measured by the amount of production of β-hexosaminidase enzyme per unit time per mg of protein, located downstream of ChiS. Total β-hexosaminidase enzyme activity in all the *V. cholerae* strains in the presence or absence of 1% mucin as a sole nutrient source was measured here. The activity of hexosaminidase enzyme in wild-type CytR⁺ strain in presence of mucin was 255 nmol/min/mg, whereas in CytR⁻ mutant strain it was 55 nmol/min/mg. CytR⁻ mutant strain was 4.6-fold less hexosaminidase activity than the wild-type CytR⁺ strain *(Fig.5.12B)*. However, the enzyme activity was negligibly small in absence of mucin in all the strains, suggesting that it is triggered in presence of mucin. On the other hand, complemented CytRᶜ strain also showed comparable hexosaminidase enzyme activity with respect to the CytR⁺ strain in presence of mucin *(Fig.5.12B)*. Furthermore, RNA expression of *chiS* in mucin supplemented M9 minimal media gets 2-fold downregulated in CytR⁻ mutant strain *(Fig.5.12A)*. Expression of chitinase genes *chiA1* and *chiA2* both gets downregulated by 10 and 3.5-fold respectively in presence of mucin *(Fig.5.12A)*.

The total activity of β–hexosaminidase was assessed with each of the strains inoculated in rabbit ileal loops. This was to evaluate whether sensor histidine kinase ChiS is also inducted by CytR in *in-vivo* conditions. In wild-type CytR⁺ strain β–hexosaminidase activity was 32 nmol/min/mg whereas the CytR⁻ strain showed activity of 8 nmol/min/mg *(Fig.5.12C)*. The CytR⁻ strain, therefore, showed 4-fold lower hexosaminidase activity compared to the wild-type CytR⁺. Induction of β–hexosaminidase activity in CytRᶜ strain was alike CytR⁺ strain. So, this indicates that CytR plays a necessary role in β–hexosaminidase activity and hence is critical for ChiS activation in the host intestine and cause pathogenesis.

5.11. CytR is essential for V. cholerae to synthesize its single monotrichous polar flagella

To further investigate the reason behind the reduced motility of CytR⁻ strain in mucin media we have done negative-stain transmission electron microscopy to check morphology of wild type CytR⁺ strain of *V. cholerae* and the mutant CytR⁻ strain. Interestingly CytR ablated *V. cholerae* strain appeared to be aflagellate. On the other hand, wild-type CytR⁺ strain showed normal flagella *(Fig.5.13A)*.
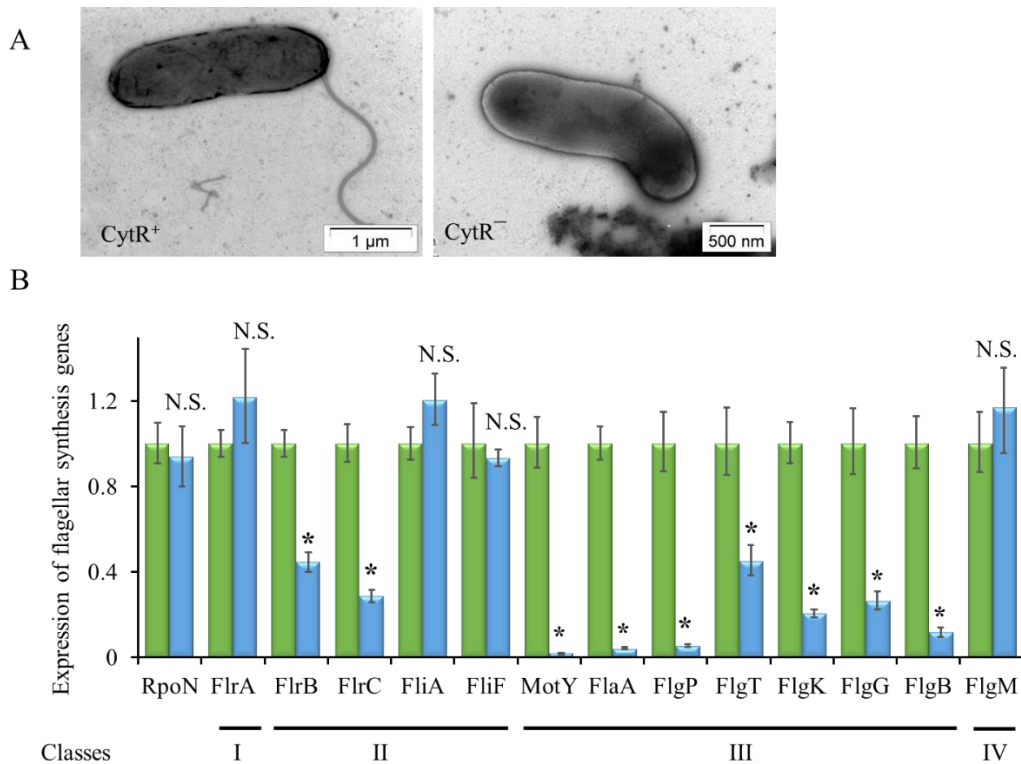
Fig. 5.13. Synthesis of flagella in *V. cholerae* is CytR dependent. (A) Representative electron micrographs of negatively stained *V. cholerae* strains CytR⁺ (wild type) (left) and CytR⁻ (isogenic CytR mutant) (right) in LB broth till mid-log phase. **(B)** Mid log phase *V. cholerae* cultures CytR⁺ (wild type) (🟩) and CytR⁻ (isogenic CytR mutant) (🟦) were subjected to RNA isolation using TriZol method and mRNA transcript levels of different flagellar synthesis genes were analyzed by qRT PCR and graphically represented, using *recA* as internal control gene. Each of the experiments was repeated three times (n=3) and the data were expressed as Mean ± SEM; †, P-value <0.05

qRT-PCR analysis of flagellar synthesis genes in CytR⁻ strain indicated decreased expression of *flrB*, a histidine kinase, and *flrC,* its response regulator by 2.3-fold and 3.5-fold, respectively *(Fig.5.13B)*. Transcriptional levels of *flrA,* master regulator and *rpoN,* alternate sigma factor remained unchanged in the mutant strain. FlrA and σ⁵⁴ -dependent transcription of other Class II genes like *fliF* (forms structural unit of MS ring) and alternate sigma factor σ²⁸, *fliA* showed no change in CytR⁻ strain when compared to the wild type *V. cholerae*. Class III genes studied here showed reduced expression in mutant strain. 55-fold, 24-fold, and 19-fold reduction in mRNA expression was observed for, *motY* (forms T ring), *flaA* (main flagellin subunit), and *flgP* (associated with H ring) genes. Other class III genes, *flgT* (H ring component), *flgK* (associated with hook-filament junction), *flgG* (distal rod), *flgB* (proximal rod)

were down by 2.2-fold, 5-fold, 4-fold, and 9-fold, respectively. However, in the mutant strain flgM, an anti-sigma factor whose transcription is σ^{28}-dependent showed no change in RNA level in CytR mutant.

5.11. Whole-genome transcriptome analysis showed CytR is important for many biological functions in V. cholerae

Till now, we have observed the role of CytR in various aspects of the pathogenesis of *V. cholerae*. To further investigate the role of this Cytoplasmic regulatory protein CytR we have done whole-genome transcriptome study taking the wild type O1 El tor N16961 *V. cholerae* and CytR deleted *V. cholerae* strain.
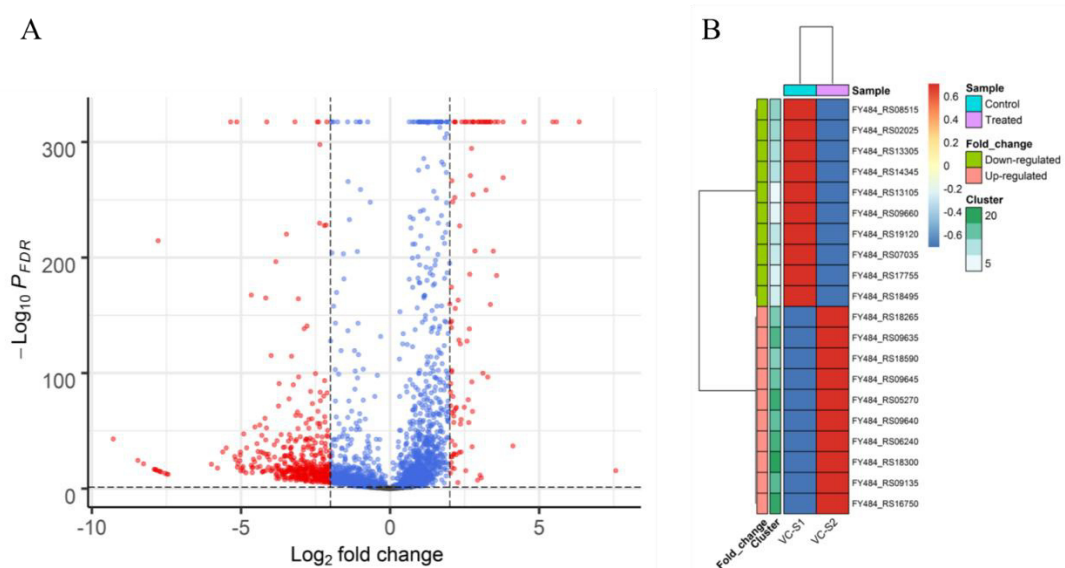
Fig.5.14. (A) Volcano plot between wild-type CytR⁺ and mutant CytR⁻ *V. cholerae* showing differential gene expression. Each point represents a specific gene in the genome, among them few genes show significant differences in fold change (●, $Log_2FC \geq 2$ and $P_{FDR} \leq 0.05$), and rest genes show lesser fold changes (●, $P_{FDR} \leq 0.05$) **(B)** Heat Map of top and bottom 10 genes of treated samples of *V. cholerae*; FC, Fold Change; FDR, False Determination Rate.

Transcriptome study showed among 3217 variable genes, 94 genes are upregulated ($Log_2FC > 2$) and 428 genes are downregulated ($Log_2FC < 2$) upon deletion of CytR *(Fig.5.14A)*. Among all these genes the top ten upregulated and downregulated genes are listed in the following figure *(Fig.5.14B)*.

Fold Change	Gene
5.582	uridine phosphorylase (udp-1)
5.457	cytidine deaminase (cdd)
3.788	C4-dicarboxylate-binding periplasmic protein (dctP-1)
3.613	outer membrane protein OmpW (ompW)
3.516	2`,3`-cyclic-nucleotide 2`-phosphodiesterase (cpdB)
3.372	aspartate ammonia-lyase (aspA)
3.366	threonine 3-dehydrogenase (tdh)
3.182	glycine cleavage system H protein (gcvH)
3.112	glycine cleavage system T protein (gcvT)
2.950	fumarate reductase, 15 kDa hydrophobic protein (frdC)
2.815	fumarate reductase, 13 kDa hydrophobic protein (frdD)
2.781	C4-dicarboxylate transporter, anaerobic (dcuC)
2.658	carbamoyl-phosphate synthase, large subunit (carB)
2.655	triosephosphate isomerase (tpiA)

Fold Change	Gene
-7.681	phosphate ABC transporter, permease protein (pstC-2)
-5.026	ribonuclease HII (rnhB)
-4.919	multidrug resistance protein D
-4.580	vibriobactin-specific isochorismatase (vibB)
-4.533	flagellar hook-associated protein FlgL (flgL)
-4.371	cholera enterotoxin, B subunit (ctxB)
-4.252	fimbrial assembly protein PilM, putative
-4.169	psp operon transcriptional activator (pspF)
-4.146	glucose-1-phosphate adenylyltransferase
-3.804	toxin co-regulated pilus biosynthesis protein T (tcpT)
-3.630	cadaverine/lysine antiporter CadB, putative
-3.599	phosphate ABC transporter, permease protein (pstA-1)
-3.377	chemotaxis protein CheD, putative
-3.369	cytochrome c-type protein TorC (torC)
-3.334	citrate (pro-3S)-lyase ligase (citC)
-3.317	flagellar protein FliL, putative
-3.289	lipid-A-disaccharide synthase (lpxB)
-3.280	2-aminoethylphosphonate:pyruvate aminotransferase (phnW)
-3.248	flagellar protein FliJ, putative
-3.115	sulfate ABC transporter, permease protein (cysT)
-3.075	citrate lyase, beta subunit (citE)
-3.057	regulatory protein RecX (recX)
-3.017	PTS system, fructose-specific IIA/FPR component (fruB)
-3.011	glycerol-3-phosphate ABC transporter, permease protein (ugpE)

Fig. 5.15. Whole-genome transcriptome analysis showing differential gene expression of few top upregulated (left column) and downregulated genes (right column) along with its fold change values.

This transcriptomic study confirms a previous report (Antonova et al., 2012; Watve et al., 2015) of upregulation of nucleoside scavenging genes like uridine phosphorylase (*udp-1*), cytidine deaminase (*cdd*) in CytR ablated *V. cholerae* strain. We have also found upregulation of several other genes related to C4-dicarboxylate (such as fumarate, succinate, L-malate, and D-malate)-binding periplasmic proteins, ribonucleic acid catabolism genes (*cpdB*), nutrient uptake, and metabolism-related genes (*aspA*, *tdh*, *gcvH/T*, *frdC/D*, *carB*, *tpiA*). On the contrary, genes that have been downregulated include different transporter genes (ABC transporter, permease), multidrug resistance protein (*mdrD*), flagella synthesis and assembly related genes (*flgL, fliL, fliJ*), cholera enterotoxin (*ctxB*), toxin co-regulated pilus biosynthesis protein (*tcpT*), chemotaxis genes (*cheD*) and others related to the metabolism of *V. cholerae* (*Fig.5.15*).

5.12. Inhibitor study to diminish V. cholerae virulence

V. cholerae uses multiple strategies to evolve itself by the frequent acquisition of extrachromosomal mobile genetic elements by horizontal gene transfer from other bacterial species and becomes drug-resistant (Narendrakumar et al., 2019). Traditional antimicrobials are usually bacteriostatic or bactericidal which may facilitate the emergence of MDR strains (Das et al., 2020; Verma et al., 2019). Therefore, alternative novel therapeutic approaches like the use of plant or herb extracts, bioactive phytochemicals, or the use of small molecules are in urgent need to fight against these pathogens by particularly targeting bacterial virulence factors.

In order to curb bacterial virulence during pathogenesis, we have selected different bioactive phytochemicals, sugars, small molecules, and chitinase inhibitors with varying functions on the growth, motility, adhesion, and cholera toxin (CT) production of *V. cholerae*. After a thorough literature study, the following inhibitors are used, Curcumin (CC), Carvacrol (CV), and Trans-cinnamaldehyde (TC) as phytochemicals; N-acetyl D-glucosamine (GlcNAc), Xylose, Xylitol, Allose and Mannitol as monosaccharide; Na-3-hydroxy Butyrate (3HB) and NH125 as small molecule; Pentoxifylline (PEN), Caffeine (CF), Dequalinium chloride (DQ) and Theophylline (TH) as Family 18 chitinase inhibitor.

5.13. Effect of the inhibitors on V. cholerae growth

Initially, we aim to determine the nature of the inhibitors whether they possess any growth inhibitory property or not. The growth study of *V. cholerae* showed that only curcumin (at 200 µg/ml) supplemented culture media does not inhibit the growth of *V. cholerae* when compared to the control. On the other hand, Carvacrol and Trans-cinnamaldehyde inhibit the growth at 150 µg/ml and 200 µg/ml respectively *(Fig.5.16A)*. Monosaccharides or sugars are also used to check whether they possess any growth inhibitory function at 0.5% (w/v) supplementation. All the sugars that are studied here (namely, Xylose, Xylitol, Allose, Mannitol, and GlcNAc) do not have any effect on the growth of *V. cholerae (Fig.5.16B)*. We have also checked the effect of two small molecules, Na-3-Hydroxy Butyrate (3HB) and NH125. Out of which only NH125 at 20µg/ml concentration showed growth inhibition. On the other hand, Sodium-3-hydroxy butyrate even at 250µg/ml did not show any growth inhibition *(Fig.5.16C)* in the culture medium. Few Family-18 chitinase inhibitors are also studied. Where,

Theophylline (TH), Pentoxifylline (PEN), and Caffeine (CF) do not possess any growth difference when compared to the control. Only Dequalinium chloride at 200µg/ml concentration possesses growth inhibition *(Fig.5.16D).*
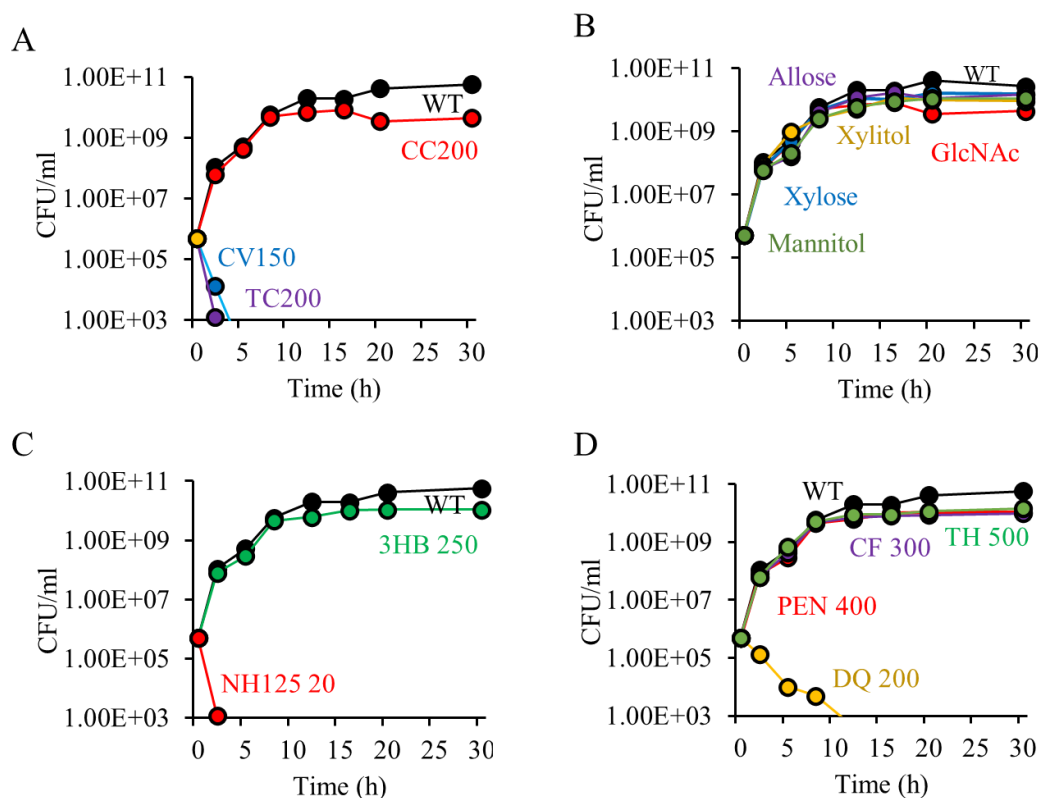
Fig. 5.16. *V. cholerae* **growth assay.** Wild type *V. cholerae* N16961 was given as an initial inoculum of 5×10^5 CFU/ml in the Luria-Bertani broth medium along with different inhibitors. The viable bacterial counts in CFU/ml were detected by plate count method taking culture samples from different time points and represented graphically. **(A) Phytochemicals** used CC, Curcumin; CV, Carvacrol; TC, Trans-cinnamaldehyde. **(B) Monosaccharides** used Xylose, Xylitol, Allose, Mannitol, and N-acetyl-D-Glucosamine (GlcNAc). **(C) Small molecules** used Na-3-Hydroxy Butyrate (3HB) and NH125. **(D) Chitinase inhibitors** used Pentoxifylline (PEN), Caffeine (CF), Dequalinium chloride (DQ), and Theophylline (TH).

5.14. Effect of the inhibitors on mucin penetrating ability of V. cholerae

Next, we have analyzed the Mucin penetrating ability of *V. cholerae* in presence of different compounds. Curcumin (CC) treated *V. cholerae* did not show any effect on mucin penetrating ability of *V. cholerae*; on the other hand, Carvacrol (CV) at 75µg/ml and Trans- cinnamaldehyde (TC) at 100µg/ml treated mucin column showed reduced mucin penetrating ability by 12-fold and 5-fold respectively *(Fig.5.17A).* Monosaccharides are also used to check whether they possess any motility inhibitory function. Results suggest that GlcNAc, Xylose, and Xylitol does not have much effect.
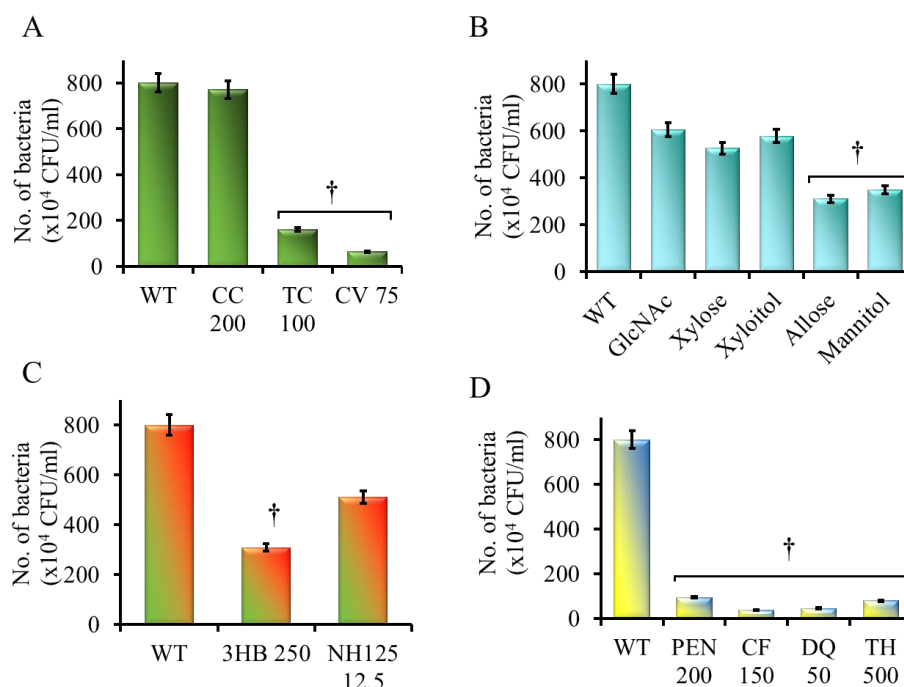
Fig.5.17. *In vitro* mucin penetration assay. Wild type *V. cholerae* N16961 was grown in LB broth till mid-log phase. 100µl of 5×10^8 CFU/ml bacterial culture were loaded on top of the 1.5% 1ml mucin column with or without the inhibitors. Bacterial samples of 100µl were collected from the bottom of the column after 1 h incubation at 37°C. The samples were serially diluted and plated on LB agar supplemented with proper antibiotics and the bacterial numbers were counted and graphically represented. **(A)** Effect of Phytochemicals **(B)** Effect of Monosaccharides **(C)** Effect of Small molecules and **(D)** Effect of Chitinase inhibitors. Each of the experiments was repeated three times (n=3) and the data were expressed as Mean ± SEM; †, P-value <0.05

But treatment with 0.5% Allose and 0.5% Mannitol reduced mucin penetration by 2.6-fold and 2.3-fold respectively *(Fig.5.17B)*. Sodium-3-hydroxy butyrate (3HB) supplemented bacterial culture reduced mucin penetration by 2.5-fold. But NH125 at 12.5µg/ml did not show any mucin penetration inhibitory function *(Fig.5.17C)*. Finally, Pentoxifylline (PEN), Caffeine (CF), Dequalinium chloride (DQ), and Theophylline (TH) all possess significantly reduced mucin penetration ability of *V. cholerae* by 8.5-fold, 22-fold, 17-fold, and 10-fold respectively at 200µg/ml, 150µg/ml, 50µg/ml and 500µg/ml concentration *(Fig.5.17D)*.

5.15. Effect of the inhibitors on V. cholerae adhesion to HT-29 cell line

Next, we have studied the *V. cholerae* adherence ability to the mucin secreting colon-carcinoma cell line HT-29 in presence of these inhibitors. Curcumin (CC) at 200µg/ml and Trans-cinnamaldehyde (TC) at 50µg/ml treated bacterial culture showed

not much adherence defect to the HT-29. But Carvacrol (CV) treated *V. cholerae* showed a 72-fold adherence defect at 50 µg/ml concentration.
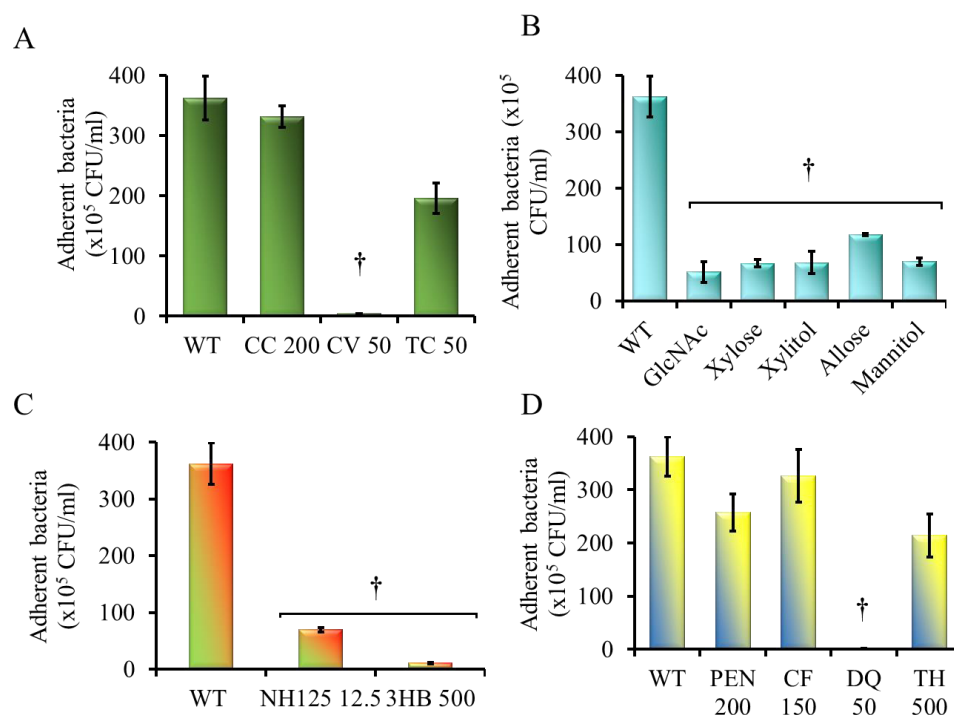
Fig.5.18. *Ex vivo* **adhesion assay of** *V. cholerae* **with HT-29 cell line in presence or absence of different inhibitors.** *V. cholerae* was grown to mid-log phase and optical density was adjusted to 1. HT-29 was grown in 12-well cell culture plate to 80% confluency. The cell line was then infected at 100 MOI of bacteria supplemented with or without the inhibitors. After incubation at humidified 37°C incubator for 1 h, cell culture plate was washed with PBS to remove unbound bacteria, and then bound bacteria were collected and enumerated by plating on streptomycin supplemented LB agar. **(A)** Effect of Phytochemicals **(B)** Effect of Monosaccharides **(C)** Effect of Small molecules and **(D)** Effect of Chitinase inhibitors. Each of the experiments was repeated three times (n=3) and the data were expressed as Mean ± SEM; †, P-value <0.05

All Monosaccharides studied here significantly reduced the adherence efficiency. It is reduced by 7-fold, 5.5-fold, 5.5-fold, 3-fold and 5.5-fold in 0.5% GlcNAc, 0.5% Xylose, 0.5% Xylitol, 0.5% Allose and 0.5% Mannitol respectively *(Fig.5.18)*. Sodium-3-hydroxy butyrate (3HB) at 500µg/ml supplemented bacterial culture reduced adherence of *V. cholerae* by 36 –fold and NH125 at 12.5µg/ml by 5-fold. Finally, chitinase inhibitors Pentoxifylline (PEN), Caffeine (CF), and Theophylline (TH) all possess no significant effect on the adhesion of *V. cholerae*. Except Dequalinium chloride (DQ) at 50µg/ml showed reduced adhesion of *V. cholerae* by 72-fold.

5.16. Effect of the inhibitors on in vitro Cholera Toxin (CT) production

We then analyzed the *V. cholerae* Cholera Toxin production by CT-ELISA in presence of these inhibitors *(Fig.5.19A-D)*. Only Carvacrol (CV) treated *V. cholerae* showed reduced CT production by 3.3-fold than the untreated control at 50 µg/ml concentration. But Curcumin (CC) and Trans-cinnamaldehyde (TC) treated bacterial culture showed not much difference in CT production than the control. Among all Monosaccharides studied here Xylose, Xylitol, Allose at 0.5% concentration significantly reduced the CT production by 13-fold, 4.7-fold and 12-fold respectively. GlcNAc and Mannitol do not have any role in *V. cholerae* CT inhibition. Sodium-3-hydroxy butyrate (3HB) at 250 µg/ml supplemented bacterial culture reduced CT of *V. cholerae* by 13–fold and NH125 at 12.5 µg/ml by 3.2-fold. Finally, chitinase inhibitors Pentoxifylline (PEN), Caffeine (CF), Dequalinium chloride (DQ), and Theophylline (TH) all possess a significant effect on CT production of *V. cholerae* by 5.2-fold, 13-fold, 7-fold, and 18-fold respectively.
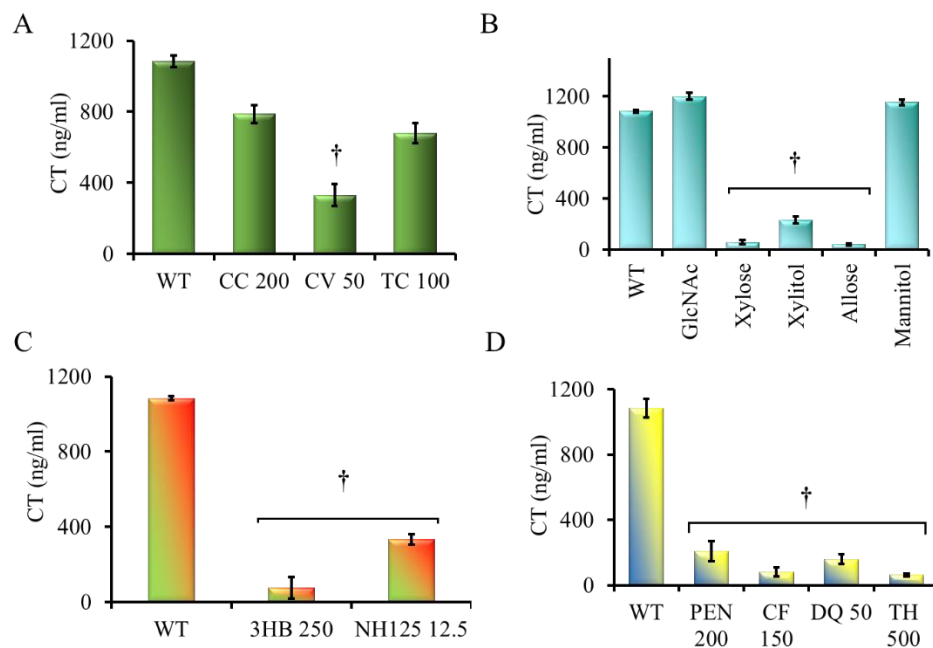
Fig. 5.19. *In vitro* **CT production assay in the presence or absence of different inhibitors.** Log phase cultures of wild type *V. cholerae* were inoculated (1:100) in AKI media with or without inhibitors and grown statically at 37°C for 18 h. Culture supernatant was collected, Cholera Toxin (CT) was measured by ELISA and represented graphically. **(A)** Effect of Phytochemicals **(B)** Effect of Monosaccharides **(C)** Effect of Small molecules and **(D)** Effect of Chitinase inhibitors. Each of the experiments was repeated three times (n=3) and the data were expressed as Mean ± SEM; †, P-value <0.05

Based on this broad spectrum of inhibitor research, the phytochemical carvacrol appears to be a strong anti-virulent agent that needs further investigation. Other features of *V. cholerae* pathogenicity will be investigated. *In-vivo* animal models will also be used to assess the role of Carvacrol.

5.17. Growth of V. cholerae at sub-MIC concentrations of carvacrol

We have first determined the Minimum Inhibitory Concentration (MIC) of carvacrol, which was found to be 150 µg/ml. Then the growth rate of *V. cholerae* was measured in Luria-Bertani (LB) medium along with exogenously added MIC and sub-MIC concentrations of Carvacrol. The result indicated that *V. cholerae* growth was completely inhibited at 150 µg/ml. No bacteria were recovered after 2 h of initial inoculum at MIC. At 75 µg/ml, the viable count of the bacteria was reduced to 60% 1h post initial inoculum.
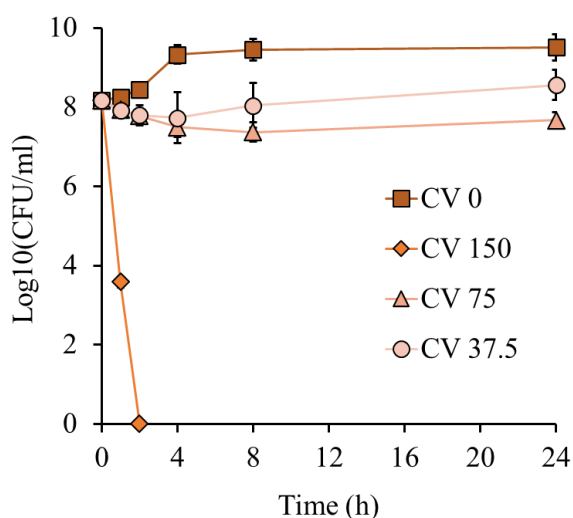
Fig.5.20. Effect of carvacrol on *V. cholerae* growth at MIC and sub-MICs. 1×10^8 cells/ml wild type *V. cholerae* N16961 was inoculated in LB broth. Treatment with carvacrol was done at 150µg/ml (CV 150 (♦); 75µg/ml (CV 75) (▲); 37.5 µg/ml (CV 37.5) (●) along with the untreated control, CV 0 (■). The cultures were grown at 37°C for 24 hours. The viable bacterial counts in CFU/ml were detected by the plate count method taking culture samples from different time points and represented graphically. Each experiment was repeated three times (n = 3) and the data were expressed as mean ± SEM.

Within the initial 8 h, the viable count of the bacteria reduced gradually to 20%. Although at 24 h, the growth of the *V. cholerae* starts resuming to a lesser extent and reaches up to 37% viability of the initial bacterial population. On the contrary, carvacrol

treatment at 37.5 µg/ml resulted in a reduction in the bacterial population to 60% within 2 h of the initial inoculum. After that *V. cholerae* resumes growth and at 24 h, the viable count of the bacteria exceeds more than five times the initial inoculum *(Fig.5.20)*. At the initial phase of the sub-MIC treatment, carvacrol showed the bactericidal effect on *V. cholerae*, subsequently, it remained bacteriostatic for the remaining viable bacteria. This suggests that *V. cholerae* remained viable and continued to grow even upon carvacrol treatment at sub-MIC concentrations.

5.18. Swarming motility and mucin penetrating ability of V. cholerae is affected by carvacrol

The ability of *V. cholerae* to penetrate the mucin layer *in vitro* in presence of carvacrol was studied. It was found that *V. cholerae* mucin penetration decreased significantly upon carvacrol treatment. Out of a total of 5×10^8 CFU/ml bacteria loaded on top of the 1.5% mucin column, 100µl of 43×10^3 CFU/ml bacteria were recovered after 1h from the bottom of the column *(Fig.5.21A)*. In the case of CV treatment at 37.5 µg/ml and 75 µg/ml, a total of 8×10^2 and 3.5×10^2 bacteria were recovered from the bottom of the column respectively.

A

B

Diameter (cm)	CV 0	CV 37.5	CV 75
Mean (± SEM)	7 (± 0.3)	0.4 (± 0)	0.4 (± 0)
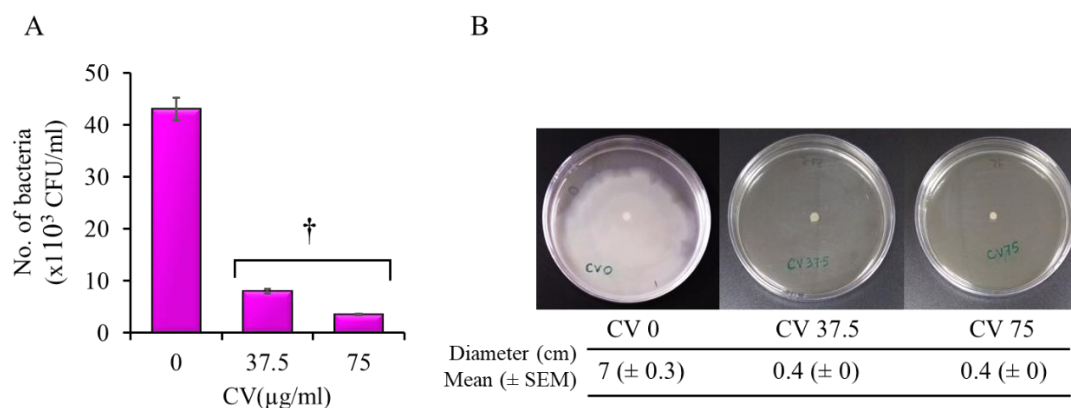
Fig.5.21. Effect of carvacrol on the motility of *V. cholerae*. (A) Mucin penetration was performed in a 1.5% mucin column in presence of different concentrations of carvacrol at 75 µg/ml and 37.5 µg/ml. Bacterial numbers eluted were counted and graphically represented. **(B)** Representative plates showing the motility zone of *V. cholerae* on 0.3% agar plates under different treatment conditions.

Which seems to have caused a 5.2-fold and 12.3-fold reduction in mucin penetration respectively. Because CV at both sub-MIC concentrations reduced the viable count of the bacteria by 40% in the initial 1 h of growth, we can say that the viable count of the bacteria must be 25.8×10^2 in the bottom 100 µl fraction of the CV

treated columns. Compared to that, 37.5 µg/ml of CV treatment showed 3.2-fold and 75 µg/ml of CV treatment showed a 7.4-fold reduction. We have also investigated the surface motility of *V. cholerae* on soft agar LB plates *(Fig.5.21B)*. We found that in the CV untreated plate *V. cholerae* showed a motility zone of 7±0.3 cm and the addition of CV resulted in complete inhibition of swarming motility after 24 h of incubation.

5.19. Carvacrol affects V. cholerae adhesion to epithelial cells

The effect of carvacrol on *V. cholerae* adherence to rabbit ileum epithelial cells was tested. The result suggested that 3.37×10^7 CFU/ml adherent *V. cholerae* was present in the untreated condition *(Fig.5.22A)*.
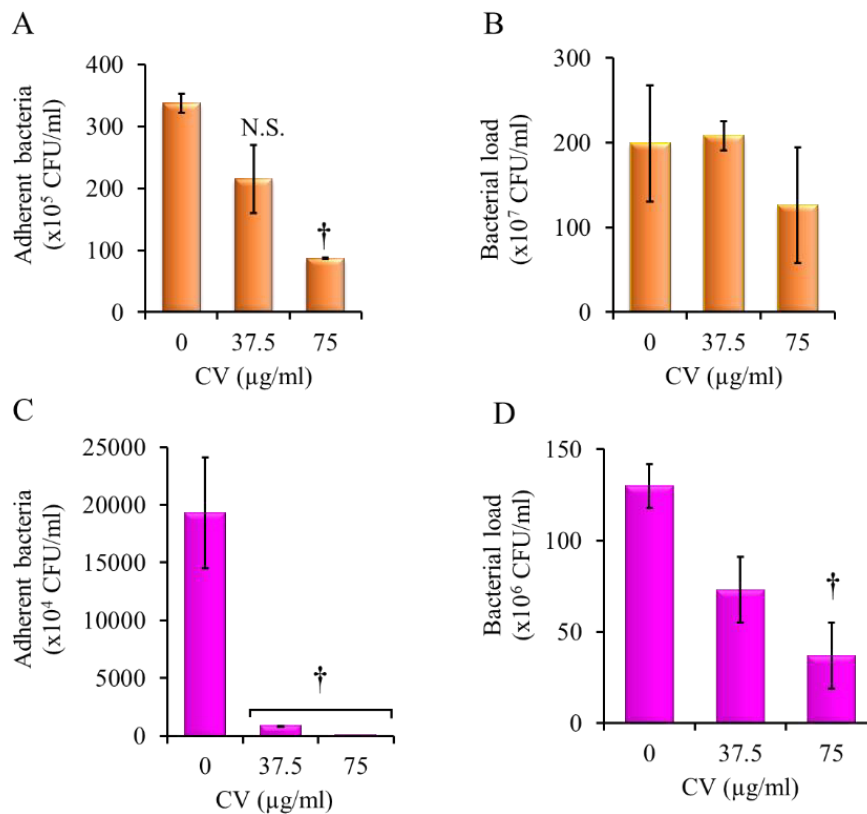
Fig.5.22. Effect of carvacrol on the adhesion of *V. cholerae* to the epithelial cells. Carvacrol at 75 µg/ml and 37.5 µg/ml were used in treating both rabbit intestine and cell culture conditions. **(A)** Adhered *V. cholerae* in the rabbit ileal loop tissue samples **(B)** Total number of *V. cholerae* count in each of the rabbit ileal loops **(C)** Adhered *V. cholerae* with the HT-29 cell line **(D)** Total number of *V. cholerae* count in each HT-29 culture samples. Each experiment was repeated three times (n = 3) and the data were expressed as mean ± SEM.

In contrast, there was only 8.7×10^6 CFU/ml and 21×10^6 CFU/ml of adherent bacteria at 75 µg/ml and 37.5 µg/ml of carvacrol treatment respectively. We have also

checked the bacterial load in each of the ileal loop samples. 1.98×10^9 CFU/ml, 2.08×10^9 CFU/ml, and 1.59×10^9 CFU/ml bacteria were recovered from the CV untreated, 37.5 µg/ml of CV treated and 75 µg/ml of CV treated ileal loop samples *(Fig. 5.22B)*. This study exhibits that only 1.7% of the total *V. cholerae* adhered to the epithelium in absence of CV. Whereas, 0.5% out of total *V. cholerae* was adhered to the epithelium in presence of 37.5 µg/ml of CV treatment, showing three times less adherence capability of *V. cholerae*. Further, the adherence capability of *V. cholerae* to the HT-29 intestinal epithelial cell line was also studied compared with the recovered viable bacteria from treated and untreated culture samples. In absence of CV, 1.47% out of total bacteria adhered to the HT-29. Whereas, only 0.12% and 0.04% bacteria out of total viable bacteria adhered at 37.5 µg/ml and 75 µg/ml of carvacrol treatment *(Fig.5.22C-D)*. Therefore, the effect of carvacrol on *V. cholerae* is more pronounced in cell culture conditions although we found significant results *in vivo* treatment.

5.20. *V. cholerae show less fluid accumulation upon carvacrol treatment*

Next, the effect of carvacrol in fluid accumulation in ligated rabbit ileal loop model was studied.
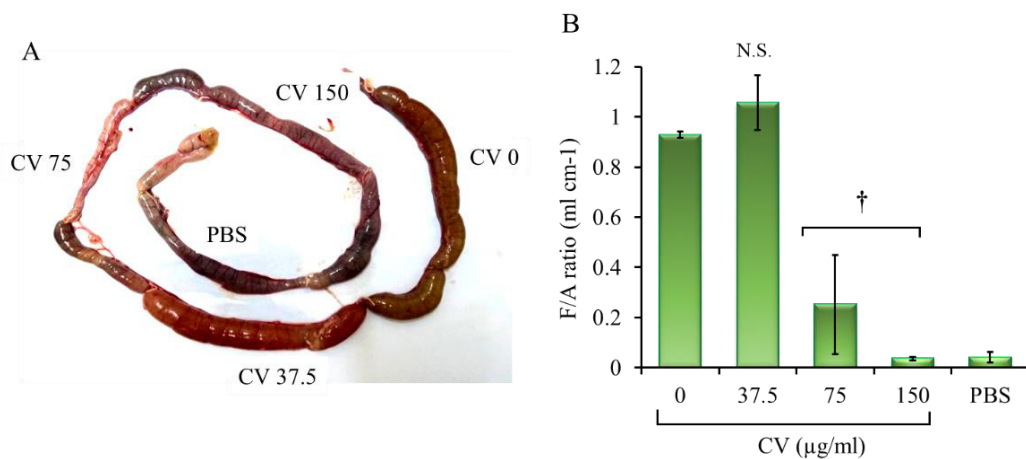
Fig.5.23. Effect of carvacrol in fluid accumulation in rabbit intestine. *V. cholerae* were grown in LB broth till mid-log phase and O.D. was adjusted to 1.0 and 1 ml of 10^9 CFU/ml were inoculated in each of the ligated loops of the rabbit intestine. Carvacrol at different concentrations, 150 µg/ml, 75µg/ml, and 37.5µg/ml were also administered in each loop. A control loop with no carvacrol was also kept (A) Retrieved rabbit intestinal portion showing infected loop 18 h post-infection. Each loop was separated by an uninfected interloop region. The negative control loop was inoculated with PBS. (B) The fluid accumulation ratio in the rabbit intestine of three different experiments was measured and represented graphically as mean ± SEM. †, P < 0.05, N.S., non-significant.

The amount of fluid accumulated per unit length (FA ratio) in each loop was measured 18 h post-infection with or without carvacrol treated *V. cholerae* culture *(Fig.5.23A)*. When quantified, the FA ratio of CV treatment showed complete obliteration of fluid accumulation upon carvacrol treatment with 150 µg/ml. At 75 µg/ml, a 3.7-fold decrease in fluid accumulation was observed compared to the control *(Fig.5.23B)*. At 37.5 µg/ml of carvacrol, the FA ratio was found to be similar to the untreated one.

5.21. Carvacrol treatment decreases cholera toxin production and virulence gene expression
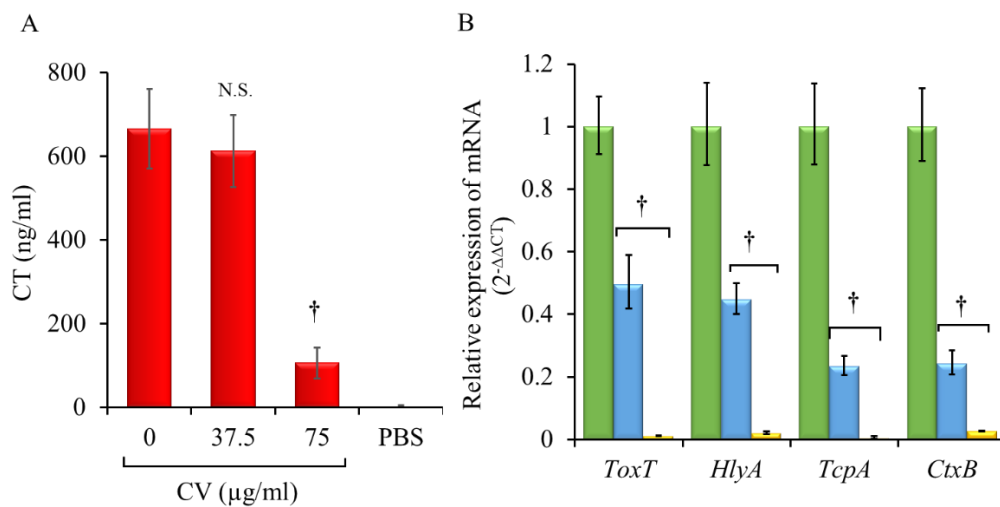
Fig.5.24. Effect of carvacrol on cholera toxin (CT) production and virulence gene expression. (A) *In vivo* CT production was measured by ELISA from the accumulated fluid samples of carvacrol treated with 75µg/ml and 37.5µg/ml) and untreated ligated rabbit ileal loops. **(B)** Relative expression of *V. cholerae* virulence genes by Real-Time PCR. RNA was isolated from the bacteria of carvacrol treated with 75µg/ml (■); 37.5µg/ml (■) or untreated (■) ileal loop fluid samples and were used for this experiment. *recA* was used as an internal control gene. Data have shown here as fold change and were calculated as $2^{-\Delta\Delta Ct}$. Each of the experiments was repeated three times (n = 3) and the data were expressed as mean ± SEM. †, P < 0.05

Cholera Toxin (CT) production in the rabbit ileal loop sample, which is primarily responsible for fluid accumulation was measured by GM_1-CT ELISA. Experimental results suggested that *V. cholerae* produced 666 ng/ml of CT in the untreated ileal loop. At 75 µg/ml of carvacrol treatment, CT production was measured to be 106.6 ng/ml resulting in 6.3-fold reduced production of CT compared to the untreated control loop *(Fig.5.24A)*. Fluid from 37.5 µg/ml carvacrol infected loop showed almost similar CT production (612 ng/ml) compared to the control loop. The

expression of different virulence genes (*toxT*, *hlyA*, *tcpA,* and *ctxB*) was also measured by qPCR. It was found that the expression of these genes was significantly reduced by 2-fold, 2.3-fold, 4.4-fold, and 4.2-fold respectively in 37.5 µg/ml carvacrol infected ileal loop samples relating to the infection with only *V. cholerae (Fig.5.24B)*. At 75 µg/ml of carvacrol treatment expression of these genes was greatly reduced compared to the control gene at the control condition.

5.22. Carvacrol affects morphology and flagellar gene synthesis in V. cholerae

Changes in bacterial morphology were observed by transmission electron microscopy upon carvacrol treatment. As shown in *Fig.5.25*, carvacrol treatment 150 µg/ml showed altered morphology with distorted shape and damaged cell membranes. Whereas at lower concentrations of carvacrol, showed the normal shape of the bacteria. Although flagella in each of the treatments were not observed in *V. cholerae*. Compared to that untreated *V. cholerae* showed a normal shape and single polar flagellum *(Fig.5.25)*.
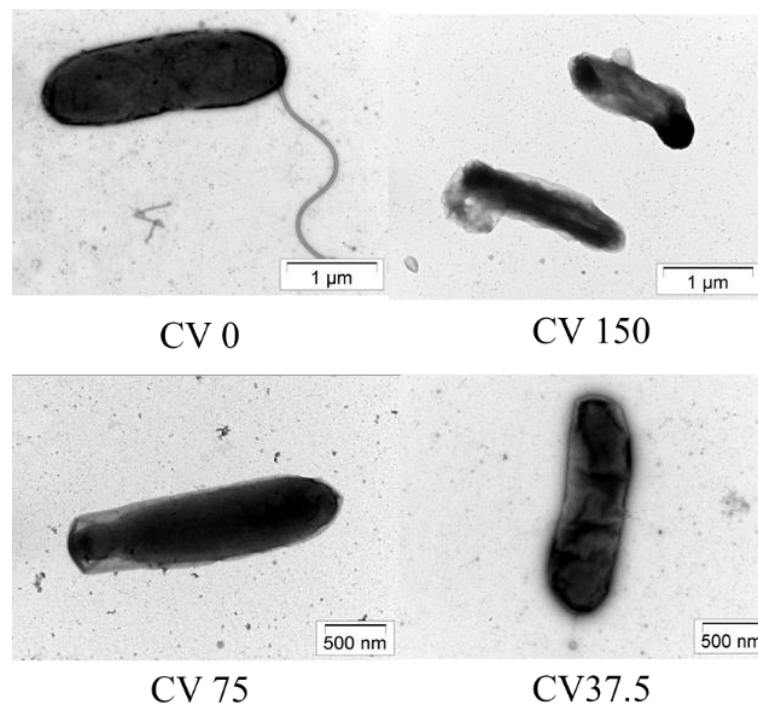
Fig.5.25. Effect of carvacrol on *V. cholerae* morphology. Representative Transmission Electron Micrographs of negatively stained *V. cholerae* in the absence and presence of different concentrations of carvacrol [150µg/ml (CV 150); 75µg/ml (CV 75); 37.5µg/ml (CV 37.5) along with the untreated control (CV 0)]

Flagella-driven bacterial motility is an important virulence trait of *V. cholerae*. Reduced mucin penetration and absence of flagella by microscopic analysis upon carvacrol treatment raised interest in whether carvacrol has any effect on flagella synthesis. Therefore, the effect of the sub-inhibitory concentration of carvacrol on *V. cholerae* flagella synthesis was assessed by measuring the transcription of flagella synthesis genes by qRT-PCR. The analysis revealed that at 37.5 µg/ml of carvacrol treatment, there was a 4-fold decreased expression of *flrC,* a response regulator (P <0.05) *(Fig.5.26)*. Transcriptional expression of master regulator *flrA,* histidine kinase *flrB,* and *fliF* (MS ring structure forming unit) was not significantly changed upon carvacrol treatment (P > 0.05). On the other hand, alternate sigma factor *fliA* (σ^{28}), *flgM,* and *RpoN* (σ^{54}) expression were downregulated by 2.5-fold, 2.9-fold, and 3.5-fold respectively.
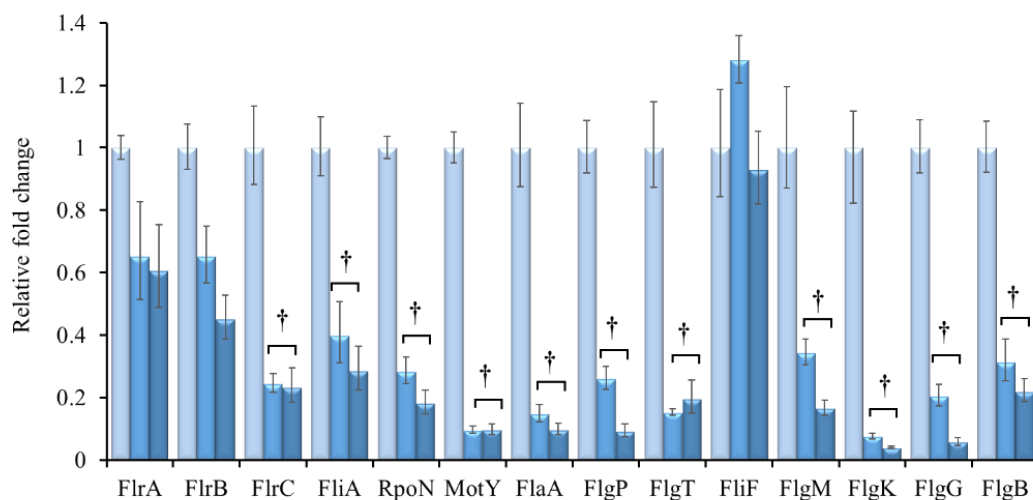
Fig.5.26. Effect of carvacrol in *V. cholerae* flagellar gene synthesis. Mid-log-phase bacterial cultures in the presence [75µg/ml (■) and 37.5µg/ml (■)] or absence of carvacrol (■) were subjected to RNA isolation using the TriZol method and mRNA transcript levels were analyzed by qRT PCR and graphically represented, using *recA* as an internal control gene. Data have shown here as fold change and were calculated as $2^{-\Delta\Delta Ct}$. Each of the experiments was repeated three times (n = 3) and the data were expressed as mean ± SEM. †, P < 0.05

Furthermore, downregulation of *motY* (T-ring motor protein), *flaA* (main flagellin subunit), *flgP* (H-ring associated protein), *flgT* (H-ring component), *flgK* (hook filament junction protein), *flgG* (distal rod), and *flgB* (proximal rod) all of which belong to Class III flagellar synthesis genes were downregulated by 10.5-fold, 7.1-fold, 3.8-fold, 6.6-fold, 33.3-fold, 5-fold and 3.2-fold respectively upon 37.5 µg/ml of

carvacrol treatment. However, inconspicuous change in the expression pattern of these flagellar synthesis genes was noticed when *V. cholerae* culture was treated with an even higher sub-inhibitory concentration 75 µg/ml of carvacrol.

5.23. Effect of carvacrol on the cytotoxicity of HT-29 cell line
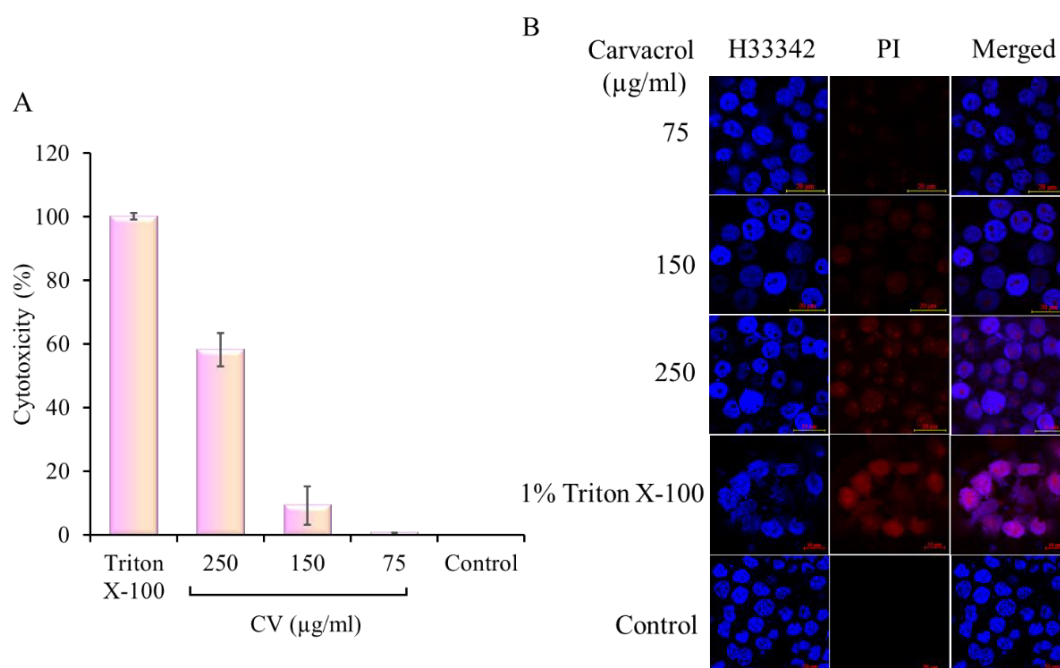
Fig.5.27. Cytotoxic activity of carvacrol in the HT-29 cell line. (A) The cytotoxic effect of carvacrol at different concentrations was measured by LDH release assay and graphically represented as percent cytotoxicity taking Triton X-100 treated cell's LDH release as a positive control. **(B)** Confocal images of HT-29 cells treated with different concentrations of carvacrol. Cells were stained with Hoechst 33342 (Blue) and counterstained with Propidium Iodide (Red). Inconspicuous red fluorescence of Propidium Iodide (PI) is visible in 75µg/ml CV treatment, indicating insignificant damage to the plasma membrane of the HT-29 cell line compared to the much higher intake of PI in triton X-100 treatment, where PI permeate easily through the damaged membrane and stains the nucleus.

Cytotoxicity of the HT-29 cell line upon carvacrol treatment was measured by LDH release assay. Different doses of carvacrol were used to treat HT-29 cells and after 12 h the supernatants were collected and assessed for the release of LDH. HT-29 cell treatment with triton X-100 showed maximum membrane damage hence considered to possess 100% cytotoxicity. The experimental result obtained here showed that carvacrol exerts 9% and <1% cytotoxicity at 75 µg/ml and 37.5 µg/ml concentration respectively, compared to the triton X-100 treated cell *(Fig.5.27A)*. So, no substantial membrane damage upon treatment at 150 µg/ml and lower concentrations of carvacrol

were observed. Although at a higher concentration 250 µg/ml carvacrol exhibited noteworthy spillage of LDH resulting in 58% cytotoxicity. Confocal microscopy images also revealed that at 150 µg/ml and below that concentration of carvacrol treatment, the permeability of propidium iodide to HT-29 cell line was very less compared to the Triton-X 100 treatment *(Fig.5.27B)*. The above results led to the conclusion that carvacrol at concentrations below 150 µg/ml is safe and does not cause human epithelial cell damage.

5.24. Carvacrol affects the formation of biofilm in vitro
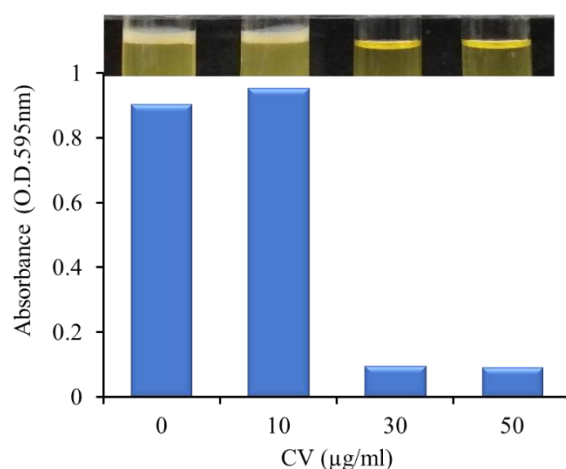
Fig.5.28. Effect of carvacrol on *V. cholerae* biofilm. *V. cholerae* was grown in Luria- Bertani broth in the presence or absence of different concentrations of carvacrol. The formation of biofilm was quantified by Crystal Violet staining and represented graphically after measuring the optical density at 595nm.

After forming microcolonies both in the environment and *in vivo*, bacteria tend to protect themselves by forming a protective sheath around them, called biofilms. In this way, they shield themselves from therapeutic interventions and remained inaccessible to the antibiotics. So, we have tested the effect of carvacrol on biofilm. The result indicates that carvacrol at 30 µg/ml completely inhibits the formation of the biofilm of *V. cholerae*. However, below the above concentration, no effect on biofilm was seen.

Chapter 6

Results

To study the effect of host intestine on CytR during pathogenesis.

Results

We have already recognized the crucial role of *V. cholerae* transcriptional regulator CytR in the environmental conditions, more specifically in the chitinous medium as well as during the pathogenesis. Now, we aim to look at how different host variables affect the expression of this transcriptional regulator.

6.1. Effect of mucin on CytR expression
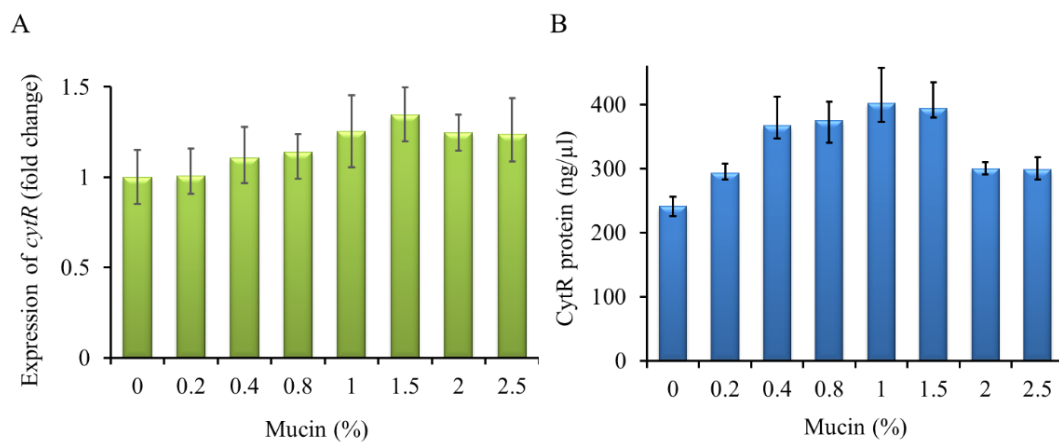
Fig.6.1. Effect of mucin on CytR expression. *V. cholerae* N16961 was grown to log phase under the varying concentration of porcine mucin. mRNA expression was analyzed by qPCR and protein levels by ELISA. **(A)** Relative mRNA expression or the fold change of cytR is represented graphically, **(B)** Relative protein level expression of cytR. Each of the experiments was repeated three times (n=3) and the data were expressed as Mean ± SEM.

Mucin is a large extracellular glycoprotein located on the surface of intestinal epithelial cells that is extensively glycosylated and contains 80% carbohydrates, primarily N-acetylglucosamine, N-acetyl galactosamine, fucose, galactose, and sialic acid, as well as quantities of mannose and sulfated sugars. It is possible that chitinases that hydrolyze the chitin polymer might also get involved in the breakdown of mucin due to structural similarity between chitin and mucin. So, *V. cholerae* was grown in different concentrations of porcine mucin (Type III) between 0 to 2.5% keeping a fixed pH 7.5 and 37°C temperature in a minimal M9 medium. First, the cytR RNA expression was studied by qRT-PCR *(Fig.6.1A)*. Analysis of cytR expression under different amounts of mucin showed 1.5% mucin was optimum for cytR expression.

Comparable expression was also observed at mucin concentrations of 1%, 2%, and 2.5%. *V. cholerae* produces 1.34-fold more cytR mRNA in presence of 1.5% mucin. Very low (0.2%) mucin concentration decreased the expression of cytR.

The CytR protein expression pattern under the varying amount of mucin was also similar to RNA expression *(Fig.6.1B)*. The expression increased with the increasing amount of mucin. At 1% mucin, the CytR protein expression was maximum measuring 402 ng/µl compared to the expression of 241 ng/µl in absence of mucin. Here comparable protein expression was observed at 0.4%, 0.8%, 1.5% of mucin concentration, which measures about 366 ng/µl, 374 ng/µl, and 394 ng/µl of CytR protein respectively.

6.2. Effect of bile salts on CytR expression
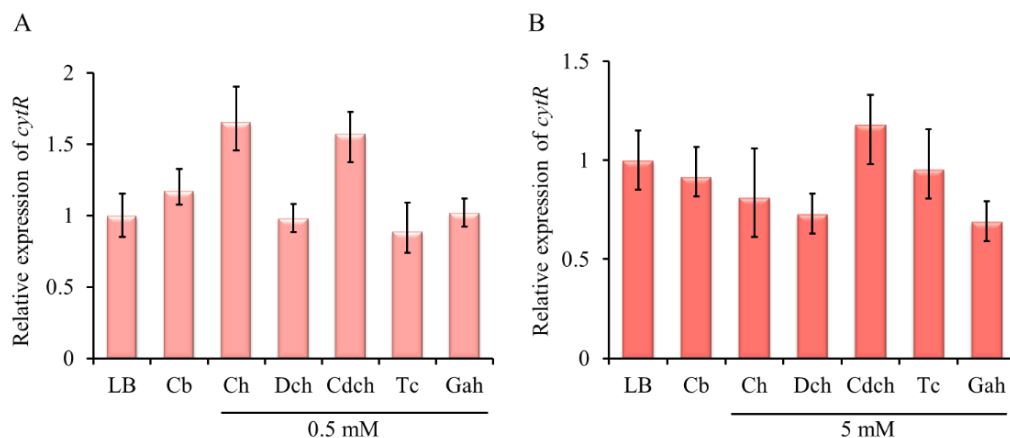
Fig.6.2. Effect of bile salts on CytR expression. *V. cholerae* N16961 was grown to log phase in presence of bile and its components at **(A)** lower concentration 0.5mM and **(B)** higher concentration 5mM, as supplements in Luria-Bertani (LB) broth medium. Log phase cultures were harvested and RNA was isolated. RNA expressional analysis was done by the quantitative real-time PCR method. Data represented as fold change of cytR gene, taking recA as an internal control. Each of the experiments was repeated three times (n=3) and the data were expressed as Mean ± SEM. Cb, Crude bile; Ch, Cholate; Dch, Deoxycholate; Cdch, Chenodeoxycholate; Tc, Taurocholate hydrate; Gah, Glycocholic acid hydrate.

Bile salts are produced in the pericentral hepatocytes of the liver from cholesterol. After production, they are stored in the gall bladder and then enter the upper intestine, where it facilitates the digestion and absorption of fats and fat-soluble vitamins. Seventeen enzymes convert cholesterol into bile acids, which are then converted into bile salts by interacting with Na+ or K+ ions. Bile acids are thought to

have antibacterial action. As a result, it is critical to investigate the effects of bile and its components on CytR. We investigated the expression of CytR in the presence of 0.1 percent crude bile and its various forms at both higher and lower concentrations. Bile salts studied here include cholate, deoxycholate, chenodeoxycholate, taurocholate hydrate, and glycocholic acid hydrate.

Our study indicated that at lower concentration i.e., at 0.5mM concentration of bile salt cholate and chenodeoxycholate, cytR expression is upregulated by 1.68-fold and 1.57-fold respectively compared to the bile salt untreated LB broth culture *(Fig.6.2A)*. However, at higher concentration i.e., at 5 mM concentration, cholate treated culture showed reduced cytR expression *(Fig.6.2B)*. On the other hand, crude bile and other bile salts like, deoxycholate, taurocholate hydrate and glycocholic acid hydrate do not seem to have a significant effect on the regulation of CytR gene expression.

6.3. Time-dependent study of Secretion of inflammatory cytokines
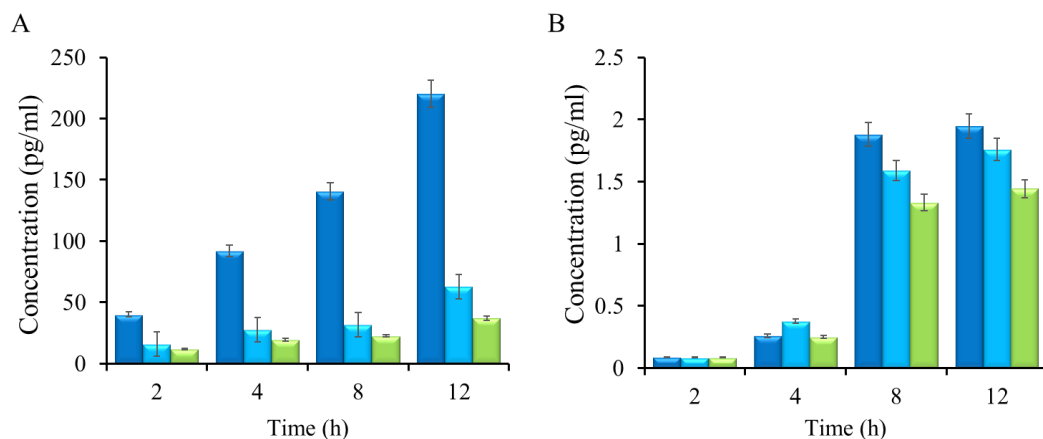
Fig.6.3. Comparison of IL-8 and TNF secretion by wild type *V. cholerae* and CytR mutant *V. cholerae* infection in Caco2 cell line at different time points. The Caco2 cell line was infected with the *V. cholerae* strains CytR⁺ (■) and CytR⁻ (■) for varying time periods from 2h to 12h. The secretion of IL-8 **(A)** and TNF **(B)** was measured by ELISA. The basal level of IL-8 and TNF secretion from the Caco2 cell line was also measured as control (■). Each of the experiments was repeated three times (n=3) and the data were expressed as Mean ± SEM.

The intestine serves as both our largest single barrier to the external environment and the host of more immune cells than any other location in our bodies. Pathogenic bacteria that penetrate the intestinal epithelial barrier stimulate an inflammatory response in the adjacent intestinal mucosa. Infection of human colon

epithelial cell monolayers with bacteria strains resulted in the coordinated expression and upregulation of a specific array of proinflammatory cytokines, IL-8, monocyte chemotactic protein-1, GM-CSF, and TNF alpha, as assessed by mRNA levels and cytokine secretion. Here, we aimed to study the secretion of cytokine IL-8 and TNF, when the Caco2 cell is treated with CytR$^+$ and CytR$^-$ *V. cholerae* strains.

80% confluent Caco2 cells were infected with 1:100 MOI of bacterial strains. The study was done at different time points from 2 h to 12 h. After 2 h onwards an increase in IL-8 concentration was observed with increasing time for wild type *V. cholerae*. At 12 h incubation with wild type *V. cholerae,* the amount of IL-8 secretion was maximum and the concentration measured was 220 pg/ml *(Fig. 6.3A)*. In contrast to the wild-type strain, infection with the CytR$^-$ strain produced a significantly lower amount of IL-8. At 12 h, the IL-8 production from the Caco2 cell line in CytR$^-$ strain measured 62 pg/ml, showing about a 3.5-fold reduction.

On the other hand, we did not notice significant production of TNF from the Caco2 cell line. Even after 12 h of incubation, the secretion measured was 1.9 pg/ml from the wild-type CytR$^+$ strain *(Fig. 6.3B)*. The CytR$^-$ strain did not cause any significant reduction in the secretion of the TNF.

Chapter 7

Discussion

Discussion

Throughout human history, cholera has remained one of the deadliest diseases, inflicting significant mortality. Since 1817, scientists have been aware of cholera outbreaks (Pollitzer, 1954). Later, in 1849, Sir John Snow demonstrated the link between cholera and contaminated water. The causative agent of the waterborne disease cholera is now well recognized as being acquired through environmental sources and persisting between outbreaks of the disease.

Recent developments in molecular biology have shown that this bacterium may be found in locations where it has not been previously isolated (Sack et al., 2004), suggesting that this bacterium has a much greater distribution outside of the endemic zone (Tall et al., 2013; Vezzulli et al., 2010). *V. cholerae* has been found in a wide range of environments, from the tropics (Bay of Bengal) to temperate regions of different parts of the world specifically Africa, Australia, North America, and South America (Albert, 1992; de Magny et al., 2011; Anwar Huq et al., 2005). This pathogen lives in the aquatic environment and infects humans via contaminated food or water (Hsiao & Zhu, 2020). In the aquatic environment, the surface of different zooplankton, copepods, mollusks, arthropods, and crustaceans are widely colonized by this pathogen (R. R. Colwell, 1996; A Huq et al., 1983; Pruzzo et al., 2008). Chitin, which is made up of β-1,4-linked GlcNAc residues, is nature's second most abundant polysaccharide after cellulose. Every year, 10^{11} metric tonnes of chitin are produced in the aquatic biosphere alone. This massive volume of insoluble, carbon-containing material is primarily recycled by chitinolytic bacteria, including members of the Vibrionaceae family. Chitin is found in all kingdoms and is the primary component of fungus cell walls and crustacean exoskeletons. Each year, copepods are believed to create billions of tonnes of chitin.

The survival and association of *V. cholerae* with zooplanktons are most likely regulated by abiotic environmental variables (Rudra Bhowmick et al., 2008; Islam et al., 2020; Lipp et al., 2002). In this study, we aim to understand how environmental parameters like temperature, pH, salinity, and chitin as a nutrient source of *V. cholerae* affect the expression of CytR. *V. cholerae* feeds on the exoskeletal chitinous coating in the aquatic environment (A. Huq et al., 1983). *V. cholerae* releases

extracellular chitinases like ChiA1 and ChiA2 and helps in breaking down the chitinous exoskeleton, thus releasing N-acetyl glucosamine (GlcNAc) residues, which are detected and internalized as a source of nutrition for *V. cholerae*. ChiS, a periplasmic two-component sensor histidine kinase of *V. cholerae*, is required for both sensing and chitinase secretion. Insoluble chitin recycling is extremely important for the environment. Another regulator of chitinases, the cytoplasmic repressor CytR (VC_2677), was recently found in *V. cholerae* (Meibom et al., 2004; Watve et al., 2015). These new studies on the regulation of chitinases and the chitin utilization pathway of *V. cholerae* opened up a wide range of research possibilities, driving us to dig more into the new chitinase regulator, CytR. So, here we aim to understand the function of CytR in presence of different environmental factors.

We found CytR expression to be affected significantly by a wide variety of environmental factors. Similarly, we found a Gaussian pattern of RNA and protein level expression of CytR in presence of chitin. With temperatures varying between 16°C to 42°C, we found the highest CytR expression at 25°C. The optimum temperature for CytR protein expression was in accordance with the RNA expression i.e., 25°C. The effect of different temperatures on *V. cholerae* growth has been studied earlier (R. Bhowmick et al., 2007; Escobar et al., 2015; Singleton et al., 1982). Rita Colwell and colleagues previously discovered a relationship between the cholera bacterium, sea surface temperature, and phytoplankton (Constantin de Magny & Colwell, 2009). Warmer surface temperatures increase the abundance of phytoplankton, which supports a large population of zooplankton and serves as a reservoir for cholera bacteria. Cholera is not only associated with climate change, but it also has an *El Niño* (unusual warming of the ocean's surface water on a regular basis) aspect. For instance, Papua New Guinea, a Pacific Ocean Island state, recorded its first cholera cases in 50 years in 2009, which also happened to be an *El Niño* year. When these conditions are combined with the rise in temperature and heavy rainfalls caused by climate change, ideal conditions for the bacterium that causes cholera to multiply are created, resulting in a global resurgence of the disease. Another study has linked cholera outbreaks to oceanographic variables such as water temperature, pH, salinity, and phytoplankton blooms, implying the possibility of predicting disease outbreaks (Jutla et al., 2011). Therefore, temperature appears to be an important factor not only for the growth of the marine bacterium but also for optimal chitinase activity.

We found pH 7.5 to be optimum for CytR expression both at the RNA and protein levels. However, the expression of CytR at pH 9 showed almost similar expression to pH 7.5. Studies have shown that higher pH results in improved colonization of *V. cholerae* on the chitinous surface of copepods in aquatic environments (Lipp et al., 2002).

Another important abiotic factor in *V. cholerae* growth and survival in aquatic environments is salinity (R. K. Colwell et al., 2008). *V. cholerae* can grow in a medium without NaCl, however, its growth is stimulated in the presence of NaCl (Reichelt & Baumann, 1974). MacLeod and his colleagues have extensively studied the basis for the salt requirement in a marine bacterium known as strain B-16, which has been described and identified as *Alteromonas haloplanktis* (Baumann et al., 1972). We observed that 300 mM salinity was optimum for maximum *cytR* expression but a very high salt concentration such as 600 mM salt caused decreased expression of CytR.

Furthermore, we found that 0.8% chitin was optimal for maximal CytR expression at both the RNA and protein levels. CytR expression was four times higher in the presence of 0.8% chitin. Indicating, when chitin is present, CytR is activated and expressed. The previous study has shown that *V. cholerae* grows and expresses its chitinase gene optimally in the presence of 0.8% chitin (Mondal et al., 2014). These data collectively indicate that among the three different conditions tested here, we found 25°C, pH 7.5 and 300mM salinity is ideal for successful growth and survival in the aquatic environment. This temperature, alkaline pH, and high salt concentration are also optimal for CytR expression, and because CytR governs chitinase gene expression, this resulted in maximum chitinase expression and activity under the same conditions that encourage *V. cholerae* development in aquatic habitats. The survival of *V. cholerae* in the environment is speculated to be regulated by CytR expression and chitinase activity.

Our lab has earlier established the importance of chitinase, ChiA2 in the survival of *V. cholerae* (Mondal et al., 2014). Therefore, it is likely that host factors would also affect CytR and its downstream-regulated enzymes, i.e., chitinases. So, we monitored the effect of host factors on the activity of sensor histidine kinase ChiS and chitinases. Significant upregulation of *V. cholerae* chitinase genes and the chitinase activity was observed in presence of 0.8% chitin in the optimum condition of abiotic

factors. Studies showed that high salt concentration is required for higher level of chitinase gene expression of *V. cholerae* (R. Bhowmick et al., 2007).
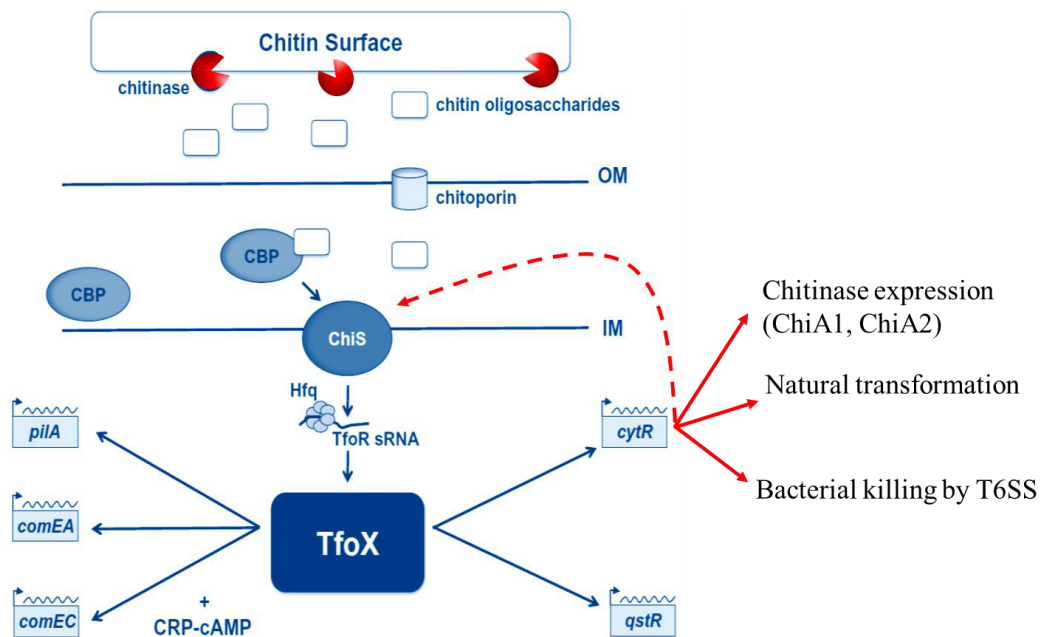
Fig.7.1. Proposed model of chitin-dependent signaling pathways in *V. cholerae* (Modified from Sun et al., 2013). Extracellular chitinases degrade chitin into oligosaccharide fragments, which enter the periplasm via a chitoporin. The sensor kinase ChiS detects the presence of chitin oligosaccharides and activates the TfoR sRNA with the help of CBP (chitin oligosaccharides binding protein). TfoR initiates translation of TfoX, the master regulator of competence in Vibrionaceae, via the RNA chaperone Hfq. As a result, TfoX increases the expression of several competence genes (such as *pilA*, *comEA*, and *comEC*) as well as two transcription factor genes (*cytR* and *qstR*). CytR, in turn, regulates the expression of chitinase genes, natural transformation genes and T6SS gene clusters, and sensor kinase ChiS. The lines connecting components of the signaling cascade represent positive regulation, but no direct interaction. The dashed line represents the proposed regulation of CytR. IM, inner membrane; OM, outer membrane.

The ability of *V. cholerae* to thrive in brackish water is probably due to increased chitinase gene expression under higher salt concentrations (R. Bhowmick et al., 2007). This finding was consistent with previous findings showing *V. cholerae* has higher levels of chitinase gene expression at alkaline pH than at acidic pH (R. Bhowmick et al., 2007). *Serratia marcescens* chitinase has been proven to have the highest activity on chitin at pH 7-8. Our study further confirmed the role of CytR in chitinase gene expression. A previous study led by another research group showed

that CytR positively regulates chitinases *chiA1*, *chiA2*, *vc0769*, and a chitodextrinase *vca0700* along with *tfoX* (Watve et al., 2015). Consistent with this finding, our study showed that deletion of CytR severely downregulates the expression of four chitinase genes (*chiA1, chiA2, vc0769*, and *vc1073*). Further, the expression of *tfoX* and *chiS* got downregulated in CytR ablated strain. A proposed model of regulation of CytR with respect to chitin utilization is depicted in *Fig. 7.1*.

We compared the growth patterns of CytR ablated *V. cholerae* strains in the presence or absence of chitin to those of wild-type *V. cholerae* to determine the involvement of CytR in *V. cholerae* chitin breakdown and utilization. In chitin supplemented media CytR ablated *V. cholerae* showed a reduced growth rate than the wild type *V. cholerae*. This corroborates with the proposed hypothesis that CytR is important for chitinase production thus helping degradation of chitin in the media. The dynamic lifestyle of *V. cholerae* includes two different habitats (Chac et al., 2021; Islam et al., 2020). *V. cholerae* primarily lives in the aquatic environment and it also colonizes in the intestinal epithelium of the human gut, where the mucus layer provides a niche for colonization because it harbors attachment sites like glycans. Mucus glycans also act as a direct source of nutrients for the bacteria (Reddi et al., 2018). *V. cholerae* chitinases act on mucus glycans to produce GlcNAc like residues which act as a nutrient source. Reports have also indicated the involvement of bacterial chitinases in pathogenesis (Frederiksen et al., 2013; Mondal et al., 2014; Tran et al., 2011). Our previous studies have shown that chitinase ChiA2 (VCA0027) is important for *V. cholerae* survival and pathogenesis (Mondal et al., 2014). *V. cholerae* ChiS (VC_0622) regulates the expression of chitinases as well as plays an important role in pathogenesis (Chourashi et al., 2016). ChiS is activated in the human intestine when mucin is present. The active ChiS helps *V. cholerae* survive in the intestine by facilitating the utilization of mucin. In the intestinal environment, ChiS promotes motility, mucin layer penetration, adhesion, and survival. Furthermore, ChiS mutant *V. cholerae* is hypovirulent, as it secretes less cholera toxin in the intestine, resulting in decreased fluid accumulation and virulence (Chourashi et al., 2016).

CytR (VC_2677) is another regulator of chitinases [like ChiA1 (Antonova et al., 2012) and ChiA2 (Mondal et al., 2014)] found in *V. cholerae* (Watve et al., 2015). Since chitinases play a role in pathogenesis, we hypothesize that CytR is also

involved in regulating the virulence cascade, which contributes to the pathogenicity of *V. cholerae* and causes disease.

CytR has an N-terminal domain that contains a helix-turn-helix (HTH) motif for DNA binding and a C-terminal domain for dimerization, inducer binding, and protein contact with cAMP Receptor Protein (CRP). Its role in the transport and utilization of nucleosides has long been studied in *Escherichia coli* (Antonova et al., 2012; Hammer-jespersen & Nygaard, 1976). In *E. coli* CytR negatively regulates a small set of nucleoside scavenging and metabolism genes including *udp*, *cdd*, *ompK,* and *cytR* itself via cAMP receptor protein (CRP)- dependent anti-activation mechanism (Valentin-Hansen et al., 1996). *V. cholerae* CytR is a functionally diverse protein and a global regulator. It represses multiple nucleoside catabolism and scavenging genes, positively regulates competence and a majority of natural transformation genes, bacterial killing by inducing Type VI secretion system (T6SS) gene clusters, and co-regulates chitinase genes along with TfoX (Watve et al., 2015).

The pathogenesis of *V. cholerae* within the human host is controlled by a complex signaling cascade of virulence genes and regulatory factors that have been the subject of intense research for several decades. During pathogenesis, *V. cholerae* has to survive in the intestinal environment, penetrate through the mucus layer, adhere to the intestinal epithelium, form colonies to secrete cholera toxin. To define the role of CytR in *V. cholerae* pathogenesis we explored the impact of CytR deletion and studied the growth of bacteria in presence of mucin, its motility due to flagellar movement in mucin, virulence genes expression, and fluid accumulation as a marker of CT production. We demonstrated that CytR positively regulates activation of sensor histidine kinase ChiS in the mucinous environment, thus affecting the secretion of chitinases and degradation of mucin. CytR deletion resulted in no flagellar synthesis which leads to reduced motility and mucin penetration.

CytR is engaged in several regulatory mechanisms in *V. cholerae*, with varying mechanisms in each case (Watve et al., 2015). A complicated signaling cascade involving numerous regulatory variables regulates *V. cholerae* pathogenesis inside the human body. CytR is also a regulator, but its role in pathogenesis is unknown. For the first time, we aimed to understand the involvement of this multifunctional transcription factor in the pathogenesis of *V. cholerae*.

Our experimental results suggest that the CytR⁻ *V. cholerae* showed inefficient growth in presence of mucin supplemented M9 minimal media. It is known that CytR upregulates four chitinase genes including *chiA1* and *chiA2*(Antonova et al., 2012; Watve et al., 2015) in presence of chitin. We showed that CytR mutant *V. cholerae* produced a significantly lower amount of RNA for both extracellular chitinase genes *chiA1* and *chiA2* in mucin which might result in decreased synthesis of the chitinase enzymes. Low levels of these chitinases result in an inefficient breakdown of complexly polymerized O-linked glycans of mucin.

As a result, the generation of GlcNAc as a nutrient is low, and the growth of CytR⁻ strain in mucin-supplemented media is hampered. Mucin has a number of GlcNAc residues on its side chains, which can be used as a source of carbon and nitrogen (Bjork et al., 1987). Depending on the environment in which it grows, *V. cholerae* can use a variety of carbon sources, including intestinal mucus. The extracellular chitinase ChiA2 cleaves the oligosaccharide moieties of mucin, releasing GlcNAc, as we previously observed (Mondal et al., 2014).

V. cholerae transports and assimilates the GlcNAc residues as nutrients (Meibom et al., 2004, 2005). It has also been observed that few pathogens can effectively use GlcNAc as a nutrition source (Chen et al., 2002). Gut mucus is used as a source of carbon and energy by a subset of intestinal microbiota in terms of nutrition. Few enteric pathogens, including *C. jejuni* (Alemka et al., 2012), *enterohemorrhagic E. coli* (EHEC) (Fabich et al., 2008), *C. difficle*, and *Salmonella enterica serotype Typhimurium*, efficiently utilise mucus derived monosaccharides. As previously indicated, *V. cholerae* mucin utilization occurs only after the sensor kinase ChiS detects GlcNAc residues in the environment, turning on downstream mucin utilization cascade components such as periplasmic -N-acetylhexosaminidases (Meibom et al., 2004). For the first time, our findings demonstrate that CytR regulates hexosaminidase activity in *V. cholerae* in the presence of mucin *in vitro* and the intestinal environment. The qRT-PCR findings demonstrated that the expression of *chiS* RNA is also CytR dependent. As a result, CytR appears to positively regulate both *chiS* expression and activity. As a result, we suggest CytR aids *V. cholerae* in breaking down the thick mucus layer using chitinases in a ChiS-dependent way, releasing primarily the GlcNAc residues from the mucus component. ChiS is also required for GlcNAc internalization and transport from the intestinal environment

(Meibom et al., 2004). We believe that in the CytR⁻ strain, GlcNAc is less transported, and to produce the clinical symptoms of cholera *V. cholerae* needs to transport sufficient titer of GlcNAc from the intestine (Ghosh et al., 2011; Naseem & Konopka, 2015; Reddi et al., 2018). However, more research into how CytR regulates ChiS expression and activity is further needed for complete understanding.

Flagella-driven motility is required for effective mucin layer penetration and colonization of intestinal epithelial cells in *V. cholerae* (Z. Liu et al., 2015). A previous study has shown that the movement of *V. cholerae* through the viscous mucus layer is promoted by mucin (Z. Liu et al., 2015). Additionally, the presence and internal degradation of N-acetylneuraminic acid and N-acetylglucosamine (GlcNAc) promote motility (Reddi et al., 2018). Our study here indicates that under experimental conditions, motility is positively regulated by CytR.

V. cholerae must simultaneously break down and remove the thick mesh of mucin side chains with the help of chitinases and proteases, as well as generate propulsion by rotation of whip-like, monotrichous polar flagella to penetrate through the mucus layer (Fleckenstein & Kopecko, 2001). The activity of chitinase ChiA2 in mucin deglycosylation in *V. cholerae* does not require any proteolytic help (Mondal et al., 2014). So, the inability to penetrate mucin by the CytR⁻ strain can be explained by the reduced expression of chitinases ChiA1 and ChiA2. Furthermore, electron microscopy demonstrated that the CytR⁻ *V. cholerae* strain does not have a polar flagellum, which explains why the CytR⁻ *V. cholerae* strain is less motile than the wild type. In *V. cholerae*, more than fifty genes are involved in the synthesis and regulation of flagella (Echazarreta & Klose, 2019). Protein synthesis and structural component assembly of the major flagellar units happened hierarchically. The transcriptional hierarchy of flagella synthesis genes in *V. cholerae* is divided into four levels (Klose & Mekalanos, 1998). The σ54 – dependent transcriptional activator FlrA is the only Class I gene in this hierarchy (Prouty et al., 2001; Syed et al., 2009).

FlrA is the master regulator of the *V. cholerae* flagellar transcription hierarchy because it is important for the expression of the rest of the flagellar genes. FlrA, along with the RpoN (sigma factor σ54), activates Class II flagellar genes. Class II flagellar protein histidine kinase FlrB and its response regulator FlrC regulates the synthesis of Class III flagellar genes which encodes the different structural components of flagella

including the major flagellin subunit (FlaA), proximal and distal transmembrane helical rod (FlgB/G), H-ring protein (FlgT), H-ring associated protein (FlgP), flagellar hook associated protein (FlgK) and T-ring motor protein (MotY). CytR⁻ strain showed reduced expression of Class II flagellar genes *flrB*, *flrC,* and several Class III genes tested. This suggests that CytR is important for the expression of *flrB* and *flrC*, except for which no other structural components of flagella in *V. cholerae* is synthesized *(Fig.7.2)*. The previous study has also shown that *flrC* mutant is defective in flagella synthesis thereby reducing motility as well as intestinal colonization of *V. cholerae* (Correa et al., 2000). Although we have observed decreased expression of *flrBC* and Class III flagellar genes in CytR⁻ strain, further study is still needed to complete the understanding of this process.
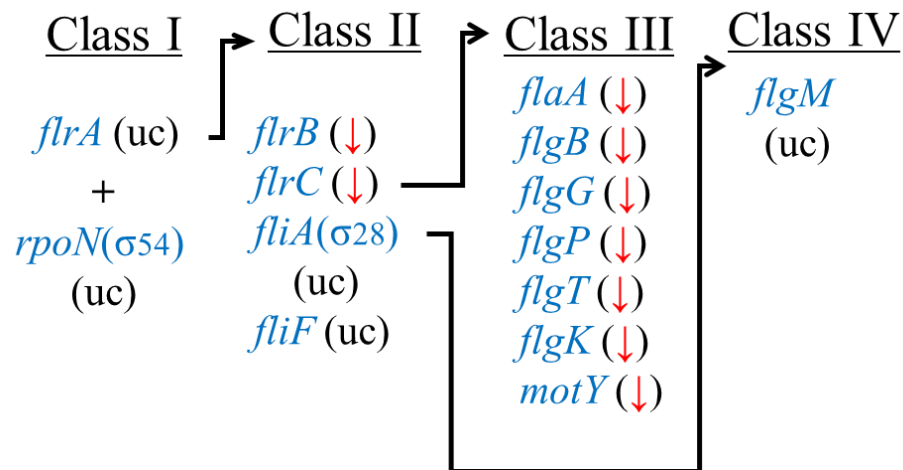
Fig. 7.2. Hierarchical regulation of *V. cholerae* flagellar gene synthesis. Down arrow (red) indicates downregulation of the respective genes in the CytR⁻ *V. cholerae* strain. uc, unchanged

Our findings further indicate that the *V. cholerae* CytR⁻ strain has a reduced ability to adhere to intestinal cells than the wild-type strain, showing a colonization defect. Colonization of *V. cholerae* in the small intestine requires the stringent activity of TcpA (Toxin Coregulated Pilus A) that also promotes adherence to intestinal cells (Krebs & Taylor, 2011). In support of this, we found that CytR⁻ *V. cholerae* express less *tcpA* during colonization. Bacterial attachment to the protective mucus layer can also be facilitated by flagellar motility in cooperation with N-acetylglucosamine binding protein A (GbpA) (Rudra Bhowmick et al., 2008). GbpA expression, on the other hand, was unaffected during colonization of the CytR⁻ strain.

The lack of flagella in CytR⁻ *V. cholerae* supports the rationale behind the colonization defect in the mutant strain. Taken together, CytR of *V. cholerae* positively regulates mucin layer penetration as well as colonization to the intestinal epithelium. After successfully colonizing the brush border lining of the intestinal epithelium, *V. cholerae* expresses CT and causes efflux of chloride ions (Cl⁻) from the cell, causing osmotic imbalance and ultimately leading to fluid loss into the intestinal lumen, which serves as one of the major aspects of *V. cholerae* virulence (Hsiao & Zhu, 2020; Kaper et al., 1995; Matson et al., 2007).

To examine the role of CytR in pathogenesis, we studied the intestinal fluid accumulation assay in the adult rabbit model. The results demonstrated that the CytR⁻ strain had less fluid buildup than the wild-type strain, which was attributed to lower cholera toxin production. Most virulence factors in *V. cholerae*, including *ctx* and *tcp*, are known to be controlled by a ToxT-dependent pathway in response to intestinal stimuli (Childers & Klose, 2007; Matson et al., 2007). Consistent with this, we found reduced expression of *toxT*, *ctxB*, and *tcpA* in the CytR⁻ strain. This could imply that the ToxT virulence regulation mechanism is affected in the CytR⁻ strain. Furthermore, *toxR/S* and *tcpP/H* control the expression of *toxT* in *V. cholerae* (Matson et al., 2007). Expression of ToxR is downregulated in the CytR⁻ strain, implying that CytR may regulate the master virulence regulator *toxT* in a *toxR*-dependent manner by a mechanism presently unknown. The expression of *tcpP*, on the other hand, was unaffected in the CytR⁻ strain. AphA/B regulates TcpP expression in wild type *V. cholerae*. As a consequence, we assume that *aphA/B* expression remained unaffected in the CytR⁻ strain.

Furthermore, the CytR⁻ strain is unable to use mucin in the intestine, which reduces GlcNAc residues within *V. cholerae* and may activate cyclic AMP (cAMP) receptor protein (CRP) (Kovacikova et al., 2004), which negatively controls the ToxR virulence regulon via the cAMP-CRP pathway (Skorupski & Taylor, 1997). However, more research is required to establish a relationship between CytR and the virulence cascade. Furthermore, effective colonization of the small intestine by *V. cholerae* is required for cholera toxin delivery to enterocytes (Ritchie et al., 2010; Taylor et al., 1987). The histology analysis confirms that the intestinal epithelium undergoes less damage when infected with the CytR⁻ strain. The CytR⁻ strain produces less CT in the ileal loop, resulting in less osmotic imbalance and less damage to the structure of

crypts and villi compared to the damage caused by the wild type strain during infection.
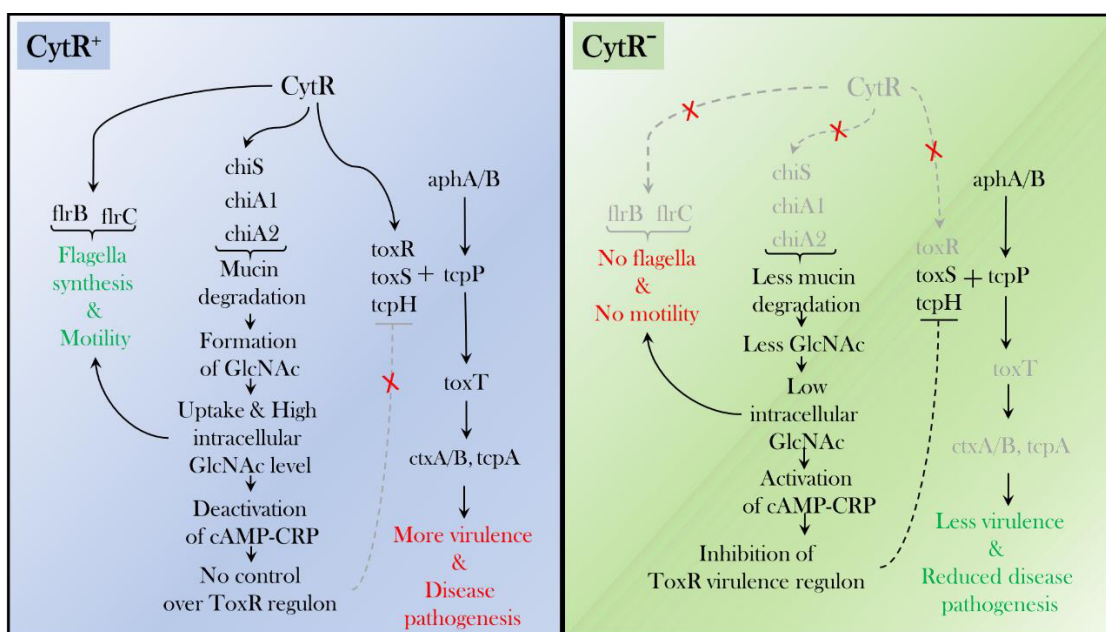
Fig. 7.3. Proposed model and mode of regulation of virulence cascade and pathogenesis by CytR in *V. cholerae*. The left panel shows the virulence regulation in wild type *V. cholerae* and the right panel indicates the effect of isogenic deletion mutation of CytR in *V. cholerae* (Please refer to the text for detailed discussion).

Our findings show that *V. cholerae* CytR positively regulates flagellar motility, adhesion, and pathogenicity in all conditions studied. Several studies have connected motility to adhesion in different Vibrios (Kim et al., 2014; Lee et al., 2002; McGee et al., 1996; Meron et al., 2009; Ormonde et al., 2000). In all the cases non-motile, non-flagellate mutants are all incapable of adhering to the host. The relationship between motility and virulence has also been studied. It was shown that the CytR homolog positively influences flagella synthesis and virulence gene production in *Erwinia carotovora*, the causal agent of soft-rot disease in plants, and plays an essential role in pathogenicity (Matsumoto et al., 2003). Similar observations were also made in our case.
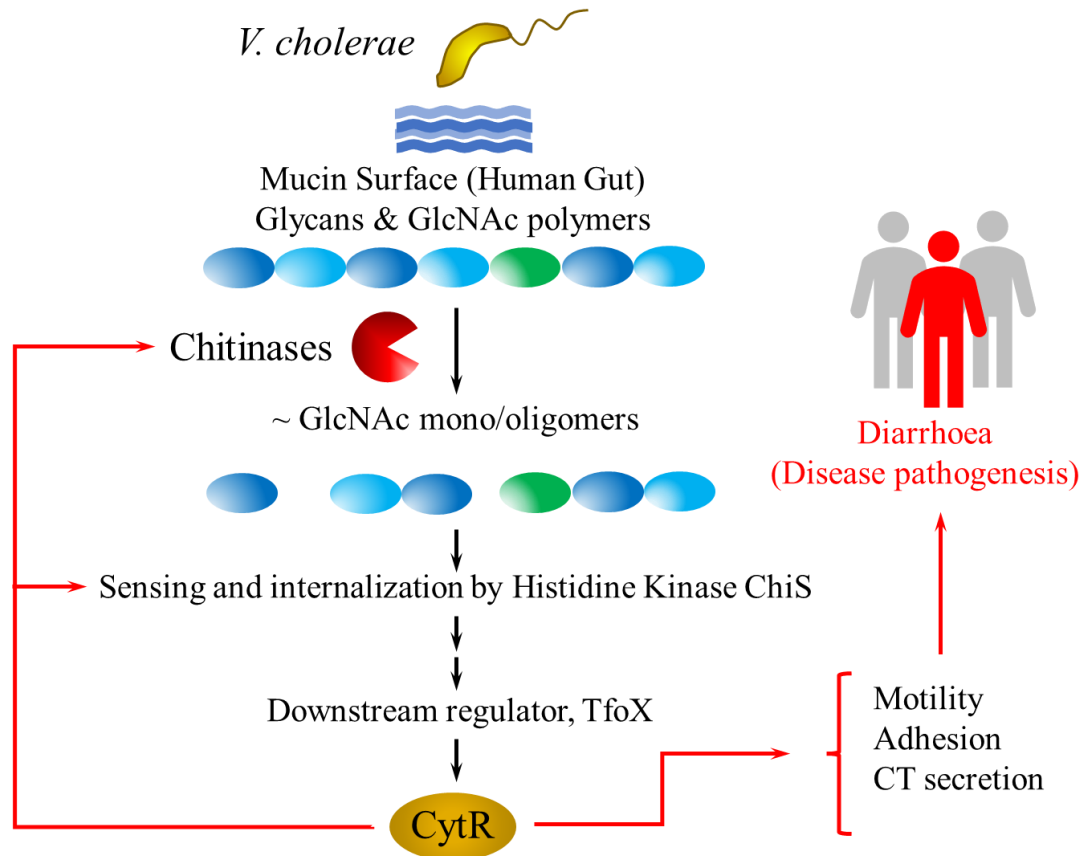
Fig. 7.4. Proposed model of mucin-dependent signalling pathways in V. cholerae. Mucin is degraded by extracellular chitinases into oligosaccharide fragments that enter the periplasm via a chitoporin. ChiS, a sensor kinase, recognises the presence of mucin oligosaccharides and eventually activates TfoX, which promotes the expression of several downstream genes including transcription factor CytR. In turn, CytR regulates the expression of sensor histidine kinase ChiS, chitinases, flagella synthesis genes, and other virulence regulatory genes.

To summarize the role of *V. cholerae* CytR during pathogenesis, it is important for the activity and expression of sensor histidine kinase ChiS and its downstream chitinases like ChiA1 and ChiA2. As a consequence, the CytR⁻ strain showed reduced mucin degradation and nutrient acquisition. CytR is also important for the expression of the Class II flagellar regulatory gene *flrB* and *flrC*. Deletion of CytR resulted in aflagellation of the bacteria. This results in reduced motility and penetration through the mucus layer by CytR⁻ strain *(Fig. 7.3)*. CytR mutation affects the expression of the virulence cascade gene *toxR*, resulting in reduced expression of the master virulence regulator *toxT*. During pathogenesis, ToxT modulates all virulence attributes, including the expression of toxin-coregulated pilus A, *tcpA*, and *ctxAB*. Reduced adherence to the epithelial cell in the CytR⁻ strain is correlated with

reduced expression of *tcpA*, and less CT synthesis resulted in reduced fluid accumulation. Furthermore, lower nutrition intake (in the form of GlcNAc) may result in reduced pathogenesis, either directly or indirectly through some undiscovered mechanisms involving the cAMP-CRP system. As a result, various regulatory pathways may exist, and CytR may be involved in this regulation directly or indirectly. Future research is needed to understand the complete regulation of virulence involving CytR in the host intestine *(Fig. 7.4)*.

Throughout the last decade, public awareness and campaigning in developing countries on the importance of adequate hygiene and sanitation, as well as the availability of safe drinking water, has helped to reduce the global prevalence of cholera. According to WHO, cholera infects about 1 million to 4 million people worldwide each year, claiming up to 21000 to 143000 lives (Ali et al., 2015). Total cholera cases were reduced by 60% in 2018 compared to the previous year (WHO, 2019). Typically, cholera treatment comprises electrolyte replacement therapy and, in certain cases, antibiotics.

However, the inappropriate and excessive use of antibiotics as a result of self-medication and indiscriminate access to medicines without a prescription has resulted in the emergence of multidrug-resistant (MDR) epidemic strains of bacteria. Antibiotic-resistant *V. cholerae* is becoming increasingly frequent among bacteria around the world (Verma et al., 2019). Kitaoka et al. performed an extensive review of countries reporting major drug-resistant *V. cholerae* strains (Kitaoka et al., 2011). *V. cholerae* develops drug resistance due to the frequent acquisition of extrachromosomal mobile genetic elements from other bacterial species through horizontal gene transfer (Das et al., 2020; Narendrakumar et al., 2019; Verma et al., 2019). Traditional antimicrobials are often bacteriostatic or bactericidal, which can promote the formation of MDR strains. As a result, novel therapeutic techniques such as the use of plant or herb extracts, bioactive phytochemicals, or the use of small molecules are urgently needed to combat these diseases by specifically targeting bacterial virulence factors.

Furthermore, probiotic treatment with *Bdellovibrio bacteriovorus* or *Micavibrio aeruginosavorus* has been shown to reduce the spread of antibiotic resistance in *V. cholerae* (Duncan et al., 2018; Dwidar et al., 2012). The usage of

bioactive chemicals derived from natural items such as herbs, spices, fruits, and seeds has numerous health benefits and has fewer adverse effects. Since ancient times, various plant parts and their derivative components have been utilized as Ayurvedic medicine in India to treat a variety of ailments, including diarrhoea. Plant-derived essential oils contain significant volatile components that have a variety of bioactivities, including antibacterial potential. The usage of essential oils such as cinnamon, cardamom, red chilli, white pepper, sweet fennel, and ginger has been well documented in recent years (Aminzare et al., 2018).

These bioactive compounds act against *V. cholerae* in various ways mainly by controlling virulence regulatory gene *toxT* (Virstatin) (Hung et al., 2005; Shakhnovich et al., 2007), inhibiting the binding of CT to GM_1 (6-Gingerol) (Saha et al., 2013), disrupting the secondary structure of CT (zinc oxide nanoparticles) (Sarwar et al., 2017) or by showing direct antimicrobial activity against the pathogen. A few carbohydrates have also been shown to suppress the cholera toxin (Kumar & Turnbull, 2018). Chitinase inhibitors have the potential to be chemotherapeutic against fungi, insects, and malaria transmission. Chitinase inhibitors have recently been suggested to have anti-inflammatory properties against asthma and allergic diseases such as atopic dermatitis and allergic rhinitis (Andersen et al., 2005).

In this study, we have screened different bioactive phytochemicals, sugar molecules (Wang et al., 2015), and enzyme inhibitors with varying functions on the growth, motility, adhesion, and cholera toxin (CT) production of *V. cholerae*. The molecules were selected as screening compounds after a literature survey. We found that phytochemical Carvacrol, an essential oil fraction of Oregano, was able to inhibit *V. cholerae* virulence both *in-vitro* and *in-vivo*. It also inhibited *V. cholerae* growth. We have done a detailed study with carvacrol and its effect on different virulence attributes during *V. cholerae* pathogenesis. Cinnamaldehyde also reduced growth and adhesion to some extent. However, Curcumin, from *Curcuma longa*, did not show much effect on *V. cholerae*. Sugar molecules like Xylose, Xylitol, Cellobiose, d-Allose, and Na-3-hydroxy butyrate mainly reduced CT production *in vitro*. 3-hydroxy butyrate distinctly reduced cellular adhesion of *V. cholerae*. Chitinases in *V. cholerae* have been demonstrated to be important for pathogenesis. Therefore, chitinase inhibitors Dequalinium chloride, Pentoxifylline, Theophylline, and Caffeine were tested for their role as anti-virulence compounds (Rao et al., 2005). The cholera toxin

was found to be 5.5-fold, 13.5-fold, 6.9-fold, and 17.5-fold less produced in presence of pentoxifylline, caffeine, dequalinium chloride, and theophylline respectively, compared to the wild type as control. These results suggest that these chitinase inhibitor molecules might prevent growth, adhesion, motility, and cholera toxin production which might ultimately reduce the pathogenicity of *V. cholerae*. The identified effective inhibitors may act as dietary additives to reduce the risk of *V. cholerae* infection. Therefore, further studies may be carried out to formulate the use of these chitinase inhibitor molecules alone or in combination at the lowest possible doses to combat *V. cholerae* pathogenesis.

Carvacrol (CV) is a naturally occurring essential oil fraction of Oregano (Origanum vulgare) that has antimicrobial activity against a variety of foodborne pathogens including *E. coli* O157: H7 (Obaidat & Frank, 2009), *Bacillus cereus* (Annemieke Ultee et al., 2000), *Shigella sp.* (Bagamboula et al., 2004), *Salmonella sp.* (Miladi et al., 2016), *Clostridium difficile* (Mooyottu et al., 2014), and also *V. cholerae* (Rattanachaikunsopon & Phumkhachorn, 2010). Studies indicated that CV possesses a variety of characteristics (Ahmad et al., 2011; Arunasree, 2010) including anti-oxidant (Aristatile et al., 2009; Slamenova et al., 2008; Slameňová et al., 2007), anti-bacterial (Nostro et al., 2009; Pérez-Conesa et al., 2011; Rattanachaikunsopon & Phumkhachorn, 2010) and anti-inflammatory properties (Hotta et al., 2010; Landa et al., 2009).

The majority of studies on the effects of carvacrol on bacteria have focused on determining the Minimum Inhibitory Concentration (MIC) at which bacterial growth is inhibited or the Minimum Bactericidal Concentration (MBC), i.e., the concentration at which > 99.9% of the bacterial population is killed (van Alphen et al., 2012). Despite considerable research on carvacrol in recent years, no report on carvacrol's anti-virulence capabilities against *V. cholerae* has been published. In this study, we have explored the impact of sub-inhibitory (sub-MIC) carvacrol concentrations on the pathogenic potential of *V. cholerae*. In this context, we evaluated carvacrol's activity on *V. cholerae* motility, transcriptional regulation of flagella synthesis genes, *in vitro* mucin penetration, adhesion to epithelial cells, and *in vivo* anti-virulence activity using rabbit ileal loop models. Traditional knowledge of herbal extracts was widely practiced as therapies to treat certain diseases around the world before the age of antibiotic discovery. However, in this antibiotic era, bacteria with resistance to

various antibiotics are becoming more common, and the slow rate of development of new medicines over the last decade has prompted researchers to seek alternative techniques to treating pathogenic diseases (Bassetti et al., 2013; Sharifi-Rad et al., 2018). After an extensive literature survey, Carvacrol (CV), an essential oil fraction of oregano was selected for the study possessing several bioactive properties on various organisms.

In this study, we looked at how the sub-inhibitory concentration of CV affected the ability of *V. cholerae* to access a wide range of biological activities under pathogenic conditions. The current experimental study results indicate that CV has a bacteriostatic as well as a bactericidal effect on *V. cholerae* at MIC. These findings are consistent with the prior investigation, although a subtle difference in MIC was also observed (Magi et al., 2015; Rattanachaikunsopon & Phumkhachorn, 2010). To assess the anti-pathogenic activity of CV against *V. cholerae*, we determined that ½ MIC is the highest concentration of CV that does not inhibit *V. cholerae* growth and remains viable. As a result, concentrations of ½ MIC and lower were employed to evaluate the inhibitory effect of carvacrol on the various virulence and pathogenic attributes of *V. cholerae*. We also ensured that at a particular optical density, CV-treated and untreated *V. cholerae* cultures had the same number of viable bacteria, eliminating the possibility of unfair analysis of the experimental results. The fecal-oral pathway is used during the transmission of *V. cholerae* in humans. *V. cholerae* must penetrate the thick mucus layer in the small intestine to colonize the underlying enterocytes (Jordan et al., 1998). CV at sub-MIC levels decreased *V. cholerae* mucin penetrating capacity in a dose-dependent manner. The rotation of the monotrichous polar flagellum of *V. cholerae* mediates motility and mucin penetration, which is considered a crucial pathogenicity component for the bacteria (Mewborn et al., 2017; Silva et al., 2003).

Our findings are also in line with previous studies where various bioactive phytochemicals or their derivatives produce anti-virulence effects against different pathogenic microorganisms by diminishing bacterial motility and flagellar protein expression (Y. Liu et al., 2017). It was previously observed that the polyphenolic fraction of Kombucha was capable of inhibiting *V. cholerae* motility because of a defect in flagellar gene biosynthesis (Bhattacharya et al., 2020). Furthermore, two separate studies showed that tea polyphenols and cranberry proanthocyanidins

decreased *P. aeruginosa* swarming motility (O'May & Tufenkji, 2011; Yin et al., 2015).

Transmission electron microscopy demonstrates that sub-MIC treatment of CV causes *V. cholerae* to become aflagellate, which explains the rationale behind the reduced motility. As per the RT-PCR data, the sub-inhibitory concentrations of CV had a significant ($P < 0.05$) downregulatory influence on *flrC*, a cytosolic response regulator that belongs to the Class II flagellar synthesis genes. Together with the histidine kinase *flrB*, *flrC* regulates the synthesis of Class III flagellar genes, which are largely involved in the production of flagellin proteins as well as structural units of the flagellar basal body (Echazarreta & Klose, 2019; Klose & Mekalanos, 1998). We have also found that sub-MIC of CV downregulates the expression of class III genes. These genes primarily include *motY*, *flaA*, *flgP*, *flgT*, *flgK*, *flgG*, *flgB*. Therefore, we speculate CV at sub-MIC inhibits the synthesis of class III genes directly by regulating their expression or by specifically modulating the expression of class II component *flrC*. Although further research is a prerequisite to gain a better insight into this mechanism. The swarming motility and mucin penetrating ability of *V. cholerae* also get inhibited by CV. Therefore, the inability to swim and penetrate the mucin layer can be explained by the absence of flagella.

V. cholerae attaches to the brush borders of epithelial cells after penetrating the thick mucus layer. We found that CV inhibited *V. cholerae* adhesion to the epithelial cells. Although, due to the lower bioavailability, a greater dose of CV was required to achieve a significant effect in vivo. Furthermore, reduced expression of toxin co-regulated pilus A (*tcpA*), one of the major adhesins of *V. cholerae*, might explain the possible reason behind decreased adhesion of *V. cholerae* to the epithelium. After adhering to the intestinal brush border epithelium *V. cholerae* starts secreting cholera toxin (CT). The fundamental determinant of cholera pathogenesis is fluid accumulation as a result of CT generation. In the rabbit ileal loop model, we have found a significant reduction in fluid accumulation upon CV treatment. This finding is also consistent with previous studies in which CV administration at 60 µg/ml was shown to inhibit diarrhoeal toxin generation by *Bacillus cereus* by 80% (A. Ultee & Smid, 2001). To investigate the inhibitory mechanisms of CV on CT production in *V. cholerae*, quantitative RT-PCR of major virulence genes such as *toxT, ctxB, tcpA*, and *hlyA* were performed. In this context, we found a significant

decrease in all virulence genes by more than 2-fold at sub-MIC levels. The expression of CT and TCP in *V. cholerae* is activated by the expression of *toxT*, the master virulence regulator, which is controlled by upstream regulators such as TcpP/TcpH and ToxR/ToxS (Matson et al., 2007).

Therefore, we assume that the reduction in transcription of *ctxB*, *tcpA* genes upon sub-MIC treatment of CV may be due to the inhibitory effect of CV on *toxT*. Notably, CV might also be involved in the regulation of the transcription of *toxT*, *tcpA*, *ctxB*, and *hlyA* by either a direct or an indirect mechanism, although further study regarding the mechanism is needed for a complete understanding of this process. The phenolic group of CV damages bacterial membranes, resulting in increased membrane fluidity and loss of protons and larger ions (Langeveld et al., 2014; Weber & De Bont, 1996). TEM micrograph demonstrated that CV at MIC produced substantial damage to the surface of *V. cholerae* and affected the bacterial morphology. At sub-MIC, membrane impairment was not noticed but as stated earlier it lacks the presence of flagella. CV causes membrane disruption and inhibits *V. cholerae* survival and growth at MIC, however *V. cholerae* retain its membrane integrity and shape at sub-MICs. This also supports the previous report where *B. cereus* was found to adapt to the non-lethal concentrations of CV (Annemieke Ultee et al., 2000). Overall, these results indicated that CV inhibited *V. cholerae* virulence in a dose-dependent manner. Bioactive phytochemicals have a wide range of health benefits. Apart from these properties, they may have cytotoxic effects on the host cells (Llana-Ruiz-Cabello et al., 2015), which should be studied. We have tested the cytotoxic activity of CV on the human cell line HT-29 and CV showed minimum membrane damage. Even after 48 hours, the ½ MIC of CV exhibited 5.12% cytotoxicity. As a result, it is thought that using CV at sub-MIC levels won't affect human intestinal cells. This is also supported by fluorescence microscopy. Earlier studies have also suggested that CV is usually nongenotoxic to the living cells (Bakkali et al., 2008) and shown to be safe for 24 h on HepG2 cell-line (Palabiyik et al., 2016).

Therefore, the present study demonstrates for the first time that CV at sub-inhibitory concentrations inhibits *V. cholerae* growth and virulence. *V. cholerae* flagellar synthesis was suppressed by CV treatment, which inhibited bacterial motility through the thick mucus layer. This was followed by reduced adherence to the

intestinal epithelium and subsequently lower expression of CT and other virulence-associated genes. Finally, these events result in less fluid accumulation in the rabbit intestine. It is plausible that CV acts on a global regulator to describe the pleiotropic effect of CV on such a wide range of virulence genes. Repression of the CT production and virulence gene transcription is affected by natural compounds *(Fig.7.5)*.

One such example includes capsaicin, a red chili extract that reduced the virulence of *V. cholerae* by regulating the expression of *hns* (Yamasaki et al., 2011). Future research is required to discover the global regulator and comprehend the cascade of the inhibitory mechanism. A previous study revealed CV to be safe for human use, and we discovered that it has a minimal cytotoxic effect at sub-MIC levels for up to 12 hours. We have also tested the long-term cytotoxicity of CV against the HT-29 cell line, and it exhibited roughly 5% cytotoxicity at ½ MIC after 48 hours (Preliminary observation). The finding of the current study emphasizes the intriguing role of CV as a novel anti-virulent chemical that can be promoted as a therapeutic agent to treat *V. cholerae* infection.

The finding of the present study highlights the potential role of CV as a novel anti-virulent compound that can be promoted as a therapeutic agent to treat *V. cholerae* infection. Further experiments on the detailed pharmacokinetics relating to human evidence may be worthy of evaluation before CV administration. Despite the fact that CV has been classified as a Generally Recognized As Safe (GRAS) substance and is allowed for usage (Hyldgaard et al., 2012), its poor solubility and bioavailability remain a concern (Suntres et al., 2015). As a result, advancements in delivery systems must be made concurrently to improve the solubility, stability, and bioavailability of this compound.

We earlier established the importance of CytR in the survival and pathogenicity of *V. cholerae*. Therefore, it is likely that host factors would also affect CytR. So, we monitored the effect of host factors on CytR. We found that at an optimum concentration of 1% mucin the CytR expression was maximum. Previous research from other laboratories has suggested that pathogenic bacteria's chitinases and chitin-binding proteins interact with the carbohydrate moiety of glycoproteins that have a chemical resemblance to chitin (Chaudhuri et al., 2010; Debroy et al., 2006).

Our findings suggest that *V. cholerae* chitinases can hydrolyze the β-1, 4-linkages that connect the GlcNAc moieties present in mucin.
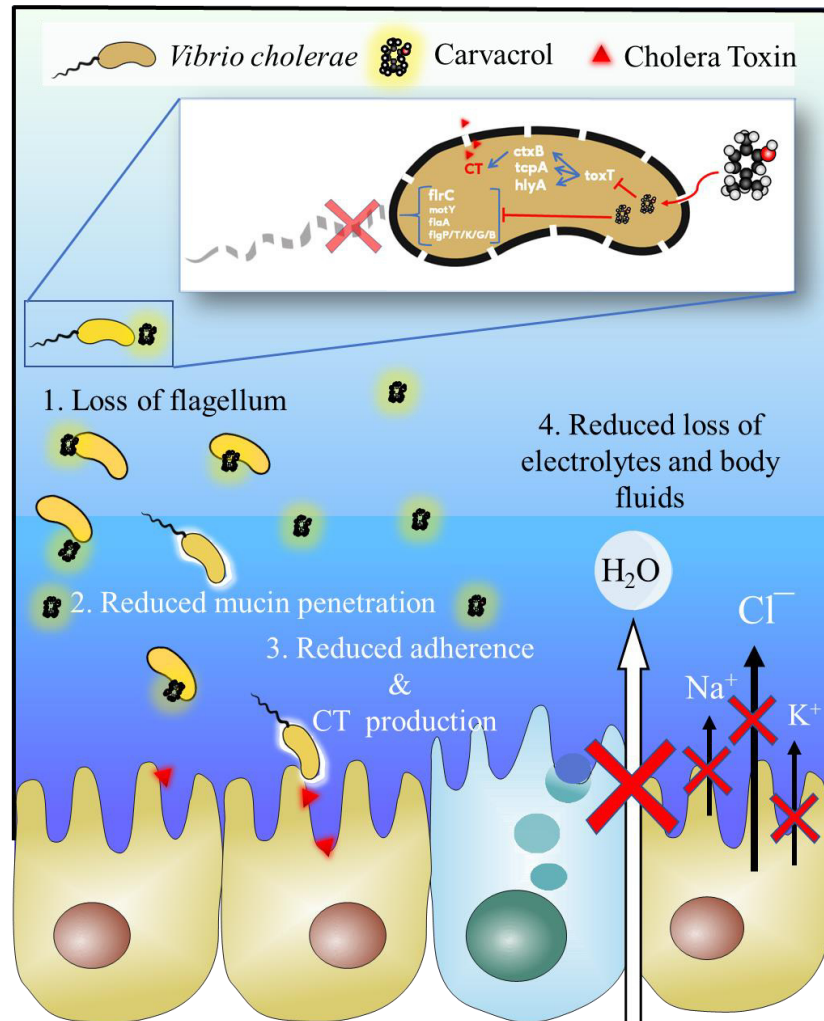
Fig. 7.5. Schematic diagram showing a proposed model for the mode of action of Carvacrol. In the intestinal environment, carvacrol inhibits the synthesis of flagella in *V. cholerae*, resulting in reduced motility and mucin penetration. This further leads to reduced adhesion to the brush border epithelial cells and less cholera toxin (CT) production. That ultimately results in reduced loss of electrolytes and body fluids, hence less pathogenesis.

When CytR is expressed in the presence of mucin, it triggers the expression of chitinases, which actively hydrolyze the GlcNAc moieties in mucin. This demonstrates that there is a mucolytic activity of bacterial chitinases, which has previously been documented but only with the assistance of proteases (Sanders et al., 2007).

Bacterial pathogens are distinguished by their ability to detect host metabolites and effectively coordinate the expression of numerous virulence factors (Elmi et al., 2018; Olive & Sassetti, 2016). Bile is a well-known host metabolite that is biosynthesized from cholesterol by hepatocytes in the liver (Joyce & Gahan, 2016). The gallbladder secretes bile into the small intestine, particularly the duodenum, jejunum, and proximal ileum (Urdaneta & Casadesús, 2017). The physiological concentration of bile in the gut can be as high as 20 mM in the duodenum, then gradually decreases to 10 mM in the jejunum, and finally drops to 4 mM in the ileum (Hofmann & Hagey, 2008; Maldonado-Valderrama et al., 2011). Bile emulsifies dietary fats and aids in the absorption of lipid elements in the intestine. Furthermore, because of the diverse composition of bile salts, bilirubin, phospholipids, cholesterol, and enzymes, bile has detergent-like toxicity and works as a potent antibacterial agent, solubilizing membrane lipids and dissociating bacterial membrane proteins (Boyer, 2013; Hofmann & Small, 1967). Bile acts as a signal for several enteric pathogens, including *E. coli* O157:H7, *Vibrio cholerae*, *Shigella flexneri*, and *Vibrio parahaemolyticus*, to modulate global gene expression of virulence components (Alam et al., 2010; Bachmann et al., 2015; Sistrunk et al., 2016). CytR expression is not significantly up-regulated when crude bile is present. We also did not find any significant change in CytR expression for individual bile salt supplements. Our experimental data also suggests CytR expression is not affected by the dose of different bile salt components. We can conclude that CytR is not directly involved in bile-induced virulence modulation in *V. cholerae*.

It has long been said that cholera is a noninflammatory diarrhoeal disease, however recent study (Rodríguez et al., 2001) have shown that *V. cholerae* upon binding with the intestinal epithelial cell lines produces pro-inflammatory cytokine (Jung et al., 1995) Interleukin-8 (IL-8), which is a potent chemoattractant for polymorphonuclear leukocytes and T lymphocytes, which further causes inflammation (Bandyopadhaya et al., 2007). Our study showed that infection with CytR⁻ *V. cholerae* reduces the production of IL-8 during *ex-vivo* infection.

Tumor necrosis factor (TNF) another regulator of inflammatory responses, is a potent lymphoid factor that is produced by a wide number of cells. TNFs play a critical role in the body's resistance to infection by inducing fever and activating macrophages and the destruction of certain tumors. However, over-production of TNF has been

associated with cytotoxic effects such as cachexia (Andrews et al., 2018). Our study showed no significant production of TNF by CaCo2 cell-line. Deletion of CytR in *V. cholerae* also did not possess any effect on the production of TNF. We conclude from our research that CytR, a transcriptional regulator, promotes *V. cholerae* survival in the natural environment as well as the host intestine, thereby favouring its existence and transmission between its dual life cycle, which includes the aquatic environment as well as the host intestine.

Chapter 8

Conclusion

Conclusion

This thesis work deals with the functional characterization of *V. cholerae* cytoplasmic regulatory protein CytR in chitin utilization and disease pathogenesis in animal models. The conclusions of the thesis are as follows –

- We studied the expression of CytR at RNA and protein levels under varying temperatures, pH, salinity, and chitin amount. We found the optimum environmental conditions for maximum CytR expression are around temperature 25°C, pH 7.5, salinity 300 mM, and chitin 0.8 %.

- *V. cholerae* CytR positively regulates the expression of all four known chitinase genes (*chiA1*, *chiA2*, *vc0769,* and *vc1073*). These chitinase helps *V. cholerae* to utilize chitin as a nutrient source from the environment.

- The expression of ChiS, which is a periplasmic sensor histidine kinase, is significantly reduced in the CytR⁻ strain of *V. cholerae*. ChiS is important for the detection and sensing of chitin oligosaccharides and plays an important role in the chitin utilization pathway by regulating the downstream genes like *tfoR* and *tfoX*. The activity of β-hexosaminidase (which is a measure of ChiS activity) also reduced greatly in the CytR ablated strain. We hypothesize that CytR controls the *V. cholerae* chitin utilization pathway by regulating ChiS.

- CytR is involved in regulating the growth of *V. cholerae* both in the chitin and mucin supplemented media. The absence of CytR in *V. cholerae* genome caused reduced production of chitinases and hence lesser breakdown of chitin or mucin occurs.

- CytR plays an important role in the adhesion of *V. cholerae* to the epithelial cells by regulating the expression of *tcpA*, one of the major adhesions of *V. cholerae*.

- In *V. cholerae*, CytR is responsible for flagella synthesis. CytR may regulate the Class II flagellar synthesis genes *flrB* and *flrC*, leading to the downregulation of downstream Class III flagellar synthesis genes. The lack of

flagella in the CytR mutant *V. cholerae* reduces the bacteria's ability to move in the thick mucinous environment.

- Deletion of CytR significantly reduced the virulence of *V. cholerae* in the rabbit ileal loop model. CytR controls the cholera toxin production by regulating the *toxR-toxT-ctxAB* virulence axis. Reduced cholera toxin production in the CytR mutant *V. cholerae* leads to reduced fluid accumulation in the rabbit intestine.

- We have mentioned previously that CytR regulates ChiS in presence of chitin. We further showed that *V. cholerae* requires CytR for the regulation of ChiS dependent utilization of mucin in the intestinal environment.

- Further, we have tested a few bioactive phytochemicals for their potential role as anti-virulence agents. We found that Carvacrol, Allose, Sodium-3-hydroxy butyrate, and Dequalinium chloride acts as potent inhibitor of cholera toxin production, adhesion to gastro-epithelial cells, and motility which ultimately reduces the pathogenicity of *V. cholerae*.

- The host factor mucin with a concentration of 1% - 1.5 % is optimum for CytR expression.

- Bile acts as a signal for several enteric pathogens, including *V. cholerae,* to modulate the global gene expression of virulence components. Bile salts do not have much significant effect on the expression of CytR. We conclude that CytR does not play a direct role in bile-induced virulence modulation in *V. cholerae*.

- CytR deletion in *V. cholerae* has no effect on TNF release from the CaCo2 cell line, but it reduces IL-8 production by 5.5-fold. When *V. cholerae* binds to intestinal epithelial cell lines, it produces the pro-inflammatory cytokine Interleukin-8 (IL-8), which is a powerful chemoattractant for polymorphonuclear leukocytes and T lymphocytes, causing inflammation. To summarise, *V. cholerae* CytR may play a role in causing gastrointestinal inflammation.

Chapter 9

References

References

Abuaita, B. H., & Withey, J. H. (2009). Bicarbonate induces *Vibrio cholerae* virulence gene expression by enhancing ToxT activity. *Infection and Immunity*, *77*(9), 4111–4120. https://doi.org/10.1128/IAI.00409-09

Ahmad, A., Khan, A., Akhtar, F., Yousuf, S., Xess, I., Khan, L. A., & Manzoor, N. (2011). Fungicidal activity of thymol and carvacrol by disrupting ergosterol biosynthesis and membrane integrity against Candida. *European Journal of Clinical Microbiology and Infectious Diseases*, *30*(1), 41–50. https://doi.org/10.1007/s10096-010-1050-8

Alam, A., Tam, V., Hamilton, E., & Dziejman, M. (2010). vttRa and vttRB encode ToxR family proteins that mediate bile-induced expression of type three secretion system genes in a non-O1/non-O139 *Vibrio cholerae* strain. *Infection and Immunity*, *78*(6), 2554–2570. https://doi.org/10.1128/IAI.0 1073-09

Alam, M., Islam, A., Bhuiyan, N., Rahim, N., Hossain, A., Khan, G. Y., Ahmed, D., Watanabe, H., Izumiya, H., Faruque, A. G., Akanda, A., Islam, S., Sack, R. B., Huq, A., Colwell, R. R., Cravioto, A., Kuna, A., Gajewski, M., Yildiz, F. H. H., … Silva, A. A. J. (2017). HHS Public Access. *Journal of Bacteriology*, *5*(2), 7273. https://doi.org/10.1128/JB.186.19.6374

Alam, M., Kasan, N. A., Sadique, A., Bhuiyan, N. A., Ahmed, K. U., Nusrin, S., Nair, G. B., Siddique, A. K., Sack, R. B., Sack, D. A., Huq, A., & Colwell, R. R. (2006). Seasonal cholera caused by *Vibrio cholerae* serogroups O1 and O139 in the coastal aquatic environment of Bangladesh. *Applied and Environmental Microbiology*, *72*(6), 4096–4104. https://doi.org/10.1128/ AEM.00066-06

Albert, M. J. (1992). *Large outbreak of clinical cholera due to*. 704.

Alemka, A., Corcionivoschi, N., & Bourke, B. (2012). Defense and adaptation: the complex inter-relationship between Campylobacter jejuni and mucus. *Frontiers in Cellular and Infection Microbiology*, *2*(February), 15. https://doi.org/10.3389/fcimb.2012.00015

Ali, M., Nelson, A. R., Lopez, A. L., & Sack, D. A. (2015). Updated global burden of cholera in endemic countries. *PLoS Neglected Tropical Diseases*, *9*(6), 1–13. https://doi.org/10.1371/journal.pntd.0003832

Alm, R. A., & Manning, P. A. (1990). Biotype-specific probe for *Vibrio cholerae* serogroup O1. *Journal of Clinical Microbiology*, *28*(4), 823–824.

https://doi.org/10.1128/jcm.28.4.823-824.1990

Al-Mekhlafi, H. M. (2018). Perspective piece: Yemen in a time of cholera: Current situation and challenges. *American Journal of Tropical Medicine and Hygiene*, *98*(6), 1558–1562. https://doi.org/10.4269/ajtmh.17-0811

Aminov, R. I. (2010). A brief history of the antibiotic era: Lessons learned and challenges for the future. *Frontiers in Microbiology*, *1*(DEC), 1–7. https://doi.org/10.3389/fmicb.2010.00134

Aminzare, M., Hashemi, M., Abbasi, Z., Mohseni, M., & Amiri, E. (2018). Vibriosis phytotherapy: A review on the most important world medicinal plants effective on Vibrio spp. *Journal of Applied Pharmaceutical Science*, *8*(1), 170–177. https://doi.org/10.7324/JAPS.2018.8126

Andersen, O. A., Dixon, M. J., Eggleston, I. M., & Van Aalten, D. M. F. (2005). Natural product family 18 chitinase inhibitors. *Natural Product Reports*, *22*(5), 563–579. https://doi.org/10.1039/b416660b

Andrews, C., McLean, M. H., & Durum, S. K. (2018). Cytokine tuning of intestinal epithelial function. *Frontiers in Immunology*, *9*(JUN). https://doi.org/10.3389/fimmu.2018.01270

Antonova, E. S., & Hammer, B. K. (2011). Quorum-sensing autoinducer molecules produced by members of a multispecies biofilm promote horizontal gene transfer to *Vibrio cholerae*. *FEMS Microbiology Letters*, *322*(1), 68–76. https://doi.org/10.1111/j.1574-6968.2011.02328.x

Antonova, E. S., Bernardy, E. E., & Hammer, B. K. (2012). Natural competence in *Vibrio cholerae* is controlled by a nucleoside scavenging response that requires CytR-dependent anti-activation. *Molecular Microbiology*, *86*(5), 1215–1231. https://doi.org/10.1111/mmi.12054

Aristatile, B., Al-Numair, K. S., Veeramani, C., & Pugalendi, K. V. (2009). Effect of carvacrol on hepatic marker enzymes and antioxidant status in d-galactosamine-induced hepatotoxicity in rats. *Fundamental and Clinical Pharmacology*, *23*(6), 757–765. https://doi.org/10.1111/j.1472-8206.2009.00721.x

Arunasree, K. M. (2010). Anti-proliferative effects of carvacrol on a human metastatic breast cancer cell line, MDA-MB 231. *Phytomedicine*, *17*(8–9), 581–588. https://doi.org/10.1016/j.phymed.2009.12.008

Bachmann, V., Kostiuk, B., Unterweger, D., Diaz-Satizabal, L., Ogg, S., & Pukatzki, S. (2015). Bile salts modulate the mucin-activated type vi secretion system of pandemic *vibrio cholerae*. *PLoS Neglected Tropical Diseases*, *9*(8), 1–22. https://doi.org/10.1371/journal.pntd.0004031

Bagamboula, C. F., Uyttendaele, M., & Debevere, J. (2004). Inhibitory effect of thyme and basil essential oils, carvacrol, thymol, estragol, linalool and p-cymene towards Shigella sonnei and S. flexneri. *Food Microbiology*, *21*(1), 33–42. https://doi.org/10.1016/S0740-0020(03)00046-7

Baker-Austin, C., Oliver, J. D., Alam, M., Ali, A., Waldor, M. K., Qadri, F., & Martinez-Urtaza, J. (2018). Vibrio spp. infections. *Nature Reviews Disease Primers*, *4*(1). https://doi.org/10.1038/s41572-018-0005-8

Baker-Austin, C., Stockley, L., Rangdale, R., & Martinez-Urtaza, J. (2010). Environmental occurrence and clinical impact of Vibrio vulnificus and Vibrio parahaemolyticus: A European perspective. *Environmental Microbiology Reports*, *2*(1), 7–18. https://doi.org/10.1111/j.1758-2229.2009.00096.x

Bakkali, F., Averbeck, S., Averbeck, D., & Idaomar, M. (2008). Biological effects of essential oils - A review. *Food and Chemical Toxicology*, *46*(2), 446–475. https://doi.org/10.1016/j.fct.2007.09.106

Bandyopadhaya, A., Sarkar, M., & Chaudhuri, K. (2007). Transcriptional upregulation of inflammatory cytokines in human intestinal epithelial cells following *Vibrio cholerae* infection. *FEBS Journal*, *274*(17), 4631–4642. https://doi.org/10.1111/j.1742-4658.2007.05991.x

Banerjee, R., Das, B., Balakrish Nair, G., & Basak, S. (2014). Dynamics in genome evolution of *Vibrio cholerae. Infection, Genetics and Evolution*, *23*(January), 32–41. https://doi.org/10.1016/j.meegid.2014.01.006

Bansil, R., & Turner, B. S. (2006). Mucin structure, aggregation, physiological functions and biomedical applications. *Current Opinion in Colloid and Interface Science*, *11*(2–3), 164–170. https://doi.org/10.1016/j.cocis.2005.11.001

Barbier, C. S., Short, S. A., & Senear, D. F. (1997). Allosteric mechanism of induction of CytR-regulated gene expression. CytR repressor-cytidine interaction. *Journal of Biological Chemistry*, *272*(27), 16962–16971. https://doi.org/10.1074/jbc.272.27.16962

Bassetti, M., Merelli, M., Temperoni, C., & Astilean, A. (2013). New antibiotics for bad bugs: Where are we? *Annals of Clinical Microbiology and Antimicrobials*, *12*(1), 1–15. https://doi.org/10.1186/1476-0711-12-22

Baudry, B., Fasano, A., Ketley, J., & Kaper, J. B. (1991). Cloning of a gene (zot) encoding a new toxin produced by *Vibrio cholerae. Infection and Immunity*, *60*(2), 428–434. https://doi.org/10.1128/iai.60.2.428-434.1992

Baumann, L., Baumann, P., Mandel, M., & Allen, R. D. (1972). Taxonomy of aerobic marine eubacteria. *Journal of Bacteriology*, *110*(1), 402–429.

https://doi.org/10.1128/jb.110.1.402-429.1972

Bear, C. E., Li, C., Kartner, N., Bridges, R. J., Jensen, T. J., Ramjeesingh, M., & Riordan, J. R. (1992). Purification and functional reconstitution of the cystic fibrosis transmembrane conductance regulator (CFTR). *Cell*, *68*(4), 809–818. https://doi.org/10.1016/0092-8674(92)90155-6

Beier, S., & Bertilsson, S. (2013). Bacterial chitin degradation-mechanisms and ecophysiological strategies. *Frontiers in Microbiology*, *4*(JUN), 1–12. https://doi.org/10.3389/fmicb.2013.00149

Bhattacharya, D., Sinha, R., Mukherjee, P., Howlader, D. R., Nag, D., Sarkar, S., Koley, H., Withey, J. H., & Gachhui, R. (2020). Anti-virulence activity of polyphenolic fraction isolated from Kombucha against *Vibrio cholerae*. *Microbial Pathogenesis*, *140*, 103927. https://doi.org/10.1016/j.micpath.2019.103927

Bhowmick, R., Ghosal, A., & Chatterjee, N. S. (2007). Effect of environmental factors on expression and activity of chitinase genes of vibrios with special reference to *Vibrio cholerae*. *Journal of Applied Microbiology*, *103*(1), 97–108. https://doi.org/10.1111/j.1365-2672.2006.03253.x

Bhowmick, Rudra, Ghosal, A., Das, B., Koley, H., Saha, D. R., Ganguly, S., Nandy, R. K., Bhadra, R. K., & Chatterjee, N. S. (2008). Intestinal adherence of *Vibrio cholerae* involves a coordinated interaction between colonization factor GbpA and mucin. *Infection and Immunity*, *76*(11), 4968–4977. https://doi.org/10.1128/IAI.01615-07

Binsztein, N., Costagliola, M. C., Pichel, M., Jurquiza, V., Ramírez, F. C., Akselman, R., Vacchino, M., Huq, A., & Colwell, R. (2004). Viable but nonculturable *Vibrio cholerae* O1 in the aquatic environment of Argentina. *Applied and Environmental Microbiology*, *70*(12), 7481–7486. https://doi.org/10.1128/AEM.70.12.7481-7486.2004

Bjork, S., Breimer, M. E., Hansson, G. C., Karlsson, K., & Leffler, H. (1987). Structures of Blood Group Glycosphingolipids of Human Small Intestine. *Journal of Biological Chemistry*, *262*(14), 6758–6765.

Blokesch, M. (2012). Chitin colonization, chitin degradation and chitin-induced natural competence of *Vibrio cholerae* are subject to catabolite repression. *Environmental Microbiology*, *14*(8), 1898–1912. https://doi.org/10.1111/j.1462-2920.2011.02689.x

Boyer, J. L. (2013). Bile formation and secretion. *Comprehensive Physiology*, *3*(3), 1035–1078. https://doi.org/10.1002/cphy.c120027

Burt, S. (2004). Essential oils: Their antibacterial properties and potential applications in foods - A review. *International Journal of Food*

Microbiology, *94*(3), 223–253. https://doi.org/10.1016/j.ijfoodmicro.2004.03.022

Butler, S. M., & Camilli, A. (2005). Going against the grain: chemotaxis and infection in *Vibrio cholerae*. *Nature Reviews Microbiology*, *3*(8), 611–620. https://doi.org/10.1038/nrmicro1207

Cash, R. A., Music, S. I., Joseph, P., Snyder, M. J., Wenzel, R. P., & Hornick, R. B. (1974). *Response of Man to Infection with Vibrio cholerae*. *129*(1), 45–52.

Castro-Rosas, J., & Escartín, E. F. (2000). Survival and growth of *Vibrio cholerae* O1 Salmonella typhi, and Escherichia coli O157:H7 in alfalfa sprouts. *Journal of Food Science*, *65*(1), 162–165. https://doi.org/10.1111/j.1365-2621.2000.tb15973.x

Chac, D., Dunmire, C. N., Singh, J., & Weil, A. A. (2021). Update on Environmental and Host Factors Impacting the Risk of *Vibrio cholerae* Infection. *ACS Infectious Diseases*, *7*(5), 1010–1019. https://doi.org/10.1021/acsinfecdis.0c00914

Chatterjee, A., Dutta, P. K., & Chowdhury, R. (2007). Effect of Fatty Acids and Cholesterol Present in Bile on Expression of Virulence Factors and Motility of *Vibrio cholerae*. *Infection and Immunity*, *75*(4), 1946–1953. https://doi.org/10.1128/IAI.01435-06

Chatterjee, S. N., & Chaudhuri, K. (2003). Lipopolysaccharides of *Vibrio cholerae*: I. Physical and chemical characterization. *Biochimica et Biophysica Acta - Molecular Basis of Disease*, *1639*(2), 65–79. https://doi.org/10.1016/j.bbadis.2003.08.004

Chaudhuri, S., Bruno, J. C., Alonzo, F., Xayarath, B., Cianciotto, N. P., & Freitag, N. E. (2010). Contribution of chitinases to listeria monocytogenes pathogenesis. *Applied and Environmental Microbiology*, *76*(21), 7302–7305. https://doi.org/10.1128/AEM.01338-10

Chen, H. C., Chang, C. C., Mau, W. J., & Yen, L. S. (2002). Evaluation of N-acetylchitooligosaccharides as the main carbon sources for the growth of intestinal bacteria. *FEMS Microbiology Letters*, *209*(1), 51–54. https://doi.org/10.1111/j.1574-6968.2002.tb11108.x

Childers, B. M., & Klose, K. E. (2007). Regulation of virulence in *Vibrio cholerae*: The ToxR regulon. *Future Microbiology*, *2*(3), 335–344. https://doi.org/10.2217/17460913.2.3.335

Chourashi, R., Mondal, M., Sinha, R., Debnath, A., Das, S., Koley, H., & Chatterjee, N. S. (2016). Role of a sensor histidine kinase ChiS of *Vibrio cholerae* in pathogenesis. *International Journal of Medical Microbiology*,

306(8). https://doi.org/10.1016/j.ijmm.2016.09.003

Colwell, R. K., Brehm, G., Cardelús, C. L., Gilman, A. C., Longino, J. T., Cardelus, C. L., Gilman, A. C., & Longino, J. T. (2008). in the Wet Tropics. *Science*, *322*(October), 258–261. http://www.sciencemag.org/cgi/doi/10.1126/science.1162547

Colwell, R. R. (1996). Global climate and infectious disease: The cholera paradigm. *Science*, *274*(5295), 2025–2031. https://doi.org/10.1126/science.274.5295.2025

Colwell, R. R. (2002). A voyage of discovery: Cholera, climate and complexity: Editorial. *Environmental Microbiology*, *4*(2), 67–69. https://doi.org/10.1046/j.1462-2920.2002.00270.x

Colwell, R. R. (2004). Infectious disease and environment: Cholera as a paradigm for waterborne disease. *International Microbiology*, *7*(4), 285–289.

Constantin de Magny, G., & Colwell, R. R. (2009). Cholera and climate: a demonstrated relationship. *Transactions of the American Clinical and Climatological Association*, *120*, 119–128.

Correa, N. E., Lauriano, C. M., McGee, R., & Klose, K. E. (2000). Phosphorylation of the flagellar regulatory protein FlrC is necessary for *Vibrio cholerae* motility and enhanced colonization. *Molecular Microbiology*, *35*(4), 743–755. https://doi.org/10.1046/j.1365-2958.2000.01745.x

Cottingham, K. L., Chiavelli, D. A., & Taylor, R. K. (2003). Environmental Microbe and Human Pathogen: The Ecology and Microbiology of *Vibrio cholerae*. *Frontiers in Ecology and the Environment*, *1*(2), 80. https://doi.org/10.2307/3868034

Coyne, V. E., & Al-Harthi, L. (1992). Induction of melanin biosynthesis in *Vibrio cholerae*. *Applied and Environmental Microbiology*, *58*(9), 2861–2865. https://doi.org/10.1128/aem.58.9.2861-2865.1992

Curriero, F. C., Patz, J. A., Rose, J. B., & Lele, S. (2001). The association between extreme precipitation and waterborne disease outbreaks in the United States, 1948-1994. *American Journal of Public Health*, *91*(8), 1194–1199. https://doi.org/10.2105/AJPH.91.8.1194

Czerkinsky, C., Russell, M. W., Lycke, N., Lindblad, M., & Holmgren, J. (1989). Oral administration of a streptococcal antigen coupled to cholera toxin B subunit evokes strong antibody responses in salivary glands and extramucosal tissues. *Infection and Immunity*, *57*(4), 1072–1077.

https://doi.org/10.1128/iai.57.4.1072-1077.1989

Das, B., Verma, J., Kumar, P., Ghosh, A., & Ramamurthy, T. (2020). Antibiotic resistance in *Vibrio cholerae*: Understanding the ecology of resistance genes and mechanisms. *Vaccine*, *38*(xxxx), A83–A92. https://doi.org/10.1016/j.vaccine.2019.06.031

Davis, B. M., Kimsey, H. H., Chang, W., & Waldor, M. K. (1999). The *Vibrio cholerae* O139 Calcutta Bacteriophage CTXφ Is Infectious and Encodes a Novel Repressor. *Journal of Bacteriology*, *181*(21), 6779–6787. https://doi.org/10.1128/JB.181.21.6779-6787.1999

de Magny, G. C., Mozumder, P. K., Grim, C. J., Hasan, N. A., Naser, M. N., Alam, M., Sack, R. B., Huq, A., & Colwell, R. R. (2011). Role of zooplankton diversity in *Vibrio cholerae* population dynamics and in the incidence of cholera in the Bangladesh sundarbans. *Applied and Environmental Microbiology*, *77*(17), 6125–6132. https://doi.org/10.1128/AEM.01472-10

De, K., Ramamurthy, T., Faruque, S. M., Yamasaki, S., Takeda, Y., Nair, G. B., & Nandy, R. K. (2004). Molecular characterisation of rough strains of *Vibrio cholerae* isolated from diarrhoeal cases in India and their comparison to smooth strains. *FEMS Microbiology Letters*, *232*(1), 23–30. https://doi.org/10.1016/S0378-1097(04)00013-8

De, S. N., & Chatterje, D. N. (1953). An experimental study of the mechanism of action ofvibrio choleræ on the intestinal mucous membrane. *The Journal of Pathology and Bacteriology*, *66*(2), 559–562. https://doi.org/10.1002/path.1700660228

Debroy, S., Dao, J., Söderberg, M., Rossier, O., & Cianciotto, N. P. (2006). Legionella pneumophila type II secretome reveals unique exoproteins and a chitinase that promotes bacterial persistence in the lung. *Proceedings of the National Academy of Sciences of the United States of America*, *103*(50), 19146–19151. https://doi.org/10.1073/pnas.0608279103

Dekker, J., Rossen, J. W. A., Büller, H. A., & Einerhand, A. W. C. (2002). The MUC family: An obituary. *Trends in Biochemical Sciences*, *27*(3), 126–131. https://doi.org/10.1016/S0968-0004(01)02052-7

DiRita, V. J., Parsot, C., Jander, G., & Mekalanos, J. J. (2006). Regulatory cascade controls virulence in *Vibrio cholerae*. *Proceedings of the National Academy of Sciences*, *88*(12), 5403–5407. https://doi.org/10.1073/pnas.88.12.5403

DiRita, Victor J. (1992). Co-ordinate expression of virulence genes by ToxR in *Vibrio cholerae*. *Molecular Microbiology*, *6*(4), 451–458.

https://doi.org/10.1111/j.1365-2958.1992.tb01489.x

Duncan, M. C., Forbes, J. C., Nguyen, Y., Shull, L. M., Gillette, R. K., Lazinski, D. W., Ali, A., Shanks, R. M. Q., Kadouri, D. E., & Camilli, A. (2018). *Vibrio cholerae* motility exerts drag force to impede attack by the bacterial predator Bdellovibrio bacteriovorus. *Nature Communications*, *9*(1). https://doi.org/10.1038/s41467-018-07245-3

Dutta, N. K., Panse, M. V., & Kulkarni, D. R. (1959). Role of cholera a toxin in experimental cholera. *Journal of Bacteriology*, *78*, 594–595. https://doi.org/10.1128/jb.78.4.594-595.1959

Dwidar, M., Monnappa, A. K., & Mitchell, R. J. (2012). The dual probiotic and antibiotic nature of Bdellovibrio bacteriovorus. *BMB Reports*, *45*(2), 71–78. https://doi.org/10.5483/BMBRep.2012.45.2.71

Echazarreta, M. A., & Klose, K. E. (2019). Vibrio flagellar synthesis. *Frontiers in Cellular and Infection Microbiology*, *9*(MAY), 1–11. https://doi.org/10.3389/fcimb.2019.00131

Elmi, A., Dorey, A., Watson, E., Jagatia, H., Inglis, N. F., Gundogdu, O., Bajaj-Elliott, M., Wren, B. W., Smith, D. G. E., & Dorrell, N. (2018). The bile salt sodium taurocholate induces Campylobacter jejuni outer membrane vesicle production and increases OMV-associated proteolytic activity. *Cellular Microbiology*, *20*(3), 1–14. https://doi.org/10.1111/cmi.12814

Erken, M., Lutz, C., & McDougald, D. (2015). Interactions of Vibrio spp. with Zooplankton . *Microbiology Spectrum*, *3*(3). https://doi.org/10.1128/microbiolspec.ve-0003-2014

Escobar, L. E., Ryan, S. J., Stewart-Ibarra, A. M., Finkelstein, J. L., King, C. A., Qiao, H., & Polhemus, M. E. (2015). A global map of suitability for coastal *Vibrio cholerae* under current and future climate conditions. *Acta Tropica*, *149*, 202–211. https://doi.org/10.1016/j.actatropica.2015.05.028

Fabich, A. J., Jones, S. A., Chowdhury, F. Z., Cernosek, A., Anderson, A., Smalley, D., McHargue, J. W., Hightower, G. A., Smith, J. T., Autieri, S. M., Leatham, M. P., Lins, J. J., Allen, R. L., Laux, D. C., Cohen, P. S., & Conway, T. (2008). Comparison of carbon nutrition for pathogenic and commensal Escherichia coli strains in the mouse intestine. *Infection and Immunity*, *76*(3), 1143–1152. https://doi.org/10.1128/IAI.01386-07

Farmer, J. J. (2006). The Family Vibrionaceae. In *The Prokaryotes* (Vol. 6, pp. 495–507). Springer New York. https://doi.org/10.1007/0-387-30746-X_17

Faruque, S. M., Abdul Alim, A. R. M., Roy, S. K., Khan, F., Nair, G. B., Sack, R. B., & Albert, M. J. (1994). Molecular analysis of rRNA and cholera toxin genes carried by the new epidemic strain of toxigenic *Vibrio cholerae*

O139 synonym bengal. *Journal of Clinical Microbiology*, *32*(4), 1050–1053. https://doi.org/10.1128/jcm.32.4.1050-1053.1994

Fasano, A., Baudry, B., Pumplin, D. W., Wasserman, S. S., Tall, B. D., Ketley, J. M., & Kaper, J. B. (1991). *Vibrio cholerae* produces a second enterotoxin, which affects intestinal tight junctions. *Proceedings of the National Academy of Sciences of the United States of America*, *88*(12), 5242–5246. https://doi.org/10.1073/pnas.88.12.5242

Finkelstein, R. A., & LoSpalluto, J. J. (1969). Pathogenesis Of Experimental Cholera. *Journal of Experimental Medicine*, *130*(1), 185–202. https://doi.org/10.1084/jem.130.1.185

Fleckenstein, J. M., & Kopecko, D. J. (2001). Breaching the mucosal barrier by stealth: An emerging pathogenic mechanism for enteroadherent bacterial pathogens. *Journal of Clinical Investigation*, *107*(1), 27–30. https://doi.org/10.1172/JCI11792

Fong, J. C. N., Syed, K. A., Klose, K. E., & Yildiz, F. H. (2010). Role of Vibrio polysaccharide (vps) genes in VPS production, biofilm formation and *Vibrio cholerae* pathogenesis. *Microbiology*, *156*(9), 2757–2769. https://doi.org/10.1099/mic.0.040196-0

Frederiksen, R. F., Paspaliari, D. K., Larsen, T., Storgaard, B. G., Larsen, M. H., Ingmer, H., Palcic, M. M., & Leisner, J. J. (2013). Bacterial chitinases and chitin-binding proteins as virulence factors. *Microbiology (United Kingdom)*, *159*(PART 5), 833–847. https://doi.org/10.1099/mic.0.051839-0

Ghosal, A., Bhowmick, R., Nandy, R. K., Ramamurthy, T., & Chatterjee, N. S. (2007). PCR-based identification of common colonization factor antigens of enterotoxigenic Escherichia coli. *Journal of Clinical Microbiology*, *45*(9), 3068–3071. https://doi.org/10.1128/JCM.00646-07

Ghosh, S., Rao, K. H., Sengupta, M., Bhattacharya, S. K., & Datta, A. (2011). Two gene clusters co-ordinate for a functional N-acetylglucosamine catabolic pathway in *Vibrio cholerae*. *Molecular Microbiology*, *80*(6), 1549–1560. https://doi.org/10.1111/j.1365-2958.2011.07664.x

Gooday, G. W. (1994). Physiology of microbial degradation of chitin and chitosan. *Biochemistry of Microbial Degradation*, *Blackwell 1988*, 279–312. https://doi.org/10.1007/978-94-011-1687-9_9

Gupta, S., & Chowdhury, R. (1997). Bile affects production of virulence factors and motility of *Vibrio cholerae*. *Infection and Immunity*, *65*(3), 1131–1134. https://doi.org/10.1128/iai.65.3.1131-1134.1997

Hall, R. H., Losonsky, G., Silveira, A. P. D., Taylor, R. K., Mekalanos, J. J., Witham, N. D., & Levine, M. M. (1991). Immunogenicity of *Vibrio*

cholerae O1 toxin-coregulated pili in experimental and clinical cholera. *Infection and Immunity*, *59*(7), 2508–2512. https://doi.org/10.1128/iai.59.7.2508-2512.1991

Hammer-Jespersen, K., & Munch-Petersen, A. (1975). Multiple regulation of nucleoside catabolizing enzymes: Regulation of the deo operon by the cytR and deoR gene products. *MGG Molecular & General Genetics*, *137*(4), 327–335. https://doi.org/10.1007/BF00703258

Hammer-jespersen, K., & Nygaard, P. (1976). *Multiple Regulation of Nucleoside Catabolizing Enzymes in Escherichia coli : 55*, 49–55.

Heidelberg, J. F., Elsen, J. A., Nelson, W. C., Clayton, R. A., Gwinn, M. L., Dodson, R. J., Haft, D. H., Hickey, E. K., Peterson, J. D., Umayam, L., Gill, S. R., Nelson, K. E., Read, T. D., Tettelin, H., Richardson, D., Ermolaeva, M. D., Vamathevan, J., Bass, S., Halving, Q., … Fraser, C. M. (2000). DNA sequence of both chromosomes of the cholera pathogen *Vibrio cholerae*. *Nature*, *406*(6795), 477–483. https://doi.org/10.1038/35020000

Higgins, D. A., Pomianek, M. E., Kraml, C. M., Taylor, R. K., Semmelhack, M. F., & Bassler, B. L. (2007). The major *Vibrio cholerae* autoinducer and its role in virulence factor production. *Nature*, *450*(7171), 883–886. https://doi.org/10.1038/nature06284

Hofmann, A. F., & Hagey, L. R. (2008). Bile acids: Chemistry, pathochemistry, biology, pathobiology, and therapeutics. *Cellular and Molecular Life Sciences*, *65*(16), 2461–2483. https://doi.org/10.1007/s00018-008-7568-6

Hofmann, A. F., & Small, D. M. (1967). Detergent properties of bile salts: correlation with physiological function. *Annual Review of Medicine*, *18*, 333–376. https://doi.org/10.1146/annurev.me.18.020167.002001

Holmgren, J. (1973). Comparison of the tissue receptors for *Vibrio cholerae* and Escherichia coli enterotoxins by means of gangliosides and natural cholera toxoid. *Infection and Immunity*, *8*(6), 851–859.

Holmgren, J., Lycke, N., & Czerkinsky, C. (1993). Cholera toxin and cholera B subunit as oral-mucosal adjuvant and antigen vector systems. *Vaccine*, *11*(12), 1179–1184. https://doi.org/10.1016/0264-410X(93)90039-Z

Honda, T., & Finkelstein, R. A. (1979). Purification and characterization of a hemolysin produced by *Vibrio cholerae* biotype El Tor: Another toxic substance produced by cholera vibrios. *Infection and Immunity*, *26*(3), 1020–1027. https://doi.org/10.1128/iai.26.3.1020-1027.1979

Hood, M. ., & Winter, P. . (2006). Attachment of *Vibrio cholerae* under various environmental conditions and to selected substrates. *FEMS Microbiology*

Ecology, *22*(3), 215–223. https://doi.org/10.1111/j.1574-6941.1997.tb00 373.x

Hotta, M., Nakata, R., Katsukawa, M., Hori, K., Takahashi, S., & Inoue, H. (2010). Carvacrol, a component of thyme oil, activates PPARα and γ and suppresses COX-2 expression. *Journal of Lipid Research*, *51*(1), 132–139. https://doi.org/10.1194/jlr.M900255-JLR200

Hsiao, A., & Zhu, J. (2020). Pathogenicity and virulence regulation of *Vibrio cholerae* at the interface of host-gut microbiome interactions. *Virulence*, *11*(1), 1582–1599. https://doi.org/10.1080/21505594.2020.1845039

Hung, D. T., Shakhnovich, E. A., Pierson, E., & Mekalanos, J. J. (2005). Small-molecule inhibitor of *Vibrio cholerae* virulence and intestinal colonization. *Science*, *310*(5748), 670–674. https://doi.org/10.1126/science.1116739

Hunt, D. E., Gevers, D., Vahora, N. M., & Polz, M. F. (2008b). Conservation of the chitin utilization pathway in the Vibrionaceae. *Applied and Environmental Microbiology*, *74*(1), 44–51. https://doi.org/10.1128/AEM.01412-07

Huq, A., Small, E. B., West, P. A., Huq, M. I., Rahman, R., & Colwell, R. R. (1983). Ecological relationships between *Vibrio cholerae* and planktonic crustacean copepods. *Applied and Environmental Microbiology*, *45*(1), 275–283.

Huq, Anwar, Sack, R. B., Nizam, A., Longini, I. M., Nair, G. B., Ali, A., Morris, J. G., Khan, M. N. H., Siddique, A. K., Yunus, M., Albert, M. J., Sack, D. A., & Colwell, R. R. (2005). Critical factors influencing the occurrence of *Vibrio cholerae* in the environment of Bangladesh. *Applied and Environmental Microbiology*, *71*(8), 4645–4654. https://doi.org/10.1128/AEM.71.8.4645-4654.2005

Hyldgaard, M., Mygind, T., & Meyer, R. L. (2012). Essential oils in food preservation: Mode of action, synergies, and interactions with food matrix components. *Frontiers in Microbiology*, *3*(JAN), 1–24. https://doi.org/10.3389/fmicb.2012.00012

Ichinose, Y., Yamamoto, K., Nakasone, N., Tanabe, M. J., Takeda, T., Miwatani, T., & Iwanaga, M. (1987). Enterotoxicity of El Tor-like hemolysin of non-O1 *Vibrio cholerae*. *Infection and Immunity*, *55*(5), 1090–1093. https://doi.org/10.1128/iai.55.5.1090-1093.1987

Inagaki, T., Moschetta, A., Lee, Y. K., Peng, L., Zhao, G., Downes, M., Yu, R. T., Shelton, J. M., Richardson, J. A., Repa, J. J., Mangelsdorf, D. J., & Kliewer, S. A. (2006). Regulation of antibacterial defense in the small intestine by the nuclear bile acid receptor. *Proceedings of the National*

Academy of Sciences of the United States of America, *103*(10), 3920–3925. https://doi.org/10.1073/pnas.0509592103

Islam, M. S., Zaman, M. H., Islam, M. S., Ahmed, N., & Clemens, J. D. (2020). Environmental reservoirs of *Vibrio cholerae*. *Vaccine*, *38*(xxxx), A52–A62. https://doi.org/10.1016/j.vaccine.2019.06.033

Johnson, C. N., Bowers, J. C., Griffitt, K. J., Molina, V., Clostio, R. W., Pei, S., Laws, E., Paranjpye, R. N., Strom, M. S., Chen, A., Hasan, N. A., Huq, A., Noriea, N. F., Grimes, D. J., & Colwell, R. R. (2012). Ecology of vibrio parahaemolyticus and vibrio vulnificus in the coastal and estuarine waters of Louisiana, Maryland, Mississippi, and Washington (United States). *Applied and Environmental Microbiology*, *78*(20), 7249–7257. https://doi.org/10.1128/AEM.01296-12

Johnson, S. B., Park, H. S., Gross, C. P., & Yu, J. B. (2018). Use of alternative medicine for cancer and its impact on survival. *Journal of the National Cancer Institute*, *110*(1), 121–124. https://doi.org/10.1093/jnci/djx145

Jordan, N., Newton, J., Pearson, J., & Allen, A. (1998). A novel method for the visualization of the in situ mucus layer in rat and man. *Clinical Science*, *95*(1), 97–106. https://doi.org/10.1042/CS19980081

Jorgensen, J. H., & Pfallerc, M. A. (2015). *Manual of Clinical Microbiology* (J. H. Jorgensen, K. C. Carroll, G. Funke, M. A. Pfaller, M. L. Landry, S. S. Richter, & D. W. Warnock (eds.)). ASM Press. https://doi.org/10.1128/9781555817381

Joyce, S. A., & Gahan, C. G. M. (2016). Bile Acid Modifications at the Microbe-Host Interface: Potential for Nutraceutical and Pharmaceutical Interventions in Host Health. *Annual Review of Food Science and Technology*, *7*(December 2015), 313–333. https://doi.org/10.1146/annurev-food-041715-033159

Jung, H. C., Eckmann, L., Yang, S. K., Panja, A., Fierer, J., Morzycka-Wroblewska, E., & Kagnoff, M. F. (1995). A distinct array of proinflammatory cytokines is expressed in human colon epithelial cells in response to bacterial invasion. *Journal of Clinical Investigation*, *95*(1), 55–65. https://doi.org/10.1172/jci117676

Jutla, A. S., Akanda, A. S., Griffiths, J. K., Colwell, R., Islam, S., & Jutla, A. S. (2011). Warming Oceans, Phytoplankton, and River Discharge: Implications for Cholera Outbreaks. *The American Journal of Tropical Medicine and Hygiene*, *85*(2), 303–308. https://doi.org/10.4269/ajtmh.2011.11-0181

Kallipolitis, B. H., & Valentin-Hansen, P. (2004). A role for the interdomain

linker region of the Escherichia coli CytR regulator in repression complex formation. *Journal of Molecular Biology*, *342*(1), 1–7. https://doi.org/10.1016/j.jmb.2004.05.067

Kaper, J. B., Morris, J. G., & Levine, M. M. (1995). *Cholera*. *8*(1), 48–86.

Keyhani, N. O., & Roseman, S. (1999). Physiological aspects of chitin catabolism in marine bacteria. *Biochimica et Biophysica Acta - General Subjects*, *1473*(1), 108–122. https://doi.org/10.1016/S0304-4165(99)00172-5

Kim, S. Y., Thanh, X. T. T., Jeong, K., Kim, S. Bin, Pan, S. O., Jung, C. H., Hong, S. H., Lee, S. E., & Rhee, J. H. (2014). Contribution of six flagellin genes to the flagellum biogenesis of Vibrio vulnificus and in vivo invasion. *Infection and Immunity*, *82*(1), 29–42. https://doi.org/10.1128/IAI.00654-13

Kirn, T. J., Jude, B. A., & Taylor, R. K. (2005). A colonization factor links *Vibrio cholerae* environmental survival and human infection. *Nature*, *438*(7069), 863–866. https://doi.org/10.1038/nature04249

Kitaoka, M., Miyata, S. T., Unterweger, D., & Pukatzki, S. (2011). Antibiotic resistance mechanisms of *Vibrio cholerae*. *Journal of Medical Microbiology*, *60*(4), 397–407. https://doi.org/10.1099/jmm.0.023051-0

Klose, K. E., & Mekalanos, J. J. (1998). Distinct roles of an alternative sigma factor during both free-swimming and colonizing phases of the *Vibrio cholerae* pathogenic cycle. *Molecular Microbiology*, *28*(3), 501–520. https://doi.org/10.1046/j.1365-2958.1998.00809.x

Koley, H., Mitra, R., Basu, A., Mukhopadhyay, A. K., Saha, P. K., Ramakrishna, B. S., Krishnan, S., Takeda, Y., & Nair, G. B. (1999). Response of wild-type mutants of *Vibrio cholerae* O1 possessing different combinations of virulence genes in the ligated rabbit ileal loop and in Ussing chambers: Evidence for the presence of additional secretogen. *Journal of Medical Microbiology*, *48*(1), 51–57. https://doi.org/10.1099/00222615-48-1-51

Kovacikova, G., Lin, W., & Skorupski, K. (2004). *Vibrio cholerae* AphA uses a novel mechanism for virulence gene activation that involves interaction with the LysR-type regulator AphB at the tcpPH promoter. *Molecular Microbiology*, *53*(1), 129–142. https://doi.org/10.1111/j.1365-2958.2004.04121.x

Krebs, S. J., & Taylor, R. K. (2011). Protection and attachment of *Vibrio cholerae* mediated by the toxin-coregulated pilus in the infant mouse model. *Journal of Bacteriology*, *193*(19), 5260–5270. https://doi.org/10.1128/JB.00378-11

Kumar, V., & Turnbull, W. B. (2018). Carbohydrate inhibitors of cholera toxin. *Beilstein Journal of Organic Chemistry*, *14*, 484–498. https://doi.org/10.3762/bjoc.14.34

Landa, P., Kokoska, L., Pribylova, M., Vanek, T., & Marsik, P. (2009). In vitro anti-inflammatory activity of carvacrol: Inhibitory effect on COX-2 catalyzed prostaglandin E2 biosynthesisb. *Archives of Pharmacal Research*, *32*(1), 75–78. https://doi.org/10.1007/s12272-009-1120-6

Langeveld, W. T., Veldhuizen, E. J. A., & Burt, S. A. (2014). Synergy between essential oil components and antibiotics: A review. *Critical Reviews in Microbiology*, *40*(1), 76–94. https://doi.org/10.3109/1040841X.2013.763219

Lee, S. H., Butler, S. M., & Camilli, A. (2002). Selection for in vivo regulators of bacterial virulence. *Proceedings of the National Academy of Sciences*, *98*(12), 6889–6894. https://doi.org/10.1073/pnas.111581598

Li, X., & Roseman, S. (2004). The chitinolytic cascade in Vibrios is regulated by chitin oligosaccharides and a two-component chitin catabolic sensor/kinase. *Proceedings of the National Academy of Sciences of the United States of America*, *101*(2), 627–631. https://doi.org/10.1073/pnas.0307645100

Lipp, E. K., Huq, A., & Colwell, R. R. (2002). Effects of global climate on infectious disease: The cholera model. *Clinical Microbiology Reviews*, *15*(4), 757–770. https://doi.org/10.1128/CMR.15.4.757-770.2002

Lippi, D., & Gotuzzo, E. (2014). The greatest steps towards the discovery of *Vibrio cholerae*. *Clinical Microbiology and Infection*, *20*(3), 191–195. https://doi.org/10.1111/1469-0691.12390

Liu, Y., McKeever, L. C., & Malik, N. S. A. (2017). Assessment of the antimicrobial activity of olive leaf extract against foodborne bacterial pathogens. *Frontiers in Microbiology*, *8*(FEB), 1–8. https://doi.org/10.3389/fmicb.2017.00113

Liu, Z., Miyashiro, T., Tsou, A., Hsiao, A., Goulian, M., & Zhu, J. (2008). Mucosal penetration primes *Vibrio cholerae* for host colonization by repressing quorum sensing. *Proceedings of the National Academy of Sciences*, *105*(28), 9769–9774. https://doi.org/10.1073/pnas.0802241105

Liu, Z., Stirling, F. R., & Zhu, J. (2007). Temporal Quorum-Sensing Induction Regulates *Vibrio cholerae* Biofilm Architecture. *Infection and Immunity*, *75*(1), 122–126. https://doi.org/10.1128/IAI.01190-06

Liu, Z., Wang, Y., Liu, S., Sheng, Y., Rueggeberg, K. G., Wang, H., Li, J., Gu, F. X., Zhong, Z., Kan, B., & Zhu, J. (2015). *Vibrio cholerae* represses

polysaccharide synthesis to promote motility in mucosa. *Infection and Immunity*, *83*(3), 1114–1121. https://doi.org/10.1128/IAI.02841-14

Livak, K. J., & Schmittgen, T. D. (2001). Analysis of relative gene expression data using real-time quantitative PCR and the 2-ΔΔCT method. *Methods*, *25*(4), 402–408. https://doi.org/10.1006/meth.2001.1262

Llana-Ruiz-Cabello, M., Pichardo, S., Maisanaba, S., Puerto, M., Prieto, A. I., Gutiérrez-Praena, D., Jos, A., & Cameán, A. M. (2015). In vitro toxicological evaluation of essential oils and their main compounds used in active food packaging: A review. *Food and Chemical Toxicology*, *81*, 9–27. https://doi.org/10.1016/j.fct.2015.03.030

Lo Scrudato, M., & Blokesch, M. (2012). The regulatory network of natural competence and transformation of *Vibrio cholerae*. *PLoS Genetics*, *8*(6). https://doi.org/10.1371/journal.pgen.1002778

Lo Scrudato, M., & Blokesch, M. (2013). A transcriptional regulator linking quorum sensing and chitin induction to render *Vibrio cholerae* naturally transformable. *Nucleic Acids Research*, *41*(6), 3644–3658. https://doi.org/10.1093/nar/gkt041

Lobitz, B., Beck, L., Huq, A., Wood, B., Fuchs, G., Faruque, A. S. G., & Colwell, R. (2000). Climate and infectious disease: Use of remote sensing for detection of *Vibrio cholerae* by indirect measurement. *Proceedings of the National Academy of Sciences of the United States of America*, *97*(4), 1438–1443. https://doi.org/10.1073/pnas.97.4.1438

Louis, V. R., Russek-Cohen, E., Choopun, N., Rivera, I. N. G., Gangle, B., Jiang, S. C., Rubin, A., Patz, J. A., Huq, A., & Colwell, R. R. (2003). Predictability of *vibrio cholerae* in chesapeake bay. *Applied and Environmental Microbiology*, *69*(5), 2773–2785. https://doi.org/10.1128/AEM.69.5.2773-2785.2003

Lutz, C., Erken, M., Noorian, P., Sun, S., & McDougald, D. (2013). Environmental reservoirs and mechanisms of persistence of *Vibrio cholerae*. *Frontiers in Microbiology*, *4*(DEC), 1–15. https://doi.org/10.3389/fmicb.2013.00375

Macfadyen, L. P., Chen, D., Vo, H. C., Liao, D., Sinotte, R., & Rosemary, J. (2001). *Competence development by hi is regulated by the availability of nucleic acid precursors*. *40*, 700–707.

Magi, G., Marini, E., & Facinelli, B. (2015). Antimicrobial activity of essential oils and carvacrol, and synergy of carvacrol and erythromycin, against clinical, erythromycin-resistant Group A Streptococci. *Frontiers in Microbiology*, *6*(MAR), 1–7. https://doi.org/10.3389/fmicb.2015.00165

Magina, M. D. A., Dalmarco, E. M., Wisniewski, A., Simionatto, E. L., Dalmarco, J. B., Pizzolatti, M. G., & Brighente, I. M. C. (2009). Chemical composition and antibacterial activity of essential oils of Eugenia species. *Journal of Natural Medicines*, *63*(3), 345–350. https://doi.org/10.1007/s11418-009-0329-5

Maldonado-Valderrama, J., Wilde, P., MacIerzanka, A., & MacKie, A. (2011). The role of bile salts in digestion. *Advances in Colloid and Interface Science*, *165*(1), 36–46. https://doi.org/10.1016/j.cis.2010.12.002

Martinez, G., Ambrosio, J., Gutierrez-cogco, L., & Flisser, A. (2001). Identi cation and Strain Differentiation of *Vibrio cholerae* by Using Polyclonal Antibodies against Outer Membrane Proteins. *Clinical and Diagnostic Laboratory Immunology*, *8*(4), 768–771. https://doi.org/10.1128/ CDLI.8.4.768

Matson, J. S., Withey, J. H., & DiRita, V. J. (2007). Regulatory networks controlling *Vibrio cholerae* virulence gene expression. *Infection and Immunity*, *75*(12), 5542–5549. https://doi.org/10.1128/IAI.01094-07

Matsumoto, H., Muroi, H., Umehara, M., Yoshitake, Y., & Tsuyumu, S. (2003). Peh production, flagellum synthesis, and virulence reduced in Erwinia carotovora subsp. carotovora by mutation in a homologue of cytR. *Molecular Plant-Microbe Interactions*, *16*(5), 389–397. https://doi.org/10.1094/MPMI.2003.16.5.389

McCarter, L. L. (2004). Dual Flagellar Systems Enable Motility under Different Circumstances. *Journal of Molecular Microbiology and Biotechnology*, *7*(1–2), 18–29. https://doi.org/10.1159/000077866

McGee, K., Hörstedt, P., & Milton, D. L. (1996). Identification and characterization of additional flagellin genes from Vibrio anguillarum. *Journal of Bacteriology*, *178*(17), 5188–5198. https://doi.org/10.1128/ jb.178.17.5188-5198.1996

Meibom, K. L., Blokesch, M., Dolganov, N. A., Wu, C. Y., & Schoolnik, G. K. (2005). Microbiology: Chitin induces natural competence in *vibrio cholerae*. *Science*, *310*(5755), 1824–1827. https://doi.org/10.1126/ science.1120096

Meibom, K. L., Kallipolitis, B. H., Ebright, R. H., & Valentin-Hansen, P. (2000). Identification of the subunit of cAMP receptor protein (CRP) that functionally interacts with CytR in CRP-CytR-mediated transcriptional repression. *Journal of Biological Chemistry*, *275*(16), 11951–11956. https://doi.org/10.1074/jbc.275.16.11951

Meibom, K. L., Li, X. B., Nielsen, A. T., Wu, C. Y., Roseman, S., & Schoolnik,

G. K. (2004). The *Vibrio cholerae* chitin utilization program. *Proceedings of the National Academy of Sciences of the United States of America*, *101*(8), 2524–2529. https://doi.org/10.1073/pnas.0308707101

Mekalanos, J. J., Swartz, D. J., Pearson, G. D. N., Harford, N., Groyne, F., & De Wilde, M. (1983). Cholera toxin genes: Nucleotide sequence, deletion analysis and vaccine development. *Nature*, *306*(5943), 551–557. https://doi.org/10.1038/306551a0

Meron, D., Efrony, R., Johnson, W. R., Schaefer, A. L., Morris, P. J., Rosenberg, E., Greenberg, E. P., & Banin, E. (2009). Role of flagella in virulence of the coral pathogen Vibrio coralliilyticus. *Applied and Environmental Microbiology*, *75*(17), 5704–5707. https://doi.org/10.1128/AEM.00198-09

Mewborn, L., Benitez, J. A., & Silva, A. J. (2017). Flagellar motility, extracellular proteases and *Vibrio cholerae* detachment from abiotic and biotic surfaces. *Microbial Pathogenesis*, *113*(October), 17–24. https://doi.org/10.1016/j.micpath.2017.10.016

Miladi, H., Zmantar, T., Chaabouni, Y., Fedhila, K., Bakhrouf, A., Mahdouani, K., & Chaieb, K. (2016). Antibacterial and efflux pump inhibitors of thymol and carvacrol against food-borne pathogens. *Microbial Pathogenesis*, *99*, 95–100. https://doi.org/10.1016/j.micpath.2016.08.008

Mondal, M., Nag, D., Koley, H., Saha, D. R., & Chatterjee, N. S. (2014). The *Vibrio cholerae* extracellular chitinase ChiA2 is important for survival and pathogenesis in the host intestine. *PLoS ONE*, *9*(9). https://doi.org/10.1371/journal.pone.0103119

Mooyottu, S., Kollanoor-Johny, A., Flock, G., Bouillaut, L., Upadhyay, A., Sonenshein, A. L., & Venkitanarayanan, K. (2014). Carvacrol and trans-cinnamaldehyde reduce Clostridium difficile toxin production and cytotoxicity in vitro. *International Journal of Molecular Sciences*, *15*(3), 4415–4430. https://doi.org/10.3390/ijms15034415

Morris, J. G., Sztein, M. B., Rice, E. W., Nataro, J. P., Losonsky, G. A., Panigrahi, P., Tacket, C. O., & Johnson, J. A. (1996). *Vibrio cholerae* 01 Can Assume a Chlorine-Resistant Rugose Survival Form that Is Virulent for Humans. *Journal of Infectious Diseases*, *174*(6), 1364–1368. https://doi.org/10.1093/infdis/174.6.1364

Narendrakumar, L., Gupta, S. Sen, Johnson, J. B., Ramamurthy, T., & Thomas, S. (2019). Molecular Adaptations and Antibiotic Resistance in *Vibrio cholerae*: A Communal Challenge. *Microbial Drug Resistance*, *25*(7), 1012–1022. https://doi.org/10.1089/mdr.2018.0354

Naseem, S., & Konopka, J. B. (2015). N-acetylglucosamine Regulates Virulence

Properties in Microbial Pathogens. *PLoS Pathogens*, *11*(7), 6–11. https://doi.org/10.1371/journal.ppat.1004947

Nesper, J., Lauriano, C. M., Klose, K. E., Kapfhammer, D., Kraiß, A., & Reidl, J. (2001). Characterization of *Vibrio cholerae* O1 El Tor galU and galE Mutants: Influence on Lipopolysaccharide Structure, Colonization, and Biofilm Formation. *Infection and Immunity*, *69*(1), 435–445. https://doi.org/10.1128/IAI.69.1.435-445.2001

Ng, W., Perez, L. J., Wei, Y., Kraml, C., Semmelhack, M. F., & Bassler, B. L. (2011). Signal production and detection specificity in Vibrio CqsA/CqsS quorum-sensing systems. *Molecular Microbiology*, *79*(6), 1407–1417. https://doi.org/10.1111/j.1365-2958.2011.07548.x

Nostro, A., Marino, A., Blanco, A. R., Cellini, L., Di Giulio, M., Pizzimenti, F., Roccaro, A. S., & Bisignano, G. (2009). In vitro activity of carvacrol against staphylococcal preformed biofilm by liquid and vapour contact. *Journal of Medical Microbiology*, *58*(6), 791–797. https://doi.org/10.1099/jmm.0.009274-0

O'May, C., & Tufenkji, N. (2011). The swarming motility of Pseudomonas aeruginosa is blocked by cranberry proanthocyanidins and other tannin-containing materials. *Applied and Environmental Microbiology*, *77*(9), 3061–3067. https://doi.org/10.1128/AEM.02677-10

Obaidat, M. M., & Frank, J. F. (2009). Inactivation of Escherichia coli O157:H7 on the intact and damaged portions of lettuce and spinach leaves by using allyl isothiocyanate, carvacrol, and cinnamaldehyde in vapor phase. *Journal of Food Protection*, *72*(10), 2046–2055. https://doi.org/10.4315/0362-028X-72.10.2046

Olive, A. J., & Sassetti, C. M. (2016). Metabolic crosstalk between host and pathogen: Sensing, adapting and competing. *Nature Reviews Microbiology*, *14*(4), 221–234. https://doi.org/10.1038/nrmicro.2016.12

Orikoshi, H., Nakayama, S., Miyamoto, K., Hanato, C., Yasuda, M., Inamori, Y., & Tsujibo, H. (2005). Roles of four chitinases (ChiA, ChiB, ChiC, and ChiD) in the chitin degradation system of marine bacterium Alteromonas sp. strain O-7. *Applied and Environmental Microbiology*, *71*(4), 1811–1815. https://doi.org/10.1128/AEM.71.4.1811-1815.2005

Ormonde, P., Hörstedt, P., O'Toole, R., & Milton, D. L. (2000). Role of motility in adherence to and invasion of a fish cell line by Vibrio anguillarum. *Journal of Bacteriology*, *182*(8), 2326–2328. https://doi.org/10.1128/JB.182.8.2326-2328.2000

Osek, J., Svennerholm, A. M., & Holmgren, J. (1992). Protection against *Vibrio*

cholerae El Tor infection by specific antibodies against mannose-binding hemagglutinin pili. *Infection and Immunity*, *60*(11), 4961–4964. https://doi.org/10.1128/iai.60.11.4961-4964.1992

Palabiyik, S. S., Karakus, E., Halici, Z., Cadirci, E., Bayir, Y., Ayaz, G., & Cinar, I. (2016). The protective effects of carvacrol and thymol against paracetamol-induced toxicity on human hepatocellular carcinoma cell lines (HepG2). *Human and Experimental Toxicology*, *35*(12), 1252–1263. https://doi.org/10.1177/0960327115627688

Pant, A., Bag, S., Saha, B., Verma, J., Kumar, P., Banerjee, S., Kumar, B., Kumar, Y., Desigamani, A., Maiti, S., Maiti, T. K., Banerjee, S. K., Bhadra, R. K., Koley, H., Dutta, S., Nair, G. B., Ramamurthy, T., & Das, B. (2020). Molecular insights into the genome dynamics and interactions between core and acquired genomes of *Vibrio cholerae. Proceedings of the National Academy of Sciences of the United States of America*, *117*(38), 23762–23773. https://doi.org/10.1073/pnas.2006283117

Pascual, M., Rodó, X., Ellner, S. P., Colwell, R., & Bouma, M. J. (2000). Cholera Dynamics and El Niño-Southern Oscillation. *Science*, *289*(5485), 1766–1769. https://doi.org/10.1126/science.289.5485.1766

Patil, R. S., Ghormade, V., & Deshpande, M. V. (2000). Chitinolytic enzymes: An exploration. *Enzyme and Microbial Technology*, *26*(7), 473–483. https://doi.org/10.1016/S0141-0229(00)00134-4

Patra, T., Koley, H., Ramamurthy, T., Ghose, A. C., & Nandy, R. K. (2012). The Entner-Doudoroff pathway is obligatory for gluconate utilization and contributes to the pathogenicity of *vibrio cholerae. Journal of Bacteriology*, *194*(13), 3377–3385. https://doi.org/10.1128/JB.06379-11

Pérez-Conesa, D., Cao, J., Chen, L., McLandsborough, L., & Weiss, J. (2011). Inactivation of Listeria monocytogenes and Escherichia coli O157:H7 biofilms by micelle-encapsulated eugenol and carvacrol. *Journal of Food Protection*, *74*(1), 55–62. https://doi.org/10.4315/0362-028X.JFP-08-403

Perini, L. T., Doherty, E. A., Werner, E., & Senear, D. F. (1996). Multiple specific CytR binding sites at the Escherichia coli deoP2 promoter mediate both cooperative and competitive interactions between CytR and cAMP receptor protein. *Journal of Biological Chemistry*, *271*(52), 33242–33255. https://doi.org/10.1074/jbc.271.52.33242

Philippe, N., Alcaraz, J. P., Coursange, E., Geiselmann, J., & Schneider, D. (2004). Improvement of pCVD442, a suicide plasmid for gene allele exchange in bacteria. *Plasmid*, *51*(3), 246–255. https://doi.org/10.1016/j.plasmid.2004.02.003

Pollitzer, R. (1954). Cholera studies. 1. History of the disease. *Bulletin of the World Health Organization*, *10*(3), 421–461.

Price, M. N., Dehal, P. S., & Arkin, A. P. (2007). Orthologous transcription factors in bacteria have different functions and regulate different genes. *PLoS Computational Biology*, *3*(9), 1739–1750. https://doi.org/10.1371/journal.pcbi.0030175

Prouty, M. G., Correa, N. E., & Klose, K. E. (2001). The novel σ54- and σ28-dependent flagellar gene transcription hierarchy of *Vibrio cholerae*. *Molecular Microbiology*, *39*(6), 1595–1609. https://doi.org/10.1046/j.1365-2958.2001.02348.x

Pruzzo, C., Vezzulli, L., & Colwell, R. R. (2008). Global impact of *Vibrio cholerae* interactions with chitin. *Environmental Microbiology*, *10*(6), 1400–1410. https://doi.org/10.1111/j.1462-2920.2007.01559.x

Rao, F. V., Andersen, O. A., Vora, K. A., DeMartino, J. A., & Van Aalten, D. M. F. (2005). Methylxanthine drugs are chitinase inhibitors: Investigation of inhibition and binding modes. *Chemistry and Biology*, *12*(9), 973–980. https://doi.org/10.1016/j.chembiol.2005.07.009

Rasko, D. A., & Sperandio, V. (2010). Anti-virulence strategies to combat bacteria-mediated disease. *Nature Reviews Drug Discovery*, *9*(2), 117–128. https://doi.org/10.1038/nrd3013

Rattanachaikunsopon, P., & Phumkhachorn, P. (2010). Assessment of factors influencing antimicrobial activity of carvacrol and cymene against *Vibrio cholerae* in food. *Journal of Bioscience and Bioengineering*, *110*(5), 614–619. https://doi.org/10.1016/j.jbiosc.2010.06.010

Rawlings, T. K., Ruiz, G. M., & Colwell, R. R. (2007). Association of *Vibrio cholerae* O1 El Tor and O139 Bengal with the copepods Acartia tonsa and Eurytemora affinis. *Applied and Environmental Microbiology*, *73*(24), 7926–7933. https://doi.org/10.1128/AEM.01238-07

Reddi, G., Pruss, K., Cottingham, K. L., Taylor, R. K., & Almagro-Moreno, S. (2018). Catabolism of mucus components influences motility of *vibrio cholerae* in the presence of environmental reservoirs. *PLoS ONE*, *13*(7), 1–16. https://doi.org/10.1371/journal.pone.0201383

Reichelt, J. L., & Baumann, P. (1974). Effect of sodium chloride on growth of heterotrophic marine bacteria. *Archives of Microbiology*, *97*(1), 329–345. https://doi.org/10.1007/BF00403071

Reyrat, J., Pelicic, V., Gicquel, B., & Rappuoli, R. (1998). Counterselectable Markers: Untapped Tools for Bacterial Genetics and Pathogenesis. *Infection and Immunity*, *66*(9), 4011–4017. https://doi.org/10.1128/

IAI.66.9.4011-4017.1998

Ritchie, J. M., Rui, H., Bronson, R. T., & Waldor, M. K. (2010). Back to the future: Studying cholera pathogenesis using infant Rabbits. *MBio*, *1*(1), 1–13. https://doi.org/10.1128/mBio.00047-10

Roberts, W. K., & Selitrennikoff, C. P. (1988). Plant and Bacterial Chitinases Differ in Antifungal Activity. *Microbiology*, *134*(1), 169–176. https://doi.org/10.1099/00221287-134-1-169

Rodríguez, B. L., Rojas, A., Campos, J., Ledon, T., Valle, E., Toledo, W., & Fando, R. (2001). Differential interleukin-8 response of intestinal epithelial cell line to reactogenic and nonreactogenic candidate vaccine strains of *Vibrio cholerae*. *Infection and Immunity*, *69*(1), 613–616. https://doi.org/10.1128/IAI.69.1.613-616.2001

Sack, D. A., Sack, R. B., Nair, G. B., & Siddique, A. (2004). Cholera (The Lancet). *The Lancet*, *363*(9404), 223–233. http://www.sciencedirect.com/science/article/pii/S0140673603153287

Saha, P., Das, B., & Chaudhuri, K. (2013). Role of 6-gingerol in reduction of cholera toxin activity in vitro and in vivo. *Antimicrobial Agents and Chemotherapy*, *57*(9), 4373–4380. https://doi.org/10.1128/AAC.00122-13

Sahai, A. S., & Manocha, M. S. (1993). Chitinases of fungi and plants: their involvement in morphogenesis and host-parasite interaction. *FEMS Microbiology Reviews*, *11*(4), 317–338. https://doi.org/10.1111/j.1574-6976.1993.tb00004.x

Sakazaki , Gomez, S. M. (1967). *Recently , McIntyre and Feeley (1965) studied 82 non-cholera vibrios isolated fromm patients with diarrhea in East Pakistan . They found two biochemical groups within the vibrios , and identified these groups as members of Vibrio and Aeromonas , respec*. *20*, 265–280.

Sakazaki, & Shimada. (1977). Additional serovars and inter o-antigenic relationships of *Vibrio cholerae*. *Japan J. Med. Sci. Biol*, *30*, 275–277.

Sanders, N. N., Eijsink, V. G. H., van den Pangaart, P. S., Joost van Neerven, R. J., Simons, P. J., De Smedt, S. C., & Demeester, J. (2007). Mucolytic activity of bacterial and human chitinases. *Biochimica et Biophysica Acta - General Subjects*, *1770*(5), 839–846. https://doi.org/10.1016/j.bbagen.2007.01.011

Sarwar, S., Ali, A., Pal, M., & Chakrabarti, P. (2017). Zinc oxide nanoparticles provide anti-cholera activity by disrupting the interaction of cholera toxin with the human GM1 receptor. *Journal of Biological Chemistry*, *292*(44),

18303–18311. https://doi.org/10.1074/jbc.M117.793240

Schultz, J., Milpetz, F., Bork, P., & Ponting, C. P. (1998). SMART, a simple modular architecture research tool: Identification of signaling domains. *Proceedings of the National Academy of Sciences of the United States of America*, *95*(11), 5857–5864. https://doi.org/10.1073/pnas.95.11.5857

Sedas, V. T. P. (2007). Influence of environmental factors on the presence of *Vibrio cholerae* in the marine environment: a climate link. *Journal of Infection in Developing Countries*, *1*(3), 224–241. https://doi.org/10.3855/jidc.359

Sernova, N. V., & Gelfand, M. S. (2012). Comparative Genomics of CytR, an Unusual Member of the LacI Family of Transcription Factors. *PLoS ONE*, *7*(9), 1–16. https://doi.org/10.1371/journal.pone.0044194

Shakhnovich, E. A., Hung, D. T., Pierson, E., Lee, K., & Mekalanos, J. J. (2007). Virstatin inhibits dimerization of the transcriptional activator ToxT. *Proceedings of the National Academy of Sciences of the United States of America*, *104*(7), 2372–2377. https://doi.org/10.1073/pnas.0611643104

Sharifi-Rad, M., Varoni, E. M., Iriti, M., Martorell, M., Setzer, W. N., del Mar Contreras, M., Salehi, B., Soltani-Nejad, A., Rajabi, S., Tajbakhsh, M., & Sharifi-Rad, J. (2018). Carvacrol and human health: A comprehensive review. *Phytotherapy Research*, *32*(9), 1675–1687. https://doi.org/10.1002/ptr.6103

Shikuma, N. J., & Hadfield, M. G. (2010). Marine bioflims on submerged surfaces are a reservoir for Escherichia coli and *Vibrio cholerae*. *Biofouling*, *26*(1), 39–46. https://doi.org/10.1080/08927010903282814

Shimada, T., Arakawa, E., Itoh, K., Okitsu, T., Matsushima, A., Asai, Y., Yamai, S., Nakazato, T., Nair, G. B., Albert, M. J., & Takeda, Y. (1994). Current Microbiology Extended Serotyping Scheme for *Vibrio cholerae*. *Current Microbiology*, *28*, 175–178. https://page-one.live.cf.public.springer.com/pdf/preview/10.1007/BF01571061

Silva, A. J., Pham, K., & Benitez, J. A. (2003). Haemagglutinin/protease expression and mucin gel penetration in El Tor biotype *Vibrio cholerae*. *Microbiology*, *149*(7), 1883–1891. https://doi.org/10.1099/mic.0.26086-0

Singer, J. T., Barbier, C. S., & Short, S. A. (1985). Identification of the Escherichia coli deoR and cytR gene products. *Journal of Bacteriology*, *163*(3), 1095–1100. https://doi.org/10.1128/jb.163.3.1095-1100.1985

Singleton, F. L., Attwell, R., Jangi, S., & Colwell, R. R. (1982). Effects of temperature and salinity on *Vibrio cholerae* growth. *Applied and Environmental Microbiology*, *44*(5), 1047–1058. https://doi.org/10.1128/

aem.44.5.1047-1058.1982

Sinha, S., Mell, J., & Redfield, R. (2013). The availability of purine nucleotides regulates natural competence by controlling translation of the competence activator Sxy. *Molecular Microbiology*, *88*(6), 1106–1119. https://doi.org/10.1111/mmi.12245

Sistrunk, J. R., Nickerson, K. P., Chanin, R. B., Rasko, D. A., & Faherty, C. S. (2016). Survival of the fittest: How bacterial pathogens utilize bile to enhance infection. *Clinical Microbiology Reviews*, *29*(4), 819–836. https://doi.org/10.1128/CMR.00031-16

Skorupski, K., & Taylor, R. K. (1996). Positive selection vectors for allelic exchange. *Gene*, *169*(1), 47–52. https://doi.org/10.1016/0378-1119(95)00793-8

Skorupski, K., & Taylor, R. K. (1997). Cyclic AMP and its receptor protein negatively regulate the coordinate expression of cholera toxin and toxin-coregulated pilus in *Vibrio cholerae*. *Proceedings of the National Academy of Sciences of the United States of America*, *94*(1), 265–270. https://doi.org/10.1073/pnas.94.1.265

Slamenova, D., Horvathova, E., Marsalkova, L., & Wsolova, L. (2008). Carvacrol given to rats in drinking water reduces the level of DNA lesions induced in freshly isolated hepatocytes and testicular cells by H 2O2. *Neoplasma*, *55*(5), 394–399.

Slameňová, D., Horváthová, E., Šramková, M., & Maršálková, L. (2007). DNA-protective effects of two components of essential plant oils carvacrol and thymol on mammalian cells cultured in vitro. *Neoplasma*, *54*(2), 108–112.

Sogaard-Andersen, L., Martinussen, J., Mollegaard, N. E., Douthwaite, S. R., & Valentin-Hansen, P. (1990). The CytR repressor antagonized cyclic AMP-cyclic AMP receptor protein activation of the deoCp2 promoter of Escherichia coli K-12. *Journal of Bacteriology*, *172*(10), 5706–5713. https://doi.org/10.1128/jb.172.10.5706-5713.1990

Sullivan, T. J., & Neigel, J. E. (2018). Effects of temperature and salinity on prevalence and intensity of infection of blue crabs, Callinectes sapidus, by *Vibrio cholerae*, V. parahaemolyticus, and V. vulnificus in Louisiana. *Journal of Invertebrate Pathology*, *151*, 82–90. https://doi.org/10.1016/j.jip.2017.11.004

Sun, S., Kjelleberg, S., & McDougald, D. (2013). Relative Contributions of Vibrio Polysaccharide and Quorum Sensing to the Resistance of *Vibrio cholerae* to Predation by Heterotrophic Protists. *PLoS ONE*, *8*(2). https://doi.org/10.1371/journal.pone.0056338

Sun, Y., Bernardy, E. E., Hammer, B. K., & Miyashiro, T. (2013). Competence and natural transformation in vibrios. *Molecular Microbiology*, *89*(4), 583–595. https://doi.org/10.1111/mmi.12307

Suntres, Z. E., Coccimiglio, J., & Alipour, M. (2015). The Bioactivity and Toxicological Actions of Carvacrol. *Critical Reviews in Food Science and Nutrition*, *55*(3), 304–318. https://doi.org/10.1080/10408398.2011.653458

Suzuki, K., Sugawara, N., Suzuki, M., Uchiyama, T., Katouno, F., Nikaidou, N., & Watanabe, T. (2002). Chitinases a, b, and c1 of serratia marcescens 2170 produced by recombinant escherichia coli: Enzymatic properties and synergism on chitin degradation. *Bioscience, Biotechnology and Biochemistry*, *66*(5), 1075–1083. https://doi.org/10.1271/bbb.66.1075

Svitil, A. L., Ní Chadhain, S. M., Moore, J. A., & Kirchman, D. L. (1997). Chitin degradation proteins produced by the marine bacterium Vibrio harveyi growing on different forms of chitin. *Applied and Environmental Microbiology*, *63*(2), 408–413. https://doi.org/10.1128/aem.63.2.408-413.1997

Switzer, R. C., Merril, C. R., & Shifrin, S. (1979). A highly sensitive silver stain for detecting proteins and peptides in polyacrylamide gels. *Analytical Biochemistry*, *98*(1), 231–237. https://doi.org/10.1016/0003-2697(79)90732-2

Syed, K. A., Beyhan, S., Correa, N., Queen, J., Liu, J., Peng, F., Satchell, K. J. F., Yildiz, F., & Klose, K. E. (2009). The *Vibrio cholerae* flagellar regulatory hierarchy controls expression of virulence factors. *Journal of Bacteriology*, *191*(21), 6555–6570. https://doi.org/10.1128/JB.00949-09

Tall, A., Hervio-Heath, D., Teillon, A., Boisset-Helbert, C., Delesmont, R., Bodilis, J., & Touron-Bodilis, A. (2013). Diversity of vibrio spp. isolated at ambient environmental temperature in the eastern english channel as determined by pyrH sequencing. *Journal of Applied Microbiology*, *114*(6), 1713–1724. https://doi.org/10.1111/jam.12181

Tamplin, M. L., Gauzens, A. L., Huq, A., Sack, D. A., & Colwell, R. R. (1990). Attachment of *Vibrio cholerae* serogroup O1 to zooplankton and phytoplankton of Bangladesh waters. *Applied and Environmental Microbiology*, *56*(6), 1977–1980. https://doi.org/10.1128/aem.56.6.1977-1980.1990

Tarsi, R., & Pruzzo, C. (1999). Role of surface proteins in *Vibrio cholerae* attachment to chitin. *Applied and Environmental Microbiology*, *65*(3), 1348–1351. https://doi.org/10.1128/aem.65.3.1348-1351.1999

Taylor, R. K., Miller, V. L., Furlong, D. B., & Mekalanos, J. J. (1987). Use of

phoA gene fusions to identify a pilus colonization factor coordinately regulated with cholera toxin. *Proceedings of the National Academy of Sciences of the United States of America*, *84*(9), 2833–2837. https://doi.org/10.1073/pnas.84.9.2833

Thomas, K. U., Joseph, N., Raveendran, O., & Nair, S. (2006). Salinity-induced survival strategy of *Vibrio cholerae* associated with copepods in Cochin backwaters. *Marine Pollution Bulletin*, *52*(11), 1425–1430. https://doi.org/10.1016/j.marpolbul.2006.04.011

Thompson, F. L., Gevers, D., Thompson, C. C., Dawyndt, P., Naser, S., Hoste, B., Munn, C. B., & Swings, J. (2005). *<Baranov, Bohme_1996_International Journal of Mass Spectrometry and Ion Processes.pdf>*. *71*(9), 5107–5115. https://doi.org/10.1128/AEM.71.9.5107

Towbin, H., Staehelin, T., & Gordon, J. (1979). Electrophoretic transfer of proteins from polyacrylamide gels to nitrocellulose sheets: Procedure and some applications. *Proceedings of the National Academy of Sciences*, *76*(9), 4350–4354.

Tran, H. T., Barnich, N., & Mizoguchi, E. (2011). Potential role of chitinases and chitin-binding proteins in host-microbial interactions during the development of intestinal inflammation. *Histology and Histopathology*, *26*(11), 1453–1464. https://doi.org/10.14670/HH-26.1453

Trucksis, M., Michalski, J., Deng, Y. K., & Kaper, J. B. (1998). The *Vibrio cholerae* genome contains two unique circular chromosomes. *Proceedings of the National Academy of Sciences*, *95*(24), 14464–14469. https://doi.org/10.1073/pnas.95.24.14464

Turner, J. W., Good, B., Cole, D., & Lipp, E. K. (2009). Plankton composition and environmental factors contribute to Vibrio seasonality. *ISME Journal*, *3*(9), 1082–1092. https://doi.org/10.1038/ismej.2009.50

Turner, J. W., Malayil, L., Guadagnoli, D., Cole, D., & Lipp, E. K. (2014). Detection of Vibrio parahaemolyticus, Vibrio vulnificus and *Vibrio cholerae* with respect to seasonal fluctuations in temperature and plankton abundance. *Environmental Microbiology*, *16*(4), 1019–1028. https://doi.org/10.1111/1462-2920.12246

Ultee, A., & Smid, E. J. (2001). Influence of carvacrol on growth and toxin production by Bacillus cereus. *International Journal of Food Microbiology*, *64*(3), 373–378. https://doi.org/10.1016/S0168-1605(00)00480-3

Ultee, Annemieke, Kets, E. P. W., Alberda, M., Hoekstra, F. A., & Smid, E. J.

(2000). Adaptation of the food-borne pathogen Bacillus cereus to carvacrol. *Archives of Microbiology*, *174*(4), 233–238. https://doi.org/10.1007/s002030000199

Urdaneta, V., & Casadesús, J. (2017). Interactions between bacteria and bile salts in the gastrointestinal and hepatobiliary tracts. *Frontiers in Medicine*, *4*(OCT), 1–13. https://doi.org/10.3389/fmed.2017.00163

Valentin-Hansen, P., Søgaard-Andersen, L., & Pedersen, H. (1996). A flexible partnership: The CytR anti-activator and the cAMP-CRF activator protein, comrades in transcription control. *Molecular Microbiology*, *20*(3), 461–466. https://doi.org/10.1046/j.1365-2958.1996.5341056.x

Valeru, S. P., Wai, S. N., Saeed, A., Sandström, G., & Abd, H. (2012). ToxR of *Vibrio cholerae* affects biofilm, rugosity and survival with Acanthamoeba castellanii. *BMC Research Notes*, *5*. https://doi.org/10.1186/1756-0500-5-33

van Alphen, L. B., Burt, S. A., Veenendaal, A. K. J., Bleumink-Pluym, N. M. C., & van Putten, J. P. M. (2012). The Natural Antimicrobial Carvacrol Inhibits Campylobacter jejuni Motility and Infection of Epithelial Cells. *PLoS ONE*, *7*(9), 1–7. https://doi.org/10.1371/journal.pone.0045343

Verma, J., Bag, S., Saha, B., Kumar, P., Ghosh, T. S., Dayal, M., Senapati, T., Mehra, S., Dey, P., Desigamani, A., Kumar, D., Rana, P., Kumar, B., Maiti, T. K., Sharma, N. C., Bhadra, R. K., Mutreja, A., Nair, G. B., Ramamurthy, T., & Das, B. (2019). Genomic plasticity associated with antimicrobial resistance in *Vibrio cholerae. Proceedings of the National Academy of Sciences of the United States of America*, *116*(13), 6226–6231. https://doi.org/10.1073/pnas.1900141116

Vezzulli, L., Pezzati, E., Repetto, B., Stauder, M., Giusto, G., & Pruzzo, C. (2007). A general role for surface membrane proteins in attachment to chitin particles and copepods of environmental and clinical vibrios. *Letters in Applied Microbiology*, *46*(1), 071018031740005-??? https://doi.org/10.1111/j.1472-765X.2007.02269.x

Vezzulli, Luigi, Pruzzo, C., Huq, A., & Colwell, R. R. (2010). Environmental reservoirs of *Vibrio cholerae* and their role in cholera. *Environmental Microbiology Reports*, *2*(1), 27–33. https://doi.org/10.1111/j.1758-2229.2009.00128.x

Wai, S. (1999). How *Vibrio cholerae* survive during starvation. *FEMS Microbiology Letters*, *180*(2), 123–131. https://doi.org/10.1016/S0378-1097(99)00454-1

Wang, S., Wang, J., Mou, H., Luo, B., & Jiang, X. (2015). Inhibition of adhesion

of intestinal pathogens (Escherichia coli, *Vibrio cholerae*, Campylobacter jejuni, and Salmonella Typhimurium) by common oligosaccharides. *Foodborne Pathogens and Disease*, *12*(4), 360–365. https://doi.org/10.1089/fpd.2014.1835

Waters, C. M., Lu, W., Rabinowitz, J. D., & Bassler, B. L. (2008). Quorum Sensing Controls Biofilm Formation in *Vibrio cholerae* through Modulation of Cyclic Di-GMP Levels and Repression of vpsT. *Journal of Bacteriology*, *190*(7), 2527–2536. https://doi.org/10.1128/JB.01756-07

Watnick, P I, Fullner, K. J., & Kolter, R. (1999). A Role for the Mannose-Sensitive Hemagglutinin in Biofilm Formation by *Vibrio cholerae* El Tor -- Watnick et al. 181 (11): 3606 -- The Journal of Bacteriology. *Journal of Bacteriology*, *181*(11), 3606–3609. http://jb.asm.org/cgi/content/abstract/181/11/3606

Watnick, Paula I., & Kolter, R. (1999). Steps in the development of a *Vibrio cholerae* El Tor biofilm. *Molecular Microbiology*, *34*(3), 586–595. https://doi.org/10.1046/j.1365-2958.1999.01624.x

Watve, S. S., Thomas, J., & Hammer, B. K. (2015). CytR is a global positive regulator of competence, type VI secretion, and chitinases in *Vibrio cholerae*. *PLoS ONE*. https://doi.org/10.1371/journal.pone.013883

Weber, F. J., & De Bont, J. A. M. (1996). Adaptation mechanisms of microorganisms to the toxic effects of organic solvents on membranes. *Biochimica et Biophysica Acta - Reviews on Biomembranes*, *1286*(3), 225–245. https://doi.org/10.1016/S0304-4157(96)00010-X

Wei, Y., Ng, W., Cong, J., & Bassler, B. L. (2012). Ligand and antagonist driven regulation of the *Vibrio cholerae* quorum-sensing receptor CqsS. *Molecular Microbiology*, *83*(6), 1095–1108. https://doi.org/10.1111/j.1365-2958.2012.07992.x

Weickert, M. J., & Adhya, S. (1992). A family of bacterial regulators homologous to gal and lac repressors. *Journal of Biological Chemistry*, *267*(22), 15869–15874. https://doi.org/10.1016/s0021-9258(19)49615-4

WHO. (2019). *Weekly epidemiological record* (Vol. 94, Issue 48). https://www.who.int/wer/2019/wer9448/en/

WHO. (2019). *Weekly epidemiological record* (Vol. 94, Issue 48). https://www.who.int/wer/2019/wer9448/en/

William, S., Feil, H., & Copeland, A. (2004). Bacterial DNA Isolation CTAB Protocol Bacterial genomic DNA isolation using CTAB Materials & Reagents. *Doe Joint Genome Institute*, 4. http://my.jgi.doe.gov/general/

protocols/JGI-Bacterial-DNA-isolation-CTAB-Protocol-2012.pdf

Withey, J. H., Nag, D., Plecha, S. C., Sinha, R., & Koley, H. (2015). Conjugated linoleic acid reduces cholera toxin production in Vitro and in Vivo by inhibiting *Vibrio cholerae* ToxT activity. *Antimicrobial Agents and Chemotherapy*, *59*(12), 7471–7476. https://doi.org/10.1128/AAC.01029-15

Yamamoto, K., Ichinose, Y., Shinagawa, H., Makino, K., Nakata, A., Iwanaga, M., Honda, T., & Miwatani, T. (1990). Two-step processing for activation of the cytolysin/hemolysin of *Vibrio cholerae* O1 biotype El Tor: Nucleotide sequence of the structural gene (hlyA) and characterization of the processed products. *Infection and Immunity*, *58*(12), 4106–4116. https://doi.org/10.1128/iai.58.12.4106-4116.1990

Yamamoto, Shigeo, Okujo, N., Fujita, Y., Saito, M., Yoshida, T., & Shinoda, S. (1993). Structures of two polyamine-containing catecholate siderophores from vibrio fluvialis. *Journal of Biochemistry*, *113*(5), 538–544. https://doi.org/10.1093/oxfordjournals.jbchem.a124079

Yamamoto, Shouji, Izumiya, H., Mitobe, J., Morita, M., Arakawa, E., Ohnishi, M., & Watanabe, H. (2011). Identification of a Chitin-Induced Small RNA That Regulates Translation of the tfoX Gene, Encoding a Positive Regulator of Natural Competence in *Vibrio cholerae*. *Journal of Bacteriology*, *193*(8), 1953–1965. https://doi.org/10.1128/JB.01340-10

Yamamoto, Shouji, Morita, M., Izumiya, H., & Watanabe, H. (2010). Chitin disaccharide (GlcNAc)2 induces natural competence in *Vibrio cholerae* through transcriptional and translational activation of a positive regulatory gene tfoXVC. *Gene*, *457*(1–2), 42–49. https://doi.org/10.1016/j.gene.2010.03.003

Yamasaki, S., Asakura, M., Neogi, S. B., Hinenoya, A., Iwaoka, E., & Aoki, S. (2011). Inhibition of virulence potential of *Vibrio cholerae* by natural compounds. *The Indian Journal of Medical Research*, *133*(February), 232–239. http://www.ncbi.nlm.nih.gov/pubmed/21415500

Yeung, A. T. Y., Parayno, A., & Hancock, R. E. W. (2012). *Mucin Promotes Rapid Surface Motility in*. *3*(3), 1–12. https://doi.org/10.1128/mBio.00073-12.Editor

Yildiz, F. H., & Visick, K. L. (2009). Vibrio biofilms: so much the same yet so different. *Trends in Microbiology*, *17*(3), 109–118. https://doi.org/10.1016/j.tim.2008.12.004

Yildiz, F. H., Liu, X. S., Heydorn, A., & Schoolnik, G. K. (2004). Molecular analysis of rugosity in a *Vibrio cholerae* O1 El Tor phase variant. *Molecular Microbiology*, *53*(2), 497–515. https://doi.org/10.1111/j.1365-

2958.2004.04154.x

Yin, H., Deng, Y., Wang, H., Liu, W., Zhuang, X., & Chu, W. (2015). Tea polyphenols as an antivirulence compound Disrupt Quorum-Sensing Regulated Pathogenicity of Pseudomonas aeruginosa. *Scientific Reports*, *5*(October), 1–12. https://doi.org/10.1038/srep16158

Zheng, J., Shin, O. S., Cameron, D. E., & Mekalanos, J. J. (2010). Quorum sensing and a global regulator TsrA control expression of type VI secretion and virulence in *Vibrio cholerae*. *Proceedings of the National Academy of Sciences*, *107*(49), 21128–21133. https://doi.org/10.1073/pnas.1014998107

Zhu, J., & Mekalanos, J. J. (2003). Quorum sensing-dependent biofilms enhance colonization in *Vibrio cholerae*. *Developmental Cell*, *5*(4), 647–656. https://doi.org/10.1016/s1534-5807(03)00295-8

Zhu, J., Miller, M. B., Vance, R. E., Dziejman, M., Bassler, B. L., & Mekalanos, J. J. (2002). Quorum-sensing regulators control virulence gene expression in *Vibrio cholerae*. *Proceedings of the National Academy of Sciences*, *99*(5), 3129–3134. https://doi.org/10.1073/pnas.052694299

Zhu, Jun, & Mekalanos, J. J. (2003). Quorum sensing-dependent biofilms enhance colonization in *Vibrio cholerae*. *Developmental Cell*, *5*(4), 647–656. https://doi.org/10.1016/s1534-5807(03)00295-8

Chapter 10

Appendix

$\mathscr{Appendix}$

Table 10.1. Bacterial strains and plasmid strains used in this study.

Strain	Relevant genotype and /or phenotype	Source / Reference
Wild Type *V. cholerae* N16961 or CytR$^+$	Wild-type, lacking *hap*R function, O1 serogroup, biotype El Tor, Str^R	Heidelberg *et al.*, 2000
Δ*CytR* or CytR$^-$	N16961 Δvc2677, Str^R	This study
CytR^c	N16961 Δvc2677, Str^R + *cytR* in pBAD-TOPO vector, amp^R (complemented strain)	This study
E. coli JM109	endA1 glnV44 thi-1 relA1 gyrA96 recA1 mcrB$^+$ Δ(lac-proAB) e14- [F' traD36 proAB$^+$ lacI^q lacZΔM15] hsdR17(r$_K^-$m$_K^+$)	Promega™
E. coli Top10	F- *mcrA* Δ(*mrr-hsd*RMS-*mcr*BC) *lac*ZΔM15 Δ *lac*X74 *rec*A1 (Str^R) *end*A1 *nup*G	Invitrogen™
E. coli DH5α λpir	endA1 hsdR17 glnV44 (= supE44) thi-1 recA1 gyrA96 relA1 Δ(lacZ)M15::Tn10 uidA::pir+	Lab stock
E. coli SM10λpir	*thi thr leu tonA lacY supE recA*::RP4-2-Tc::Mu *pir R6K*; Kan^R	Skorupski and Taylor, 1996
E. coli BL21 (DE3)	F$^-$ *ompT hsd*S$_B$(r$_B^-$ m$_B^-$) *gal dcm* (DE3)	Skorupski and Taylor, 1996
pCVD442	Suicidal conjugation vector carrying *sacB*, Amp^R	Lab stock, Gift from Dr. Sun Nyunt Wai and Dr. Sridhar Elluri, Department of Molecular Biology, Umea University, Sweden
pGEM®T-Easy vector	pUC/M13 T7 RNA pol transcription initiation site, lac operon, Amp^R	Promega™
pBAD-TOPO	TA-cloning vector, Amp^R	Promega™
pET-151	pBR322 ori, directional TOPO™, His Tag (6X), TEV protease recognition site, Amp^R	Invitrogen™
pGFPuv	GFP expressing plasmid, Amp^R	Clontech™

Table 10.2. Different media used in this study.

Media	Constituents	pH
Luria broth (LB)	1 % Bactopeptone (Difco, USA), 0.5 % Yeast Extract (Difco, USA), and 0.5 - 1.0 % NaCl dissolved in distilled water followed by sterilization at 15 psi for 15 min.	7.2
Luria Agar or LA (for plate)	LB containing 1.5 % Bactoagar (Difco, USA), sterilization was done at 15 psi for 15 min.	7.2

M9 minimal (M9M) medium	5X M9M salts [(Difco, USA), 56.4 g dissolved in distilled water followed by sterilization at 10 lb for 10 min] as a stock, from 5X stock solution 1X complete M9M medium was prepared by using sterile distilled water followed by addition of filter sterilized 2 mM $MgSO_4$, 0.4 % glucose or 0.5% Na-DL-Lactate, 0.1 mM $CaCl_2$. To prepare M9M agar, 1.5% agar was added in 1X M9M complete medium followed by sterilization at 10 psi for 10 min.	7.4
Thiosulphate-Citrate-Bile salt-Sucrose (TCBS) agar	Dehydrated medium from Difco containing 0.5 % Yeast Extract, 1 % Peptone, 1 % Sodium Citrate, 0.7 % Sodium Thiosulphate, 0.5 % Oxgall, 0.3 % Sodium Cholate, 0.2 % Saccharose, 1 % Sodium Chloride, 0.1 % Ferric Citrate, 0.004 % Bromothymol blue, 0.004 % Thymol blue, 1.5 % Agar. To prepare TCBS agar 89 g was dissolved in distilled water followed by boiling and pouring in plates.	8.6
AKI medium	1.5 % Bactopeptone (Difco), 0.4% Yeast Extract (Difco), 0.5 % NaCl and 0.3 % $NaHCO_3$ dissolved in distilled water.	7.2
Defined Artificial Sea Water (DASW) media	460 mM NaCl, 10 mM KCl, 9 mM $CaCl_2$, 36 mM $MgCl_2$, 17 mM $MgSO_4$, 10 mM HEPES-NaOH.	8.2
Sucrose Selection plate	1% Tryptone, 0.5% Yeast extract, 1.8% Bacto Agar followed by autoclaving at 15 lb for 15 min. 10% Sucrose was added to the autoclaved media before plate pouring.	
SOC Medium	Tryptone 2%, Yeast extract 0.5%, NaCl (1M) 1%, KCl (1M) 0.25%, Mg^{+2} stock [(2M) filter sterile - 20% $MgCl_2$, 25% $MgSO_4$] 1%, filter sterile 20 mM Glucose	-

Table 10.3. Different buffers and solutions used in this study.

For isolation of bacterial genomic DNA

Proteinase K	Proteinase K was dissolved at a concentration of 20 mg/ml in sterile 50 mM Tris (pH 8.0), 1.5 mM calcium acetate.
CTAB (Cetyltrimethyl ammonium bromide)/NaCl (S buffer)	10 % CTAB in 0.7 M NaCl; 4.1 g NaCl was dissolved in 80 ml water followed by slow addition of 10 g CTAB while heating and constant stirring. The volume was finally adjusted to 100 ml.
1X TE	0.01 M Tris-HCl (pH 8.0), 0.001 M ethylenediaminetetraacetic acid (EDTA; pH 8.0); the solution was sterilized at 15 psi for 15 min.
Normal saline	0.9% NaCl; 9g/L of distilled water and sterilization at 15 psi for 15 min.
5 N NaCl	292.5 g NaCl in distilled water and volume made upto 1 L.
10 % Sodium dodecyl sulfate (SDS)	10 % (w/v) SDS solution prepared in distilled water.

RNaseA solution (20 mg/ml)	Pancreatic RNase (RNase A) was dissolved in 10 mM sodium acetate (pH 5.4), the solution was heated to 100°C for 15 min and allowed to cool slowly to room temperature, pH was adjusted to 7.4 and then stored at -20°C.

For isolation of plasmid DNA from bacterial cells

Cell Resuspension Solution (CRS)	50 mM Tris-HCl (pH 7.5), 10 mM EDTA, 100 μg/ml RNase A
Cell Lysis Solution (CLS)	0.2 M NaOH, 1% SDS
Neutralization Solution (NS)	1.32 M Potassium Acetate (pH 4.8)
Column Wash Solution (CWS)	80 mM Potassium acetate, 8.3 mM Tris – HCl (pH 7.5), 40 μM EDTA, 55% 95% Ethanol

For agarose gel electrophoresis of DNA

50X TAE	242 g Tris base in double-distilled H_2O, 57.1 ml Glacial acetic acid, 100 ml 0.5 M EDTA solution (pH 8.0). Adjust final volume to 1 L. [Molarity in 1X TAE – EDTA disodium salt, 1 mM; Tris, 40 mM; Glacial acetic acid, 20 mM]
10X DNA gel loading dye	0.25 % (w/v) Bromophenol blue, 0.25 % (w/v) Xylene cyanol, 50 mM EDTA, 50 % (v/v) glycerol, 10% SDS in distilled water.
Gel staining solution	Ethidium bromide stock solution (10 mg/ml) in distilled water. The final working solution was of 0.5 μg/ml concentration, which was used for staining DNA fragments.

For transformation of *E. coli* cells with plasmid DNA

Transformation buffer	10 mM Tris-HCl, 100 mM $CaCl_2.2H_2O$ (pH 7.6); sterilized at 15 lb for 15 min

For electroporation of *V. cholerae* cells with plasmid DNA

Electroporation buffer	272 mM sucrose, 1 mM HEPES (pH 8.0), 10% Glycerol in Milli-Q water; sterilized at 15 psi for 15 min

For Selection of recombinants

Isopropyl- -D-thiogalactopyranoside (IPTG) stock solution	0.1 M IPTG prepared in sterile distilled water and stored at -20°C.
5-Bromo-4-chloro-3-D-galactoside (X-gal) stock solution	40 mg/ml X-gal dissolved) in N,N'- dimethyl formamide (DMF) and stored at -20°C in a dark container.

LA plate with antibiotics/IPTG/X-Gal

1.5% of LA plate was incubated at 37 °C for 30 min and 100 μl of 100 mM IPTG and 20 μl of 40 mg/ml X-Gal were spread on the LA plate. The plate was incubated for 30 min at 37 °C.

L-arabinose solution	20 % (w/v) L-arabinose in water and filter sterilized, stored at -20°C.

For SDS-PAGE

Solution A	29.2% Acrylamide, 0.8% Bis-acrylamide dissolved in Elix water. The solution was stored in light resistant container.
Solution B	1.5 M Tris HCl (pH 8.8), 0.4% SDS
Solution C	0.5 M Tris HCl (pH 6.8), 0.4% SDS
Gel Running buffer	0.025 M Tris base, 0.192 M Glycine, 0.1% SDS dissolved in Elix Water. pH 8.3
5X Gel loading Dye	100 mM Tris-HCl pH 6.8, 4% (w/v) SDS, 0.2% (w/v) Bromophenol blue, 20% (v/v) Glycerol, 200 mM β-mercaptoethanol.
Staining Solution	0.25 % (w/v) Coomassie Blue (R-250) was dissolved in a solution of 50 % methanol (v/v), 40 % water and 10 % acetic acid (v/v) and the solution was filtered through Whatman filter paper (No. 1).
Destaining Solution	40 % methanol (v/v), 10 % acetic acid (v/v) and 50 % (v/v) water.

For Western blotting

Transfer Buffer	25 mM Tris, 192 mM glycine, 0.05% Glycine, 20 % (v/v) methanol.
Washing Buffer (TBS and TBS-T buffer)	Solution TBS was prepared by adding 10 mM Tris and 150 mM NaCl and adjusting pH to 7.4. To this solution 0.1 % (v/v) Tween 20 was added to get the TBS-T solution.
Blocking Buffer	5 % (w/v) BSA dissolved in TBST buffer.
Bicarbonate buffer	168 mg $NaHCO_3$, 4.06 mg $MgCl_2$ for 20 ml, pH adjusted to 9.8 with NaOH
Ponceau S	1 % (w/v) Ponceau S in 7 % (v/v) acetic acid.

For M9M medium preparation

1 M $MgSO_4$	24.65 g of $MgSO_4.7H_2O$ was dissolved in 100 ml of water and filter sterilized.
0.1 M $CaCl_2$	0.11 g $CaCl_2$ was dissolved in 100 ml of water and filter sterilized.

For AKI medium preparation

3% NaHCO$_3$	3% (w/v) NaHCO$_3$ in distilled water and filter sterilized.

For ELISA

1X PBS buffer	137 mM NaCl, 2.7 mM KCl, 10 mM Na$_2$HPO$_4$, 2 mM KH$_2$PO$_4$ (pH 7.4).
PBS Tween-20 (PBS-T) solution	0.05 % (v/v) Tween-20 in 1X PBS.

For isolation of cytoplasmic fraction of recombinant proteins from the inclusion bodies

Cell Resuspension Buffer (CRB)	50 mM Tris-HCl, 50 mM NaCl, 0.5 mM EDTA (3.72 mg / 20 ml), 1 mM TCEP (make 1 M TCEP stock and store at -80°C.), 5% Glycerol, add protease inhibitor cocktail or 1 mM PMSF (final concentration), pH 8.0
Inclusion Wash Buffer (IWB)	50 mM Tris-HCl, 50 mM NaCl, 0.5 mM EDTA (3.72 mg / 20 ml), 1 mM TCEP (make 1 M TCEP stock and store at -80°C.), 5% Glycerol, 0.125 M NDSB-201 (make 1.5 M NDSB stock solution and store at -80°C), pH 8.0
Denaturation Buffer (DB)	50 mM Tris-HCl, 0.2 M NaCl, 20 mM EDTA, 8 M Urea, pH 8.0
Cell lysis buffer	50 mM Potassium phosphate buffer pH 7.8 [prepare the potassium phosphate buffer by mixing 0.3 ml KH$_2$PO$_4$ and 4.7 ml K$_2$HPO$_4$ from their respective 1 M stock], 400 mM NaCl, 100 mM KCl, 10% Glycerol, 0.5% Triton X-100, 10 mM Imidazole
Sonication buffer	20 mM Tris-HCl pH 7.4, 5 mM PMSF, 1 mM DTT, 20% v/v Glycerol

For Bacterial periplasmic fraction extraction

Periplasmic extraction buffer	30 mM Tris-HCl pH 7.4, 5 mM EDTA, 25% Sucrose, 1.5 mg/ml Lysozyme

For maintenance of tissue culture cells

Dulbecco's Modified Eagle's Medium (DMEM) Complete media	13.5 g/L DMEM, 3.7 g/L Sodium Bicarbonate, 100 ml FBS, 10 ml Antibiotics (Penicillin-Streptomycin), 10 ml Non-Essential Amino Acid, volume adjusted to 1 L with MilliQ water, pH 7.4
Dulbecco's Modified Eagle's Medium (DMEM) Incomplete media	13.5 g/L DMEM, 3.7 g/L Sodium Bicarbonate, 5 ml FBS, 10 ml Non-Essential Amino Acid, volume adjusted to 1 L with MilliQ water, pH 7.4

For Purification of DNA from Agarose gel	
Membrane Wash Solution (MWS)	10 mM Potassium acetate (pH 5.0), 80% 95% Ethanol, 16.7 μM EDTA (pH 8.0)
Membrane Binding Solution (MBS)	4.5 M Guanidine Isothiocyanate, 0.5 M Potassium acetate (pH 5.0)

Table 10.4. Sequence of oligonucleotides used in this study

Primer Name	Primer Sequence (5' - 3')	T_m (ºC)	Amplicon Length (bp)
CytR Internal FP	TTGCGCCGTAATGAATCG	54	653
CytR Internal RP	CCGACCACAGAGAGATCT	56	
CytR RT FP	GGACAGATTTGCCGTTTGATG	62	158
CytR RT RP	CCCAAGCTGAGTGAGATAGTTT	62	
RecA RT FP	GTCGCAAGCAATGCGTAAAC	63	158
RecA RT RP	CCAAACGAACAGAAGCGTAGA	62	

Table 10.5. Sequence of oligonucleotides used for CytR deletion and Complementation

Primer Name	Primer Sequence (5'- 3')	T_m (ºC)	Amplicon Length (bp)
CytR FP *XbaI* (A)	**CAGCTCTAGA**GCAAAGCGCACGTCCAGC *XbaI*	60 ºC	450
CytR RP Fusion (B)	**CCCATCCACTATAAACTAACA**AGACACGGTCGCGG TTGA	58 ºC	
CytR FP Fusion(C)	**TGTTAGTTTATAGTGGATGGG**GTACGTGCTGGAT CGCGT	58 ºC	483
CytR RP *SacI* (D)	**GAATCGAGCTC**GGGCGGTAGCGTTTCTGT *SacI*	58 ºC	
CytR comp pBad FP	ATGGCGACAATGAAGGATGT	58 ºC	1008
CytR comp pBad RP	TTACTTCTTGCTTGGCGGCG	62 ºC	

Table 10.6. Sequence of oligonucleotides used for CytR recombinant protein expression

Primers	Sequence (5' – 3')	T_m
pET151 d-TOPO Forward Primer	**CACC**<u>ATG</u>GCGACAATGAAG	58°C
pET151 d-TOPO Reverse Primer	CTTCTTGCTTGGCGGCGC	60°C

Table 10.7. Sequence of oligonucleotides used for Real time PCR

Primers	Sequence (5' – 3')	Gene Locus[1]
FlrA RT FP	GAGCGTATGGTCATCCTGTATC	VC2137
FlrA RT RP	AAATGCCTTCCAACACATCAC	
FlrB RT FP	CCTATTGCAGTCACGGATCA	VC2136
FlrB RT RP	CGAGTAGCAGGCGGTAAAT	
FlrC RT FP	CACAATGCCTCTCCTCGTAAA	VC2135
FlrC RT RP	CCTTGGGCTTGTTCAAACTTAC	
RpoN RT FP	ATGCGGAGAGCAACTACATC	VC2529
RpoN RT RP	CTTCATCGCCTCTTCTCCATAC	
FliA RT FP	GATAGAGGATCTCGGTGTTTCTG	VC2066
FliA RT RP	GCGAAAGTACCAAAGCTTCAC	
MotY RT FP	CAACCAATACTCCGTTGGAATG	VC1008
MotY RT RP	CTAGGCTGACATTACGGGTATC	
FlaA RT FP	GGGTGGCCAATCCTTTATT	VC2188
FlaA RT RP	TCTTCAATGTCATCACCATCTT	
FlgP RT FP	CTGAGCAGGTGTATGGTATG	VC2206
FlgP RT RP	GTTCAGTGACATAGCTGTCC	
FlgT RT FP	CCTTAGAAGATGCGCTGTATAA	VC2208
FlgT RT RP	CGCTTTGCGTTCTTCAATC	
FliF RT FP	CAGTAGAGCAGACACGTAAAG	VC2133
FliF RT RP	TACATCTTGCGGAATTGAGG	
FlgM RT FP	CACCAATGTGCGTTCTTCT	VC2204
FlgM RT RP	CTGGGTCTTGAAGCCATTT	
FlgK RT FP	ACCTTACAGTCACAAGGTTTAG	VC2191
FlgK RT RP	AGCTGGCTAACATCTTCAATAA	
FlgG RT FP	AGCACTATGGGTCAGTAAGA	VC2195

FlgG RT RP	CCCGGCTGGTTAATGTTT	
FlgB RT FP	CAATACGCCGGGATTTAAGG	VC2200
FlgB RT RP	CGGTACGCGGTAAAGAATTT	
ToxT RT FP	TTACTGATGATCTTGATGCTATGGA	VC0838
ToxT RT RP	ATTCTCTAAACTTTACTCCTCGAGAC	
ToxR RT FP	GACGAATAAATCGGCTCCAAAC	VC0984
ToxR RT RP	AGGGTGGTTATTCGGCATATT	
CtxB RT FP	TGTGCAGAATACCACAACAC	VC1456
CtxB RT RP	TGTGAATCTATATGTTGACTACCT	
TcpA RT FP	CGAAACTCTGCAGCGAATAAAG	VC0828
TcpA RT RP	CGTTTCGAAATCACCAAGATCAG	
ChiA1 RT FP	GCCGAGCATTGAAGCAAATC	VC1952
ChiA1 RT RP	ATTCCACTGTAGGCAACCATAC	
ChiA2 RT FP	CTACCGCCCAGTTTACTTATCC	VCA0027
ChiA2 RT RP	AACCATCGGTATCCGCAATAG	
VC0769 RT FP	GTGGGAAGTGGGTAAGGTTTAT	VC0769
VC0769 RT RP	TTGGCGTTGGCTCAGTT	
VC1073 RT FP	GGAAAGCCAGTGGTGGAATA	VC1073
VC1073 RT RP	TAAAGCTCATGCTTGGGTAAGA	
ChiS RT FP	CGGATCGGGTGACCAAATAA	VC0622
ChiS RT RP	GTTCTAAGTAAGCCCAGTGGTAG	
TfoX RT FP	GCCTTAGGGTGCGAGAAATA	VC1153
TfoX RT RP	CGTTGAAATTCCCGCTGATTC	
GbpA RT FP	GATACCGCAGCTTCCTTCTAC	VC0811
GbpA RT RP	GCCAATGCTGAGATCCATACT	
TcpP RT FP	CAGCTCTGAAAGTCTAACTCAGG	VC0826
TcpP RT RP	GACTACAGTCAGCTTCATCAACA	
ToxR RT FP	GACGAATAAATCGGCTCCAAAC	VC0984
ToxR RT RP	AGGGTGGTTATTCGGCATATT	
RecA RT FP	GTCGCAAGCAATGCGTAAAC	VC0543
RecA RT RP	CCAAACGAACAGAAGCGTAGA	

* The amplicon length of all of these above oligos for Real time PCR lies within 158 ± 4 bp range.

[1] Locus number of specific gene specified here according to Heidelberg *et al*., 2000.
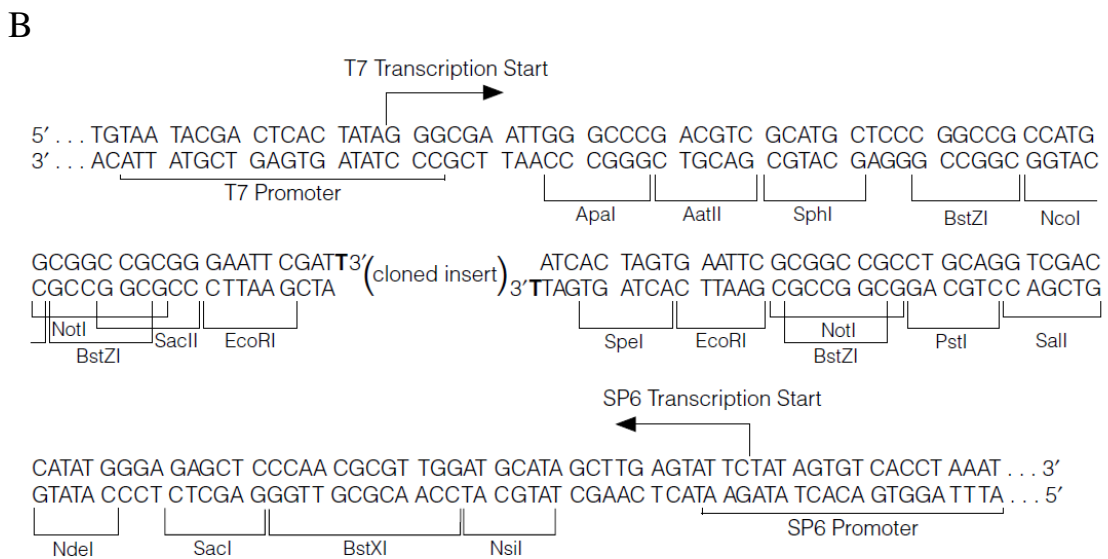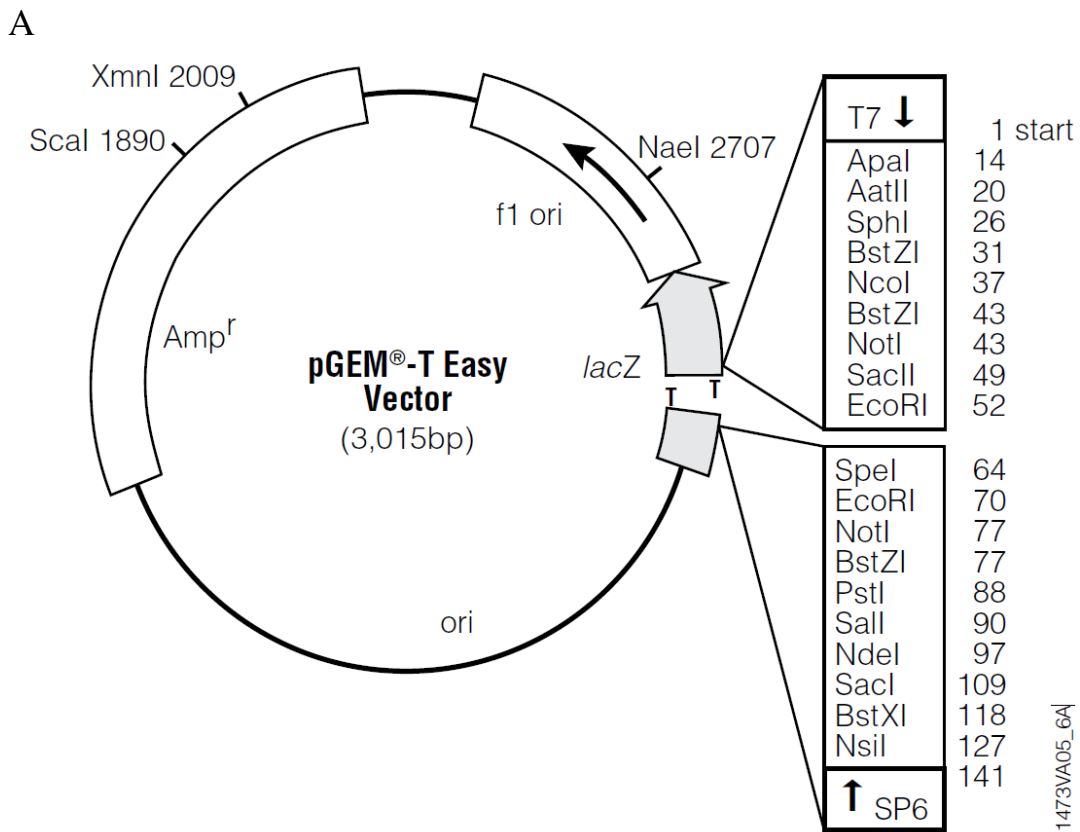
Cloning vectors used in this study

A

B

Fig.10.1. (A) pGEM®-T Easy Vector (Promega) Map, (B) The promoter and multiple cloning sequence of the pGEM®-T Easy Vector. The top strand shown corresponds to the RNA synthesized by T7 RNA polymerase. The bottom strand corresponds to the RNA synthesized by SP6 RNA polymerase.
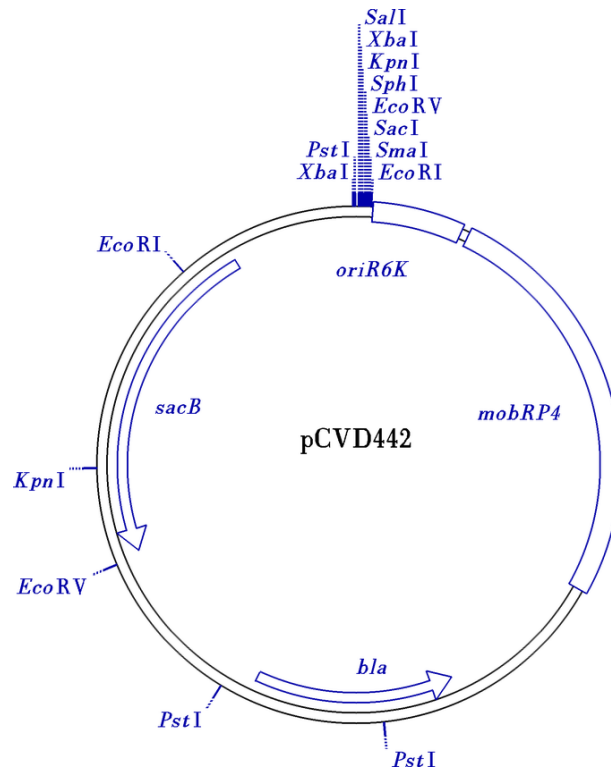
Fig.10.2. Suicidal vector pCVD442 (addgene) map. This suicide vector was created to engineer mutations in host strains via allelic exchange. The important properties of this vector are:

1) a pir dependent origin of replication from plasmid R6K,
2) the *bla* gene encoding resistance to ampicillin,
3) the *mob* region allowing efficient transfer by conjugation from strains containing the *tra* locus, and
4) the *sacB* gene conferring sensitivity to sucrose in Gram-negative bacteria.

Plasmid pCVD442 was created by cloning the *sacB* gene on a PstI fragment from plasmid pUM24 (Ried and Collmer. Gene 57:239-46, 1987) into plasmid pGP704 (Miller and Mekalanos. J.Bacteriol. 170:2575-83, 1988) that had been partially digested with *PstI*. Plasmid pCVD442 and its derivatives can only grow in strains that have the pir gene encoding the Pi protein, which is necessary for replication of R6K plasmids. The pir gene is usually supplied by a lambda lysogen. Such strains include DH5alpha-lambdapir, SY327-lambdapir, SM10-lambdapir, and S17-lambdapir. The last two strains supply the tra genes for efficient conjugation. Sucrose sensitivity is far from absolute. The strain carrying the plasmid grows well on sucrose plates. To detect sucrose sensitivity make serial dilutions of the bacteria and plate both on plates containing and lacking 5% sucrose. There should be substantially fewer colonies and the colonies are smaller on the sucrose plates.
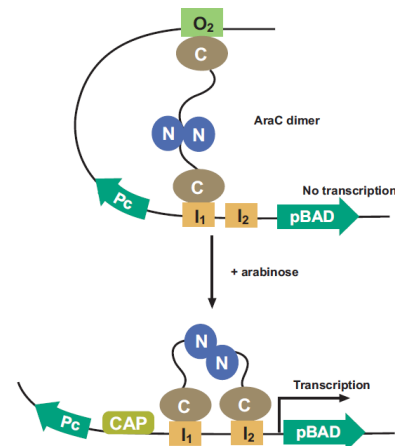
A
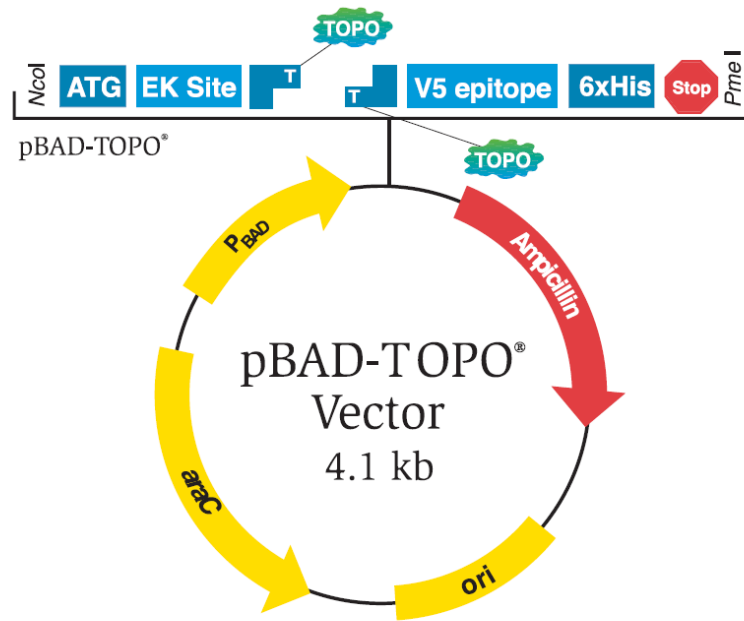
TOPO Represents covalently bound topoisomerase I

B
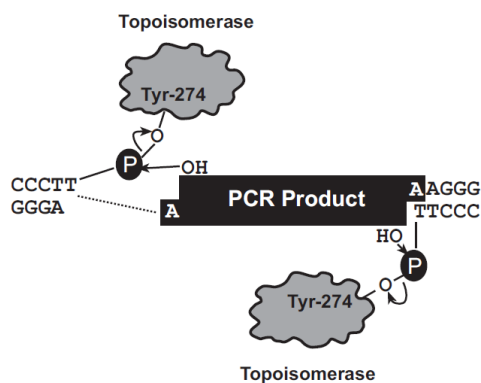
C

Fig.10.3. (A) Vector map of pBAD TOPO® (Invitrogen). (B) TOPO®-cloning reaction. (C) Regulation by L-arabinose. The *ara*BAD promoter used in pBAD-TOPOR is both positively and negatively regulated by the product of the *ara*C gene (Ogden *et al.*, 1980; Schleif, 1992). AraC is a transcriptional regulator that forms a complex with L-arabinose. In the absence of L-arabinose the AraC dimer contacts the O_2 and I_1 half sites of the *ara*BAD operon, forming a 210 bp DNA loop. First, L-Arabinose binds to AraC and causes the protein to release the O_2 site and bind the I_2 site which is adjacent to the I1 site. This releases the DNA loop and allows transcription to begin and second, The cAMP activator protein (CAP)-cAMP complex binds to the DNA and stimulates binding of AraC to I_1 and I_2.
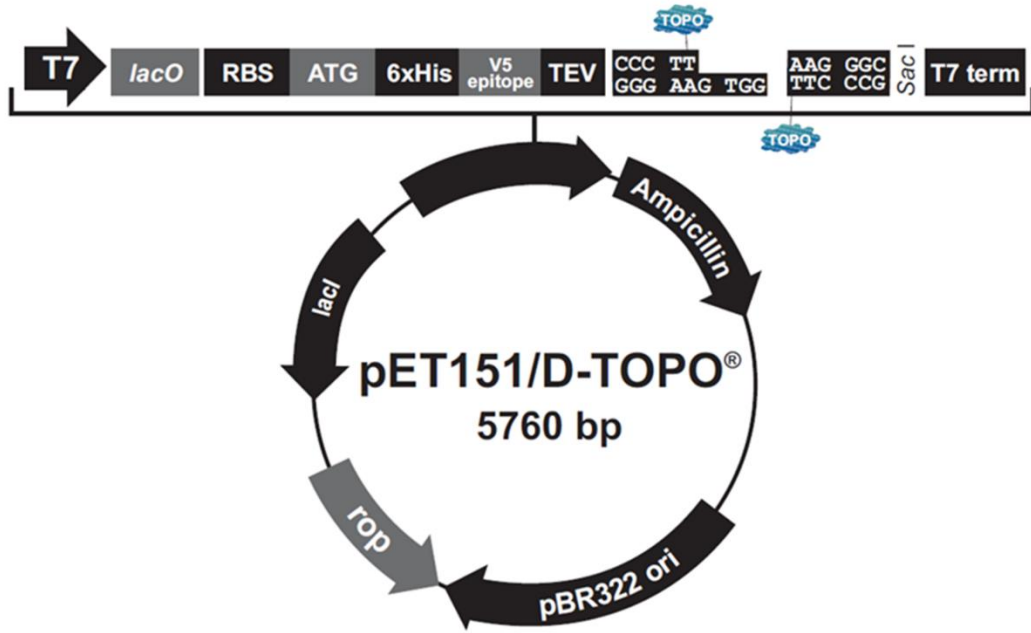
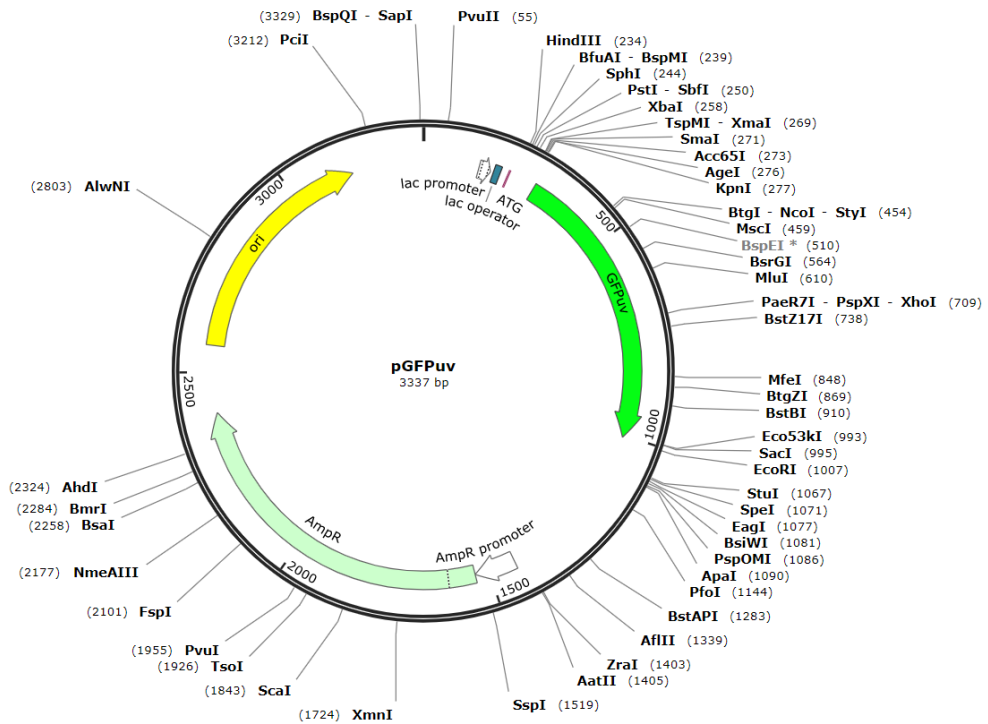**Fig.10.4. Vector map of pET-151/D-TOPO® (Invitrogen).** This vector is used for recombinant protein expression.

Fig.10.5. Vector map of pGFPuv (Snapgene). This vector is used for expressing GFP in bacteria.

Chapter 11

Publications

&

Conferences

Journal articles published

- **Das S, Chourashi R, Mukherjee P, Gope A, Koley H, Dutta M, Mukhopadhyay AK, Okamoto K, Chatterjee NS.** Multifunctional transcription factor CytR of *Vibrio cholerae* is important for pathogenesis. *Microbiology* (Reading). **2020** Nov 4. doi: 10.1099/mic.0.000949. Epub ahead of print. PMID: 33150864.

- **Das S, Chourashi R, Mukherjee P, Kundu S, Koley H, Dutta M, Mukhopadhyay AK, Okamoto K, Chatterjee NS.** Carvacrol abrogates pathogenesis in *Vibrio cholerae*. *Journal of Applied Microbiology*. Jan **2021**. doi: 10.1111/jam.15022.

- **Chourashi R, Das S, Dhar D, Okamoto K, Mukhopadhyay AK, Chatterjee NS.** Chitin-induced T6SS in Vibrio cholerae is dependent on ChiS activation. *Microbiology* (Reading). 2018 May; 164(5):751-763. doi: 10.1099/mic.0.000656. Epub **2018** Apr 10. PMID: 29633936.

- **Chourashi R, Mondal M, Sinha R, Debnath A, Das S,** Koley H, Chatterjee NS. Role of a sensor histidine kinase ChiS of Vibrio cholerae in pathogenesis. International Journal of Medical Microbiology. 2016 Dec;306(8): 657-665. doi: 10.1016/j.ijmm.2016.09.003. Epub **2016** Sep 19. PMID: 27670078.

Conference attended

- Presented a poster on "*Essential oil fraction of oregano abrogates V. cholerae pathogenesis*" and participated in the ISCBC NIPICON- 2020 International Conference on "Integrating Chemical, Biological and Pharmaceutical Sciences for Innovations in Health Care" held at Institute of Pharmacy, Nirma University, Ahmedabad during *January, 22-24, 2020*.

- Presented a poster on "*Role of Vibrio cholerae regulatory protein CytR in pathogenesis*" in the 15th Asian conference on Diarrhoeal disease and Nutrition (ASCODD) held at the Pan Pacific Sonargaon hotel, Dhaka, Bangladesh from *28th Jan to 30th Jan 2020* organized by ICDDR,B.

Multifunctional transcription factor CytR of *Vibrio cholerae* is important for pathogenesis

Suman Das[1], Rhishita Chourashi[1], Priyadarshini Mukherjee[2], Animesh Gope[3], Hemanta Koley[2], Moumita Dutta[4], Asish K. Mukhopadhyay[2], Keinosuke Okamoto[5] and Nabendu Sekhar Chatterjee[1,*]

Abstract

Vibrio cholerae, the Gram-negative facultative pathogen, resides in the aquatic environment and infects humans and causes diarrhoeagenic cholera. Although the environment differs drastically, *V. cholerae* thrives in both of these conditions aptly and chitinases play a vital role in their persistence and nutrient acquisition. Chitinases also play a role in *V. cholerae* pathogenesis. Chitinases and its downstream chitin utilization genes are regulated by sensor histidine kinase ChiS, which also plays a significant role in pathogenesis. Recent exploration suggests that CytR, a transcription factor of the LacI family in *V. cholerae,* also regulates chitinase secretion in environmental conditions. Since chitinases and chitinase regulator ChiS is involved in pathogenesis, CytR might also play a significant role in pathogenicity. However, the role of CytR in pathogenesis is yet to be known. This study explores the regulation of CytR on the activation of ChiS in the presence of mucin and its role in pathogenesis. Therefore, we created a CytR isogenic mutant strain of *V. cholerae* (CytR⁻) and found considerably less β-hexosaminidase enzyme production, which is an indicator of ChiS activity. The CytR⁻ strain greatly reduced the expression of chitinases *chiA1* and *chiA2* in mucin-supplemented media. Electron microscopy showed that the CytR⁻ strain was aflagellate. The expression of flagellar-synthesis regulatory genes *flrB*, *flrC* and class III flagellar-synthesis genes were reduced in the CytR⁻ strain. The isogenic CytR mutant showed less growth compared to the wild-type in mucin-supplemented media as well as demonstrated highly retarded motility and reduced mucin-layer penetration. The CytR mutant revealed decreased adherence to the HT-29 cell line. In animal models, reduced fluid accumulation and colonization were observed during infection with the CytR⁻ strain due to reduced expression of *ctxB*, *toxT* and *tcpA*. Collectively these data suggest that CytR plays an important role in *V. cholerae* pathogenesis.

INTRODUCTION

Cholera is an acute diarrhoeal disease caused by facultative, Gram-negative pathogenic bacteria *Vibrio cholerae* [1, 2]. The world has witnessed seven pandemics of cholera to date. The current seventh cholera pandemic started in 1992 and still, outbreaks are reported mainly from Africa, Asia, America, and it is predominantly caused by the O1 El tor biotypes of *V. cholerae* [3].

The dynamic lifestyle of *V. cholerae* includes two different habitats. They live primarily in the aquatic environment either as a free-living bacterium or in association with phyto-, zooplanktons, mollusks, crustaceans and arthropods. In the aquatic environment, *V. cholerae* feeds on their exoskeletal chitinous covering [4]. *V. cholerae* releases extracellular chitinases ChiA1 and ChiA2 to degrade the chitinous exoskeleton by breaking the β–1,4 glycosidic linkage of the chitin polymer releasing N-acetyl glucosamine (GlcNAc) residues, which are sensed and internalized by *V. cholerae* as a source of the nutrient. The regulation of sensing and chitinase secretion is ChiS dependent, which is a periplasmic two-component sensor histidine kinase [5, 6]. *V. cholerae* also colonizes in the intestinal epithelium of the human gut, where the mucus layer provides a niche for colonization because it harbours attachment sites like glycans [7]. Mucus glycans also act as a direct source of nutrients for the bacteria [8].

V. cholerae chitinases act on mucus glycans to produce GlcNAc-like residues, which act as a nutrient source. Reports have also indicated the involvement of bacterial chitinases in pathogenesis [9–11]. Our studies have shown that the chitinase ChiA2 (VCA0027) is important for *V. cholerae* survival and pathogenesis [11, 12].

V. cholerae ChiS (VC0622) regulates the expression of chitinases and it plays an important role in pathogenesis [12]. In the host intestine, ChiS gets activated in the presence of mucin. The activated ChiS contributes to the utilization of mucin and helps *V. cholerae* to survive in the intestine. ChiS also promotes motility, mucin-layer penetration, adherence and survival in the intestinal environment. Moreover, ChiS mutant *V. cholerae* shows hypovirulent characteristics as it secretes less cholera toxin (CT) in the intestine, and hence shows less fluid accumulation and less virulence [12].

There is another regulator of chitinases in *V. cholerae* known as CytR (VC2677) [13]. Since chitinases play a role in pathogenesis, we speculate that CytR might also be involved in controlling virulence cascade, which is ultimately attributed to the pathogenicity of *V. cholerae* and causes the disease. CytR is a 37 KDa cytoplasmic protein belonging to the LacI family transcriptional regulator present in some gamma proteobacteria including *V. cholerae* [14, 15]. CytR has an N-terminal domain that contains a helix-turn-helix (HTH) motif for DNA binding and a C-terminal domain for dimerization, inducer binding and protein contact with cAMP Receptor Protein (CRP). Its role in transport and utilization of nucleosides have long been studied in *Escherichia coli* [16, 17]. In *E. coli* CytR negatively regulates a small set of nucleoside scavenging and metabolism genes including *udp*, *cdd*, *ompK* and *cytR* itself via cAMP receptor protein (CRP)-dependent anti-activation mechanism [18]. *V. cholerae* CytR is a functionally diverse protein and a global regulator. It represses multiple nucleoside catabolism and scavenging genes, positively regulates competence and a majority of natural transformation genes, bacterial killing by inducing type VI secretion system (T6SS) gene clusters, and co-regulates chitinase genes along with TfoX [13].

Recently it has been discovered that among many other roles, CytR is involved in the regulation of *V. cholerae* extracellular chitinase ChiA1 (17) and ChiA2 (13). Therefore, it is possible that CytR might be involved in *V. cholerae* pathogenesis.

The pathogenesis of *V. cholerae* within the human host is controlled by a complex signalling cascade of virulence genes and regulatory factors that have been the subject of intense research for several decades. During pathogenesis, *V. cholerae* has to survive in the intestinal environment, penetrate through the mucus layer, adhere to the intestinal epithelium, form colonies to secrete CT [1, 19–21]. To define the role of CytR in *V. cholerae* pathogenesis we explored the impact of CytR deletion and studied the growth of bacteria in the presence of mucin, its motility due to flagellar movement in mucin, virulence-gene expression and fluid accumulation as a marker of CT production. We demonstrated that CytR positively regulates activation of sensor histidine

kinase ChiS in the mucinous environment, thus affecting the secretion of chitinases and degradation of mucin. CytR deletion resulted in no flagellar synthesis, which leads to reduced motility and mucin penetration. Furthermore, CytR not only has a marked effect on the adhesion to the intestinal epithelial cells but also positively controls CT secretions and other virulence traits. Therefore, a distinct regulatory pattern may exist, which leads to the reduced pathogenicity in the CytR-ablated strain.

METHODS

Ethics statement

Animal experiments were conducted following the standard operating procedure framed by the Committee for the Purpose of Control and Supervision of Experiments on Animal (CPCSEA), Government of India. All the animal experiments performed here were approved by the Institutional Animal Ethics Committee of National Institute of Cholera and Enteric Diseases (registration no: PRO/120/April 2016–March 2019). Intestinal colonization competitive index assay was performed using 4- to 5-day-old infant Swiss mice. For fluid accumulation and other *in vivo* studies, New Zealand white rabbits weighing about 2.5 kg were used. Animals were euthanized in a CO_2 chamber assuring minimum pain to the animals during the intestinal harvest.

Bacterial strains culture conditions and DNA manipulations

Streptomycin-resistant *V. cholerae* (O1 El Tor Inaba) N16961 was used in all the experiments performed here [22]. The *V. cholerae* strain N16961 used is denoted as the wild-type (WT or CytR$^+$); the CytR-deleted N16961 strain is denoted as the CytR mutant (CytR$^-$) and the complemented CytR$^-$ as strain CytR^c. These strains were cultured in Luria–Bertani (LB) medium (BD, Difco) at 37 °C under constant shaking at 180 r.p.m. or under the static condition on Petri plates containing LB agar supplemented with suitable antibiotics streptomycin (100 µg ml^{-1}) or ampicillin (100 µg ml^{-1}) whenever necessary. For enzymatic assay and *in vitro* RNA analysis, bacteria were also grown in minimal-lactate media containing M9 minimal medium (BD Difco), 50 mM HEPES (pH 7.5) (Sigma), filter sterile 0.2% $MgSO_4$ (Merck) and 0.01% $CaCl_2$ (SRL) with or without 1% porcine mucin (sigma) as a sole source of carbon [12]. Sodium lactate (Sigma) at 0.5% was also added to support equal growth of wild-type and mutant strains during RNA analysis and enzymatic assay [12]. Bacteria were also cultured in AKI media containing 0.4% yeast extract (BD Difco), 1.5% Bacto peptone (BD Difco), 0.5% NaCl and 0.3% freshly prepared $NaHCO_3$ (Merck) pH 7.2 at 37 °C under static condition for CT analysis. Plasmid DNA was isolated by plasmid DNA purification kit (Promega). DNA manipulations were done using restriction enzymes (New England Biolabs), DNA ligation kit (Promega) and *Taq* DNA polymerase (Promega) for PCR amplification.

Construction of the deletion mutant of CytR and its complement

The isogenic deletion mutant of *cytR* was constructed as described previously [23]. In brief, genomic DNA was first isolated from N16961 *V. cholerae*. The 500 bp fragment upstream and downstream of the *cytR* gene (VC_2677 of NCBI reference sequence, NC_002505.1) was PCR-amplified using primer pairs *cytR* Ext Xba1 FP (A) and *cytR* Fus RP (B) *cytR* Fus FP (C) and *cytR* Ext Sac1 RP (D) (Table S1, available in the online version of this article). The amplicons AB and CD were then fused and amplified with the primer pair A and D to generate a 954 bp amplicon with an in-frame deletion of the 876 bp region of the *cytR* gene. This fusion product was amplified and subcloned into pGEM-T Easy vector (Promega). The DNA fragments containing the deleted gene were digested with *Xba*1 and *Sac*1 restriction enzymes and ligated into the counter selectable suicide plasmid pCVD442 [22]. To harbour these deleted genes in *V. cholerae*, the resultant chimeric plasmid was transformed into *E. coli* SM10λpir and was conjugally transferred to N16961. The transconjugants were selected in ampicillin-streptomycin double-antibiotic LB agar plates and then grown in sucrose selection media (1% tryptone, 0.5% yeast extract, 10% sucrose and 1.5% agar) to identify the clones where pCVD442 plasmid loss had occurred [24]. Isogenic deletion of the *cytR* gene was confirmed by PCR using external primer pairs A and D, showing a 954 bp amplicon in the isogenic deletion *cytR* mutant and internal primers *cytR* Int FP and *cytR* Int RP amplify the 653 bp region in the WT strain and show no amplification in the mutant strain [25] (Fig. S1) . The *cytR* mutant strain was complemented with the cytR^c plasmid to generate a complemented strain following a previously described procedure [26]. cytR^c was generated by cloning the *cytR* gene in pBAD-TOPO TA expression vector (Invitrogen) along with its signal sequence using the primers *cytR* Comp FP and *cytR* Comp RP (Table S1).

Generation of a *V. cholerae* growth curve

Cultures of wild-type *V. cholerae* CytR$^+$, CytR$^-$ mutant and its complement CytR^C were taken from the log phase and centrifuged, washed in PBS and OD was adjusted to 1×10^9 cells ml^{-1}. An inoculum of 1×10^5 cells ml^{-1} was given in fresh mucin supplemented (1%) M9 minimal medium, as the presence of 1% mucin in medium showed maximum *cytR* expression (Fig. S2). The cultures were grown at 37 °C under constant shaking at 180 r.p.m. for 60 h [11]. The viable cell counts were enumerated by dilution plating of the cultures at different time points (between 0 to 60 h) onto LB agar plates supplemented with streptomycin followed by colony count [27].

RNA isolation and quantitative Reverse Transcriptase – PCR

Bacterial cultures were grown to the mid-logarithmic phase of growth (OD$_{600}$−0.5) in LB medium and minimal-lactate media with or without 1% porcine mucin at 37 °C with constant shaking. Total RNA was extracted using Trizol (Invitrogen) following the manufacturer's protocol. Extracted

RNA was frozen in RNase-free water at −80 °C until use. RNA concentrations were determined using V-660 UV-VIS spectrophotometer (Jasco). DNase treatment was performed using DNA-free kit (Ambion) for the elimination of contaminating genomic DNA. Then, 1 µg of RNA from each sample was subjected to cDNA synthesis using the Reverse Transcription kit (Promega) according to the manufacturer's protocol. The mRNA transcript levels were quantified by quantitative PCR (qPCR) using 2×SYBR green PCR master mix (AB Applied Biosystems) and 0.2 µM of specific forward and reverse primers designed using PrimerQuest from Integrated DNA Technologies (IDT) for each transcript (Table S2). Data analysis was done using a 7500 Real Time PCR detection system (Applied Biosystems, Foster City, CA, USA) with 40 cycles of a two-step cycle followed by a melting curve. The relative expression of the target transcripts was calculated according to Livak's $2^{-\Delta\Delta C_T}$ method [28] using *recA* (VC_0543) as an internal control.

β-hexosaminidase assay

The activity of β-hexosaminidase enzyme was estimated by a previously described procedure [29] with *p*-nitrophenyl-*β*, D-*N*-acetylglucosaminide (PNP-GlcNAc) (Sigma). In brief, *V. cholerae* cells' wild-type CytR$^+$, mutant CytR$^-$, and its complement CytR^C were grown in minimal-lactate media with or without 1% porcine mucin up to the log phase. The bacterial cell density was adjusted to 5×10^8 cells ml^{-1}, they were washed and treated with toluene at a ratio of 10 µl ml^{-1} of culture. After vigorous shaking for 10 s, the mixture was kept at room temperature for 20 mins. Next, 0.1 ml of these treated cultures were mixed 0.1 ml of 1 mM PNP-GlcNAc in 20 mM Tris-HCl (pH 7.5) and incubated at 37 °C for 60 mins. The reaction was stopped with 0.8 ml of 1M Tris base (pH 11). Cell debris was removed by centrifugation and the optical density of the supernatant was analysed at 400 nm. Total hexosaminidase activity was analysed after measuring total protein by Lowry's method and then expressed as *p*-nitrophenol produced per minute per mg of protein. For determining *in vivo* hexosaminidase activity, rabbit ileal loop intestinal fluid was collected after incubation. The samples were then washed and centrifuged to collect the bacterial cells and total hexosaminidase activity was measured as described above [12].

Mucin penetration assay

The assay was performed according to a previously published method [30]. In brief, mucin columns were prepared in 1 ml syringes by adding different concentrations of porcine mucin (1, 1.5 and 2%) (Sigma). Bacteria were grown up to mid-log phase and their concentration was adjusted to 5×10^8 cells ml^{-1} using PBS. 0.1 ml of the culture were loaded on the top of the mucin columns. Columns were then allowed to settle for 1 h at 37 °C under static conditions. Thereafter, 100 µl fractions were collected from the bottom of the columns. Bacterial numbers were measured by serially diluting the samples and plating them onto LB agar and counting the c.f.u.

Motility assay

The surface motility of all *V. cholerae* strains used in this study was done by a previously described procedure [31]. Bacterial strains were grown up to the mid-log phase in LB broth. The culture was resuspended in PBS and OD adjusted to 5×10^8 cells ml^{-1}. In total, 1 µl of this culture was spotted on soft agar plates containing 0.4% porcine mucin (Sigma) in minimal M9 media (BD Difco) and 0.3% bacto agar (BD Difco). And the plates were incubated for 18 h at 37 °C. Bacterial motility was analysed by measuring the diameter of the motility zone on the plate surface.

Cell culture

In this study mucin-secreting human adenocarcinoma cell line HT-29 (National Centre for Cell Sciences, Pune, India) was used. Cells were maintained in Dulbecco's Modified Eagle's Medium (DMEM) (Sigma), supplemented with 10% FBS (PAN Biotech, Germany), 1% non-essential amino acid (Sigma) and 1% penicillin/streptomycin (Sigma) mixture at 37 °C under 5% CO_2 in a humidified incubator [11].

Adhesion assay

Adhesion of *V. cholerae* (WT CytR$^+$, mutant CytR$^-$ and its complement CytR^c) to the human colon adenocarcinoma cell line HT-29 was done according to the previously described method [12]. As mentioned earlier HT-29 cells were split into 12-well cell-culture plates and maintained in DMEM with 10% FBS. Upon reaching 80% confluency, 1.2×10^8 freshly grown mid-log phase bacterial inoculum (washed in PBS, numerated by c.f.u. counting, ratio, 100 bacteria:1 HT-29 cell, m.o.i. 100) was given to 1.2×10^6 cells in DMEM culture medium with 0.5% FBS and without antibiotics. Adhesion assay was conducted by incubating the bacteria/cell at 37 °C for 1 h under conditions 5% CO_2 and 90% relative humidity. Cells were washed thrice with prewarmed PBS pH 7.4 and were detached using 0.1% Triton X-100. Adherent bacteria were counted after serial dilution by plating on LB agar plates supplemented with 100 µg ml^{-1} streptomycin. *In vivo* adhesion of bacterial strains with the rabbit intestinal lumen was also evaluated. Intestinal loop sections recovered 18 h after the rabbit ileal loop experiment was washed in PBS three times and then homogenized and serially diluted in PBS. The adherent bacterial count was determined by plating and counting these bacterial cultures on LB agar supplemented with 100 µg ml^{-1} streptomycin. For fluorescence microscopy, all *V. cholerae* strains (WT CytR$^+$, mutant CytR$^-$, and its complement CytR^c) were transformed with ampicillin-resistant GFP-expressing plasmid, pGFPuv (Clontech, TaKaRa bioscience) by electroporation. Adhesion assay with this GFP expressing *V. cholerae* strain was done on a grease-free, sterile coverslip, washed in PBS, and mounted with VECTASHIELD antifade mounting medium (Vector laboratories) to view under a fluorescence microscope.

Suckling mouse colonization competition assay

The *in vivo* infant mouse colonization assay was performed as described previously [32]. Log-phase culture of the *V.*

cholerae mutant strain (LacZ$^-$) was mixed with each of the wild-type strains (LacZ$^+$), i.e. CytR$^+$, CytR$^-$, and CytR^c at a ratio of 1:1. Then, 2 h prior to giving the inoculum to 4- to 5-day-old suckling Swiss albino mice were separated from their mothers. Each mouse was then orally gavaged with 50 µl of 5×10^8 c.f.u. ml^{-1} of the mixed bacterial culture. Negative control mice were fed with 50 µl PBS. Mice were kept at 26 °C in isolation. Then, 18 h after infection they were sacrificed and intestines were harvested, washed in PBS, mechanically homogenized and diluted serially to a plate on the LB agar supplemented with 100 µg ml^{-1} streptomycin. Competitive index (CI) was calculated by the following equation: - ratio out $_{\text{(mutant/wild-type)}}$ / ratio in $_{\text{(mutant/wild-type)}}$. The CI value of <1 indicates a defect in fitness and that of >1 indicates an increased fitness. Seven mice per group were used in this study.

Ligated rabbit ileal loop assay for fluid accumulation and bacterial recovery

This assay was performed in New Zealand White Rabbits weighing approx. 2.5 kg by a detailed method described previously [33]. In brief, a bacterial inoculum of all three strains was adjusted to 1×10^9 c.f.u. ml^{-1} and 1 ml of these cultures was introduced into the ligated loops of the ileum. The negative control loop was inoculated with PBS. The animal was sacrificed after about 18 h and loops were taken out. The volume of the accumulated fluid and the length of the loops were measured. The extent of the fluid accumulation (FA) was expressed as loop fluid volume (ml)/length (cm) ratio. Using the same model, bacterial colonization, β-hexosaminidase assay, quantitative RT-PCR of different genes from recovered bacteria, estimation of *in vivo* CT, and histopathology were also performed.

GM1 enzyme-linked immunosorbent assay

The ability to secrete CT by *V. cholerae* strains was assayed by GM1 ELISA following the previously described method [34] with minor modifications [35, 36]. CT expression was measured by cell-free culture supernatants from AKI grown *V. cholerae* cultures harvested after 12 h of static incubation at 37 °C as well as from *in vivo* rabbit ileal loop culture. Culture supernatants were added to the wells of MaxiSorp ELISA plates (Nunc) that were coated with GM1 ganglioside (Sigma). Wells were subsequently treated with polyclonal anti-CT antibody (Sigma). In each set of assays, known amounts of purified CT were used in different concentrations to generate a standard curve. The amount of CT secreted by *V. cholerae* strains was done by extrapolating the optical density value of the samples at 492 nm in the standard curve. The OD$_{492}$ average obtained from triplicate wells of each experimental sets were considered to estimate the amount of CT present and expressed as ng of CT ml^{-1}.

Transmission electron microscopy

Negatively stained whole-cell mounts were prepared to visualize bacterial morphology. In brief CytR$^+$, CytR$^-$ strains of *V. cholerae* were grown in LB broth and 5 µl of bacterial suspension was gently placed on a glow-discharged carbon-coated

300 mesh copper grid. After about 1 min, the remaining solution on the grids was wicked away with the help of a filter paper followed by washing with two drops of distilled water. The grid was then stained with 2% (w/v) uranyl acetate and air-dried. The negatively stained cells were visualized with a FEI Tecnai 12 BioTWIN Transmission electron microscope (FEI, Hillsboro, OR, USA) at an operating voltage of 100 kV.

Histological studies

Histological analysis was done by collecting tissue samples from rabbit ileal loop assays. They were fixed in 10% neutral buffered formalin. Further, the samples were embedded in paraffin. Then, 3–4 µm thin sections were cut in a microtomy rotor (Leica, Germany) and were stained with haematoxylin and eosin and examined under a compound light microscope. Photographs were taken under different magnifications with a Carl Zeiss PrimoStar microscope (Oberkochen, Germany), equipped with a digital imaging system.

Statistical analysis

All the experiments were analysed by Student's *t*-test. Each of the experiments was repeated at least three times. Data were represented as mean±SEM. Statistical analysis and data plotting for suckling mice colonization competition assay were done by two-way ANOVA using GraphPad Prism software (Version 5). A '*P*' value of <0.05 was considered as statistically significant.

RESULTS

CytR plays a role in *V. cholerae* mucin utilization

To evaluate the role of CytR in mucin utilization for growth of *V. cholerae*, we first measured the growth rate of all the *V. cholerae* in M9 minimal media in the presence (Fig. 1b)
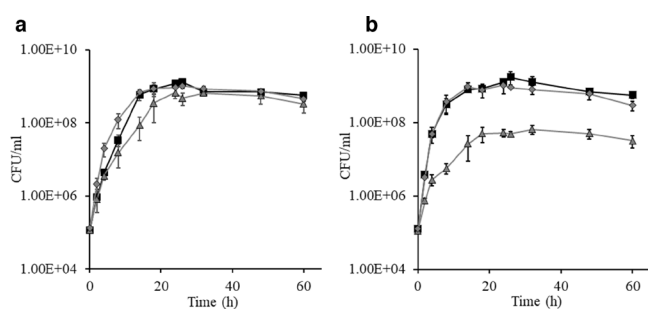

Fig. 1. CytR helps *V. cholerae* to utilize mucin as a sole nutrient source. All *V. cholerae* N16961 strains, CytR⁺ (wild-type), CytR⁻(isogenic CytR mutant) and CytRᶜ (CytR⁻strain complemented with CytR clone) strains were inoculated separately in (a) M9 minimal media with 0.5% sodium lactate as the sole carbon source and (b) M9 minimal media supplemented with 1% (w/v) porcine mucin only. The viable bacterial counts in c.f.u. ml⁻¹ were detected by the plate count method taking culture samples from different time points and represented graphically. The CytR⁻ mutant showed a reduction in growth rate in the presence of mucin. Each experiment was repeated three times (*n*=3) and the data were expressed as mean±SEM.

or absence of mucin (Fig. 1a). The CytR⁻ mutant strain grew poorly in mucin-supplemented M9 minimal media compared to the wild-type CytR⁺ strain. At 60 h, the total viable count of wild-type *V. cholerae* CytR⁺ strain in mucin-supplemented media was $5.57×10^8$ c.f.u. ml⁻¹, whereas it was $3.18×10^7$ c.f.u. ml⁻¹ in the CytR⁻ mutant strain, showing a 17.5-fold difference in growth. The complemented CytRᶜ strain showed similar growth as the wild-type CytR⁺ strain in mucin-supplemented media. In contrast, all the strains showed almost similar growth patterns in the presence of sodium-lactate-supplemented M9 minimal media in the absence of mucin (Fig. 1a), which indicates equal fitness of all the strains. This result indicates *V. cholerae* could utilize mucin as a sole nutrient source and CytR contributes to utilizing it.

CytR is important for motility and mucin penetration

Next, we investigated the surface motility of different *V. cholerae* strains on soft agar mucin plates. We found that CytR⁻ strain showed reduced motility with a zone of 0.36±0.03 cm, whereas CytR⁺ strain showed a motility zone of 3.8±0.14 cm (Fig. 2a, b). Therefore, the motility of CytR⁻ strain was reduced to 10.5-fold compared to the CytR⁺ strain. The complemented CytRᶜ strain showed a similar motility zone of 3.4±0.11 cm when compared to the wild type strain.

Further, the *in vitro* mucin-layer penetration experiment supports our above observation. Here we also observed that motility of CytR⁻ *V. cholerae* strain decreased severely. Out of the total $5×10^8$ c.f.u. ml⁻¹ bacteria loaded on top of the mucin column, $4.89×10^7$ c.f.u. ml⁻¹, wild-type CytR⁺ bacteria were able to penetrate through the 1% mucin column after 1 h incubation (Fig. 2c). However, only $1.3×10^6$ c.f.u. ml⁻¹ mutant CytR⁻ bacteria were able to penetrate the 1% mucin column. This clearly showed that the CytR⁻ strain was 38-fold less competent in motility than the wild-type bacteria, whereas the CytRᶜ strain showed almost similar mucin-penetration ability compared to the CytR⁺ strain.

V. cholerae CytR plays a significant role in adhesion to epithelial cells

Adhesion of *V. cholerae* to the intestinal epithelial cells is a major step in its pathogenesis. Therefore, we have studied the effect of CytR in the adherence capability of *V. cholerae* to HT-29 intestinal epithelial cell line in tissue culture conditions. Adherent *V. cholerae* wild-type CytR⁺ strain count after 1 h incubation with the HT-29 cell was $2.7×10^8$ c.f.u. ml⁻¹, whereas for the CytR⁻ strain it was $2.6×10^7$ c.f.u. ml⁻¹ (Fig. 3a). Therefore, the CytR⁻ *V. cholerae* strain was 10.5-fold less adherent with HT-29 cells than the wild-type. CytRᶜ complemented strain showed similar adhering ability when compared to the wild-type CytR⁺. GFP-labelled CytR⁻ mutant bacteria were less visible in adhered form when compared to the wild-type CytR⁺ strain under fluorescence microscopy (Fig. 3b), whereas the complemented CytRᶜ strain adhered similarly like the wild-type *V. cholerae*.
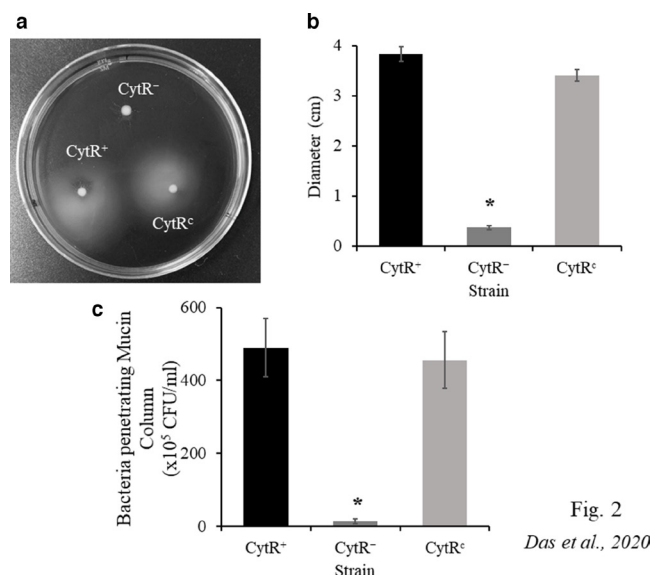
Fig. 2. Surface motility and mucin penetration are fostered by CytR in *V. cholerae*. CytR+ (wild-type), CytR− (isogenic CytR mutant) and CytRᶜ (CytR−strain complemented with CytR clone) were grown separately in LB broth till mid-log phase. Then, 1 µl of 5×10⁸ c.f.u. ml⁻¹ different bacterial samples were spotted on 0.3% agar plates containing 0.4% mucin. Plates were incubated at 37 °C for 18 h. (a) Plate showing the motility zone of different bacteria. (b) The diameter of bacterial surface motility zones is graphically represented as mean±SEM by measuring the zone of three independent biological replicates. (c) The 100 µl of 5×10⁸ c.f.u. ml⁻¹ bacterial culture CytR+ (wild-type), CytR− (isogenic CytR mutant) and CytRᶜ (CytR−strain complemented with CytR clone) were loaded on top of the 1 ml mucin column of containing 1% porcine mucin. Bacterial samples of 100 µl were collected from the bottom of the column after 1 h incubation at 37 °C. The samples were serially diluted and plated on LB agar supplemented with proper antibiotics and the bacterial numbers were counted and graphically represented. Each of the experiments was repeated three times (*n*=3) and the data were expressed as mean±SEM. *, *P* <0.05.
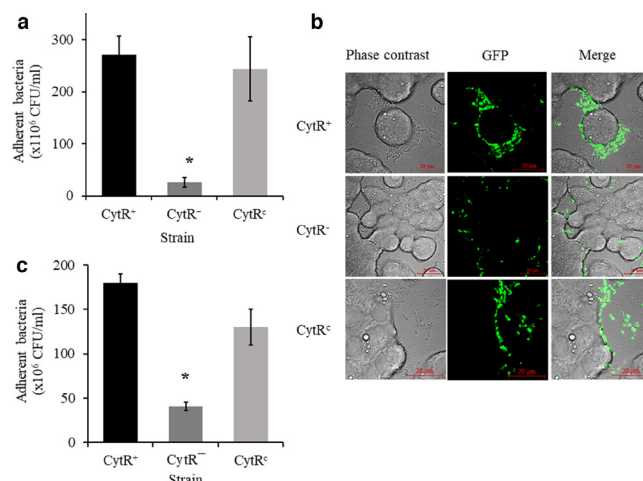

Fig. 3. CytR plays an important role for *V. cholerae* in adhesion with the epithelial cell. All three experimental strains were grown to mid-log phase and optical density was adjusted to 1. The HT-29 cell line was grown in a 12-well cell-culture plate to 80% confluency. The cell line was then infected at 100 m.o.i. After incubation at humidified 37 °C incubator for 1 h, the cell-culture plate was washed with PBS to remove unbound bacteria and bound bacteria were collected and enumerated by plating on streptomycin-supplemented LB agar. (a) Graphical representation of different strain of *V. cholerae* bound to HT-29 under cell-culture conditions. (b) Fluorescent microscopy images of bound bacteria with HT-29 cell. (c) Bacterial adhesion was assayed from the samples recovered from *in vivo* rabbit ileal loop tissue samples, where the bound bacterial count was determined after washing and homogenizing the tissue samples. Bound bacteria were collected, plated and the number of bacteria was enumerated by the plate count method. The result is shown as the mean±SEM of three biological replicates (*n*=3). *, *P* <0.05.

We further tested the adherence in rabbit ileal loop conditions. Our result suggested that 1.8×10⁸ c.f.u. ml⁻¹ wild-type CytR+ *V. cholerae* adhered to the intestinal lumen (Fig. 3c). In contrast, only 4.0×10⁷ c.f.u. ml⁻¹ CytR− bacteria were adherent, showing ~ 4.5-fold decrease in adherence efficiency of the CytR− mutant compared to the wild-type bacteria. The CytRᶜ-complemented strain adhered similarly to the wild-type CytR+. These results indicated clearly that CytR is important for adhesion of *V. cholerae* in the intestinal environment.

CytR mutant *V. cholerae* displays colonization defect in suckling mice

To further examine the role of CytR in colonization, we used the 5–6-day-old suckling mice for the intestinal colonization ability of the mutant CytR− strain along with complemented CytRᶜ and the wild-type *V. cholerae* N16961 (CytR+LacZ−). During bacterial infection, the input ratio of mutant (CytR−) to wild-type N16961 (CytR+LacZ−) was 1:1. The CytR− strain showed an output ratio (CI) (CytR− LacZ+/ CytR+ LacZ−) of 0.034±0.01 at 18 h post-infection (Fig. 4). Whereas, CI

between CytR+ LacZ−/ CytR+ LacZ+ was 0.84±0.06, indicating no or negligibly low fitness defect of the LacZ− mutant strain over wild-type LacZ+ *V. cholerae*. This indicates that deletion in CytR in *V. cholerae* significantly decreased its colonization fitness to 24.5-fold. In contrast, the complemented CytRᶜ strain showed CI, CytRᶜ LacZ+/ CytR+ LacZ− value of 0.71±0.07 with almost no competitive disadvantage.

V. cholerae shows less fluid accumulation in the absence of CytR

We studied fluid accumulation by *V. cholerae* in the rabbit ligated ileal loop model as an indicator of pathogenesis. In this experiment, we measured the amount of fluid secreted per unit area (FA ratio) in each loop 18 h post-infection. Infection with CytR− strain showed threefold less fluid accumulation compared to the wild-type CytR+ strain (Fig. 5). Infection with CytRᶜ complemented strain showed fluid accumulation similar to CytR+.

CytR plays a role in virulence-gene expression and cholera-toxin production

To understand the reason behind the decreased fluid accumulation, we analysed the expression levels of different virulence
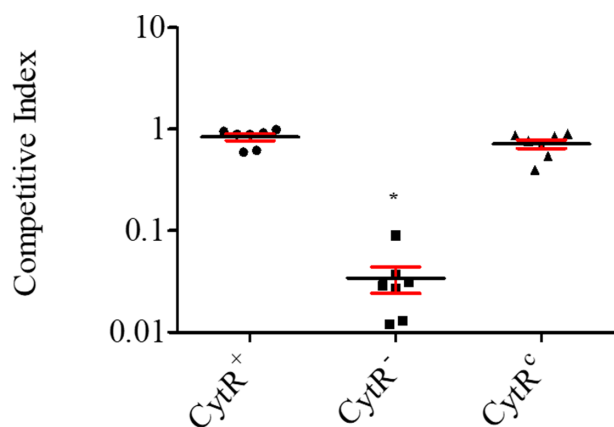
Fig. 4. CytR plays a role *in vivo* colonization of *V. cholerae*. Competitive indices of the CytR deletion mutant show less colonization fitness compared to wild-type *V. cholerae*. Comparative colonization study of three experimental strains was done in 5–6-day-old suckling mice. Then, 50 µl of 5×10^8 c.f.u. ml^−1 bacteria of the *V. cholerae* (LacZ^−) strain were mixed at a ratio of 1:1 with each of the strains, i.e. CytR^+ (LacZ^+), CytR^− (LacZ^+) and CytR^c (LacZ^+) and orally gavaged to each mouse. After 18 h incubation, the mouse intestine was harvested, washed, homogenized, serially diluted and plated on LB agar. The CI was calculated and plotted to represent in the graph. CI=ratio out_(mutant/wild-type)/ratio in_(mutant/wild-type). Each data point represents an individual animal infected with *V. cholerae*. Seven animals were sacrificed in each set. Horizontal bars indicate the mean±SEM. CI <1 indicates fitness defect; CI >1 indicates increased fitness, whereas CI≈1 indicates no fitness defect. *, *P* <0.05.

Fig. 6. Virulence-gene expression and CT production are affected by CytR mutation. (a) Relative expression of virulence genes from rabbit ileal loop samples CytR^+ (wild-type), CytR^− (isogenic CytR mutant) and CytR^c (CytR^−strain complemented with CytR clone) was measured by quantitative RT-PCR. Data were represented by the comparative ΔΔC_T method, using *recA* as an internal control. (b) *In vivo* CT production was also measured by ELISA from the accumulated fluid samples of ligated rabbit ileal loops. The result is shown as the mean±SEM of three biological replicates (*n*=3). *, *P* <0.05, N.S., non-significant.

genes in the post-infected wild-type CytR^+ and CytR^− mutant strain by qPCR. We found the expression of *toxT*, *tcpA* and *ctxB* were significantly reduced by 5-fold, 3.5-fold and 4.5-fold, respectively, in the CytR^− mutant with respect to the wild-type *V. cholerae*. The deletion of CytR did not affect the expression of *tcpP*, but the expression of *toxR* was reduced by 3.6-fold (Fig. 6a). We also found reduced expression of
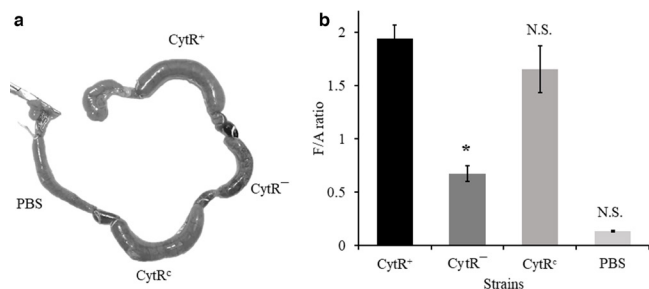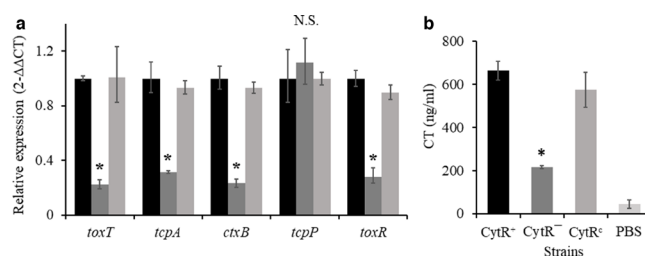
toxT, *tcpA* and *ctxB in vitro* AKI grown culture media for the CytR^− mutant strain (Fig. S5a).

We also measured CT production, which is primarily responsible for fluid accumulation in the rabbit intestine. We found that the rabbit ileal loop samples infected with the CytR^− mutant contained threefold less CT (215 ng ml^−1) than the fluid from the wild-type CytR^+-infected loop (665 ng ml^−1) (Fig. 6b). Fluid from the CytR^c-infected loop showed similar CT (574 ng ml^−1) production compared to the wild-type. Reduced CT production was also seen in the AKI media culture soup in the CytR^− mutant strain (Fig. S5b).

CytR mutant causes less damage to the rabbit intestine compared to the infection with wild-type *V. cholerae*

Intestinal fluid-accumulation assay results encouraged us to investigate the microscopic changes of the rabbit intestinal tissues. Histological staining of rabbit ileum revealed that the wild-type CytR^+ *V. cholerae* strain caused a gross structural alteration with distorted villus epithelium, extensive damage to the mucosa, sub-mucosa and lamina propria (Fig. 7). Haemorrhage in muscularis mucosa was also seen. In contrast, the intestinal loop section infected with the CytR^− strain displayed almost normal villi structure, although dilated and extended lamina propria with scattered haemorrhagic changes were observed. Mucosa and sub-mucosal layers did not show much noticeable damage. Tissue section from the intestinal loop infected with complemented CytR^c strain showed an effect on villi and mucosal structure similar to the tissues infected wild-type *V. cholerae*. PBS-treated ileal loop tissue showed normal crypts and villi structure and did not show any alteration to the gut mucosae.

CytR controls flagella synthesis

To further investigate the reason behind reduced motility of the CytR^− strain in mucin media we have done negative-stain transmission electron microscopy to analyse the morphology

Fig. 5. CytR plays a role in fluid accumulation in the rabbit intestine. All *V. cholerae* experimental strains were grown separately in LB broth till mid-log phase and OD was adjusted to 1.0 and 1 ml of 10^9 c.f.u. ml^−1 were inoculated in each of the ligated loops of rabbit intestine. (a) Retrieved rabbit intestinal portion showing infected loop 18 h post-infection. Each loop was separated by an uninfected interloop region. The negative control loop was inoculated with PBS. (b) Fluid accumulation ratio in the rabbit intestine of three different experiments was measured and represented graphically as mean±SEM. *, *P* <0.05; N.S., non-significant.
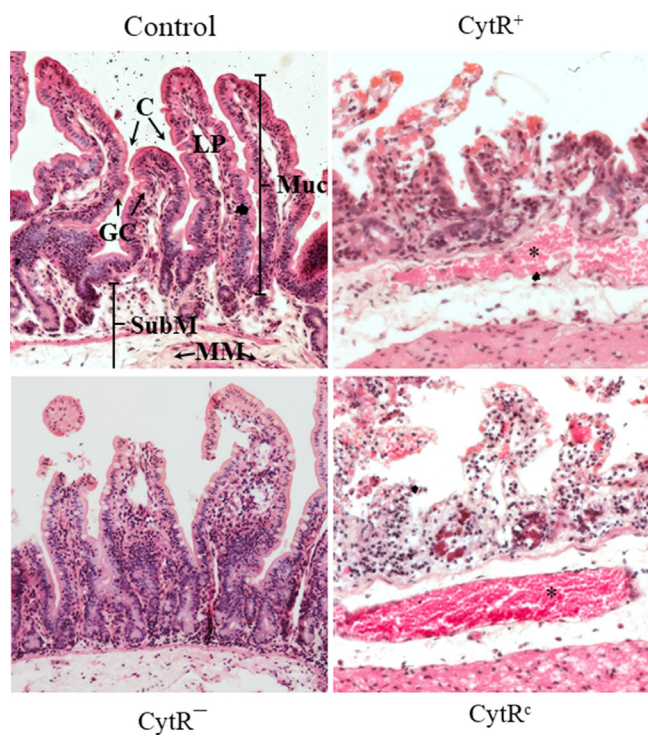
Fig. 7. Histological examination of the rabbit intestine showed the CytR mutant infected loop causes less damage to the intestinal lining. All *V. cholerae* strains CytR+ (wild-type), CytR− (isogenic CytR mutant) and CytR^c (CytR−strain complemented with CytR clone) were grown separately in LB broth till mid-log phase and OD was adjusted to 1.0 and 1 ml of 10^9 c.f.u. ml^{-1} were inoculated in each of the ligated loops of rabbit intestine. Then, 18 h post-infection tissue sections from each loop were collected, processed and stained with haematoxylin and eosin. Representative images were taken under a 20×objective lens. The PBS-treated ileal loop was considered as control. C, Crypts; GC, Goblet Cells; LP, Lamina Propria; Muc, Mucosa; MM, Muscularis Mucosae; SubM, Submucosa, *, indicating the site of haemorrhage.

Fig. 8. *V. cholerae* flagella synthesis is CytR dependent. (a) Electron micrographs of negatively stained *V. cholerae* strain CytR+ (wild-type) (left) and CytR− (isogenic CytR mutant) (right) in LB broth till mid-log phase. (b) Mid-log-phase bacterial cultures were subjected to RNA isolation using the TriZol method and mRNA transcript levels were analysed by quantitative RT PCR and graphically represented, using *recA* as an internal control gene. Each of the experiments was repeated three times (*n*=3) and the data were expressed as mean±SEM. *, *P* <0.05; N.S., non-significant.

flgK (associated with hook-filament junction), *flgG* (distal rod), *flgB* (proximal rod) showed meagre downregulation by 2.2-fold, 5-fold, 4-fold and 9-fold, respectively. However, the mutant strain class IV gene *flgM* (σ^{28}-dependent anti-sigma factor) did not show any change in RNA level in the CytR mutant compared to the wild-type *V. cholerae*.

DISCUSSION

CytR is involved in multiple regulations in *V. cholerae* and varying mechanisms appear to exist in each case [13]. The pathogenesis of *V. cholerae* inside the human host is regulated by a complex signalling cascade, which includes several regulatory factors. CytR, also being a regulator, its function in pathogenesis is still not known. Here, we for the first time aimed to understand the role of this multifunctional transcription factor in *V. cholerae* pathogenesis.

Our experimental results suggest that the CytR− *V. cholerae* showed inefficient growth in the presence of mucin-supplemented M9 minimal media. It is known that CytR upregulates four chitinase genes including *chiA1* and *chiA2* (13,17) in the presence of chitin. We showed that the CytR mutant *V. cholerae* produced a significantly lower amount of RNA for both extracellular chitinase genes *chiA1* and *chiA2* in mucin-supplemented media (Fig. S3), which might result in decreased synthesis of the chitinase enzymes. Low levels of these chitinases result in an inefficient breakdown of complexly polymerized O-linked glycans of mucin. Therefore, production of GlcNAc as a nutrient is low and the growth of CytR− strain in mucin-supplemented media is

of the wild-type CytR+ strain of *V. cholerae* and the isogenic mutant CytR− strain. The wild-type CytR+ strain showed normal flagella. However, the CytR-ablated *V. cholerae* strain appeared to be aflagellate (Fig. 8a).

The quantitative RT-PCR analysis of flagellar-synthesis genes in CytR− strain indicated decreased expression of *flrB* (a histidine kinase) and *flrC* (the response regulator of FlrB) by 2.3-fold and 3.5-fold, respectively, when compared to the wild-type *V. cholerae* (Fig. 8b). RNA expression levels of *flrA* (the master regulator) and *rpoN* (the alternate sigma factor σ^{54}) remained unchanged in the mutant strain. Transcription of other class II genes like *fliF* (forms structural unit of MS ring) and *fliA* (alternate sigma factor σ^{28}) showed no change in CytR− strain when compared to the wild-type *V. cholerae*. We also analysed the RNA expression of some class III genes, which showed reduced expression in the mutant strain. Three genes *motY* (forms T ring), *flaA* (main flagellin subunit) and *flgP* (associated with H ring) showed greater downregulation of RNA expression by 55-fold, 24-fold and 19-fold, respectively. Four other class III genes *flgT* (H ring component),
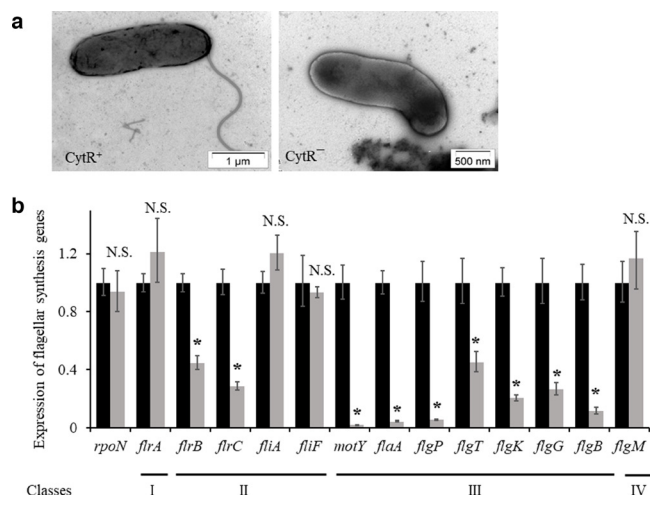
compromised. The side chains of mucin are rich in GlcNAc residues that can act as a source of carbon and nitrogen [37]. *V. cholerae* can utilize a diverse pool of carbon source depending upon the environment it thrives in, including intestinal mucin. It has been previously reported by us that the extracellular chitinase ChiA2 cleaves the oligosaccharide moieties of mucin-releasing GlcNAc [11]. The GlcNAc residues are then transported and assimilated by *V. cholerae* as a nutrient [5]. It has also been reported that few pathogens can utilize GlcNAc efficiently as a nutrient source [38]. From the nutritional point of view, gut mucus is used as a source of carbon and energy by a subset of intestinal microbiota. *C. jejuni* [39], enterohemorrhagic *E. coli* (EHEC) [40], *C. difficile*, *Salmonella enterica* serotype Typhimurium [41] are among few enteric pathogens, which efficiently utilizes mucus-derived monosaccharides.

As stated earlier, mucin utilization by *V. cholerae* proceeds only after the sensor kinase ChiS senses the presence of GlcNAc residues in the environment and hence switching on the downstream mucin utilization cascade components including periplasmic *β*-N-acetylhexosaminidases [5]. Our results suggest for the first time that CytR positively controls hexosaminidase activity in *V. cholerae* in the presence of mucin (Fig. S4) *in vitro* as well as in the intestinal environment (Fig. S6). The expression of *chiS* RNA is also CytR dependent as revealed by the qRT-PCR data (Fig. S4). Thus, it indicates that CytR positively regulates both *chiS* expression and its activity. Therefore, we speculate that CytR helps *V. cholerae* to breakdown the thick mucus layer with the help of chitinases in a ChiS- dependent manner and release primarily the GlcNAc residues from the mucus component. Internalization and transport of GlcNAc from the intestinal environment is also ChiS dependent [5]. We believe that in the CytR⁻ strain, GlcNAc is less transported, and to produce the clinical symptoms of cholera *V. cholerae* needs to transport sufficient titre of GlcNAc from the intestine [8, 42, 43]. However, the mechanism of how CytR controls the expression and activity of ChiS needs further study.

To successfully carry out mucin-layer penetration [24] and to colonize the intestinal epithelial cells, flagella-driven motility plays an important role in *V. cholerae*. A previous study has shown that the movement of *V. cholerae* through the viscous mucus layer is promoted by mucin [24]. Additionally, motility is further triggered by the presence and internal catabolism of *N*-acetylneuraminic acid and *N*-acetylglucosamine (GlcNAc) [8]. Our study here indicates that under experimental conditions, motility is positively regulated by CytR. To pass through the mucus layer, *V. cholerae* simultaneously needs to degrade and loosen the thick mesh of mucin side chains with help of chitinases and proteases along with the generation of propulsion through rotation of whip-like, monotrichous polar flagella to move forward. In *V. cholerae*, the activity of chitinase ChiA2 in mucin deglycosylation does not require any proteolytic help [11]. So, the inability to penetrate mucin by the CytR⁻ strain can be explained by reduced expression of chitinases ChiA1 and ChiA2. Moreover, electron microscopic observation revealed that CytR⁻ *V. cholerae* strain completely

lacks the presence of a polar flagellum, which further explains why CytR⁻ *V. cholerae* is less motile than the wild-type.

More than 50 genes are involved in the synthesis and regulation of flagella in *V. cholerae* [44]. Protein synthesis and structural component assembly of the major flagellar units happened hierarchically. The expression of flagella-synthesis genes in *V. cholerae* is categorized into a four-tier transcriptional hierarchy [45]. The σ54-dependent transcriptional activator FlrA is the only class I gene in this hierarchy [46, 47]. FlrA is the master regulator of the *V. cholerae* flagellar transcription hierarchy because it is important for the expression of the rest of the flagellar genes. FlrA, along with the RpoN (sigma factor σ54), activates class II flagellar genes. Class II flagellar protein histidine kinase FlrB and its response regulator FlrC regulates the synthesis of class III flagellar genes, which encodes the different structural component of flagella including the major flagellin subunit (FlaA), proximal and distal transmembrane helical rod (FlgB/G), H-ring protein (FlgT), H-ring-associated protein (FlgP), flagellar-hook-associated protein (FlgK) and T-ring motor protein (MotY).

CytR⁻ strain showed reduced expression of class II flagellar genes *flrB*, *flrC*, and several class III genes tested. This suggests that CytR is important for expression of *flrB* and *flrC*, except when no other structural components of flagella in *V. cholerae* are synthesized. Previous study has also shown that the *flrC* mutant is defective in flagella-synthesis thereby reducing motility as well as intestinal colonization of *V. cholerae* [48]. Although we have observed decreased expression of *flrBC* and class III flagellar genes in CytR⁻ strain, further study is still needed to complete the understanding of this process.

Our results also suggest that *V. cholerae* CytR⁻ strain showed reduced adhering capability to the intestinal cells than the wild-type strain depicting colonization defect. Colonization of *V. cholerae* in the small intestine requires the stringent activity of TcpA (Toxin Coregulated Pilus A) that also promotes adherence to intestinal cells [49]. In support of this, we found that CytR⁻ *V. cholerae* express less *tcpA* during colonization. Bacterial attachment to the protective mucus layer can also be facilitated by flagellar motility in cooperation with N-acetylglucosamine binding protein A (GbpA) [50]. However, expression of GbpA was not affected during colonization in CytR⁻ strain (Fig. S7). The absence of flagella in CytR⁻ *V. cholerae* also supports the reason behind colonization defect of the mutant strain. Taken together, CytR of *V. cholerae* positively controls the mucin-layer penetration as well as colonization to the intestinal epithelium.

Upon reaching the brush border lining of the intestinal epithelium and following successful colonization, *V. cholerae* expresses CT and causes efflux of chloride ions (Cl⁻) from the cell, that causes osmotic imbalance and ultimately leads to the loss of fluid into the intestinal lumen, which serves as one of the major aspects of virulence of *V. cholerae* [1, 51]. To examine the role of CytR in the pathogenesis, we studied the intestinal fluid-accumulation assay in the adult rabbit model. Results showed that CytR⁻ strain showed reduced fluid accumulation than the wild-type strain, which is due

to the reduced CT production. It is well established that in response to intestinal stimuli, most of the virulence factors in *V. cholerae,* e.g. *ctx* and *tcp* are regulated by ToxT-dependent pathway [51, 52]. Consistent with this, we found reduced expression of *toxT*, *ctxB* and *tcpA* in CytR⁻ strain. This might indicate that ToxT virulence regulatory pathway gets affected in the CytR⁻ strain. Further, *toxR/S* and *tcpP/H* act in conjunction to regulate the expression of *toxT* in *V. cholerae* [51]. Expression of *toxR* is downregulated in CytR⁻ strain, suggesting that CytR may regulate the master virulence regulator *toxT* in *toxR*-dependent way by a mechanism presently unknown. However, the expression of *tcpP* remained unaffected in the CytR⁻ strain. In the wild-type *V. cholerae*, expression of TcpP is regulated by AphA/B. Therefore, we speculate that the expression of *aphA/B* remained unaltered in the CytR⁻ strain.

Additionally, CytR⁻ strain is unable to utilize mucin in the intestine, which decreases GlcNAc residues inside *V. cholerae,* which might activate cyclic AMP (cAMP) receptor protein (CRP) [53], which negatively regulates the ToxR virulence regulon via cAMP-CRP pathway [54]. However, further experiments are needed to establish a link between CytR and the virulence cascade. Furthermore, CT delivery by *V. cholerae* to the enterocytes requires successful colonization in the small intestine [55, 56]. The histological study supports the evidence that less damage occurs to the intestinal epithelium when infected with the CytR⁻ strain. A lower amount of CT is produced by the CytR⁻ strain in the ileal loop, which results in less osmotic imbalance and less damage in the structure of crypts and villi compared to the damage caused by the wild-type strain during infection.

Taken together, our data indicate that *V. cholerae* CytR positively controls flagellar motility, adhesion and virulence in all conditions tested. In several studies, motility has been linked to the adhesion in different Vibrios [57–61]. In all the cases non-motile, non-flagellate mutants are defective to adhere to the host. Relationship between the motility and virulence has also been explained. In *Erwinia carotovora*, the causative agent of soft-rot disease in plants, it was observed that the CytR homologue positively controls flagella synthesis and virulence-gene production and plays an important role in pathogenicity [62]. In our case also similar observations were made. To summarize the role of *V. cholerae* CytR during pathogenesis, it is important for the activity and expression of sensor histidine kinase ChiS and its downstream chitinases like ChiA1 and ChiA2. As a consequence, the CytR⁻ strain showed reduced mucin degradation and nutrient acquisition. CytR is also important for the expression of class II flagellar regulatory genes *flrB* and *flrC*. Deletion of CytR resulted in aflagellation of the bacteria. This results in reduced motility and penetration through the mucus layer by the CytR⁻ strain. The expression of virulence cascade gene *toxR* is also affected by CytR mutation, which results in lower expression of master virulence regulator *toxT*. ToxT, which in turn regulates all virulence attributes including expression of toxin coregulated pilus A, *tcpA* and *ctxAB* during pathogenesis. In the CytR⁻ strain reduced adhesion to the epithelial cell is correlated

with the reduced expression of *tcpA* and less CT production resulted in reduced fluid accumulation. Besides, reduced nutrient uptake (in the form of GlcNAc), may directly or indirectly by some unknown mechanisms involving the cAMP-CRP pathway results in reduced pathogenesis. So multiple regulatory pathways may exist and CytR may directly or indirectly be involved in this regulation. Future research is needed to understand the complete regulation of virulence involving CytR in the host intestine.

Conflicts of interest

The authors declare that there are no conflicts of interest.

References

1. Kaper JB, Morris JG, Levine MM. Cholera. *Clin Microbiol Rev* 1995;8:48–86.

2. Morris JG. Cholera—Modern pandemic disease of ancient lineage. *Emerg Infect Dis* 2011;17:2099–2104.

3. Mutreja A, Kim DW, Thomson NR, Connor TR, Lee JH *et al*. Evidence for several waves of global transmission in the seventh cholera pandemic. *Nature* 2011;477:462–465

4. Huq A, Small EB, West PA, Huq MI, Rahman R *et al*. Ecological relationships between Vibrio cholerae and planktonic crustacean copepods. *Appl Environ Microbiol* 1983;45:275–283.

5. Meibom KL, Li XB, Nielsen AT, Wu CY, Roseman S *et al*. The Vibrio cholerae chitin utilization program. *Proc Natl Acad Sci U S A* 2004;101:2524–2529.

6. Orikoshi H, Nakayama S, Miyamoto K, Hanato C, Yasuda M *et al*. Roles of four chitinases (chia, ChiB, chiC, and ChiD) in the chitin degradation system of marine bacterium Alteromonas sp. strain O-7. *Appl Environ Microbiol* 2005;71:1811–1815.

7. Harel J, Fairbrother J, Forget C, Desautels C, Moore J. Virulence factors associated with F165-positive Escherichia coli strains isolated from piglets and calves. *Vet Microbiol* 1993;38:139–155.

8. Reddi G, Pruss K, Cottingham KL, Taylor RK, Almagro-Moreno S. Catabolism of mucus components influences motility of *Vibrio cholerae* in the presence of environmental reservoirs. *PLoS One* 2018;13:1–16.

9. Tran HT, Barnich N, Mizoguchi E. Potential role of chitinases and chitin-binding proteins in host-microbial interactions during the development of intestinal inflammation. *Histol Histopathol* 2011;26:1453–1464.

10. Frederiksen RF, Paspaliari DK, Larsen T, Storgaard BG, Larsen MH *et al*. Bacterial chitinases and chitin-binding proteins as virulence factors. *Microbiology* 2013;159:833–847.

11. Mondal M, Nag D, Koley H, Saha DR, Chatterjee NS. The Vibrio cholerae extracellular chitinase ChiA2 is important for survival and pathogenesis in the host intestine. *PLoS One* 2014;9:e103119.

12. Chourashi R, Mondal M, Sinha R, Debnath A, Das S *et al*. Role of a sensor histidine kinase ChiS of Vibrio cholerae in pathogenesis. *Int J Med Microbiol* 2016;306:657–665.

13. Watve SS, Thomas J, Hammer BK. CytR is a global positive regulator of competence, type VI secretion, and chitinases in Vibrio cholerae. *PLoS One* 2015;10:e0138834.

14. Price MN, Dehal PS, Arkin AP. Orthologous transcription factors in bacteria have different functions and regulate different genes. *PLoS Comput Biol* 2007;3:e175–50.

15. Sernova NV, Gelfand MS. Comparative genomics of CytR, an unusual member of the lacI family of transcription factors. *PLoS One* 2012;7:e44194–16.

16. Hammer-jespersen K, Nygaard P. Multiple regulation of nucleoside catabolizing enzymes in Escherichia coli 1976;55:49–55.

17. Antonova ES, Bernardy EE, Hammer BK. Natural competence in *Vibrio cholerae* is controlled by a nucleoside scavenging response that requires CytR-dependent anti-activation. *Mol Microbiol* 2012;86:1215–1231.

18. Valentin-Hansen P, Søgaard-Andersen L, Pedersen H. A flexible partnership: The CytR anti-activator and the cAMP-CRF activator protein, comrades in transcription control. *Mol Microbiol* 1996;20:461–466.

19. Silva AJ, Benitez JA. Vibrio cholerae biofilms and cholera pathogenesis. *PLoS Negl Trop Dis* 2016;10:e0004330–25.

20. Conner JG, Teschler JK, Jones CJ, Yildiz FH. VMBF-0015-2015_ Vibrio review. 2016:1–32.

21. Nelson EJ, Harris JB, Glenn Morris J, Calderwood SB, Camilli A. Cholera transmission: the host, pathogen and bacteriophage dynamic. *Nat Rev Microbiol* 2009;7:693–702.

22. Philippe N, Alcaraz JP, Coursange E, Geiselmann J, Schneider D. Improvement of pCVD442, a suicide plasmid for gene allele exchange in bacteria. *Plasmid* 2004;51:246–255.

23. Skorupski K, Taylor RK. Positive selection vectors for allelic exchange. *Gene* 1996;169:47–52.

24. Liu Z, Wang Y, Liu S, Sheng Y, Rueggeberg KG *et al*. *Vibrio cholerae* represses polysaccharide synthesis to promote motility in mucosa. *Infect Immun* 2015;83:1114–1121.

25. Herrera CM, Crofts AA, Henderson JC, Pingali SC, Davies BW *et al*. Virulence through endotoxin modification 2014;5:1–13.

26. Bansil R, Turner BS. Mucin structure, aggregation, physiological functions and biomedical applications. *Curr Opin Colloid Interface Sci* 2006;11:164–170.

27. Vercruysse M, Köhrer C, Davies BW, Arnold MFF, Mekalanos JJ *et al*. The highly conserved bacterial RNase YbeY is essential in *Vibrio cholerae*, playing a critical role in virulence, stress regulation, and RNA processing. *PLoS Pathog* 2014;10:e1004175.

28. Livak KJ, Schmittgen TD. Analysis of relative gene expression data using real-time quantitative PCR and the 2−ΔΔCT method. *Methods* 2001;25:402–408.

29. Li X, Roseman S. The chitinolytic cascade in vibrios is regulated by chitin oligosaccharides and a two-component chitin catabolic sensor/kinase. *Proc Natl Acad Sci U S A* 2004;101:627–631.

30. Miyashiro T, Hsiao A, Liu Z, Tsou A, Zhu J *et al*. Mucosal penetration primes *Vibrio cholerae* for host colonization by repressing quorum sensing. *Proc Natl Acad Sci* 2008;105:9769–9774.

31. Yeung ATY, Parayno A, Hancock REW. Mucin promotes rapid surface motility in 2012;3:1–12.

32. Zheng J, Shin OS, Cameron DE, Mekalanos JJ. Quorum sensing and a global regulator TsrA control expression of type VI secretion and virulence in *Vibrio cholerae*. *Proc Natl Acad Sci U S A* 2010;107:21128–21133.

33. Koley H, Mitra R, Basu A, Mukhopadhyay AK, Saha PK *et al*. Response of wild-type mutants of *Vibrio cholerae* O1 possessing different combinations of virulence genes in the ligated rabbit ileal loop and in Ussing chambers: evidence for the presence of additional secretogen. *J Med Microbiol* 1999;48:51–57.

34. Holmgren J. Comparison of the tissue receptors for *Vibrio cholerae* and *Escherichia coli* enterotoxins by means of gangliosides and natural cholera toxoid. *Infect Immun* 1973;8:851–859.

35. De K, Ramamurthy T, Faruque SM, Yamasaki S, Takeda Y *et al*. Molecular characterisation of rough strains of *Vibrio cholerae* isolated from diarrhoeal cases in India and their comparison to smooth strains. *FEMS Microbiol Lett* 2004;232:23–30.

36. Patra T, Koley H, Ramamurthy T, Ghose AC, Nandy RK. The Entner-Doudoroff pathway is obligatory for gluconate utilization and contributes to the pathogenicity of *Vibrio cholerae*. *J Bacteriol* 2012;194:3377–3385.

37. Bjork S, Breimer ME, Hansson GC, Karlsson K, Leffler H. Structures of blood group glycosphingolipids of human small intestine. *J Biol Chem* 1987;262:6758–6765.

38. Chen H, Chang CC, Mau WJ, Yen LS. Evaluation of N-acetylchitooligosaccharides as the main carbon sources for the growth of intestinal bacteria. *FEMS Microbiol Lett* 2002;209:51–54.

39. Alemka A, Corcionivoschi N, Bourke B. Defense and adaptation: the complex inter-relationship between Campylobacter jejuni and mucus. *Front Cell Infect Microbiol* 2012;2:15.

40. Fabich AJ, Jones SA, Chowdhury FZ, Cernosek A, Anderson A *et al*. Comparison of carbon nutrition for pathogenic and commensal Escherichia coli strains in the mouse intestine. *Infect Immun* 2008;76:1143–1152.

41. KM N, Ferreyra JA, Higginbottom SK, Lynch JB, Kashyap PC *et al*. Microbiota-liberated host sugars facilitate post-antibiotic expansion of enteric pathogens. *Nature* 2013;502:96–99

42. Ghosh S, Rao KH, Sengupta M, Bhattacharya SK, Datta A. Two gene clusters co-ordinate for a functional N-acetylglucosamine catabolic pathway in *Vibrio cholerae*. *Mol Microbiol* 2011;80:1549–1560.

43. Naseem S, Konopka JB. *N*-acetylglucosamine regulates virulence properties in microbial pathogens. *PLoS Pathog* 2015;11:e1004947–11.

44. Echazarreta MA, Klose KE. *Vibrio flagellar* synthesis. *Front Cell Infect Microbiol* 2019;9:1–11.

45. Klose KE, Mekalanos JJ. Distinct roles of an alternative sigma factor during both free-swimming and colonizing phases of the *Vibrio cholerae* pathogenic cycle. *Mol Microbiol* 1998;28:501–520.

46. Prouty MG, Correa NE, Klose KE. The novel sigma54- and sigma28-dependent flagellar gene transcription hierarchy of Vibrio cholerae. *Mol Microbiol* 2001;39:1595–1609.

47. Syed KA, Beyhan S, Correa N, Queen J, Liu J *et al*. The *Vibrio cholerae* flagellar regulatory hierarchy controls expression of virulence factors. *J Bacteriol* 2009;191:6555–6570.

48. Correa NE, Lauriano CM, McGee R, Klose KE. Phosphorylation of the flagellar regulatory protein FlrC is necessary for Vibrio cholerae motility and enhanced colonization. *Mol Microbiol* 2000;35:743–755.

49. Krebs SJ, Taylor RK. Protection and attachment of Vibrio cholerae mediated by the toxin-coregulated pilus in the infant mouse model. *J Bacteriol* 2011;193:5260–5270.

50. Bhowmick R, Ghosal A, Das B, Koley H, Saha DR *et al*. Intestinal adherence of Vibrio cholerae involves a coordinated interaction between colonization factor GbpA and mucin. *Infect Immun* 2008;76:4968–4977.

51. Matson JS, Withey JH, DiRita VJ. Regulatory networks controlling Vibrio cholerae virulence gene expression. *Infect Immun* 2007;75:5542–5549.

52. Childers BM, Klose KE. Regulation of virulence in *Vibrio cholerae* : the ToxR regulon. *Future Microbiol* 2007;2:335–344.

53. Kovacikova G, Lin W, Skorupski K. Vibrio cholerae AphA uses a novel mechanism for virulence gene activation that involves interaction with the LysR-type regulator AphB at the tcpPH promoter. *Mol Microbiol* 2004;53:129–142.

54. Skorupski K, Taylor RK. Cyclic AMP and its receptor protein negatively regulate the coordinate expression of cholera toxin and toxin-coregulated pilus in Vibrio cholerae. *Proc Natl Acad Sci U S A* 1997;94:265–270.

55. Taylor RK, Miller VL, Furlong DB, Mekalanos JJ. Use of phoA gene fusions to identify a pilus colonization factor coordinately regulated with cholera toxin. *Proc Natl Acad Sci U S A* 1987;84:2833–2837.

56. Ritchie JM, Rui H, Bronson RT, Waldor MK. Back to the future: studying cholera pathogenesis using infant rabbits. *MBio* 2010;1:1–13.

57. Kim SY, Thanh XTT, Jeong K, Kim SB, Pan SO *et al*. Contribution of six flagellin genes to the flagellum biogenesis of Vibrio vulnificus and in *vivo* invasion. *Infect Immun* 2014;82:29–42.

58. Meron D, Efrony R, Johnson WR, Schaefer AL, Morris PJ *et al*. Role of flagella in virulence of the coral pathogen Vibrio coralliilyticus. *Appl Environ Microbiol* 2009;75:5704–5707.

59. McGee K, Hörstedt P, Milton DL. Identification and characterization of additional flagellin genes from Vibrio anguillarum. *J Bacteriol* 1996;178:5188–5198.

60. Ormonde P, Hörstedt P, O'Toole R, Milton DL. Role of motility in adherence to and invasion of a fish cell line by Vibrio anguillarum. *J Bacteriol* 2000;182:2326–2328.

61. Lee SH, Butler SM, Camilli A. Selection for *in vivo* regulators of bacterial virulence. *Proc Natl Acad Sci USA* 2001;98:6889–6894.

62. Matsumoto H, Muroi H, Umehara M, Yoshitake Y, Tsuyumu S. S. Peh production flagellum synthesis, and virulence reduced in Erwinia carotovora subsp. carotovora by mutation in a homologue of cytR. *Mol Plant-Microbe Interact* 2003;16:389–397.

Edited by: J. Stülke and H. Strahl

ORIGINAL ARTICLE

Inhibition of growth and virulence of *Vibrio cholerae* by carvacrol, an essential oil component of *Origanum* spp.

S. Das[1], R. Chourashi[1], P. Mukherjee[2], S. Kundu[1], H. Koley[2], M. Dutta[3], A.K. Mukhopadhyay[2], K. Okamoto[4] and N.S. Chatterjee[1] (iD)

1 Division of Biochemistry, ICMR-National Institute of Cholera and Enteric Diseases, Kolkata, India
2 Division of Bacteriology, ICMR-National Institute of Cholera and Enteric Diseases, Kolkata, India
3 Division of Electron Microscopy, ICMR-National Institute of Cholera and Enteric Diseases, Kolkata, India
4 Collaborative Research Center of Okayama University for Infectious Diseases at NICED, Kolkata, India

Abstract

Aims: In the age where bacterial resistance to conventional antibiotics is increasing at an alarming rate, the use of the traditional plant, herb extracts or other bioactive constituents is gradually becoming popular as an anti-virulence agent to treat pathogenic diseases. Carvacrol, a major essential oil fraction of Oregano, possesses a wide range of bioactivities. Therefore, we aimed to study the effect of sub-inhibitory concentrations of carvacrol on major virulence traits of *Vibrio cholerae*.

Methods and Results: We have used *in vitro* as well as *ex vivo* models to access the anti-pathogenic role of carvacrol. We found that the sub-inhibitory concentration of carvacrol significantly repressed bacterial mucin penetrating ability. Carvacrol also reduced the adherence and fluid accumulation in the rabbit ileal loop model. Reduction in virulence is associated with the downregulated expression of *tcpA*, *ctxB*, *hlyA* and *toxT*. Furthermore, carvacrol inhibits flagellar synthesis by downregulating the expression of *flrC* and most of the class III genes.

Conclusions: Carvacrol exhibited anti-virulence activity against *V. cholerae*, which involved many events including the inhibition of mucin penetration, adhesion, reduced expression of virulence-associated genes culminating in reduced fluid accumulation.

Significance and Impact of the Study: These findings indicate that carvacrol possesses inhibitory activity against *V. cholerae* pathogenesis and might be considered as a potential bio-active therapeutic alternative to combat cholera.

Introduction

Vibrio cholerae is a comma-shaped, Gram-negative, facultatively anaerobic bacterium that causes severe food and waterborne diarrhoeal disease cholera. The disease cholera causes gastrointestinal ailments with characteristic non-bloody watery diarrhoea leading to the loss of body fluids and the consequent electrolyte imbalance results in the death of the individual if left untreated. Infection of *V. cholerae* in humans is caused by the ingestion of contaminated water and food (Kaper *et al.* 1995). After reaching the small intestine, *V. cholerae* confronts the thick mucus barrier of the intestine, where it penetrates the thick mucus barrier by the simultaneous action of flagellar movement and release of different proteases and chitinases. As a result, *V. cholerae* subverts the protective mucus layer and then adheres to the epithelial cell. After the adherence, colonization of *V. cholerae* occurs by forming microcolonies. *Vibrio cholerae* then produces cholera toxin (CT) and other virulence factors and cause disease (Matson *et al.* 2007; Das *et al.* 2020). WHO estimates that each year cholera infects nearly 1–4 million people worldwide and claims up to 21 000–143 000 lives (Ali *et al.* 2015).

Throughout the last decade, awareness and campaigning among the people of developing nations about the practice of proper hygiene and sanitation and the availability of uncontaminated drinking water has reduced the global burden of cholera. In 2018, total cases of cholera were reduced by 60% than the previous year (World Health Organization 2019). Typically, treatment of cholera includes electrolyte replacement therapy and sometimes antibiotics. However, the inappropriate and overuse of antibiotics through self-medication and indiscriminate access to antibiotics without prescription has led to the emergence of multidrug-resistant epidemic strains of bacteria. Among bacteria, antibiotic-resistant *V. cholerae* is becoming worryingly common across the globe (Verma *et al.* 2019). Countries reporting major drug-resistant *V. cholerae* strains are reviewed extensively by Kitaoka et al. (Kitaoka *et al.* 2011). *Vibrio cholerae* becomes drug resistant by the frequent acquisition of extrachromosomal mobile genetic elements by horizontal gene transfer from other bacterial species. (Narendrakumar *et al.* 2019; Verma *et al.* 2019; Das *et al.* 2020).

Traditional antimicrobials are usually bacteriostatic or bactericidal which may facilitate the emergence of MDR strains. Therefore, alternative novel therapeutic approaches like the use of plant or herb extracts, bioactive phytochemicals or the use of small molecules are in urgent need to fight against these pathogens by particularly targeting bacterial virulence factors. Furthermore, the use of *Bdellovibrio bacteriovorus* or *Micavibrio aeruginosavorus* as probiotic treatment has also been reported to decrease the spread of antibiotic resistance in *V. cholerae* (Dwidar *et al.* 2012; Duncan *et al.* 2018). The use of bioactive compounds from natural products such as herbs, spices, fruits and seeds has many beneficial effects on our health and possess lesser side effects.

In India, various plant parts and their derivative components have been used as Ayurvedic medicine since ancient times to treat various diseases including diarrhoea. Plant-derived essential oils possess important volatile components with diverse bioactivities including antimicrobial potential. Over the past few years, the use of essential oils from cinnamon, cardamom, red chili, white pepper, sweet fennel and ginger has been well documented (Aminzare *et al.* 2018). These bioactive compounds act against *V. cholerae* in various ways mainly by controlling virulence regulatory gene *toxT* (Virstatin) (Hung 2005; Shakhnovich *et al.* 2007), inhibiting the binding of CT to GM_1 (6-Gingerol) (Saha *et al.* 2013), disrupting the secondary structure of CT (zinc oxide nanoparticles) (Sarwar *et al.* 2017) or by showing direct antimicrobial activity against the pathogen.

Carvacrol (CV) is a naturally occurring essential oil fraction of Oregano (*Origanum vulgare*) and it exhibits antimicrobial activity against a variety of foodborne pathogens such as *Escherichia coli* O157: H7 (Obaidat and Frank 2009), *Bacillus cereus* (Ultee *et al.* 1999), *Shigella*sp. (Bagamboula *et al.* 2004), *Salmonella*sp. (Miladi *et al.* 2016), *Clostridium difficile* (Mooyottu *et al.* 2014) and also *V. cholerae* (Rattanachaikunsopon and Phumkhachorn 2010). Studies indicated that CV possesses a variety of characteristics (Ahmad *et al.* 2010; Arunasree 2010) including anti-oxidant (Slameňová *et al.* 2007; Slamenova *et al.* 2008; Aristatile *et al.* 2009), antibacterial (Nostro *et al.* 2009; Rattanachaikunsopon and Phumkhachorn 2010; Pérez-Conesa *et al.* 2011) and anti-inflammatory properties (Landa *et al.* 2009; Hotta *et al.* 2009).

Most of the studies on the effects of carvacrol on bacteria have focussed on determining the minimum inhibitory concentration (MIC) at which growth arrest of the bacterial culture occurs, or on the minimum bactericidal concentration (MBC), that is, the concentration at which >99·9% of the bacterial population are killed (van Alphen *et al.* 2012). Despite extensive research on carvacrol in recent years, there is still no report regarding the anti-virulence properties of carvacrol against *V. cholerae*. In this study, we investigated the potential effects of sub-inhibitory (sub-MIC) concentration of carvacrol on the virulence potential of *V. cholerae*. In this context, we have evaluated the activity of carvacrol on *V. cholerae* motility, transcriptional regulation of flagella synthesis genes, *in vitro* mucin penetration, adhesion to epithelial cells followed by studying the *in vivo* anti-virulence activity of carvacrol using the rabbit ileal loop models. Here, we report for the first time the anti-virulence activity of carvacrol against pathogenic *V. cholerae*. Our results indicate that at concentrations that do not affect the bacterial growth CV can inhibit *V. cholerae* motility, mucin penetration, adhesion, toxin production and virulence which may limit bacterial infection and disease pathogenesis within the human host.

Materials and methods

Ethics statement

Animal experiments were carried on following the guideline proposed by the Committee for the Purpose of Control and Supervision of Experiments on Animal (CPCSEA), Government of India. All animal experiments performed here were subjected to the approval (registration no: PRO/120/April 2016–March 2019) by the Institutional Animal Ethics Committee of the National Institute of Cholera and Enteric Diseases. For *in vivo* fluid accumulation study, New Zealand white rabbits of about 2·5 kg were used. At the time of harvesting the

intestine, animals were euthanized in the CO chamber assuring minimum pain to the animals.

Bacterial strains and culture conditions

Streptomycin-resistant O1 El Tor Inaba *V. cholerae* strain N16961 was used in all the experiments performed here. This strain was cultured in Luria–Bertani (LB) medium at 37°C with 180 rev min^{-1} constant shaking or at static conditions on Petri plates containing LB agar supplemented with appropriate antibiotics streptomycin (100 μg ml^{-1}). Bacteria were also cultured in AKI media containing 0·4% yeast extract (BD Difco, San Diego, CA), 1·5% Bacto peptone (BD Difco, San Diego, CA), 0·5% NaCl and 0·3% freshly prepared NaHCO$_3$ (Merck, Burlington, MA) pH 7·2 at 37°C under static condition for CT analysis.

Determination of MIC and MBC of Carvacrol

The study compound carvacrol, a major constituent of essential oil fraction of oregano (*O. vulgare*), was purchased from Sigma-Aldrich, St. Louis, MO. A stock solution of carvacrol with a concentration of 50 mg ml^{-1} was prepared by diluting it in DMSO before use. These stocks were stored at 4°C in the dark until required and diluted stocks are used for not more than 1 week.

The MIC of carvacrol was determined by the broth microdilution method according to CLSI guidelines (Clinical Laboratory Standards Institute 2012) in 96-well flat-bottomed polystyrene microtiter plates (Costar Corning, Corning, NY). Bacterial strain suspension was adjusted to optical density values 0·08–0·12 at 600 nm (equivalent to 0·5 McFarland standard turbidity) with a spectrophotometer. In total, 200 μl of cell suspensions was inoculated into the wells of 96-well microplates and carvacrol was dissolved in DMSO and then in Muller Hinton Broth (MHB) as required and transferred to the microplate well to obtain a twofold serial dilution ranging from 1200 to 1 μg ml^{-1}. MHB only and MHB with bacteria containing wells were used as negative and positive controls, respectively. Plates were incubated for 24 h at 37°C and bacterial growth was evaluated by the presence of turbidity and a pellet on the bottom. The MIC value was recorded as the lowest concentration of the tested compound that had no macroscopically visible growth of bacteria (Burt 2004). To determine the MBC values, 100 μl of each well medium with no visible growth was inoculated in Muller Hinton Agar plates. After 24 h of incubation at 37°C, the number of surviving organisms was determined. MBC was defined as the lowest concentration of compounds at which 99% of the bacteria were killed. Each experiment was repeated twice

separately (Magina *et al.* 2009). To verify that the antimicrobial effect was from the carvacrol and not from DMSO (that was used as the solvent for carvacrol), we used DMSO as negative control and it did not inhibit bacterial growth.

Vibrio cholerae growth assay

For growth curve analysis, overnight grown log-phase cultures of *V. cholerae* N16961 were collected, centrifuged, washed in PBS, and cell number was adjusted to 1×10^9 cells per ml using LB medium. The growth curve was done in a nutrient-rich LB medium. Carvacrol was supplemented to the culture media at different concentrations (150, 75 and 37·5 μg ml^{-1}). A starting inoculum of 1×10^8 cells per ml was given to the fresh LB broth medium. Cultures were grown at 37°C under constant shaking at 180 rev min^{-1} for up to 24 h (Chourashi *et al.* 2016). The viable cell counts were enumerated by dilution plating of the bacterial cultures at different time points onto LB agar plates supplemented with streptomycin followed by colony count.

RNA isolation and quantitative RT-PCR

To determine the effect of carvacrol on *V. cholerae* toxin gene associated virulence gene and flagellar gene expression, total RNA was isolated from the mid-logarithmic-phase (O. D$_{600}$ values 0·5–0·6) bacterial culture. Carvacrol-treated and -untreated bacterial cultures were harvested either from in vitro samples grown in AKI and LB broth or from *in vivo* rabbit ileal loop. After extracting the total RNA using Trizol (Invitrogen, Carlsbad, CA) method, it was dissolved in RNase-free water at −80°C until use. Contaminating genomic DNA was eliminated by DNase treatment using a DNA-free kit (Ambion, Austin, TX). 1 μg of RNA from each sample was subjected to cDNA synthesis using a Reverse Transcription kit (Promega, Madison, WI) following the manufacturer's protocol. The mRNA transcript levels were quantified by quantitative PCR (qPCR) using 2 × SYBR green PCR master mix (AB Applied Biosystems, Foster City, CA) and 0·2 μmol l^{-1} of specific forward and reverse primers designed using PrimerQuest from Integrated DNA Technologies (IDT) for each transcript (Table S1). Data analysis was done using a 7500 Real-Time PCR detection system (Applied Biosystems, Foster City, CA) with 40 cycles of a two-step cycle followed by a melting curve. The relative expression of the target transcripts was calculated according to Livak's $2^{-\Delta\Delta C_T}$ method (Livak and Schmittgen 2001) using *recA* (VC_0543) as an internal control.

Mucin penetration assay

Mucin penetration study was performed according to the previously described method (Liu *et al.* 2008). In brief, mucin columns were prepared by adding 1·5% porcine mucin (Sigma-Aldrich) in 1-ml syringes. Different concentrations of carvacrol (75 and 37·5 μg ml^{-1}) were added to each of the mucin columns. The untreated mucin column was used as control. *Vibrio cholerae* was grown up to mid-log phase and the concentration was adjusted to 5×10^8 cells per ml using PBS. On top of the mucin columns, 0·1 ml of the culture was loaded and allowed to settle for 1 h at 37°C under static conditions (Chourashi *et al.* 2016). In all, 100 μl of culture fractions was collected from the bottom of the columns. Bacterial numbers were measured by serially diluting the samples and plating them onto LB agar and counting the colony forming units (CFU).

Motility assay

The surface motility of *V. cholerae* was done by the previously described method (Yeung *et al.* 2012). Bacteria were grown up to the mid-log phase in LB broth. The culture was resuspended in PBS and OD$_{600}$ adjusted to 0·5. In total, 1 μl of this culture was spotted on soft agar plates containing different concentrations of carvacrol (75 and 37·5 μg ml^{-1}) in LB media and 0·3% bacto agar. The plates were incubated for 24 h at 37°C. Bacterial motility was analysed by measuring the diameter of the motility zone on the plate surface.

Cell culture

Human adenocarcinoma cell line HT-29 (ATCC HTB-38) was used to study the effect of carvacrol in ex vivo conditions. HT-29 cells were maintained in Dulbecco's modified Eagle's medium (DMEM) (Sigma-Aldrich, St. Louis, MO), supplemented with 10% foetal bovine serum (PAN Biotech, Aidenbach, BY), 1% non-essential amino acid (Sigma-Aldrich, St. Louis, MO) and 1% penicillin/streptomycin (Sigma-Aldrich, St. Louis, MO) mixture at 37°C under 5% CO_2 in a humidified incubator (Mondal *et al.* 2014).

Adhesion assay

Vibrio cholerae adhesion to HT-29 was done according to the method described previously (Chourashi *et al.* 2016). HT-29 cells were split into 12-well cell culture plates and grown up to 80% confluency. *Vibrio cholerae* grown till mid-log phase was taken and $1·2 \times 10^8$ bacteria were (1 : 100 MOI) inoculated to HT-29 cells. Carvacrol at different concentrations (75 and 37·5 μg ml^{-1}) was added to the DMEM in each well. Adhesion assay was done by incubating the bacteria/cell at 37°C for 1 h. The cells were then washed three times with pre-warmed PBS pH 7·4 to remove unbound bacteria. Adhered bacteria were detached using 0·1% Triton X-100 in each treatment group and were counted after serial dilution by plating on LB agar plates supplemented with 100 μg ml^{-1} streptomycin. *In vivo* adhesion of bacterial strains with the rabbit intestinal lumen was also evaluated. Intestinal loop sections recovered 18 h after the rabbit ileal loop experiment were washed in PBS three times, homogenized and serially diluted in PBS. The adherent bacterial count was determined by plating these bacterial cultures on LB agar supplemented with 100 μg ml^{-1} streptomycin.

Ligated rabbit ileal loop assay for fluid accumulation and bacterial recovery

New Zealand white rabbit was used to study intestinal fluid accumulation assay. In total, 1 ml of 1×10^9 CFU per ml *V. cholerae* culture with or without carvacrol (at 150, 75, 37·5 μg ml^{-1}) was introduced into each ileal loop. The negative control loop was inoculated with PBS. After 18 h, the animal was sacrificed and the loops were taken out and the volume of the accumulated fluid and the length of the loops were measured. The amount of the accumulated fluid (FA) was expressed as a loop fluid volume (ml)/length (cm) ratio (Chourashi *et al.* 2016). The accumulated fluid was also used for bacterial adhesion, CT production and virulence gene expression studies.

GM1 enzyme-linked immunosorbent assay

The amount of CT in the culture supernatant was quantified by GM1 enzyme-linked immunosorbent assay (ELISA) as described by Holmgren (1973) with minor alterations (De *et al.* 2004; Patra *et al.* 2012). *Vibrio cholerae* grown in AKI media for 18 h was harvested and cell-free culture supernatant was pulled out by centrifugation. Culture supernatants were added to the wells of MaxiSorp ELISA plates (Nunc, Rochester, NY) and pre-coated with GM1 ganglioside (Sigma-Aldrich, St. Louis, MO). Subsequently, each well was treated with a polyclonal anti-CT antibody (Sigma-Aldrich, St. Louis, MO). In each set of assays, known amounts of purified CT were used in different concentrations to generate a standard curve. The amount of CT secreted by *V. cholerae* strains was done by extrapolating the optical density value of the samples at 450nm in the standard curve. The average of OD$_{450}$ values obtained from triplicate wells of each experimental set was considered to estimate the amount of CT

present and expressed as ng of CT per ml. The amount of CT produced *in vivo* rabbit ileal loop culture was also measured by this method.

Transmission electron microscopy

Whole-cell mounts of *V. cholerae* were negatively stained and bacterial morphology was visualized. In brief, wild-type *V. cholerae* was grown in LB broth with or without carvacrol at different concentrations (150, 75 and 37·5 μg ml^{-1}). In total, 5 μl of bacterial suspension was gently placed on a carbon-coated 300 mesh copper grid. After about 1 min, the remaining solution on the grids was wicked away with the help of a filter paper followed by washing with two drops of distilled water. The grid was then stained with 2% (w/v) uranyl acetate and air-dried. The negatively stained cells were visualized with an FEI Tecnai 12 BioTWIN transmission electron microscope (FEI, Hillsboro, OR) at an operating voltage of 100 kV.

LDH cytotoxicity assay

The effect of carvacrol on the cytotoxicity of the HT-29 cell line was estimated by lactate dehydrogenase (LDH) release assay following the manufacturer's protocol (LDH cytotoxicity detection kit, TaKaRa Biosciences). In brief, HT-29 cells were grown in six-well cell culture plates up to 80% confluency and then co-incubation with carvacrol at different concentrations was done for 12 h at 37°C humid cell culture incubator. Cell culture supernatants were analysed for the release of LDH. The percent cytotoxicity value was calculated using the following formula:

$$\text{Cytotoxicity}(\%) = \left(\frac{\text{EX} - \text{LC}}{\text{HC} - \text{LC}} - \text{BC}\right) \times 100,$$

where EX is the experimental value, LC the low control or spontaneous LDH release from the untreated normal HT-29 cells, HC the high control or maximum releasable LDH in the HT-29 cells by the addition of 1% Triton X-100 and BC the background control or LDH activity in the assay medium. Treatment with 1% (v/v) Triton X-100 represented maximum LDH release, hence represented 100% cytotoxicity.

Cell staining and fluorescence microscopy

The effect of carvacrol on human adenocarcinoma cell line HT-29 was visualized by fluorescence microscopy. HT-29 cells were seeded on sterile borosilicate cover glass (Blue star, Mumbai, MH) in six-well cell culture plates. Upon reaching 80% confluency, HT-29 cells were incubated in serum-free DMEM and carvacrol treatment at

different concentrations (0–250 μg ml^{-1}) was done for 4 h. After removing the media, HT-29 cells were washed in PBS and stained with Hoechst 33342 (5 μg ml^{-1}) (Sigma-Aldrich) for 10 min. Cells were then washed in PBS twice and subsequently counterstained and mounted with PI containing mounting medium (VectaShield, Vector Laboratories, Burlingame, CA). Both carvacrol-treated and -untreated cells were visualized under a confocal laser scanning microscope. Propidium iodide (PI) is a membrane impermeant dye, whereas Hoechst H33342 is a membrane-permeable stain; therefore, HT-29 cells exhibiting membrane permeability upon carvacrol treatment display red (PI) intensity.

Statistical analysis

All the experiments were performed independently in triplicates, and the data obtained were analysed by Student's *t* test. Data were represented as mean ± standard error of mean (SEM). A $P < 0.05$ was considered as statistically significant.

Results

Determination of MIC and growth of *V. cholerae* at sub-MIC concentrations of carvacrol

The antibacterial activities in terms of MIC of carvacrol against *V. cholerae* were found to be 150 μg ml^{-1}. In this concentration of carvacrol, no visible growth of *V. cholerae* was seen in the broth dilution assay. Also, in line with the definition of MBC (Helander *et al.* 1998), its value was found to be the same as MIC, as no viable bacteria were found in this concentration of carvacrol. Furthermore, all the experiments of this study were performed at sub-MIC concentrations of carvacrol (at ½ MIC (75 μg ml^{-1}) and ¼ MIC (37·5 μg ml^{-1})). MIC of carvacrol was also used in some experiments to compare the effect with other treatment groups. The effect of carvacrol on *V. cholerae* growth in a time-dependent manner was examined by counting the viable cells on the plates. The growth rate of *V. cholerae* was measured in LB medium along with exogenously added MIC and sub-MIC concentrations of carvacrol. The result indicated that *V. cholerae* growth was completely inhibited at MIC (150 μg ml^{-1}). No bacteria were recovered after 2 h of initial inoculum at MIC. At ½ MIC (75 μg ml^{-1}), the viable count of the bacteria was reduced to 60% 1 h post-initial inoculum. Within the initial 8 h, the viable count of the bacteria reduced gradually to 20%. At 24 h, the growth of the *V. cholerae* starts resuming to a lesser extent and reaches up to 37% viability of the initial bacterial population. On the contrary, carvacrol treatment at

¼ MIC (37·5 μg ml^{-1}) resulted in a reduction in the bacterial population to 60% within 2 h of the initial inoculum. After that *V. cholerae* resumes growth and at 24 h, the viable count of the bacteria exceeds more than five times the initial inoculum (Fig. 1). At the initial phase of the sub-MIC treatment, carvacrol showed the bactericidal effect on *V. cholerae*; subsequently, it remained bacteriostatic for the remaining viable bacteria. This suggests that *V. cholerae* remained viable and continued to grow even upon carvacrol treatment at sub-MIC concentrations.

Swarming motility and mucin penetrating ability of *V. cholerae* is reduced by carvacrol

The ability of *V. cholerae* to penetrate the mucin layer *in vitro* in the presence of carvacrol was investigated. It was found that *V. cholerae* mucin penetration decreased significantly upon carvacrol treatment. Out of a total of 5×10^8 CFU per ml bacteria loaded on top of the 1·5% mucin column, 100 μl of 43×10^3 CFU per ml bacteria was recovered after 1 h from the bottom of the column (Fig. 2a). In case of CV treatment at ¼ MIC (37·5 μg ml^{-1}) and ½ MIC (75 μg ml^{-1}), a total of 8×10^2 and $3·5 \times 10^2$ bacteria were recovered from the bottom of the column, respectively, which seems to have caused a 5·2-fold and 12·3-fold reduction in mucin
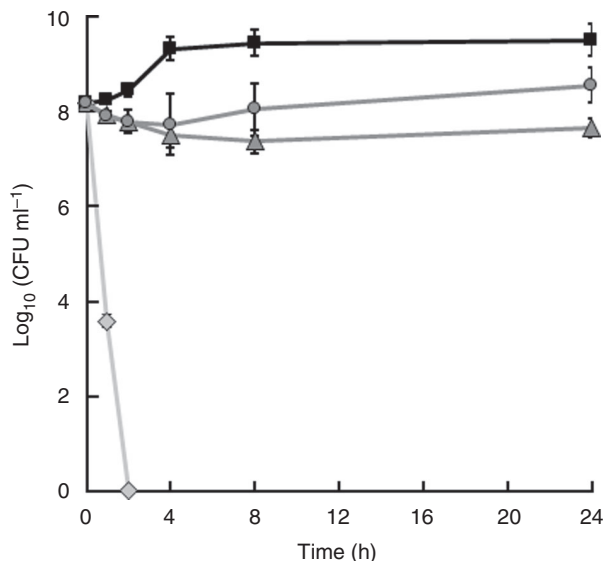

Figure 1 Effect of carvacrol on *Vibrio cholerae* growth at MIC and sub-MICs. Wild-type *V. cholerae* N16961 were grown in LB broth along with carvacrol at MIC (150 μg ml^{-1}), CV 150 (◇); ½ MIC (75 μg ml^{-1}), CV 75 (▲); ¼ MIC (37·5 μg ml^{-1}), CV 37·5 (○) along with the untreated control, CV 0 (□). The viable bacterial counts in CFU per ml detected by the plate count method were represented graphically. Each experiment was repeated three times (*n* = 3) and the data were expressed as mean ± SEM.

penetration, respectively. Because CV at both sub-MIC concentrations reduced the viable count of the bacteria by 40% in the initial 1 h of growth, we can say that the viable count of the bacteria must be $25·8 \times 10^2$ in the bottom 100 μl fraction of the CV-treated columns. Compared to that, ¼ MIC of CV treatment showed 3·2-fold and ½ MIC of CV treatment showed a 7·4-fold reduction. We have also investigated the surface motility of *V. cholerae* on soft agar LB plates (Fig. 2b). We found that in the CV-untreated plate *V. cholerae* showed a motility zone of $7 \pm 0·3$ cm and the addition of CV resulted in complete inhibition of swarming motility after 24 h of incubation.

Adhesion to epithelial cells is affected by carvacrol

The effect of carvacrol on *V. cholerae* adherence to rabbit ileum epithelial cells was tested. The result suggested that $3·37 \times 10^7$ CFU per ml adherent *V. cholerae* was present in the untreated condition (Fig. 3a). In contrast, there was only $8·7 \times 10^6$ CFU per ml and 21×10^6 CFU per ml of adherent bacteria at ½ MIC (75 μg ml^{-1}) and ¼ MIC (37·5 μg ml^{-1}) of carvacrol treatment, respectively. We have also checked the bacterial load in each of the ileal loop samples. $1·98 \times 10^9$ CFU per ml, $2·08 \times 10^9$ CFU per ml and $1·59 \times 10^9$ CFU per ml bacteria were recovered from the CV-untreated, ¼ MIC of CV-treated and ½ MIC of CV-treated ileal loop samples (Fig. 3b). This study exhibits that only 1·7% of the total *V. cholerae* adhered to the epithelium in the absence of CV. Whereas 0·5% out of total *V. cholerae* was adhered to the epithelium in the presence of ½ MIC of CV treatment, showing three times less adherence capability of *V. cholerae*. Furthermore, the adherence capability of *V. cholerae* to the HT-29 intestinal epithelial cell line was also studied comparing with the recovered viable bacteria from treated and untreated culture samples. In the absence of CV, 1·47% out of total bacteria adhered to the HT-29. Whereas only 0·12 and 0·04% bacteria out of total viable bacteria adhered at ¼ and ½ MIC of carvacrol treatment (Fig. 3c,d). Therefore, the effect of carvacrol on *V. cholerae* is more pronounced in cell culture conditions although we found significant results *in vivo* treatment.

Vibrio cholerae show less fluid accumulation upon carvacrol treatment

Next, the effect of carvacrol in fluid accumulation in ligated rabbit ileal loop model was studied. The amount of fluid accumulated per unit length (FA ratio) in each loop was measured 18 h post-infection with or without carvacrol-treated *V. cholerae* culture (Fig. 4a). When quantified, the FA ratio of CV treatment showed
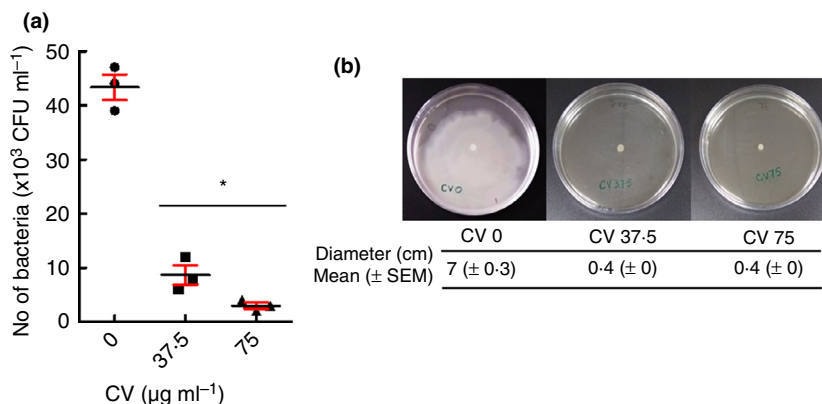
Figure 2 Effect of carvacrol on motility of *Vibrio cholerae*. (a) Mucin penetration was performed in a 1·5% mucin column in the presence of different concentrations of carvacrol at ½ MIC (75 μg ml^{-1}) and ¼ MIC (37·5 μg ml^{-1}). Please see Materials and methods for details. Bacterial numbers eluted were counted and graphically represented. (b) Representative plates showing the motility zone of *V. cholerae* on 0·3% agar plates under different treatment conditions. Each of the experiments was repeated three times ($n = 3$) and the data were expressed as mean $\pm$ SEM. *$P < 0.05$.

complete obliteration of fluid accumulation upon treatment with MIC of carvacrol (i.e. 150 μg ml^{-1}). At ½ MIC (75 μg ml^{-1}), a 3·7-fold decrease in fluid accumulation was observed compared to the control (Fig. 4b). At ¼ MIC (37·5 μg ml^{-1}) of carvacrol, the FA ratio was found to be similar to the untreated one.

CT production and virulence gene expression is decreased by carvacrol

CT production in the rabbit ileal loop sample, which is primarily responsible for fluid accumulation, was measured by GM$_1$-CT ELISA. Experimental results suggested that *V. cholerae* produced 666 ng ml^{-1} of CT in the untreated ileal loop. At ½ MIC (75 μg ml^{-1}) of carvacrol treatment, CT production was measured to be 106·6 ng ml^{-1} resulting in 6·3-fold reduced production of CT compared to the untreated control loop (Fig. 5a). Fluid from ¼ MIC (37·5 μg ml^{-1}) carvacrol-infected loop showed almost similar CT production (612 ng ml^{-1}) compared to the control loop. The expression of different virulence genes (*toxT*, *hlyA*, *tcpA* and *ctxB*) was also measured by qPCR. It was found that the expression of these genes was significantly reduced by twofold, 2·3-fold, 4·4-fold and 4·2-fold, respectively, in ¼ MIC carvacrol (37·5 μg ml^{-1})-infected ileal loop samples relating to the infection with only *V. cholerae* (Fig. 5b). At ½ MIC (75 μg ml^{-1}) of carvacrol treatment, expression of these genes was greatly reduced compared to the control gene at the control condition. Carvacrol also reduced CT production as well as the expression of virulence genes *in vitro* AKI media (Fig. S1).

Negligible cytotoxic effect was seen at sub-MIC concentrations of carvacrol

Cytotoxicity of the HT-29 cell line upon carvacrol treatment was measured by LDH release assay. Different doses of carvacrol were used to treat HT-29 cells and after 12 h the supernatants were collected and assessed for the release of LDH. HT-29 cell treatment with triton X-100 showed maximum membrane damage, hence considered to possess 100% cytotoxicity. The experimental result obtained here showed that carvacrol exerts 9% and <1% cytotoxicity at MIC and ½ MIC (75 μg ml^{-1}), respectively, compared to the triton X-100 treated cell (Fig. 6a). So, no substantial membrane damage upon treatment at MIC (150 μg ml^{-1}) and sub-MIC concentrations carvacrol is observed. Although at higher concentration (250 μg ml^{-1}), carvacrol exhibited noteworthy spillage of LDH resulted in 58% cytotoxicity. Confocal microscopy images also revealed that at MIC and sub-MIC treatment of carvacrol, the permeability of PI to HT-29 cell line was very less compared to the Triton-X 100 treatment (Fig. 6 b). The above results led to the conclusion that carvacrol at sub-MIC is safe and does not cause human epithelial cell damage.

Morphology and flagellar synthesis in *V. cholerae* is affected by carvacrol

Changes in bacterial morphology were observed by transmission electron microscopy upon carvacrol treatment. As shown in Fig. 7, carvacrol treatment at MIC (150 μg ml^{-1}) showed altered morphology with distorted shape and damaged cell membranes, whereas lower
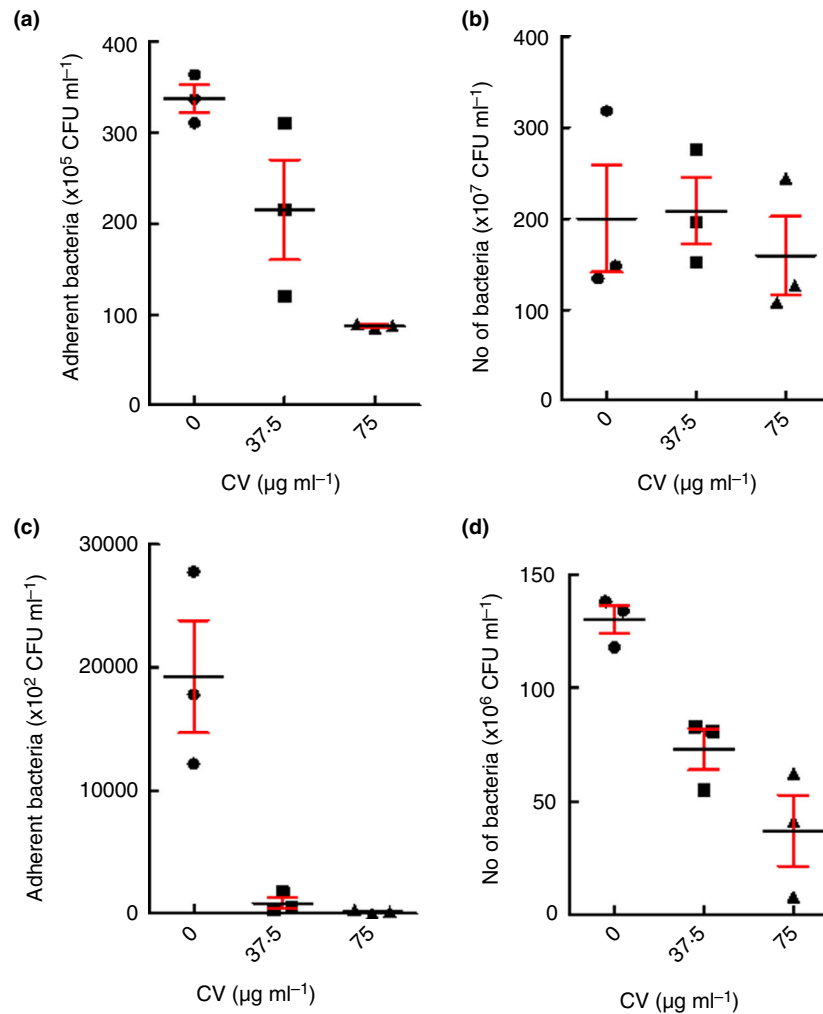
Figure 3 Effect of carvacrol on the adhesion of *Vibrio cholerae* to the epithelial cells. Carvacrol at ½ MIC (75 μg ml^{-1}) and ¼ MIC (37·5 μg ml^{-1}) were used in treating both rabbit intestine and cell culture conditions. (a) Adhered *V. cholerae* in the rabbit ileal loop tissue samples. (b) Total number of *V. cholerae* count in each of the rabbit ileal loops. (c) Adhered *V. cholerae* with the HT-29 cell line. (d) Total number of *V. cholerae* count in each HT-29 culture samples. The result is shown as the mean ± SEM of three biological replicates ($n = 3$).

concentrations of carvacrol showed the normal shape of the bacteria. Although flagella in each of the treatments was not observed in *V. cholerae*. Compared to that untreated *V. cholerae* showed a normal shape and single polar flagellum (Fig. 7). Flagella-driven bacterial motility is an important virulence trait of *V. cholerae*. Reduced mucin penetration and absence of flagella by microscopic analysis upon carvacrol treatment raised interest in whether carvacrol has any effect on flagella synthesis. Therefore, the effect of the sub-inhibitory concentration of carvacrol on *V. cholerae* flagella synthesis was assessed by measuring the transcription of flagella synthesis genes by qRT-PCR. The analysis revealed that at ¼ MIC (37·5 μg ml^{-1}) of carvacrol treatment, there was a

fourfold decreased expression of *flrC*, a response regulator ($P < 0.05$) (Fig. 8). Transcriptional expression of master regulator *flrA*, histidine kinase *flrB* and *fliF* (MS ring structure forming unit) was not significantly changed upon carvacrol treatment ($P > 0.05$). On the other hand, alternate sigma factor *fliA* (σ^{28}), *flgM* and *RpoN* (σ^{54}) expressions were downregulated by 2·5-fold, 2·9-fold, and 3·5-fold, respectively. Furthermore, downregulation of *motY* (T-ring motor protein), *flaA* (main flagellin sub-unit), *flgP* (H-ring-associated protein), *flgT* (H-ring component), *flgK* (hook filament junction protein), *flgG* (distal rod) and *flgB* (proximal rod) all of which belong to Class III flagellar synthesis genes were downregulated by 10·5-fold, 7·1-fold, 3·8-fold, 6·6-fold, 33·3-fold, 5-fold
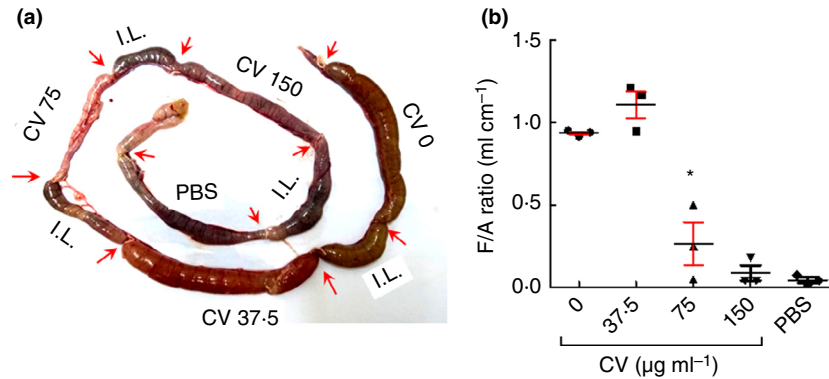
Figure 4 Effect of carvacrol in fluid accumulation in rabbit intestine. (a) Representative image of retrieved rabbit intestinal portion showing infected loop 18 h post-infection. The negative control loop was inoculated with PBS. Arrow showing the location of ligations in the loop. I.L., Inter Loop. (b) Fluid accumulation ratio in the rabbit intestine of three different experiments was measured and represented graphically as mean ± SEM. *$P < 0.05$.
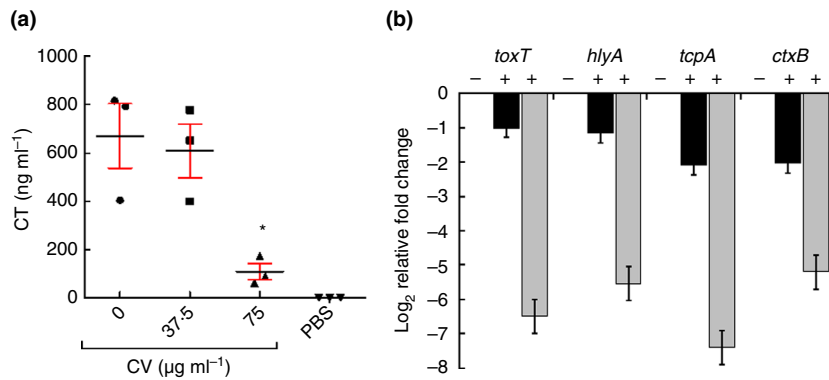

Figure 5 Effect of carvacrol on cholera toxin (CT) production and virulence gene expression. (a) *In vivo* CT production was measured by ELISA from the accumulated fluid samples of carvacrol treated (with ½ MIC (75 μg ml^{-1}), ¼ MIC (37·5 μg ml^{-1})) and untreated ligated rabbit ileal loops. (b) Relative expression of *Vibrio cholerae* virulence genes by real-time PCR. RNA was isolated from the untreated (−) or carvacrol treated (+) (¼ MIC (37·5 μg ml^{-1}) CV, (□) and ½ MIC (75 μg ml^{-1}), (□)) ileal loop bacterial samples. *recA* was used as an internal control gene. Data showed here as the log$_2$-transformed values of relative fold change. Each of the experiments was repeated three times ($n = 3$) and the data were expressed as mean ± SEM.

and 3·2-fold, respectively, upon ¼ MIC (37·5 μg ml^{-1}) of carvacrol treatment. However, inconspicuous change in the expression pattern of these flagellar synthesis genes was noticed when *V. cholerae* culture was treated with even higher sub-inhibitory concentration, that is, ½ MIC (75 μg ml^{-1}) of carvacrol.

Discussion

Preceding the age of antibiotic discovery, traditional knowledge of herbal extracts was widely practiced as remedies to treat certain diseases around the world. However, in this antibiotic era, bacteria with resistance to various antibiotics are emerging increasingly, along with the declined rate of development of new antibiotics during

the last decade compelled researchers to look for alternative approaches to treat pathogenic infections (Bassetti *et al.* 2013; Sharifi-Rad *et al.* 2018). After an extensive literature survey, Carvacrol (CV), an essential oil fraction of oregano, was selected for the study possessing several bioactive properties on various organisms.

In this study, we have investigated the effect of the sub-inhibitory concentration of CV on *V. cholerae* to access the spectrum of biological activities under pathogenic conditions. Our experimental result from the present study suggests that CV possesses bacteriostatic as well as the bactericidal effect on *V. cholerae* at MIC. These findings are in accordance with the previous study, although a minor difference in MIC was also observed (Rattanachaikunsopon and Phumkhachorn 2010; Magi
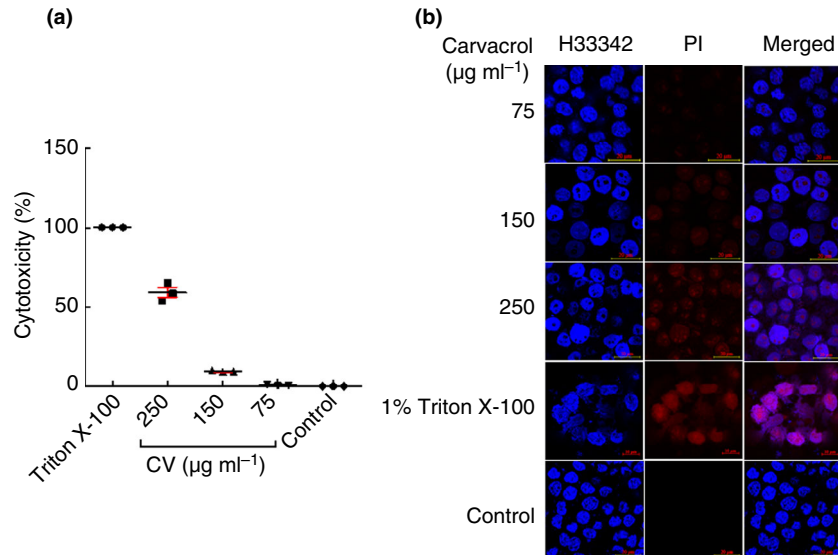
(a)

(b)

Figure 6 Cytotoxic activity of carvacrol in the HT-29 cell line. (a) The cytotoxic effect of carvacrol at different concentrations was measured by LDH release assay in HT-29 cells and graphically represented as percent cytotoxicity. Triton X-100 treated cell's LDH release as a positive control. (b) Confocal images of HT-29 cells treated with different concentrations of carvacrol. Cells were stained with Hoechst 33342 (Blue) and counterstained with propidium iodide (Red).
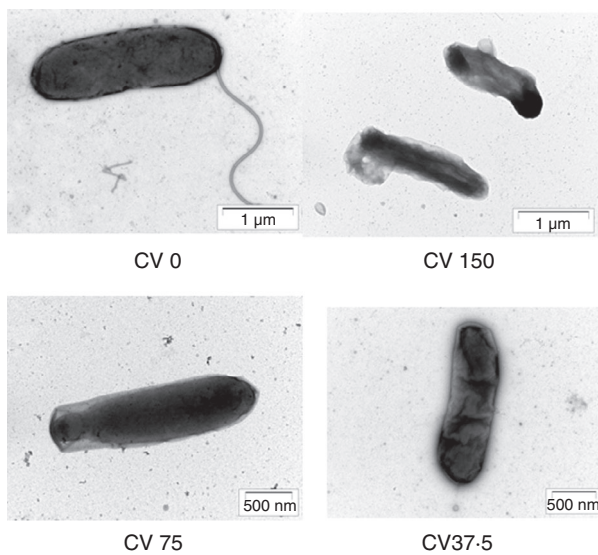

Figure 7 Effect of carvacrol on *Vibrio cholerae* morphology. Transmission electron micrographs of negatively stained *V. cholerae* in the absence and presence of different concentrations of carvacrol.

et al. 2015). To find out the anti-pathogenic role of CV against *V. cholerae*, we determined that ½ MIC is the highest concentration of CV that does not inhibit the growth of *V. cholerae* and it remained viable. Therefore, the concentration of ½ MIC and lower was used to assess the inhibitory effect of carvacrol on the different virulence and pathogenic attributes of *V. cholerae*. We have

also ensured that at a particular optical density of CV-treated or -untreated *V. cholerae* cultures possess equal viable bacteria, thereby eliminating the possibility of unfair analysis of the experimental results (Preliminary observation).

Transmission of *V. cholerae* in humans involves the faecal-oral route. After reaching the small intestine, *V. cholerae* need to penetrate through the thick mucus layer to successfully colonize the underlying enterocytes (Jordan *et al.* 1998). We found that CV at sub-MIC inhibited *V. cholerae* mucin penetrating ability in a dose-dependent manner. *Vibrio cholerae* motility and mucin penetration are mediated by the rotation of its monotrichous polar flagellum and is considered as a significant virulence factor for the bacteria (Silva 2003; Mewborn *et al.* 2017). Our findings are also in line with previous studies where various bioactive phytochemicals or their derivatives produce anti-virulence effect against different pathogenic micro-organisms by diminishing bacterial motility and flagellar protein expression (Liu *et al.* 2017). It was also previously reported that the polyphenolic fraction of Kombucha was able to inhibit the motility of *V. cholerae* as a result of the disruption in flagellar gene biosynthesis (Bhattacharya *et al.* 2020). Furthermore, two separate studies showed swarming motility of *Pseudomonas aeruginosa* was inhibited by tea polyphenols and cranberry proantocyanidins (O'May and Tufenkji 2011; Yin *et al.* 2015).
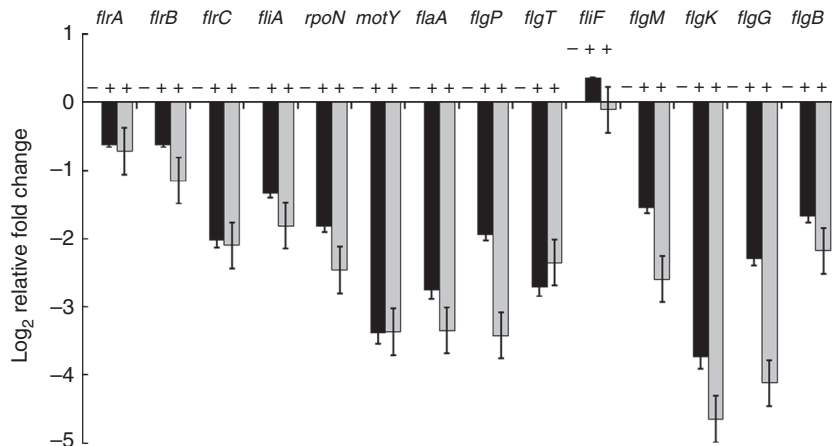
Figure 8 Effect of carvacrol in *Vibrio cholerae* flagellar gene synthesis. Mid-log-phase bacterial cultures in the presence (+) (¼ MIC (37·5 μg ml^{-1}), (■) and ½ MIC (75 μg ml^{-1}) (■)) or absence (−) of carvacrol were subjected to RNA isolation using the TriZol method and mRNA transcript levels were analysed by qRT PCR and graphically represented, using *recA* as an internal control gene. Data showed here as the log$_2$-transformed values of relative fold change. Each of the experiments was repeated three times (*n* = 3) and the data were expressed as mean ± SEM.

Transmission electron microscopy reveals that sub-MIC treatment of CV causes *V. cholerae* to become aflagellate, which further explains the rationale behind the reduced motility. RT-PCR results showed that the sub-inhibitory concentrations of CV had a significant (*P* < 0·05) downregulatory effect on *flrC*, which is a cytosolic response regulator and belongs to the Class II flagellar synthesis genes. *flrC* along with the histidine kinase *flrB* regulates the synthesis of Class III flagellar gene which are mostly associated with the synthesis of flagellin proteins as well as the structural units of the flagellar basal body (Klose and Mekalanos 1998; Echazarreta and Klose 2019). We have also found that sub-MIC of CV downregulates the expression of class III genes. These genes primarily include *motY*, *flaA*, *flgP*, *flgT*, *flgK*, *flgG* and *flgB*. Therefore, we speculate CV at sub-MIC inhibits the synthesis of class III genes directly by regulating their expression or by specifically modulating the expression of class II component *flrC*. Although further research is a prerequisite to gain a better insight into this mechanism. The swarming motility and mucin penetrating ability of *V. cholerae* also get inhibited by CV. Therefore, the inability to swim and penetrate the mucin layer can be explained by the absence of flagella.

After penetrating the thick mucus layer, *V. cholerae* adheres to the brush borders of epithelial cells for colonization. We found that CV reduced adherence of *V. cholerae* to the epithelial cells. Although to attain a significant effect under *in vivo* conditions, a higher dose of CV was needed, probably due to the lesser bioavailability. Furthermore, reduced expression of toxin co-regulated pilus A (*tcpA*), one of the major adhesin of *V.*

cholerae, might explain the possible reason behind decreased adhesion of *V. cholerae* to the epithelium. After adhering to the intestinal brush border epithelium, *V. cholerae* starts secreting CT. Fluid accumulation as a result of CT production is the primary determinant of cholera pathogenesis. In the rabbit ileal loop model, we have found a significant reduction in fluid accumulation upon CV treatment. This observation also corroborates with earlier works where CV treatment at 60 μg ml^{-1} has been reported to reduce 80% diarrhoeal toxin production by *B. cereus* (Ultee and Smid 2001).

To analyse the inhibitory mechanisms of CV on CT production in *V. cholerae*, quantitative RT-PCR of major virulence genes including *toxT*, *ctxB*, *tcpA* and *hlyA* were performed. In this context, we found a significant decline in all of the virulence genes by more than twofold at sub-MIC. In *V. cholerae*, expression of CT and TCP is activated by the expression of ToxT, the master virulence regulator, which, in turn, is controlled by upstream regulators such as TcpP/TcpH and ToxR/ToxS (Matson *et al.* 2007). Therefore, we assume that the reduction in transcription of *ctxB*, *tcpA* genes upon sub-MIC treatment of CV may be due to the inhibitory effect of CV on *toxT*. Notably, CV might also be involved in the regulation of the transcription of *toxT*, *tcpA*, *ctxB* and *hlyA* by either a direct or an indirect mechanism, although further study regarding the mechanism is needed for a complete understanding of this process.

The phenolic group of CV causes bacterial membrane damage and results in increased membrane fluidity (Weber and De Bont 1996) and loss of protons and bigger ions (Langeveld *et al.* 2013). TEM micrographs

demonstrated that CV at MIC caused severe damage to the surface of *V. cholerae* and altered the bacterial morphology. At sub-MIC, membrane impairment was not noticed but as stated earlier it lacks the presence of flagella. It is evident that CV at MIC causes membrane disruption and affects *V. cholerae* survival and growth, but at sub-MIC *V. cholerae* can retain its membrane integrity and shape. This also supports the previous report where *B. cereus* was found to adapt to the non-lethal concentrations of CV (Ultee *et al.* 2000). Altogether, these data indicated that CV exhibited a dose-dependent virulence inhibitory effect on *V. cholerae*.

Bioactive phytochemicals possess many beneficial effects. Besides these properties, they might also have potential cytotoxic effects on the host cells (Llana-Ruiz-Cabello *et al.* 2015), which is needed to be evaluated. We have tested the cytotoxic activity of CV on the human cell line HT-29 and CV showed minimum membrane damage. Even after 48 h, ½ MIC of CV showed 5·12% cytotoxicity. Therefore, it is expected that the use of CV at sub-MIC may not pose any harm to the human intestinal cells. Fluorescence microscopy also supports this observation. Earlier studies have also suggested that CV is usually nongenotoxic to the living cells (Bakkali *et al.* 2008) and shown to be safe for 24 h on HepG2 cell-line (Palabiyik *et al.* 2016).

In conclusion, the present study shows for the first time that the sub-inhibitory concentrations of CV inhibit growth and virulence in *V. cholerae*. CV treatment suppressed *V. cholerae* flagellar synthesis, thereby inhibiting the bacterial motility through the thick mucus layer followed by reduced adhesion to the intestinal epithelium and finally reduced expression of CT and other virulence-associated genes. These events finally lead to reduced fluid accumulation in the rabbit intestine. To understand the pleiotropic effect of CV on such a wide range of virulence genes, it is possible that CV could act on a global regulator. Repression of the CT production and virulence gene transcription is affected by natural compounds (Hyldgaard *et al.* 2012). One such example includes capsaicin, a red chili extract that reduced the virulence of *V. cholerae* by regulating the expression of *hns* (Yamasaki *et al.* 2011). Future study is needed to identify the global regulator and understand the cascade of the inhibitory mechanism. A previous study demonstrated that the use of CV to be safe for human use and we have also showed that it has a negligible cytotoxic effect at sub-MIC up to 12 h. We have also checked the long exposure of CV to HT-29 cell line and it showed around 5% cytotoxicity at ½ MIC after 48 h (Preliminary observation). The findings of the present study highlight the promising role of CV as a novel anti-virulent compound and can be promoted as a therapeutic agent to treat *V. cholerae* infection.

The findings of the present study highlight the promising role of CV as a novel anti-virulent compound and can be promoted as a therapeutic agent to treat *V. cholerae* infection. Further experiments on the detailed pharmacokinetics relating to human evidence may be worthy of evaluation before CV administration. Although CV has been categorized as a Generally Recognized As Safe (GRAS) compound and approved for safe use (U.S. Food and Drug Administration 1998; Hyldgaard *et al.* 2012), its poor solubility and bioavailability remain a problem (Suntres *et al.* 2015). So, the advancement of the delivery systems needs to be developed in parallel which will improve the solubility, stability and bioavailability of this compound.

Acknowledgements

Author contributions

SD, RC and NSC conceptualized the study. SD, RC, PM, SK, HK and MD performed the experiments. SD, AKM and NSC prepared the original draft of the manuscript. AKM and KO collaborated with this study. All authors did data analysis, draft review, editing and approval.

Conflict of Interest

The authors declare that they have no competing interests.

References

Ahmad, A., Khan, A., Akhtar, F., Yousuf, S., Xess, I., Khan, L.A. and Manzoor, N. (2010) Fungicidal activity of thymol and carvacrol by disrupting ergosterol biosynthesis and membrane integrity against Candida. *Eur J Clin Microbiol Infect Dis* **30**, 41–50.

Ali, M., Nelson, A.R., Lopez, A.L. and Sack, D.A. (2015) Updated global burden of cholera in endemic countries. *PLoS Negl Trop Dis* **9**, e0003832.

van Alphen, L.B., Burt, S.A., Veenendaal, A.K.J., Bleumink-Pluym, N.M.C. and van Putten, J.P.M. (2012) The natural

antimicrobial carvacrol inhibits *Campylobacter jejuni* motility and infection of epithelial cells. *PLoS One* **7**, e45343.

Aminzare, M., Hashemi, M., Abbasi, Z., Mohseni, M. and Amiri, E. (2018) Vibriosis phytotherapy: a review on the most important world medicinal plants effective on Vibrio spp. *J Appl Pharm Sci* **8**, 170–177.

Aristatile, B., Al-Numair, K.S., Veeramani, C. and Pugalendi, K.V. (2009) Effect of carvacrol on hepatic marker enzymes and antioxidant status in d-galactosamine-induced hepatotoxicity in rats. *Fundam Clin Pharmacol* **23**, 757–765.

Arunasree, K.M. (2010) Anti-proliferative effects of carvacrol on a human metastatic breast cancer cell line, MDA-MB 231. *Phytomedicine* **17**, 581–588.

Bagamboula, C.F., Uyttendaele, M. and Debevere, J. (2004) Inhibitory effect of thyme and basil essential oils, carvacrol, thymol, estragol, linalool and p-cymene towards *Shigella sonnei* and *S. flexneri*. *Food Microbiol* **21**, 33–42.

Bakkali, F., Averbeck, S., Averbeck, D. and Idaomar, M. (2008) Biological effects of essential oils – a review. *Food Chem Toxicol* **46**, 446–475.

Bassetti, M., Merelli, M., Temperoni, C. and Astilean, A. (2013) New antibiotics for bad bugs: where are we? *Ann Clin Microbiol Antimicrob* **12**, 22.

Bhattacharya, D., Sinha, R., Mukherjee, P., Howlader, D.R., Nag, D., Sarkar, S., Koley, H., Withey, J.H. *et al.* (2020) Anti-virulence activity of polyphenolic fraction isolated from Kombucha against *Vibrio cholerae*. *Microb Pathog* **140**, 103927.

Burt, S. (2004) Essential oils: their antibacterial properties and potential applications in foods—a review. *Int J Food Microbiol* **94**, 223–253.

Chourashi, R., Mondal, M., Sinha, R., Debnath, A., Das, S., Koley, H. and Chatterjee, N.S. (2016) Role of a sensor histidine kinase ChiS of *Vibrio cholerae* in pathogenesis. *Int J Med Microbiol* **306**, 657–665.

Clinical and Laboratory Standards Institute. (2012) Methods for Dilution Antimicrobial Susceptibility Tests for Bacteria That Grow Aerobically; Approved Standard—Ninth Edition, pp. 1–68, Vol. 32, M07-A9. Wayne, PA: Clinical and Laboratory Standards Institute. www.clsi.org

Das, B., Verma, J., Kumar, P., Ghosh, A. and Ramamurthy, T. (2020) Antibiotic resistance in *Vibrio cholerae*: understanding the ecology of resistance genes and mechanisms. *Vaccine* **38**, 83–92.

Das, S., Chourashi, R., Mukherjee, P., Gope, A., Koley, H., Dutta, M., Mukhopadhyay, A.K., Okamoto, K. *et al.* (2020) Multifunctional transcription factor CytR of *Vibrio cholerae* is important for pathogenesis. *Microbiology* **166**, 1136–1148.

De, K., Ramamurthy, T., Faruque, S.M., Yamasaki, S., Takeda, Y., Nair, G.B. and Nandy, R.K. (2004) Molecular characterisation of rough strains of *Vibrio cholera* isolated from diarrhoeal cases in India and their comparison to smooth strains. *FEMS Microbiol Lett* **232**, 23–30.

Duncan, M.C., Forbes, J.C., Nguyen, Y., Shull, L.M., Gillette, R.K., Lazinski, D.W., Ali, A., Shanks, R.M.Q. *et al.* (2018) *Vibrio cholerae* motility exerts drag force to impede attack by the bacterial predator *Bdellovibrio bacteriovorus*. *Nat Commun* **9**(1), 1–9.

Dwidar, M., Monnappa, A.K. and Mitchell, R.J. (2012) The dual probiotic and antibiotic nature of *Bdellovibrio bacteriovorus*. *BMB Rep* **45**, 71–78.

Echazarreta, M.A. and Klose, K.E. (2019) Vibrio flagellar synthesis. *Front Cell Infect Microbiol* **9**, 1–11.

Helander, I.M., Alakomi, H.-L., Latva-Kala, K., Mattila-Sandholm, T., Pol, I., Smid, E.J., Gorris, L.G.M. and von Wright, A. (1998) Characterization of the action of selected essential oil components on gram-negative bacteria. *J Agric Food Chem* **46**, 3590–3595.

Holmgren, J. (1973) Comparison of the tissue receptors for *Vibrio cholerae* and *Escherichia coli* enterotoxins by means of gangliosides and natural cholera toxoid. *Infect Immun* **8**, 851–859.

Hotta, M., Nakata, R., Katsukawa, M., Hori, K., Takahashi, S. and Inoue, H. (2009) Carvacrol, a component of thyme oil, activates PPARα and γ and suppresses COX-2 expression. *J Lipid Res* **51**, 132–139.

Hung, D.T. (2005) Small-molecule inhibitor of *Vibrio cholerae* virulence and intestinal colonization. *Science* **310**, 670–674.

Hyldgaard, M., Mygind, T. and Meyer, R.L. (2012) Essential oils in food preservation: mode of action, synergies, and interactions with food matrix componetns. *Front Microbiol* **3**, 1–24.

Jordan, N., Newton, J., Pearson, J. and Allen, A. (1998) A novel method for the visualization of the in situ mucus layer in rat and man. *Clin Sci* **95**, 97.

Kaper, J.B., Morris, J.G. and Levine, M.M. (1995) Cholera. *Clin Microbiol Rev* **8**, 48–86.

Kitaoka, M., Miyata, S.T., Unterweger, D. and Pukatzki, S. (2011) Antibiotic resistance mechanisms of *Vibrio cholerae*. *J Med Microbiol* **60**, 397–407.

Klose, K.E. and Mekalanos, J.J. (1998) Distinct roles of an alternative sigma factor during both free-swimming and colonizing phases of the *Vibrio cholerae* pathogenic cycle. *Mol Microbiol* **28**, 501–520.

Landa, P., Kokoska, L., Pribylova, M., Vanek, T. and Marsik, P. (2009) In vitro anti-inflammatory activity of carvacrol: inhibitory effect on COX-2 catalyzed prostaglandin E2 biosynthesisb. *Arch Pharm Res* **32**, 75–78.

Langeveld, W.T., Veldhuizen, E.J.A. and Burt, S.A. (2013) Synergy between essential oil components and antibiotics: a review. *Crit Rev Microbiol* **40**, 76–94.

Liu, Y., McKeever, L.C. and Malik, N.S.A. (2017) Assessment of the antimicrobial activity of olive leaf extract against foodborne bacterial pathogens. *Front Microbiol* **8**, 1–8.

Liu, Z., Miyashiro, T., Tsou, A., Hsiao, A., Goulian, M. and Zhu, J. (2008) Mucosal penetration primes *Vibrio cholerae* for host colonization by repressing quorum sensing. *Proc Natl Acad Sci USA* **105**, 9769–9774.

Livak, K.J. and Schmittgen, T.D. (2001) Analysis of relative gene expression data using real-time quantitative PCR and the 2−ΔΔCT Method. *Methods* **25**, 402–408.

Llana-Ruiz-Cabello, M., Pichardo, S., Maisanaba, S., Puerto, M., Prieto, A.I., Gutiérrez-Praena, D., Jos, A. and Cameán, A.M. (2015) In vitro toxicological evaluation of essential oils and their main compounds used in active food packaging: a review. *Food Chem Toxicol* **81**, 9–27.

Magi, G., Marini, E. and Facinelli, B. (2015) Antimicrobial activity of essential oils and carvacrol, and synergy of carvacrol and erythromycin, against clinical, erythromycin-resistant Group A Streptococci. *Front Microbiol* **6**, 1–7.

Magina, M.D.A., Dalmarco, E.M., Wisniewski, A., Simionatto, E.L., Dalmarco, J.B., Pizzolatti, M.G. and Brighente, I.M.C. (2009) Chemical composition and antibacterial activity of essential oils of Eugenia species. *J Nat Med* **63**, 345–350.

Matson, J.S., Withey, J.H. and DiRita, V.J. (2007) Regulatory networks controlling *Vibrio cholerae* virulence gene expression. *Infect Immun* **75**, 5542–5549.

Mewborn, L., Benitez, J.A. and Silva, A.J. (2017) Flagellar motility, extracellular proteases and *Vibrio cholerae* detachment from abiotic and biotic surfaces. *Microb Pathogenesis* **113**, 17–24.

Miladi, H., Zmantar, T., Chaabouni, Y., Fedhila, K., Bakhrouf, A., Mahdouani, K. and Chaieb, K. (2016) Antibacterial and efflux pump inhibitors of thymol and carvacrol against food-borne pathogens. *Microb Pathogenesis* **99**, 95–100.

Mondal, M., Nag, D., Koley, H., Saha, D.R. and Chatterjee, N.S. (2014) The *Vibrio cholerae* extracellular chitinase ChiA2 is important for survival and pathogenesis in the host intestine. *PLoS One* **9**, e103119.

Mooyottu, S., Kollanoor-Johny, A., Flock, G., Bouillaut, L., Upadhyay, A., Sonenshein, A. and Venkitanarayanan, K. (2014) Carvacrol and trans-cinnamaldehyde reduce *Clostridium difficile* toxin production and cytotoxicity in vitro. *Int J Mol Sci* **15**, 4415–4430.

Narendrakumar, L., Gupta, S.S., Johnson, J.B., Ramamurthy, T. and Thomas, S. (2019) Molecular adaptations and antibiotic resistance in *Vibrio cholerae*: a communal challenge. *Microb Drug Resist* **25**, 1012–1022.

Nostro, A., Marino, A., Blanco, A.R., Cellini, L., Di Giulio, M., Pizzimenti, F., Roccaro, A.S. and Bisignano, G. (2009) In vitro activity of carvacrol against staphylococcal preformed biofilm by liquid and vapour contact. *J Med Microbiol* **58**, 791–797.

O'May, C. and Tufenkji, N. (2011) The swarming motility of *Pseudomonas aeruginosa* is blocked by cranberry proanthocyanidins and other tannin-containing materials. *Appl Environ Microb* **77**, 3061–3067.

Obaidat, M.M. and Frank, J.F. (2009) Inactivation of *Escherichia coli* O157:H7 on the intact and damaged portions of lettuce and spinach leaves by using allyl isothiocyanate, carvacrol, and cinnamaldehyde in vapor phase. *J Food Protect* **72**, 2046–2055.

Palabiyik, S., Karakus, E., Halici, Z., Cadirci, E., Bayir, Y., Ayaz, G. and Cinar, I. (2016) The protective effects of carvacrol and thymol against paracetamol-induced toxicity on human hepatocellular carcinoma cell lines (HepG2). *Hum Exp Toxicol* **35**, 1252–1263.

Patra, T., Koley, H., Ramamurthy, T., Ghose, A.C. and Nandy, R.K. (2012) The Entner-Doudoroff pathway is obligatory for gluconate utilization and contributes to the pathogenicity of *Vibrio cholerae*. *J Bacteriol* **194**, 3377–3385.

Perez-Conesa, D., Cao, J., Chen, L., McLandsborough, L. and Weiss, J. (2011) Inactivation of *Listeria monocytogenes* and *Escherichia coli* O157:H7 biofilms by micelle-encapsulated eugenol and carvacrol. *J Food Protect* **74**, 55–62.

Rattanachaikunsopon, P. and Phumkhachorn, P. (2010) Assessment of factors influencing antimicrobial activity of carvacrol and cymene against *Vibrio cholerae* in food. *J Biosci Bioeng* **110**, 614–619.

Saha, P., Das, B. and Chaudhuri, K. (2013) Role of 6-gingerol in reduction of cholera toxin activity in vitro and in vivo. *Antimicrob Agents Chemother* **57**, 4373–4380.

Sarwar, S., Ali, A., Pal, M. and Chakrabarti, P. (2017) Zinc oxide nanoparticles provide anti-cholera activity by disrupting the interaction of cholera toxin with the human GM1 receptor. *J Biol Chem* **292**, 18303–18311.

Shakhnovich, E.A., Hung, D.T., Pierson, E., Lee, K. and Mekalanos, J.J. (2007) Virstatin inhibits dimerization of the transcriptional activator ToxT. *Proc Natl Acad Sci USA* **104**, 2372–2377.

Sharifi-Rad, M., Varoni, E.M., Iriti, M., Martorell, M., Setzer, W.N., del Mar Contreras, M., Salehi, B., Soltani-Nejad, A. *et al.* (2018) Carvacrol and human health: a comprehensive review. *Phytother Res* **32**, 1675–1687.

Silva, A.J. (2003) Haemagglutinin/protease expression and mucin gel penetration in El Tor biotype *Vibrio cholerae*. *Microbiology* **149**, 1883–1891.

Slameňová, D., Horváthová, E., Šramková, M. and Maršálková, L. (2007) DNA-protective effects of two components of essential plant oils carvacrol and thymol on mammalian cells cultured in vitro. *Neoplasma* **54**, 108–112.

Slamenova, D., Horvathova, E., Marsalkova, L. and Wsolova, L. (2008). Carvacrol given to rats in drinking water reduces the level of DNA lesions induced in freshly isolated hepatocytes and testicular cells by H_2O_2. *Neoplasma*, **55**, 394.

Suntres, Z.E., Coccimiglio, J. and Alipour, M. (2015) The bioactivity and toxicological actions of carvacrol. *Crit Rev Food Sci* **55**, 304–318.

U.S. Food and Drug Administration (1998). EAFUS: a food additive database. pp. 1–153. http://www.usc.es/caa/Edulc Web/EAFUS

Ultee, A., Kets, E.P.W. and Smid, E.J. (1999) Mechanisms of action of carvacrol on the food-borne pathogen *Bacillus cereus*. *Appl Environ Microb* **65**, 4606–4610.

Ultee, A., Kets, E.P.W., Alberda, M., Hoekstra, F.A. and Smid, E.J. (2000) Adaptation of the food-borne pathogen *Bacillus cereus* to carvacrol. *Arch Microbiol* **174**, 233–238.

Ultee, A. and Smid, E.J. (2001) Influence of carvacrol on growth and toxin production by *Bacillus cereus*. *Int J Food Microbiol* **64**, 373–378.

Verma, J., Bag, S., Saha, B., Kumar, P., Ghosh, T.S., Dayal, M., Senapati, T., Mehra, S. *et al.* (2019) Genomic plasticity associated with antimicrobial resistance in *Vibrio cholerae*. *Proc Natl Acad Sci USA* **116**, 6226–6231.

Weber, F.J. and de Bont, J.A.M. (1996). Adaptation mechanisms of microorganisms to the toxic effects of organic solvents on membranes. *Biochimica et Biophysica Acta (BBA) – Reviews on Biomembranes* **1286**, 225–245.

World Health Organization (2019). Weekly epidemiological record – cholera 2018. pp. 561–580. https://www.who.int/wer/2019/wer9448

Yamasaki, S., Asakura, M., Neogi, S.B., Hinenoya, A., Iwaoka, E. and Aoki, S. (2011) Inhibition of virulence potential of

Vibrio cholerae by natural compounds. *Indian J Med Res* **133**, 232–239.

Yeung, A.T.Y., Parayno A. and Hancock, R.E.W. (2012) Mucin promotes rapid surface motility in Pseudomonas aeruginosa. *mBio* **3**(3), 1–12.

Yin, H., Deng, Y., Wang, H., Liu, W., Zhuang, X. and Chu, W. (2015) Tea polyphenols as an antivirulence compound disrupt quorum-sensing regulated pathogenicity of *Pseudomonas aeruginosa*. *Sci Rep UK* **5**, 1–11.

Supporting Information

Additional Supporting Information may be found in the online version of this article:

Figure S1. Effect of carvacrol on cholera toxin (CT) production and virulence gene expression.

Table S1. List of primers used in quantitative real time PCR experiment.

Chitin–induced T6SS in *Vibrio cholerae* is dependent on ChiS activation

Rhishita Chourashi,[1] Suman Das,[1] Debarpan Dhar,[2] Keinosuke Okamoto,[3] Asish K. Mukhopadhyay[4] and Nabendu Sekhar Chatterjee[1,*]

Abstract

Vibrio cholerae regularly colonizes the chitinous exoskeleton of crustacean shells in the aquatic region. The type 6 secretion system (T6SS) in *V. cholerae* is an interbacterial killing device. This system is thought to provide a competitive advantage to *V. cholerae* in a polymicrobial community of the aquatic region under nutrient-poor conditions. *V. cholerae* chitin sensing is known to be initiated by the activation of a two-component sensor histidine kinase ChiS in the presence of $GlcNAc_2$ (N,N′-diacetylchitobiose) residues generated by the action of chitinases on chitin. It is known that T6SS in *V. cholerae* is generally induced by chitin. However, the effect of ChiS activation on T6SS is unknown. Here, we found that ChiS inactivation resulted in impaired bacterial killing and reduced expression of T6SS genes. Active ChiS positively affected T6SS-mediated natural transformation in *V. cholerae*. ChiS depletion or inactivation also resulted in reduced colonization on insoluble chitin surfaces. Therefore, we have shown that *V. cholerae* colonization on chitinous surfaces activates ChiS, which promotes T6SS-dependent bacterial killing and horizontal gene transfer. We also highlight the importance of chitinases in T6SS upregulation.

INTRODUCTION

Vibrio cholerae is a natural inhabitant of the aquatic environment [1]. It resides on the chitinous exoskeleton of planktonic copepods and utilizes chitin, a polymer of *N*-acetyl glucosamine (GlcNAc), as a sole carbon source. Chitin utilization in *V. cholerae* is controlled by a sensor histidine kinase ChiS (VC0622), which is an inner-membrane protein [2]. ChiS is a 133 kDa sensor histidine kinase that belongs to the 'two-component system' (TCS). The other part of the TCS is a response regulator that has not yet been identified for ChiS. ChiS has a short N-terminal peptide chain in the cytoplasm, a membrane domain, a periplasmic domain, a second membrane domain and finally a long polypeptide chain extending into the cytoplasm [2]. It remains in an inactive form through a chitin oligosaccharide binding protein known as CBP, which binds to the periplasmic domain of ChiS and forms a ChiS-CBP complex. After being hydrolyzed from chitin by the action of chitinases, GlcNAc residues bind to CBP. CBP then detaches itself from ChiS [2]. Free ChiS then becomes active, which in turn activates the cytoplasmic response regulator that interacts with

downstream genes. Recently, we demonstrated that ChiS plays a role in *V. cholerae* pathogenesis [3].

The downstream genes of ChiS include the *chb* operon, which consists of a cluster of 10 contiguous genes (VC0620–VC0611) that are involved in chitin utilization [4]. The other downstream effector is an activator protein known as TfoX. ChiS provides an as yet unidentified signal that activates another sensor, TfoS, which upregulates the transcription of *tfoR* [5]. This TfoR, in the next step, upregulates the translation of TfoX, leading to competence induction [6, 7]. TfoX (VC1153) is one of the major regulators required for natural competence activation in the presence of GlcNAc residues [6]. TfoX, in conjunction with another regulator known as HapR, controls the expression of natural competence genes, i.e. *pilA* and *comEA*, which are required for DNA uptake and stabilization, respectively [8–10]. Another regulator CytR is also required alongside TfoX and HapR [11, 12]. The production of TfoX, in turn, is controlled by chitin. TfoX and CytR induce two extracellular chitinase genes, *chiA1* and *chiA2* [6, 11–13].

TfoX activates a molecular mechanism known as the type VI secretion system (T6SS) in *V. cholerae* [14]. The T6SS is a molecular cell puncturing device that injects toxic factors into non-immune bacteria as well as eukaryotic cells causing cell lysis [15–18]. Consequently, it induces the uptake of genetic material from lysed bacteria, leading to horizontal gene transfer [14, 19]. This system is present in many Gram-negative bacterial genomes [16, 20]. The T6SS consists of multiple components, including the transcriptional regulator, VasH. VasH promotes the production of haemolysin-coregulated protein (Hcp). The Hcp is a small 17.4 kDa protein that forms a tube-like structure. Hcp hexamers form the inner tube of T6SS and its secretion only occurs in the presence of a structural component of T6SS, i.e. VasK. T6SS structurally resembles a phage tail-like spike with cell puncturing ability [21]. The Hcp inner tube complex is connected to a phage-like base plate. This phage-like base plate, along with a membrane-spanning unit, constitutes the structural apparatus of the T6SS [22]. The inner tube is decorated on the outside with a contractile sheath structure made up of VipA and VipB proteins in *V. cholerae*. When the sheath contracts, the inner tube propels into neighbouring cells, delivering effector toxins inside the bacteria and leading to killing of the cells [15, 23].

It was already known that in the aquatic environment *V. cholerae* ChiS is activated by (GlcNAc)$_2$ [2]. This (GlcNAc)$_2$ is also present in the chitinous sources of the aquatic environment. T6SS in *V. cholerae* is also induced by growth on chitinous surfaces [14]. T6SS helps *V. cholerae* to compete with the neighbouring bacterial community, survive under nutrient-poor conditions and utilize chitin as a nutrient source. Hence, we speculated that ChiS might be important in the upregulation of T6SS. Here, we show that ChiS is activated in the presence of chitin, as shown previously [5, 24]. The chitinases release GlcNAc residues that help in the initiation of ChiS activation, leading to chitin utilization. We found that, upon activation, ChiS positively controlled the expression of T6SS genes. We also found that ChiS is involved in T6SS-mediated bacterial killing and natural competence in *V. cholerae* in the presence of chitin. Therefore, activated ChiS upregulates T6SS in *V. cholerae*. In this context, we can also say that chitinases control T6SS through the activation of ChiS. We demonstrate the importance of *V. cholerae* chitinases in T6SS for the first time here.

METHODS

Bacterial strains and culture conditions

In this study, we used the streptomycin-resistant *V. cholerae* C6706 El Tor strain as the wild-type (WT). We constructed isogenic mutants of *chiS*, *chiA1* and *chiA2*, and double mutants of both *chiA1* and *chiA2*, and designated them as Δ*chiS*, Δ*chiA1*, Δ*chiA2* and Δ*chiA1*Δ*chiA2* throughout this paper. The details of each strain are listed in Table 1. The WT and mutant strains (Δ*chiS*, Δ*chiA1*, Δ*chiA2* and Δ*chiA1*Δ*chiA2*) were grown overnight in LB (Luria Bertini) medium (BD Difco) at 37 °C with

appropriate antibiotics. The bacteria were then grown in defined artificial seawater media (DASW) containing 0.5 % sodium lactate and supplemented with 0.8 % coarse chitin (sigma) or 0.6 mM of GlcNAc$_2$ at 30 °C. The composition of DASW was as follows: 234 mM NaCl, 27.5 mM MgSO$_4$, 1.5 mM NaHCO$_3$, 4.95 mM CaCl$_2$, 5.15 mM KCl, 0.07 mM Na$_2$B$_4$O$_7$, 0.05 mM SrCl, 0.015 mM NaBr, 0.001 mM NaI, 0.013 mM LiCl, 18.7 mM NH$_4$Cl, 0.187 mM K2HPO4, 50 mM HEPES, pH 7.4. Sodium lactate was added to the DASW to support the equal growth of WT and mutant strains in all of the experiments.

Construction of genetically modified strains in *V. cholerae*

In-frame deleted mutant strains of *chiS, chiA1, chiA2* and *chiA1chiA2* were generated by allelic exchange using the suicidal plasmid pCVD442 as mentioned previously [3]. Mutants were confirmed by a PCR-based method using the primers that are mentioned in the supplementary material (Table S1, available in the online version of this article).

Recombinant DNA techniques

All DNA manipulations were performed using standard molecular biology-based methods. For the transcriptional and translational assay, we used the β-galactosidase-expressing plasmid pTL61T. We cloned *tfoX* and *tfoR* promoter genes in this plasmid. In short, the genes were amplified from genomic DNA by PCR using the primers mentioned in the supplementary material (Table S1). The gene inserts were cloned into plasmid pTL61T to generate plasmid-borne fusions by using the restriction enzymes Xho1 and Xba1 (New England Biolabs) to generate the restriction sites in both the insert and the vector. DNA ligase was used (Promega) for the ligation reaction. The fusion plasmid was then transformed in all the strains of *V. cholerae* (Table 1).

β-hexosaminidase activity assay

β-hexosaminidase activity was estimated by a previously followed procedure [2] with p-nitrophenyl, *N*-acetyl-β-D-glucose (PNP-GlcNAc) (Sigma). To analyse β-hexosaminidase activity, WT *V. cholerae* C6706 and its deletion mutants Δ*chiS*, Δ*chiA1*, Δ*chiA2* and Δ*chiA1*Δ*chiA2* were grown in 0.5 % sodium lactate containing DASW media individually supplemented with 0.8 % coarse chitin or 0.6 mM GlcNAc$_2$. The bacteria were diluted to 1×10^5 c.f.u ml^{-1} and washed and treated with toluene at a ratio of 10 µl ml^{-1} of culture. The mixture was shaken vigorously and kept at RT for 20 min. Then 0.1 ml of these treated bacteria were mixed with 0.1 ml of 1 mM substrate, i.e PNP-GlcNAc, in 20 mM Tris-HCl (pH 7.5) and incubated for 60 min at 37 °C. Following this, 0.8 ml of 1 M Tris-base was added to stop the reaction. The reaction mixture was centrifuged to separate the cell debris and the optical density of the supernatant was measured at 400 nm. The total enzymatic activity was determined by measuring the total protein by the Lowry method and then calculated as p-nitrophenol produced per minute per mg of total protein.

Table 1. List of strains and plasmids used in this study

Strains or plasmids	Description and role	Source
Strains		
Escherichia coli		
SM10 λpir	*E. coli*, λpir host for R6K origin plasmids and mobilizing strain, Kan^R	[27]
V. cholerae C6706	WT*Vibrio cholerae* O1 El Tor, Str^R	[6]
C6706 Δ*chiS*	Δ*vc0622*, Str^R, ChiS – sensor kinase	This study
C6706 Δ*chiA1*	Δ*vc1952*, Str^R, ChiA1 – extracellular chitinase	This study
C6706 Δ*chiA2*	Δ*vc0027*, Str^R, ChiA2 – extracellular chitinase	This study
C6706 Δ*chiA1* Δ*chiA2*	Δ*vc1952*Δ*vc0027*, Str^R	This study
WTTX	P$_{tfoR}$–*LacZ* transcriptional fusion into WT *V. cholerae* C6706	This study
Δ*chiS* TX	P$_{tfoR}$–*LacZ* transcriptional fusion into the deletion mutant of *chiS* in C6706	This study
Δ*chiA1* TX	P$_{tfoR}$–*LacZ* transcriptional fusion into the deletion mutant of *chiA1* in C6706	This study
Δ*chiA2* TX	P$_{tfoR}$–*LacZ* transcriptional fusion into the deletion mutant of *chiA2* in C6706	This study
Δ*chiA1*Δ*chiA2* TX	P$_{tfoR}$–*LacZ* transcriptional fusion into the deletion mutant of *chiA1and chiA2* in C6706	This study
WTTL	P$_{tfoX}$–*LacZ* translational fusion into WT *V. cholerae* C6706	This study
Δ*chiS* TL	P$_{tfoX}$–*LacZ* translational fusion into the deletion mutant of *chiS* in C6706	This study
Δ*chiA1* TL	P$_{tfoX}$–*LacZ* translational fusion into the deletion mutant of *chiA1* in C6706	This study
Δ*chiA2* TL	P$_{tfoX}$–*LacZ* translational fusion into the deletion mutant of *chiA2* in C6706	This study
Δ*chiA1*Δ*chiA2* TL	P$_{tfoX}$–*LacZ* translational fusion into the deletion mutant of *chiA1* and *chiA2* in C6706	This study
Plasmids		
pGEM-T easy	TA-cloning vector, Amp^R	Promega
pCVD442	Suicidal conjugation vector carrying *sacB*, Amp^R	[3]
pTL6IT	LacZ β-galactosidase reporter assay vector, Amp^R. The promoters of *tfoX* (P$_{tfoX}$) and *tfoR* (P$_{tfoR}$) were cloned upstream of the reporter gene (*LacZ*) of the plasmid pTL6IT and then used for the reporter assay.	[40]

Resistance to Amp^R, ampicillin-resistant; Str^R, streptomycin-resistant; WT*, wild-type.

Escherichia coli killing assay

An *E. coli* killing assay was performed by modifying previously mentioned protocols [14]. Briefly, overnight cultures of all *V. cholerae* strains and the prey bacteria, i.e. an *E. coli* DH5α strain carrying the ampicillin-resistant (100 µg ml^{-1}) plasmid pBR322, were grown in LB at 37 °C. All of the *V. cholerae* strains were grown to log phase in sodium lactate-supplemented DASW medium containing either 0.8 % chitin or 0.6 mM GlcNAc$_2$. The prey bacteria were also grown to log phase.The prey cells were then mixed with WT and mutant strains of *V. cholerae* at a ratio of 1 : 10, and 30 µl of the mixture was spotted in LB agar plates and grown statically at 30 °C for 5 h. *E. coli* prey bacteria were also spotted in LB agar plates in the absence of predator bacteria. Bacterial spots were then harvested and plated on LB agar plates containing 100 µg ml^{-1} ampicillin to enumerate the surviving *E. coli* prey cells. In the above experiment, Δ*tfoX* was used as a negative control.

T6SS-dependent natural transformation in mixed communities

To quantify T6SS-dependent natural transformation, the bacterial strains, i.e. *V. cholerae* and the *E. coli* DH5α strain carrying the ampicillin-resistant (100 µg ml^{-1}) plasmid pBR322, were grown as a co-culture on sodium lactate-supplemented DASW media containing 0.8 % coarse chitin or 0.6 mM GlcNAc$_2$ (Sigma) [14]. The mixture was vortexed and incubated statically for 10 h at 30 °C. The bacteria were detached from the chitin surfaces by rigorous vortexing. Serial dilutions were spread on LB agar plates containing either streptomycin 100 µg ml^{-1} (to selected predator cells, i.e. *V. cholerae*) or ampicillin 100 µg ml^{-1} and streptomycin 100 µg ml^{-1} (to selected transformants). The transformation frequencies were calculated by dividing the number of transformants by the total number of predator colony-forming units (c.f.u.s). Further, the transformed bacteria were also enumerated from LB agar plates containing ampicillin and streptomycin.

To confirm that the transformed colonies of *V. cholerae* were only due to natural transformation, *V. cholerae* WT strain bacteria were incubated with 10 µg ml^{-1} plasmid pBR322 in the presence and absence of 30 µg ml^{-1} DNAse in DASW media containing sodium lactate and supplemented with chitin or GlcNAc$_2$. To show that the plasmid pBR322 is transferred by T6SS-induced natural transformation from the prey bacteria to the predator in the mixed culture medium, we also showed the effect of DNAse in a co-culture of the *E. coli* DH5α (prey) strain harbouring pBR322 and WT *V. cholerae* (predator) in DASW media containing sodium lactate and supplemented with or

without chitin-based sources, i.e. chitin or $GlcNAc_2$. After 10 h of static incubation, the transformed bacteria were enumerated by the plate count method after spread plating on LB agar with appropriate antibiotics. Here, we also used WT *V. cholerae* N16961, which is already known to be defective in chitin-induced natural transformation and T6SS, as a control strain [6, 14]. For further confirmation, the co-cultured samples were also subjected to plasmid purification, and the plasmid was digested with EcoR1 and applied to 0.8 % (w/v) agarose/Tris-acetate-EDTA (TAE) gel. The transformed plasmid was detected by subjecting the mixed culture medium samples to PCR by using primers (Table S1) that amplify the 227 bp region of the plasmid, which contains the ampicillin-resistant gene.

Total RNA isolation and real-time PCR

WT *V. cholerae* C6706 and its deletion mutants Δ*chiS*, Δ*chiA1*, Δ*chiA2* and Δ*chiA1*Δ*chiA2* were grown in sodium lactate-supplemented DASW media with 0.8 % coarse chitin or $GlcNAc_2$ (from shrimp shells; Sigma) and harvested from the mid-log phase. Bacterial pellets were washed three times with PBS and then used for RNA isolation. Total RNA was isolated using TriZol (Invitrogen) following the manufacturer's protocol. DNase treatment was performed using the DNA-free kit (Ambion) for the elimination of contaminating genomic DNA. cDNA synthesis was performed with a Reverse Transcription kit (Promega) using 1 μg of total RNA according to the manufacturer's protocol. The mRNA transcript levels were quantified by real-time PCR using 2×SYBR Green PCR Master Mix (Applied Biosystems) and 0.2 μM of specific real-time primers for the competence genes (*tfoX*, *PilA* and *comEA*) and T6SS gene cluster (*vipA*, *vipB*, *vasH*, *vasD*, *vasK*), which were designed using IDT and are mentioned in the supplementary material (Table S1). Data analysis was performed using the 7500 Real-Time PCR Detection System (Applied Biosystems). The relative expression of the target transcripts was calculated according to the Livak method [25]. RecA was used as an internal control.

Miller assays

Miller assays were used to measure the LacZ activity of the transcriptional reporter strains as previously described [26]. In short, overnight cultures of all of the strains were grown up to log phase in LB at 37 °C. Next, bacteria were finally transferred to sodium lactate-supplemented DASW media containing 0.8 % coarse chitin or 0.6 mM $GlcNAc_2$. They were grown to mid-log phase at 30 °C under static conditions for 16–24 h. Bacteria were collected and washed with PBS and then placed on ice for 30 min. Then 200 μl of the culture was resuspended in 'Z' buffer (16.1 g Na_2HPO_4.$7H_2O$, 5.5 g NaH_2PO_4.H_2O, 0.75 g KCl, 0.246 g $MgSO_4$.$7H_2O$ dissolved in distilled water to make a final volume of 1L; β-ME is added to obtain a final concentration of 0.27 % before use). After this, 30 μl 0.1 % SDS and 60 μl of chloroform were added to each sample and vortexed for 10 s. Next, 200 μl of substrate, i.e. ONPG (o-nitrophenyl – β-D-galactoside) solution, was added and incubated at 28 °C.

The reaction was stopped by adding 500 μl of 1 M Na_2CO_3 as soon as the reaction mixture turned turn yellow. The OD_{420} and OD_{550} values were recorded and β-galactosidase activity was expressed as Miller units, which are calculated using the equation,

$$\text{Miller units} = 1000 \times [OD_{420} - (1.75 \times OD_{550})/t \times v \times OD_{600}],$$

where v is the initial volume of the culture and t is the total time of the reaction.

Generation of growth curve

Log phase cultures of WT *V. cholerae* C6706 (WT) and its deletion mutants Δ*chiS*, Δ*chiA1*, Δ*chiA2* and Δ*chiA1*Δ*chiA2* were harvested by centrifugation and washed three times in PBS. The cell number was adjusted to 1×10^5 c.f.u. ml^{-1} and inoculated in DASW media supplemented with 0.5 % sodium lactate as the only carbon source. DASW media was also individually supplemented with 0.8 % chitin flakes or with 0.6 mM $GlcNAc_2$ (sigma) as the only carbon source. The cultures were maintained at 30 °C under constant shaking at 150 r.p.m. for 48 h [27]. For the analysis of viable counts, cultures were vortexed to detach any bound bacteria and diluted, and viable bacteria were plated on LB agar plates supplemented with streptomycin.

Chitin colonization assay

The chitin colonization assay was analysed by following a modified procedure from a previously mentioned protocol [28]. All strains of *V. cholerae* C6706 were grown overnight and log phase cultures at a dilution of 1×10^5 c.f.u. ml^{-1} were mixed with prewashed chitin beads at a ratio of 1.1. The samples were kept at 30 °C under static conditions for 18 h. The bacteria were passed through an 8 μm membrane filter (HiMedia) to wash out unbound bacteria. Chitin beads were resuspended in PBS and vortexed to harvest bound bacteria and then serially diluted to plate on LB agar plates containing streptomycin.

For qualitative analysis of bacterial colonization, all strains of *V. cholerae* were GFP-tagged following a previously mentioned protocol [28]. In short, chitin beads were inoculated with GFP-tagged bacteria for 18 h at 30 °C under static conditions. The chitin beads were mounted on glass slides and visualized under a confocal microscope (LSM 710 Axio Observer, Carl Zeiss) to show the GFP-labelled bacteria bound to the surface of the chitin beads.

Statistical analysis

All of the experiments were analysed by Student's *t*-test. Each of the experiments was performed in triplicate and the results are represented as mean±SEM. A *P* value of <0.05 was considered statistically significant.

RESULTS

ChiS-dependent β-hexosaminidase activity is enhanced in presence of chitin

We first measured ChiS-dependent β-hexosaminidase activity. Since β-hexosaminidase is directly controlled by

ChiS, measuring its activity shows that the ChiS is activated [2]. So, we first measured the β-hexosaminidase activity of the WT and an isogenic mutant of *chiS* ($\Delta chiS$) grown in sodium lactate-supplemented DASW media containing either chitin or GlcNAc$_2$. We found that the β-hexosaminidase activity increased in the presence of chitin in the WT strain, with an activity of 145 nmoles min^{-1} mg^{-1} compared to 16.4 nmoles min^{-1} mg^{-1} in the case of $\Delta chiS$. This shows that the β-hexosaminidase activity in $\Delta chiS$ has been reduced by ninefold compared to that in the WT (Fig. 1a). We also found that in the presence of 0.6 mM GlcNAc$_2$, the β-hexosaminidase activity of the WT strain was 149.3 nmoles min^{-1} mg^{-1} compared to 19 nmoles min^{-1} mg^{-1} in the case of $\Delta chiS$, showing a 7.8-fold reduction. Next, we measured β-hexosaminidase activity in the

mutants, i.e. the $\Delta chiA1$, $\Delta chiA2$ and $\Delta chiA1\Delta chiA2$ strains, in the presence of chitin or 0.6 mM GlcNAc$_2$. The mutant strains with $\Delta chiA1$, $\Delta chiA2$ and $\Delta chiA1\Delta chiA2$ showed β-hexosaminidase activity of 74, 31, 33 nmoles min^{-1} mg^{-1}, respectively. Therefore, the $\Delta chiA1$, $\Delta chiA2$ and $\Delta chiA1\Delta chiA2$ strains showed 2.2, 4.6- and 4.3-fold reductions, respectively, compared to the WT strain in the presence of chitin. However, all of these mutant strains ($\Delta chiA1$, $\Delta chiA2$ and $\Delta chiA1\Delta chiA2$) showed ChiS-dependent β-hexosaminidase activity that was almost similar to that of the WT in the presence of GlcNAc$_2$ when it was added exogenously (Fig. 1b). When DASW media were supplemented solely with sodium lactate and did not contain chitin or GlcNAc$_2$, negligible β-hexosaminidase activity was found in all the strains. This shows that chitin
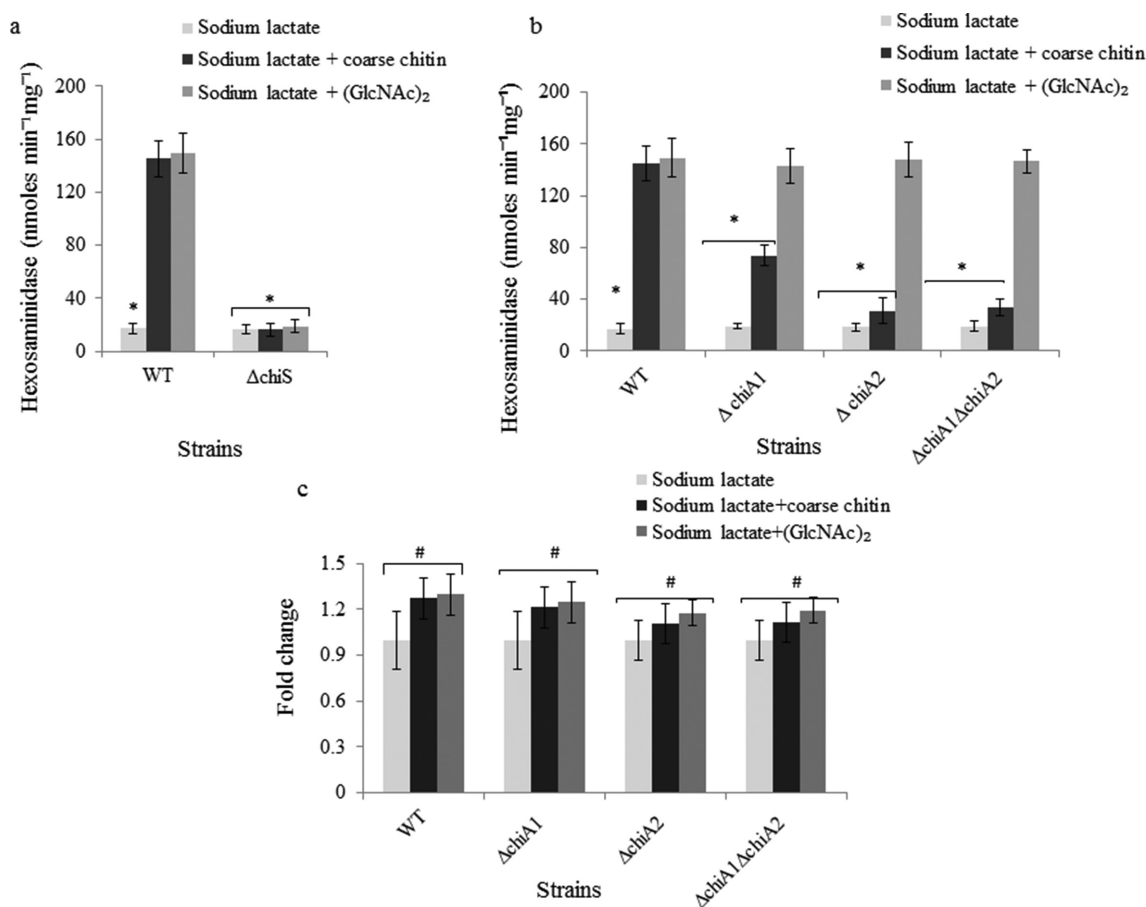

Fig. 1. Activation of ChiS is promoted in the presence of chitin. Bacteria were grown in DASW media supplemented with 0.8 % coarse chitin or 0.6 mM GlcNAc$_2$, with 0.5 % sodium lactate being added to each medium to obtain similar bacterial growth. Log phase cultures were taken to measure the total hexosaminidase (ChiS-regulated periplasmic enzyme) activity in (a) the WT (*V. cholerae* C6706) and $\Delta chiS$ (isogenic ChiS mutant) strains, and (b) the $\Delta chiA1$ (isogenic *chiA1* mutant), $\Delta chiA2$ (isogenic *chiA2* mutant) and $\Delta chiA1\Delta chiA2$ (isogenic *chiA1* and *chiA2* double-mutant) strains grown in DASW media individually supplemented with (▨) sodium lactate, (■) sodium lactate+coarse chitin and (▦) sodium lactate+GlcNAc$_2$. Each of the experiments was repeated three times (*n*=3). All the data are expressed as means±SEM. *, *P*<0.05. (c) Log phase cultures of the WT, $\Delta chiA1$, $\Delta chiA2$ and $\Delta chiA1\Delta chiA2$ strains were also used for total RNA isolation, while *chiS* gene expression was measured by qRT-PCR. Log-phase cultures were taken from DASW media individually supplemented with (▨) sodium lactate, (■) sodium lactate+coarse chitin and (▦) sodium lactate+GlcNAc$_2$. All the data are expressed as means±SEM. #, *P*>0.05, not significant.

activates the chitin utilization pathway by inducing ChiS. It was the $GlcNAc_2$ residues released from chitin following hydrolysis by the chitinases ChiA1 and ChiA2 that initiated the ChiS activation.

We also measured the ChiS mRNA levels by qPCR in the different media mentioned above. We found similar mRNA expression in the cases of the WT and the Δ*chiA1*, Δ*chiA2* and Δ*chiA1*Δ*chiA2* mutant strains, respectively (Fig. 1c). This shows that there is no change in ChiS expression level, while it is only activated in the presence of $GlcNAc_2$ which results in the upregulation of ChiS-controlled downstream genes.

ChiS promotes T6SS in *V. cholerae*

We next investigated the effect of ChiS, ChiA1 and ChiA2 on T6SS. The Δ*chiS* strain showed significant downregulation of *vasH, vasD, vasK, vipA, vipB* genes compared to the WT strain in the presence of chitin ($P<0.05$) (Fig. 2a). This

supported our hypothesis that ChiS controls the expression of T6SS genes. The T6SS genes (*vasH, vasD, vasK, vipA* and *vipB*) were also downregulated in Δ*chiA1*, Δ*chiA2* and Δ*chiA1*Δ*chiA2* mutants compared to the WT levels ($P<0.05$) in the presence of chitin. However, the expression levels reverted back to levels that were close to those of the WT in the presence of $GlcNAc_2$ (Fig. 2b). This indicated that ChiS-induced expression of T6SS genes was initiated by $GlcNAc_2$ when released by chitinases from chitin.

We also explored the effect of bacterial killing of *E. coli* DH5α (prey) by T6SS in all the strains of *V. cholerae* (predator). We found that in the presence of chitin in sodium lactate-supplemented DASW media, the mutants led to increased survival of the prey bacteria compared to the WT *V. cholerae*. The number of prey bacteria that survived was 3.5×10^7, 3×10^6, 1×10^7 and 1.36×10^7 c.f.u. ml^{-1} for Δ*chiS*, Δ*chiA1*, Δ*chiA2* and Δ*chiA1*Δ*chiA2*-treated prey bacteria, respectively. The number of prey bacteria
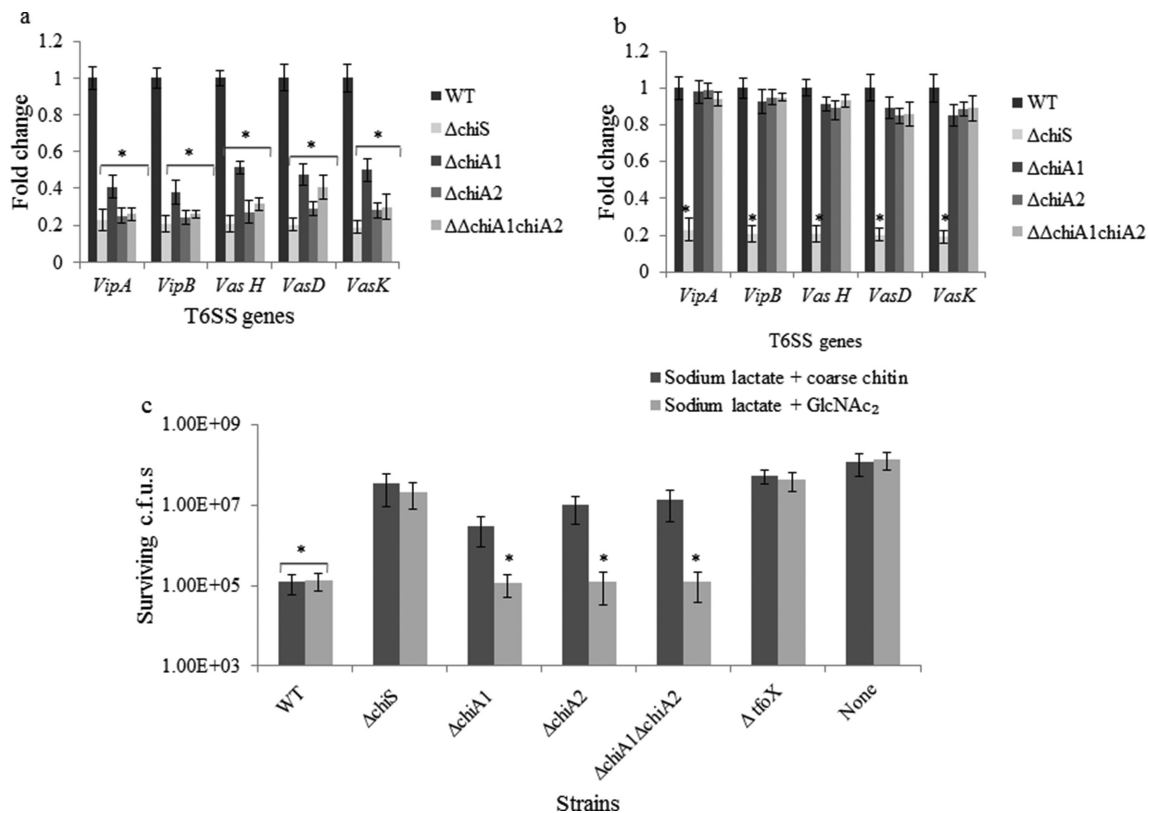

Fig. 2. ChiS contributes in T6SS in *V. cholerae*. Bacteria were grown in DASW media supplemented with 0.8 % coarse chitin or 0.6 mM $GlcNAc_2$, with 0.5% sodium lactate being added to each medium to obtain similar bacterial growth. Log-phase cultures were taken from DASW media individually supplemented with (a) coarse chitin or (b) $GlcNAc_2$, with total RNA being isolated and T6SS gene expression being measured by qRT-PCR. (c) *E. coli* killing assay: log-phase cultures of the prey bacteria, i.e. the *E. coli* DH5α strain with the ampicillin-resistant plasmid pBR322 grown in the presence of ampicillin (100 µg ml^{-1}), were mixed with all the indicated *V. cholerae* strains at a ratio of 1 : 10, with 30 µl being spotted on an LB plate and then incubated statically at 30 °C for 10 h. All the indicated *V. cholerae* strains were pregrown to log phase in (■) sodium lactate+coarse chitin or (■) sodium lactate+$GlcNAc_2$-supplemented DASW media. Bacterial samples were harvested from the spots and plated on LB agar plates containing 100 µg ml^{-1} ampicillin to enumerate the surviving *E. coli* prey cells. Each of the experiments was repeated three times (*n*=3). All the data are expressed as means ±SEM. *, $P<0.05$.
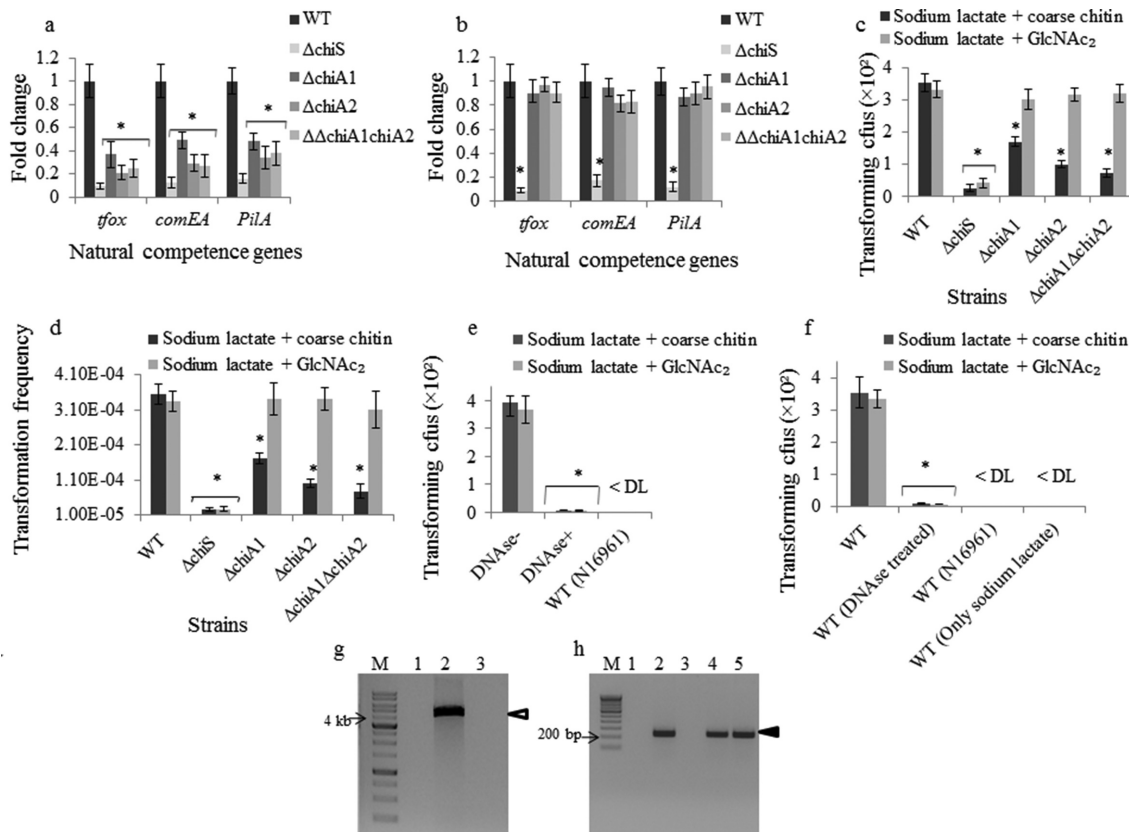
Fig. 3. ChiS promotes T6SS-induced natural transformation in *V. cholerae*. Bacteria were grown in DASW media supplemented with 0.8 % coarse chitin or 0.6 mM GlcNAc$_2$, with 0.5% sodium lactate being added to each medium to obtain similar bacterial growth. The bacterial cultures were washed, total RNA was isolated and the expression of natural competence genes was measured by qRT-PCR in the presence of (a) (■) sodium lactate+coarse chitin or (b) (■) sodium lactate+GlcNAc$_2$. (c) T6SS-induced natural transformation was analysed by co-culturing all the strains of *V. cholerae* and the *E. coli* DH5α strain carrying the ampicillin-resistant plasmid pBR322 in (■) sodium lactate+coarse chitinor and (■) sodium lactate+GlcNAc$_2$-supplemented DASW media, and then incubating them statically for 10 h at 30 °C. The transformed bacteria were enumerated by plating on LB agar plates containing ampicillin and streptomycin. (d) The transformation frequencies were calculated by dividing the number of transformants by the total number of predator c.f.u.s and are represented graphically. (e) Quantification of natural transformation with the purified plasmid (10 µg ml^{-1}) in the WT *V. cholerae* strain in the presence or absence of DNAse (30 µg ml^{-1}) in the DASW media supplemented with (■) sodium lactate+coarse chitin or (■) sodium lactate+GlcNAc$_2$. (f) Measurement of T6SS-induced natural transformation in the presence or absence of DNAse in the mixed culture medium of the *E. coli* DH5α strain carrying the ampicillin-resistant plasmid pBR322 and *V. cholerae* in (■) sodium lactate+coarse chitin or (■) sodium lactate+GlcNAc$_2$-supplemented DASW media. WT *V. cholerae* N16961 is used as a negative control. Each of the experiments was repeated three times (*n*=3). The absence of bars indicates outcomes that were below the detection limit, shown as <DL. All the data are expressed as means±SEM. *, *P*<0.05. (g) Confirmation of the workability of DNAse in DASW medium. DNAse (30 µg ml^{-1}) were added to the co-culture of the *E. coli* DH5α strain (prey) harbouring pBR322 and *V. cholerae* (predator), and incubated statically for 10 h at 30 °C. Plasmid DNA was isolated and digested with EcoR1 and applied to 0.8 % agarose/TAE gel. Lane M, 1 kb marker; lane 1, control (DNA free); lane 2, plasmid pBR322 isolated from the sample of the co-culture of the prey and predator; lane 3, plasmid isolated from the sample with DNAse added in the co-culture of the prey and predator. The arrowheads show the plasmid pBR322 (4.6 kb). (h) Detection of the plasmid. Samples were used directly for PCR and applied to 1.5 % agarose TAE gel electrophoresis. Lane M, 100 bp marker; lane 1, medium sample from the co-culture without PCR; lane 2, positive control – PCR product from the purified pBR322 DNA; lane 3, PCR product from DNase-treated mixed sample of prey and predator; lane 4, PCR product from sample of *E. coli* DH5α strain harbouring pBR322 and *V. cholerae*; lane 5, PCR product from positive colony of T6SS-induced naturally transformed *V. cholerae*.

that survived in the presence of the WT was 1.2×10^5 c.f.u. ml^{-1}. Therefore, the survival of the prey increased by 270-, 25-, 83- and 113-fold in the case of Δ*chiS*, Δ*chiA1*, Δ*chiA2* and Δ*chiA1*Δ*chiA2*, respectively, compared to prey survival when mixed with the WT strain. We also found that in the

presence of GlcNAc$_2$ the effect of Δ*chiA1*, Δ*chiA2* and Δ*chiA1*Δ*chiA2* mutants on prey survival was nullified (Fig. 2c). This showed that chitinases have their own role in initiating ChiS activation, which is important for T6SS-mediated bacterial killing. The prey bacteria showed normal

growth in the absence of any predator bacteria. Moreover, when mixed with Δ*tfoX*, the prey bacteria showed significantly higher survival, which is in agreement with previous studies that reported that *tfoX* positively controls T6SS [14]. Therefore, ChiS is the regulator that induced T6SS via the *tfoX*-dependent pathway of *V. cholerae* (predator), which led to a lower number of surviving *E. coli* prey bacteria in the presence of chitin-based media.

ChiS promotes T6SS-induced natural transformation in *V. cholerae*

We showed that T6SS is regulated by ChiS. Next, we examined the role of ChiS, ChiA1 and ChiA2 in T6SS-induced natural transformation. The Δ*chiS* strain showed 10.1-, 7.6- and 6.2-fold downregulation of natural competence genes, i.e. *tfoX*, *pilA* and *comEA*, respectively, compared to the WT strain in the presence of chitin (Fig. 3a). This showed that ChiS also controlled T6SS-induced natural

transformation in *V. cholerae*. We also found downregulation of natural competence genes (*tfoX*, *pilA* and *comEA*) in the case of Δ*chiA1*, Δ*chiA2* and Δ*chiA1*Δ*chiA2* mutants. However, this downregulation of the natural competence genes reverted back to WT expression levels in the case of the mutants in the presence of GlcNAc$_2$ (Fig. 3b). Earlier studies have shown the effects of ChiS on natural transformation and on the transcription of *pilA* [5]. Here we have shown the effects of ChiA1 and ChiA2 on the expression of natural competence genes, which had not been covered previously. Therefore, taken together, our results suggest that the chitinases initiated ChiS-dependent upregulation of T6SS-induced natural competence.

We further estimated the naturally transformed bacterial count of *V. cholerae* and also measured the transformation frequency. The number of naturally transformed bacteria in the case of the WT, Δ*chiS*, Δ*chiA1*, Δ*chiA2* and
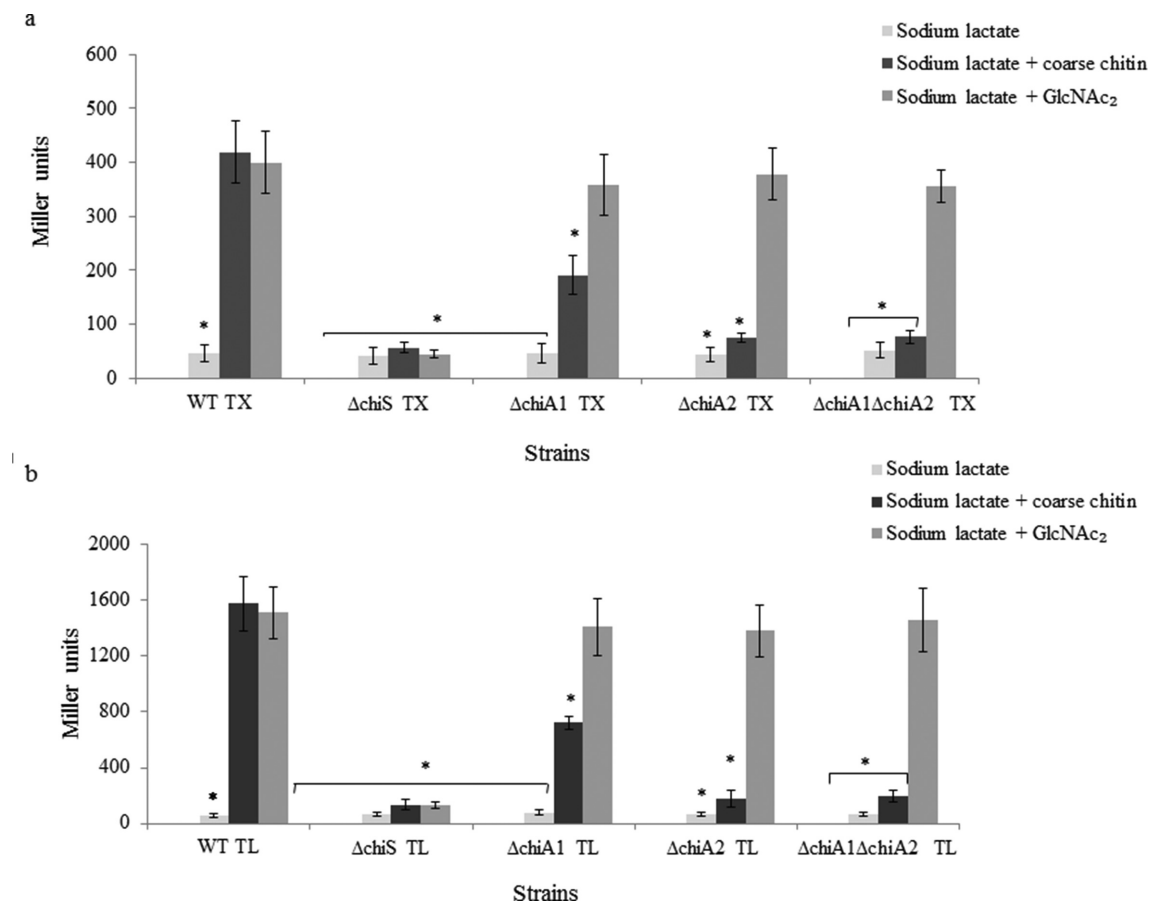

Fig. 4. ChiS activation upregulates the competence regulators *tfoX* and *tfoR* in *V. cholerae.* All of the strains were grown in DASW media supplemented with 0.8 % coarse chitin or 0.6 mM GlcNAc$_2$, with 0.5% sodium lactate being added to each medium to obtain similar bacterial growth. The bacteria were collected from DASW media individually supplemented with (▨) sodium lactate, (■)sodium lactate+coarse chitin and (■) sodium lactate+GlcNAc$_2$. Samples were washed with PBS and used for Miller assays. Miller assays were performed using the indicated strains containing (a) the *tfoR* transcriptional fusion TX and (b) the *tfoX* translational fusion TL with LacZ in the plasmid pTl61T. Each of the experiments was repeated three times (*n*=3). All of the data are expressed as means±SEM. *, *P*<0.05.

$\Delta chiA1\Delta chiA2$ was 35×10^{10} c.f.u. ml^{-1}, 2×10^{10} c.f.u. ml^{-1}, 17×10^{10} c.f.u. ml^{-1}, 10×10^{10} c.f.u. ml^{-1} and 10×10^{10} c.f.u. ml^{-1}, respectively. Therefore, $\Delta chiS$, $\Delta chiA1$, $\Delta chiA2$ and $\Delta chiA1\Delta chiA2$ showed 17-, 2-, 3.5- and 4.8-fold less T6SS-induced natural transformation from ChiS compared to the WT. This indicated that ChiS regulated T6SS and therefore affected T6SS-induced natural transformation in *V. cholerae*. In addition to this, we also found that in the presence of GlcNAc$_2$ the effect of $\Delta chiA1$, $\Delta chiA2$ and $\Delta chiA1\Delta chiA2$ mutants on natural transformation was nullified (Fig. 3c, d). Therefore, this showed that chitinases are also important for T6SS-induced bacterial horizontal gene transfer.

When we further investigated the transformation mechanism by monitoring natural transformation in the presence of DNAse, we found that both direct plasmid transfer by natural competence and T6SS-induced natural transformation were severely affected compared to the plasmid transfer in the absence of DNAse in the culture medium (Fig. 3e, f). In both of the above cases, we used the

V. cholerae El Tor strain N16961 as a negative control. Plasmid purification and PCR from the mixed culture samples also confirmed that it is the plasmid pBR322 that is released from the prey after T6SS-induced killing by *V. cholerae*, and this is taken up by the WT *V. cholerae* itself due to T6SS-induced natural transformation (Fig. 3g, h). Therefore, this indicates that in the presence of chitin, ChiS activation gives rise to upregulation of T6SS and T6SS-induced natural transformation.

Expression of the competence regulators tfoX and tfoR in *V. cholerae* requires activation of ChiS

Here, we investigated the effect of ChiS, ChiA1 and ChiA2 on the activity of the *tfoX* and *tfoR* promoters by β-galactosidase activity assay. We found that the mutants, i.e. $\Delta chiS$, $\Delta chiA1$, $\Delta chiA2$ and $\Delta chiA1\Delta chiA2$, showed lower transcriptional activity, i.e. 134, 746, 175 and 193 Miller units, respectively, in the case of *tfoX* as compared to the *tfoX* promoter activity of 1576 Miller units in the WT in the presence of chitin (Fig. 4a). Therefore, $\Delta chiS$, $\Delta chiA1$, $\Delta chiA2$
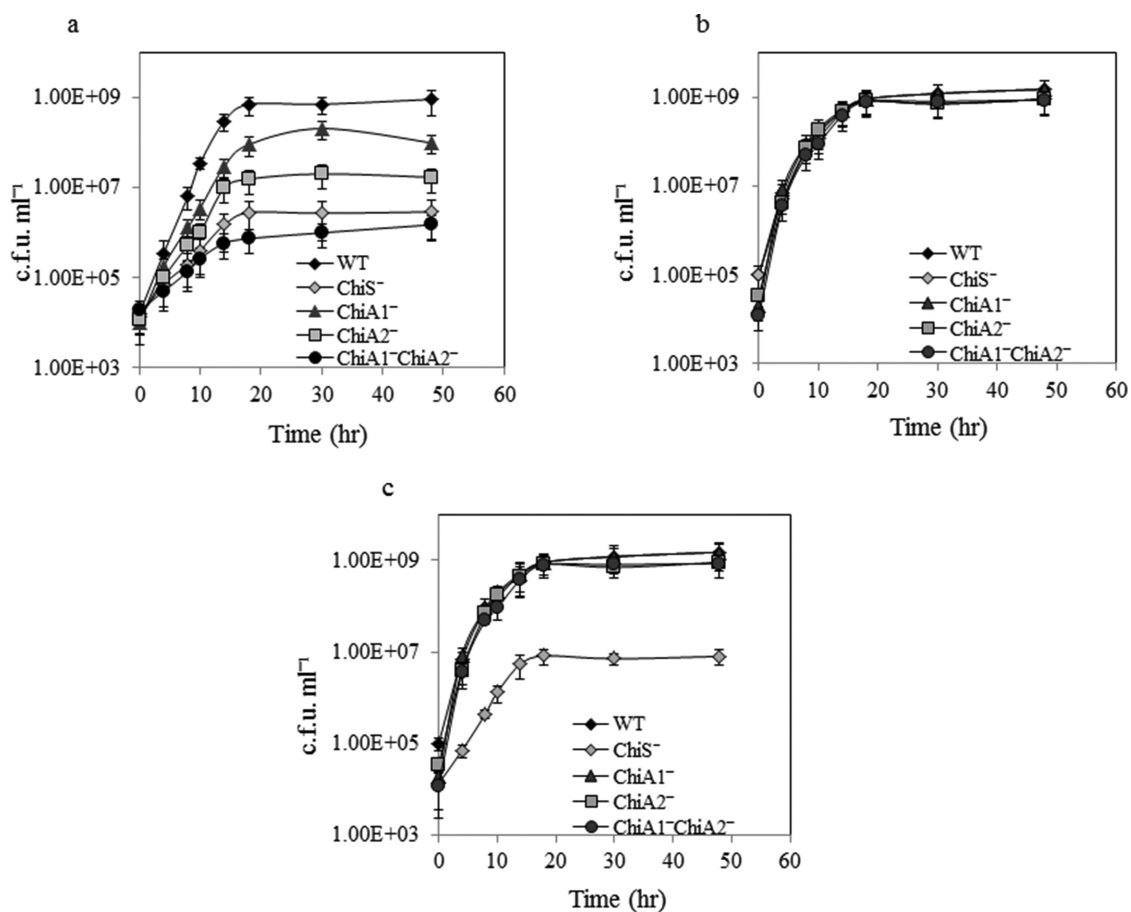

Fig. 5. *V. cholerae* growth on chitin requires ChiS induction. All of the indicated strains were grown in DASW media individually supplemented with (a) 0.8 % coarse chitin, (b) 0.5 % sodium lactate and (c) 0.6 mM GlcNAc$_2$. The viable bacterial counts were detected by the plate count method and are represented graphically. Each of the experiments was repeated three times (*n*=3). All of the data are expressed as mean±SEM. *, *P*<0.05.

and $\Delta chiA1\Delta chiA2$ showed 11.7-, 2.1-, 9-, 8.1-fold lower activity of the *tfoX* promoter.

The transcriptional activity of *tfoR* was also lowered, with an activity of 44, 191, 71 and 76 Miller units for $\Delta chiS$, $\Delta chiA1$, $\Delta chiA2$ and $\Delta chiA1\Delta chiA2$, respectively, compared to the WT, which showed an activity of 418 Miller units in the presence of chitin (Fig. 4b). The effect of the $\Delta chiA1$, $\Delta chiA2$ and $\Delta chiA1\Delta chiA2$ strains on the transcriptional activity of *tfoX* and *tfoR* was restored to normal levels (i.e. comparable to those of the WT strain) in the presence of GlcNAc$_2$ in DASW media. The transcriptional activity of both *tfoX* and *tfoR* was insignificant in the absence of chitin or GlcNAc$_2$ in DASW media supplemented solely with sodium lactate. Therefore, these data indicated that ChiA1 and ChiA2 were only required for GlcNAc$_2$ generation from chitin, which activated ChiS, which further promoted the expression of *tfoX* and *tfoR*. The downregulation of *tfoR* due to *chiS* deletion has been already shown by Yamamoto *et al.* in 2014 [5], but the effect of chitinases ChiA1 and ChiA2 on *tfoR* was not known previously.

V. cholerae growth on chitin requires ChiS induction

Chitin utilization is an important phenomenon that helped *V. cholerae* to feed on the chitinous exoskeleton of crustaceans in the aquatic region. Here, we used all of the aforementioned mutants in a growth curve analysis in which chitin was present or absent as a sole carbon source in DASW media. We observed a drastic reduction in growth for each of these mutants compared to the WT. The growth rate of the WT, $\Delta chiS$, $\Delta chiA1$, $\Delta chiA2$ and $\Delta chiA1\Delta chiA2$ was 9×10^{8}, 2.9×10^{6}, 9.9×10^{7}, 1×10^{7} and 1.5×10^{6} c.f.u. ml^{-1} after 48 h, respectively (Fig. 5a). Therefore, the mutants $\Delta chiS$, $\Delta chiA1$, $\Delta chiA2$ and $\Delta chiA1\Delta chiA2$ showed a 473-, 9-, 90- and 600-fold lower growth rate compared to the WT strain. However, the growth pattern of all the strains showed a similar pattern in sodium lactate-containing DASW medium (Fig. 5b). On the addition of 0.6 mM GlcNAc$_2$ instead of chitin in the growth medium, with the exception of $\Delta chiS$, all of the mutants, i.e. $\Delta chiA1$, $\Delta chiA2$ and $\Delta chiA1\Delta chiA2$, followed the WT growth rate (Fig. 5c). Therefore, it was clearly evidenced that the chitinases
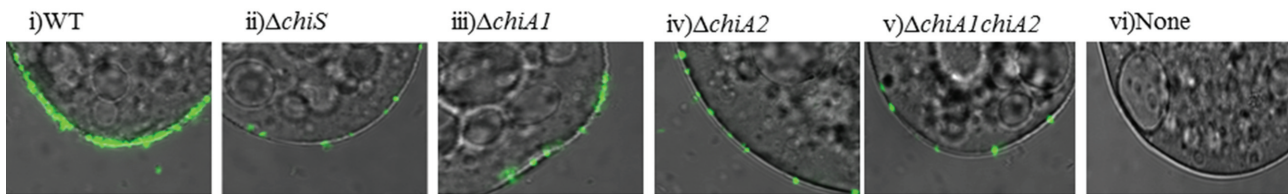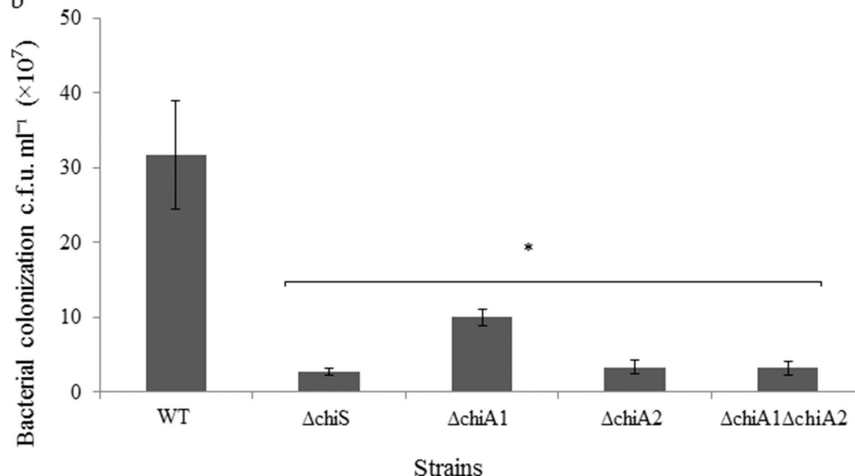

Fig. 6. ChiS helps in the chitin colonization of *V. cholerae*. Colonization assays were performed for all of the indicated strains by mixing log phase (1×10^{5} c.f.u. ml^{-1}) cultures and prewashed insoluble chitin beads at a ratio of 1.1. (a) Fluorescent images of GFP-labelled bacteria bound to chitin beads seen under phase contrast. Chitin beads bound with (i) WT strain, (ii) $\Delta chiS$ strain, (iii) $\Delta chiA1$, (iv) $\Delta chiA2$, (v) $\Delta chiA1\Delta chiA2$ strain and (vi) nothing. (b) Colonization was also quantified. The unbound bacteria were passed through an 8 µm membrane filter to wash out unbound bacteria and then the bound bacterial counts were detected by the plate count method and represented graphically. Each of the experiments was repeated three times (*n*=3). All of the data are expressed as means±SEM. *, *P*<0.05.

initially release GlcNAc$_2$ residues from chitin, which activate ChiS to induce growth on chitin.

V. cholerae colonization on chitin requires ChiS

Next, we investigated the colonization of *V. cholerae* WT, Δ*chiS*, Δ*chiA1*, Δ*chiA2* and Δ*chiA1*Δ*chiA2* strains on chitin. We performed a qualitative analysis by visualizing bacterial colonization under a confocal microscope, and the mutants were considerably reduced in chitin colonization compared to the WT strain (Fig. 6a). We also performed a quantitative assay and found bacterial colonization to be 41×10^7 c.f.u. ml^{-1}, 2.7×10^7 c.f.u. ml^{-1}, 10×10^7 c.f.u. ml^{-1}, 3.3×10^7 c.f.u. ml^{-1}, 3.2×10^7 c.f.u. ml^{-1} for the WT, Δ*chiS*, Δ*chiA1*, Δ*chiA2* and Δ*chiA1*Δ*chiA2*, respectively. Therefore, the mutant strains Δ*chiS*, Δ*chiA1*, Δ*chiA2* and Δ*chiA1*Δ*chiA2* showed 15-, 4.1-, 12.4- and 12.8-fold, reduced efficiency, respectively, for the colonization of chitinous surfaces compared to the WT strain (Fig. 6b). Hence, the results were in agreement with those of the qualitative assay. This indicates that ChiS, ChiA1 and ChiA2 are individually important for colonization on chitinous surfaces. Therefore, ChiS, in addition to chitinases individually, promotes chitin colonization.

DISCUSSION

In this study, we explore the role of ChiS, a member of the two-component system (TCS) in T6SS function. Here, we report that under ChiS-inactivated conditions, the T6SS genes in *V. cholerae* are downregulated. This also results in functional disruption of T6SS. ChiS is activated in the presence of GlcNAc$_2$. These GlcNAc$_2$ residues are released from chitin by chitinases. Therefore, chitinases are also important in upregulating T6SS. In each of the experiments performed, we have used chitinase mutants along with a ChiS mutant to show that ChiS activation by chitinases is also involved in inducing T6SS in *V. cholerae*. Activation of ChiS in the presence of GlcNAc$_2$ had already been discussed [5, 24], but direct evidence for the effect of *V. cholerae* chitinases on ChiS activation and their link with T6SS induction in the presence of chitin had not yet been shown. The role of two-component sensor kinases in T6SS was studied earlier in *Pseudomonas aeruginosa*, where TCS-like RetS/LadS reciprocally regulates the expression of T6SS genes [29, 30]. In fact, T6SS is also found to be regulated by a TCS pmrA-pmrB in an enteric pathogen, i.e. *Salmonella typhi* [31].
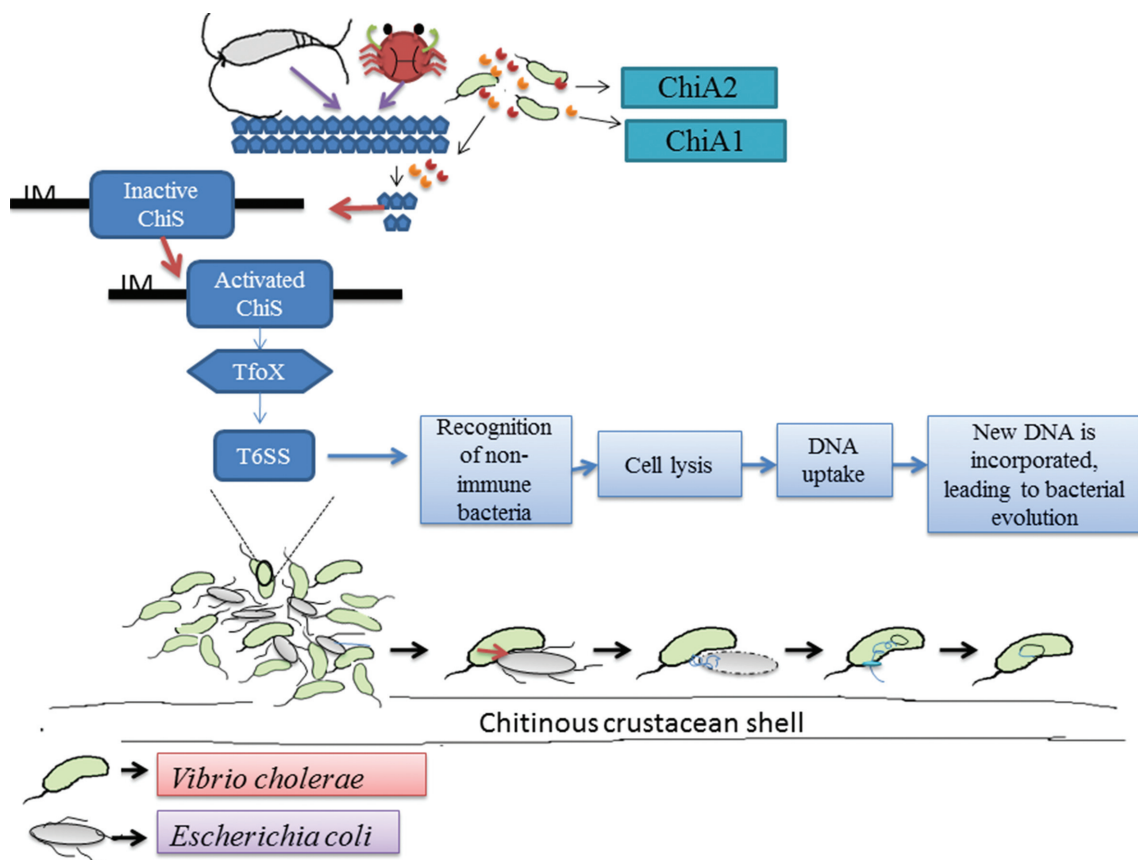

Fig. 7. Schematic diagram showing ChiS affecting T6SS. This diagram shows that ChiS controls T6ss in *V. cholera* and helps it to survive under harsh environmental conditions in the marine region. ChiS promotes T6SS-induced DNA uptake and horizontal gene transfer.

The aforementioned effect of ChiS on T6SS can be explained by the fact that chitin sensing by ChiS induces TfoX, which results in T6SS upregulation. T6SS in C6706 and in some other *V. cholerae* strains is known to be part of the natural competence regulon and is induced via TfoX [6, 14]. However recent reports indicated that T6SS induction also occurs independently of chitin [32, 33]. Downregulation of natural competence genes such as the *tfoX* and *PilA* genes in the Δ*chiS* strain was shown earlier [5]. However, we have shown that Δ*chiS* also has the same effect on another natural competence gene, *comEA*, along with the *tfoX* and *PilA* genes. We also showed reduced expression of the natural competence genes under ChiS-inactivated conditions in chitinase-deleted mutants. We also found that inactive ChiS leads to reduced T6SS-mediated natural transformation in *V. cholerae*. Hence, we might conclude that when the GlcNAc$_2$ residues of chitin activate ChiS, it upregulates natural competence, upon which T6SS is also induced. Thereafter, *V. cholerae* uses the T6SS device to cause the lysis of non-immune bacteria present in its vicinity, which results in the release of their DNA. This DNA is then taken up by the well-known machinery of natural competence in *V. cholerae*, leading to horizontal gene transfer. We have represented our findings through a schematic diagram (Fig. 7). Therefore, on the one hand, *V. cholerae* uses T6SS to kill other non-immune bacteria, while on the other hand, it helps to acquire their DNA, as shown earlier [14]. T6SS has also been found to show antibacterial activity in *S. typhimurium* that kills gut microflora and establishes infection [34].

ChiS leads to the upregulation of *tfoR* transcription, which promotes *tfoX* translation [7]. In this context, we show that it is the GlcNAc$_2$ residues that are released by the chitinases from chitin that activate ChiS, and this ChiS activation results in the upregulation of the T6SS via the activation of natural competence regulators, i.e. *tfoR* and *tfoX*. Therefore, this suggests that chitinases are also important for T6SS in *V. cholerae*. Chitin-induced natural transformation had been studied earlier in other *Vibrio* species, including *V. vulnificus* [35]. One research group found that chitin-induced natural transformation in *Vibrio fischeri* requires *tfoX* and *tfoY* [36].

Here we also demonstrated that ChiS inactivation leads to reduced growth and colonization in *V. cholerae*. This is due to the downregulation of *tfoX* because of ChiS-inactivated conditions, as shown previously [5]. TfoX induces the chitoporin ChiP chitin oligosaccharide uptake, as well as the chitinases [6]. This helps in chitin utilization and growth of the organism. In 2003, Uchiyama *et al.* reported that in *Serratia marcescens* the expression of chitinases and chitin-binding proteins, which are essential for nutrient supply to the bacteria via the chitin degradation pathway in the aquatic environment, is induced by GlcNAc$_2$ [37]. However, its effect on T6SS in *S. marcescens* is not yet known. We speculate that *V. cholerae* colonization on the chitinous surface increases its access to chitin, enhancing the probability of chitin degradation and growth. This growth on chitinous surface induces natural competence as well as T6SS. This facilitates the chance of T6SS-dependent bacterial killing and horizontal gene transfer. Therefore, colonization is important for chitin-induced T6SS upregulation in *V. cholerae*. Here, we show that this chitin surface colonization is dependent on active ChiS. Earlier reports have shown the complex circuit connecting colonization and natural competence in *V. cholerae* [28].

Here, we provide a model of how T6SS operates in the aquatic region under nutrient-poor conditions. Under these conditions, *V. cholerae* uses ChiS to upregulate the chitin utilization programme for nutrient acquisition. We speculate that ChiS-activated T6SS might act as an antibacterial weapon to clear the niche of competing bacteria. A recent work showed such effects of T6SS in *V. cholerae* [38]. In *Burkholderia thailandensis*, a close relative of the human pathogen *Burkholderia pseudomallei*, T6SS plays an important role in inter-bacterial interaction and provides a fitness advantage in the polymicrobial community [39]. Similarly, T6SS-dependent killing of non-immune bacteria increases the probability of chitin degradation, which facilitates *V. cholerae* growth. Taken together, we have highlighted the importance of ChiS activation for *V. cholerae*'s inter-bacterial competitiveness, with T6SS being used to promote its growth, survival and horizontal gene transfer under harsh environmental conditions, which may have implications for *V. cholerae* evolution.

Conflicts of interest
The authors declare that there are no conflicts of interest.

References
1. Huq A, Small EB, West PA, Huq MI, Rahman R *et al.* Ecological relationships between *Vibrio cholerae* and planktonic crustacean copepods. *Appl Environ Microbiol* 1983;45:275–283.
2. Li X, Roseman S. The chitinolytic cascade in Vibrios is regulated by chitin oligosaccharides and a two-component chitin catabolic sensor/kinase. *Proc Natl Acad Sci USA* 2004;101:627–631.
3. Chourashi R, Mondal M, Sinha R, Debnath A, das S *et al.* Role of a sensor histidine kinase ChiS of *Vibrio cholerae* in pathogenesis. *Int J Med Microbiol* 2016;306:657–665.
4. Hunt DE, Gevers D, Vahora NM, Polz MF. Conservation of the chitin utilization pathway in the Vibrionaceae. *Appl Environ Microbiol* 2008;74:44–51.
5. Yamamoto S, Mitobe J, Ishikawa T, Wai SN, Ohnishi M *et al.* Regulation of natural competence by the orphan two-component system sensor kinase ChiS involves a non-canonical transmembrane regulator in *Vibrio cholerae*. *Mol Microbiol* 2014;91:326–347.
6. Meibom KL, Blokesch M, Dolganov NA, Wu CY, Schoolnik GK. Chitin induces natural competence in *Vibrio cholerae*. *Science* 2005; 310:1824–1827.

7. **Yamamoto S, Izumiya H, Mitobe J, Morita M, Arakawa E** *et al.* Identification of a chitin-induced small RNA that regulates translation of the *tfoX* gene, encoding a positive regulator of natural competence in *Vibrio cholerae*. *J Bacteriol* 2011;193:1953–1965.

8. **Lo Scrudato M, Blokesch M.** The regulatory network of natural competence and transformation of *Vibrio cholerae*. *PLoS Genet* 2012;8:e1002778.

9. **Lo Scrudato M, Blokesch M.** A transcriptional regulator linking quorum sensing and chitin induction to render *Vibrio cholerae* naturally transformable. *Nucleic Acids Res* 2013;41:3644–3658.

10. **Seitz P, Blokesch M.** DNA-uptake machinery of naturally competent *Vibrio cholerae*. *Proc Natl Acad Sci USA* 2013;110:17987–17992.

11. **Antonova ES, Bernardy EE, Hammer BK.** Natural competence in *Vibrio cholerae* is controlled by a nucleoside scavenging response that requires CytR-dependent anti-activation. *Mol Microbiol* 2012; 86:1215–1231.

12. **Watve SS, Thomas J, Hammer BK.** CytR is a global positive regulator of competence, type VI secretion, and chitinases in *Vibrio cholerae*. *PLoS One* 2015;10:e0138834.

13. **Meibom KL, Li XB, Nielsen AT, Wu CY, Roseman S** *et al.* The *Vibrio cholerae* chitin utilization program. *Proc Natl Acad Sci USA* 2004; 101:2524–2529.

14. **Borgeaud S, Metzger LC, Scrignari T, Blokesch M.** The type VI secretion system of *Vibrio cholerae* fosters horizontal gene transfer. *Science* 2015;347:63–67.

15. **Ho BT, Dong TG, Mekalanos JJ.** A view to a kill: the bacterial type VI secretion system. *Cell Host Microbe* 2014;15:9–21.

16. **Pukatzki S, Ma AT, Sturtevant D, Krastins B, Sarracino D** *et al.* Identification of a conserved bacterial protein secretion system in *Vibrio cholerae* using the *Dictyostelium* host model system. *Proc Natl Acad Sci USA* 2006;103:1528–1533.

17. **Pukatzki S, McAuley SB, Miyata ST.** The type VI secretion system: translocation of effectors and effector-domains. *Curr Opin Microbiol* 2009;12:11–17.

18. **Russell AB, Peterson SB, Mougous JD.** Type VI secretion system effectors: poisons with a purpose. *Nat Rev Microbiol* 2014;12:137–148.

19. **Thomas J, Watve SS, Ratcliff WC, Hammer BK.** Horizontal gene transfer of functional type VI killing genes by natural transformation. *MBio* 2017;8:e00654-17–.

20. **Boyer F, Fichant G, Berthod J, Vandenbrouck Y, Attree I.** Dissecting the bacterial type VI secretion system by a genome wide in silico analysis: what can be learned from available microbial genomic resources? *BMC Genomics* 2009;10:104.

21. **Pukatzki S, Ma AT, Revel AT, Sturtevant D, Mekalanos JJ.** Type VI secretion system translocates a phage tail spike-like protein into target cells where it cross-links actin. *Proc Natl Acad Sci USA* 2007;104:15508–15513.

22. **Costa TR, Felisberto-Rodrigues C, Meir A, Prevost MS, Redzej A** *et al.* Secretion systems in Gram-negative bacteria: structural and mechanistic insights. *Nat Rev Microbiol* 2015;13:343–359.

23. **Basler M, Pilhofer M, Henderson GP, Jensen GJ, Mekalanos JJ.** Type VI secretion requires a dynamic contractile phage tail-like structure. *Nature* 2012;483:182–186.

24. **Dalia AB, Lazinski DW, Camilli A.** Identification of a membrane-bound transcriptional regulator that links chitin and natural competence in *Vibrio cholerae*. *MBio* 2014;5:e01028-13.

25. **Livak KJ, Schmittgen TD.** Analysis of relative gene expression data using real-time quantitative PCR and the 2(-Delta Delta C(T)) Method. *Methods* 2001;25:402–408.

26. **Miller J.** *Experiments in Molecular Genetics*. New York: Cold Spring Harbor Laboratory; 1972. pp. 352–355.

27. **Mondal M, Nag D, Koley H, Saha DR, Chatterjee NS.** The *Vibrio cholerae* extracellular chitinase ChiA2 is important for survival and pathogenesis in the host intestine. *PLoS One* 2014;9:e103119.

28. **Blokesch M.** Chitin colonization, chitin degradation and chitin-induced natural competence of *Vibrio cholerae* are subject to catabolite repression. *Environ Microbiol* 2012;14:1898–1912.

29. **Bordi C, Lamy MC, Ventre I, Termine E, Hachani A** *et al.* Regulatory RNAs and the HptB/RetS signalling pathways fine-tune *Pseudomonas aeruginosa* pathogenesis. *Mol Microbiol* 2010;76: 1427–1443.

30. **Ventre I, Goodman AL, Vallet-Gely I, Vasseur P, Soscia C** *et al.* Multiple sensors control reciprocal expression of *Pseudomonas aeruginosa* regulatory RNA and virulence genes. *Proc Natl Acad Sci USA* 2006;103:171–176.

31. **Wang M, Luo Z, Du H, Xu S, Ni B** *et al.* Molecular characterization of a functional type VI secretion system in *Salmonella enterica* serovar Typhi. *Curr Microbiol* 2011;63:22–31.

32. **Metzger LC, Stutzmann S, Scrignari T, van der Henst C, Matthey N** *et al.* Independent regulation of type VI secretion in *Vibrio cholerae* by TfoX and TfoY. *Cell Rep* 2016;15:951–958.

33. **Bernardy EE, Turnsek MA, Wilson SK, Tarr CL, Hammer BK.** Diversity of clinical and environmental isolates of *Vibrio cholerae* in natural transformation and contact-dependent bacterial killing indicative of type VI secretion system activity. *Appl Environ Microbiol* 2016;82:2833–2842.

34. **Sana TG, Flaugnatti N, Lugo KA, Lam LH, Jacobson A** *et al.* *Salmonella* Typhimurium utilizes a T6SS-mediated antibacterial weapon to establish in the host gut. *Proc Natl Acad Sci USA* 2016; 113:E5044–E5051.

35. **Gulig PA, Tucker MS, Thiaville PC, Joseph JL, Brown RN.** USER friendly cloning coupled with chitin-based natural transformation enables rapid mutagenesis of *Vibrio vulnificus*. *Appl Environ Microbiol* 2009;75:4936–4949.

36. **Pollack-Berti A, Wollenberg MS, Ruby EG.** Natural transformation of *Vibrio fischeri* requires *tfoX* and *tfoY*. *Environ Microbiol* 2010;12: 2302–2311.

37. **Uchiyama T, Kaneko R, Yamaguchi J, Inoue A, Yanagida T** *et al.* Uptake of N,N'-diacetylchitobiose [(GlcNAc)$_2$] via the phosphotransferase system is essential for chitinase production by *Serratia marcescens* 2170. *J Bacteriol* 2003;185:1776–1782.

38. **McNally L, Bernardy E, Thomas J, Kalziqi A, Pentz J** *et al.* Killing by Type VI secretion drives genetic phase separation and correlates with increased cooperation. *Nat Commun* 2017;8:14371.

39. **Schwarz S, West TE, Boyer F, Chiang WC, Carl MA** *et al.* Burkholderia type VI secretion systems have distinct roles in eukaryotic and bacterial cell interactions. *PLoS Pathog* 2010;6:e1001068–14.

40. **Abuaita BH, Withey JH.** Bicarbonate Induces *Vibrio cholerae* virulence gene expression by enhancing ToxT activity. *Infect Immun* 2009;77:4111–4120.

Edited by: P. Langford and M. Whiteley

Role of a sensor histidine kinase ChiS of *Vibrio cholerae* in pathogenesis

Rhishita Chourashi[a], Moumita Mondal[a], Ritam Sinha[b], Anusuya Debnath[a], Suman Das[a], Hemanta Koley[b], Nabendu Sekhar Chatterjee[a],[*]

[a] *Division of Biochemistry, National Institute of Cholera and Enteric Diseases, Kolkata 700010, India*
[b] *Division of Bacteriology, National Institute of Cholera and Enteric Diseases, Kolkata 700010, India*

ARTICLE INFO

ABSTRACT

Vibrio cholera survival in an aquatic environment depends on chitin utilization pathway that requires two factors, chitin binding protein and chitinases. The chitinases and the chitin utilization pathway are regulated by a two-component sensor histidine kinase ChiS in *V. cholerae*. In recent studies these two factors are also shown to be involved in *V. cholerae* pathogenesis. However, the role played by their upstream regulator ChiS in pathogenesis is yet to be known. In this study, we investigated the activation of ChiS in presence of mucin and its functional role in pathogenesis. We found ChiS is activated in mucin supplemented media. The isogenic *chiS* mutant (ChiS−) showed less growth compared to the wild type strain (ChiS+) in the presence of mucin supplemented media. The ChiS− strain also showed highly retarded motility as well as mucin layer penetration *in vitro*. Our result also showed that ChiS was important for adherence and survival in HT-29 cell. These observations indicate that ChiS is activated in presence of intestinal mucin and subsequently switch on the chitin utilization pathway. In animal models, our results also supported the *in vitro* observation. We found reduced fluid accumulation and colonization during infection with ChiS− strain. We also found ChiS− mutant with reduced expression of *ctxA, toxT* and *tcpA*. The cumulative effect of these events made *V. cholerae* ChiS− strain hypovirulent. Hence, we propose that ChiS plays a vital role in *V. cholerae* pathogenesis.

© 2016 Published by Elsevier GmbH.

1. Introduction

Vibrio cholerae causes the fatal diarrheal disease cholera. *V. cholerae* normally resides in the aquatic environment, where it colonizes on the chitinous surface of crustaceans (Huq et al., 1983) and utilize chitin as nutrient source. Chitin is an un-branched long chain polymer of β-1, 4 linked *N*-acetylglucosamine residues (Glc-NAc). In *V. cholerae,* a two-component sensor histidine kinase, ChiS (VC0622) located in the inner membrane controls the expression of genes involved in chitin degradation. These include $(GlcNAc)_2$ catabolic operon (*chb*), two extracellular chitinase genes *chiA1* and *chiA2*, and an outer membrane chitoporin gene *chiP* (Meibom et al., 2004). ChiA1 and ChiA2 hydrolyze the β-1, 4 linkages between the GlcNAc residues in chitin, yielding soluble $GlcNAc_n$ oligosaccharides, where n = 2–6 (Svitil et al., 1997; Meibom et al., 2004; Orikoshi et al., 2005) which enter through chitoporin and are utilized sequentially via a downstream cascade of catabolic operon

(*chb*) (Hunt et al., 2008). It has been recently known that ChiS also regulate chitin induced natural competence through the involvement of another transmembrane regulator TfoS (Yamamoto et al., 2014).

ChiS is a 133 kDa sensor histidine kinase which belongs to the 'Two component system' (TCS). It has a short N-terminal peptide chain in the cytoplasm, a membrane domain, a periplasmic domain, a second membrane domain, and finally a long polypeptide chain extending into the cytoplasm (Li and Roseman., 2004). ChiS remains inactive by a periplasmic chitin oligosaccharide binding protein, CBP through the ChiS-CBP complex formation. The presence of GlcNAc oligosaccharides as an environmental signal leads to the dissociation of ChiS-CBP complex by mediating asociation of CBP with GlcNAc, thereby activating ChiS. Like other TCS, a conserved histidine residue in the cytoplasmic domain of the active ChiS is autophosphorylated followed by the transfer of the phosphoryl group to a conserved aspartate residue of the cytoplasmic response regulator which is not yet characterized for ChiS. This regulator finally interacts with the genes under ChiS regulation. This typically activates an output domain which includes chitinolytic genes of chitin utilization pathway (Li and Roseman, 2004).

* Corresponding author at: Division of Biochemistry, National Institute of Cholera and Enteric Diseases, P33 C.I.T. Road, Scheme XM, Beliaghata, Kolkata 700 010, India.
  E-mail addresses: nschatterjee@rediffmail.com, chatterjeens@icmr.org.in (N.S. Chatterjee).

TCS in various other pathogenic bacteria are reported to control virulence. VieSAB, a TCS of *V. cholerae* is reported to contribute to its motility and biofilm regulation (Hector et al., 2008). Another *V. cholerae* TCS, VprA-VprB is found to be involved in virulence through its endotoxin modification in host intestine (Herrera et al., 2014). Similarly, TCS PhoP-PhoQ in *Salmonella enteric* is involved in LPS modification and resistance to antimicrobial peptides (Groisman, 2001; Shi et al., 2004). CpxR-CpxA in *Shigella sonnei* is found to be involved in the activation of the master virulence gene regulator virF (Gal-Mor and Segal, 2003).

Several reports indicate that *V. cholerae* chitinase and chitin binding protein are also important for pathogenesis apart from their role in chitin utilization program (Bhowmick et al., 2008; Mondal et al., 2014). GbpA, a chitin binding protein, helps in adherence of *V. cholerae* to the intestinal epithelial cells through a coordinated interaction with mucin (Bhowmick et al., 2008). A recent study shows that ChiS dependent chitinase, ChiA2 is important for survival and pathogenesis of *V. cholerae* within the host intestine (Mondal et al., 2014). Since TCS are found to be involved in virulence, it is important to explore the role of ChiS in *V. cholerae* pathogenesis. In this study, we determined the effect of intestinal mucin on ChiS activation. Further, in order to define the role of ChiS in *V. cholerae* pathogenesis, we explore the impact of *chiS* deletion. We found that isogenic *chiS* mutant (ChiS⁻) showed repression in mucin utilization. We also demonstrated that disruption of *chiS* gene has marked effects on survival, motility, mucin penetration and utilization, expression of virulence in *V. cholerae*.

2. Materials and methods

2.1. Ethics statement

All the animal experiments were done according to the guidelines provided by Committee for the Purpose of Supervision and Control Experiments on Animals (CPCSEA), Government of India. The protocols followed for the animal experiments were approved by the Institutional Animal Ethics Committee of National Institute of Cholera and Enteric Diseases (Registration no: PRO/106/May, 2014–September 2017). Four to five days old infant Swiss mice were used for intestinal colonization studies. New Zealand white rabbits were used for fluid accumulation assay. Animals were euthanized in CO_2 chamber assuring minimum pain to the animals during the intestinal harvest.

2.2. Bacterial strains, plasmids used and culture conditions

In this study, streptomycin resistant *V. cholerae* N16961 (O1El Tor Inaba) was used as a wild type strain. The suicide vector pCVD442 was maintained in *E. coli* strain DH5αlpir (Philippen et al., 2004). For TA cloning, we used pGEMT Easy vector (Promega) was used and maintained in *E. coli* JM109 (Table S1). Strains were grown in LB medium (BD, Difco) at 37 °C with appropriate antibiotics. For β-hexosaminidase assay, bacteria were grown in minimal–lactate media containing M9 minimal medium (BD Difco); 0.5% sodium lactate (Sigma); 50 mM HEPES, pH 7.5 (Sigma), filter sterile 0.2% $MgSO_4$ (Merck) and 0.01% $CaCl_2$ (SRL) with or without mucin (Sigma) as a sole source of carbon. Sodium lactate was added to support equal growth of wild type and mutant strains. To study the expression of virulence genes, bacteria were cultured in AKI media containing 0.5% NaCl, 0.3% NaHCO₃ (Merck), 0.4% yeast extract and 1.5% peptone (BD Difco) pH 7.2 at 37 °C under static condition.

2.3. Construction of deletion mutants of ChiS and CBP

Construction of isogenic mutants were done following earlier mentioned procedure (Skorupski and Taylor, 1996). In brief, *V.*

cholerae N16961 was used for genomic DNA isolation. Almost 500 bps of flanking sequences of both the genes (*chiS* and *cbp*) were amplified by PCR using primers (Table S1). The flanking sequences were then annealed by fusion PCR using primers (Table S2) to get in-frame 3017 base pairs and 1509 base pairs deleted constructs for *chiS* and *cbp* mutants respectively. These unmarked fusion products were amplified and subcloned into pGEM-T Easy vector (Promega). The DNA fragments containing the unmarked deleted gene were digested with Xba1 and Sac1 restriction enzymes and ligated into the counter selectable *sacB*-based suicidal plasmid pCVD442 (Philippen et al., 2004). To harbour these deleted genes in *V. cholerae*, the resultant chimeric plasmid was transformed into *E. coli* SM10λpir (Philippen et al., 2004) and were conjugally transferred to N16961. The transconjugants were selected in ampicillin-streptomycin double antibiotic Luria Bertani (LB) agar plates. The unmarked gene replacements were done by double-crossover recombination mutation using the sucrose plates (Liu et al., 2015). Isogenic deletions and insertions of the unmarked gene were confirmed by using PCR based assay (Fig. S1) from the genomic DNA of the respective mutants using primers mentioned (Table S1) (Herrera et al., 2014).

V. cholerae strains were denoted as wild type (ChiS⁺) and *chiS* isogenic mutant strain (ChiS⁻). A constitutive mutant of *chiS* was constructed by deleting the *cbp* gene (chitin oligosaccharide binding protein) from *V. cholerae* and was denoted as ChiS* in all the experiments.

2.4. Complementation of chiS mutant

For complementation of *chiS* mutant, the open reading frame of *chiS* was PCR amplified by using Taq polymerase and Pfu polymerase (Promega) at a ratio of 2:1 and primers mentioned in Table S1 and cloned into pBAD-TOPO TA expression vector as previously mentioned protocol (Mondal et al., 2014). The cloned vector was transformed into *chiS* mutant strain (ChiS⁻) and the complemented strain was denoted as ChiSᶜ. The complemented strain was induced by 0.2% arabinose (Sigma).

2.5. β-hexosaminidase assay

β-hexosaminidase activity was estimated by previously followed procedure (Li and Roseman, 2004) with PNP-GlcNAc (*p*-nitrophenyl-, *N*-acetyl-β-D-glucosa) purchased from Sigma. To analyse its activity wild type *V. cholerae* (ChiS⁺), ChiS⁻, its constitutive mutant ChiS* and ChiSᶜ were grown up to log phase in minimal–lactate media with or without mucin as mentioned previously. In case of *in vivo* hexosaminidase assay bacteria were collected from intestinal samples. Equal amount of bacteria (1×10^8 c.f.u/ml) were taken from each sample, washed and treated with toluene at a ratio of 10 μl/ml of culture. The mixture was shaken vigorously and kept at RT for 20 min. 0.1 ml of each of these treated bacteria was mixed with 0.1 ml of 1 mM substrate i.e PNP-GlcNAc in 20 mM Tris-HCl (pH 7.5). The reaction mixture was incubated at 37 °C for 60 min. 0.8 ml of 1 M Tris-base was added to stop the reaction. The reaction mixture was centrifuged to separate the cell debris and optical density of the supernatant was measured at 400 nm. Total enzymatic activity was analyzed after measuring total protein by Lowry method and then calculated as *p*-nitrophenol produced per minute per mg of total protein.

2.6. Generation of V. cholerae growth curve

Log phase cultures of wild type *V. cholerae* ChiS⁺, ChiS⁻, its constitutive mutant ChiS* and ChiSᶜ were harvested by centrifugation, washed three times with PBS, cell number was adjusted to 1×10^8 c.f.u/ml and mixed in a ratio of 1:1000 either lactate or

mucin supplemented minimal medium. The cultures were maintained at 37 °C under constant shaking at 180 rpm for 72 h (Mondal et al., 2014). For analysis of viable counts cultures were diluted and plated on LB agar supplemented with streptomycin (Vercruysse et al., 2014).

2.7. In vitro growth assay in HT-29 cell line

Mucin secreting human intestinal cell line HT-29 cells were maintained in Dulbecco's Modified Eagle's Medium (DMEM, Sigma), supplemented with 10% fetal bovine serum (FBS) (HiMedia), 1% (vol/vol) non-essential amino acid and 1% (vol/vol) penicillin/streptomycin (Sigma) mixture at 37 °C under 5% CO_2. The survival of V. cholerae in the presence of mucin secreting HT-29 cells were analysed by using previously described protocol (Mondal et al., 2014). The 80% confluent, serum starved HT-29 cells in 12-well plate were infected with log phase cultures of all V. cholerae strains at an infectious dose of 10^7 c.f.u/ml. After 12 h of incubation unbound cells were collected from the supernatant and cells were then treated with 0.1% Triton X-100 for 2–3 min to detach the bound bacteria. Both the unbound and the bound bacteria were collected, washed in PBS, serially diluted and plated on to LB agar to get viable bacterial count.

2.8. Motility assay on semi solid agar

Motility of all V. cholerae strains were examined on soft agar plates by a previously mentioned protocol (Yeung et al., 2012). The soft agar plates contained minimal media supplemented with 0.4% porcine mucin and 0.3% agar. All the strains were grown to log phase and 1 μl of each of the cultures were spotted on soft agar plates and incubated at 37 °C for 15 h. Motility were analysed by measuring the diameter of the surface motility zone.

2.9. Mucin penetration assay

The assay was performed according to previously described protocol (Liu et al., 2008). In brief, 1% mucin columns were prepared in 1 ml syringes. Log phase cultures were taken, washed and 0.1 ml of culture containing equal number bacteria (10^8 c.f.u/ml) were added from the top of 1% mucin columns. Columns were then kept at 37 °C under static conditions. After 30 min of incubation 500 μl fractions were collected from the bottom of the columns, serially diluted and plated onto LB agar to measure the bacterial count.

2.10. HT-29 cell adhesion assay

For detection of bound bacteria in HT-29 cell, we followed a modified procedure from previously used protocol was followed (Debnath et al., 2015). 80% confluent HT-29 cells maintained in DMEM as mentioned before in 12 well plates and were serum starved overnight before treatment. These were then treated with log phase cultures of all three strains of V. cholerae at a dilution of 10^7 c.f.u/ml and incubated at 37 °C for 1 h in 5% CO_2, cells were washed three times with PBS and detached using 0.1% Triton X-100. Adherent bacteria were counted after serial dilution by plating on LB agar plates.

For qualitative analysis of bacterial adhesion we used GFP labelled bacterial strains and followed a previously mentioned protocol (Debnath et al., 2015). HT-29 cells were cultured on glass coverslips in 12 well plates until (70–80) % confluent and infected with 10^7 c.f.u/ml of GFP labelled strains. After 1 h of incubation, bound bacteria were washed 3 times with PBS and mounted on glass slides with mounting medium. Glass slides were observed under fluorescence microscope (Olympus AX-70) to show the GFP labelled bacteria bound to HT-29 cells.

2.11. Suckling mouse colonization

Bacterial colonization in suckling mice intestine were assessed by in vivo competition assay in the procedure described before (Ding et al., 2004). Log phase cultures of wild type V. cholerae (LacZ⁻) strain was mixed at a ratio of 1:1 with each of the strains i.e ChiS⁺, ChiS⁻, ChiS* and complemented ChiS^c strains (LacZ⁺). The mixed cultures were orally inoculated at a concentration of approximately 5×10^7 c.f.u/ml into five day old infant mice and incubated for 18 h. Mice intestine were then harvested, homogenized, washed and serially diluted to plate on LB agar supplemented with streptomycin (100 μg/ml). Competitive index was calculated by the following equation:- ratio out$_{(mutant/wild-type)}$/ratio in$_{(mutant/wild-type)}$. The competitive Index (CI) value of CI < 1 indicates a fitness defect and that of CI > 1 indicates an increased fitness.

2.12. Fluid accumulation in ileal–ligated rabbit model and bacterial recovery from rabbit intestine

New Zealand rabbits were used for the fluid accumulation assay. Rabbit weighing approximately 2.5 kg was used for the assay as described (Mondal et al., 2014; Debnath et al., 2015). Bacterial inoculums of each of the strains were adjusted to 10^9 c.f.u/ml and introduced in rabbit ileum. Fluid accumulation was measured after 18 h infection in rabbit. Fluid accumulation was calculated as FA ratio = volume of fluid accumulation (ml)/intestinal length (cm). PBS was used as a negative control. Bacteria were counted by homogenizing the intestinal sections in 1 ml PBS. To determine the actual bacterial c.f.u at the time of intestinal harvest, bacteria were collected from the intestine, washed, serially diluted and plated on LB agar supplemented with streptomycin (100 μg/ml). β-hexosaminidase assay were also performed under in vivo conditions by collecting bacteria from intestinal samples of rabbit during ileal loop experiment.

2.13. RNA isolation and quantitative RT-PCR in vitro and in vivo

Bacteria were also harvested from rabbit intestinal loops (in vivo) after infecting with all the V. cholerae strains separately in each loop. Bacterial pellets were washed thrice in PBS and then used for RNA isolation. Total RNA was isolated using Trizol (Invitrogen) following the manufacterer's protocol. DNase treatment was performed using DNA free kit (Ambion) for elimination of contaminating genomic DNA followed by cDNA synthesis using reverse transcription kit (Promega) according to the manufacter's protocol with 1 μg of total RNA for each of the 20 μl reactions. The mRNA transcript levels were quantified by quantitative PCR (qPCR) using 2×SYBR green PCR master mix (Applied Biosystems) and 0.2 μM of specific primers (toxT, tcpA, ctxA) designed using IDT for each transcripts (Table S1). Data analysis was done using 7500 Real Time PCR detection system (Applied Biosystems, Foster City, California). The relative expression of the target transcripts were calculated according to Livak method (Livak and Schmittgen, 2001) using recA as an internal control.

2.14. GM1 ELISA for CT estimation in vivo

The ability of V. cholerae strains to express cholera toxin (CT) in vivo was assayed by GM1 enzyme-linked immunosorbent assay (ELISA) (Holmgren., 1973) using polyclonal anti-CT antibody (Sigma). CT was detected in the intestinal fluid accumulated in rabbit ligated ileal loop. The fluid collected was centrifuged and filtered using 0.45 μm membrane filter (Millipore). The amount of CT produced was determined using a standard curve obtained with purified CT and absorbance was measured at 492 nm. The average OD_{492} obtained from triplicate wells of each experimental sets were
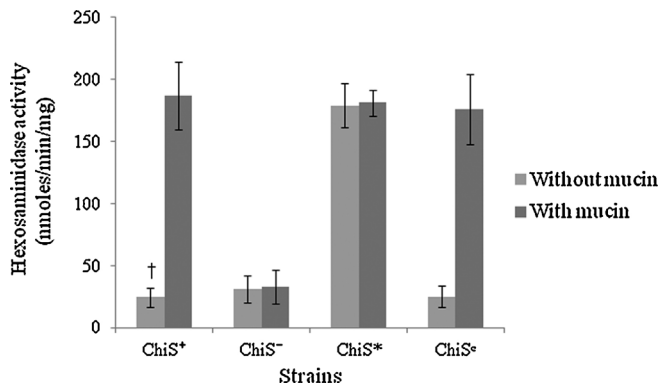
Fig. 1. Activation of ChiS is promoted in the presence of mucin: Bacteria were grown in minimal medium supplemented with or without porcine mucin. 0.5% of sodium lactate was added in each medium to obtain similar bacterial growth. Log phase cultures were taken to measure the total hexosaminidase (ChiS regulated periplasmic enzyme) activity in ChiS+ (V. cholerae N16961 wild type), ChiS− (isogenic ChiS mutant), ChiS* (cbp mutant expressing ChiS constitutively) and ChiS^c (complement of ChiS−) strains in presence (■) or absence (▪) of 2% mucin. †, P < 0.05. Error bars represent standard errors from three biological replicates (n = 3).

considered to estimate the amount of CT present in the samples using the standard curve (Patra et al., 2012).

2.15. Statistical analysis

The suckling mice colonization data were graphically plotted by using Graphpad Prism software and analysed by using one way ANOVA. Rest of the experiments were analysed by student's *t*-test. Each of the experiments were done in triplicates and the results were represented as mean ± SEM. A *P* value of <0.05 was considered statistically significant.

3. Results

3.1. Activation of ChiS in the presence of mucin

β-hexosaminidase activity is a measure of ChiS activation and its effect on the chitin utilization pathway (Li and Roseman, 2004). Here, we measured the total β-hexosaminidase activity in all the *V. cholerae* strains in presence or absence of mucin as a sole nutrient source. Total hexosaminidase activity in the ChiS+ strain in the presence of mucin was 180.5 nmol/min/mg compared to 24 nmol/min/mg in the absence of mucin. So, in the presence of mucin, ChiS activation was induced 7.4 fold higher in ChiS+ strain in the presence of mucin (Fig. 1). However, the ChiS− strain showed negligible activity of the enzyme in presence or absence of mucin. On the other hand, the ChiS* strain showed constitutive activation of β-hexosaminidase without requiring any induction by mucin. The ChiS^c strain also showed similar activation to the ChiS+ strain in presence of mucin. Additionally, we also found RNA expression of ChiA2 was 5 fold less and total mucinase activity to be 9 fold less in ChiS− strain than the ChiS+ strain in mucin supplemented media (Figs. S1 and S2). Therefore, this indicated that mucin induced the activation of ChiS which further turned on the chitin utilization pathway genes as well as the extracellular chitinase ChiA2.

3.2. ChiS helps V. cholerae to utilize mucin

Next, we measured the growth rate of all the strains in minimal media supplemented with mucin (Fig. 2A) or sodium lactate (Fig. 2B). The growth rate of the ChiS+ strain in mucin supplemented minimal medium after 72 h was 6.1×10^8 c.f.u/ml compared to the ChiS− strain with that of 3×10^7 c.f.u/ml. So, the growth rate of
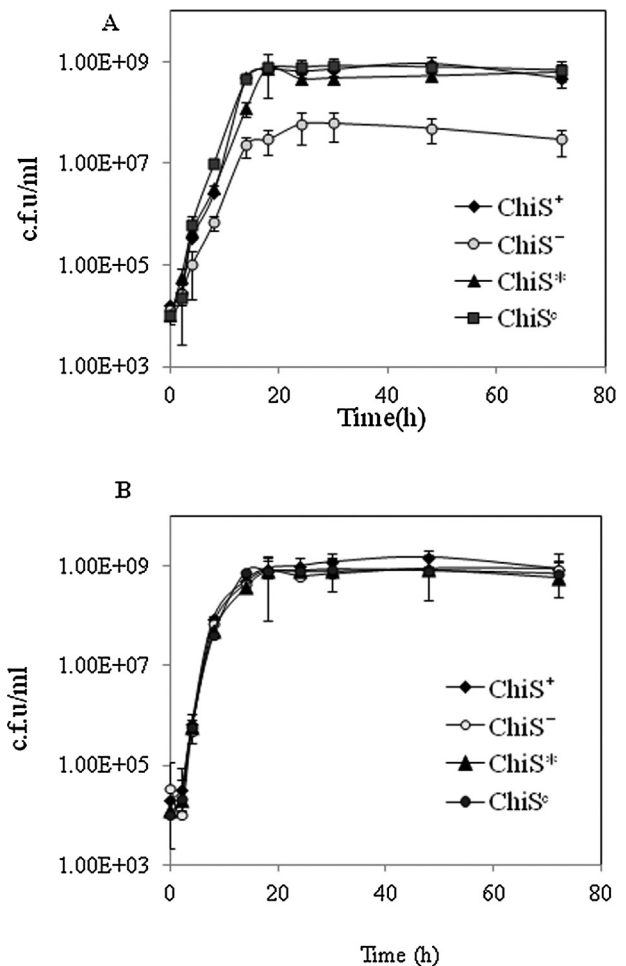

Fig. 2. ChiS contributes in utilization of mucin as a sole nutrient source. ChiS+ (*V. cholerae* N16961 wild type), ChiS− (isogenic *ChiS* mutant), ChiS* (*cbp* mutant expressing ChiS constitutively) and ChiS^c (complement of ChiS−) strains were inoculated separately in (A) minimal media supplemented with 2% (w/v) porcine mucin and (B) 0.5% sodium lactate as the only carbon source. The viable bacterial counts were detected by plate count method and represented graphically. Each of the experiment was repeated three times (n = 3) and the data were expressed as mean ± SEM.

the ChiS− strain was severely 20 fold diminished compared to the ChiS+ strain. The ChiS* and ChiS^c strains showed similar growth as of the ChiS+ strain in mucin supplemented medium. However, the growth rate of all the strains were similar in sodium lactate supplemented minimal medium indicating equal fitness of all the strains. This indicated ChiS is an important factor for utilizing mucin as a sole nutrient source.

3.3. Motility and mucin penetration depends on ChiS

We investigated the motility of different *V. Cholerae* strains in presence of mucin (Fig. 3A and B). In plate assay, we found all the strains except ChiS− showed similar motility. However, we found that motility zone in case of the ChiS− strain was 0.36 ± 0.07 cm and that of the ChiS+ strain was 1.8 ± 0.11 cm. Therefore, motility of the ChiS− strain was reduced to 5 fold compared to the ChiS+ strain (*P* < 0.05). Taken together, this indicates ChiS is required to promote motility in *V. Cholerae* in the presence of mucin.

Next, we investigated the role of ChiS on mucin layer penetration *in vitro* (Fig. 3C). Out of all the loaded bacterial cells 2.6×10^7 c.f.u/ml ChiS+ viable cells penetrated through mucin layer, whereas, 2×10^6 c.f.u/ml ChiS− strain was detected following mucin penetration. Therefore, our data showed 13 fold reduction in
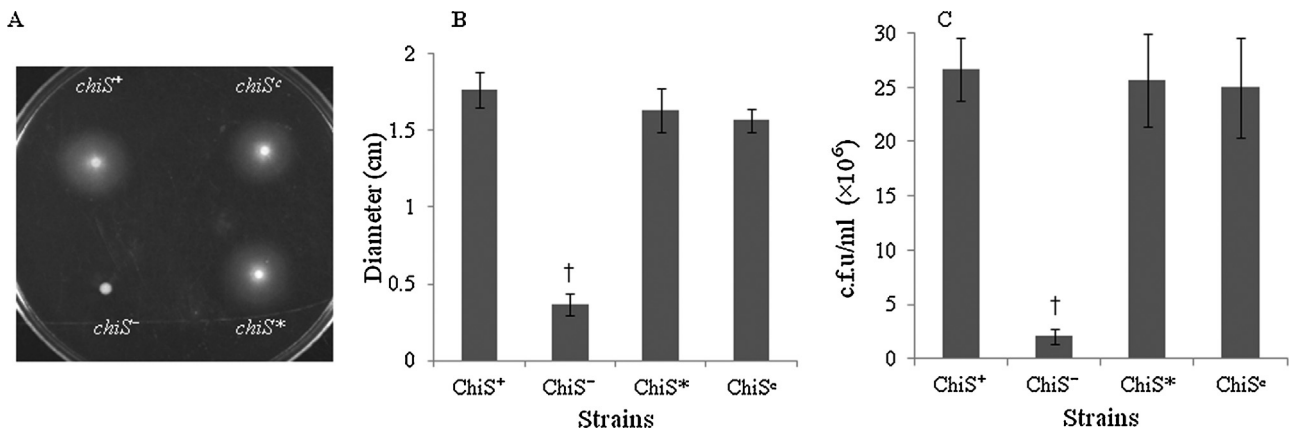
Fig. 3. Motility and mucin penetration is promoted by ChiS in *V. cholerae*: ChiS+ (*V. cholerae* N16961 wild type), ChiS− (isogenic *ChiS* mutant), ChiS* (*cbp* mutant expressing ChiS constitutively) and ChiSc (complement of ChiS−) strains were separately grown in LB till log phase. (A) Soft agar plates showing differences in motility between ChiS− strain and all other strains. 1 μl of each of the cultures were spotted on plates containing minimal media supplemented with 0.4% porcine mucin and 0.3% agar. Plates were incubated for 15 h at 37 °C. (B) Diameter of the surface motility zones are graphically represented. Motility were analysed by measuring the diameter of the surface motility zone. †, $P < 0.05$. The result shown is a mean of ±SEM of three biological replicates (n = 3). (C) 10^7 c.f.u/ml of ChiS+ (*V. cholerae* N16961 wild type), ChiS− (isogenic *ChiS* mutant), ChiS* (*cbp* mutant expressing ChiS constitutively) and ChiSc (complement of ChiS−) were loaded on top of 1 ml mucin (1%) columns and were allowed to penetrate. Bacteria were collected from the bottom of the columns, serially diluted and plated on LB agar to obtain the bacterial number by plate count method. †, $P < 0.05$. The result shown is a mean of ±SEM of three biological replicates (n = 3).
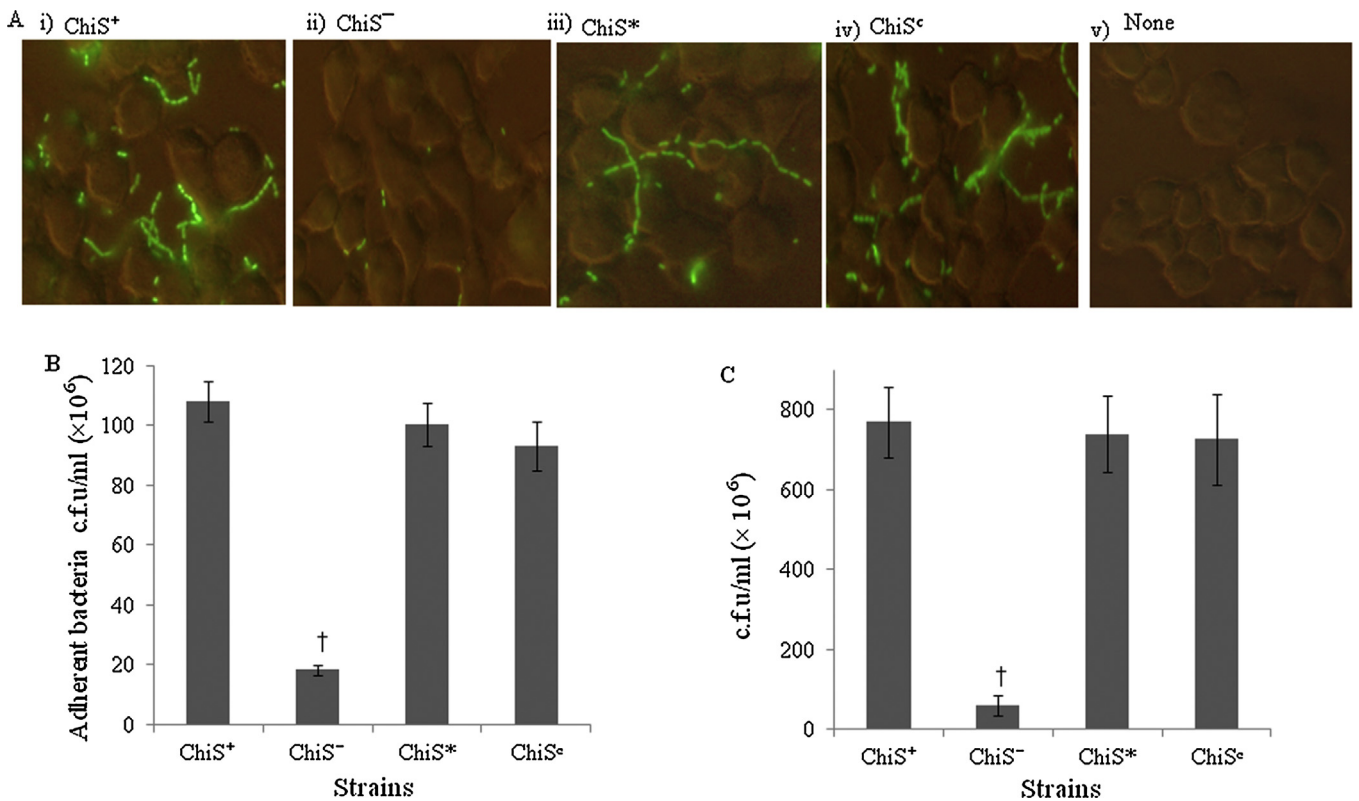

Fig. 4. ChiS is important for bacterial adhesion and survival in presence of HT-29 cells. ChiS+ (*V. cholerae* N16961 wild type), ChiS− (isogenic *ChiS* mutant), ChiS* (*cbp* mutant expressing ChiS constitutively) and ChiSc (complement of ChiS−) strains were grown to log phase and adjusted to 1 O.D. 80% confluent HT-29 cells were then infected with 10^7 c.f.u/ml of each strain and incubated at 37 °C in 5% humidified CO_2 incubator. A) Fluorescent Images of GFP labeled bacteria bound to HT-29 cells seen under Phase contrast. i) HT-29 cells infected with ChiS+ strain, ii) HT-29 cells infected with ChiS− strain, iii) HT-29 cells infected with ChiS*, iv) HT-29 cells infected with ChiSc and v) Non-infected HT-29 cells. (B) Adhesion assay: HT-29 epithelial cells were infected with *V. cholerae* strains for 1 h. Bound bacteria were collected and plated. †, $P < 0.05$. Each of the experiment was repeated three times (n = 3) and the data were expressed as mean ± SEM. (C) Both bound and unbound bacteria were collected after 12 h incubation with HT-29 cells. Samples were washed and serially diluted to plate on LB agar. Number of bacteria were enumerated by plate count method. †, $P < 0.05$. The result shown is mean of ±SEM of three biological replicates (n = 3).

mucin penetration ability by the ChiS− mutant strain compared to the ChiS+ wild type strain ($P < 0.05$). ChiS* and ChiSc showed almost similar mucin penetration compared to ChiS+ strain. This indicates that ChiS helps *V. cholerae* to penetrate the mucin layer *in vitro*.

3.4. Adhesion and survival of V. cholerae in the presence of HT-29 cells is dependent on ChiS

After penetration through the mucin layer of the intestine *V. cholerae* needs to adhere to the epithelial cells in the intestine to

initiate the infection. We studied the effect of ChiS on initial adherence of *V. cholerae* to HT-29 cells under fluorescence microscopy (Fig. 4A). The GFP labelled ChiS− strain was less visible in adhered form with HT-29 cells compared to the ChiS⁺ strain. We also studied the adhesion assay quantitatively (Fig. 4B). The bacterial count for ChiS⁺ bound to HT-29 cells was 1.08×10^8 c.f.u/ml and that of ChiS⁻ was 1.83×10^7 c.f.u/ml. Therefore, we found that the ChiS⁻ strain to be 6 fold more defective to adhere to the HT-29 cells when compared to the ChiS⁺ strain ($P < 0.05$). ChiS* and ChiS^c showed adherence almost similar to the ChiS⁺ strain.

Here, the impact of ChiS on survival of *V. cholerae* was also analysed by infecting mucin secreting HT-29 cells (Fig. 4C). After 12 h of infection, the viable counts for the ChiS⁺ strain was 7.7×10^7 c.f.u/ml and that of the ChiS− strain was 5.9×10^6 c.f.u/ml in the presence of HT-29 cells. Our result showed that the ChiS− strain was 13 fold less efficient to survive when compared to the ChiS⁺ strain ($P < 0.05$). ChiS* and ChiS^c strains showed survival similar to that of the ChiS⁺ strain. This indicated that ChiS was important for *V. cholerae* survival in the presence of HT-29 cells.

3.5. ChiS affects suckling mice colonization in mice

Bacterial binding to intestinal epithelial cell facilitates bacterial colonization in the intestine. We have already showed the ChiS− strain to be defective in adhesion *in vitro*. Therefore, we next examined the role of ChiS in colonization of suckling mice by using competition assay (Fig. 5). The input ratio during bacterial infection was 1:1 of mutants or complemented strains (LacZ⁺) competing with wild type N16961 (LacZ⁻) *V. cholerae*. After 18 h, the output ratio (competitive index CI) of ChiS⁻lacZ⁺/ChiS⁺LacZ⁻ was ≈0.0001 indicating a high fitness defect for the ChiS⁻ strain ($P < 0.05$). In contrast, ChiS^c and ChiS* strains showed almost no compet-
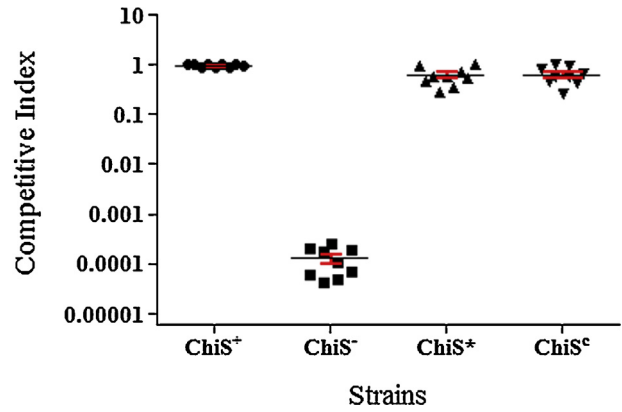

Fig. 5. ChiS helps in *invivo* colonization of *V. cholerae*: Comparative study of colonization of ChiS⁺ (*V. cholerae* N16961 wild type), ChiS⁻ (isogenic *ChiS* mutant), ChiS* (*cbp* mutant expressing ChiS constitutively) and ChiS^c (complement of ChiS⁻) strains in 5 days old suckling mice is presented here. Mice were orally inoculated with 5×10^7 c.f.u/ml of wild type *V. cholerae* (LacZ⁻) strain mixed at a ratio of 1:1 with each of the strains i.e ChiS⁺ (LacZ⁺), ChiS⁻ (LacZ⁺), ChiS* (LacZ⁺) and complemented ChiS^c (LacZ⁺) strains and incubated for 18 h. Mice intestine were harvested, homogenized, washed, serially diluted and plated onto LB agar. Competitive index (CI) = ratio out(mutant/wild-type)/ratio in(mutant/wild-type). The competitive Index (CI) value of CI < 1 indicates the a fitness defect, CI > 1 indicates an increased fitness and CI ≈ 1 indicates no fitness defect. $P < 0.05$. Each of the experiment was repeated three times (n = 3) and the data were expressed as mean ± SEM.

itive disadvantage. Additionally, we determined the CI between ChiS⁺LacZ⁻/ChiS⁺LacZ⁺ and we found CI ≈ 1 indicating no fitness defect of the LacZ⁻ mutant over LacZ⁺. Taken together, this indicated that the ChiS⁺ strain outcompeted ChiS⁻ strain in the infant mice colonization. Therefore, we concluded that *V. cholerae* ChiS contributes in intestinal colonization.
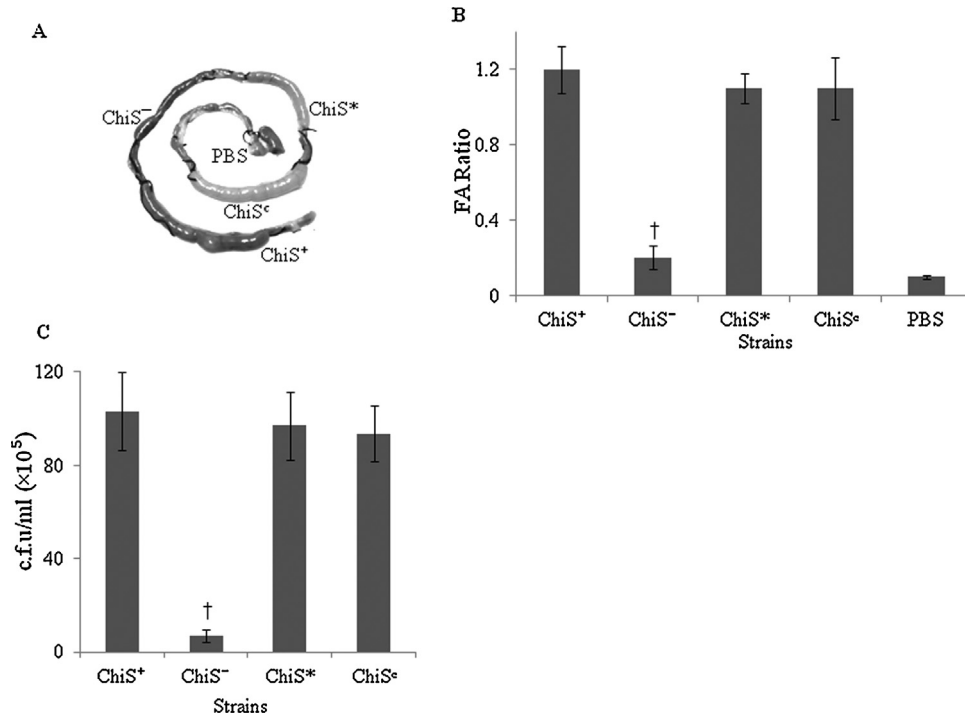

Fig. 6. *V. cholerae* ChiS contributes in fluid accumulation as well as colonization in rabbit intestine: Log phase cultures of ChiS⁺ (*V. cholerae* N16961 wild type), ChiS⁻ (isogenic *ChiS* mutant), ChiS* (*cbp* mutant expressing ChiS constitutively) and ChiS^c (complement of ChiS⁻) strains were adjusted to 1 O.D and 10^9 c.f.u/ml were inoculated into the intestinal ligated loops of a rabbit. (A) A representative rabbit intestine is presented here. Effects of V. cholerae strains in fluid accumulation are shown. PBS is used as a negative control. (B) Fluid accumulation ratio in rabbit ligated ileal loop were determined and represented graphically. †, $P < 0.05$. The result shown is a mean ± SEM of three biological replicates. (C) Rabbit intestinal samples were also harvested, homogenized, washed, serially diluted and plated onto LB agar to enumerate the intestinal colonization and the recovered c.f.u of each strain are graphically represented. †, $P < 0.05$. Each of the experiment was repeated three times (n = 3) and the data were expressed as mean ± SEM.
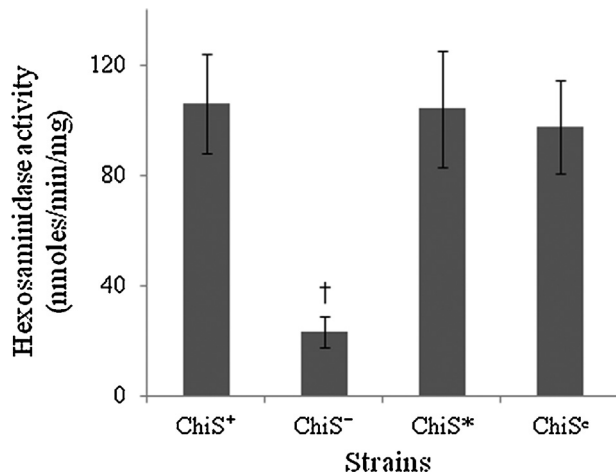
Fig. 7. *V. cholerae* ChiS is activated in the intestine: Log phase cultures of ChiS+ (*V. cholerae* N16961 wild type), ChiS− (isogenic *ChiS* mutant), ChiS* (*cbp* mutant expressing ChiS constitutively) and ChiSᶜ (complement of ChiS−) strains were adjusted to 1 O.D and 10^9 c.f.u./ml were inoculated into the rabbit intestinal ligated loops. *In vivo* hexosaminidase assay was performed by the samples collected from fluid accumulated in the intestinal loops. †, $P < 0.05$. Each of the experiment was repeated three times (n = 3) and the data were expressed as mean ± SEM.

3.6. ChiS depletion in V. cholerae results in reduced pathogenesis in rabbit intestine

Till now, we have shown that ChiS affects *V. cholerae* colonization efficiency. In this experiment, we have qualitatively shown and measured the intestinal fluid accumulation in rabbit ileal ligated model by evaluating FA ratio (Fig. 6A and B). In rabbit intestine, infection with the ChiS− strain showed 6 fold reduction in fluid accumulation compared to the wild type *V. cholerae* ChiS+ after 18 h of infection ($P < 0.05$). Infection with ChiS* and ChiSᶜ strain showed fluid accumulation similar to the ChiS+ strain. We also measured the c.f.u recovered from the rabbit intestine (Fig. 6C). In case of the ChiS+ strain, bacteria recovered was 1.03×10^7 c.f.u/gm of intestine and that of the ChiS− strain was 7×10^5 c.f.u/gm of intestine. Therefore, we found upto 15 fold less recovery in case of the ChiS− strain ($P < 0.05$).This indicated that ChiS is involved in colonization of *V. cholerae* and fluid accumulation in the host intestine, which is one of the critical aspects of its pathogenesis.

3.7. Activation of ChiS in the host intestine

We also analysed total β-hexosaminidase activity to evaluate ChiS induction in each strains *in vivo* from fluid accumulated samples in the rabbit intestine (Fig. 7). β-hexosaminidase activity in ChiS+ was 102 nmoles/min/mg whereas the ChiS− strain showed activity of 23 nmoles/min/mg. The ChiS+ strain therefore, showed 4.4 fold higher β-hexosaminidase activity compared to the ChiS+ strain ($P < 0.05$). Induction of β-hexosaminidase activity in ChiS* and ChiSᶜ strains were similar to ChiS+ strain. Therefore, this indicated that ChiS is activated in the host intestine and thus affects pathogenesis of *V. cholerae*.

3.8. ChiS contributes in virulence gene expression and cholera toxin (CT) production in V. cholerae

Since we found differential colonization and less fluid accumulation in rabbit intestine, we analyzed the virulence gene expression (*ctxA, toxT,* and *tcpA*) in *V. cholerae* strains harvested from rabbit ileal loop samples (Fig. 8A). We found *ctxA, toxT,* and *tcpA* RNA levels to be significantly reduced by 3 fold, 4.5 fold and 4 folds less, respectively, in the ChiS− strain when compared to the ChiS+ wild

type ($P < 0.05$). ChiS* and ChiSᶜ showed *ctxA, toxT,* and *tcpA* RNA levels similar to the ChiS+ strain. We also measured cholera toxin production of all the strains of *V. cholerae* in the intestinal fluid samples from the rabbit ileal loop after 18 h of infection (Fig. 8B). We found fluid from the ChiS− infected ileal loop sample to contain less cholera toxin (210 ng/ml) with a difference of 6.5 fold compared to the ChiS+ (1220 ng/ml) ($P < 0.05$). Additionally, in AKI media ChiS− strain showed significant decrease in the RNA levels of these virulence genes (*ctxA, toxT,* and *tcpA*) compared to ChiS+ strain (Fig. S4).

4. Discussion

It has been previously reported that there are many TCS in pathogenic bacteria that contributes to virulence. ChiS is a component of TCS in *V. cholerae*. Although ChiS is the regulator of *V. cholerae* extracellular chitinases like ChiA2 (Meibom et al., 2004), its function in pathogenesis is still unknown. Therefore, in this study we have aimed to understand its role in pathogenesis.

It is known that, *V. cholerae* ChiS is activated in the presence of GlcNAc oligosaccharides of chitin in the aquatic environment (Li and Roseman., 2004). The activation of ChiS promotes the expression of downstream chitin utilization pathway components like periplasmic-β-N-acetylglucosminidase, etc. (Meibom et al., 2004). Our results showed that ChiS is also activated in the presence of intestinal mucin. Most probably the GlcNAc oligosaccharide residues of mucin activates ChiS in the same way as it does in the aquatic environment. This leads to the activation of the chitin utilization pathway in a similar manner as mentioned before and results into the expression of extracellular chitinases like ChiA2.

The activation of ChiS is governed by chitin oligosaccharide binding protein (CBP) that binds to keep ChiS in a deactivated mode in the absence of GlcNAc residues. Once CBP when binds to GlcNAc residues, it is released from ChiS leaving the sensor kinase in activated mode (Li and Roseman., 2004). We also observed that activation and deactivation cycle of ChiS takes place in presence of intestinal mucin. In absence of CBP, ChiS remains constitutively active even in the absence of GlcNAc oligosaccharides (Li and Roseman., 2004). In our case also, the induction by mucin was not required in the *cbp* mutant strain (ChiS*). Therefore, we confirmed that *V. cholerae* ChiS is induced in the presence of mucin.

V. cholerae can utilize mucin as a sole nutrient source (Mondal et al., 2014). Our results here showed that mucin utilization by *V. cholerae* depends upon ChiS. In absence of ChiS, *V. cholerae* showed poor growth even in presence of mucin in minimal media as well as in the mucin secreting intestinal cells. This suggests that ChiS contributes in utilization of mucin by *V. cholerae* which helps the bacteria to survive in mammalian host intestine. There are many intestinal microbes that utilize mucin as an energy source (Chen et al., 2002; Deplancke et al., 2002; Derrien et al., 2010). *Clostridium perfringens*, an opportunistic intestinal pathogen was able to grow on medium with mucin as a substrate (Deplancke et al., 2002) and (GlcNAc)₂ (Chen et al., 2002). Other intestinal microbes like *Bacteroides fragilis* could utilize GlcNAc; *Escherichia coli*, *Lactococcus lactis* and *Proteus vulgaris* could utilize (GlcNAc)$_{1-6}$ (Chen et al., 2002). *Bifidobacterium adolescentis* and *Eubacterium limosum* could use (GlcNAc)$_{1-6}$ to some extent as their main carbon source (Chen et al., 2002).

Earlier, it has been shown that *V. cholerae* utilizes mucin by the help of an extracellular chitinase ChiA2 (Mondal et al., 2014). ChiA2 cleaves the oligosaccharide moieties of mucin (Mondal et al., 2014). These residues then help to switch on the chitin utilization pathway that results in catabolism of GlcNAc residues of mucin. ChiS contributes in the utilization of mucin as nutrient source by inducing the extracellular chitinases like ChiA2. Additionally, here we
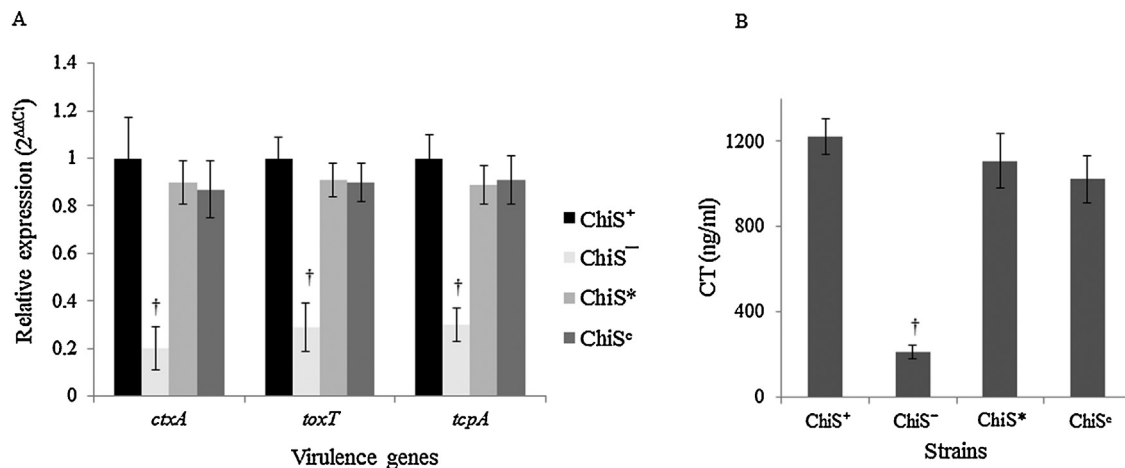
Fig. 8. *V. cholerae* ChiS affects cholera toxin production and virulence gene expression in the intestine: Log phase cultures of ChiS⁺ (*V. cholerae* N16961 wild type), ChiS⁻ (isogenic *ChiS* mutant), ChiS* (*cbp* mutant expressing ChiS constitutively) and ChiSᶜ (complement of ChiS⁻) strains were adjusted to 1 O.D and 10^9 c.f.u./ml were inoculated into the intestinal loops. (A) Bacteria were harvested from rabbit intestinal ligated loops after infection for 18 h, RNA was isolated and virulence gene expression was measured by qRT-PCR. †, $P < 0.05$. Each of the experiment was repeated three times (n = 3) and the data expressed as means ± SEM. (B) *in vivo* cholera toxin production was also analyzed from the accumulated fluid samples of ligated ileal loop assay. †, $P < 0.05$. Each of the experiment was repeated three times (n = 3) and the data expressed as means ± SEM.

also found significant differences in RNA expression of ChiA2 and chitinase activity assay between ChiS⁺ and ChiS⁻ strain in mucin supplemented media (Figs. S2 and S3).

When *V. cholerae* reaches the small intestine, the mucosal layer acts as a barrier. Thus trespassing this mucosal barrier is one of its aspects of virulence. Motility is important for *V. cholerae* in order to carryout mucin penetration (Liu et al., 2015). In this study, we found ChiS is important for *V. cholerae* motility in mucin and its penetration. This can be explained by the fact that when ChiS is activated by mucin ChiA2 is induced along with other chitinases to remove the sugar residues from mucin. This weakens the integrity of mucin. This provides easy access for the proteases to degrade mucin (Sanders et al., 2007). This leads *V. cholerae* to swim faster as well as penetrate into mucin layer to reach the intestinal epithelium for successful colonization. Our result suggested that the ChiS⁻ strain showed reduced adherence to intestinal cells, leading to defective colonization. Therefore, ChiS, a component of TCS, is found to be important for intestinal colonization by *V. cholerae*. A previous study with VprAB which is also a *V. cholerae* TCS has been found to contribute to its intestinal colonization (Herrera et al., 2014).

The ChiS⁻ strain in rabbit intestine showed reduced fluid accumulation, which is due to the reduced cholera toxin production. This was in accordance with our result, where we found reduced expression of *ctxA*. Decreased expression of *ctxA* along with *tcpA* was due to reduced expression of *toxT*. It is well established that lower *toxT* expression is linked to reduced *ctxA* and *tcpA* (DiRita et al., 1991). This indicates that ToxR regulon might be affected in the ChiS⁻ strain. The unability to utilize mucin by *V. cholerae* in the intestine decreases GlcNAc residues in the ChiS⁻ strain which might activate cyclic AMP (cAMP) receptor protein (CRP) (Kovacokova et al., 2004). This negatively regulates the ToxR regulon via cAMP-CRP pathway (Skorupski and Taylor, 1997). *In vitro*, we have also observed decreased production of virulence genes in AKI media (Fig. S4). However, further experiments are needed to establish the link between ChiS and ToxR regulon.

Additionally, delivery of the cholera toxin requires successful *V. cholerae* colonization in the small intestine (Taylor et al., 1987; Ritchie et al., 2010). Reduced colonization by ChiS⁻ leads to decreased cholera toxin production as well as less fluid accumulation.

Taken together, our data indicate that *V. cholerae* ChiS gets activated in the host intestine by mucin. It contributes to mucin

utilization by the bacteria which helps *V. cholerae* to survive in the intestine. On the other hand, ChiS plays a role in *V. cholerae* pathogenesis, probably through nutrient acquisition from mucin in the intestine during infection. However, further studies are needed for a complete understanding of the function of ChiS in this event.

Conflict of interest

The authors have no conflict of interest.

Appendix A. Supplementary data

Supplementary data associated with this article can be found, in the online version, at http://dx.doi.org/10.1016/j.ijmm.2016.09.003.

References

Bhowmick, R., Ghosal, A., Das, B., Koley, H., Saha, D.R., Ganguly, S., Nandy, R.K., Bhadra, R.K., Chatterjee, N.S., 2008. Intestinal Adherence of *Vibrio cholerae* involves a coordinated interaction between colonization factor GbpA and mucin. Infect. Immun. 76, 4968–4977.

Chen, H.C., Chang, C.C., Mau, W.J., Yen, L.S., 2002. Evaluation of *N*-acetylchitooligosaccharides as the main carbon sources for the growth of intestinal bacteria. FEMS Microbiol. Lett. 209, 53–56.

Debnath, A., Wajima, T., Sabui, S., Hamabata, T., Ramamurthy, T., Chatterjee, N.S., 2015. Two specific amino acid variations in colonization factor CS6 subtypes of enterotoxigenic *Escherichia coli* results in differential binding and pathogenicity. Microbiology 161, 865–874.

Deplancke, B., Vidal, O., Ganessunker, D., Donovan, S.M., Mackie, R.I., 2002. Selective growth of mucolytic bacteria including *Clostridium perfringens* in

neonatal piglet model of total parenteral nutrition. Am. J. Clin. Nutr. 76, 1117–1125.

Derrien, M., Passel, M.W., Bovenkamp, J.H., Schipper, R.G., Vos, W.M., 2010. Mucin-bacterial interactions in the human oral cavity and digestive tract. Gut Microbes 1, 254–268.

DiRita, V.J., Parsot, C., Jander, G., Mekalanos, J.J., 1991. Regulatory cascade controls virulence in Vibrio cholerae. Proc. Natl. Acad. Sci. U. S. A. 88, 5403–5407, Ding.

Ding, Y., Davis, B.M., Waldor, M.K., 2004. Hfq is essential for Vibrio cholerae virulence and downregulates σ^E expression. Mol. Microbiol. 53, 345–354.

Gal-Mor, O., Segal, G., 2003. Identification of CpxR as a positive regulator of icm and dot virulence genes of Legionella pneumophila. J. Bacteriol. 185, 4908–4919.

Groisman, E.A., 2001. The pleiotropic two-component regulatory system PhoP-PhoQ. J. Bacteriol. 183, 1835–1842.

Hector, M.W., Tamayo, R., Tischler, A.D., Lazinski, D.W., Camilli, A., 2008. The Vibrio cholerae hybrid sensor kinase VieS contributes to motility and biofilm regulation by altering the cyclic diguanylate level. J. Bacteriol. 190, 6439–6447.

Herrera, C.M., Crofts, A.A., Henderson, J.C., Pingali, Davies, B.W., Trent, M.S., 2014. The Vibrio cholerae VprA-VprB two-component system controls virulence through endotoxin modification. mBio 5, e02283-14.

Holmgren, J., 1973. Comparison of the tissue receptors for Vibrio cholerae and Escherichia coli enterotoxins by means of gangliosides and natural cholera toxoid. Infect. Immun. 8, 851–859.

Hunt, D.E., Gevers, D., Vahora, N.M., Polz, M.F., 2008. Conservation of chitin utilization pathway in Vibrionaceae. Appl. Environ. Microbiol. 74, 44–51.

Huq, A., Small, E.B., West, P.A., Huq, M.I., Rahman, R., Colwell, R.R., 1983. Ecological relationships between Vibrio cholerae and planktonic crustacean copepods. Appl. Environ. Microbiol. 45, 275–283.

Kovacokova, G., Lin, W., Skorupski, K., 2004. Vibrio cholerae AphA uses a novel mechanism virulence gene activation that involves interaction with the LysR-type regulator AphB at the tcpPH promoter. Mol. Microbiol. 53, 129–142.

Li, X., Roseman, S., 2004. The chitinolytic cascade in vibrios is regulated by chitin oligosaccharides and a two-component chitin catabolic sensor/kinase. Proc. Natl. Acad. Sci. U. S. A. 101, 627–631.

Liu, Z., Miyashiro, T., Tsou, A., Hsiao, A., Goulian, M., Zhu, J., 2008. Mucosal penetration primes Vibrio cholerae for host colonization by repressing quorum sensing. Proc. Natl. Acad. Sci. U. S. A. 105, 9769–9774.

Liu, Z., Wang, Y., Liu, S., Sheng, Y., Rueggeberg, K.G., Wang, H., Li, J., Frank, X., Zhong, G.Z., Kan, B., Zhu, J., 2015. Vibrio cholerae represses polysaccharide synthesis to promote motility in mucosa. Infect. Immun. 83, 1114–1121.

Livak, K.J., Schmittgen, D.T., 2001. Analysis of relative gene expression data using real- time quantitative PCR and the 2(-Delta DeltaC(T)) method. Methods 25, 402–408.

Meibom, K.M., Li, X.B., Neilson, A.T., Wu, C.Y., Roseman, S., 2004. The Vibrio cholerae chitin utilization program. Proc. Natl. Acad. Sci. U. S. A. 101, 2524–2529.

Mondal, M., Nag, D., Koley, H., Saha, D.R., Chatterjee, N.S., 2014. The Vibrio cholerae extracellular chitinase ChiA2 is important for survival and pathogenesis in the host intestine. PLoS One 9, e103119.

Orikoshi, H., Nakayama, S., Miyamoto, K., Hanato, C., Yasuda, M., Inamori, Y., Tsujibo, H., 2005. Roles of four chitinases (ChiA, ChiB, ChiC and ChiD) in the chitin degradation system of marine bacterium Alteromonas sp. Strain O-7. Appl. Environ. Microbiol. 71, 1811–1815.

Patra, T., Koley, H., Ramamurthy, T., Ghose, A.C., Nandy, R.K., 2012. The Entner-Doudoroff pathway is obligatory for gluconate utilization and contributes to the pathogenicity of Vibrio cholerae. J. Bacteriol. 194, 3377–3385.

Philippen, N., Alcaraz, J.P., Counsage, E., Geiselmann, J., Schneider, D., 2004. Improvement of pCVD442, a suicide plasmid for gene allele exchange in bacteria. Plasmid 51, 246–255.

Ritchie, J.M., Rui, H., Bronson, R.T., Waldor, M.K., 2010. Back to the future: studying cholera pathogenesis using infant rabbits. mBio 1, e00047–10.

Sanders, N.N., Eijsink, V.G., van den Pangaart, P.S., Joost van Neerven, R.J., Simons, P.J., De Smedt, S.C., Demeester, J., 2007. Mucolytic activity of bacterial and human chitinases. Biochim. Biophys. Acta 1770, 839–846.

Shi, Y., Cromie, M.J., Hsu, F.F., Turk, J., Groisman, E.A., 2004. PhoP- regulated salmonella resistance to the antimicrobial peptides magainin 2 and polymixin B. Mol. Microbiol. 53, 229–241.

Skorupski, K., Taylor, R.K., 1996. Positive selection of vectors for allelic exchange. Gene 169, 47–52.

Skorupski, K., Taylor, R.K., 1997. Cyclic AMP and its receptor protein negatively the coordinate expression of cholera toxin and toxin-coregulated pilus in Vibrio cholerae. Proc. Natl. Acad. Sci. U. S. A. 94, 265–270.

Svitil, A.L., Chadhain, S., Moore, J.A., Kirchman, D.L., 1997. Chitin degradation proteins produced by the marine bacterium Vibrio harveyi growing on different forms of chitin. Appl. Environ. Microbiol. 63, 408–413.

Taylor, R.K., Miller, V.L., Furlong, D.B., Mekalanos, J.J., 1987. Use of phoA gene fusions to identify a pilus colonization factor coordinately regulated with cholera toxin. Proc. Natl. Acad. Sci. U. S. A. 84, 2833–2837.

Vercruysse, M., Kohrer, C., Davies, B.W., Arnold, M.F.F., Mekalanos, J.J., RajBhandary, U.L., Walker, G.C., 2014. The highly conserved bacterial RNase YbeY is essential in Vibrio cholerae, playing a critical role in virulence, stress regulation, and RNA processing. PLoS Pathog. 10, e1004175.

Yamamoto, S., Mitobe, J., Ishikawa, T., Wai, S.N., Ohnishi, M., Watanabe, H., Izumiya, H., 2014. Regulation of natural competence by the orphan two component system sensor kinase ChiS involves a non-canonical transmembraneregulator in Vibrio cholerae. Mol. Microbiol. 91, 326–347.

Yeung, A.T., Parayno, A., Hancock, R.E., 2012. Mucin promotes rapid surface motility in Pseudomonas aeruginosa. mBio 3, e00073-12.